Studies on Sustainable Oxidation, Azidation, Rearrangement, and Annulation Reactions towards Heterocyclic Scaffolds under Batch and Continuous Flow

A Thesis

Submitted in Partial Fulfillment of the Requirements

Of the Degree of

Doctor of Philosophy

By

Akanksha M. Pandey

(ID: 20183576)

INDIAN INSTITUTE OF SCIENCE EDUCATION AND RESEARCH PUNE

This Thesis is Dedicated to my Mother, Father, Mother-in-law, and Father-in-law for Loving and Supporting Me Unconditionally

DECLARATION

I declare that this written submission represents my ideas in my own words and where others' ideas have been included, I have adequately cited and referenced the original sources. I also declare that I have adhered to all principles of academic honesty and integrity and have not misrepresented or fabricated or falsified any idea/data/fact/source in my submission. I understand that violation of the above will be cause for disciplinary action by the Institute and can also evoke penal action from the sources which have thus not been properly cited or from whom proper permission has not been taken when needed.

Date: 13.04.2023

Akanksha M. Pandey

Roll No. 20183576

CERTIFICATE

Certified that the work incorporated in the thesis entitled "*Studies on Sustainable Oxidation, Azidation, Rearrangement, and Annulation Reactions toward Heterocyclic Scaffolds under Batch and Continuous Flow*" submitted by Akanksha M. Pandey was carried out by the candidate, under my supervision. The work presented here or any part of it has not been included in any other thesis submitted previously for the award of any degree or diploma from any other University or institution.

Date: 13.04.2023

Supervisor

Dr. Boopathy Gnanaprakasam

Associate Professor

ACKNOWLEDGMENTS

I want to express my heartfelt appreciation to everyone who helped make these five years possible. First and foremost, I would like to express my profound thanks to my advisor, Dr. Boopathy Gnanaprakasam, for providing me with all the opportunities, support, suggestion, and encouragement I needed to succeed in my Ph.D. studies. He deserves my sincere thanks, which I'm not sure I'll ever be able to convey adequately. I am grateful to Dr. Ramnath Mallah for his support during my CSIR-NET exam preparation and career guidance.

No gratitude can express how much my devoted parents, Mrs. Asha Pandey and Mr. Mahendrakumar Pandey, have meant to me throughout my life. I feel blessed to learn life lessons from my strong grandparents, Mrs. Ashrafi Pandey, Mr.Lalchand Pandey, Nirmala Upadhyay and Rambali Upadhyay. I am fortunate that my spouse Mr. Navinkumar Tiwari and my in-laws, Mrs. Nirmala Tiwari and Mr. Jayprakash Tiwari, supported me during this trip. I always had tremendous support from my dear brothers Agnivesh, Nityavesh, and Praveen. I also appreciate my sister-in-law Richa and Rusham for their support. As a bonus, my nephews, Tejomya and Trayaksh deserve my gratitude for always making me smile in stressful situations.

I am very grateful to Prof. K. N. Ganesh and Prof. Jayant Udgaonkar, our former directors, and Prof. Sunil Bhagwat, our current director, for providing top-notch research facilities, funding and platforms at the Indian Institute of Science Education and Research (IISER), Pune, India. Additionally, I would like to thank Dr. S. G. Srivatsan and Dr. Ravindar Kontham for their insightful comments during my RAC meetings. I wish to thank Prof. M. Jayakannan and Prof. H. N. Gopi, the former chairs of chemistry, and Dr. Nirmalya Ballav, the current chair, for their help and support with Chemsymphoria and other departmental initiatives. I appreciate the XPS analysis and hydrogen gas evolution tests performed by Dr. C. P. Vinod and Dr.Chinnakonda S. Gopinath from CSIR-NCL, Pune. I also thank Dr. S. K. Ghosh for the BET isotherm. I also thank the IISER Pune faculties for carrying out departmental activities. I thank the instrument operators and the administrative team (Dr. Sandeep Kanade, Mahesh, Yathish, Ravindra, Ganesh, Mayuresh, Megha, Bhagyashree, Sanjay, Tushar, Sayalee, Dr. Sandeep Mishra, Nitin, Chinmay).

I am glad this journey made me meet fantastic friends, Pragati, Pooja, Vishnu, Himan, Jabed, Utreshwar, Pragalbh, and Priya, who have improved my personal and professional lives. I am amazingly fortunate to get the cheerful and friendly lab members: Dr. Sandip, Dr. Moreshwar, Dr. Girish, Nirmala, Akash Ubale, Moseen, Akash Jamdade, Dashrath Sutar, Shankhajit, Gokul, Palvi, Somnath, Parvathalu, Navin, Nilima, Prabu, Gourishankar, Shahrukh, and Writam for making good lab ambiance. I thank all the labs for their support, especially Dr. Debanjan for catalysis and its characterization-related queries, Himan and Vishnu for SCXRD, and Yogesh for PXRD studies.

The IISER-Pune, Trimurti Fabricators, and Twenty-Twenty Interior Design Software Research Grant 2021-202 are recognized for their financial support. Lastly, I express my gratitude to the omnipotent god, without whom nothing is possible.

AKANKSHA M. PANDEY

TABLE OF CONTENTS

ABBREVIATION

Ac	Acetyl
Ar	Aryl
atm	Atmospheric
Aq	Aqueous
Bn	Benzyl
bs	Broad singlet
Bu	Butyl
bpy	Bipyridyl
°C	Degrees Celsius
calcd.	Calculated
cat.	Catalytic
conc.	Concentrated
$CDCl_3$	Deuterated chloroform
DBU	1,8-Diazabicyclo[5.4.0]undec-7-ene
DCM	Dichloromethane
DCE	Dichloroethane
THF	Tetrahydrofuran
DEPT	Distortionless enhancement by polarization transfer
DMF	*N*, *N*-Dimethyl formamide
DMSO	Dimethyl sulfoxide
DMSO-d_6	Duterated dimethyl sulfoxide
DMA	*N,N'*-Dimethylacetmide
dppf	1,1′-Bis(diphenylphosphino)ferrocene
DMAP	4-Dimethylaminopyridine
DTBP	Di-tert-butyl peroxide
dr	Diastereomeric ratio
ee	Enantiomeric excess
equiv.	Equivalents

ESI TOF	Electrospray ionization time-of-flight
EI	Electron impact
ESI	Electron spray ionization
Et	Ethyl
EtOAc	Ethyl acetate
FTIR	Fourier-transform infrared spectroscopy
Fg	Functional group
gm	gram(s)
GC	Gas chromatography
GC-MS	Gas chromatography-mass spectrometry
h	Hour (s)
Hz	Hertz
HRMS	High-resolution mass spectroscopy
IR	Infra-red
J	Coupling constant in NMR
L	Ligand
LA	Lewis-acid
M	Molar solution
m/z	mass to charge ratio
m	multiplet (in NMR)
Me	Methyl
MS	Mass spectroscopy
Mp	Melting point
mg	Milligram
mmol	Millimoles
NMR	Nuclear magnetic resonance
OAc	Acetate
Ph	Phenyl
PTSA	*Para*-toluenesulfonic acid
rt	Room temperature
Sn	Tin
tert	Tertiary

TBHP	*tert*-butyl hydroperoxide
TLC	Thin layer chromatography
TMS	Tetramethyl silane
THF	Tetrahydrofuran
TON	Turnover number
TOF	Turnover frequency
t_R	Residence time (in flow)
TS	Transition state

PREFACE

Chemistry paved the path for making modern society livable by fulfilling the basic needs of daily life through rapid industrialization. However, the toxic waste produced by chemical industries vitiates the environment profoundly and affects the ecosystem. Still, industrialization is the only way to cope with the plenty of resources of society. Hence, the quest for new sustainable methods that eliminate hazardous waste generation or deliver useful waste is required in the chemical industry. In this context, twelve green chemistry principles play a pivotal role in making the process sustainable. Therefore, the selection of reactions, chemicals, and processes, which are sustainable and green at the same time, should be preferred for the design and innovation of any chemical operation. Therefore, the utilization of green chemistry tools such as green solvents, green catalysis, solvent free-catalyst free reactions (SF-CF), or the use of alternative technologies (microwave, flow, mechanochemistry, photochemistry, etc.) can be an ideal choice for making the process sustainable. In this direction, this thesis describes research findings in the development of "*Studies on Sustainable Oxidation, Azidation, Rearrangement, and Annulation Reactions toward Heterocyclic Scaffolds under Batch and Continuous Flow*," and which comprises of five chapters.

Chapter 1: Introduction to sustainable chemistry

At the outset, the studies and development of various chemical operations have been depicted utilizing several tools of green chemistry to make the process sustainable. Subsequently, the general overview of sustainable and green chemistry has been briefly discussed. The selected representative examples using tools of green chemistry are also summarized in this chapter. Finally, the aim and rationale for the thesis work are described.

Chapter 2: Benzylic sp^3 C-H oxidation under batch and continuous flow

Functional group transformation is one of the major challenging aspects of organic synthesis. For the direct transformation of methylene groups to afford ketone, several homogeneous catalysts of Cr, Mn, Co, Bi, Ru, Rh, and Fe are reported. Tragically, there are limitations that exist in this transformation, such as the decomposition of the metal catalysts, the problems of catalyst extraction and recycling as well as product purification makes them less suitable for the synthesis of fine chemicals where product contamination with heavy metal is highly

undesirable in large-scale synthesis. Hence to surrogate the drawbacks associated with the heterogenization of the catalyst, we envisioned the synthesis of Mn-based magnetic nanoparticles because Mn is known to be a good oxidizing agent. The catalyst was fully characterized FESEM, TEM, PXRD, XPS, MPAES analysis. However, metal catalyst reacting with TBHP oxidant may produce a rigorous reaction. Therefore, we have integrated the catalyst into continuous flow conditions for mitigating safety hazards and scale-up issues. This strategy offers the opportunity for using heterogeneous 0.424 % $MnO_2@Fe_3O_4$ nanoparticles as a magnetically retrievable catalyst which shows no significant loss in its catalytic activity even after ten cycles with good TON and TOF.

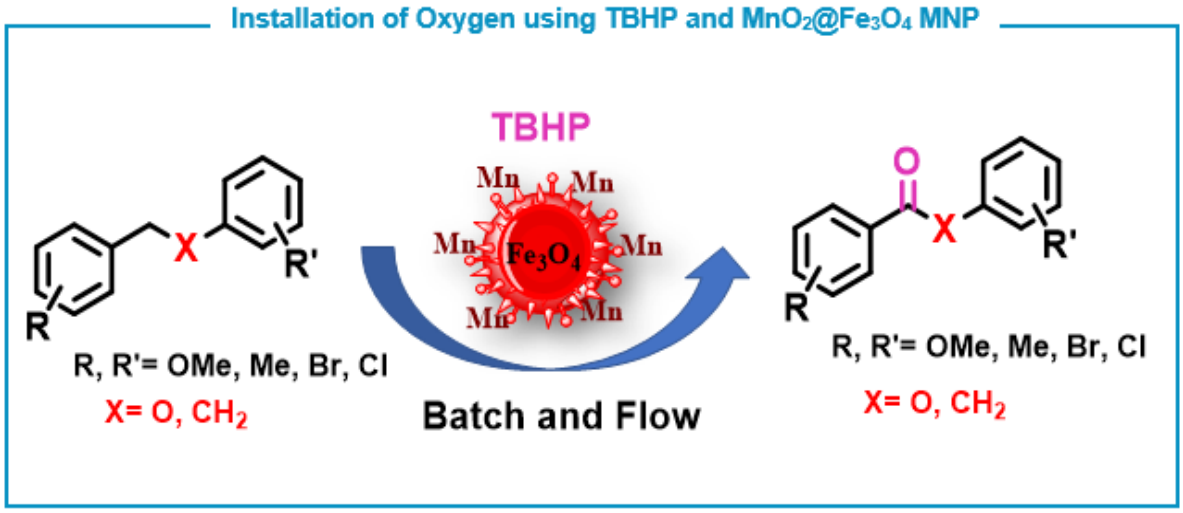

Scheme 1. Benzylic sp^3 C-H oxidation using heterogeneous $MnO_2@Fe_3O_4$ nanoparticles

Chapter 3: Continuous flow direct azidation of alcohols and peroxides towards the synthesis of heterocyclic scaffolds

Traditionally, direct azidation of alcohols required activation of hydroxy to make it as a good leaving group for feasible nucleophilic reaction. Notably, direct installation of azides from alcohols has also been reported using Lewis acid or Bronsted acid catalysts. However, large-scale production has been an issue under batch conditions. This issue can be dealt with by integrating it into a continuous flow. The literature report on azidation in flow is not adequate when sustainability parameters are concerned as it is limited to propargylic alcohols and produces stoichiometric waste generation from azide precursor. Thus, we proposed to develop an energy-efficient, room temperature, recyclable heterogeneous Bronsted acid catalyst for

direct azidation of alcohols to generate hitherto unknown azides. A further application was studied towards the synthesis of drugs and the development of new organic transformations.

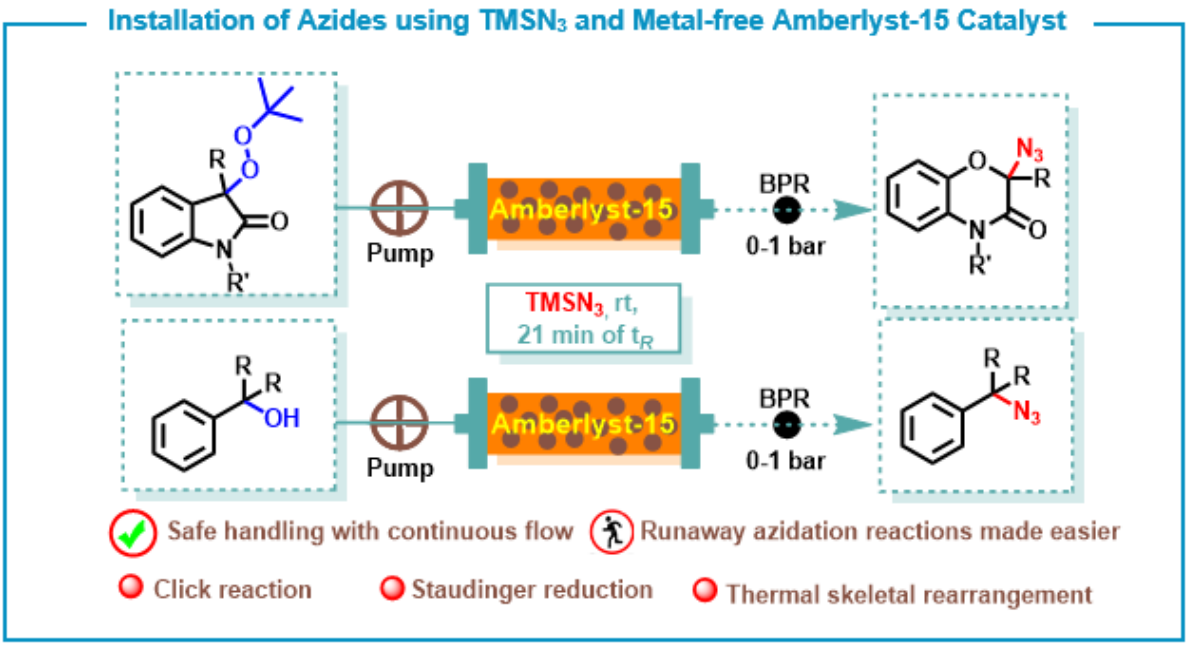

Scheme 2. Continuous flow direct azidation, rearrangement, and its applications toward heterocyclic scaffolds generation

Chapter 4: Skeletal editing through solid state melt rearrangement of azides

Organic azides deliver various organic reactions that have been extensively studied in chemical biology, pharmaceuticals, medicinal, and agricultural areas. Furthermore, the rearrangement of azide is a key operation in generating numerous heterocyclic scaffolds. The heterocyclic scaffolds such as phenanthridines are prevalent core in several natural products and staining agents that could be assembled in various manners. However, to the best of our knowledge, the skeletal editing of azides for the synthesis of phenanthridines is not reported in the literature. Additionally, the available reports demanded the use of catalysts, high temperatures, solvents, additives, and bases. As outlined SFCF reactions, we hypothesized to study SFCF rearrangement for constructing phenanthridine derivatives which includes a skeletal editing process by using azides as a starting material.

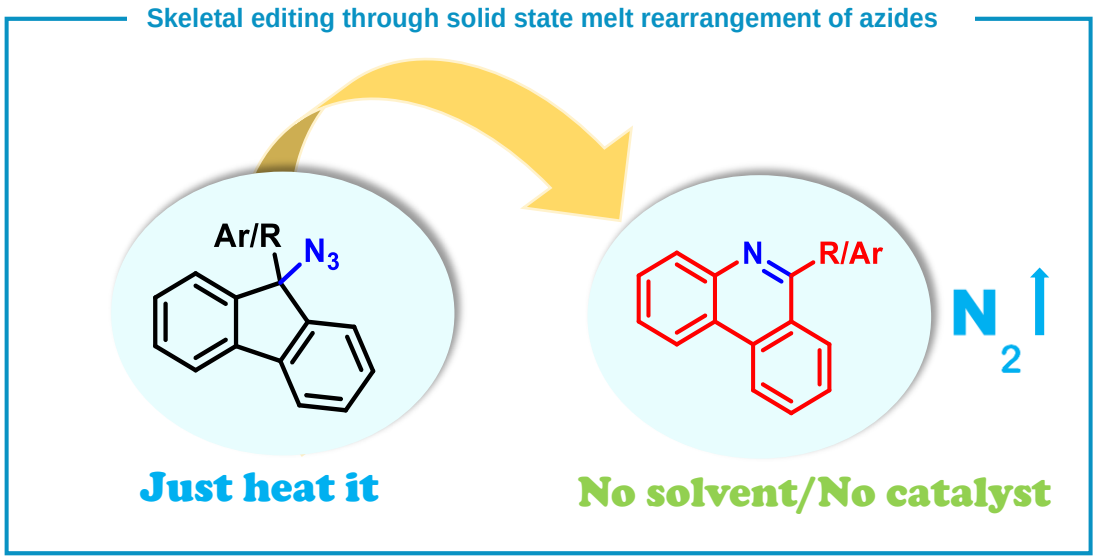

Scheme 3. Skeletal editing through solid-state melt rearrangement of azides

Chapter 5: Catalytic acceptorless dehydrogenation strategy for annulation under neutral conditions

In continuation to heterocycle synthesis, this chapter is focused on developing the Domino reaction strategy. In literature, numerous approaches have been developed for the synthesis of heterocycles that involves traditional metal and metal-free conditions. Despite the fact that these methods provide interesting catalytic reaction steps and synthetically useful approaches, the generated copious waste, multistep synthesis, and limited feedstock chemicals are the disadvantages of these traditional methods. As a result, acceptorless dehydrogenation (AD) has become a widely applied method for chemical synthesis because it has several attractive characteristics for the formation of C–C and C–X bonds. This process generates water and molecular hydrogen as a byproduct and retains a high atom economy which contributes towards green synthesis. Although several research groups have extensively employed the AD strategy for the synthesis of pyrrole and pyridine core, it still suffers from the use of a specially designed complex and requires a stoichiometric base for annulation which generates copious waste. Consequently, this decreases the atom economy and makes it less sustainable. In this direction, we aimed to develop an annulation strategy to get tetrahydroindolones and tetrahydroacrindones which avoid the need for base, ligands, and additives. Further, we propose to apply this process for the synthesis of molindone core under solvent-free conditions.

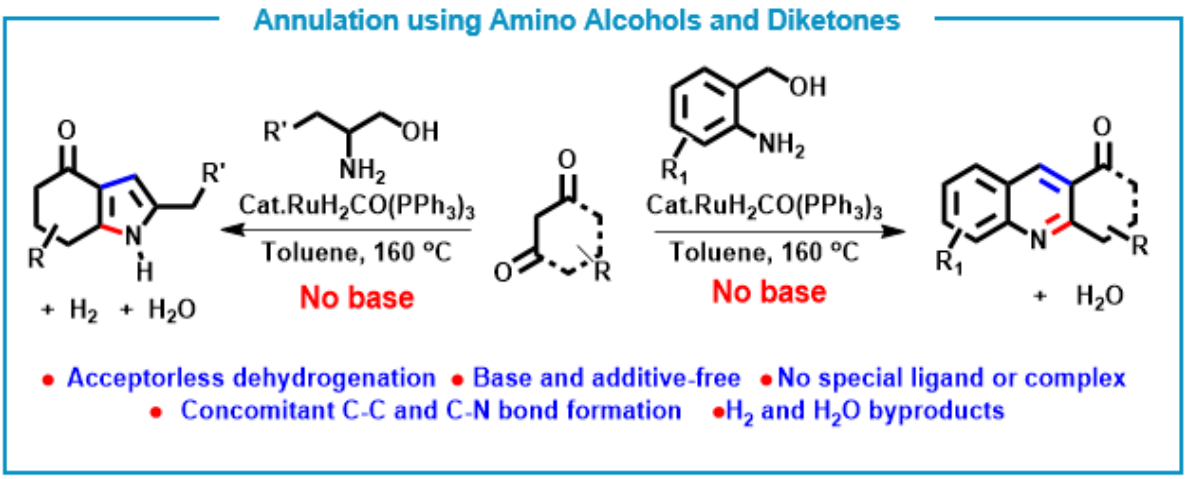

Scheme 4. Annulation through acceptorless dehydrogenation strategy under neutral condition

Overall, the research work in this thesis is aimed to develop sustainable oxidation, azidation, rearrangement, and annulation reactions toward various heterocyclic scaffolds under batch and continuous flow. To get a clear understanding, the introduction and literature background of each chapter are written separately following the current general introduction.

Chapter I: Introduction to Sustainable Chemistry

Introduction to Sustainable Chemistry

1.1. Abstract

In this chapter, studies and development of various chemical operations have been depicted utilizing several tools of green chemistry to make the process sustainable. Subsequently, the general overview of sustainable and green chemistry has been briefly discussed. The selected representative examples using tools of green chemistry are also summarized in this chapter. Finally, the aim and rationale for the thesis work are described.

1.2. Introduction to sustainable chemistry and green chemistry

Chemistry has employed widespread applications for humans through expeditious industrialization. Moreover, the toxic waste produced by chemical industries pollutes the environment profoundly and affects the ecosystem.[1] However, the demand for the majority of chemical transformations and industrial waste generation is interrelated with each other. This leads the scientific community to ponder global concerns.[2] Therefore, the concept of sustainable development was introduced in the 1980s. In "The World Commission on Environment and Development" sustainable development was described as "To meet the needs of the present without compromising the ability of future generations to meet their own needs".[3] This can be simplified as "Energy and resources should be replaced naturally as fast as it is consumed".[4]

In the context of the development of chemical transformations, *sustainable chemistry* can be defined as the development of chemical operations that envisions industrial processes to generate products with lesser pollutants for industrial profitability which can be used for human endeavors. In contrast, *green chemistry* deals with the development of reactions by designing safer approaches using environmentally benign feedstocks without considering industrial processes or profitability (Figure 1.2.1). Hence, "*Green chemistry is an integral part of sustainable chemistry*" with the "*More and better*" approach. Hence, the target of design and innovation for any chemical reactions following a sustainable and green procedure should be preferred.[5] Additionally the amalgamation of sustainable and green chemistry could accomplish the quest for new sustainable developments. Thereby twelve green chemistry principles can be considered, developed by Paul T. Anastas and John C. Warner in 1991 and published in 1998 as *Green Chemistry: Theory and Practice*, Oxford University Press, New

York. These principles focus mainly on three aspects: (1) *Avoiding toxic chemicals*, (2) *Reducing chemicals and energy consumption*, and (3) *Preventing accidents*.

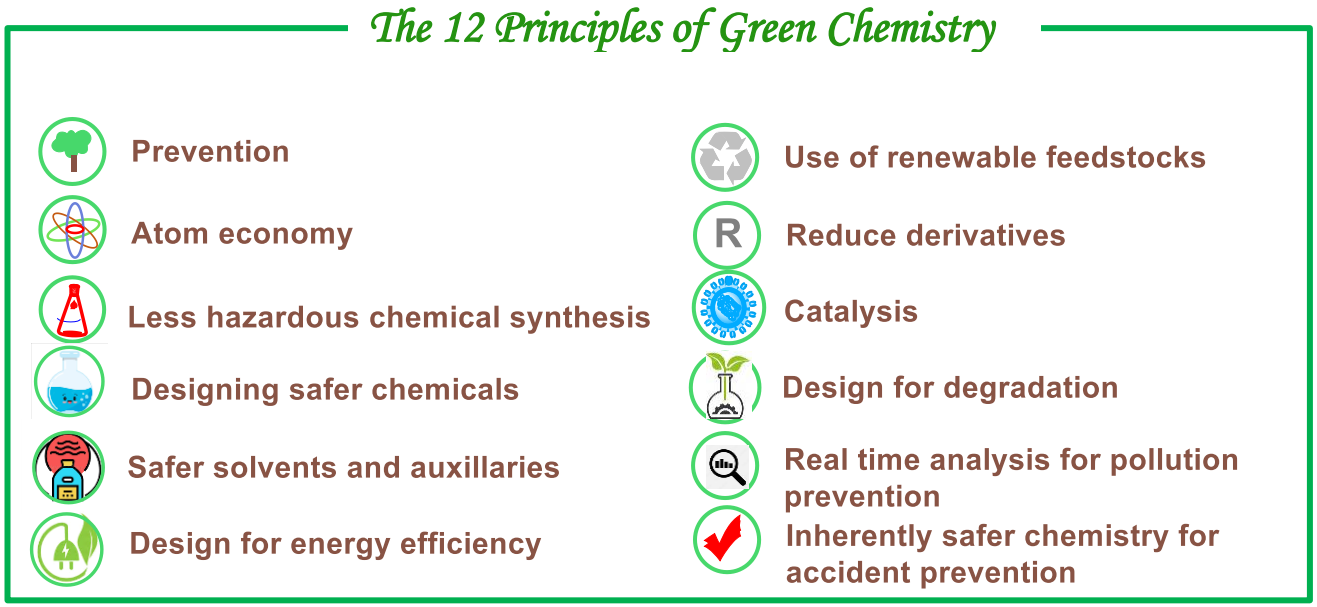

Figure 1.2.1: Twelve principles of green chemistry (Adopted from the book: "*Green Chemistry: Theory and Practice"*, Oxford University Press, New York)

The principles of green chemistry could be accomplished by using green chemistry tools.

1.3. Tools of green chemistry

To make an energy-efficient process having a "Benign by design" approach utilizing green chemistry tools can be an ideal choice.

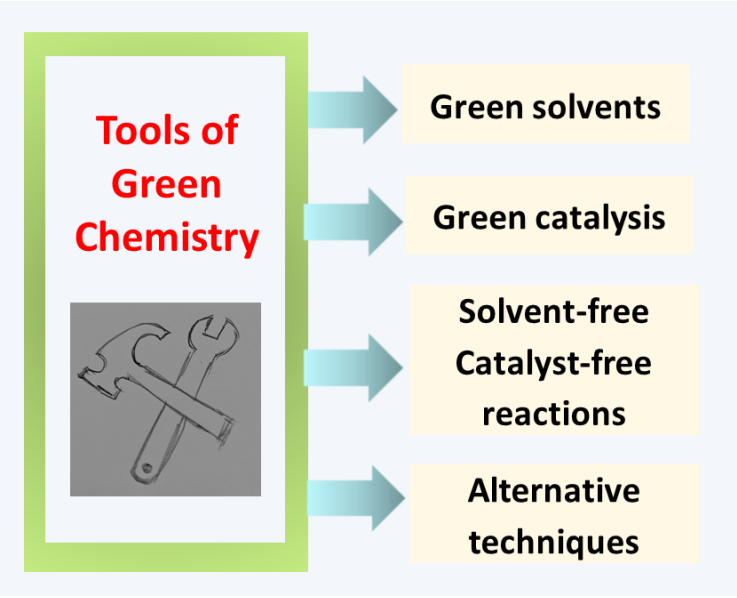

Figure 1.3.1: Tools of green chemistry

1.3.A Green solvents in organic synthesis

Organic solvents are indispensable in dissolving and extracting solutes in industries or academia, which may or may not participate in chemical reactions based on the type of reaction performed. The dissolving capacity of solute into solvents depends on the physical properties and molecular structure of both the solute and the solvent. However, organic solvents generate tremendous amount of waste which is highly undesired in chemical industries. Therefore, the most straightforward approach could be redesigning syntheses or using less solvent. In this regard, the utilization of green solvents can be imposed. The goal of the green solvent is to reduce the environmental impact associated with the use of solvents. The characteristics of green solvents are low toxicity, easy biodegradability, high boiling point, and easy recyclability. In the literature, various examples such as ionic liquids, water, supercritical fluids and polyethylene glycols (PEG) as a green solvents have been described (Figure 1.3.2).[6]

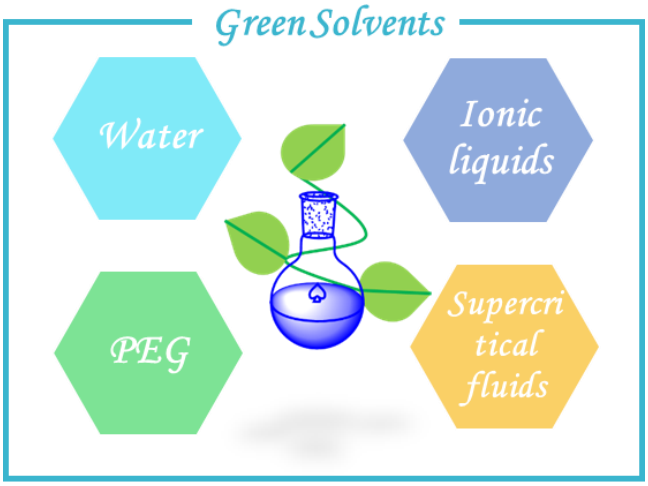

Figure 1.3.2: Green solvents

Ionic liquids are salts made up of bulky organic cations and inorganic anions. It exists in a liquid state at ambient temperature that usually does not need an external heat source to be melted. In 1914, ethylammonium nitrate was reported by Paul Walden as the first ionic liquid. The ionic liquids gained much attention in recent decades amongst the scientific community. It has been exploited as a catalyst and solvent. Several organic transformations have been performed by taking ionic liquid as a solvent. The synthesis of Pravadoline **5**, a potential nonsteroidal anti-inflammatory drug, is one of the example where ionic liquids are used as a solvent.[7] After the first stage, the second stage was carried out in [bmim]PF_6 as a solvent for the synthesis of **5**. However, due the high reactivity, the substituted indole

3 undergoes an acylation reaction without any Lewis acid. The simple product separation and solvent recovery are its key features (Scheme 1.3.1).

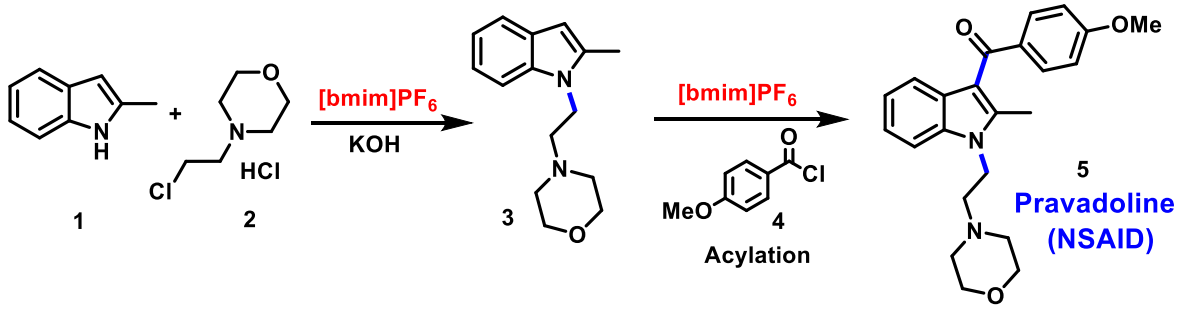

Scheme 1.3.1: Synthesis of Pravadoline **5** in ionic liquid

Water is a great solvent because of its polarity and ability to form hydrogen bonds which allows it to dissolve many molecules. One pot synthesis of indole **8** is demonstrated from indole carboxylic acid esters **6** with water as a solvent (Scheme 1.3.2).[7] Initially, at 200 ^{o}C, indole carboxylic acid esters rapidly hydrolyzed in the presence of small amounts of the base to give carboxylic acids **7**. On further increasing the temperature at 255 ^{o}C, decarboxylation takes place to afford indole **8**.

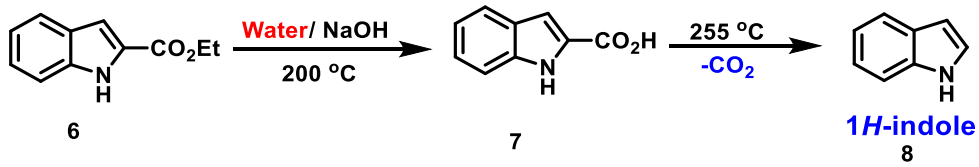

Scheme 1.3.2: Indole synthesis in water at high temperature

Isaacs and Keating performed the Diels-Alder reaction of p-benzoquinone **10** and cyclopentadiene **9** in liquid and supercritical CO_2 was studied for the synthesis of product **11** (Scheme 1.3.3).[8] By using liquid and supercritical CO_2 ($scCO_2$), more product formation was obtained than those in diethyl ether solvent.

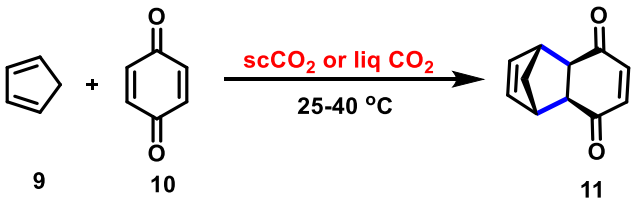

Scheme 1.3.3: Diels–Alder reaction using liquid and supercritical CO_2 ($scCO_2$)

Next, PEG-400 i.e. Poly(ethylene glycol)-400 known as an eco-friendly solvent have widespread applications in solvents, as an dispersing agents, suppository bases, pharmaceuticals, and in cosmetics industries. Thus, the sustainable protocol for the synthesis of aromatic esters by a carbonylative method

using palladium catalyst in PEG-400 as a greener and recyclable solvent has been demonstrated. The reaction was carried out at room temperature using CO in a balloon. The good to excellent yield of various esters **14** was observed by direct insertion of CO moiety leading to the high atom and step economy (Scheme 1.3.4).[9]

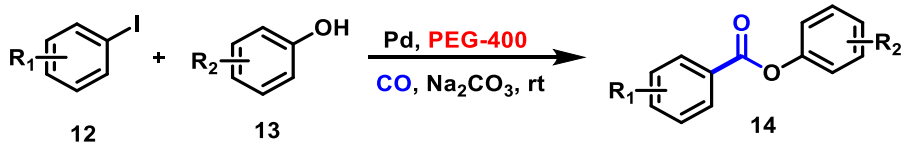

Scheme 1.3.4: Palladium catalysed synthesis of aromatic esters in PEG-400 as solvent

1.3.B. Green catalysis in organic synthesis

Catalytic reagents and stoichiometric reagents are typically the two types of reactants needed for a chemical transformation. Chemical reactants that are consumed during a reaction are known as stoichiometric reagents. As a result, a stoichiometric reagent takes an active part in the chemical process but generates a tremendous amount of byproduct. In contrast, catalytic reagents are reactants in a particular chemical transformation which doesn't get consumed during the reaction. Catalyst is a substance that alters the rate of a particular chemical reaction. In particular, the process of increasing the rate of reaction is known as catalysis. The catalytic reactions are classified as homogeneous or heterogeneous catalytic reactions.

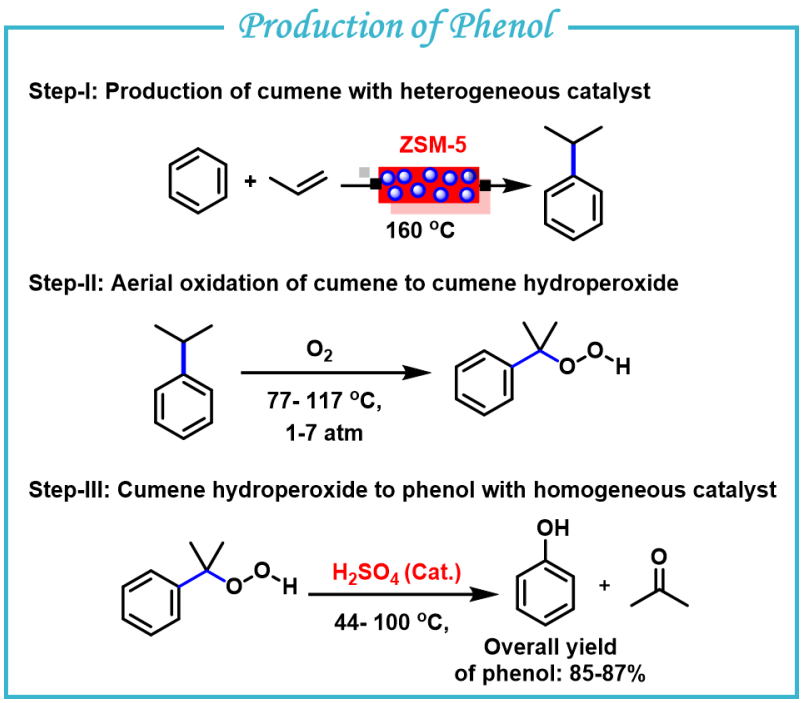

Scheme 1.3.5: Industrial production of phenol

In homogeneous catalysis, the reactants and catalyst have same phase of matter. On the other hand, in heterogeneous catalysts, the reactants have a different phase of matter than the catalyst. However, the green catalysis is focused on energy-efficient synthesis to achieve maximum atom efficiency by surrogating the need for a stoichiometric reactant to homogenous and heterogeneous catalytic reactions where organic, inorganic, and biocatalysts can be used for environmental protection and economic benefit.[6] The industrial production of phenol **19** is one of the example that includes both homogeneous and heterogeneous catalysis (Scheme 1.3.5).[10] In the first step, the production of cumene **17** from benzene **15** and 1-propene **16** using ZSM-5 as a heterogeneous catalyst was developed by heating the reaction mixture at 160 ^{o}C. In the proceeding step, cumene **17** undergoes aerial oxidation to give cumene hydroperoxide **18**. Later, cumene hydroperoxide **18** undergoes sequential rearrangement in the presence of the catalytic amount of sulphuric acid as a homogeneous catalyst to give phenol **19** and acetone **20**. Although the process is not completely green but it follows many green chemistry principles (Figure 1.2.1). To date, Scheme 1.3.5 is known to be a sustainable process for the industrial production of phenol **19**.

1.3.C. Solvent-free Catalyst-free (SF-CF) reactions in organic synthesis

It is noteworthy that small to large industries have incorporated key elements of green chemistry to move towards sustainability. Moreover, it is difficult to follow all these twelve principles to carry out any chemical reaction. Thereby, legitimate changes have been made recently to avoid the extensive use of hazardous and toxic solvents or reagents, harsh reaction condition, or expensive and complicated catalytic systems.[11] Therefore, the "*Prevention of waste*" principle could be directly achieved by eliminating solvents in the reaction. The elimination of solvent from the reaction is economical and environmentally benign that can reduce large batch volume for capital investment.[12] Thus, it received substantial attention towards pollution reduction. Besides solvents usage, catalysts that are costly and challenging to recycle raise manufacturing costs and contribute to environmental damage. Hence, a catalyst-free organic synthesis has been developed from the perspective of a practical, affordable method for simple separation and purification. Moreover, conducting an experiment under SF-CF condition at room temperature, conventional heating, or using alternative energy methods such as microwave heating, sonication, mechanochemical mixing, and high-speed ball milling is highly desired.[13a] The reaction at room temperature under SF-CF reaction is fascinating from a green perspective. Various examples have been known in the literature for the allylation of ketones, synthesis of amides, diazo-(2-ethoxy-2-oxoethyl)-1,2-dihydroquinolines, dithiocarbamates, imidazopyridines, etc at room temperature.[12] On the other hand, conventional heating is one of the oldest techniques to

conduct any organic reaction by applying direct heat to the reaction vessel for performing the reaction. By using it, several interesting reactions have been developed towards the synthesis of boronate-based cages, borasiloxane-based macrocycles, thiophenes, dithiocarbamates, 3,3'-(benzylene)-bis(4-hydroxy-2*H*-chromen-2-one), allyl phosphonates, quinazolinones, sulfones, and dihydropyrimidines, etc.[13a] The use of alternative techniques for SF-CF reactions is described under the alternative techniques in organic synthesis.

1.3.D. Alternative technique in organic synthesis

The conventional methods may affect the productivity and selectivity of the product by generating large amount of waste. Thereby, use of alternative technique has been introduced to overcome through the limitations of conventional chemical processes. In literature, several technologies are as follows;

- Microwave-assisted synthesis[13a]
- Ultrasound irradiation[13a]
- Mechanochemical mixing[13a]
- Photochemical
- Continuous flow

Each technique is shortly described further with respective examples.

1.3.D.1. Microwave-assisted synthesis:

Microwave (MW) irradiation offers rapid heating at the rotational molecular level, homogeneity in the reaction mixture, selective heating, and high temperature.

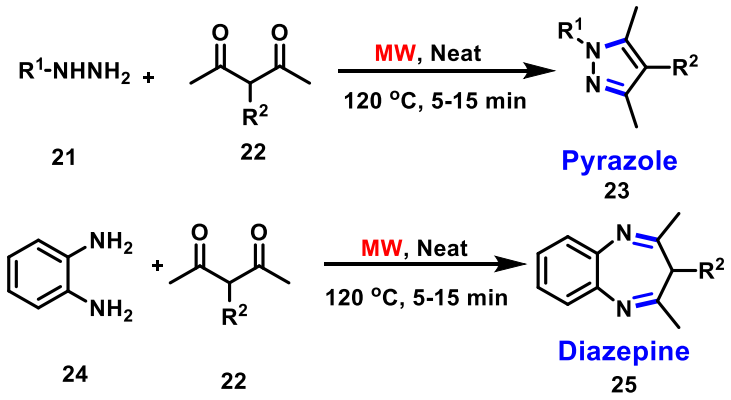

Scheme 1.3.6: Pyrazoles **23** and diazepines **25** synthesis under microwave heating

Several examples have been demonstrated under SF-CF condition using MW reaction for the synthesis of pyrazoles **23**, diazepines **25**, ring-fused aminals **28**, and many other heterocycles. A few representative examples are illustrated for the synthesis of pyrazoles **23** and diazepines **25** were studied under MW irradiation and SF–CF conditions. After grinding the reaction mixture in mortar and pestle, it was subjected to microwave irradiation at 120 °C for 5–15 min, afforded excellent yields of the products **23** and **25** (Scheme 1.3.6).[13a]

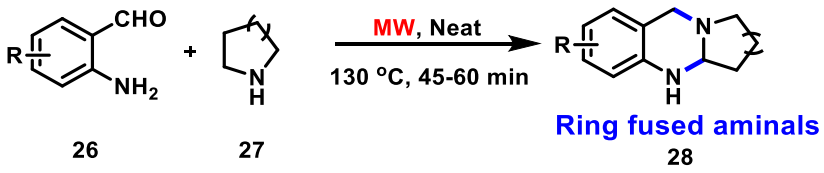

Scheme 1.3.7: Synthesis of ring-fused aminals under microwave heating

The above protocol could be used for the synthesis of other ring-fused aminals **28**. Polshettiwar and Varma achieved the high-yield synthesis of ring-fused aminals by α-amination reaction using a series of cyclic amines **27** and amino benzaldehydes **26**.[13b]

1.3.D.2. Ultrasound irradiation:

Ultrasound irradiation promoted organic reactions provide a specific activation based on acoustic cavitation. The examples in literature are the synthesis of Michael adduct **31**, rhodanine **35**, and 6*H*-1-benzopyrano[4,3-*b*]quinolin-6-ones **38**, etc. Furthermore, Yang et al. successfully demonstrated a simple, efficient Michael addition of ferrocenylenones **29** to aliphatic amines **30** under solvent and catalysts-free conditions at room temperature for 0.5-2 h reaction time using ultrasound irradiation to get desired Michael adducts (Scheme 1.3.8).

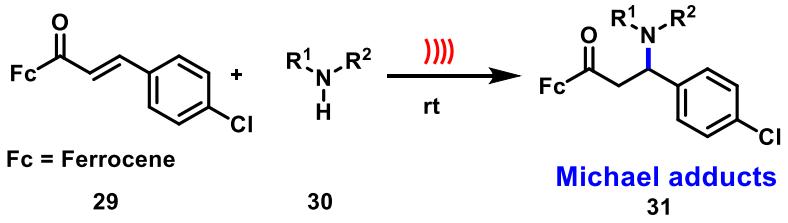

Scheme 1.3.8: Synthesis of Michael adducts under ultrasound irradiation

Next, Rostamnia and Lamei developed the synthesis of Rhodanine derivatives that have potential pharmacological and biological applications. The ultrasound-promoted reaction was carried out in the water by mixing dimethyl or ethyl acetylene dicarboxylate **34**, an amine **32**, and carbon disulfide **33**

provided excellent yields of Rhodanines in short reaction times by simple filtration method (Scheme 1.3.9).

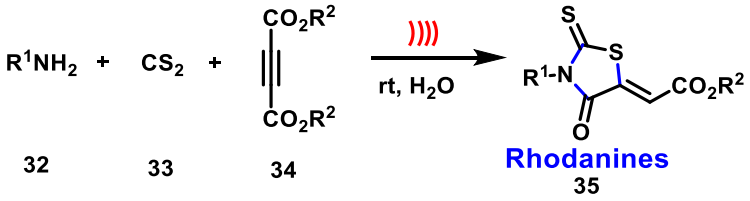

Scheme 1.3.9: Synthesis of Rhodanine derivatives under ultrasound irradiation

The synthesis of 6*H*-1-benzopyrano[4,3-*b*]quinolin-6-ones **38** from 4-chloro-2-oxo-2*H*-chromene-3-carbaldehyde **36** and aromatic amines **37** under batch was reported by Mulakayala and coworkers at very short reaction time (5-9 min) gave high yield of **38** (Scheme 1.3.10).

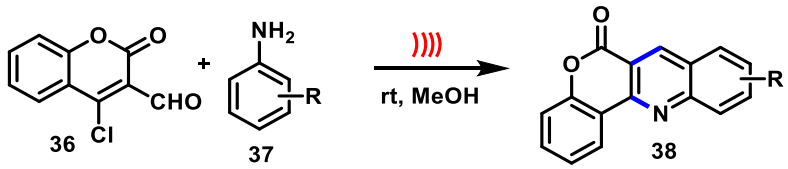

Scheme 1.3.10: Synthesis of 6*H*-1-benzopyrano[4,3-*b*]quinolin-6-one derivatives under ultrasound irradiation

1.3.D.3. Mechanochemical reactions: [13a]

The reaction is facilitated by employing mechanical grinding by ball milling which is also considered among the top techniques for performing green processes. Various heterocycles such as hexahydroquinolines, 1,4- dihydropyridines, hexahydrobenzo[*b*]-[1,8]naphthyridines, nitroamines, nitrosulfides, 2,4-disubstituted thiazoles, pyrano[2,3-*d*]pyrimidine-2,4(1*H*,3*H*)-diones, dipeptides, phenylhydrazones, etc. have been synthesized. Mokhtari and coworkers synthesized phenylhydrazones **41** from substituted aldehydes and ketones **39** into their oxime hydrochloride hydraPtes **40**, and 2,4-dinitrophenylhydrazones **41** under SF–CF condition by ball-milling (Scheme 1.3.11).

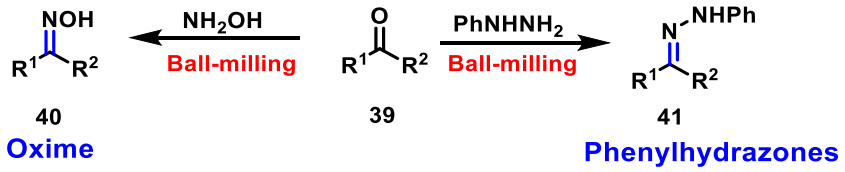

Scheme 1.3.11: Synthesis of phenylhydrazone derivatives under mechanochemical mixing

Moreover, Mashkouri and Naimi-Jamal utilized ball milling approach for the preparation of pyrano[2,3-*d*]pyrimidine-2,4(1*H*,3*H*)-diones **45** by taking a stoichiometric mixture of an aldehyde **42**, malononitrile **43**, and barbituric acid **44** (Scheme 1.3.12).

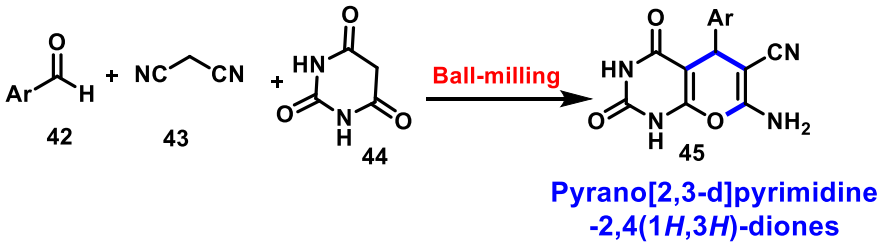

Scheme 1.3.12: Synthesis of **45** under mechanochemical mixing

The synthesis of dipeptides **49 or 50** under solvent-free conditions was reported Hernμndezand Juaristi with urethane-protected β-amino acid *N*-carboxyanhydrides **46** and α-or β-amino esters **47** or **48** (Scheme 1.3.13).

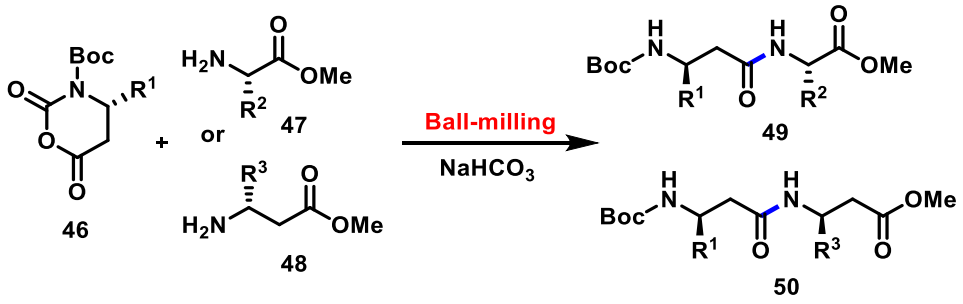

Scheme 1.3.13: Multicomponent synthesis of α,β-dipeptides and β,β-dipeptides by mechanochemical mixing

1.3.D.4. Photochemical reactions:

The primary energy source for the photochemical reaction to provide photons is light radiation which may or may not require photocatalyst to achieve desired selectivity. In the case of photocatalyzed reaction, catalyst absorbs light to reach to an electronically excited state, where it triggers a single-electron transfer (SET) process. Consequently, it produces highly reactive species in a controlled way. The sustainability aspect, such as the less hazardous, safer synthetic routes, easy disposal of less toxic or polluting by-products, and its tolerance towards various functional groups, makes photoredox catalysis highly demanding. Additionally, it enhances the atom economy using renewable feedstocks.[14] In literature, several chemical transformations such as [2 + 2] enone cycloadditions, [4 + 2] cycloadditions of photochemically generated strained alkenes, [4 + 4] cycloadditions, rearrangements,

Norrish−Yang reaction, photo-Friedel−Crafts reaction, photo-oxygenation, diazonium mediated reductive annulation, matallophotoredox decarboxylation, etc has been reported.[15-16]

In 2008, Yoon and coworkers disclosed photoredox catalyzed intramolecular [2 + 2] enone cycloaddition reaction to give cyclized product **52** (Scheme 1.3.14).[17]

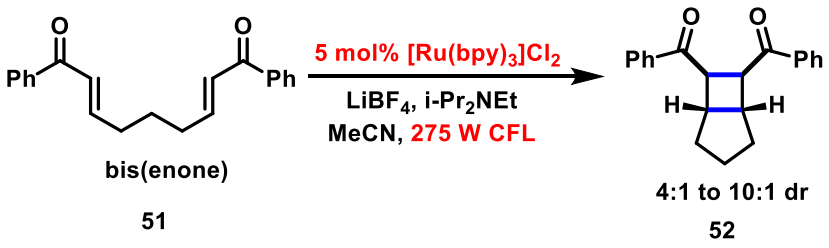

Scheme 1.3.14: [2+2] Enone cycloaddition under the photocatalytic condition

Furthermore, visible light mediated alkyne annulation with diazonium salt **53** to give the benzothiophene **54** core of raloxifene was reported by König group in 2012 (Scheme 1.3.15).[18] The reactions were carried out with 5 mol% organophotocatalyst eosin Y, with green LED providing the key step for the synthesis of raloxifenes. Additionally, this report circumvented regioselectivity issues by providing single regioisomers of benzothiophene.

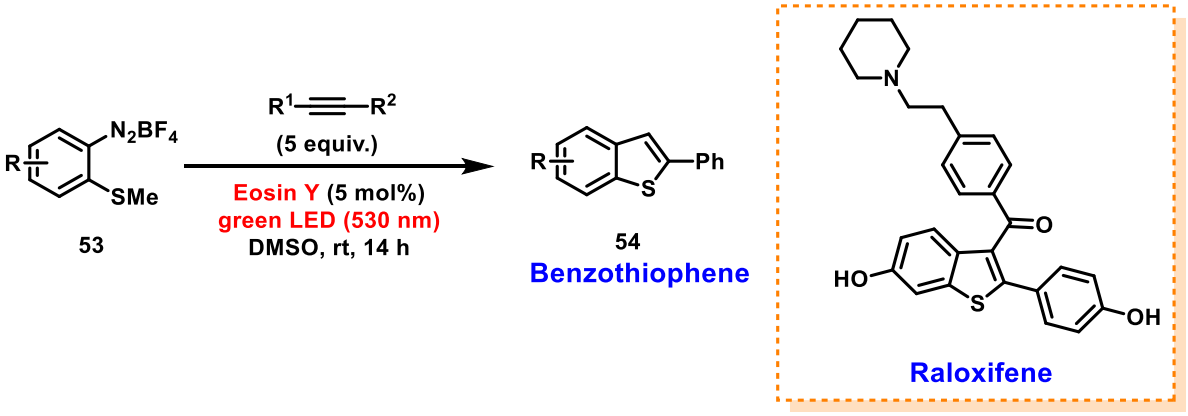

Scheme 1.3.15.: Diazonium reductive annulation under photocatalytic condition

Further, the metallophotoredox decarboxylation approach was developed, where photocatalyst generates reactive radical species and modulation of the oxidation state on nickel for the synthesis of Fenofibrate **57** (used in the treatment of hypercholesterolemia and hypertriglyceridemia) (Scheme 1.3.16).[19] With the optimized conditions, MacMillan and coworkers coupled keto acid **55** to aryl iodide **56** after irradiation for 96 h using $[Ir(dF(CF_3)ppy)_2(dtbbpy)]PF_6$ as a photocatalyst and $NiCl_2$·dtbbpy as a coupling agent provided 71% yield of **57** at 0.5 mmol scale.

The scalability of this method has not been performed due to an insufficient photon source. However, the challenges associated with scalability can be addressed with continuous flow.

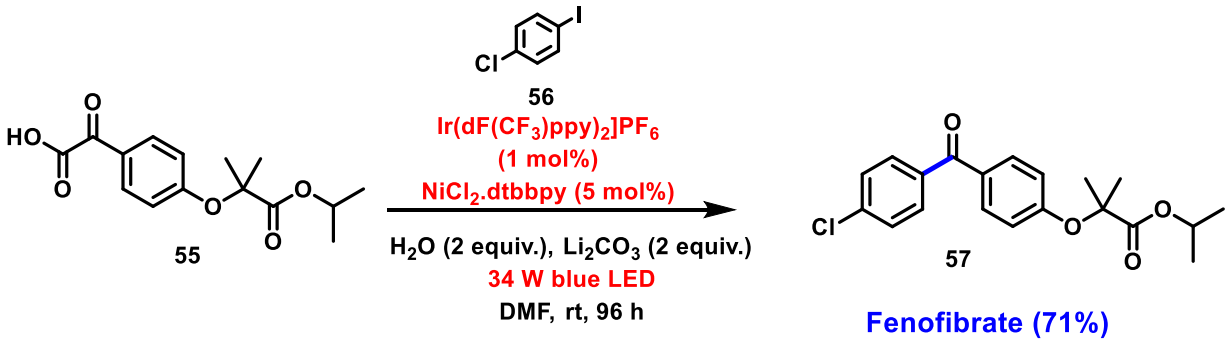

Scheme 1.3.16: Fenofibrate synthesis through meatallophotoredox decarboxylation

1.3.D.5. Continuous flow technique:

In continuous flow, the reactions are performed by pumping reagents to the reactors of various type to get the desired product in a continuous manner. Moreover, the driving force behind the need for the adoption of continuous manufacturing is improved heat/mass transfer, smaller footprint, better yields, and selectivity as well as allowing access to variable temperature and pressure. Thus, making the flow a popular choice that is difficult to do under batch conditions. The past few decades have witnessed the translation of various batch processes into continuous flow processes for large-scale synthesis (Figure 1.3.3).[20-21]

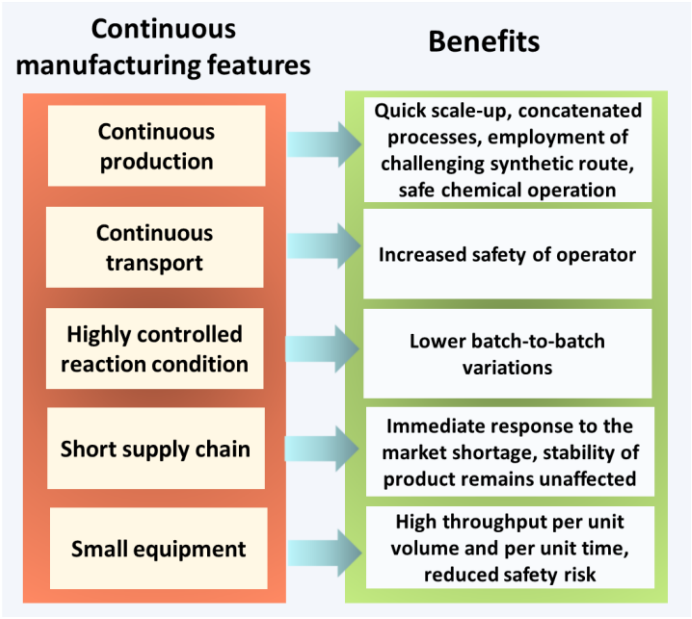

Figure 1.3.3: Advantages of flow chemistry towards industrial applications[22]

Moreover, continuous flow process have been recently expanded in photochemical and electrochemical reaction condition for the synthesis of active pharmaceutical agents, small molecules, polymers, and nanoparticles.[23-24] Few examples of continuous flow drug synthesis has been presented in the literature. A semi-continuous flow with Fischer indole strategy has been demonstrated for synthesizing Ondansetron by Gnanaprakasam and coworkers under metal-free conditions. In this process, cyclohexane-1,3-dione **58** (0.1 M in water) and *N*-methyl phenylhydrazine **59** (0.1 M in ethanol) were flown with the flow rate of 0.1 mL min^{-1} each into SS tubular reactor heated at 100 °C to give hydrazone derivative which then passes through Omnifit® (6.6 × 150 mm^2) prepacked with Amberlyst®-15 at 110 °C afforded 9-methyl-1,2,3,9-tetrahydro-4*H*-carbazol-4-one **61**. Further, the Mannich reaction gave Ondansetron **63** in 65% of the overall yield (Scheme 1.3.17).[25]

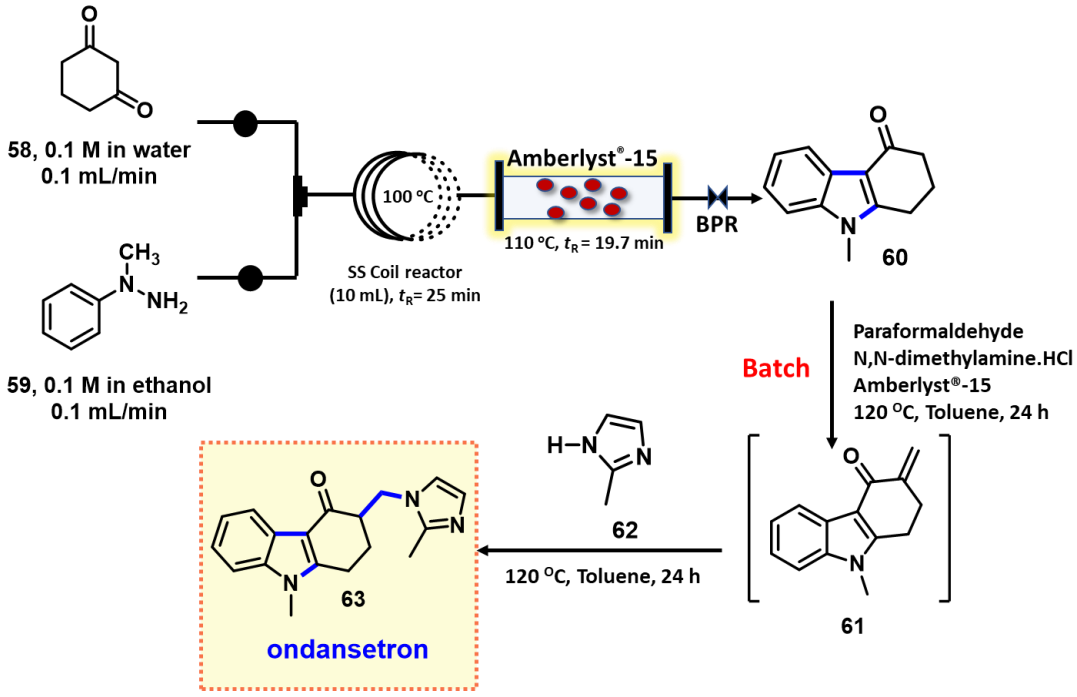

Scheme 1.3.17: Amberlyst®-15 mediated synthesis of ondansetron under semi-continuous flow process

Next, Modafinil an anti-narcoleptic drug used for the treatment of excessive daytime sleepiness associated with shift-work disorder. From 1976, around 20 articles have been published. However, Monbaliu and coworkers performed continuous flow synthesis of **64** in 3 steps by avoiding intermediate purification through column chromatography. The product purification was done by precipitation, filtration, and washing with NaCl and $NaHSO_4$ that gives innocuous side products. Finally, a fully concatenated procedure for the preparation of modafinil **64** using PFA coil reactors was demonstrated (Scheme 1.3.18).[26]

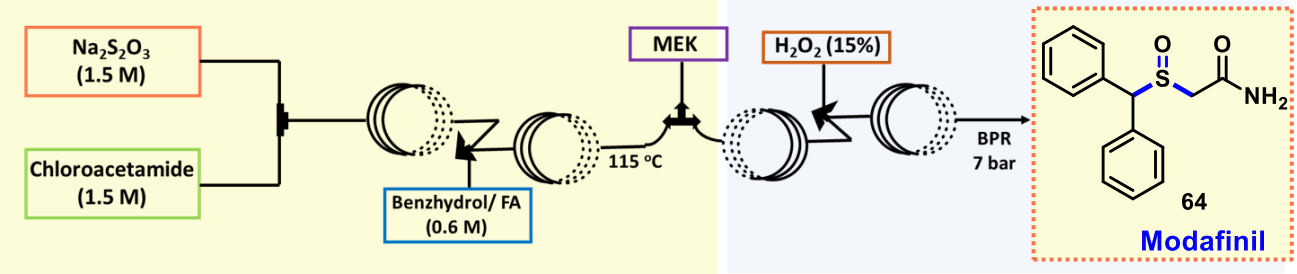

Scheme 1.3.18: Flow chart for the concatenated process in Corning AFR mesofluidic setup for the synthesis of Modafinil drug

1.4. Aim and rationale of thesis work

Rapid industrialization made modern society livable by providing many active pharmaceutical reagents, drugs and products of day to day life manufactured by chemical transformation. During majority of chemical transformation, the toxic waste produced affects the environment and ecosystem. However, with the emergence of green chemistry principles and sustainable development goals, better economy and safer process development could be acheived. In this regard, oxidation and azidation reactions that play crucial role and has extensive applications towards natural products, drugs, and API synthesis has been studied. The oxidation reactions create or modify functional groups, whereas azides are key precursors for generating heterocyclic motifs. However, it is difficult to adhere to all green principles.

In this direction, we have envisioned the use of safer tools such as continuous flow technique for oxidation and azidation reactions. Additionally, solvent and catalyst-free reactions and green catalysis have been employed for skeletal editing by solid state melt rearrangement and annulation reactions respectively.

1.5. Objectives of the thesis

1.5.A. Benzylic sp3 C-H oxidation under batch and continuous flow

Functional group transformation is one of the major challenging aspects of organic transformation. For the direct transformation of methylene groups to afford ketone, several homogeneous catalysts of Cr, Mn, Co, Bi, Ru, Rh, and Fe are reported. Tragically, there are limitations exist in this transformation, such as the decomposition of the metal catalysts, exothermic reactions, the problems of catalyst extraction and recycling as well as product purification makes them less suitable for the synthesis of fine chemicals where the product contamination with heavy metal is highly undesirable in large scale synthesis. Hence to surrogate the drawbacks associated with the heterogenization of the catalyst, we

envisioned the synthesis of Mn-based magnetic nanoparticles since Mn is well known for oxidation reactions. However, metal catalyst when reacts with TBHP may produce a rigorous reaction with difficulty in scale up. Therefore, we aimed to install oxygen at the methylene group to give ketones and ester under safer continuous flow conditions by keeping industrial benefit and sustainable reaction development approach in mind.

1.5.B. Continuous flow direct azidation of alcohols and peroxides towards the synthesis of heterocyclic scaffolds

Traditionally, direct azidation of alcohols required activation of hydroxy to make it as a good leaving group for feasible nucleophilic reaction. Notably, direct installation of azides from alcohols has also been reported using Lewis acid or Bronsted acid catalysts. However, large-scale production has been an issue under batch conditions. This issue can be dealt with by integrating it into a continuous flow. The literature report on azidation in flow is not adequate when sustainability parameters are concerned as it is limited to propargylic alcohols and produces stoichiometric waste generation from azide precursor. Thus, we proposed to develop an energy-efficient, room temperature, recyclable heterogeneous Bronsted acid catalyst for direct azidation of alcohols to generate hitherto unknown azides. A further application were studied towards the synthesis of drugs and the development of new organic transformations.

1.5.C. Skeletal editing through solid state melt rearrangement of azides

Organic azides deliver various organic reactions that have been extensively studied in chemical biology, pharmaceuticals, medicinal, and agricultural areas. Furthermore, the rearrangement of azide is a key operation in generating numerous heterocyclic scaffolds. The heterocyclic scaffolds such as phenanthridines are prevalent core in several natural products and staining agents that could be assembled in various manners. However, to the best of our knowledge, the skeletal editing of azides for the synthesis of phenanthridines is not reported in the literature. Additionally, the available reports demanded the use of catalysts, high temperatures, solvents, additives, and bases. As outlined SFCF reactions, we hypothesized to study SFCF rearrangement for constructing phenanthridine derivatives which includes a skeletal editing process by using azides as a starting material.

1.5.D. Catalytic acceptorless dehydrogenation strategy for annulation under neutral conditions

In continuation to heterocycle synthesis, this chapter is focused on developing the Domino reaction strategy. In literature, numerous approaches have been developed for the synthesis of heterocycles that

involves traditional metal and metal-free conditions. Despite the fact that these methods provide interesting catalytic reaction steps and synthetically useful approaches, the generated copious waste, multistep synthesis, and limited feedstock chemicals are the disadvantages of these traditional methods. As a result, acceptorless dehydrogenation (AD) has become a widely applied method for chemical synthesis because it has several attractive characteristics for the formation of C–C and C–X bonds. This process generates water and molecular hydrogen as a byproduct and retains a high atom economy which contributes towards green synthesis. Although several research groups have extensively employed the AD strategy for the synthesis of pyrrole and pyridine core, it still suffers from the use of a specially designed complex and requires a stoichiometric base for annulation which generates copious waste. Consequently, this decreases the atom economy and makes it less sustainable. In this direction, we aimed to develop an annulation strategy to get tetrahydroindolones and tetrahydroacrindones which avoid the need for base, ligands, and additives. Further, we propose to apply this process for the synthesis of molindone core under solvent-free conditions.

Overall, the research work in this thesis is aimed to develop sustainable oxidation, azidation, rearrangement, and annulation reactions toward various heterocyclic scaffolds under batch and continuous flow. To get a clear understanding, the introduction and literature background of each chapter are written separately following the current general introduction.

Chapter II: Benzylic sp^3 C-H Oxidation under Batch and Continuous Flow

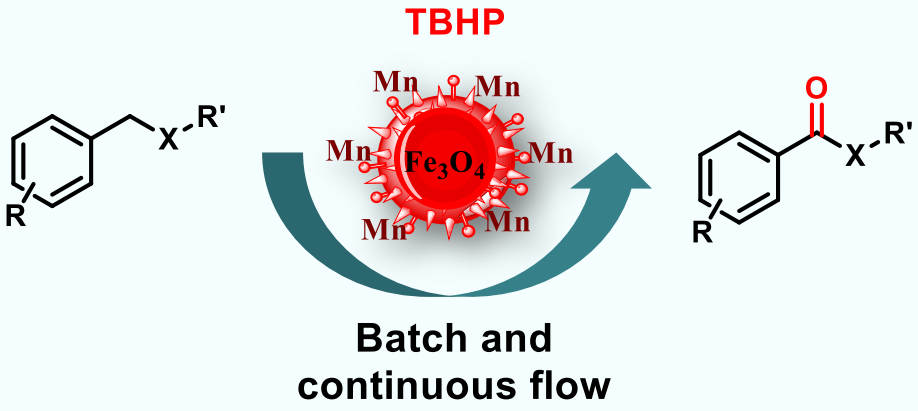

Benzylic sp^3 C-H Oxidation under Batch and Continuous Flow

2.1. An introduction to continuous flow chemistry

Chemical laboratories have relied on flasks for centuries due to their durability, versatility, thermal and chemical resistance, and affordability makes it quintessential for conducting chemical reactions on a milligram-to-gram scale. However, it becomes inefficient and unviable in large-scale production of petrochemical, polymer, and bulk chemicals. Thus, to cope with issues related to the lifetime of projects, introducing continuous flow reactions for sustainable process development gained much attention. In continuous flow, the reactants are flown through continuously flowing streams rather than relying on flasks to minimize the problems associated with overheating and mixing. Besides significant heat management and mixing, it also offers energy efficiency, scalability, innocuous waste generation, the safety of the process, and access to a broad range of reaction conditions opening windows for catalysis, multistep reactions, and more.[27-29]

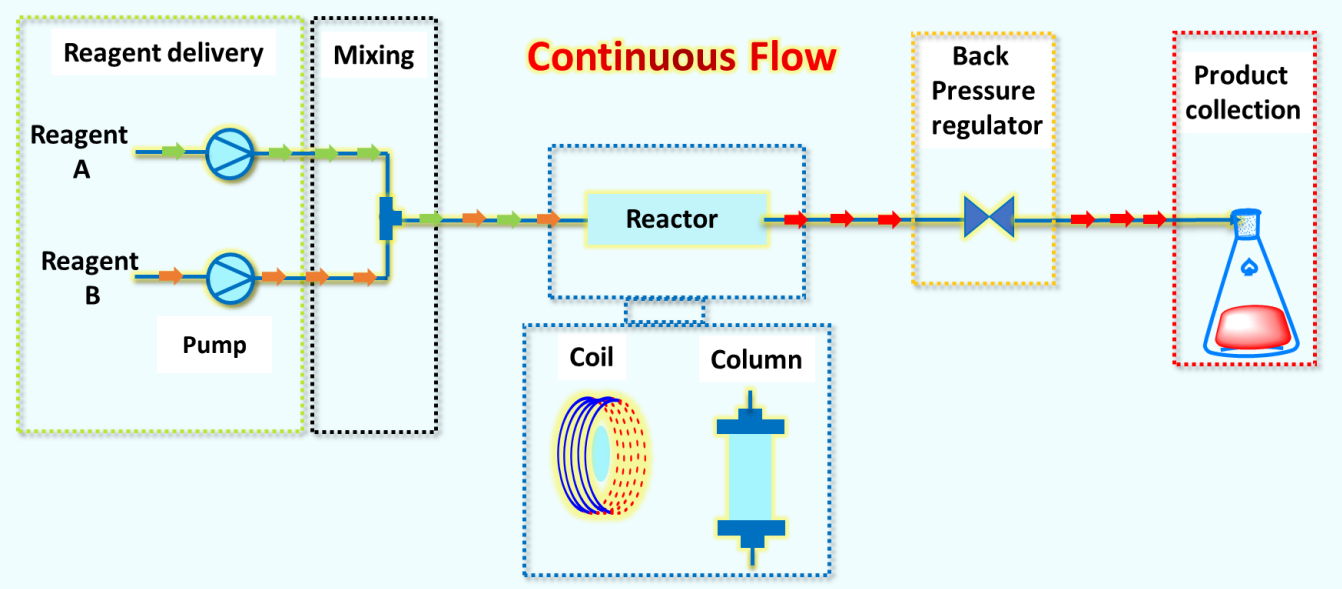

Figure 2.1.1: Schematic representation of continuous flow

Continuous processing was deemed the most important area of green chemistry and engineering research in the pharmaceutical industries.[30] Furthermore, flow chemistry has evolved into a powerful synthesis tool for handling obnoxious or hazardous materials and exothermic reactions to prevent

stockpiling and transporting such hazardous reagents with greater safety. Instead, it allows on-site production of the required amount of desired product. It also saves time and energy by direct loading and unloading chemicals to be utilized. As a result, no special cleaning is required for the reactor. The basic parameters of continuous flow are described in Figure 2.1.1.

Basic parameters of continuous flow:

(a) **Pumps** transport reagents, reactants, or solvents from vessels or bottles into reaction loops. The typical continuous flow reactor pumps include piston, peristaltic, and syringe pumps.

(b) **Reaction loops** carry the reagents or solvent to a mixing junction.

(c) **T-piece** is the initial mixing point where two reagent streams get mixed and proceeds into a reactor.

(d) **Flow rate** can be given for chemical reactions after optimizing stoichiometry, temperature, mixing, and reaction time.

(d) **Reactors** are *the heart of chemical processes* that lead to significant chemical operations for chemical plants by maintaining the heating or cooling of reaction and retention time. Based on the type of reactions there are two types of the reactor;

(i) **Column reactor** is a vertical glass or metal tube in which a solid heterogeneous catalyst or reactants can be filled.

(ii) **Coil reactor**s are used for conducting homogeneous reactions in a loop.

(e) **Back pressure regulator** maintains the pressure of the system and hence heating of solvent beyond its boiling point becomes possible.

(g**)** The **Downstream unit** can be integrated with IR, UV, NMR, etc. instruments for monitoring the progress of the reaction.

(h) **Telescoped reaction** can be easily performed by connecting a series of reactors.

(i) The term "**Residence time**" refers to the amount of time a molecule spends inside a reactor that has been calculated as the difference between the time it enters and departs the reactor.

Residence time = Volume of the reactor/flow rate

2.2. Introduction to benzylic sp^3 C-H oxidation

Developing a sustainable chemical process for functional group transformations is a significant challenge in organic synthesis.[31] Metal-catalyzed functionalization of the C-H bond to carbonyl compounds using oxidant is significantly increased in the past few decades among synthetic chemists for generating sustainable chemical processes. The literature reports disclosed the demand for oxygen containing drugs and natural products. Furthermore, oxidation of a saturated sp^3 C-H bond can rapidly install an oxygen atom on a carbon atom and has attracted considerable attention (Figure 2.2.1).[32] In recent decades, several methodologies have been developed for the direct benzylic sp^3 C-H bond oxidation to access its respective products.[33] However, the reported conditions include stoichiometric quantities of transition metal complexes which retain problems in terms of atom economy, toxicity, and increases cost of production.[34]

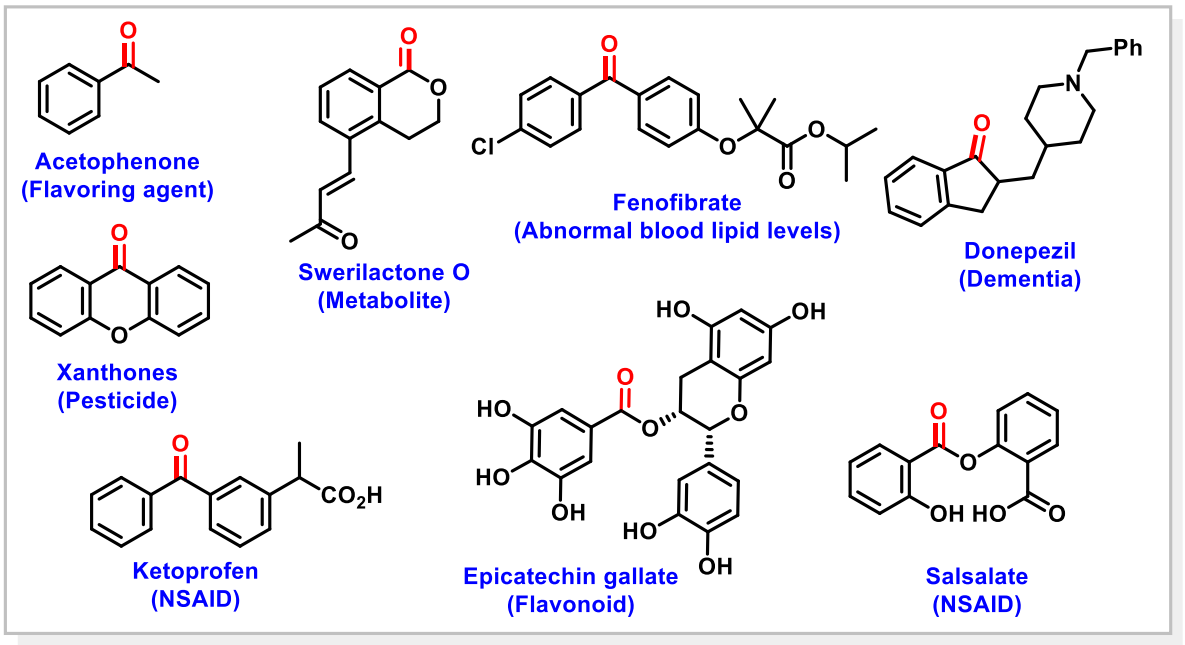

Figure 2.2.1: Benzylic C=O bond containing core moieties

Non-precious transition metals such as Cr,[35] Mn,[36] Co,[37] Ru,[38] Rh,[39] Fe,[40] Re,[41] and Bi,[42] etc. in a catalytic amount have been reported for selective benzylic oxidation (Scheme 2.2.1). However, industries use heterogeneous catalysts to circumvent the drawbacks of homogeneous catalysts (Scheme 2.2.1). The reported homogeneous transition metal catalysts have several advantages for the direct oxidation of an activated methylene group **65** to afford the ketone in excellent yields. However, it suffers from metal catalyst decomposition, the lack of regio- and stereoselectivity, difficulty in catalyst extraction, recycling, and product purification which makes it a less ideal choice for fine chemicals

synthesis. A product with heavy metal contamination is undesirable because it can elevate environmental and economic concerns during scale-up.[43] Thus, finding more sustainable catalysts that assist catalytic transformation under more realistic and environmentally benign conditions are of great interest.

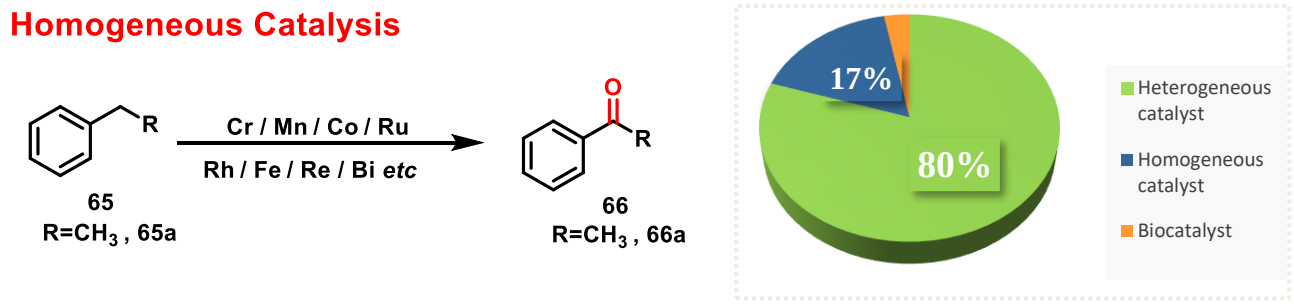

Scheme 2.2.1: Metal catalyzed oxidation of benzylic sp^3 C-H in literature

Further, the transition metal-free benzylic sp^3 C-H bond oxidation of activated methylene group to form ketone or ester in presence of external additive $NaNO_2$ and HCl is also reported (Scheme 2.2.2).[44]

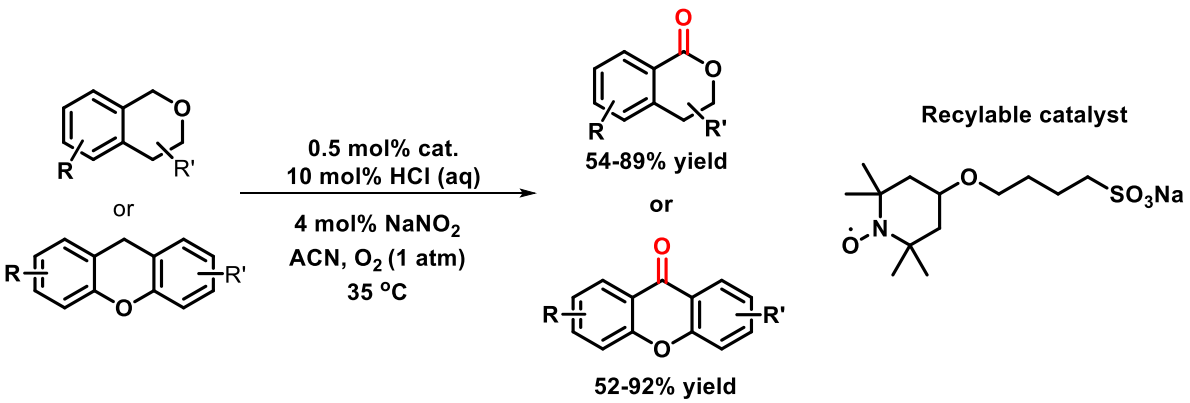

Scheme 2.2.2: Oxidation of benzylic sp^3 C-H in literature by Wang and coworkers

In 2017, Tan and coworkers showed *tert*-butyl hydrogen peroxide (TBHP) mediated direct oxidation reaction of benzylic sp^3 C-H bonds to ketones at high temperatures.[45] However, the problems associated with the use of expensive and/or toxic heavy metal homogeneous complexes could be resolved by making heterogeneous version of it.

In this direction, various materials such as activated carbon,[46] mesoporous silica,[47] biomass,[48] polymers,[49] etc. have been used as a support to generate a heterogeneous catalytic system. In 2013, Murugesan and coworkers reported Mn-Ti-SBA-15 and TBHP mediated oxidation of the active methylene group of **65** to afford **66** (Scheme 2.2.3).[50a] Later, Han and coworkers developed bioderived $Cu_3(PO_4)_2$ catalyst to access **66** using molecular oxygen as an oxidant (Scheme 2.2.3).[50b] Recently,

Sekar et.al. reported the oxidation of alkylarene **65** using binaphthyl-stabilized Pt nanoparticles (Pt-BNP) as a catalyst (Scheme 2.2.3).[50c]

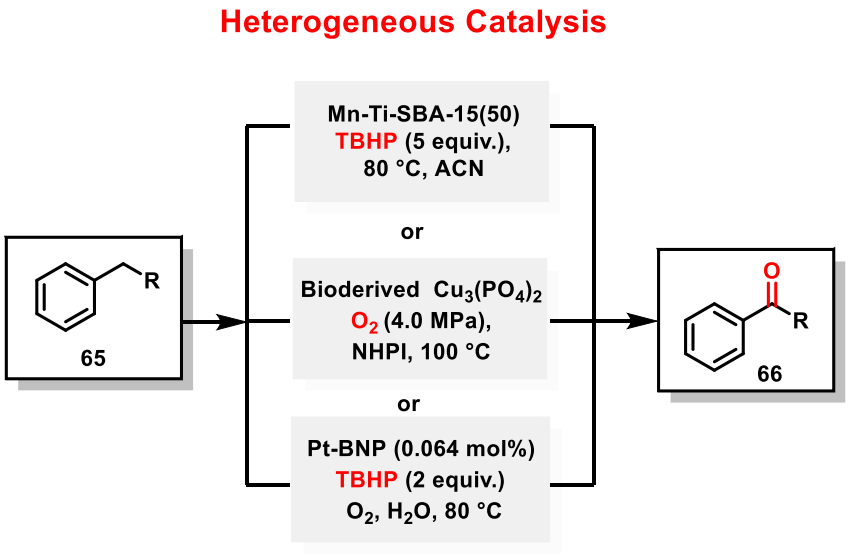

Scheme 2.2.3: Oxidation of benzylic sp^3 C-H using heterogeneous catalyst literature[50]

Advantageously, these supported catalyst systems can be effectively recycled and reused with the inherent catalytic activity. However, complete recovery of the catalyst by filtration and centrifugation is still a difficult task. Hence, we envisioned magnetic nanomaterial based catalyst synthesis so that the catalyst can be retrieved by magnet completely. Additionally, magnetic nanomaterials are found to be more effective and selective than conventional heterogeneous materials as a robust, readily available, extremely small size, and large surface area of the heterogeneous catalyst support.[51-52] Advantageously, the magnetically retrievable catalyst eliminates the need for catalyst filtration or centrifugation after the completion of the reaction.[53] In literature, Fe_3O_4 nanoparticles are used for the selective oxidation of allylic and benzylic bonds C-H to carbonyl compounds using TBHP as an oxidant.[54] However, manganese based catalysts have attracted considerable research interest because it is cheap, mild, and nontoxic oxidative reagent that oxidizes various functional groups selectively.[55]

A further implication of catalysis in the continuous flow technology has the potential to open new doors for performing the chemical reactions. Few approaches under continuous flow have been developed in this direction. Further, Yu and coworkers developed oxidation of benzylic sp^3 C-H with substrate:TBHP:NaClO in 1:10:8 proportion. The reactants are passed through a microchannel reactor to accomplish desired product **66** in excellent yield. However, this process requires use of additional oxidant and it suffers from workup issues that provided limited ketones derivatives (Scheme 2.2.4).[56]

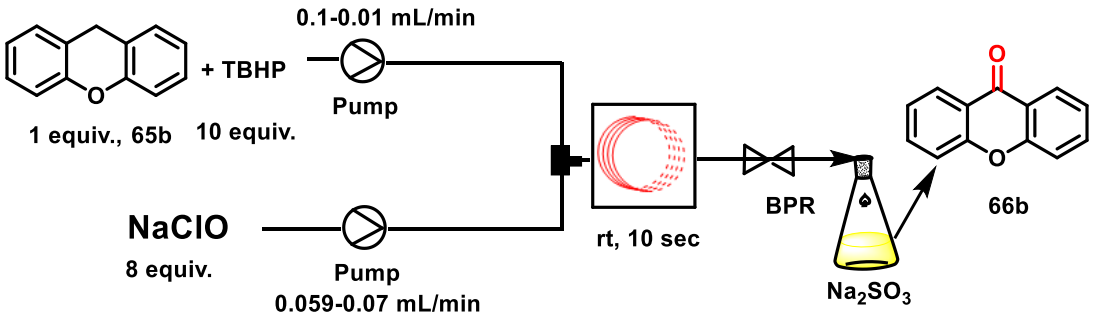

Scheme 2.2.4: Benzylic sp^3 C-H oxidation in literature by Yu and coworkers

In 2013, Kappe and coworkers reported the oxidation of ethylbenzene **65a** with molecular oxygen or H_2O_2 catalyzed by cobalt bromide in acetic acid as a solvent (Scheme 2.2.5). A tubular gas-liquid reactor was used in a continuous flow process where the reactor was heated at 110 to 120 °C by maintaining an oxygen pressure of ~12 bar to deliver acetophenone **66a** (66%) in 6 to 7 min of residence time. Increasing the temperature to 150 °C and time to 16 min afforded 71% of benzoic acid **67**.[57]

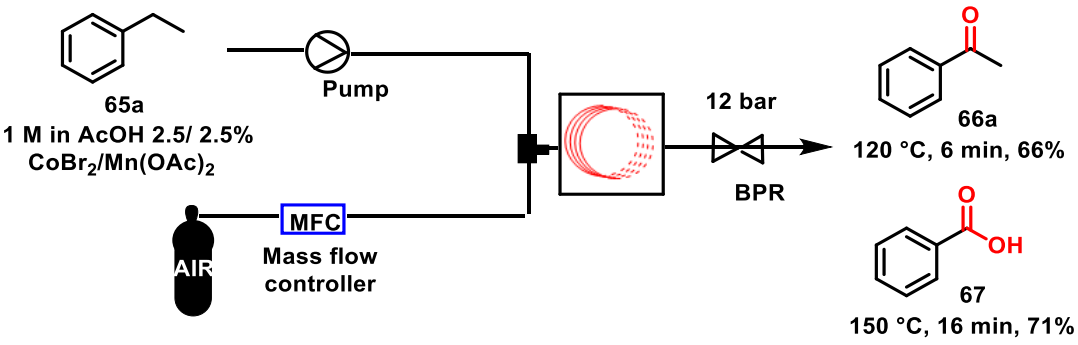

Scheme 2.2.5: Benzylic sp^3 C-H oxidation by Kappe and coworkers

Although these reports were efficient for oxidation, the use of homogeneous catalysts leads to unwanted waste generation affecting the atom economy of the process. Additionally, to the best of our knowledge, no reports for benzylic sp^3 C-H oxidation for ester and ketone using Mn supported on magnetic nanoparticles under continuous flow were found in the literature.

2.3. The rationale of the present work

Developing an Mn supported on Fe_3O_4 for benzylic sp^3 C-H oxidation of ether and methylene compound is highly desirable approach that will allow finding a more environmentally benign and economical procedure. The literature survey also revealed that to date, $MnO_2@Fe_3O_4$ MNP catalyst in

the synthesis of ester and ketone from benzylic sp^3 C-H group using TBHP as an oxidant has not been demonstrated. Therefore, we envisioned facile and atom-economical methodology for oxidation of benzylic sp^3 C-H bond using magnetically retrievable $MnO_2@Fe_3O_4$ catalyst under flow conditions (Scheme 2.3.1)

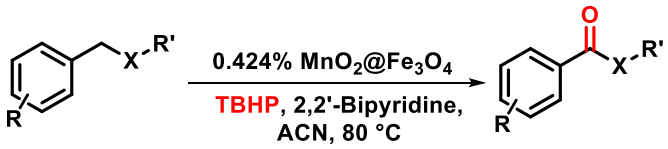

Scheme 2.3.1: General protocol for the benzylic sp^3 C-H oxidation using $MnO_2@Fe_3O_4$ MNP catalyst.

2.4. Results and discussion

Catalyst synthesis and characterizations: The synthesis of nano-sized $MnO_2@Fe_3O_4$ was accomplished by following the procedure reported for the synthesis of $Fe(OH)_3@Fe_3O_4$ by Heydari and coworkers.[58]

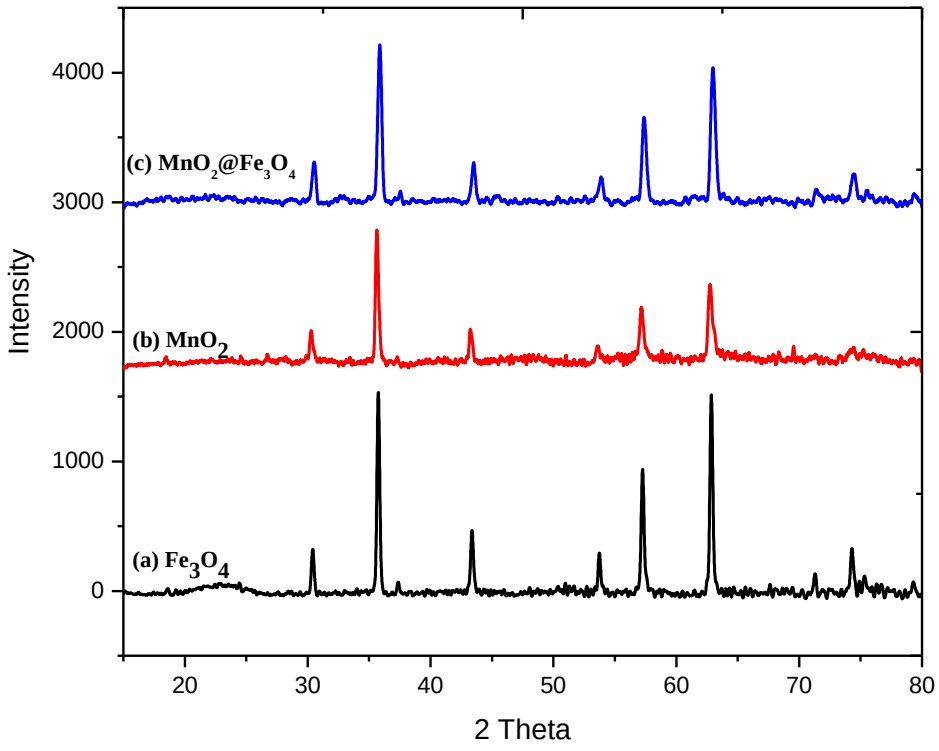

Figure 2.4.1: Powder X-ray diffraction data of (a) Fe_3O_4; (b) MnO_2; (c) $MnO_2@Fe_3O_4$

The % of Mn on Fe_3O_4 support was determined by microwave plasma atomic emission spectroscopy (MP-AES) analysis which showed that the catalyst contains 0.424% of Mn. Moreover, Figure 2.4.1 represents the X-ray diffraction pattern of 0.424% MnO_2@Fe_3O_4 nanocomposites, showing peaks corresponding to both Fe_3O_4 and MnO_2 appearing along with enhanced peak intensity caused by overlapping of both peaks (Figure 2.4.1). The diffraction peaks correspond entirely to the standard pattern characteristic peaks of the magnetite cubic inverse spinel structure (JCPDS 01-074-2435).

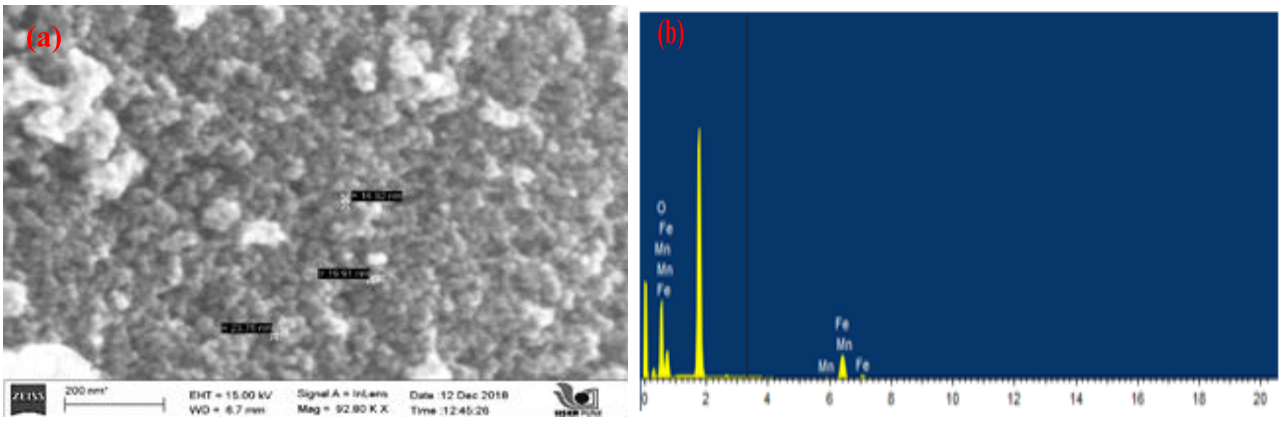

Figure 2.4.2: (a) FESEM; (b) EDAX images of MnO_2@Fe_3O_4 catalyst

The field emission scanning electron microscopy (FESEM) image suggested the formation of spherical particles with an average particle size of 14-23 nm range (Figure 2.4.2). The energy-dispersive X-ray analysis (EDAX) revealed the presence of Fe, O, and Mn as the main elements present with Fe being the most abundant in the selected field.

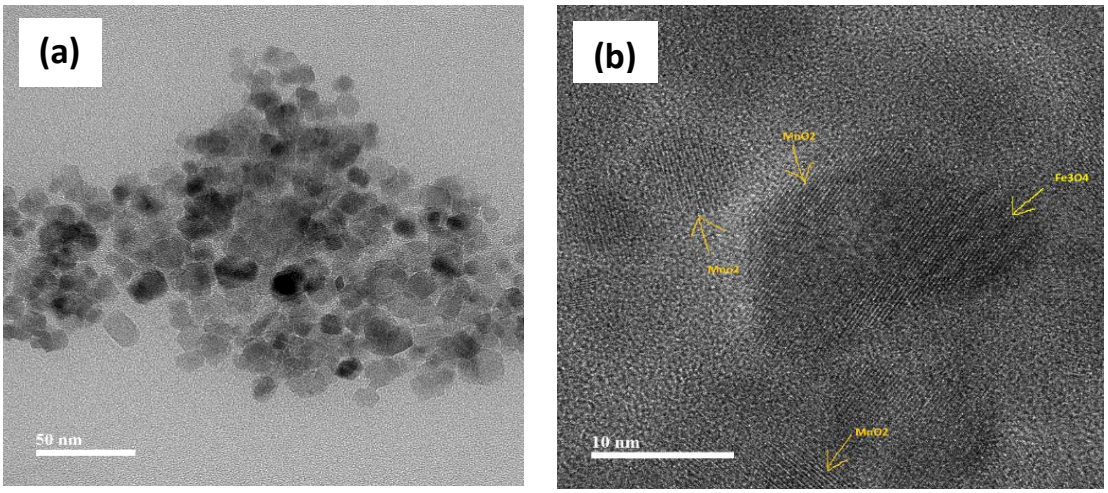

Figure 2.4.3: (a) TEM images of fresh MnO_2@Fe_3O_4 catalyst; (b) Lattice fringes of fresh MnO_2@Fe_3O_4 catalyst

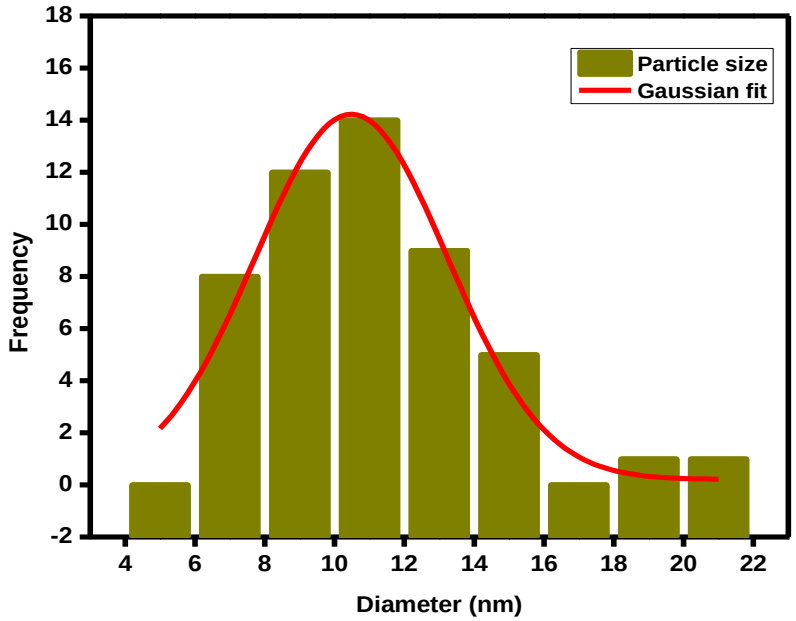

Figure 2.4.4: Histograms of fresh MnO_2@Fe_3O_4 generated from the TEM images

The morphology of the fresh MnO_2@Fe_3O_4 catalyst was evaluated by transmission electron microscopy (TEM) which suggested the average particle size of the fresh catalyst is 10.48 nm. (Figure 2.4.3-2.4.4).

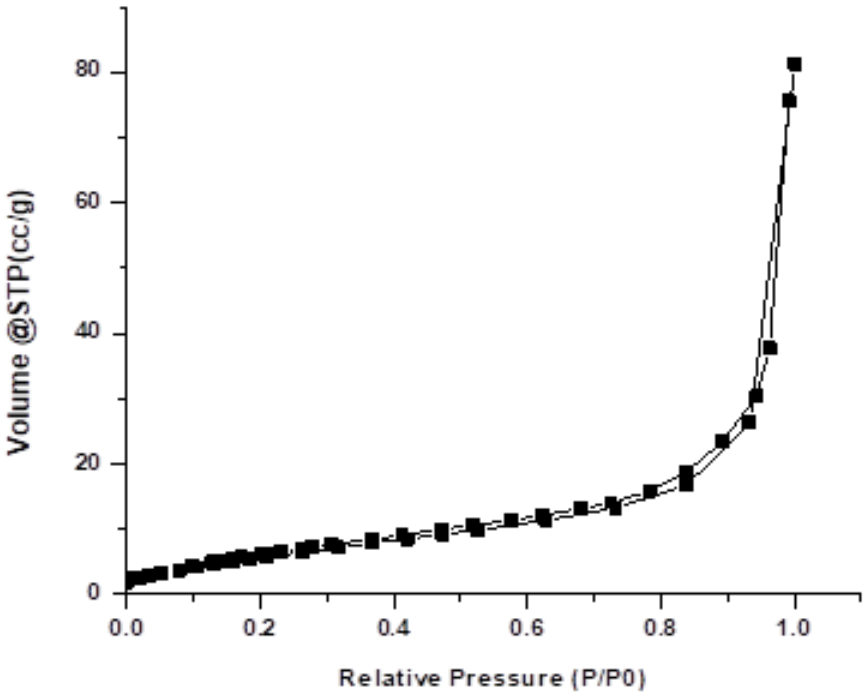

Figure 2.4.5: BET isotherm of MnO_2@Fe_3O_4 catalyst

The N_2 adsorption-desorption isotherms and pore size distribution of fresh $MnO_2@Fe_3O_4$ catalyst exhibited isotherm of type IV, which revealed a typical characteristic of the mesoporous material.[59] The pore size distribution is obtained by means of the Barrett-Joyner-Halenda (BJH) method equation using the adsorption isotherm branch, and specific surface area (SBET) was calculated by employing the Brunauer-Emmett-Teller (BET) method. The graph shows that the volume adsorbed increases with increasing relative pressures for all isotherms, which are due to the volume filling of micropores in the Fe_3O_4 membrane (Figure 2.4.5). BET-specific surface area and the pore diameter of $MnO_2@Fe_3O_4$ were found to be 13.19 m^2/g and 0.059 cm^3/g, respectively.

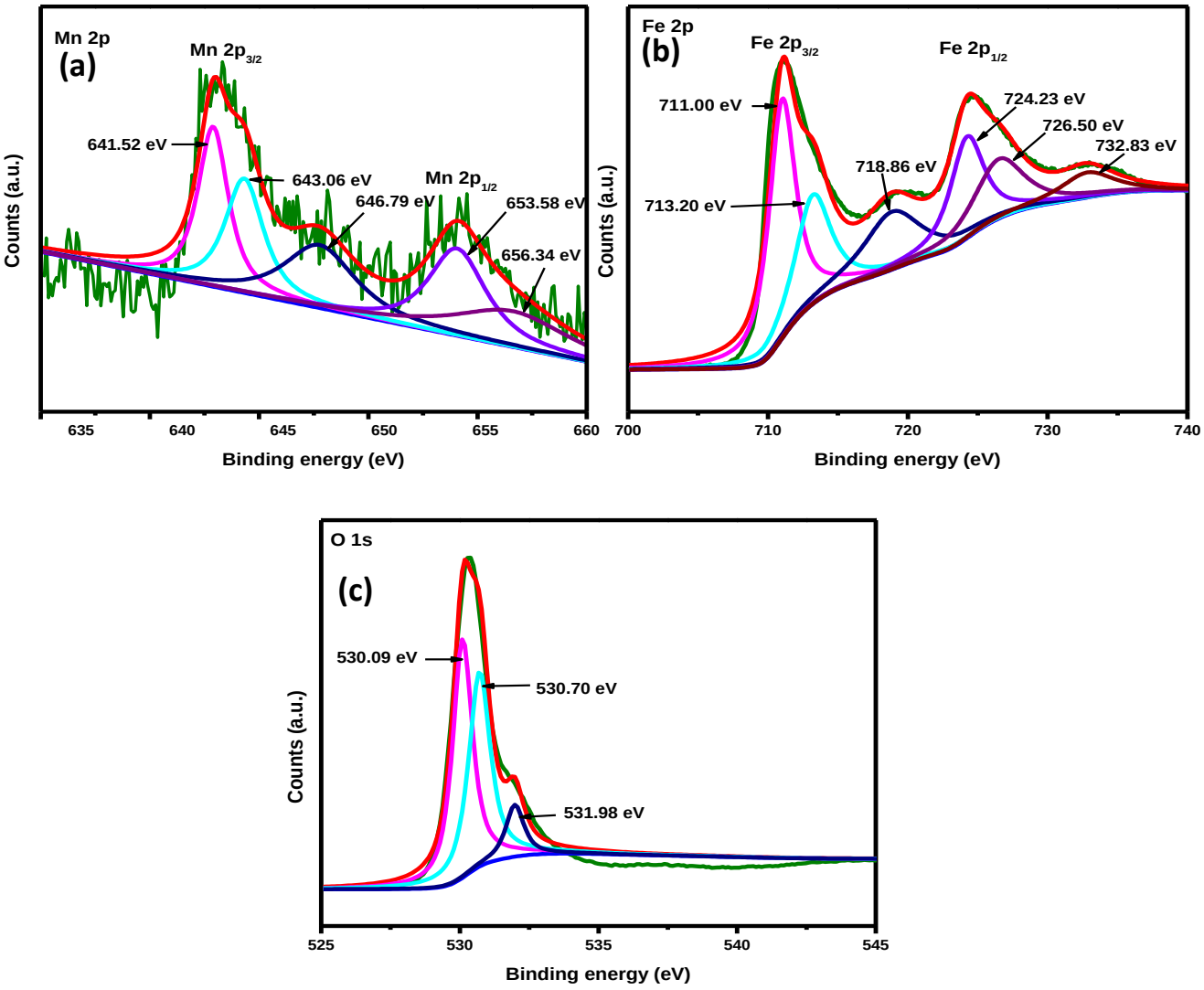

Figure 2.4.6: XPS for fresh $MnO_2@Fe_3O_4$ MNP catalyst of (a) Mn $2p_{3/2}$ and $2p_{1/2}$; (b) Fe $2p_{3/2}$ and $2p_{1/2}$; (c) O 1s

The compositions and valence states of fresh catalyst were then examined by X-ray photoelectron spectroscopy (XPS) in order to validate the PXRD results. In Figure 2.4.7a, Mn peak is divided into two portions at 641.52 and 643.06 eV for Mn $2p_{3/2}$, and 653.58 and 656.34 eV for Mn $2p_{1/2}$. Whereas Mn^{3+} is represented by the peaks at 641.52 and 643.06 eV, and Mn^{4+} is represented by the peaks at 653.58 and 656.34 eV. (Figure 2.4.6a).[60-61] Additionally, Figure 2.4.6b depicts the analysis of the Fe spectrum with two dominant peaks at 711.0 and 724.23 eV that are in agreement with the Fe $2p_{3/2}$ and Fe $2p_{1/2}$ spin-orbit peaks. Moreover, other peaks that are consistent with the typical Fe_3O_4 XPS spectrum that represents Fe is present in the form of Fe^{2+} and Fe^{3+}. Further, three major peaks can be found in the O 1s XPS spectra (Figure 2.4.6c). The peaks are situated at 530.09, 530.70, and 531.98 eV.36.[62]

2.5. Optimization studies and substrate scope in batch and flow

Initially, (benzyloxy)benzene **68a** was chosen as a model substrate by using 7 mmol of TBHP (5-6 M in decane) as an oxidant in acetonitrile (ACN) as a solvent at room temperature for 24 h. To identify the role of the catalyst for the oxidation of (benzyloxy)benzene **68a**, a blank control experiment was performed (Table 2.5.1, entry 1), which did not produce phenyl benzoate **69a**. Heating **68a** in ACN by using 5 mol% $Mn(OAc)_3.2H_2O$ as a homogeneous catalyst gave 23% of phenyl benzoate **69a** (Table 2.5.1, entry 2). In another control experiment with Fe_3O_4, a moderate yield of 33% for phenyl benzoate **69a** was observed at 80 °C (Table 2.5.1, entry 3). Next, with the synthesized heterogeneous $MnO_2@Fe_3O_4$, a 38% yield of **69a** was obtained at room temperature (Table 2.5.1, entry 4). Whereas, heating **68a** in ACN solvent using 50 mg of 0.424 % $MnO_2@Fe_3O_4$ MNP delivered 55% of **69a** (Table 2.5.1, entry 5). Further, increasing the temperature up to 100 °C has no specific influence on the outcome of the product (Table 2.5.1, entry 6).

However, the solvents were optimized with dichloroethane (DCE), dichloromethane (DCM), chlorobenzene, diethyl carbonate (DEC), and dimethylsulfoxide (DMSO) shown no improvement in the yield (Table 2.5.1, entry 7-11). However, no product formation was observed with 1,4-dioxane, dimethoxyethane (DME), and acetone solvents (Table 2.5.1, entry 12-14).

The effect of various oxidants and additives on the oxidation reaction has also been studied. The oxidants such as 4-methyl pyridine-*N*-oxide, $K_2S_2O_8$, TEMPO, and NHPI failed to deliver or gave less yield of phenyl benzoate **69a** (Table 2.5.2, entries 2-5).

Table 2.5.1: Optimization of the reaction conditions (solvent) for the benzylic sp^3 C-H group

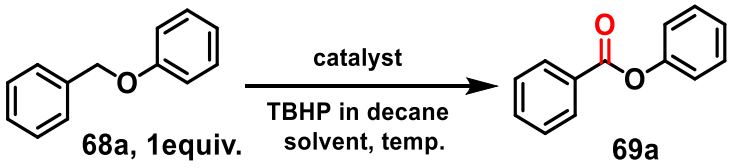

Entry	Catalyst (50 mg)	Solvent (2mL)	Temp (°C)	Yield of 69a (%)
1	–	ACN	80	nd
2	$Mn(OAc)_3.2H_2O$ (5 mol%)	ACN	80	23
3	Fe_3O_4	ACN	80	33
4	$MnO_2@Fe_3O_4$	ACN	rt	38
5	$MnO_2@Fe_3O_4$	ACN	80	55
6	$MnO_2@Fe_3O_4$	ACN	100	55
7	$MnO_2@Fe_3O_4$	DCE	80	48
8	$MnO_2@Fe_3O_4$	DCM	80	30
9	$MnO_2@Fe_3O_4$	Chlorobenzene	80	50
10	$MnO_2@Fe_3O_4$	DEC	80	50
11	$MnO_2@Fe_3O_4$	DMSO	80	55
12	$MnO_2@Fe_3O_4$	1,4-Dioxane	80	nd
13	$MnO_2@Fe_3O_4$	DME	80	nd
14	$MnO_2@Fe_3O_4$	Acetone	80	nd

Reaction conditions: (benzyloxy)benzene **68a** (1 mmol), TBHP in decane (7 mmol), and 50 mg of catalyst were stirred at various temperatures (see table 2.5.1) for 24 h.

The literature reports suggest that the role of the nitrogen-containing base was pivotal in the benzylic sp^3 C-H oxidation reaction.[63] This is because nitrogen-containing bases such as pyridine, 2,2'-bipyridine, and triethylamine could behave as a hydrogen acceptor with TBHP to speed up the formation of the tert-butoxyl radicals. This radical could abstract the hydrogen from a benzylic carbon atom.[64] However, no product formation was observed when triethylamine was used as a base (Table 2.5.2, entry 6). Moreover, a good conversion of about 66% of **69a** was obtained when 10 mol% of pyridine was used as a base (Table 2.5.2, entry 7). Other oxidants did not affect the conversion of (benzyloxy)benzene when pyridine is used as a base (Table 2.5.2, entries 8-10). The reactions proceeded smoothly using TBHP as the oxidizing agent and 2,2'-bipyridine as an additive in ACN

solvent to achieve the desired product **69a** in 80% yield (Table 2.5.2, entry 12). Several other supported catalysts, such as $Mn@Al_2O_3$ and $Ru@Fe_3O_4$ under similar reaction conditions delivered esters **69a** in good yield (Table 2.5.2, entries 13-14). After the optimal screening, the best reaction condition was obtained by reacting (benzyloxy)benzene **68a** (1 mmol), 50 mg of 0.424% $MnO_2@Fe_3O_4$ MNP as a catalyst, 10 mol% 2,2'-bipyridine as an additive and 5-6 M TBHP in decane (7 mmol) as an oxidant in ACN solvent (2.0 mL) at 80 °C for 24 h.

Table 2.5.2: Optimization of the reaction conditions (oxidant/additive) for the benzylic sp^3 C-H group

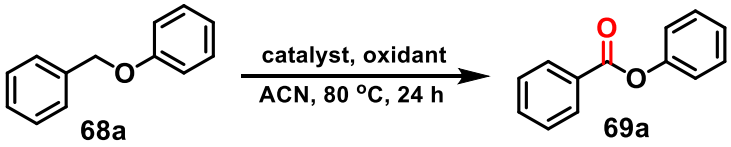

Entry	Catalyst (50 mg)	Oxidant	Additive/ligand	Yield of 69a (%)
1	$MnO_2@Fe_3O_4$	TBHP	-	55
2	$MnO_2@Fe_3O_4$	4-Methyl pyridine-*N*-oxide	-	n.d.
3	$MnO_2@Fe_3O_4$	$K_2S_2O_8$	-	n.d.
4	$MnO_2@Fe_3O_4$	TEMPO	-	n.d.
5	$MnO_2@Fe_3O_4$	NHPI	-	30
6	$MnO_2@Fe_3O_4$	TBHP	NEt_3	n.d.
7	$MnO_2@Fe_3O_4$	TBHP	Pyridine	66
8	$MnO_2@Fe_3O_4$	4-Methyl pyridine-*N*-oxide	Pyridine	n.d.
9	$MnO_2@Fe_3O_4$	$K_2S_2O_8$	Pyridine	n.d.
10	$MnO_2@Fe_3O_4$	TEMPO	Pyridine	n.d.
11	$MnO_2@Fe_3O_4$	NHPI	Pyridine	60
12	$MnO_2@Fe_3O_4$	TBHP	2,2'-bipyridine	80
13	$Mn@Al_2O_3$	TBHP	2,2'-bipyridine	75
14	$Ru@Fe_3O_4$	TBHP	2,2'-bipyridine	72

Reaction conditions: (benzyloxy)benzene **68a** (1 mmol), oxidant (7 mmol), additive (10 mol%), and catalyst (50 mg) were stirred at 80 °C for 24 h in ACN (2 mL).

To understand the generality of substrate scope, the reaction was investigated with various benzylic ethers and the results are summarized in Scheme 2.5.1. Various electron-donating substituents (**69b-69d**) were well tolerated. It is noteworthy that, the reaction conditions were compatible with halogenated substituents, which hold the potential for further functionalization. Interestingly, benzylic aliphatic ethers **68k-n** are smoothly converted into corresponding ester **69k-n** in excellent yields. This reaction is highly chemoselective towards benzylic ethers providing corresponding esters in excellent yields. However, there is no ester formation with alkylated phenol **68o** and allylic ether **68p**.

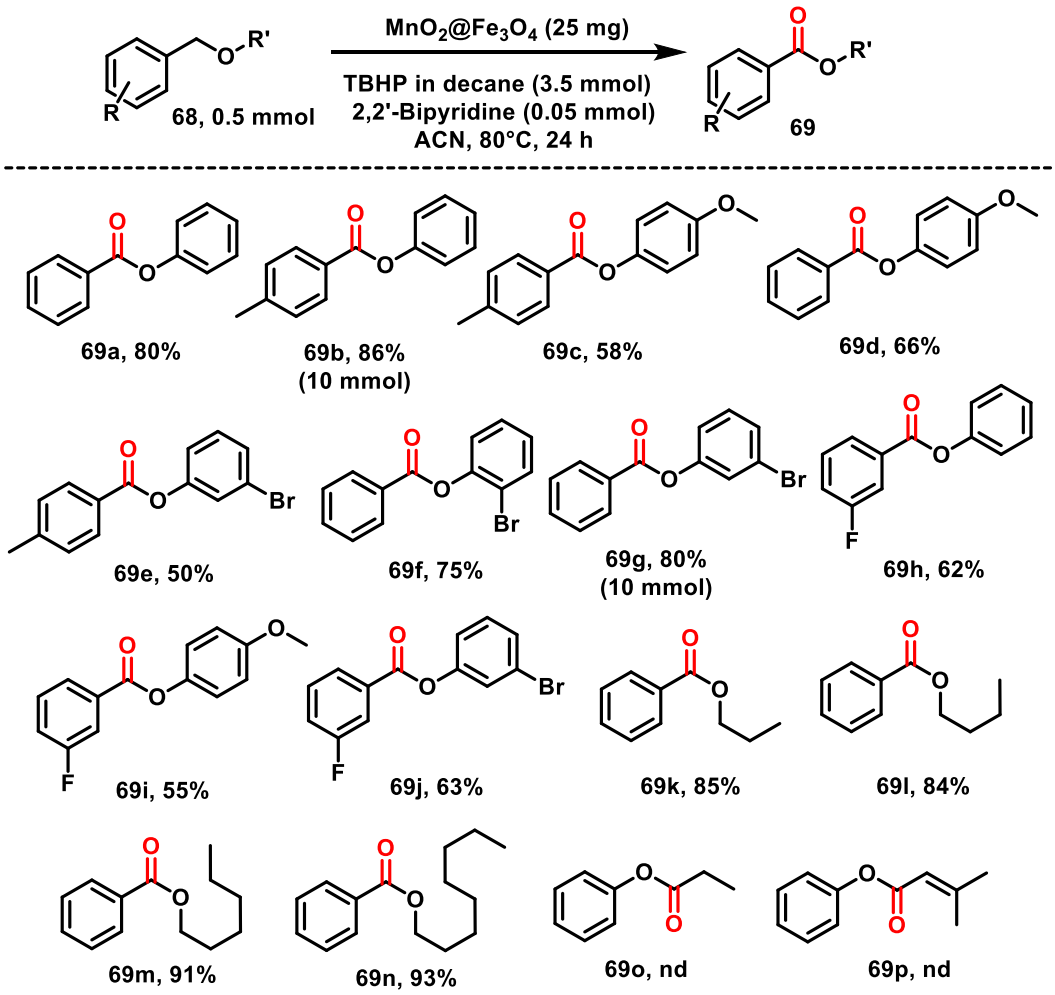

Scheme 2.5.1: The substrate scope for ester synthesis in batch condition

In order to demonstrate the general utility of this synthetic strategy, we carried out gram-scale reactions in batch (Scheme 2.5.1). Two representative benzyloxy benzene, one with a methyl-substituted **68b** and the other with a halogen-substituted **68g** were chosen to react with TBHP in presence of supported MnO_2@Fe_3O_4 MNP catalyst under optimized reaction conditions. The reactions were performed in 10 mmol scale using 0.500 g of MnO_2@Fe_3O_4 at 80 ^oC for 24 h and delivered **69b** and **69g** in 86% and

80% yields, with TON = 358.33; TOF = 14.93 h^{-1} and TON = 335.7; TOF = 13.98 h^{-1} respectively (Scheme 2.5.1).

To expand this reaction for a sustainable continuous flow process, the optimized batch reaction condition was translated to a continuous flow reactor. In continuous flow, the catalyst is filled in the column reactor, which can be separated easily after the reaction without any mechanical degradation of the supported catalyst. This further enhances efficiency and safety for performing TBHP-mediated reactions. The complete setup of continuous flow reactions using the Holmarc syringe pump (Model no.-HO-SPLF-2D) and catalyst bed in the Omnifit column reactor is depicted in Figure 2.5.1.

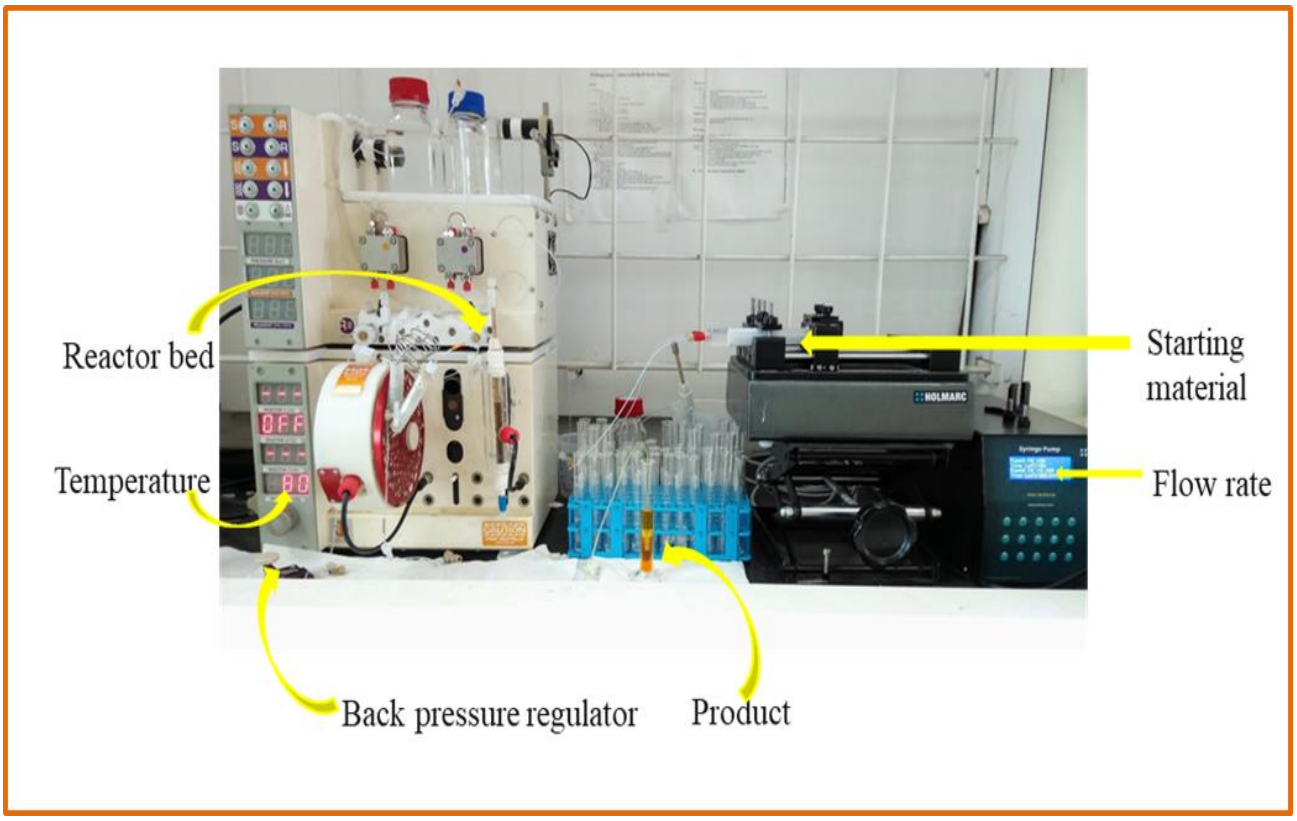

Figure 2.5.1: Continuous flow set up for benzylic sp^3 C-H oxidation

We started screening reaction conditions by taking (benzyloxy)benzene **68a** as a model substrate with that a set of reaction conditions were attempted (Table 2.5.3). Initially, 0.05:0.25 M solution of **68a**: TBHP in presence of 0.10 mmol of 2,2′-bipyridine as a ligand in acetonitrile solvent was flown through the Omnifit fixed bed reactor containing 0.424% MnO_2@Fe_3O_4 catalyst (1.0 g; void volume 1.7 mL; flow rate 0.1 mL/min) at room temperature gave 10 % of product **69a** after one cycle (Table 2.5.3, entry 1). However, increasing the molar concentration of TBHP up to 0.35 does not improve the outcome of the reaction at room temperature (Table 2.5.3, entry 2). Moreover, heating 0.05:0.35 M of

substrate:TBHP at 80 °C improved the yield of **69a** upto 50% after two cycles (Table 2.5.3, entry 3). However, the yield remained 50% when reactor bed was heated at 100 °C (Table 2.5.3, entry 4). Therefore, we concluded that the effect of temperature has a great influence for esterification of ether **68a**.

Further increasing the molar concentration of TBHP has no effect on improvement of the product formation (Table 2.5.3, entry 5). Therefore, we concluded entry 3 in table 2.5.3 as an optimum reaction condition to access **69a**.

Table 2.5.3: Optimization of the reaction conditions for the benzylic sp^3 C-H group to esters in continuous flow

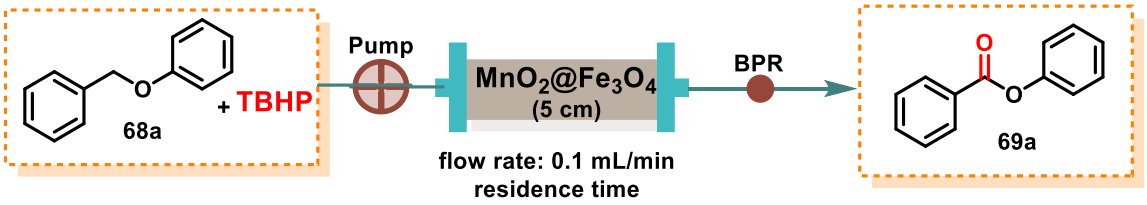

Entry	Catalyst/Additive[a]	Substrate (68a): TBHP	Flow rate (ml/min)	Temp (°C)	t_R(min)/ cycle	Yield of 69a (%)[b]
1	$MnO_2@Fe_3O_4$	0.05:0.25	0.1	rt	17.10/1	10
2	$MnO_2@Fe_3O_4$	0.05:0.35	0.1	rt	17.10/1	10
3	$MnO_2@Fe_3O_4$	0.05:0.35	0.1	80	34.20/2	50
4	$MnO_2@Fe_3O_4$	0.05:0.35	0.1	100	34.2/2	50
5	$MnO_2@Fe_3O_4$	0.05:0.45	0.1	80	34.2/2	50

Reaction conditions: 0.05 M solution of **68a** + 0.25-0.45 M solution of TBHP (5.0−6.0 M in decane) prepared in 20 mL ACN and flown throgh 0.424% $MnO_2@Fe_3O_4$ catalyst loaded bed reactor with the help of syringe pump (Model no.-HO-SPLF-2D). [a]0.1 mmol of 2,2′-bipyridine ligand used, t_R = residence time. [b]Isolated yields.

Having established the optimal reaction conditions in hand, various benzylic ethers (**68a-n**) were tested in a continuous flow to explore the generality of oxidation reaction. However, the protocol for oxidation of ethers to esters in continuous flow was found to be incompatible. With the optimized conditions, 15 to 50% yield of the ester product after 2 runs were obtained with (benzyloxy)benzene and (benzyloxy)alkanes derivatives (Scheme 2.5.2).

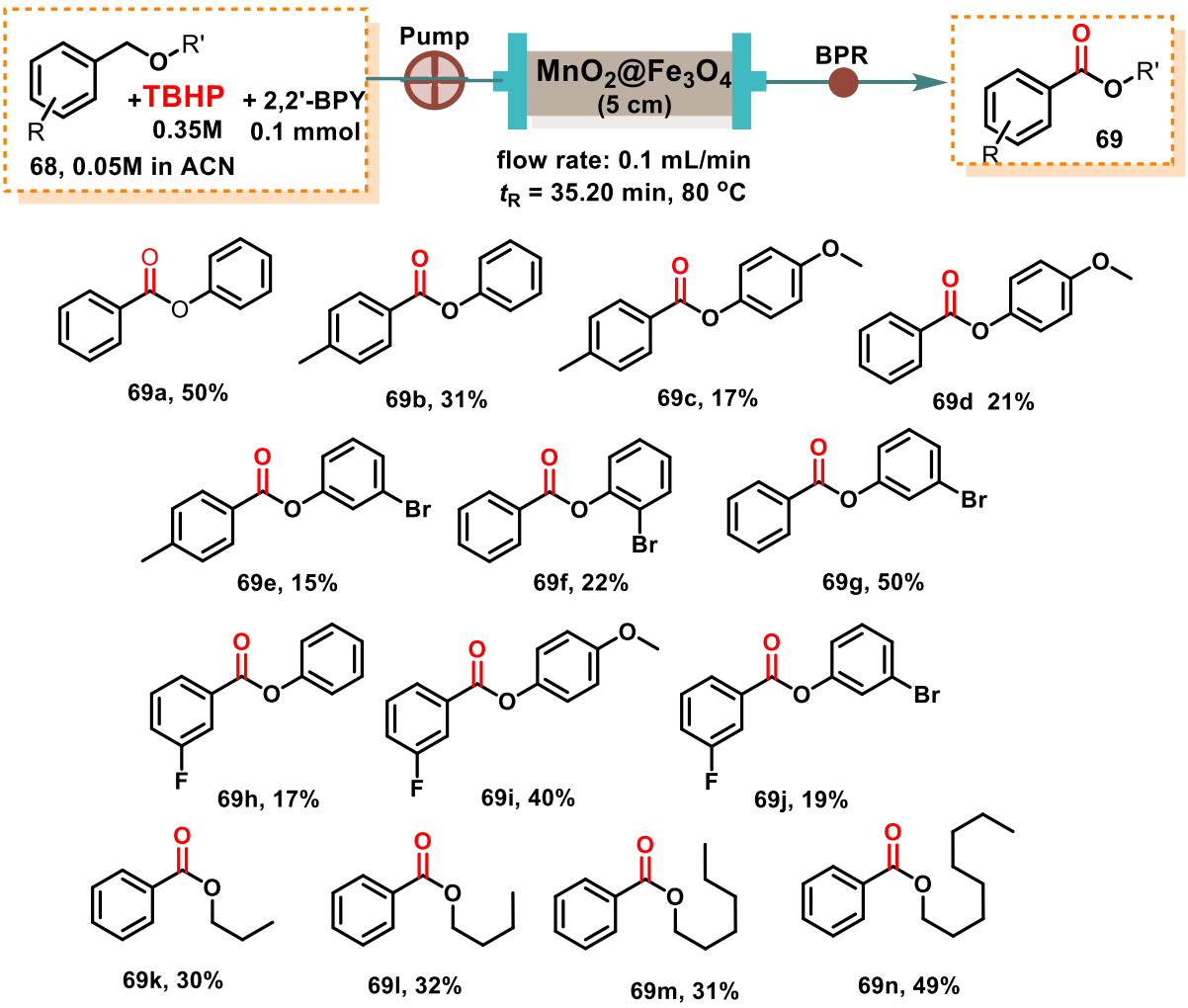

Scheme 2.5.2: Continuous flow setup and substrate scope for ester synthesis

To understand synthetic applicability and catalytic activity of $MnO_2@Fe_3O_4$ catalyst, we further investigated ketone synthesis using respective benzylic sp^3 C-H bond containing substrates in batch and continuous flow reactor. We started screening reaction condition with ethylbenzene **65a** as a model substrate and TBHP as an oxidant.

In batch condition, the oxidation of ethylbenzene (1 mmol) **65a** to acetophenone **66a** was carried out using 5 mmol of TBHP (5-6 M in decane) in 2.0 mL acetonitrile at 80 °C for 7 h (Table 2.5.4). The controlled catalytic experiments of ethylbenzene **65a** were performed with $Mn(OAc)_3.2H_2O$ and Fe_3O_4 (Table 2.5.4, entries 1-2) and under the same reaction conditions giving 72% and 48% of **66a**. Whereas, 0.424% $MnO_2@Fe_3O_4$ was found to be superior in affording acetophenone **66a** in 83% yield when heated at 80 °C for 7 h (Table 2.5.4, entries 3).

Table 2.5.4: Optimization table for sp^3 benzylic oxidation of ethyl benzene under batch

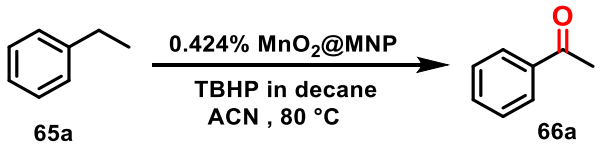

Entry	Catalyst	Solvent	Temp (°C)	Time (h)	Yield of 66a (%)
1[a]	$Mn(OAc)_3.2H_2O$	ACN	80	7	72
2	Fe_3O_4	ACN	80	7	48
3	0.424% $MnO_2@Fe_3O_4$	ACN	80	7	83

Reaction conditions: Ethylbenzene **65a** (1 mmol), TBHP in decane (5 mmol), and 50 mg of catalyst were stirred at 80 °C (see above Table) for 7 h in ACN (2 mL). [a]5 mol % catalyst was used.

The batch process was then translated into a continuous flow to perform the benzylic sp^3 C-H oxidation reaction of ethylbenzene **65a**. The solvents such as toluene and methanol resulted in a low yield for the synthesis of product **66a**. Further, a mixture of a 0.05 M solution of ethylbenzene **65a** and a 0.25 M solution of TBHP (5-6 M in decane) was passed through the catalyst bed with a flow rate of 0.1 mL/min.

Table 2.5.5. Optimization for benzylic sp^3 C-H oxidation of ethyl benzene in flow

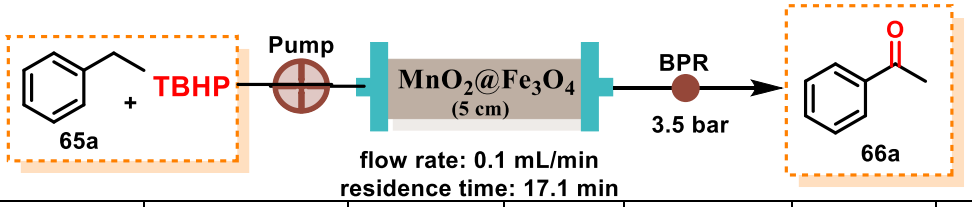

Entry	Catalyst	Substrate (65a):TBHP	Solvent	Temp (°C)	Flow rate (mL/min)	t_R(min)/ cycle	Yield of 66a(%)
1	$MnO_2@Fe_3O_4$	0.05:0.25	Toluene	Rt	0.1	17.10/1	20
2	$MnO_2@Fe_3O_4$	0.05:0.25	Toluene	80	0.1	17.10/1	55
3	$MnO_2@Fe_3O_4$	0.05:0.25	Methanol	80	0.1	17.10/1	nd
4	$MnO_2@Fe_3O_4$	0.05:0.25	ACN	80	0.1	17.10/1	95
5	$MnO_2@Fe_3O_4$	0.05:0.25	ACN	100	0.1	17.10/1	95

Reaction conditions: 0.05 M solution of **65a** + 0.25 M solution of TBHP (5.0−6.0 M in decane) was flown through 0.424% $MnO_2@Fe_3O_4$ catalyst loaded on Omnifit fixed bed reactor with the help of syringe pump (Model no.-HO-SPLF-2D).

The best-optimized condition afforded 95% of product **66a** with a residence time of 17.10 min (Table 2.5.5). Following the optimized batch and continuous flow reaction conditions, the generality of substrates and the catalytic activity of the MnO_2@Fe_3O_4 MNP catalyst were investigated (Scheme 2.5.3). The product **66a** was produced in both batch and continuous flow operations with ease, utilizing acetonitrile as the solvent and TBHP as the oxidizing agent. The yields were generally comparable to batch reactions. However, under continuous flow conditions the reactions are completed faster in 17.10 minutes than requires 7 h under batch conditions.

Other substrates, such as 9*H*-xanthene, diphenylmethane, 1,2,3,4-tetrahydronaphthalene, 2,3-dihydro-1*H*-indene, 9*H*-fluorene, and 2-ethylnaphthalene, gave good to excellent yields of the desired ketones (**66b-g**). With respect to electron-donating substituted ethylbenzene, 72-90% yields of products **66h-I** was observed. On the other hand, *N*-containing substrates such as 1-*H*-oxindole and 1-methyl oxindole transformed into their corresponding ketones (**66j-k**) with excellent yield.

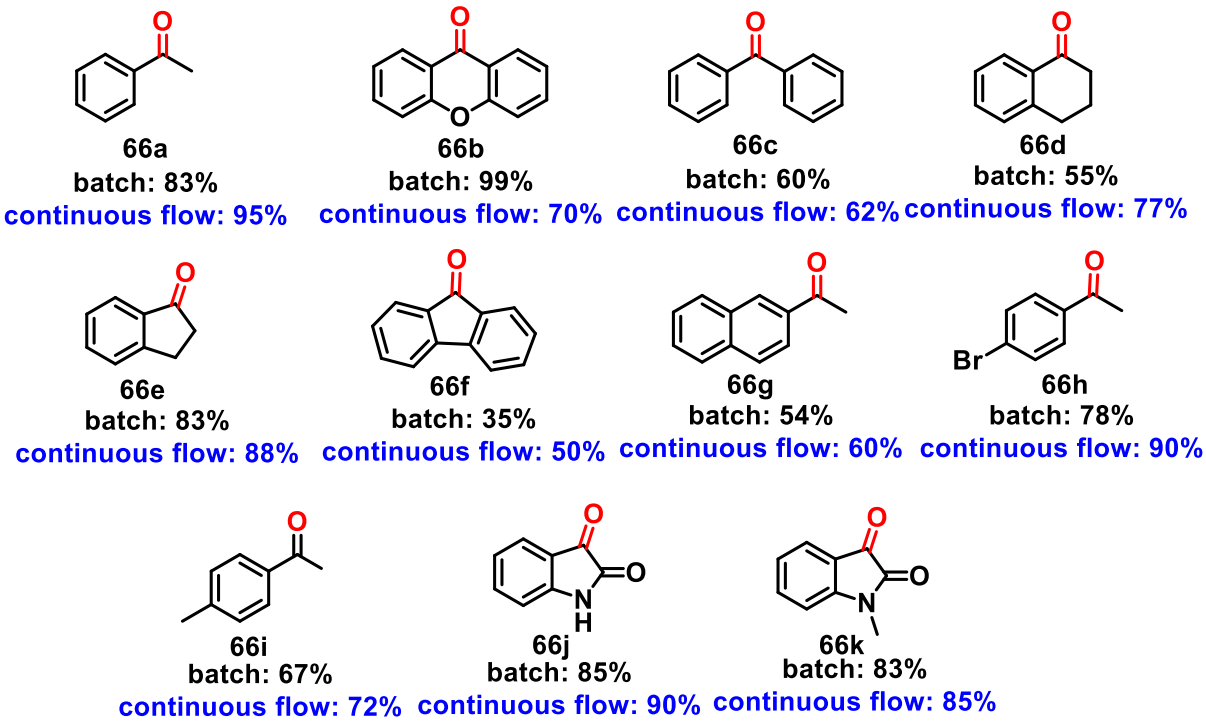

Scheme 2.5.3: The substrate scope for ketone synthesis in a batch and continuous flow

Additionally, a long-time experiment was performed in a continuous flow to check the stability and productivity of the heterogeneous MnO_2@Fe_3O_4 catalyst. For instance, 11 mmol of **65a** were continuously pumped for 12 h at a flow rate of 0.1 mL/min to obtain 10.43 mmol of product **66a**. The

formation of product **66a** was tracked through ^{1}H-NMR. This further revealed that the current catalyst is extremely effective and productive.

To confirm the morphology and oxidation state of the used $MnO_2@Fe_3O_4$ catalyst, the catalyst was magnetically retrieved after the reaction. The catalyst was then subjected to TEM analysis and XPS analysis. Moreover, TEM analysis revealed the average particle size to be 12.34 nm observed from the histogram of TEM images (Figure 2.5.2).

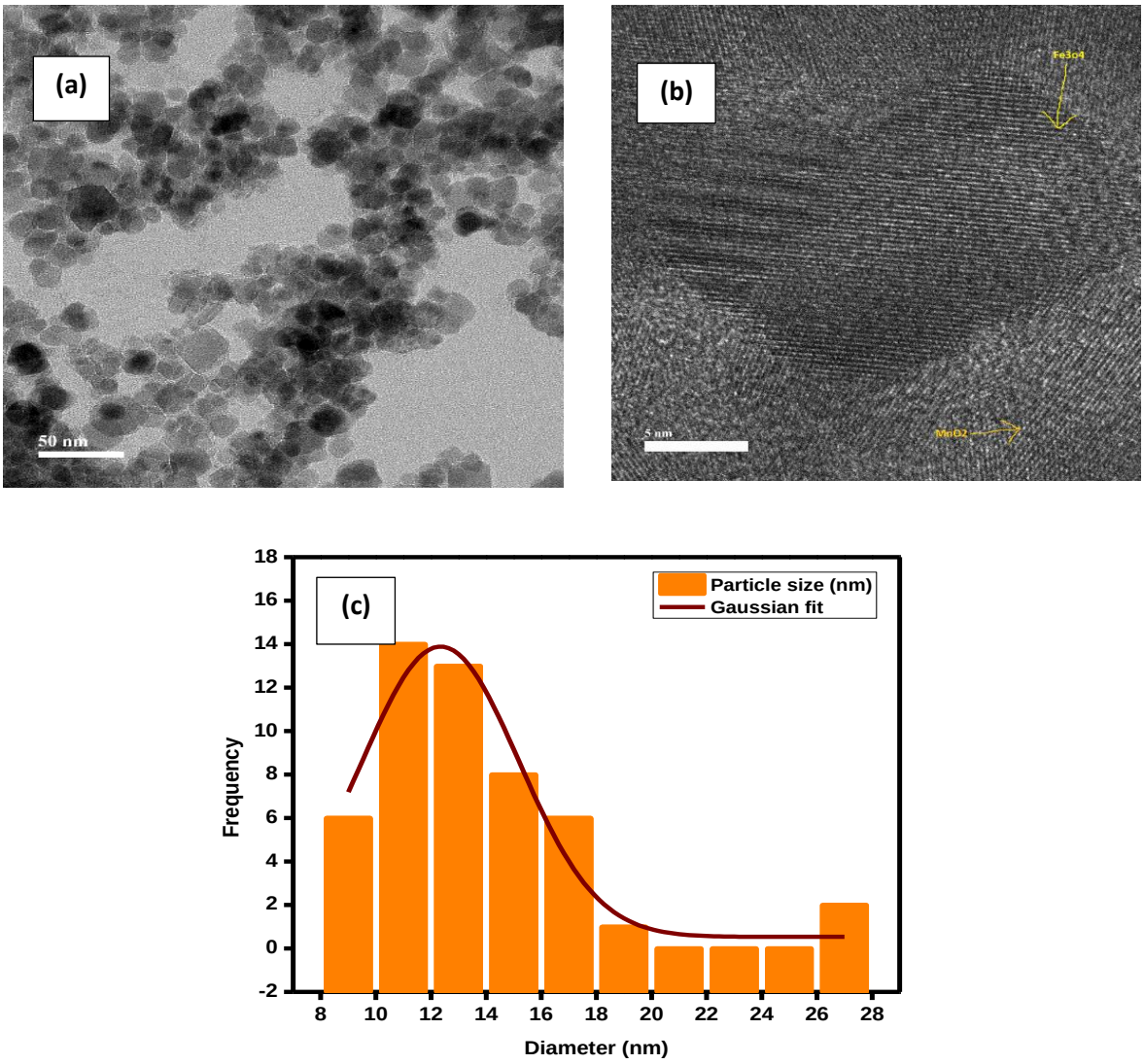

Figure 2.5.2: (a) TEM images of used $MnO_2@Fe_3O_4$ catalyst; (b) Lattice fringes of fresh $MnO_2@Fe_3O_4$ catalyst; (c) Histograms of fresh $MnO_2@Fe_3O_4$ generated from the TEM images

In Figure 2.5.2a, Mn peak is divided into two portions at 641.08 and 642.44 eV for Mn $2p_{3/2}$, and 652.90 and 654.13 eV for Mn $2p_{1/2}$. Whereas Mn^{3+} is represented by the peaks at 641.08 and 642.44

eV, and Mn^{4+} is represented by the peaks at 652.90 and 654.13 eV. (Figure 2.5.3a).[60-61] Additionally, Figure 2.5.3b depicts analysis of the Fe spectrum with two dominant peaks at 711.15 and 724.26 eV that are in agreement with the Fe $2p_{3/2}$ and Fe $2p_{1/2}$ spin-orbit peaks. Moreover, other peaks that are consistent with the typical Fe_3O_4 XPS spectrum that represents Fe is present in the form of Fe^{2+} and Fe^{3+}. Further, three major peaks can be found in the O 1s XPS spectra (Figure 2.5.3c), and they are situated at 530.10, 530.70, and 531.97 eV.36.[62] This validates no change in the oxidation state of Mn, Fe and O after it was used in the reaction.

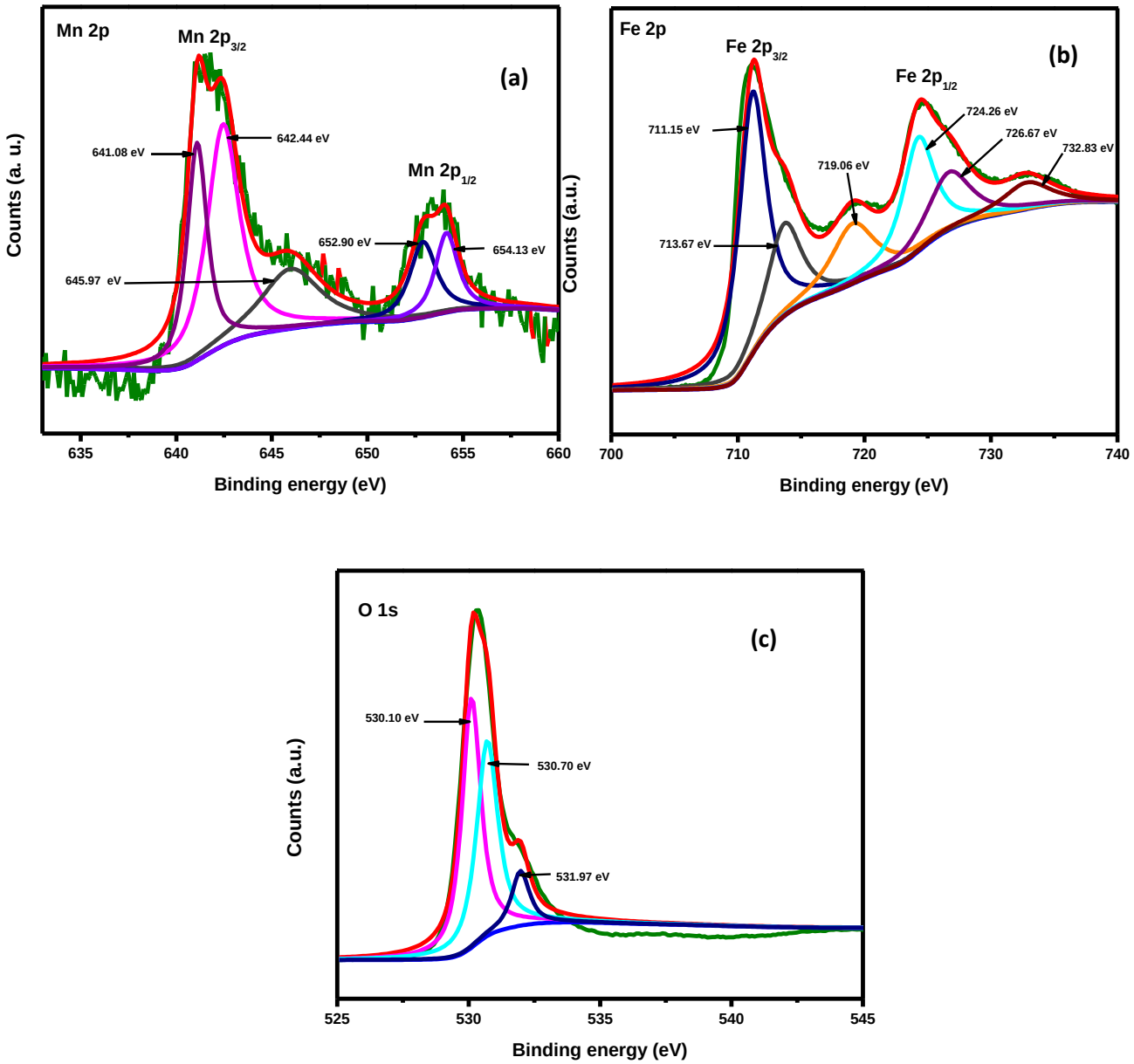

Figure 2.5.3: XPS for used MnO_2@Fe_3O_4 MNP catalyst of (a) Mn $2p_{3/2}$ and $2p_{1/2}$; (b) Fe $2p_{3/2}$ and $2p_{1/2}$; (c) O 1s

2.6. Recyclability of the catalyst

The recovery and recyclabilty of catalyst is an important application in catalysis for developing the sustainable processes for any chemical transformation. Therefore, we have examined the reusability and recyclability of the $MnO_2@Fe_3O_4$ MNP catalyst for the benzylic sp^3 C-H oxidation. The studies were peformed with compounds **68b** (Figure 2.6.1) and **65b** (Figure 2.6.2) with ten and twelve catalytic cycles, respectively, under batch conditions. After the completion of each cycle, the catalyst was simply removed from the reaction mixture using a magnetic needle retriever and washed three times with acetonitrile and ethyl acetate, dried at 100 °C for two hours. The catalyst was then used immediately for the following cycle. Further, demonstrating reaction for the same time, the product yield remained constant. These results exemplified the catalyst was highly efficient with comparable yield throughout the series of reactions.

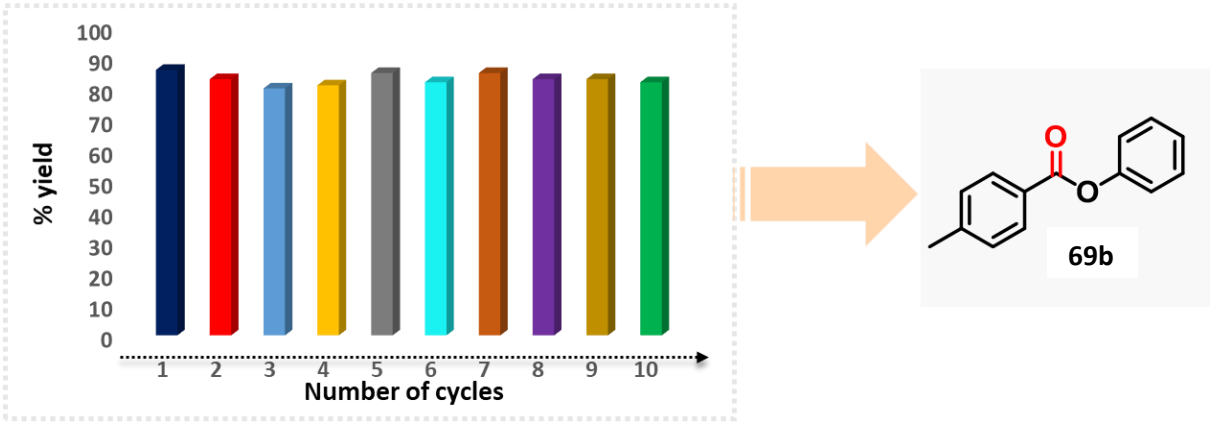

Figure 2.6.1: Recyclability of $MnO_2@Fe_3O_4$ MNP for the synthesis of **69b**

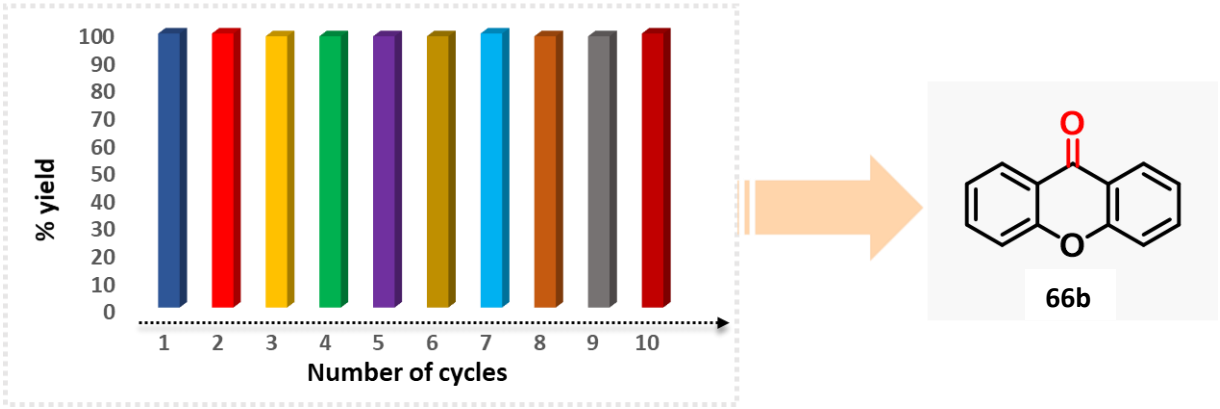

Figure 2.6.2. Recyclability of $MnO_2@Fe_3O_4$ MNP for the synthesis of **66b**

2.7. Hot filtration test

A hot filtration test was conducted for the benzylic sp^3 C-H oxidation of **68a** in order to understand the heterogeneity of the catalyst which suggests homogeneous or heterogeneous nature of the catalyst. The test was performed with ether **68a**. After 16 h of reaction time, the catalyst was extracted using a magnetic retriever. Moreover, only 60% of product **69a** was isolated. This confirms no additional improvement in production of **69a** after the MNP catalyst was separated from the reaction mixture. Additionally, analysis of the filtrate using microwave plasma atomic emission spectroscopy revealed that Mn was not present in the supernatant solution of the reaction mixture. According to this investigation, there was no leaching during the catalytic reaction and Mn was mainly intact with the heterogeneous support.

2.8. Conclusion

In conclusion, we demonstrated $MnO_2@Fe_3O_4$ MNP as an efficient heterogeneous catalyst for the direct benzylic sp^3 C-H oxidation of ethers by using TBHP as an oxidant to afford the ester in a higher yield. This method is also compatible for the synthesis of ketone derivatives in batch and continuous flow modules. The key benefits of this process include mild reaction conditions and demonstrations in batch and continuous flow modules with scalable synthesis and high TOF values, simple product isolation, and catalyst recycling for more than 10 cycles. Therefore, we anticipate that the present catalyst will be useful in a variety of industrial and organic synthesis processes.

2.9. Experimental sections

Materials and characterization:

All the chemicals are purchased from Sigma Aldrich or Alfa-Aesar. Deuterated solvents were used as received. All the solvents used were dry grade. Column chromatographic separations performed over 100−200 Silica-gel. Visualization was accomplished with UV light and phosphomolybdic acid (PMA), Ceric ammonium molybdate (CAM) stain followed by heating. The iron (III) chloride (product number: 44939) was purchased from Sigma Aldrich. All the experiments were carried out without maintaining the inert condition. The flow chemistry experiments were carried out on the Holmarc syringe pump (Model no.-HO-SPLF-2D). ^1H and ^{13}C NMR spectra were recorded on 400 and 100 MHz, respectively, using Bruker 400 MHz or JEOL 400 MHz spectrometers. The chemical shift (δ) and coupling constant (*J*) values are given in parts per million and hertz, respectively. Abbreviations used in the NMR follow-up experiments: b, broad; s, singlet; d, doublet; t, triplet; q, quartet; m,

multiplet. High-resolution mass spectra were recorded with Waters-synapt G2 using electrospray ionization (ESI-TOF). Fourier-transform infrared (FTIR) spectra were obtained with a Bruker Alpha-E Fourier transform infrared spectrometer. Powder X-ray diffraction (PXRD)patterns were measured on Bruker D8 Advanced X-ray diffractometer at room temperature using Cu Kαradiation (λ= 1.5406 Å) with a scan speed of 0.5° min^{-1} and a step size of 0.01° in 2θ. BET was recorded on Quantachrome Instruments. The Hi-Resolution Transmission Electron Microscopy (HRTEM) imaging was performed using Jeol JEM2200FS (200 kV) HRTEM instrument. The XPS was collected using a Thermo Scientific Kalpha+ spectrometer using a monochromated Al Kalpha (1486.6 eV) source. The base pressure of the spectrometer was always better than 5x 10^{-9} mbar. The electron flood gun was on during acquisition for charge neutralization. The wide area spectrum was collected using 200 eV pass energy and individual core levels at 50 eV.

A. General procedure for the synthesis of MnO_2@Fe_3O_4 MNP catalyst: A mixture of $FeCl_3.6H_2O$ (4320.0 mg, 16 mmol) and $FeCl_2.4H_2O$ (1600.0 mg, 8 mmol) was dissolved in 40 mL of deionized water. The resultant solution was left to be stirred for 30 min at 80° C. Then ammonia solution (25% (w/w)) was added in a drop-wise manner over 5 min to the stirring mixture to maintain the reaction pH of about 11. The resulting black dispersion was stirred vigorously for 1 h at room temperature and then refluxed for 1 h. The black magnetite Fe_3O_4 nanoparticles were isolated by magnetic decantation, washed several times with deionized water, and then dried at 80 °C for 4 h. To introduce reactive Mn on the surface of the magnetic nanoparticle (MNP), 600.0 mg of dried Fe_3O_4 nanoparticles were suspended in a mixture of 50 mL ethanol and then, 600.0 mg of $Mn(OAc)_3.2H_2O$ was ultrasonically dispersed. After complete dissolution and dispersion, the nanoparticles were separated from the ethanol solution by magnetic decantation and dried at 80 °C for 4 h. MnO_2@Fe_3O_4 magnetic nanoparticles were obtained by drop-wise addition of aqueous ammonia (25% (w/w)) to the dried brown nanoparticles under vigorous stirring. Finally, the MnO_2@Fe_3O_4 MNP were magnetically separated, washed with water, and dried in an oven at 100 ^oC for overnight.

B. General procedure for the synthesis of the esters from sp^3 C-H oxidation of (benzyloxy)benzene derivatives 68 in batch: In a 20 mL glass seal tube, catalyst (25.0 mg), (benzyloxy)benzene derivatives **68** (0.5 mmol, 1 equiv.) in ACN (2 mL) were added TBHP (5-6 M in decane, 3.5 mmol, 7 equiv), 0.05 mmol of 2,2′-bipyridine and the tube was sealed by using a crimper. The mixture was stirred at 80 °C for 24 h. After completion, the reaction mixture was allowed to cool to room temperature. It was then diluted with EtOAc and the catalyst was separated with an external magnet and washed twice with EtOAc. The mixture was extracted with EtOAc, the volatiles was

removed under reduced pressure, and the crude product was purified by column chromatography on silica gel directly (EtOAc:hexane in 2:98) to afford the ester products. All of the esters **69** were identified by spectral comparison with literature data.

C. General procedure for the synthesis of the esters from sp^3 C-H oxidation of (benzyloxy)benzene derivatives 68 in a continuous flow: 0.05 M solution of substrate **68** and 0.35 M of 5.0-6.0 M TBHP in decane and 0.1 mmol of 2,2′-bipyridine in 20 mL of ACN solvent was pumped through a syringe pump packed with 1500.0 mg of 0.424% MnO_2@Fe_3O_4 (up to 5 cm) is heated at 80 °C with the flow rate of 0.1 mL min^{-1}. A 3.5 to 3.8 bar back pressure regulator was placed after the reactor. The collected organic layer was concentrated under reduced pressure and the crude product was purified by column chromatography on silica gel directly (EtOAc:hexane in 2:98) to afford the ester **69** product.

D. General procedure for oxidation of benzylic sp^3 C-H group of methylene derivatives 65 to the ketone 66 in batch: In a 20 mL glass seal tube, catalyst (50.0 mg), alkyl benzene **65** (1 mmol, 1 equiv.) in ACN (2 mL) was added TBHP (5-6 M in decane, 5 mmol, 5 equiv.) and the tube was sealed by using a crimper. The mixture was stirred at 80 °C for 7 h. After completion, the reaction mixture was allowed to cool to room temperature. It was then diluted with EtOAc and the catalyst was separated with an external magnet and washed twice with EtOAc. The mixture was extracted with EtOAc, the volatiles was removed under reduced pressure, and the crude product was purified by column chromatography on silica gel directly (EtOAc:hexane in 2:98) to afford the desired product **66**.

E. General procedure for oxidation of benzylic sp^3 C-H group of methylene derivatives 65 to the ketone 66 in a continuous flow: 0.05 M solution of the substrate **65** and 0.25 M of 5.0-6.0 M TBHP in decane in 20 mL of ACN solvent was pumped through a syringe pump packed with 1500.0 mg of 0.424% MnO_2@Fe_3O_4 (up to 5 cm) is heated at 80 °C with the flow rate of 0.1 mL min^{-1}. A 3.5 to 3.8 bar back pressure regulator was placed after the reactor. The collected organic layer was concentrated under reduced pressure and the crude product was purified by column chromatography on silica gel directly (EtOAc:hexane in 2:98) to afford the desired product **66**.

F. Study of a lifetime of the catalyst and gram-scale synthesis of benzylic sp^3 C-H group of methylene derivatives to the ketone in a continuous flow: 0.05 M solution of the substrate **65a** (1166.0 mg, 10.99 mmol) and 0.25 M of TBHP (5.0-6.0 M in decane, 7080.0 mg, 54.99 mmol) in 110 mL of ACN solvent was pumped through a syringe pump packed with 1300 mg of 0.424% MnO_2@Fe_3O_4 (up to 3 cm) is heated at 80 °C with the flow rate of 0.1 mL min^{-1} at 3.5 bar pressure

for 12 h. The reaction mixture was monitored at regular intervals by ^{1}H-NMR analysis. The entire reaction fraction was concentrated in a rotary evaporator to afford 1250 mg of acetophenone **66a** as a yellowish oil.

G. General procedure for catalyst recovery for the synthesis of the esters from (benzyloxy)benzene derivatives 68b in batch: In a 20 mL glass seal tube, catalyst (25.0 mg), **68b** (0.5 mmol, 1 equiv.) in ACN (2 mL) were added TBHP (5-6 M in decane, 3.5 mmol, 7 equiv), 0.05 mmol of 2,2′-bipyridine and the tube was sealed by using a crimper. The mixture was stirred at 80 °C for 24 h. After completion, the reaction mixture was allowed to cool to room temperature; the supported catalyst was separated by an external magnet and washed with acetonitrile and ethyl acetate three times, then dried and directly used in the next run.

H. General procedure for catalyst recovery for the synthesis of the ketone from 65b in batch: In a 20 mL glass seal tube, catalyst (25.0 mg), **65b** (0.5 mmol, 1 equiv.) in ACN (2 mL) were added TBHP (5-6 M in decane, 3.5 mmol, 7 equiv), 0.05 mmol of 2,2′-bipyridine and the tube was sealed by using a crimper. The mixture was stirred at 80 °C for 7 h. After completion, the reaction mixture was allowed to cool to room temperature; the supported catalyst was separated by an external magnet and washed with acetonitrile and ethyl acetate three times, then dried and directly used in the next run.

2.10.A. Analytical data for product:

acetophenone ***(66a)*****:**[41]

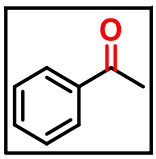

Prepared according to the general procedure (**D**) and (**E**), using ethylbenzene to afford acetophenone **66a** (Batch: 100.0 mg, 83%; TON = 341.6; TOF = 48.8 h^{-1}; Continuous flow: 114.0 mg, 95%) respectively as a yellowish liquid. ^{1}H NMR (400 MHz, $CDCl_3$) δ 7.39 (dt, *J* = 8.0 Hz and 1.96 Hz, 2H), 7.53 (t, *J* = 8.46 Hz, 1.28 Hz, 1H), 7.42 (m, 2H), 2.56 (s, 3H). ^{13}C NMR (100 MHz, $CDCl_3$) δ 198.2, 137.1, 133.1, 128.6, 128.3, 77.5, 76.8, 26.6. FT-IR: 3362, 2940, 2245, 2245, 1680, 1024, 769 cm^{-1}. HRMS (ESI-TOF) m/z: $[M + H]^+$ calcd for C_8H_8O: 121.0655; found: 121.0653.

9H-xanthen-9-one **(66b):**[42a]

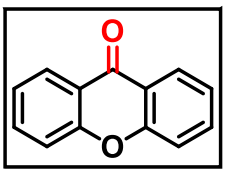

Prepared according to the general procedure (**D**) and (**E**), using 9*H*-xanthene to afford 9*H*-xanthen-9-one **66b** (Batch: 194.0 mg, 99%; TON = 405.6; TOF = 57.9 h^{-1}; Continuous flow: 137.0 mg, 70%) respectively as a white solid. ^{1}H NMR (400

MHz, $CDCl_3$) δ 8.35 (dd, *J* = 8.0 Hz and 1.6 Hz, 2H), 7.74 (ddd, *J* = 8.6, 7.2 Hz and 1.7 Hz, 2H), 7.51 (d, *J* = 8.3 Hz, 2H), 7.39 (m, 2H). ^{13}C NMR (100 MHz, $CDCl_3$) δ 177.4, 156.3, 135.0, 126.9, 124.1, 122.0, 118.1. FT-IR: 3019, 2400, 1654, 1618, 1460, 1215, 763, 669 cm^{-1}. HRMS (ESI-TOF) m/z: $[M + H]^+$ calcd for $C_{13}H_8O_2$: 197.0602; found: 197.0604.

benzophenone **(66c):**[42a]

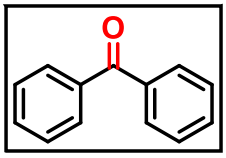

Prepared according to the general procedure (**D**) and (**E**), using diphenylmethane to afford benzophenone **66c** (Batch: 109.0 mg, 60%; TON = 245.2; TOF = 35.1 h^{-1}; Continuous flow: 112.0 mg, 62%) respectively as a white solid. ^1H NMR (400 MHz, $CDCl_3$) δ 7.81 (m, 4H), 7.59 (m, 2H), 7.48 (m, 4H). ^{13}C NMR (100 MHz, $CDCl_3$) δ 196.9, 137.7, 132.6, 130.2, 128.4. FT-IR: 3018, 1656, 1619, 1447, 1318, 1279, 1281, 772 cm^1. HRMS (ESI-TOF) m/z: $[M + H]^+$ calcd for $C_{13}H_{10}O$: 183.0812; found: 183.0810.

3,4-dihydronaphthalen-1(2H)-one **(66d):**[42a]

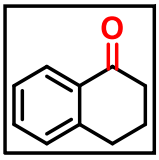

Prepared according to the general procedure (**D**) and (**E**), using 1,2,3,4-tetrahydronaphthalene to afford 3,4-dihydronaphthalen-1(2*H*)-one **66d** (Batch: 77.0 mg, 55%; TON = 216.1; TOF = 30.9 h^{-1}; Continuous flow: 112.0 mg, 77%) respectively as a pale yellow liquid. ^1H NMR (400 MHz, $CDCl_3$) δ 8.0 (d, *J* = 8.0 Hz, 1H), 7.43 (td, *J* = 8.0 Hz and 1.2 Hz, 1H), 7.24 (m, 2H), 2.93 (t, 2H), 2.62 (t, 2H), 2.10 (m, 2H). ^{13}C NMR (100 MHz, $CDCl_3$) δ 198.1, 144.2, 133.1, 132.3, 128.5, 126.9, 126.3, 38.9, 29.4, 23.0. FT-IR: 3023, 2402, 1521, 1426, 1215, 771, 672 cm^{-1}. HRMS (ESI-TOF) m/z: $[M + H]^+$ calcd for $C_{10}H_{10}O$: 147.0812; found: 147.0811.

2,3-dihydro-1H-inden-1-one **(66e):**[41]

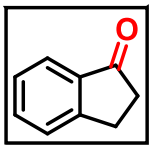

Prepared according to the general procedure (**D**) and (**E**), using 2,3-dihydro-1*H*-indene to afford 2,3-dihydro-1*H*-inden-1-one **66e** (Batch: 110.0 mg, 83%; TON = 341.7; TOF = 48.8 h^{-1}; Continuous flow: 116.0 mg, 88%) respectively as a white solid. ^1H NMR (400 MHz, $CDCl_3$) δ 7.76 (d, *J* = 7.8 Hz, 1H), 7.59 (t, *J* = 7.4 Hz, 1H), 7.48 (d, *J* = 7.2 Hz, 1H), 7.37 (t, *J* = 7.4 Hz, 1H), 3.15 (m, 2H), 2.69 (m, 2H). ^{13}C NMR (100 MHz, $CDCl_3$) δ 207.2, 155.8, 137.4, 135.1, 128.3, 127.0, 124.0, 36.5, 26.3. IR (neat): 3567, 3031, 2927, 1701, 1603, 1280, 754 cm^{-1}. HRMS (ESI-TOF) m/z: $[M + H]^+$ calcd for C_9H_8O: 133.0653; found: 133.0658.

9H-fluoren-9-one **(66f):**[41]

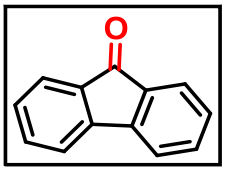

Prepared according to the general procedure (**D**) and (**E**), using 9*H*-fluorene to afford 9*H*-fluoren-9-one **66f** (Batch: 63.0 mg, 35%; TON = 143.6; TOF = 20.5 h^{-1}; Continuous flow: 90.0 mg, 50%) respectively as a yellow solid. ^{1}H NMR (400 MHz, $CDCl_3$) δ 7.64 (d, *J* = 4.0 Hz, 2H), 7.48 (m, 4H), 7.29 (m, 2H). ^{13}C NMR (100 MHz, $CDCl_3$) δ 194.4, 144.9, 135.1, 134.8, 134.6, 129.5, 124.7, 120.7. FT-IR: 3020, 1715, 1218, 772 cm^{-1}. HRMS (ESI-TOF) m/z: $[M + H]^+$ calcd for $C_{13}H_8O$: 181.0655; found: 181.0653.

1-(naphthalen-2-yl)ethan-1-one **(66g):**[50b]

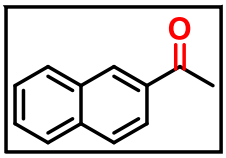

Prepared according to the general procedure (**D**) and (**E**), using 2-ethylnaphthalene to afford 1-(naphthalen-2-yl)ethan-1-one **66g** (Batch: 92.0 mg, 54%; TON = 221.9; TOF = 31.7 h^{-1}; Continuous flow: 102.0 mg, 60%) respectively as a pale yellow liquid. ^{1}H NMR (400 MHz, $CDCl_3$) δ 8.47 (s, 1H), 8.04 (dd, *J* = 8.6 Hz and 1.7 Hz, 1H), 7.97 (d, *J* = 7.9 Hz, 1H), 7.89 (m, 2H), 7.59 (m, 2H), 2.74 (s, 3H). ^{13}C NMR (100 MHz, $CDCl_3$) δ 198.5, 136.0, 134.9, 132.9, 130.6, 129.9, 128.8, 128.2, 127.2, 124.3, 27.1. FT-IR: 3352, 2940.56, 2842, 1676, 1219, 1032, 771 cm^{-1}. HRMS (ESI-TOF) m/z: $[M + H]^+$ calcd for $C_{12}H_{10}O$: 171.0810; found: 171.0812.

1-(4-bromophenyl)ethan-1-one **(66h):**[41]

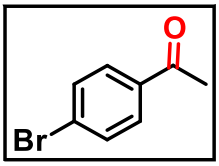

Prepared according to the general procedure (**D**) and (**E**), using 1-bromo-4-ethylbenzene to afford 1-(4-bromophenyl)ethan-1-one **66h** (Batch: 154.0 mg, 78%; TON = 320.3; TOF = 45.8 h^{-1}; Continuous flow: 179.0 mg, 90%) respectively as a white solid. ^{1}H NMR (400 MHz, $CDCl_3$) δ 7.9 (m, 2H), 7.58 (m, 2H), 2.56 (s, 3H). ^{13}C NMR (100 MHz, $CDCl_3$) δ 196.6, 135.5, 131.5, 129.7, 129.9, 127.9, 26.2. IR (neat): 3508, 1682, 1581, 1259, 819, 586 cm^{-1}. HRMS (ESI-TOF) m/z: $[M + H]^+$ calcd for C_8H_7OBr: 198.9760; found: 198.9758.

1-(p-tolyl)ethan-1-one **(66i):**[41]

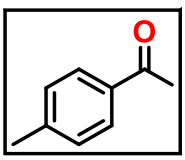

Prepared according to the general procedure (**D**) and (**E**), using 1-ethyl-4-methylbenzene to afford 1-(*p*-tolyl)ethan-1-one **66i** (Batch: 90.0 mg, 67%; TON = 275.2; TOF = 39.3 h^{-1}; Continuous flow: 97.0 mg, 72%) respectively as a pale yellow liquid. ^{1}H NMR (400 MHz, $CDCl_3$) δ 7.84 (d, *J* = 8.0 Hz, 2H), 7.24 (d, *J* = 8.0 Hz, 2H), 2.87 (s, 3H), 2.39 (s, 3H). ^{13}C NMR (100 MHz, $CDCl_3$) δ 198.3, 144.3, 135.1, 129.6, 129.0, 27.0, 22.0. FT-IR:

3009, 1681, 1605, 1217, 1182, 771 cm^{-1}. HRMS (ESI-TOF) m/z: $[M + H]^+$ calcd for $C_9H_{10}O$: 135.0809; found: 135.0810.

indoline-2,3-dione **(66j):**[71]

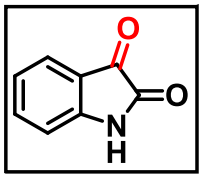

Prepared according to the general procedure (**D**) and (**E**), using indolin-2-one to afford indoline-2,3-dione **66j** (Batch: 125.0 mg, 85%; TON = 348.6; TOF = 49.8 h^{-1}; Continuous flow: 133.0 mg, 90%) respectively as an orange solid. ^1H NMR (400 MHz, $CDCl_3$) δ 8.0 (s, 1H), 7.63 (m, 1H), 7.57 (m, 1H), 7.13 (m, 1H), 6.92 (m, 1H). FT-IR: 3385, 1610, 1442, 1219, 1042, 772 cm^{-1}. HRMS (ESI-TOF) m/z: $[M + H]^+$ calcd for $C_8H_5O_2N$: 148.0398; found: 148.0401.

1-methylindoline-2,3-dione **(66k):**[71]

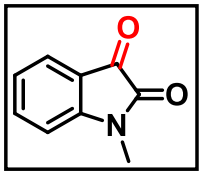

Prepared according to the general procedure (**D**) and (**E**), using 1-methylindolin-2-one to afford 1-methylindoline-2,3-dione **66k** (Batch: 134.0 mg, 83%; TON = 341.2; TOF = 48.75 h^{-1}; Continuous flow: 137.0 mg, 85%) respectively as an orange solid. ^1H NMR (400 MHz, $CDCl_3$) δ 7.60 (t, *J* = 8.0Hz, 2H), 7.12 (t, *J* = 8.0 Hz, 1H), 6.89 (d, *J* = 8.0 Hz, 1H), 3.24 (s, 3H). ^{13}C NMR (100 MHz, $CDCl_3$) δ 183.5, 158.4, 151.6, 138.5, 125.4, 124.0, 117.6, 110.1, 26.4. FT-IR: 3019, 2400, 1744, 1612, 1216, 771, 669 cm^{-1}. HRMS (ESI-TOF) m/z: $[M + H]^+$ calcd for $C_9H_7O_2N$: 162.0555; found: 162.0555.

phenyl benzoate **(69a):**[65]

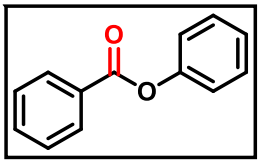

Prepared according to the general procedure (**B**) and (**C**), using (benzyloxy)benzene to afford phenyl benzoate **69a** (Batch: 79.0 mg, 80%; TON = 326.0; TOF = 13.58 h^{-1}; Continuous flow: 49.0 mg, 50%) respectively as a white solid. ^1H NMR (400 MHz, $CDCl_3$) δ 8.22 (m, 2H), 7.65 (tt, *J* = 7.4, 1.3 Hz, 1H), 7.52 (m, 2H), 7.44 (m, 2H), 7.30 (m, 1H), 7.22 (m, 2H). ^{13}C NMR (100 MHz, $CDCl_3$) δ 165.7, 151.4, 134.1, 130.6, 130.0, 129.9, 129.0, 126.4, 122.2. IR (neat): 3062, 1724, 1253, 1178, 1064, 1010, 689 cm^{-1}. HRMS (ESI-TOF) m/z: $[M + H]^+$ calcd for $C_{13}H_{10}O_2$: 199.0759; found: 199.0760.

phenyl-4-methylbenzoate **(69b):**[65]

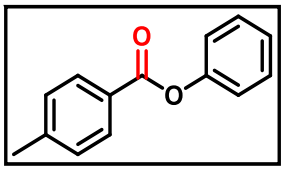

Prepared according to the general procedure (**B**) and (**C**), using 1-methyl-4-(phenoxymethyl)benzene to afford phenyl-4-methylbenzoate **69b** (Batch: 1823.0 mg (for 10 mmol scale, 86%, TON = 358.3; TOF = 14.93 h^{-1});

Continuous flow: 36.0 mg, 31% respectively as a white solid. ^{1}H NMR (400 MHz, $CDCl_3$) δ 8.10 (dt, *J* = 8.2 Hz and 1.8 Hz, 2H), 7.43 (m, 2H), 7.31 (d, *J* = 8.4 Hz, 2H), 7.28 (m, 1H), 7.22 (m, 1H), 7.20 (m, 1H), 2.46 (s, 3H). ^{13}C NMR (100 MHz, $CDCl_3$) δ 165.7, 151.5, 144.9, 130.7, 129.8, 130.0, 127.2, 126.3, 122.2, 22.2. IR (neat): 2924, 1724, 1259, 1182, 1066, 736 cm^{-1}. HRMS (ESI-TOF) m/z: $[M + H]^+$ calcd for $C_{14}H_{12}O_2$: 213.0915; found: 213.0920.

4-methoxyphenyl-4-methylbenzoate **(69c):**[65]

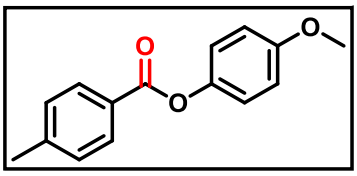

Prepared according to the general procedure (**B**) and (**C**), using 1-methoxy-4-((4-methylbenzyl)oxy)benzene to afford 4-methoxyphenyl-4-methylbenzoate **69c** (Batch: 71.0 mg, 58%; TON = 240.4; TOF = 10.0 h^{-1}; Continuous flow: 21.0 mg, 17%) respectively as a white solid. ^{1}H NMR (400 MHz, $CDCl_3$) δ 8.08 (dt, *J* = 8.4 Hz and 1.9 Hz, 2H), 7.30 (d, *J* = 8.3 Hz, 2H), 7.12 (dt, *J* = 10.3 Hz and 3.6 Hz, 2H), 6.94 (dt, *J* = 10.3 Hz and 3.6 Hz, 2H), 3.82 (s, 3H), 2.45 (s, 3H). ^{13}C NMR (100 MHz, $CDCl_3$) δ 166.4, 158.0, 145.2, 145.1, 130.9, 130.0, 127.6, 123.3, 115.3, 56.4, 22.5. IR (neat): 2929, 2851, 2120, 1723, 1500, 1250, 1178, 1065, 1020, 746.61 cm^{-1}. HRMS (ESI-TOF) m/z: $[M + H]^+$ calcd for $C_{15}H_{14}O_3$: 243.1021; found: 243.1027.

4-methoxyphenyl benzoate **(69d):**[65]

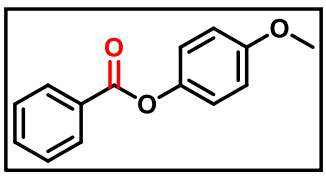

Prepared according to the general procedure (**B**) and (**C**), using 1-(benzyloxy)-4-methoxybenzene to afford 4-methoxyphenylbenzoate **69d** (Batch: 75.0 mg, 66%; TON = 270.7; TOF = 11.3 h^{-1}; Continuous flow: 24.0 mg,21%) respectively as a white solid. ^{1}H NMR (400 MHz, $CDCl_3$) δ 8.20 (m, 2H), 7.63 (tt, *J* = 6.8 Hz and 1.2Hz, 1H), 7.51 (m, 2H), 7.13 (m, 2H), 6.94 (m, 2H), 3.83 (s, 3H). ^{13}C NMR (100 MHz, $CDCl_3$) δ 165.5, 157.4, 144.5, 133.6, 130.2, 129.7, 128.6, 122.5, 114.5, 55.7. IR (neat): 2925.66, 1727.73, 1500.21, 1252.99, 1183.89, 1067.38, 1028.28, 710.77 cm^{-1}. HRMS (ESI-TOF) m/z: $[M + H]^+$ calcd for $C_{14}H_{12}O_3$: 229.0864; found: 229.0865.

3-bromophenyl 4-methylbenzoate **(69e):**[65]

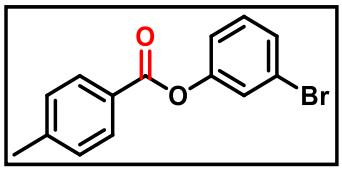

Prepared according to the general procedure (**B**) and (**C**), using 1-bromo-3-((4-methylbenzyl)oxy)benzene to afford 3-bromophenyl-4-methylbenzoate **69e** (Batch: 72.0 mg, 50%; TON = 205.0; TOF = 8.5 h^{-1}; Continuous flow: 22.0 mg, 15%) respectively as a white solid. ^{1}H

NMR (400 MHz, $CDCl_3$) δ 8.07 (dt, *J* = 8.2 Hz and 1.7 Hz, 2H), 7.41 (m,2H), 7.30 (m, 3H), 7.17 (m, 1H), 2.46 (s, 3H). ^{13}C NMR (100 MHz, $CDCl_3$) δ 164.8, 151.5, 144.8, 130.5, 130.2, 129.4, 129.0, 126.3, 125.3, 122.4, 120.7, 21.8. IR (neat): 2927, 1735, 1255, 1192, 1061, 732 cm^{-1}. HRMS (ESI-TOF) m/z: $[M + H]^+$ calcd for $C_{14}H_{11}BrO_2$: 291.0020; found: 291.0023.

2-bromophenyl benzoate **(69f):**[66]

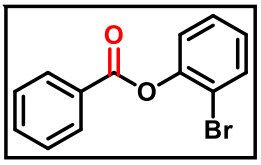

Prepared according to the general procedure (**B**) and (**C**), using 1-(benzyloxy)-2-bromobenzene to afford 2-bromophenylbenzoate **69f** (Batch: 104.0 mg, 75%; TON = 310.1; TOF = 12.92 h^{-1}; Continuous flow: 29.0 mg, 22%) respectively as a white solid. ^1H NMR (400 MHz, $CDCl_3$) δ 8.25 (m, 2H), 7.66 (m, 2H), 7.53 (m, 2H), 7.39 (td, *J* = 8.2 Hz and 3.1 Hz, 1H), 7.29 (dd, *J* = 8.1 Hz and 1.5 Hz, 1H), 7.17 (td, *J* = 7.6 Hz and 1.7 Hz, 1H). ^{13}C NMR (100 MHz, $CDCl_3$) δ 164.7, 148.9, 134.3, 133.8, 130.8, 130.0, 129.4, 129.0 (d, *J* = 15.2 Hz), 127.8, 124.4, 124.1, 116.7, 41.6. IR (neat): 2930, 1740, 1251, 1205, 1052, 694 cm^{-1}. HRMS (ESI-TOF) m/z: $[M + H]^+$ calcd for $C_{13}H_9BrO_2$: 276.9864; found: 276.9864.

3-bromophenyl benzoate **(69g):**[65]

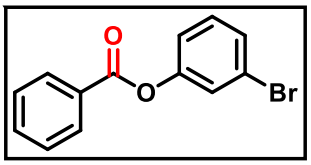

Prepared according to the general procedure (**B**) and (**C**), using 1-(benzyloxy)-3-bromobenzene to afford 3-bromophenylbenzoate **69g** (Batch: 2216.0 mg (for 10 mmol scale), 80%; TON = 335.7; TOF = 13.9 h^{-1}; Continuous flow: 69.0 mg, 50%) respectively as a white solid. ^1H NMR (400 MHz, $CDCl_3$) δ 8.19 (m, 2H), 7.66 (t, *J* = 8 Hz, 1H), 7.52 (t, *J* = 7.8 Hz, 2H), 7.42 (m, 2H), 7.33 (m, 1H), 7.19 (m, 1H). ^{13}C NMR (100 MHz, $CDCl_3$) δ 165.2, 151.8, 134.3, 131.0, 130.6, 129.5, 129.1, 125.7, 122.9, 121.1. IR (neat): 2925, 1730, 1243, 1190, 1058, 699 cm^{-1}. HRMS (ESI-TOF) m/z: $[M + H]^+$ calcd for $C_{13}H_9BrO_2$: 276.9864; found: 276.9866

phenyl-3-fluorobenzoate **(69h):**[67]

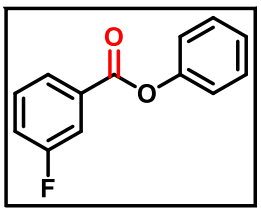

Prepared according to the general procedure (**B**) and (**C**), using 1-fluoro-3-(phenoxymethyl)benzene to afford phenyl-3-fluorobenzoate **69h** (Batch: 67.0 mg, 62%, TON = 254.3; TOF = 10.6 h^{-1}; Continuous flow: 18.0 mg, 17%) respectively as a white solid. ^1H NMR (400 MHz, $CDCl_3$) δ 8.01 (dt, *J* =7.8, 1.4, 1H), 7.89 (ddd, *J*= 9.3, 2.6 and 1.6 Hz, 1H), 7.47 (m, 3H), 7.35 (m, 1H), 7.29 (tt, *J* = 6.97 Hz and 1.04 Hz, 1H), 7.23 (m, 1H), 7.21 (m, 1H). ^{13}C NMR (100 MHz, $CDCl_3$) δ 164.1 (d, *J* C-F = 24.7 Hz), 161.5, 150.9, 131.8 (d, *J* C-F = 6.8 Hz), 130.4 (d, *J* C-F = 7.6 Hz), 129.7,126.3, 126.0 (d, *J* C-F = 2.81

Hz), 121.7, 120.8 (d, *J* C-F = 21.1 Hz), 117.1 (d, *J* C-F = 23.1 Hz). IR (neat): 2923, 1734, 1269, 1186, 740 cm^{-1}. HRMS (ESI-TOF) m/z: $[M + H]^+$ calcd for $C_{13}H_9FO_2$: 217.0667; found: 217.0666.

2-methoxyphenyl-3-fluorobenzoate **(69i):**

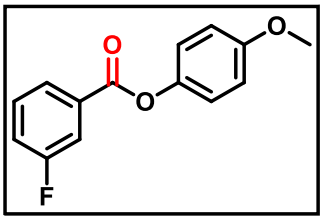

Prepared according to the general procedure (**B**) and (**C**), using 1-fluoro-3-((4-methoxyphenoxy)methyl)benzene to afford 2-methoxyphenyl-3-fluorobenzoate **69i** (Batch: 68.0 mg, 55%; TON = 226.4; TOF = 9.4 h^{-1}; Continuous flow: 49.0 mg, 40%) respectively as a white solid. ^{1}H NMR (400 MHz, $CDCl_3$) δ 7.99 (dt , *J* = 7.8 Hz and 1.2, 1H), 7.88 (m, 1H), 7.49 (td, *J* = 8.0 Hz and 5.5 Hz, 1H), 7.33 (m, 1.0 Hz, 1H), 7.13 (td, *J*= 10.4 Hz and 3.6Hz, 2H), 6.95 (td, *J*=10.4 Hz and 3.6 Hz, 2H), 3.83 (s, 3H). ^{13}C NMR (100 MHz, $CDCl_3$) δ 164.4 (d, *J* = 57.3 Hz), 161.6, 157.7, 144.5, 132.1 (d, *J* C-F = 7.5 Hz), 130.5 (d, *J* C-F = 7.7 Hz), 126.2 (d, *J* C-F = 3.1 Hz), 122.6, 120.9 (d, *J* C-F = 21.1 Hz), 117.3(d, *J* C-F = 23.06 Hz), 117.2, 114.9, 55.9. IR (neat): 2961, 2923, 1731, 1497, 1442, 1270, 1194, 805, 746 cm^{-1}. HRMS (ESI-TOF) m/z: $[M + H]^+$ calcd for $C_{14}H_{11}FO_3$: 247.0770; found: 247.0770.

3-bromophenyl-3-fluorobenzoate **(69j):**

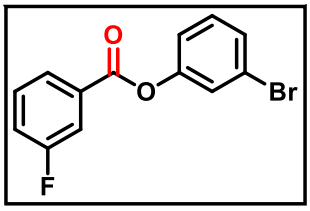

Prepared according to the general procedure (**B**) and (**C**), using 1-bromo-3-((3-fluorobenzyl)oxy)benzene to afford 3-bromophenyl-3-fluorobenzoate **69j** (Batch: 93.0 mg, 63%; TON = 260.1; TOF = 10.8 h^{-1}; Continuous flow: 27.0 mg, 19%) respectively as a white solid. ^{1}H NMR (400 MHz, $CDCl_3$) δ 7.98 (d, *J* = 6.9 Hz, 1H), 7.86 (dt, *J* = 9.2 Hz and 2.4 Hz, 1H), 7.50 (m, 1H), 7.43 (m, 2H), 7.34 (m, 2H), 7.18 (m, 1H). ^{13}C NMR (100 MHz, $CDCl_3$) δ 163.9 (d, *J* C-F = 29.9 Hz), 161.5, 151.3, 131.3 (d, *J* C-F = 7.5 Hz), 130.7, 130.5 (d, *J* C-F = 7.7 Hz), 129.4, 126.1 (d, *J* C-F = 3.1 Hz), 125.3, 122.6, 121.1 (d, *J* C-F = 11.1 Hz), 120.6, 117.2 (d, *J* C-F = 23.1 Hz). IR (neat): 2930, 1741, 1268, 1191, 749 cm^{-1}. HRMS (ESI-TOF) m/z: $[M + H]^+$ calcd for $C_{13}H_8BrFO_2$: 294.9770; found: 294.9772.

propyl benzoate **(69k):**[68]

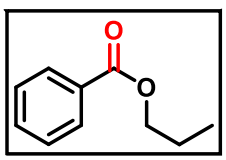

Prepared according to the general procedure (**B**) and (**C**), using (propoxymethyl)benzene to afford propyl benzoate **69k** (Batch: 69.0 mg, 85%; TON = 344.5; TOF = 14.4 h^{-1}; Continuous flow: 49.0 mg, 30%) respectively as a colorless liquid. ^{1}H NMR (400 MHz, $CDCl_3$) δ 8.05 (dd, *J* = 8.08 Hz and 1.08 Hz, 2H), 7.54(t, *J* = 7.8Hz,1H), 7.43 (t, *J* = 7.84 Hz, 2H), 4.28 (t, *J* = 6.64 Hz, 2H), 1.79 (m, 2H), 1.03 (t, *J* = 7.44 Hz,

3H). ^{13}C NMR (100 MHz, $CDCl_3$) δ 166.8, 133.0, 130.6, 129.6, 128.3, 66.6, 22.2, 10.6. IR (neat): 2965, 1718, 1270, 1108, 755 cm^{-1}. HRMS (ESI-TOF) m/z: $[M + Na]^+$ calcd for $C_{10}H_{12}O_2Na$: 187.0734; found: 187.0740.

butyl benzoate **(69l):**[68]

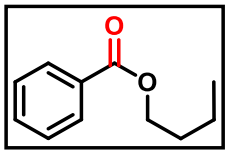

Prepared according to the general procedure (**B**) and (**C**), using (butoxymethyl)benzene to afford butyl benzoate **69l** (Batch: 75.0 mg, 84%; TON = 350.3; TOF = 14.6 h^{-1}; Continuous flow: 56.0 mg,32%) respectively as a colorless liquid. ^{1}H NMR (400 MHz, $CDCl_3$) δ 8.0 (m, 2H), 7.54(t, *J* = 8.0 Hz,1H), 7.43 (t, *J* = 8.0 Hz, 2H), 4.32 (t, *J* = 8.0 Hz, 2H), 1.75 (m, 2H), 1.48 (m, 2H), 0.98 (t, *J* = 8.0 Hz, 3H). ^{13}C NMR (100 MHz, $CDCl_3$) δ 166.8, 132.9, 130.7, 129.6, 128.4, 64.8, 30.9, 19.4, 13.7. IR (neat): 2958, 1719, 1272, 1109, 710 cm^{-1}. HRMS (ESI-TOF) m/z: $[M + H]^+$ calcd for $C_{11}H_{14}O_2$: 179.1072; found: 179.1070.

hexyl benzoate **(69m):**[69]

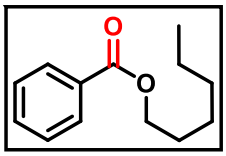

Prepared according to the general procedure (**B**) and (**C**), using ((hexyloxy)methyl)benzene to afford hexyl benzoate **69m** (Batch: 94.0 mg, 91%; TON = 374.2; TOF = 15.6 h^{-1}; Continuous flow: 63.0 mg, 31%) respectively as a colorless liquid. ^{1}H NMR (400 MHz, $CDCl_3$) δ 8.04 (m, 2H), 7.54 (m,1H), 7.43 (m, 2H), 4.3 (t, *J* = 6.92 Hz, 2H), 1.76 (m, 2H), 1.44 (m, 2H), 1.33 (m, 4H), 0.90 (t, *J* = 7.2 Hz, 3H). ^{13}C NMR (100 MHz, $CDCl_3$) δ 167.3, 133.2, 130.9, 130.1, 128.8, 65.6, 32.1, 29.2, 26.2, 23.0, 14.5. IR (neat): 2928, 1720, 1268, 1108, 709 cm^{-1}. HRMS (ESI-TOF) m/z: $[M + Na]^+$ calcd for $C_{13}H_{18}O_2Na$: 229.1204; found: 229.1202.

octyl benzoate **(69n):**[70]

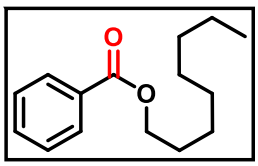

Prepared according to the general procedure (**B**) and (**C**), using ((octyloxy)methyl)benzene to afford octyl benzoate **69n** (Batch: 108.0 mg, 93%; TON = 378.2; TOF = 15.7 h^{-1}; Continuous flow: 114.0 mg, 49%) respectively as a colorless liquid. ^{1}H NMR (400 MHz, $CDCl_3$) δ 8.05 (m, 2H), 7.55 (t, *J* = 6.76 Hz and 1.36 Hz, 1H), 7.44 (m, 2H), 4.31 (t, *J* = 6.68 Hz, 2H), 1.76 (m, 2H), 1.44 (m, 2H), 1.28 (m, 8H), 0.88 (t, *J* =7.04 Hz, 3H). ^{13}C NMR (100 MHz, $CDCl_3$) δ 166.8, 132.9, 130.7, 129.6, 128.4, 64.8, 30.9, 19.4, 13.7. IR (neat): 2925, 1720, 1268, 1108, 708 cm^{-1}. HRMS (ESI-TOF) m/z: $[M + Na]^+$ calcd

for $C_{15}H_{22}O_2Na$: 257.1517; found: 257.1519.

2.10.B. Copies of ^{1}H and ^{13}C NMR spectra of representative compounds

Entry	Figure No	Data	Page No
66a	2.10.B.1-2.10.B.2	^{1}H and ^{13}C	66
66b	2.10.B.3-2.10.B.4	^{1}H and ^{13}C	67
66g	2.10.B.5-2.10.B.6	^{1}H and ^{13}C	68
66h	2.10.B.7-2.10.B.8	^{1}H and ^{13}C	69
69a	2.10.B.9-2.10.B.10	^{1}H and ^{13}C	70
69b	2.10.B.11-2.10.B.12	^{1}H and ^{13}C	71
69i	2.10.B.13-2.10.B.14	^{1}H and ^{13}C	72
69n	2.10.B.15-2.10.B.16	^{1}H and ^{13}C	73

acetophenone (66a):

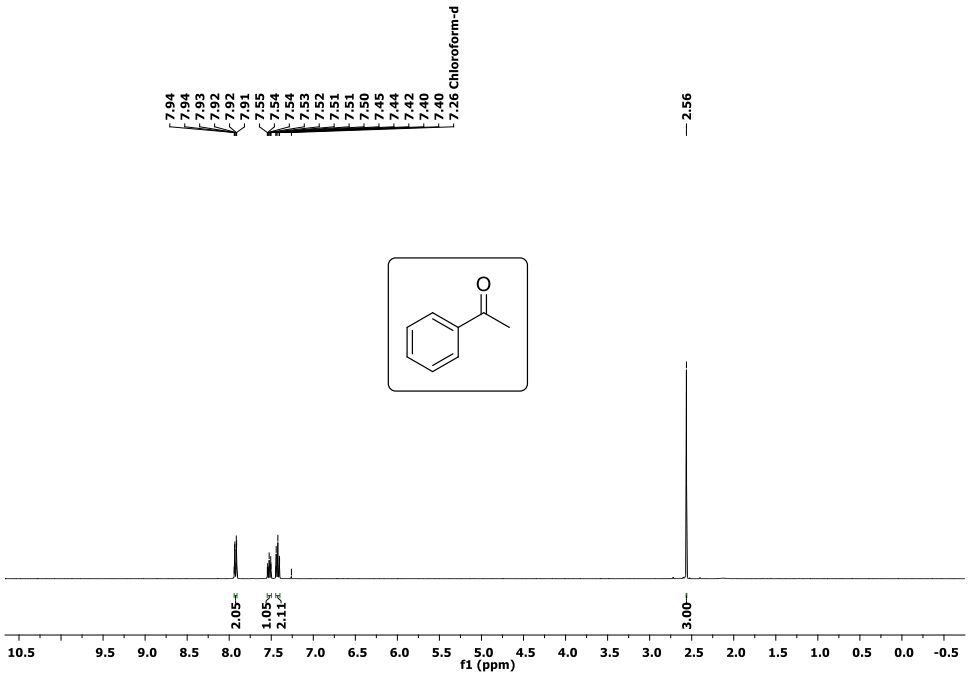

Figure 2.10.B.1: ^{1}H NMR of **66a**, 400 MHz, $CDCl_3$

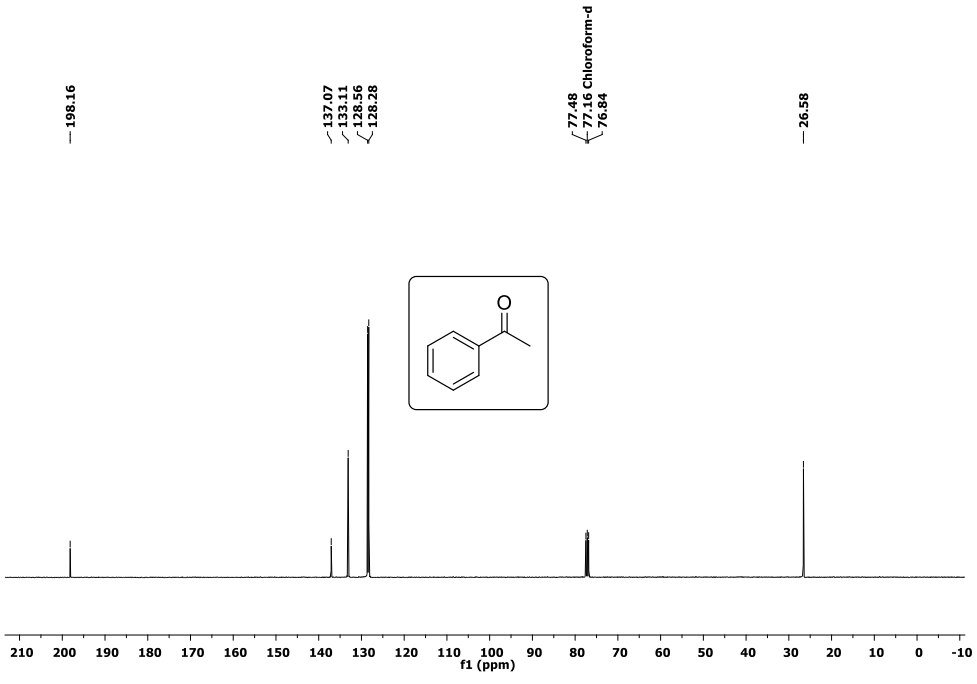

Figure 2.10.B.2: ^{13}C NMR of **66a**, 100 MHz, $CDCl_3$

9*H*-xanthen-9-one (66b):

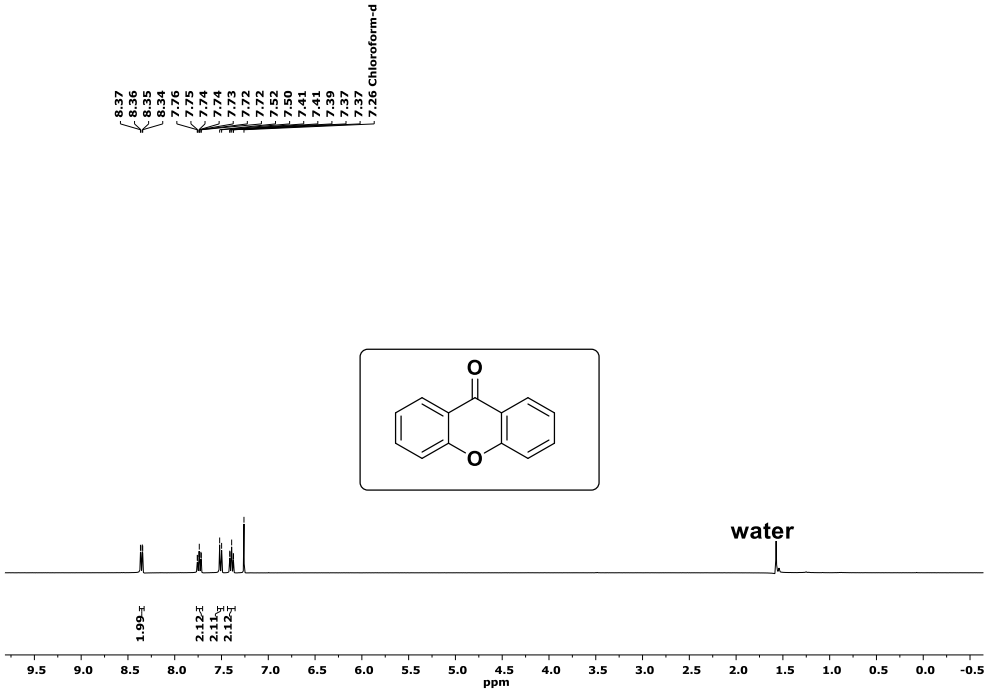

Figure 2.10.B.3: ^{1}H NMR of **66b**, 400 MHz, $CDCl_3$

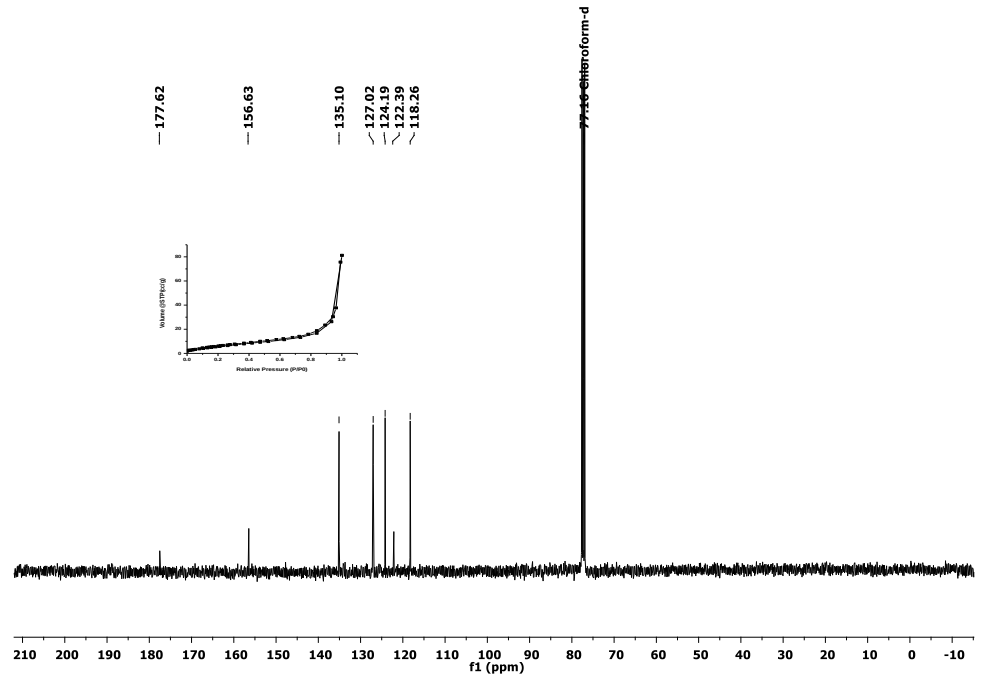

Figure 2.10.B.4: ^{13}C NMR of **66b**, 100 MHz, $CDCl_3$

1-(naphthalen-2-yl)ethan-1-one (66g):

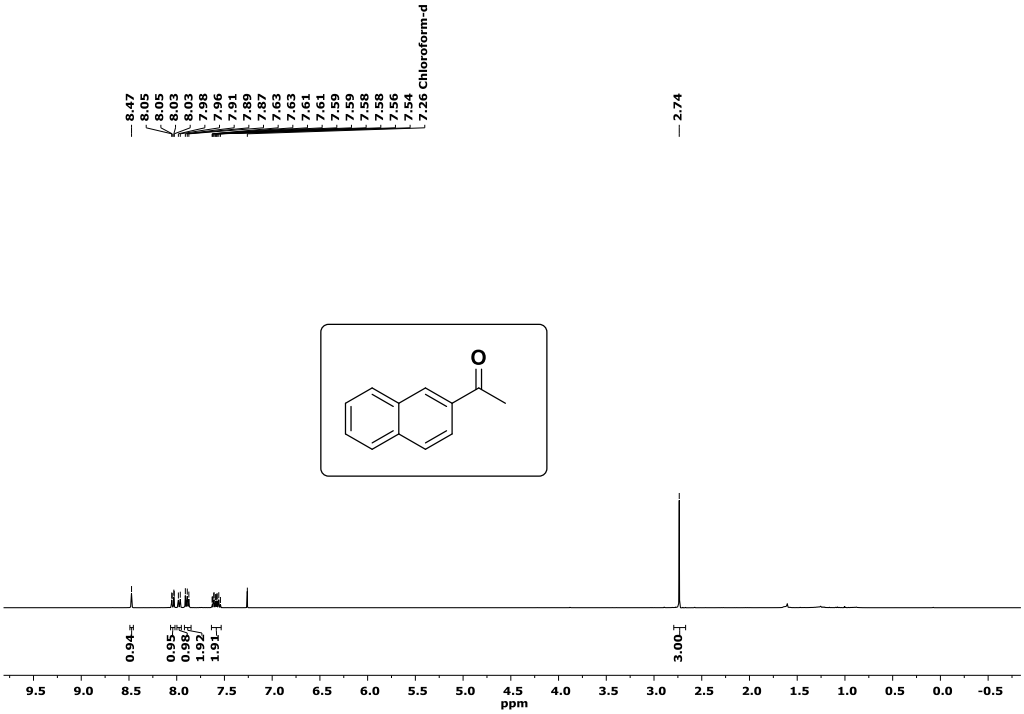

Figure 2.10.B.5: ^{1}H NMR of **66g**, 400 MHz, $CDCl_3$

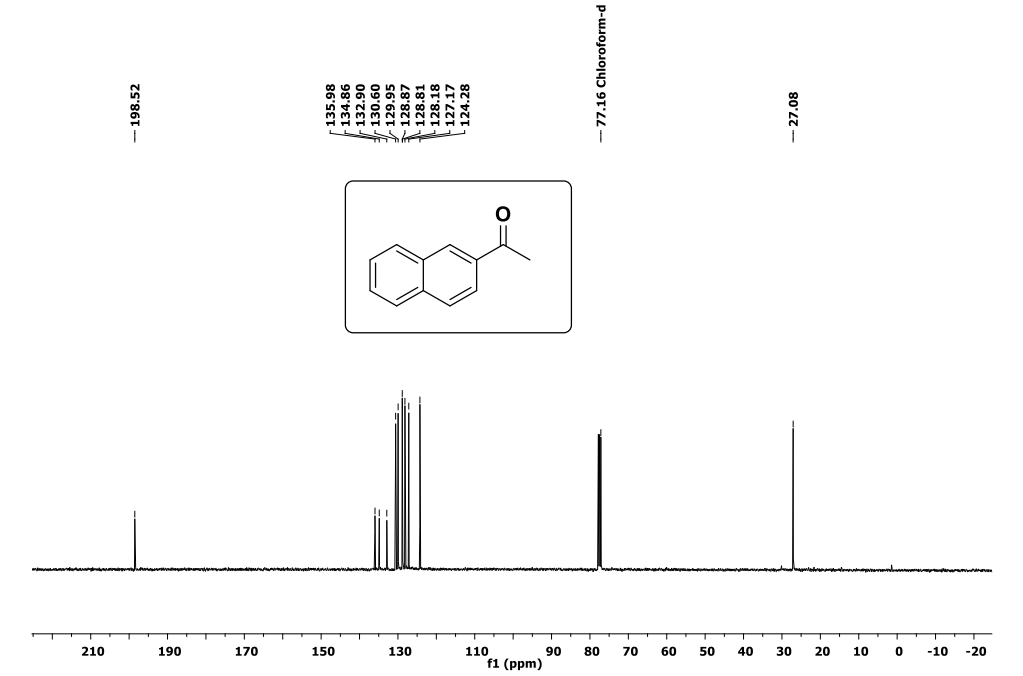

Figure 2.10.B.6: ^{13}C NMR of **66g**, 100 MHz, $CDCl_3$

1-(4-bromophenyl)ethan-1-one (66h):

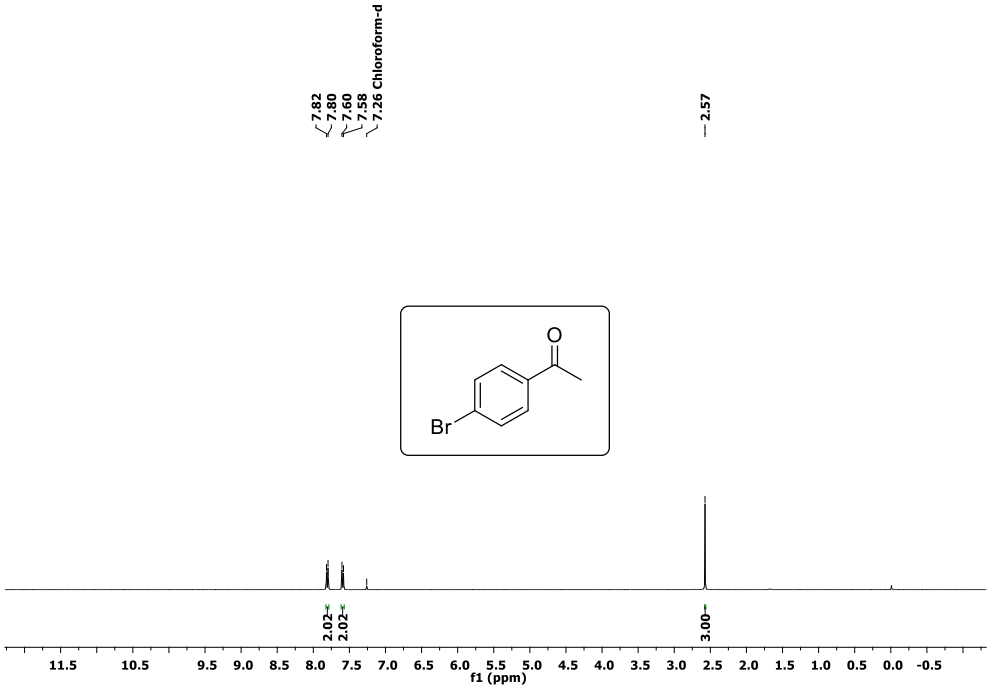

Figure 2.10.B.7: ^{1}H NMR of **66h**, 400 MHz, $CDCl_3$

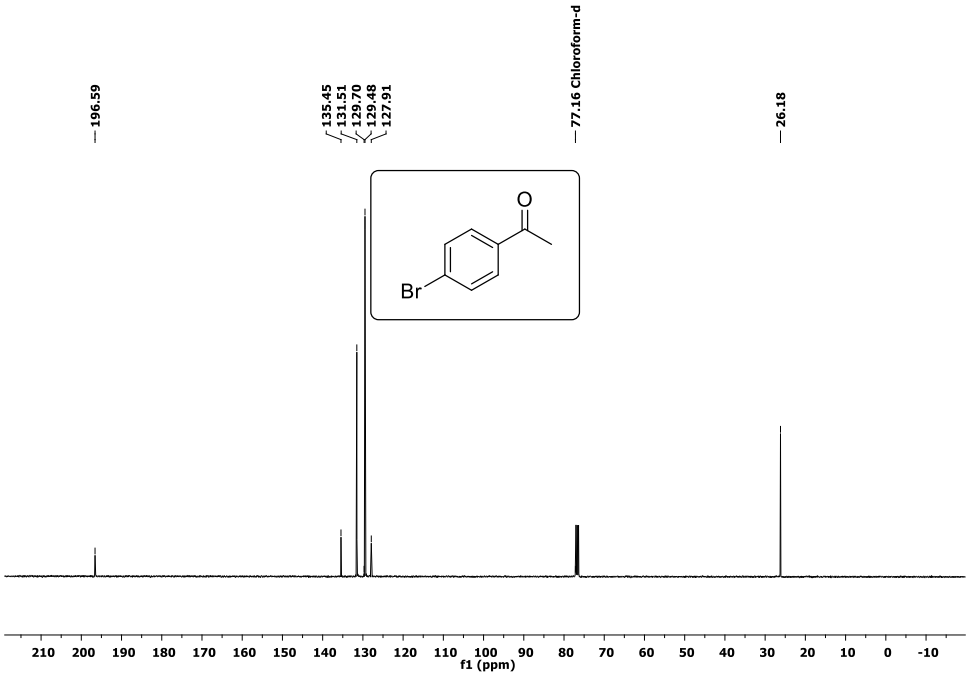

Figure 2.10.B.8: ^{13}C NMR of **66h**, 100 MHz, $CDCl_3$

phenyl benzoate (69a):

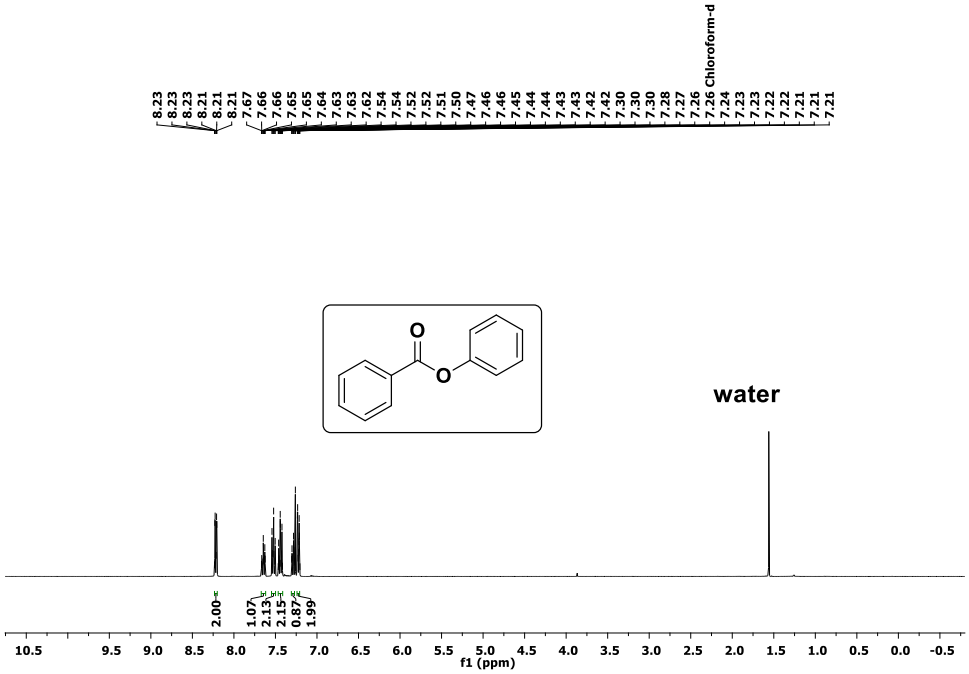

Figure 2.10.B.9: ^{1}H NMR of **69a**, 400 MHz, $CDCl_3$

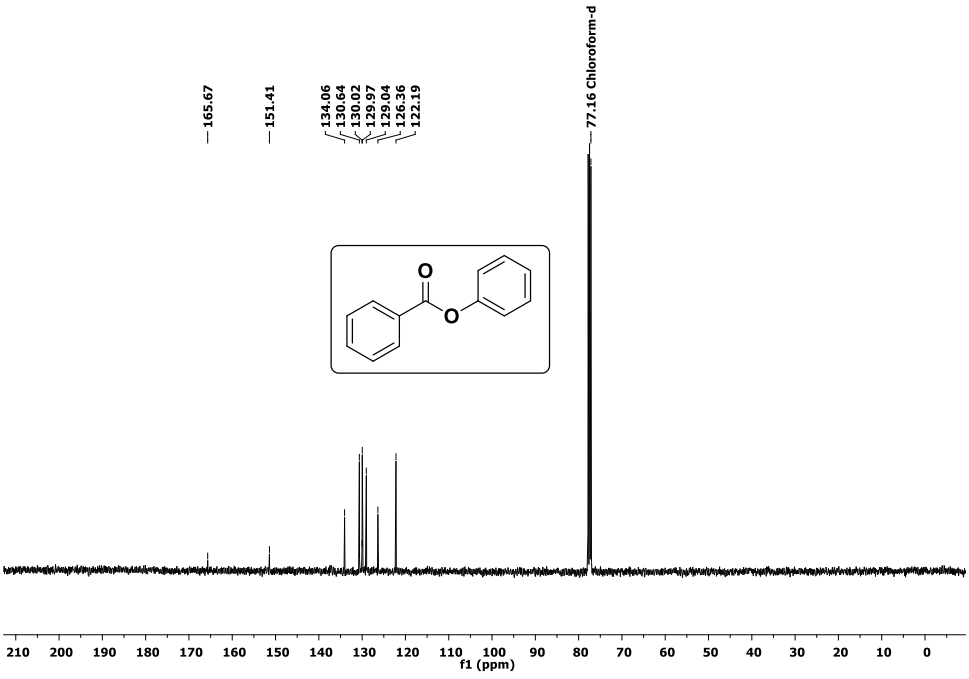

Figure 2.10.B.10: ^{13}C NMR of **69a**, 100 MHz, $CDCl_3$

phenyl-4-methylbenzoate (69b):

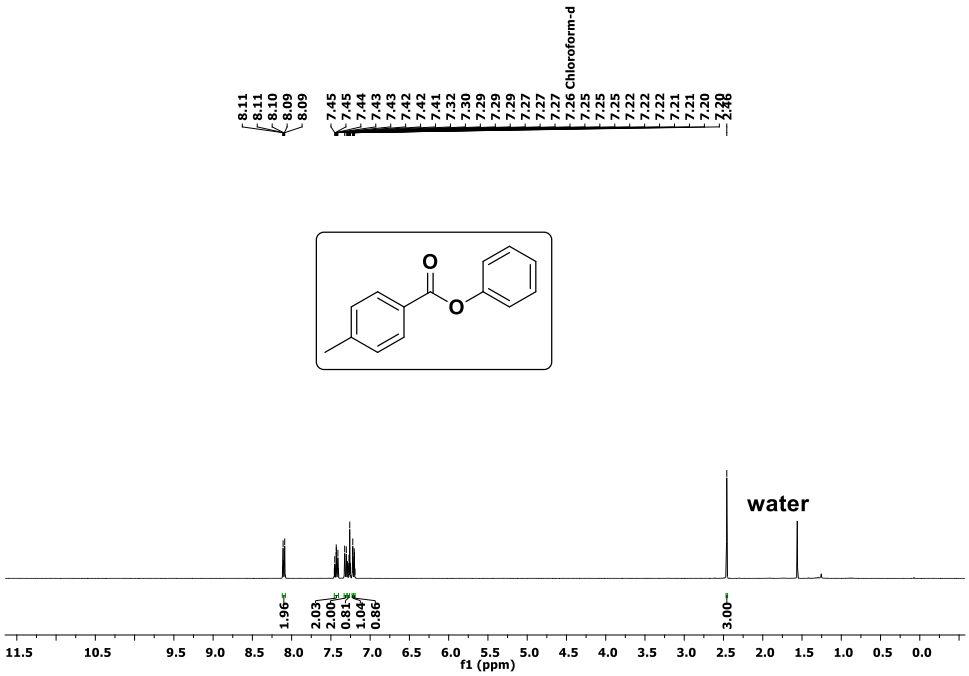

Figure 2.10.B.11: ^{1}H NMR of **69b**, 400 MHz, $CDCl_3$

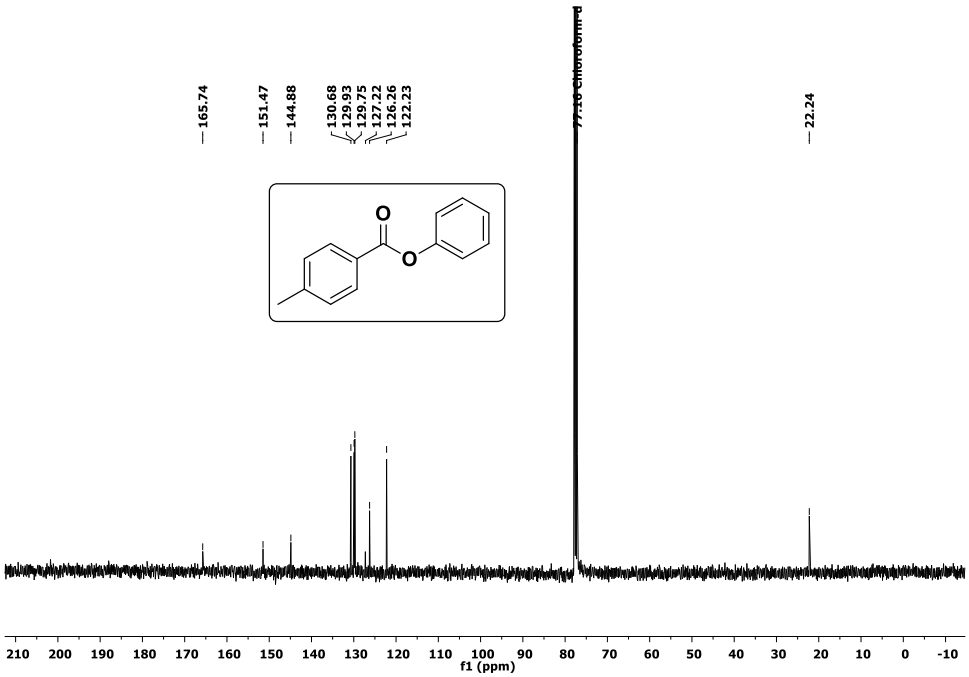

Figure 2.10.B.12: ^{13}C NMR of **69b**, 100 MHz, $CDCl_3$

4-methoxyphenyl-3-fluorobenzoate (69i):

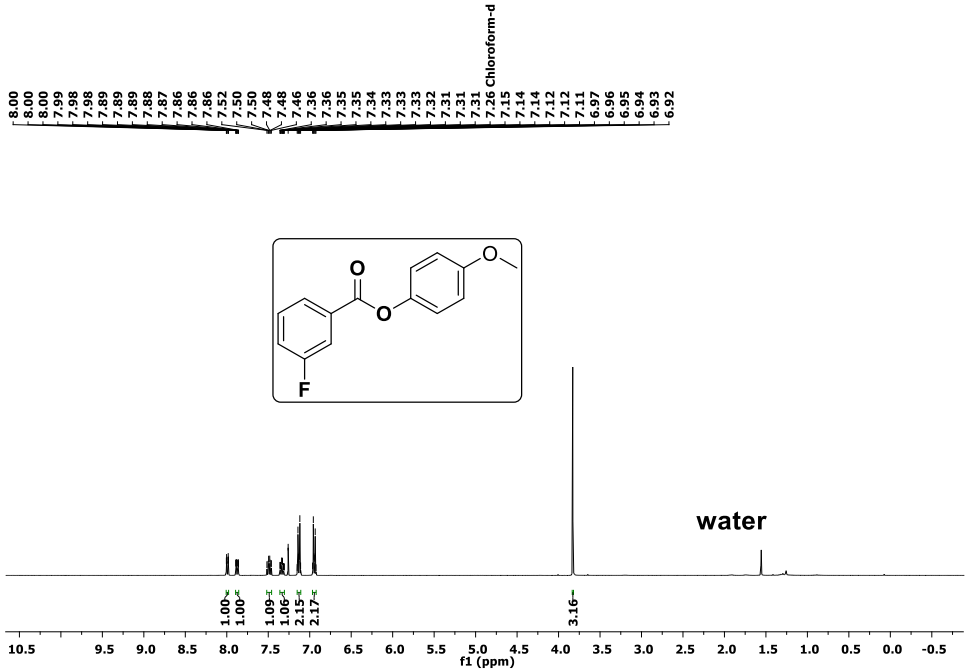

Figure 2.10.B.13: ^{1}H NMR of **69i**, 400 MHz, $CDCl_3$

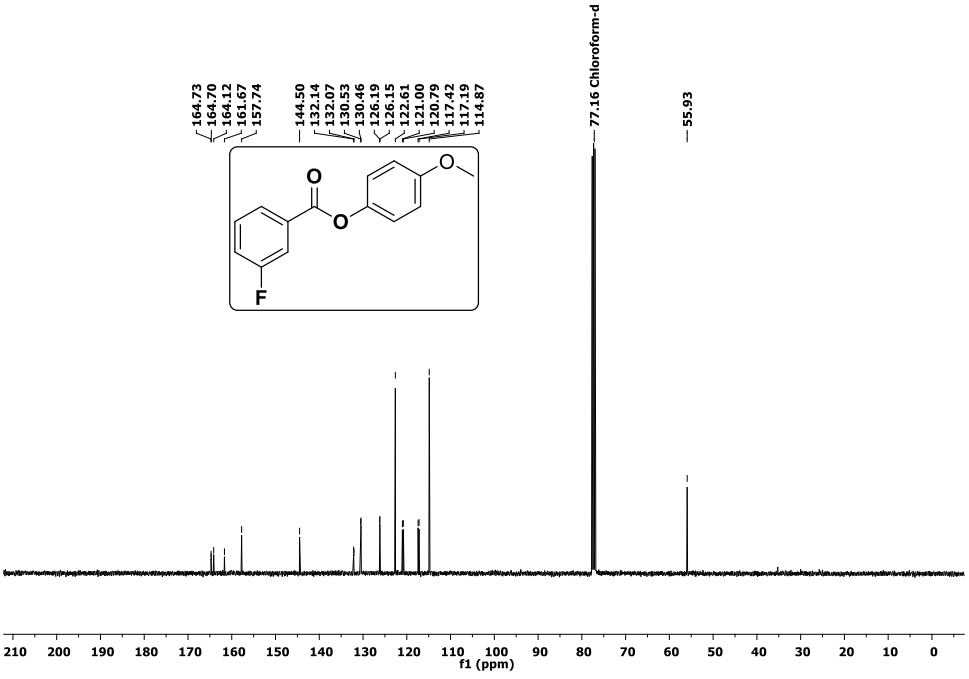

Figure 2.10.B.14: ^{13}C NMR of **69i**, 100 MHz, $CDCl_3$

octyl benzoate (69n):

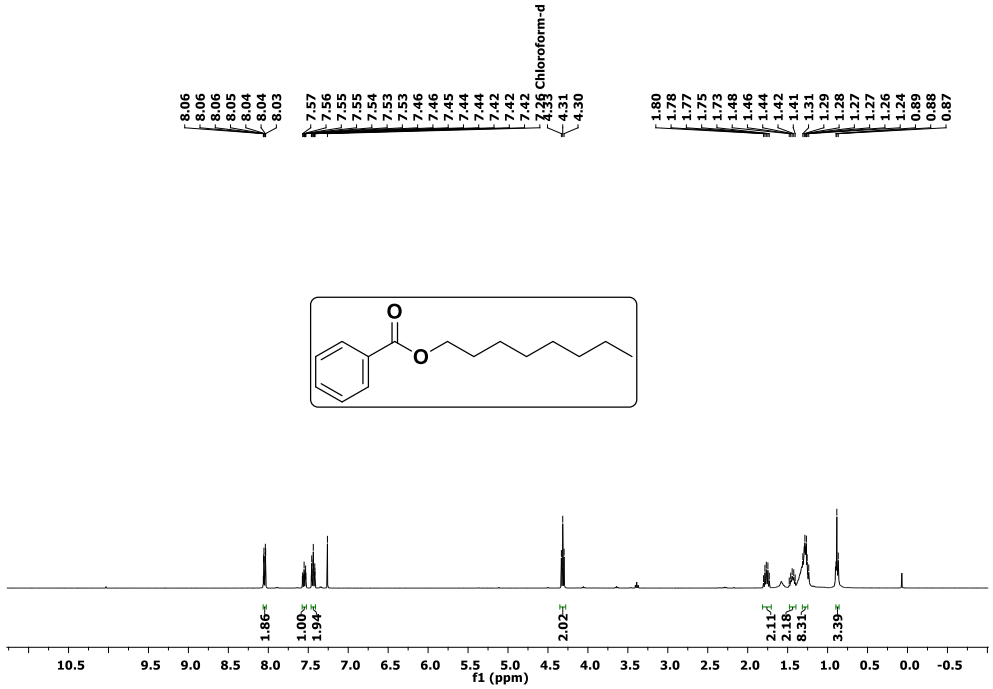

Figure 2.10.B.15: ^{1}H NMR of **69n**, 400 MHz, $CDCl_3$

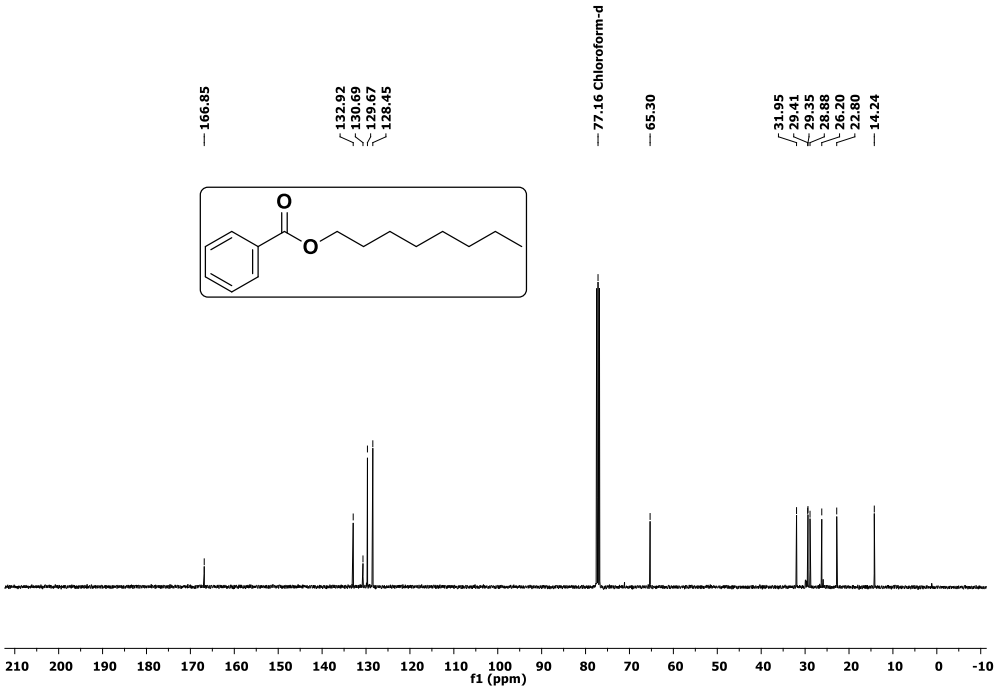

Figure 2.10.B.16: ^{13}C NMR of **69n**, 100 MHz, $CDCl_3$

2.11. List of works by other groups published after this work

(1) Nilforoushan, S.; Ghiaci, M.; Hosseini, S. M.; Laurent, S.; Muller, R. N. Selective liquid phase oxidation of ethyl benzene to acetophenone by palladium nanoparticles immobilized on a g-C_3N_4–rGO composite as a recyclable catalyst. *New J. Chem.* **2019**, 43, 6921-6931.

(2) Mohammadpour, P.; Safaei, E. Catalytic C-H aerobic and oxidant-induced oxidation of alkylbenzenes (including toluene derivatives) over VO^{2+} immobilized on core-shell Fe_3O_4@SiO_2 at room temperature in water. *RSC Adv.* **2020**, *10*, 23543-23553.

(3) Mittal, R.; Awasthi, S. K. Metal-Organic Framework-Derived Mn_3O_4/Co_3O_4/C/SiO_2 Nanostructures for Catalytic Oxidation Reactions. *ACS Appl. Nano Mater.* **2022**, *5*, *6*, 7831-7840.

Chapter III: Continuous Flow Direct Azidation of Alcohols and Peroxides towards the Synthesis of Heterocycles

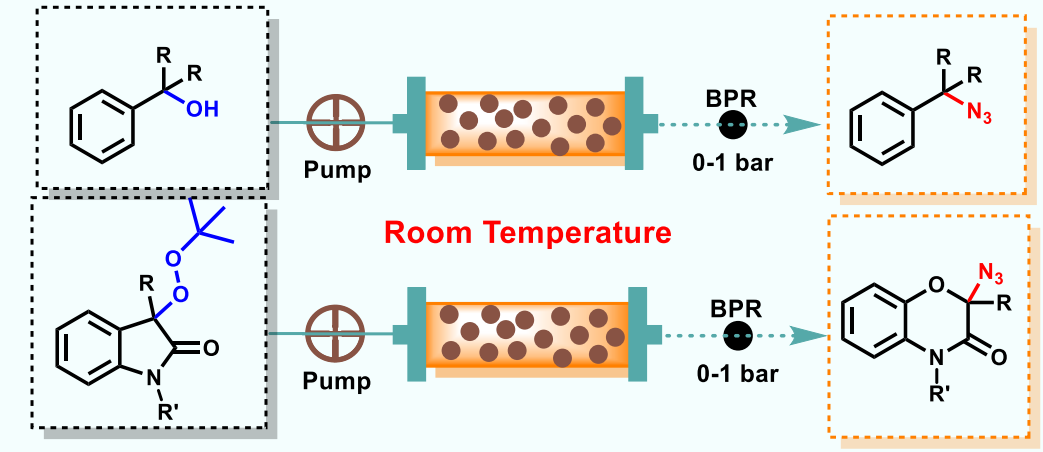

Application: Click reaction, Staudinger reduction, Thermal skeletal rearrangement in flow

Continuous Flow Direct Azidation of Alcohols and Peroxides towards the Synthesis of Heterocycles

3.1. Introduction to azidation

Heterocyclic compounds containing nitrogen have shown to be quite valuable for therapeutic applications. For instance, organic azides or hydrazides generate many 1,2,3- or 1,2-nitrogen enriched heterocycles via click reactions or condensation chemistry. Additionally, it has been used in chemical biology, material science, and medicine development. Other heterocycles such as 2*H*-1,4-benzoxazin-3(4*H*)-one and quinoxalin-2(1*H*)-ones have also shown application in medicinal chemistry (Figure 3.1.1).[72]

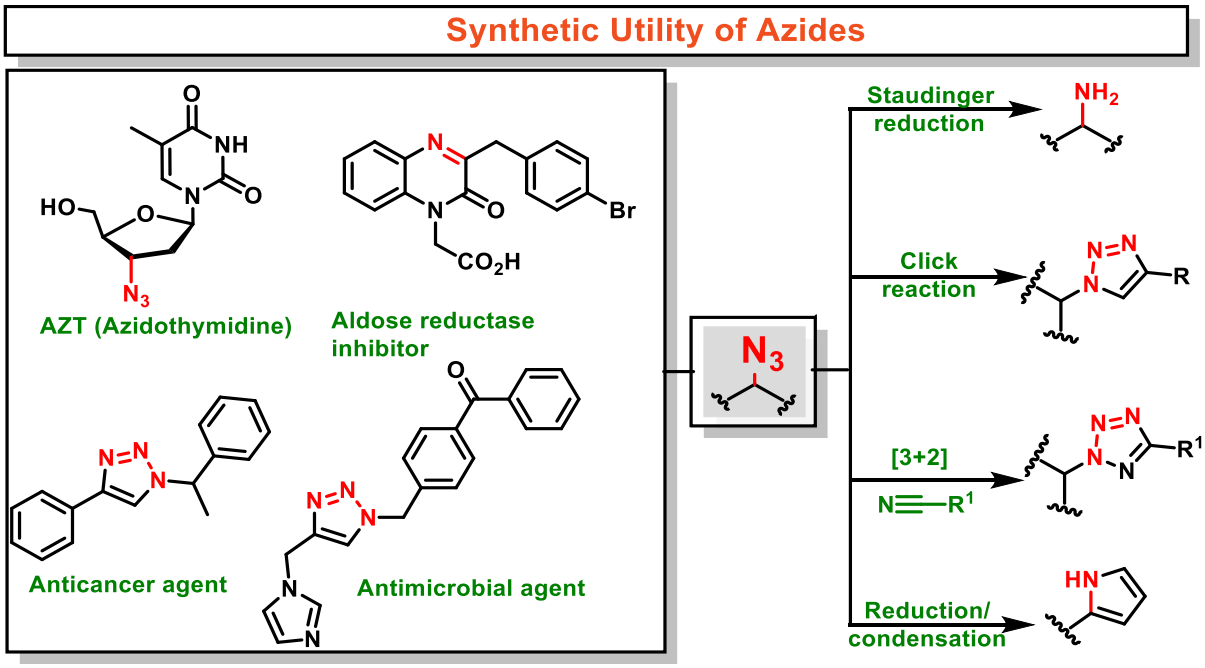

Figure 3.1.1: The synthetic utility of azides

Moreover, recent years have seen an astonishing library of potent named reactions using azides as an indispensable tool for several chemical processes (Figure 3.1.1).[73,74] The bioconjugation of

proteins uses these energy-rich intermediates as building blocks.[75] These are also known as efficient ammonia surrogates[76] and easily transformed to *N*-heterocycles[77-78] (Figure 3.1.1). In addition, organic azides were employed for the construction of tetrazole moiety by [3+2] cycloaddition with nitriles. Moreover, these organic azides generate essential bioactive compounds such as anticancer, antibacterial medicines, and aldose reductase inhibitors (Figure 3.1.1).[79-82] Although these azides have many uses, their explosive behavior in large-scale production raises serious safety issues. Azides with C/N ≥ 3 are generally stable to handle (Table 3.1.1).[83] Thus, the safety risk in azide synthesis and the relevant linked chemical transformation demands safer process technology.

Table 3.1.1: Maximum storage capacity of azides

C/N ratio	Maximum storage capacity
3	Up to 20 gm (Pure form)
1-3	Up to 5 gm (1 M or less concentrated solution)
<1	Up to 1 gm (intermediate)

Moreover, the traditional batch procedures for the synthesis alkyl azide **72** require two stages: (i) conversion to a good leaving group; (ii) substitution reaction with NaN_3. After the -OH group is activated, it can be converted into genotoxic alkyl halides,[84] sulfonates,[85] or acetates,[86] which reacts with NaN_3 to produce azides **72** (Scheme 3.1.1). It can also be obtained by utilizing other precursors such as amines, hydrazines, etc.[76,83] However, the laborious workup and safety issues in the scale-up of the reaction make the process quite challenging. Therefore, the ideal strategy to reduce the number of synthetic processes and eliminate waste formation is to design a direct azidation method from alcohol **70**.

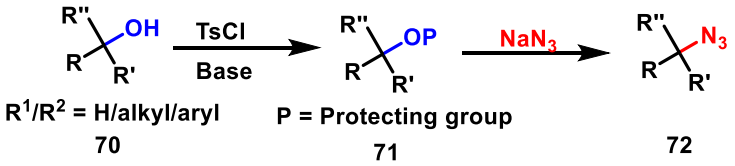

Scheme 3.1.1: Traditional approach for azidation of alcohols

The Mitsunobu reaction, which utilizes hydrazoic acid to produce azides **72**, demonstrates the direct substitution of the hydroxyl group.[87] In light of potential safety issues related to sodium azide and hydrazoic acid, $TMSN_3$ was an economically viable, and safe azide source to examine new methodologies. To perform this chemical reaction, several Lewis acid catalysts such as $BF_3{\cdot}OEt_2$,[88] $NaAuCl_4$,[88] $Cu(OTf)_2$,[89] AgOTf,[90] $FeCl_3$,[91] $MoCl_5$,[92] $InBr_3$,[93] and $Bi(OTf)_3$,[94] which promotes the substitution by the direct activation of the alcohols **70** has been exploited. However, compared to Lewis acid-mediated azidation reactions, fewer methods have been developed utilizing a Brønsted acid catalyst. Sodium azide and acidic ionic liquid [H-NMP]HSO_4 were used by Hajipour in this reaction.[95] Whereas Onaka used montmorillonite clay and a mixture of TMSCl and $TMSN_3$ to produce azides.[96] Similarly, Rode achieved it by using a solid povidone and phosphotungstic acid hybrid as a heterogeneous catalyst for direct azidation of alcohols **70**.[97] More recently, Zhou and Regier demonstrated it with aqueous perchloric acid[98] and $HBF_4{\cdot}OEt_2$,[99] respectively (Scheme 3.1.2).

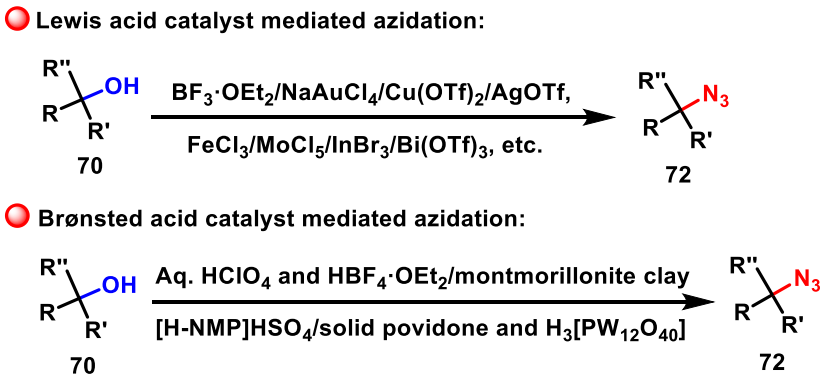

Scheme 3.1.2: Traditional approach of azidation of alcohols

On the other hand, the continuous flow has emerged as a green tool with improved heat and mass transfer, precise residence time control, faster process times, enhanced safety, reproducibility, better product quality, and easy scale-up. Therefore, the continuous flow has gained much attention in academia and industry.[100] The potential of continuous flow azidation has been investigated further by using imidazole-1-sulfonyl azide hydrochloride as a diazotransfer reagent for benzyl amine **73** to azide transfer reaction.[101] However, Baumann and coworkers developed a telescoped process to obtain propargyl amine from propargyl alcohol **75.** In this process, DPPA was used as

an azidation source to produce azide **76** which after reduction gives an amine product (Figure 3.1.1).[102] Furthermore, an essential step in the entire synthesis of oxomaritidine was azidation of **77** with azide exchange resin to give **78**.[103] Whereas aqueous sodium azide has been utilized as azidation source for C-3 azidation of mesyl shikimate **79** (Scheme 3.1.3).[104] All the developed continuous flow method requires heating conditions, and high pressure with difficulty in scale-up process.

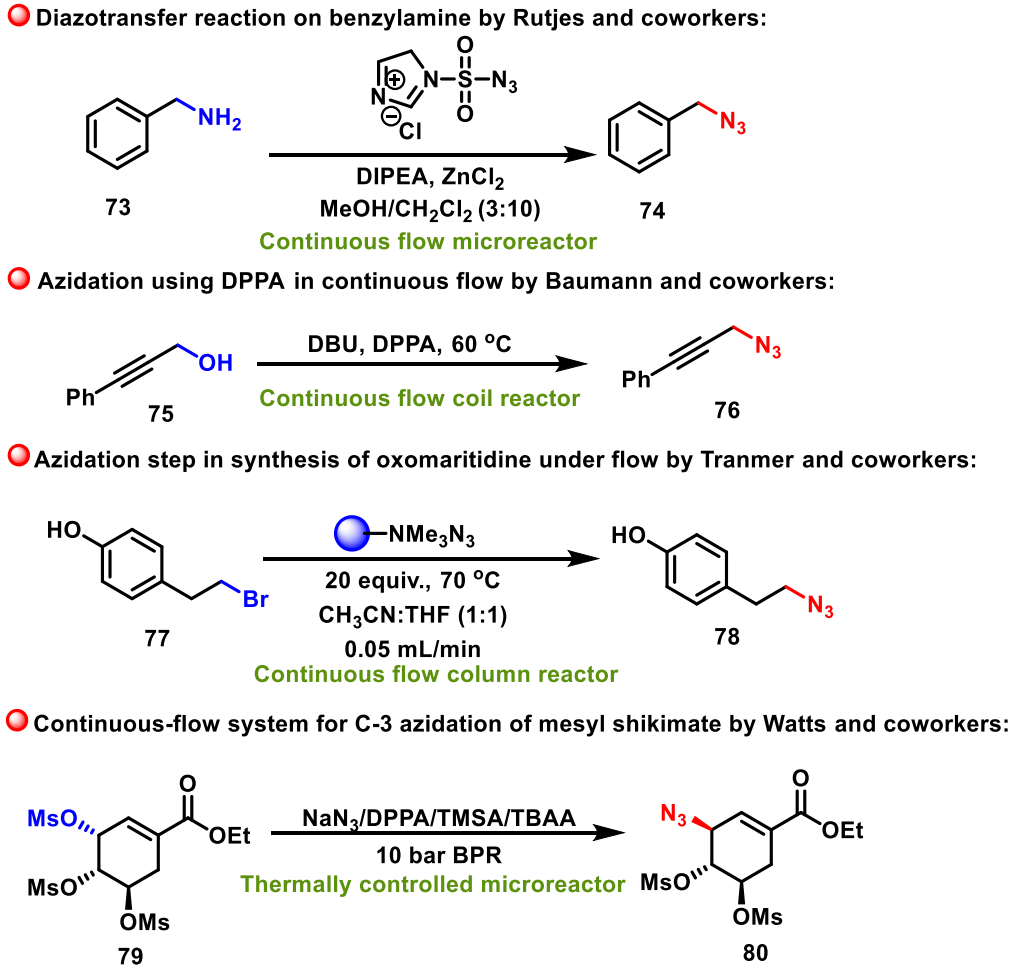

Scheme 3.1.3: Literature precedents of azidation under continuous flow

3.2. The rationale of the present work

Azides are usually explosive and high-energy molecules that decompose with heat, light, and shock. However, it has been widely used as an organic building blocks for the construction of

various heterocyclic scaffolds. Therefore, it becomes important to study azidation reaction. In literature, direct azidation of alcohols to azides by using homogeneous or heterogeneous Lewis or Brønsted acid catalyst have been reported under batch conditions. Whereas employing azidation under batch condition may led to a runaway reaction during scale up process. Therefore, the direct azidation of alcohols necessitates safer process development. Hence, introducing continuous flow can be advantageous to minimize the safety hazards associated with this process. Moreover, the continuous flow protocol would enable and streamline the assembly and delivery of these entities by mitigating any safety concerns associated with it. Therefore, we proposed the continuous-flow direct azidation of different alcohols and peroxides in the presence of Amberlyst®-15 as a catalyst. In order to make it simple to recover catalysts by conducting the reaction at room temperature, we envisioned a safe scale up approach for the azidation without using specially designed catalysts. In the case of peroxides, a sequential skeletal rearrangement has been reported by our group previously. By keeping this concept in mind, we envisioned to execute the skeletal rearrangement of azides followed by azidation to develop azide substituted 2*H*-1,4-benzoxazin-3(4*H*)-one derivative. We also sought to investigate its application in continuous flow Staudinger reduction, [3+2] cycloaddition, and rearrangement reactions.

3.3. Results and discussion

Initially, diphenylmethanol and azidotrimethylsilane was taken as a model substrate to study the direct azidation of alcohols in batch condition. A control experiment was conducted without a catalyst at room temperature and 60 ^{o}C resulted in no product formation (Table 3.3.1, entries 1,2). Next, to achieve (azidomethylene)dibenzene **83a**, we used homogeneous and heterogeneous Lewis and Brønsted acid catalysts. With 5 mol% $In(OTf)_3$ at room temperature for 12 h produced 73% of product **83a**. Whereas azidation of **81a** with 5 mol% $Bi(NO_3)_3$ produced 95% yield of the desired product (Table 3.3.1, entries 3,4). However, when this reaction was examined using Amberlyst®-15, a 98% yield of **83a** was obtained (Table 3.3.1, entry 5). The Amberlyst®-15 is a metal free polymeric resin that serves as an excellent acid source and can be recovered and reused several times. When 1:1 equivalent and 1:2 equivalent of **81a:82** were employed at rt with Amberlyst®-15 (w/w with respect to **81a)**, it provided 69% and 50% yield of **83a,** respectively (Table 3.3.1, entries 6,7). Furthermore, when three equivalents of $TMSN_3$ were employed, this

reaction produced 98% of **83a** in 30 minutes (Table 3.3.1, entry 8). After establishing batch-optimized conditions, we investigated the efficacy of this approach for the other substrates. The wide range of substrate scope ensures the tolerance and reliability of the safer azidation process for differently substituted alcohols.

Table 3.3.1: Optimization of reaction conditions for the azidation of alcohols under batch

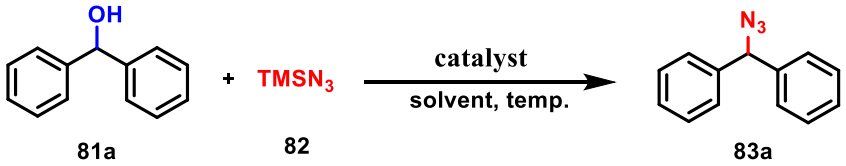

Entry	Equiv. (81a:82)	Catalyst	Temp. (ºC)	Yield (%)
1	1:3	-	rt	n.d.
2	1:3	-	60	n.d.
3[a]	1:3	$Bi(NO_3)_3$	rt	95
4[a]	1:3	$In(OTf)_3$	rt	73
5	1:3	Amberlyst®-15	rt	98
6	1:2	Amberlyst®-15	rt	69
7	1:1	Amberlyst®-15	rt	50
8[b]	1:3	Amberlyst®-15	rt	98

Reaction conditions: 81a (0.5 mmol), $TMSN_3$ (see table), Amberlyst®-15 (w/w with respect to **81a**), and DCM (2 mL) were stirred at room temperature for 12 h. [a]5 mol % catalyst is used. [b]30 min. The reported yields are isolated yields.

Thus, 50-99% yield of products **83a-p** was produced by the reaction of primary, secondary, and tertiary alcohols, with $TMSN_3$ (Scheme 3.3.1). This approach was tolerant to both electron-withdrawing groups and electron-donating groups, including alcohols in order to get the corresponding azide via direct nucleophilic substitution reaction. Furthermore, more sterically hindered tertiary alcohols were effectively azidated to generate **83f** and **83g** in 86% and 80% yield, respectively. All azides were characterized by spectroscopic analysis. The structure of **83g** was

validated further by X-ray structure (Scheme 3.3.1). Next, the azidation process was conducted smoothly on quaternary 3-hydroxy-2-oxindole derivatives delivered corresponding azides **83h-p** in high yields. The X-ray structure validated the structure of **83p** (Scheme 3.3.1).

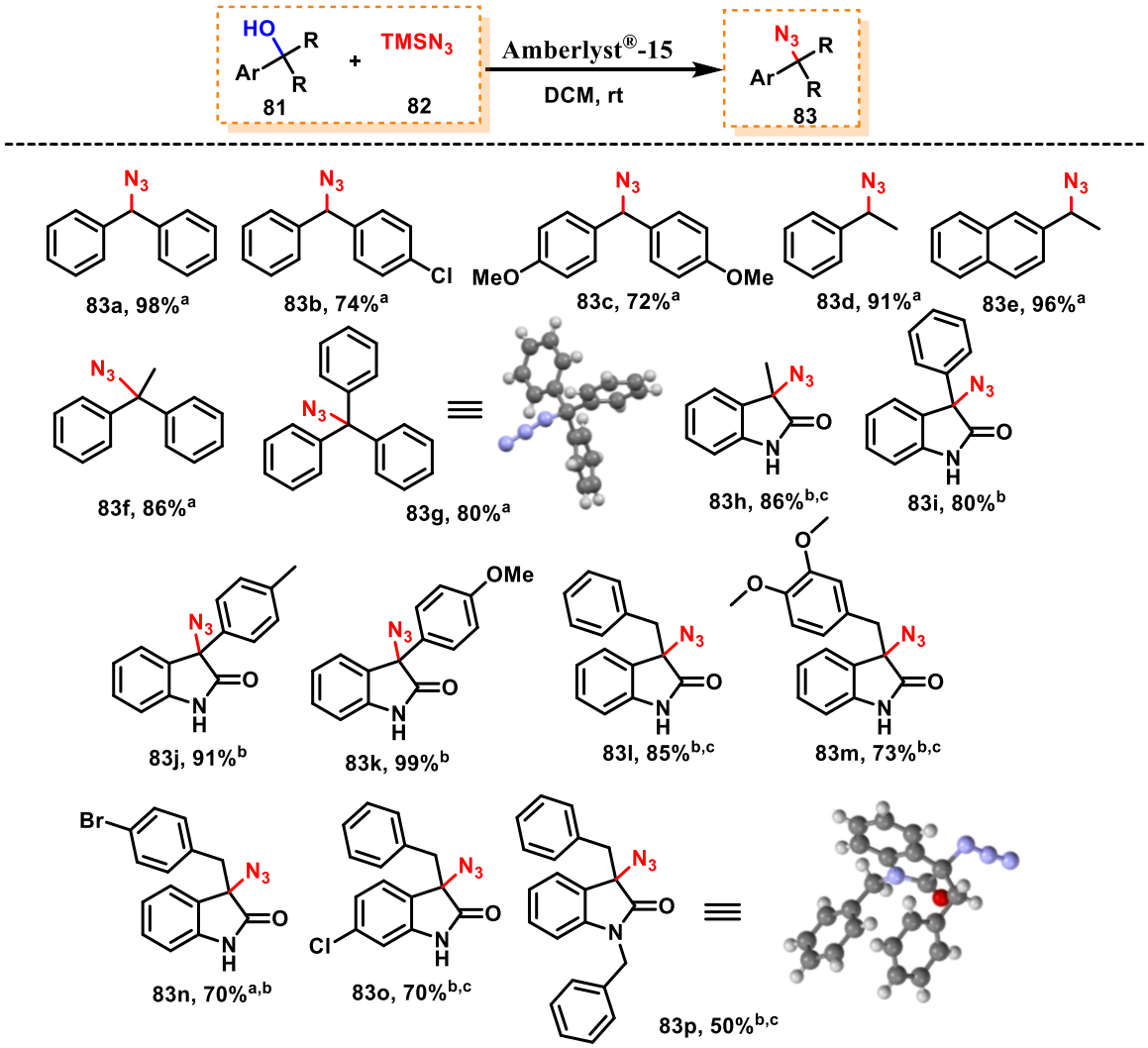

Reaction conditions: 81 (0.5 mmol), **82** (1.5 mmol), Amberlyst®-15 (w/w with respect to **81**), and DCM (2 mL) were stirred at rt for [a]30 min, [b]1 h, [c]80 °C in DCE; the reported yields were the isolated yields.

Scheme 3.3.1. Substrate scope for the azidation of alcohols under batch condition

To avoid the safety risks associated with batch reactions, we integrated this reaction under continuous flow to enable a faster and safer synthesis of different azide derivatives. We filled the

Amberlyst®-15 in the Omnifit column and connected it with the Vaportec R-series pump or Vaportec SF-10 pump to optimize the reaction conditions (Figure 3.3.1 and Table 3.3.2)

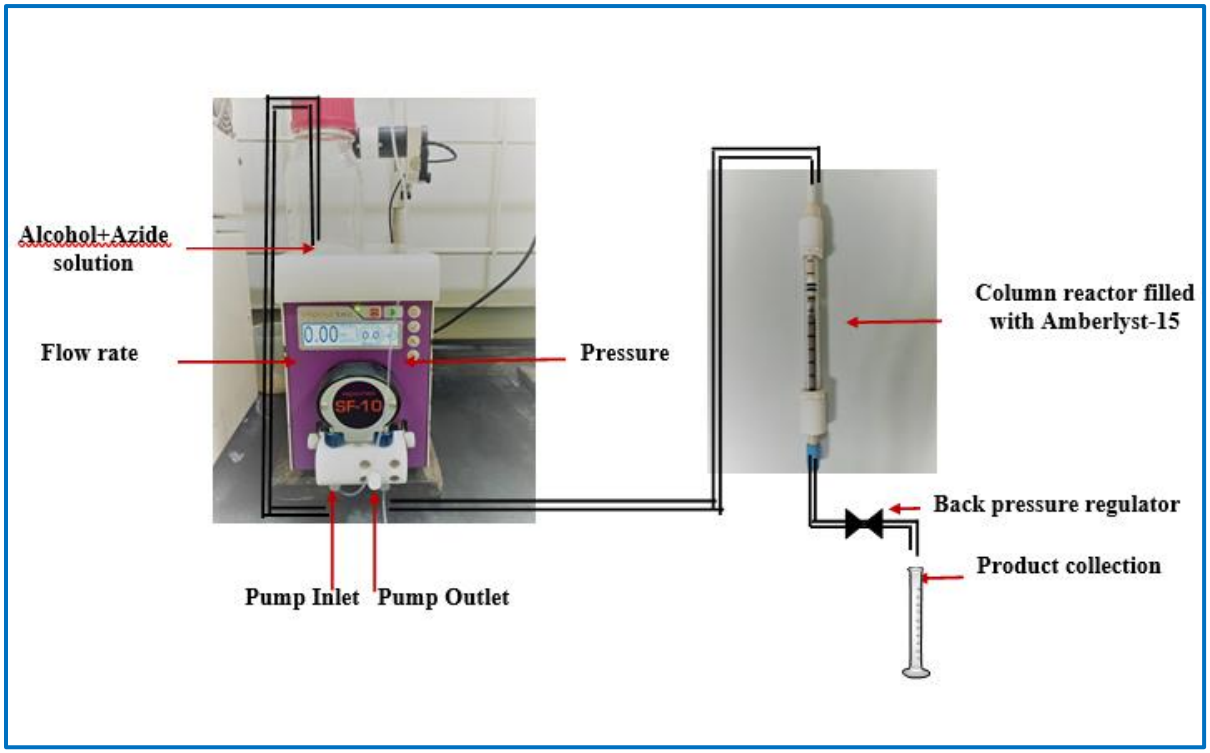

Figure 3.3.1: Setup for the azidation reaction using Vaportec SF-10 pump

To optimize the reaction conditions, several concentrations of azide and alcohol in DCM were flown through the Amberlyst®-15 at different flow rates. Initially, 0.025 M:0.075 M of **81a:82** in DCM solvent at room temperature was flown through the catalyst at a rate of 0.1 mL/min to afford 96% isolated yield of the product **83a** (Table 3.3.2, entry 1). A series of reaction conditions were conducted to test the influence of solvent, flow rate, and concentration, and the findings are reported in Table 3.3.2 (entries 2-11). The solvents such as EtOAc, acetone, THF, ACN, MeOH, and 1,4-dioxane failed to produce **83a** (Table 3.3.2, entries 2-7). As a result, DCM was proven to be the optimum solvent. Next, we optimized the flow rate. Lower yields of **83a** were reported at 0.3 mL and 0.5 mL flow rates of **81a** (Table 3.3.2, entries 8-9). Finally, this reaction was examined at different concentrations of **81a:82.** With a 0.1:0.3 M and 0.3:0.9 M concentration of **81a:82,** 98% and 90% of desired product **83a** were observed (Table 3.3.2, entries 10-11).

Table 3.3.2: Continuous-flow optimization of reaction conditions for the azidation of alcohols

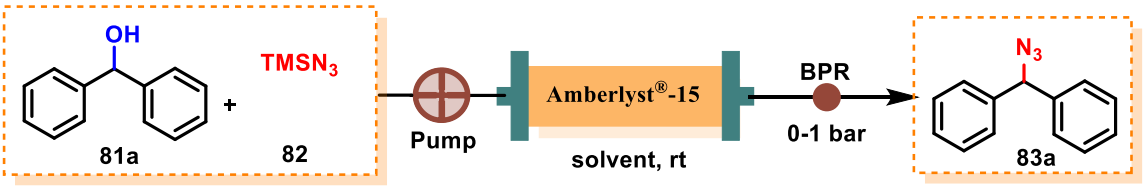

Entry	Substrate concentration (M) 81a:82	Flow rate (mL/min)	Solvent	t_R(min)/Number of runs	Yield of 83a (%)
1	0.025:0.075	0.1	DCM	21/1	96
2	0.025:0.075	0.1	EtOAc	21/1	n.d.
3	0.025:0.075	0.1	Acetone	21/1	traces
4	0.025:0.075	0.1	THF	21/1	n.d.
5	0.025:0.075	0.1	ACN	21/1	traces
6	0.025:0.075	0.1	MeOH	21/1	n.d.
7	0.025:0.075	0.1	1,4-Dioxane	21/1	n.d.
8	0.025:0.075	0.3	DCM	07/1	89
9	0.025:0.075	0.5	DCM	04/1	83
10	0.1:0.3	0.1	DCM	21/1	99
11	0.3:0.9	0.1	DCM	21/1	90

Reaction conditions: 0.1 M solution of **81a** and 0.3 M solution of **82** was prepared and flown through the 6.6 × 150 mm Omnifit packed bed reactor (1gm of Amberlyst®-15, 6 cm bed height) (Vaportec SF-10 pump) at room temperature; t_R = residence time in minutes. The mentioned yields are isolated yields.

Following the optimal continuous flow conditions, azidation on various alcohols was studied. Next, when 0.1:0.3 M concentrations of **81a:82** were flown through a catalyst bed with 0.1 mL per minute flow rate at room temperature improved the yield of azide products **83a**, **83b**, **83c**, **83d**, **83f**, and **83g** with 99%, 97%, 80%, 94%, 91%, and 86% yields (Scheme 3.3.2). Further, heating benzyl substituted 3-hydroxy-2-oxindoles at 80 °C in DCE solvent gave 93% yield of azide **83l**.

Gratifyingly, primary alcohols such as piperonyl alcohol, 6-chloropiperonyl alcohol, and pyrene methanol reacted with $TMSN_3$ afforded 91%, 97%, and 80% of **83q**, **83r**, and **83s** respectively (Scheme 3.3.2).

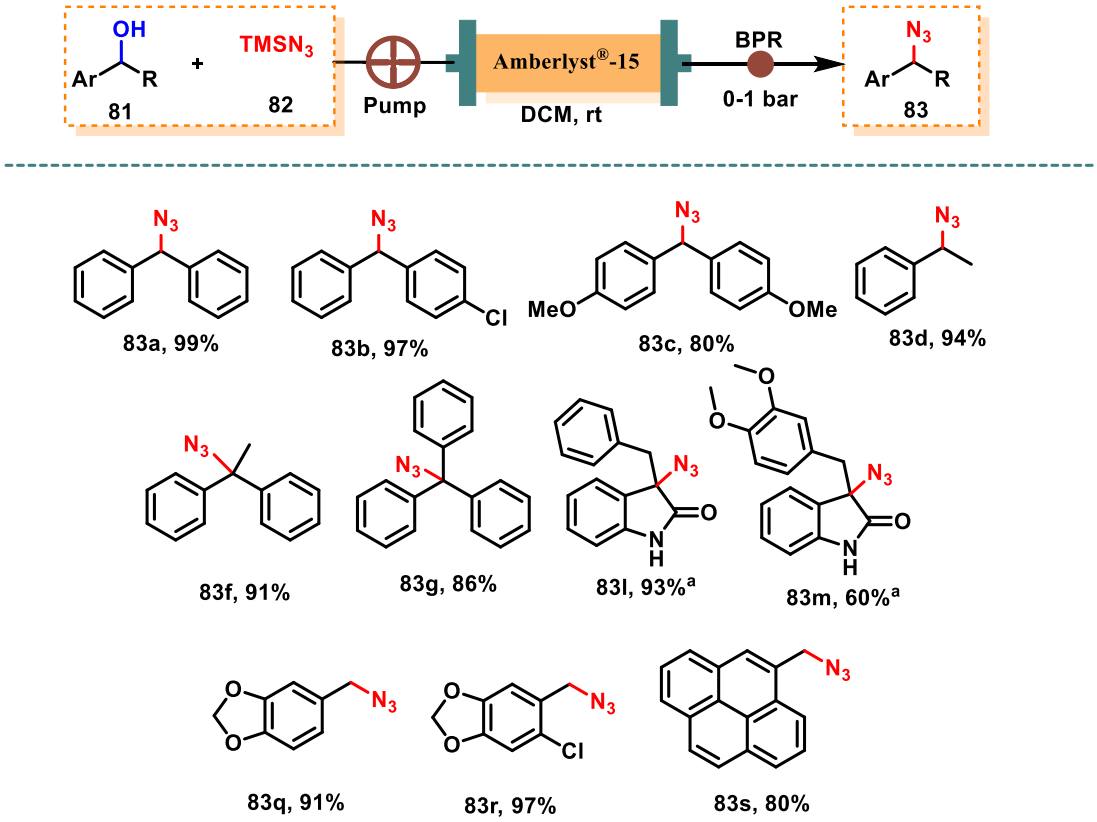

Reaction conditions: 0.1 M solution of **81a** and 0.3 M solution of $TMSN_3$ **82** in DCM was prepared and flown through the 6.6 × 150 mm Omnifit packed bed reactor (1gm of Amberlyst®-15, 6cm bed height) (Vaportec SF-10 pump) with 0.1 mL/min flow rate at room temperature; t_R = 21min; [a]80 °C in DCE (Vapourtec R-series); The mentioned yields are isolated yields.

Scheme 3.3.2: Substrate scope for the azidation of alcohols under flow conditions

Next, we investigated the azidation reaction on peroxyoxindoles that can undergo skeletal rearrangement and subsequent azidation to deliver the product. The optimized condition was established with model peroxide **84a**. At first, various concentrations of **84a** were passed through catalyst bed that directly impacts the yield of product **85a** (Table 3.3.3).

Table 3.3.3: Optimization of reaction condition for the azidation of peroxyoxindoles under flow

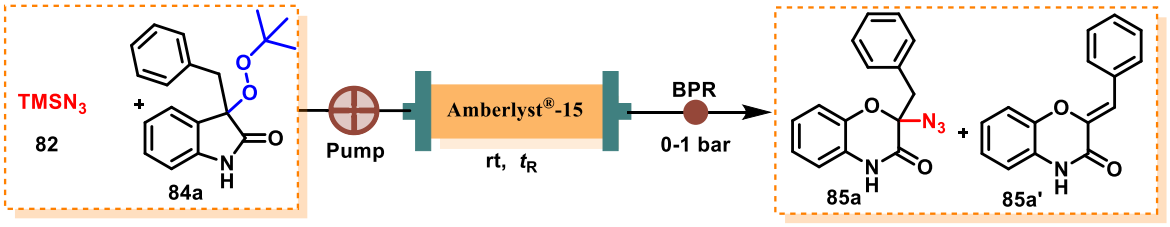

Entry	Substrate concentration (M) 84a:82	Flow rate (mL/min)	t_R (min)/Number of runs	Yield of 85a (%)
1	0.05:0.15	0.1	21/1	38
2	0.1:0.3	0.1	21/1	60
3	0.1:0.5	0.1	21/1	61
4	0.3:0.9	0.1	21/1	40
5[a]	0.1:0.3	0.1	21/1	nd
6[b]	0.1:0.3	0.1	10/1	63
7[b]	0.1:0.3	0.2	05/1	68
8[c]	0.1:0.3	0.1	03/1	38

Reaction conditions: A solution of **84a** and solution of $TMSN_3$ **82** in DCM was prepared and flown through the 6.6 × 150 mm Omnifit packed bed reactor (1gm of Amberlyst®-15, 6 cm bed height) (Vaportec SF-10 pump) at a specified temperature; t_R = residence time in minutes. [a] 60 °C. [b] 0.5 gm of Amberlyst®-15, 3 cm bed height. [c] 0.2 gm of Amberlyst®-15, 1 cm bed height. The mentioned yields are isolated yields.

Thus, increasing the molar concentration of **84a** from 0.05 M to 0.1 M increased the yield of **85a** from 38% to 60% (Table 3.3.3, entries 1-2). While 0.1:0.5 M of **84a:82** gave 61% of **85a**. As there was not much difference in product yield (Table 3.3.3, entries 2 and 3), 0.1:0.3 M was chosen as the optimal concentration for the azidation reaction. Heating the reaction to 60 °C produced only rearranged product **85a'** and no azidation product **85a**. Further, with 3 cm bed height and 0.2 mL per min flow rate 68% yield of **85a** was observed (Table 3.3.3, entry 7). Thus, the competitive

product **85a'** was minimized by controlling the flow. The generality of the reaction was studied using a range of peroxides to generate a library of 2*H*-1,4-benzoxazin-3(4*H*)-one derivatives (Scheme 3.3.3).

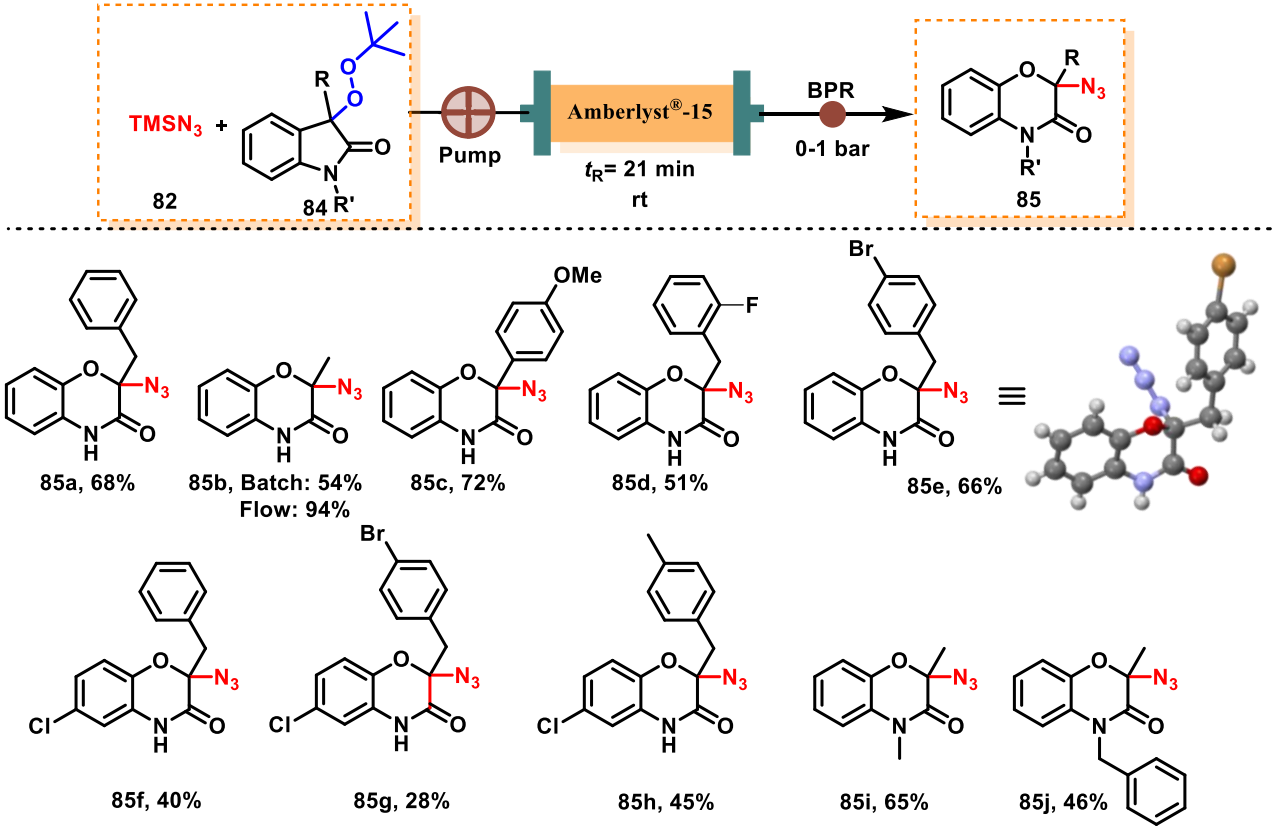

Reaction conditions: 0.1 M solution of peroxide **84** and 0.3 M solution of $TMSN_3$ in DCM was prepared and flown through the 6.6 × 150 mm Omnifit packed bed reactor (1 gm of Amberlyst®-15, 6 cm bed height) (Vaportec SF-10 pump) with 0.1 mL/min flow rate at a room temperature; t_R= 21min; The mentioned yields are isolated yields.

Scheme 3.3.3: Substrate scope for the azidation of peroxides under flow

Interestingly, this sequential rearrangement-azidation process with 3-methyl-3-peroxyoxindoles gave 94% yield (54% in batch condition). Several additional C3-substituted peroxides were also subjected to this tandem reaction, providing similar compounds **85c-e** in moderate yields (Scheme 3.3.3). However, with chloro substituted peroxyoxindole, the yield of corresponding heterocyclic

quaternary azide **85f-h** was lowered to a moderate level. Similarly, *N*-substituted peroxyoxindoles gave the rearranged azides **85i** and **85j** in 65% and 46% yield, respectively (Scheme 3.3.3).

The product of direct azidation of alcohol **81h** and peroxyoxindole **84b** were monitored by using ^{13}C NMR spectra. The direct azidation of **81h** provided **83h** which was confirmed by presence of quaternary carbon peak at 63.9 ppm. However, **84b** underwent skeletal rearrangement followed by azidation of peroxyoxindoles to achieve **85b** which was confirmed by a shift in quaternary carbon peak to 90.3 ppm. (Figure 3.3.2).

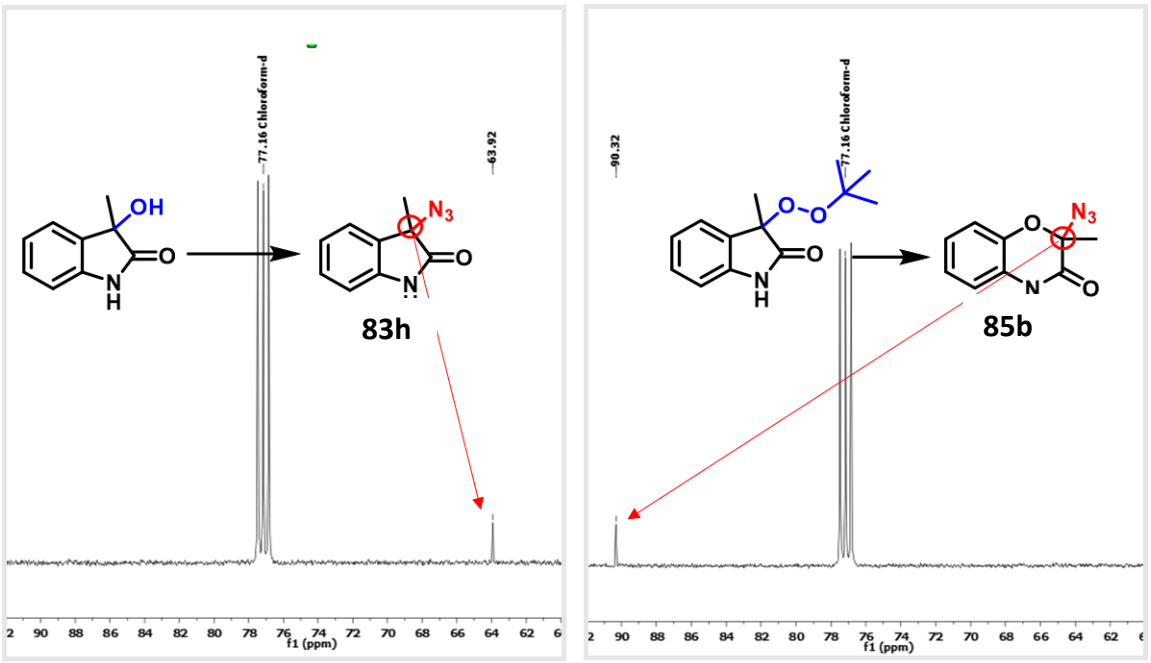

Figure 3.3.2: ^{13}C NMR spectrum of **83h** and **85b**

Next, we demonstrated a long-time continuous flow experiment to illustrate the feasibility of our process for upscaling as well as to study the stability and efficiency of the Amberlyst®-15 catalyst. For this reason, substrates **81a** and $TMSN_3$ were chosen as a model substrate. For instance, 30.0 mmol of the **81a** was pumped continuously for 50 h at a flow rate of 0.1 mL/min furnished 29.38 mmol of product with TON = 9.24 and TOF = 0.185 h^{-1} (Scheme 3.3.4). After flowing **81a** for 50 h under continuous flow, the product was isolated by column chromatography giving 6.144 gm of **83a** with a 98% yield. Even though we stopped the reaction after 50 h, the catalyst was still active for further reactions.

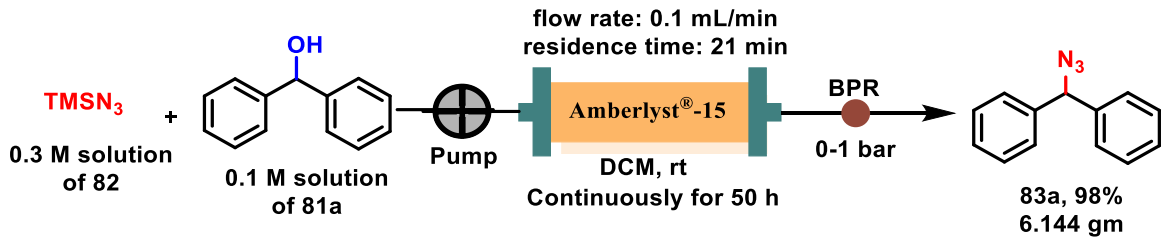

Scheme 3.3.4: Gram-scale and catalyst lifetime

The appeal of the azidation reaction is augmented by the potential application of the azide unit. The synthetic utility of azides for Staudinger reaction is well explored under batch conditions in literature. However, Baumann and coworkers demonstrated azide reduction under flow condition.[104] Following the continuous flow approach, we performed reduction of azide by preparing 1 M solution of **83a** and 2 M solution of PPh_3 in THF:H_2O (9:1). Both the solutions were flown through pump 1 and pump 2 with 0.1 and 0.3 mL/min flow rate respectively and passed through Vaportec SS coil reactor heated at 60 ^oC to deliver **87a** with 58% yield. (Scheme 3.3.5).

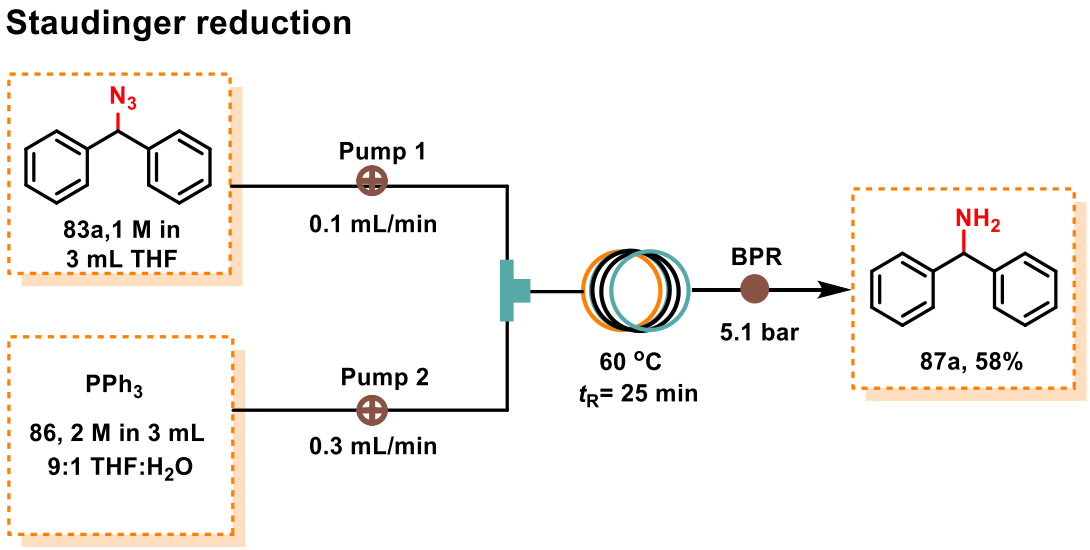

Scheme 3.3.5: The synthetic utility of azides for Staudinger reduction

Next, [3+2] copper catalyzed alkyne azide cycloaddition was performed under continuous flow by flowing solution through PTFE tubing at room temperature. A 0.12 M solution of **83a** and 0.1 M solution of ethynylbenzene with 1 mol% of $CuSO_4.5H_2O$ and 10 mol% Na-ascorbate in H_2O:*t*-

BuOH were flown through PTFE tubing of 7 mL to give 73% of desired product **89a**. However, under the similar reaction conditions 4-phenyl-1-(1-phenylethyl)-1*H*-1,2,3-triazole **89b** was synthesized starting from **83d** and ethynylbenzene provided 62% yield (Scheme 3.3.6).[107]

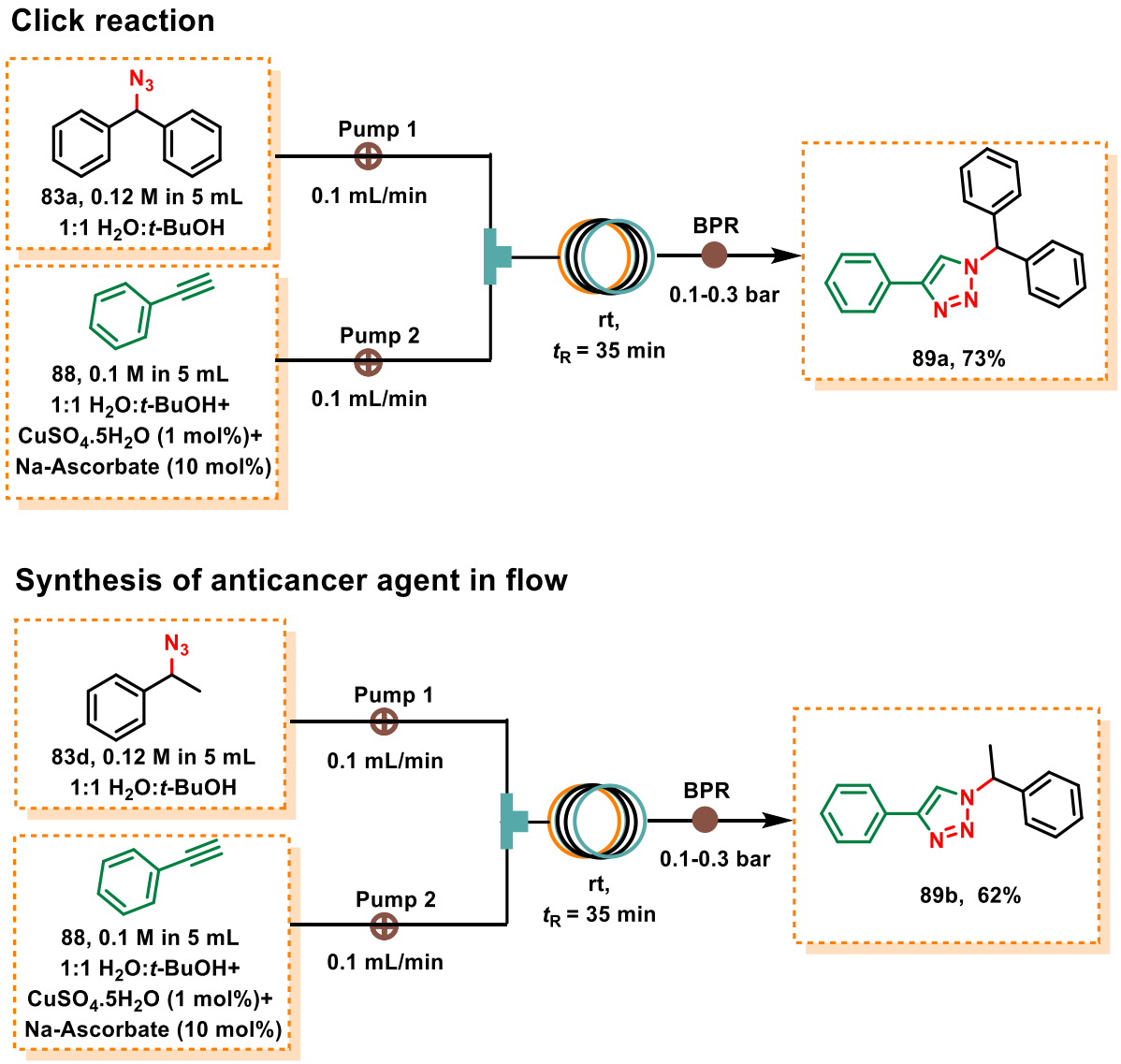

Scheme 3.3.6: The synthetic utility of azides for Click reaction in flow

Furthermore, the synthetic utility of azide **83** was illustrated by employing a 0.1 M solution of **83** at 180 ^{o}C in a Vapourtec HT reactor to produce quinoxalin-2(1*H*)-one derivative in 100 minutes. The 3-methyl and 3-benzyl substituted 3-azide-2-oxindoles provided **90i** and **90l** in 83% and 79%

yields, respectively. In the case of -Me and -OMe aryl substituted 3-azide-2-oxindoles, 70% and 83% of **90j** and **90k** were obtained respectively (Scheme 3.3.7). Moreover, azide **90n** with bromo substitution on the C-3 benzyl core was synthesized in 81% yield. Furthermore, **90n** can be transformed into an aldose reductase inhibitor in a single step.

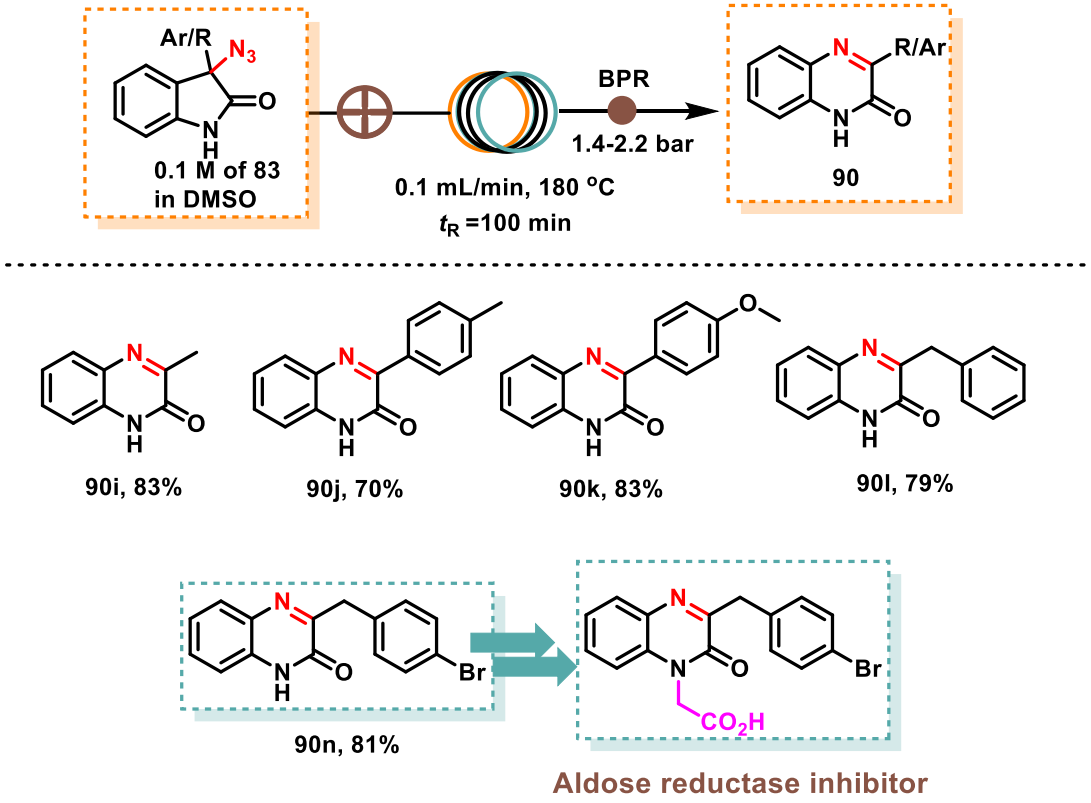

Scheme 3.3.7: Thermal skeletal rearrangement of azides to quinoxalin-2(1*H*)-one derivatives in flow

To shed light on the mechanism, Amberlyst®-15 initially protonates the hydroxyl group of alcohols **81** to make it a better leaving group. The desired azide **83a** is produced by N_3^- attack, followed by the expulsion of a water molecule. It should be noted that the nucleophilic attack can occur via the S_N1 pathway. In the case of peroxyoxindole azidation, Amberlyst®-15 initially undergoes *t*-butyl group deprotection of **84** to give **A**.[108] The distant oxygen atom of **A** gets protonated by Brønsted acid source Amberlyst®-15. Next, the protonated species undergoes skeletal rearrangement to generate in situ carbocation species **B** by expulsion of water molecule**.** Further, water molecule

attacks on Si atom of $TMSN_3$ to form trimethylsilyl alcohol (Confirmed by GCMS) and N_3^- becomes free. Finally, N_3^- attacks on electrophilic center **B** to provide the azide **85**. (Scheme 3.3.8).

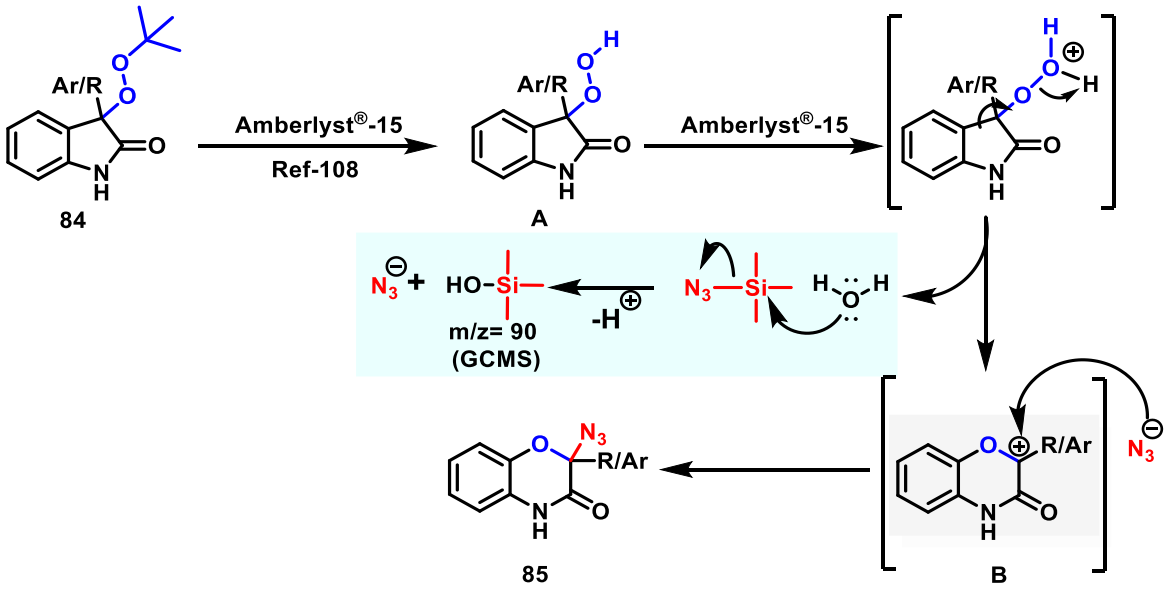

Scheme 3.3.8: A plausible mechanism for azidation reaction of peroxyoxindoles via in situ ring expansion

3.4. Conclusion

In conclusion, we demonstrated safer azidation of different alcohols and peroxides in the presence of Amberlyst®-15 utilizing $TMSN_3$ as an azidation reagent under batch and continuous flow conditions. A continuous flow azidation scale-up process was accomplished on a gram scale (6.14 gm) with 98% yield. Furthermore, continuous flow azidation of quaternary hydroxy oxindole afforded a diverse range of quaternary azides. The azidation of peroxides was accomplished by successive deprotection-bond migration-nucleophilic substitution to provide ring expansion followed by azide transfer to generate several substituted-2-azido-2*H*-benzo[b][1,4]oxazin-3(4*H*)-ones. In a continuous flow, rearranged azide products were synthesized in 21 minutes. This approach was tolerant towards many functional groups and demonstrated a broad substrate scope in high yield. It is a safer procedure for longer and larger-scale operations. The application of azides was demonstrated in a continuous flow click reaction that used alkyne and azide to produce a biologically significant triazole scaffold. Furthermore, this (azidomethylene)dibenzene was

effectively reduced under continuous flow to produce diphenylmethanamine. Finally, a thermolytic rearrangement of quaternary oxindole azide was developed under a continuous flow module to generate a diverse range of 2*H*-1,4-benzoxazin-3(4*H*)-one derivative in t_R = 100 minutes utilizing an SS coil reactor.

3.5. Experimental sections

General information and data collection:

All the chemicals were purchased from Sigma-Aldrich and SD Fine Chemicals and used without further modification. All solvents were purchased from Rankem and Finar Chemicals. Deuterated solvents were used as received. Column chromatographic separations were performed over 100−200 silica-gel. Visualization was accomplished with UV light. The ^{1}H and ^{13}C NMR spectra were recorded on 400 and 100 MHz, respectively, using Bruker or JEOL spectrometers. The chemical shift (δ) and coupling constant (*J*) values are given in parts per million and hertz, respectively. Abbreviations used in the NMR follow-up experiments: b, broad; s, singlet; d, doublet; t, triplet; q, quartet; td, dd doublet of triplet and double doublet; m, multiplet, tt, triplet of triplets and ddd, doublet of doublet of doublets. The flow chemistry experiments were carried out on Vapourtec R-series and Vaportec SF-10 pump with glass column (Omntifit, 6.6 x 150 mm) and Vapourtec Rseries with SS coil reactor (10 ml). HRMS spectra were obtained with Waters-synapt G2 using electrospray ionization (ESI-TOF). Infrared (ATIR) spectra were obtained with a Bruker Alpha-E infrared spectrometer. Single-crystal diffraction analysis data were collected at 100K with a BRUKER KAPPA APEX III CCD Duo diffractometer (operated at 1500 W power: 50 kV, 30 mA) using graphite monochromatic Mo Kα radiation and Cu-Kα radiation.

A. General procedure for azidation of alcohols in batch condition: To an oven dried 20 mL resealable pressure tube (equipped with rubber septum) were added alcohol **83** (0.5 mmol), azidotrimethylsilane (1.5 mmol), and Amberlyst®-15 (w/w with respect to alcohol) in dichloromethane (2 mL) and then the mixture was stirred at room temperature (25 ºC) for 30 min to 1 h. The reaction progress was monitored through the TLC until the completion of the reaction. The volatile solvents were removed using a vacuum, and the crude reaction mixture was purified by column chromatography on silica gel (EtOAc:hexane = 0:100 to 5:95).

Note: "Caution should be exercised when using azides. Both organic and inorganic azides can be heat- and shock-sensitive and can explosively decompose with little input of external energy." Use small amount of $TMSN_3$ when performing batch reaction. To evaluate the stability of azide use (^{N}Carbon + ^{N}Oxygen) / ^{N}Nitrogen ≥ 3) formula.

B. General procedure for azidation of alcohols in continuous-flow: In a typical procedure, the 0.1 M solution of alcohol derivative **83** in dichloromethane and 3 equivalents of azidotrimethylsilane was premixed and flown through Omnifit (6.6 x 150 mm) packed bed with Amberlyst®-15 filled up to 5 cm height (1.0 g, swollen up to 6 cm after passing solvent) at room temperature and 0-1 bar pressure with 0.1 mL/min flow rate. After reaction completion, the catalyst bed was washed with dichloromethane. A volatile component was evaporated using a vacuum. The residue was directly purified by silica gel chromatography (EtOAc:hexane = 1:99 to 5:95). Amberlyst®-15 bed was recycled by washing with DCM and reused for the other substrates.

Note: For preventive measurement, we have filtered the solution through a syringe filter before pumping it through pumps. (Filtration carried out using nylon syringe filter (0.22 µm)). Time mentioned in flow is residence time (t_R); residence time can be calculated by following formula: reactor volume/flow rate.

C. General procedure for azidation of peroxides in continuous-flow: The 0.1 M solution of peroxide derivatives **84** in dichloromethane and 3 equivalent of azidotrimethylsilane was premixed and flown through Omnifit® (6.6 x 150 mm)) packed bed with Amberlyst®-15 filled up to 5 cm height (1.0 g, swollen up to 6 cm after passing solvent) at room temperature and 0-1 bar pressure with 0.1 mL/min flow rate. After reaction completion, the catalyst bed was washed with dichloromethane. A volatile component was evaporated using a vacuum. The residue was directly purified by silica gel chromatography (EtOAc:hexane = 10:90).

D. Experimental procedure for long-time experiment of azidation of diphenylmethanol in continuous-flow: Diphenylmethanol (30 mmol, 5.52 gm) in 300 mL dichloromethane and 3 equivalent azidotrimethylsilane (90 mmol, 10.35 gm) was premixed and flown through the Omnifit (6.6 x 150 mm) packed bed column (1 gm of Amberlyst®-15, bed height= 5 cm, swollen to 6 cm) at room temperature with 0.1 mL/min flow rate with 0-2 bar pressure for 50 h. The conversion was

monitored by TLC and NMR. After 50 h reaction was stopped and the reaction mixture was concentrated under a vacuum and then subjected to column chromatography on silica gel chromatography (hexane). Product **3a** was isolated with 6.144 gm in 98% yield with TON= 9.24 and TOF= $0.185h^{-1}$.

E. General procedure for the synthesis of diphenylmethanamine:[104] To perform the Staudinger reduction in a flow process, the stream of 1.0 M solution of (azidomethylene)dibenzene **83a** was combined in a T-piece with a stream of triphenylphosphine (2 equiv.) in aqueous THF (THF/water, 9:1) at 0.1 mL/min of **3a** and 0.3 mL/min of triphenylphosphine. The resulting mixture was allowed to react in Vapourtec R-series SS coil reactor (10 mL, 60 ^{o}C, residence time 25 min) before passing through back-pressure regulator and collection in a flask. The volatile component of crude mixture was evaporated using a vacuum and then it is extracted with DCM. The residue was purified by silica gel chromatography (EtOAc:hexane = 40:60).

F. General procedure of click reaction in flow:[107] The azides **83** (0.12 M in 5 mL of *t*-BuOH:H_2O) and phenylacetylene (0.1 M in 5 mL of *t*-BuOH:H_2O and 1 mol% $CuSO_4.5H_2O$ and 10 mol% Na-ascorbate) was flown through PTFE tubing (7 mL) at room temperature with 0.1-0.3 bar pressure maintaining 0.1 mL/min flow rate each. The reaction mixture was collected continuously after 35 min. The reaction mixture was extracted with EtOAc (10 ml x 3). The solvent evaporated under vacuum and residue was subjected to column chromatography for purification using EtOAc/n-hexane (20:80) to afford the corresponding 1,2,3-triazole derivatives in good yields.

G. General procedure for ring expansion of quaternary 2-oxindole azides in flow: The tertiary azide of 2-oxindole (0.1 M, 5 mL of DMSO) was flown through Vapourtec R series 10 mL SS coil reactor with a flow rate of 0.1 mL/min at 180 ^{o}C at 1.4 - 2.2 bar pressure. The reaction mixture was collected continuously after 100 min. To the reaction mixture, 50 mL water and 2 mL EtOAc was added and left to precipitate overnight. Next, the precipitate formed was filtered, washed with water several times, and then dissolved in methanol and passed through bed of sodium sulfate to afford the corresponding quinoxalin-2(1*H*)-ones derivatives.

3.6.A. Analytical data for product:

*(azidomethylene)dibenzene **(83a):***[97]

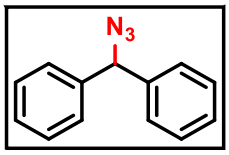

Batch condition: Prepared according to the general procedure (**A**), using diphenyl methanol (184.0 mg, 1.0 mmol) to (azidomethylene)dibenzene **83a** (204.8 mg, 98%) as a colourless oil after purification by column chromatography on silica gel (hexane).

Flow condition: Prepared according to the general procedure **(D)**, a solution of 0.1 M diphenyl methanol (5520.0 mg, 30 mmol) in 300 mL dichloromethane was flown through the packed bed of Amberlyst®-15 (bed height 6.0 cm) with 0-1 bar at 0.1 mL/min to afford (azidomethylene)dibenzene **83a** (6144.0 mg, 98%) as a colourless oil after purification by column chromatography on silica gel (hexane). ^{1}H NMR (400 MHz, $CDCl_3$) δ 7.40 (m, 10H), 5.79 (s, 1H). ^{13}C NMR (100 MHz, $CDCl_3$) δ 139.7, 128.8, 128.1, 127.5, 68.6. IR (neat): 2096, 1455, 1238 cm^{-1}. HRMS (ESI-TOF) m/z: $[M + H]^+$ calcd for $C_{13}H_{12}N$: 182.0966; found: 182.0970.

*1-(azido(phenyl)methyl)-4-chlorobenzene **(83b):***[97]

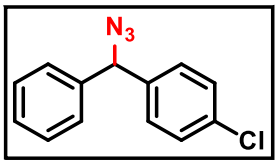

Batch condition: Prepared according to the general procedure **(A)**, using (4-chlorophenyl)(phenyl)methanol (109.0 mg, 0.50 mmol) to afford 1-(azido(phenyl)methyl)-4-chlorobenzene **83b** (89.9 mg, 74%) as a pale yellow oil after purification by column chromatography on silica gel (EtOAc:hexane = 1:99).

Flow condition: Prepared according to the general procedure **(B)**, a solution of 0.1 M (4-chlorophenyl)(phenyl)methanol (109.0 mg, 0.50 mmol) in 5 mL dichloromethane was flown through the packed bed of Amberlyst®-15 (bed height 6.0 cm) with 0-1 bar at 0.1 mL/min to afford 1-(azido(phenyl)methyl)-4-chlorobenzene **83b** (117.8 mg, 97%) as a pale yellow oil after purification by column chromatography on silica gel (EtOAc:hexane = 1:99). ^{1}H NMR (400 MHz, $CDCl_3$) δ 7.26 (m, 9H), 5.63 (s, 1H). ^{13}C NMR (100 MHz, $CDCl_3$) δ 139.2, 138.3, 134.0, 128.9, 128.4, 127.5, 67.9. IR (neat): 2098, 1659, 1495, 1087, 703 cm^{-1}. HRMS (ESI-TOF) m/z: $[M + H - N_2]^+$ calcd for $C_{13}H_{11}ClN$: 216.0571; found: 216.0580.

4,4'-(azidomethylene)bis(methoxybenzene) ***(83c):***[97]

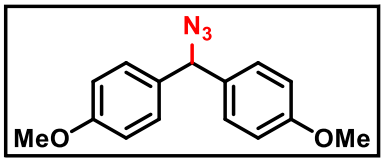

Batch condition: Prepared according to the general procedure (**A**), using bis(4-methoxyphenyl)methanol (122.0 mg, 0.50 mmol) to afford 4,4'-(azidomethylene)bis(methoxybenzene) **83c** (96.8 mg, 72%) as a pale yellow oil after purification by column chromatography on silica gel (EtOAc:hexane = 1:99).

Flow condition: Prepared according to the general procedure **(B)**, a solution of 0.1 M bis(4-methoxyphenyl)methanol (122.0 mg, 0.50 mmol) in 5 mL dichloromethane was flown through the packed bed of Amberlyst®-15 (bed height 6.0 cm) with 0-1 bar at 0.1 mL/min to afford 4,4'-(azidomethylene)bis(methoxybenzene) **83c** (107.6 mg, 80%) as a pale yellow oil after purification by column chromatography on silica gel (EtOAc:hexane = 1:99). ^{1}H NMR (400 MHz, $CDCl_3$) δ 7.25 (dq, *J* = 6.7, 2.4 Hz, 4H), 6.91 (m, 4H), 5.66 (s, 1H), 3.82 (s, 6H). ^{13}C{^{1}H} NMR (100 MHz, $CDCl_3$) δ 159.3, 132.1, 128.7, 114.1, 67.7, 55.3. IR (neat): 2092, 1611, 1508, 1243 cm^{-1}. HRMS (ESI-TOF) m/z: $[M + H - N_2]^+$ calcd for $C_{15}H_{16}NO_2$: 242.1181; found: 242.1174.

(1-azidoethyl)benzene ***(83d):***[110]

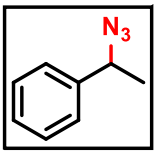

Batch condition: Prepared according to the general procedure **(A)**, using 1-phenylethan-1-ol (61.0 mg, 0.50 mmol) to afford (1-azidoethyl)benzene **83d** (133.2 mg, 91%) as a colourless oil after purification by column chromatography on silica gel (hexane).

Flow condition: Prepared according to the general procedure **(B)**, a solution of 0.1 M 1-phenylethan-1-ol (61.0 mg, 0.50 mmol) in 5 mL dichloromethane was flown through the packed bed of Amberlyst®-15 (bed height 6.0 cm) with 0-1 bar at 0.1 mL/min to afford (1-azidoethyl)benzene **83d** (138.0 mg, 94%) as a colourless oil after purification by column chromatography on silica gel (hexane). ^{1}H NMR (400 MHz, $CDCl_3$) δ 7.37 (m, 5H), 4.63 (m, 1H), 1.54 (d, *J* = 6.7 Hz, 3H). ^{13}C NMR (100 MHz, $CDCl_3$) δ 141.0, 128.9, 128.5, 126.5, 61.2, 21.7. IR (neat): 2099, 1246 cm^{-1}.

2-(1-azidoethyl)naphthalene ***(83e):***[97]

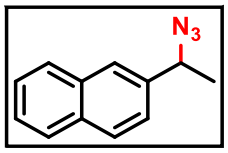

Prepared according to the general procedure **(A)**, using 1-(naphthalen-2-yl)ethan-1-ol (86.0 mg, 0.50 mmol) to afford 2-(1-azidoethyl)naphthalene **83e** (97.6 mg, 99%) as a colourless oil after purification by column chromatography on silica gel (EtOAc:hexane = 0:100) as a colourless oil. ^{1}H NMR (400 MHz, $CDCl_3$) δ 8.16 (dd, *J* = 8.2, 3.4 Hz, 1H), 7.92 (ddd, *J* = 11.2, 8.0, 2.7 Hz, 2H), 7.59 (m, 4H), 5.40 (m, 1H), 1.78 (dd, *J* = 6.8, 2.8 Hz, 3H). ^{13}C NMR (100 MHz, $CDCl_3$) δ 136.2, 134.0, 130.6, 129.1, 128.8, 126.5, 125.9, 125.4, 123.6, 123.1, 57.6, 20.7. IR (neat): 2009, 1508, 1241 cm^{-1}. HRMS (ESI-TOF) m/z: $[M + H - N_2]^+$ calcd for $C_{12}H_{12}N$: 170.0970; found: 170.0968.

(1-azidoethane-1,1-diyl)dibenzene ***(83f):***[99]

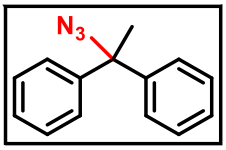

Batch condition: Prepared according to the general procedure **(A)**, using 1,1-diphenylethan-1-ol (198.0 mg, 1.0 mmol) to afford (1-azidoethane-1,1-diyl)dibenzene **83f** (191.8 mg, 86%) as a pale yellow oil after purification by column chromatography on silica gel (hexane).

Flow condition: Prepared according to the general procedure **(B)**, a solution of 0.1 M 1,1-diphenylethan-1-ol (198.0 mg, 1.0 mmol) 10 mL dichloromethane was flown through the packed bed of Amberlyst®-15 (bed height 6.0 cm) with 0-1 bar at 0.1 mL/min to afford (1-azidoethane-1,1-diyl)dibenzene **83f** (203.0 mg, 91%) as a pale yellow oil after purification by column chromatography on silica gel (hexane). ^{1}H NMR (400 MHz, $CDCl_3$) δ 7.35 (m, 10H), 2.07 (s, 3H). ^{13}C NMR (100 MHz, $CDCl_3$) δ 144.3, 128.5, 127.6, 126.7, 69.5, 27.5. IR (neat): 2087, 1492, 1444, 1238 cm^{-1}. HRMS (ESI-TOF) m/z: $[M + H - N_2]^+$ calcd for $C_{14}H_{14}N$: 196.1126; found: 196.1129.

(azidomethanetriyl)tribenzene ***(83g):***[99]

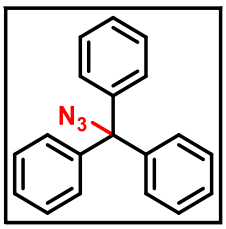

Batch condition: Prepared according to the general procedure **(A)**, using triphenylmethanol (130.0 mg, 0.5 mmol) to afford (azidomethanetriyl)tribenzene **83g** (114.0 mg, 80%) as a white solid after purification by column chromatography on silica gel (hexane).

Flow condition: Prepared according to the general procedure **(B)**, a solution of 0.1 M triphenylmethanol (130.0 mg, 0.5 mmol) 5 mL dichloromethane was flown through the packed bed of Amberlyst®-15 (bed height 6.0 cm) with 0-1 bar at 0.1 mL/min to afford (azidomethanetriyl)tribenzene **83g** (122.5 mg, 86%) as a white solid after purification by column chromatography on silica gel (hexane). Melting point: 67-69 °C. ^{1}H NMR (400 MHz, $CDCl_3$) δ 7.32 (m, 15H). ^{13}C NMR (100 MHz, $CDCl_3$) δ 143.3, 128.6, 128.3, 127.8. IR (neat): 2096, 1455, 1238 cm^{-1}. HRMS (ESI-TOF) m/z: $[M + H- N_2]^+$ calcd for $C_{19}H_{16}N$: 258.1283; found: 258.1290. Crystal preparation: The crystal is grown by the simple recrystallization method. The pure compound isolated after column chromatography is dissolved in dichloromethane and layered with hexane and kept at room temperature for 2 days to get the pure crystal.

3-azido-3-methylindolin-2-one ***(83h)*****:**[113]

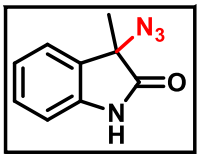

Prepared according to the general procedure **(A)**, using 3-hydroxy-3 methylindolin-2-one (81.5 mg, 0.5 mmol) at 80 °C in dichloroethane to afford 3-azido-3-methylindolin-2-one **83h** (80.5 mg, 86%) as a yellow solid after purification by column chromatography on silica gel (EtOAc:hexane = 5:95). Melting point: 94-96 °C. ^{1}H NMR (400 MHz, $CDCl_3$) δ 8.69 (s, 1H), 7.31 (t, *J* = 8.2 Hz, 2H), 7.11 (t, *J* = 7.6 Hz, 1H), 6.96 (d, *J* = 7.7 Hz, 1H), 1.70 (s, 3H). ^{13}C NMR (100 MHz, $CDCl_3$) δ 177.4, 140.1, 130.3, 129.3, 124.0, 123.5, 110.8, 63.9, 21.6. IR (neat): 2089, 1716, 1620, 1472, 1201 cm^{-1}. HRMS (ESI-TOF) m/z: $[M + H - N_2]^+$ calcd for $C_9H_9N_2O$: 161.0715; found: 161.0709.

3-azido-3-phenylindolin-2-one ***(83i)*****:**[113]

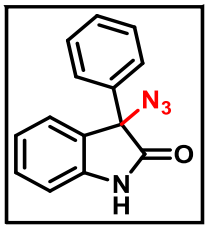

Prepared according to the general procedure (**A**), using 3-hydroxy-3-phenylindolin-2-one (45.0 mg, 0.5 mmol) to afford 3-azido-3-phenylindolin-2-one **83i** (40.0 mg, 80%) as a pale yellow solid after purification by column chromatography on silica gel (EtOAc:hexane = 5:95). Melting point: 328-330 °C. ^{1}H NMR (400 MHz, $CDCl_3$) δ 8.77 (s, 1H), 7.39 (m, 6H), 7.26 (m, 1H), 7.12 (td, *J* = 7.6, 1H), 7.00 (d, *J* = 7.8 Hz, 1H). ^{13}C NMR (100 MHz, $CDCl_3$) δ 176.0, 140.7, 136.3, 130.6, 129.1, 129.0, 128.9, 126.6, 125.6, 123.8, 111.1, 70.4. IR (neat): 3249, 2101, 1730, 1717, 1622, 1476 cm^{-1}. HRMS (ESI-TOF) m/z: $[M + Na]^+$ calcd for $C_{14}H_{10}N_4ONa$: 273.0753; found: 273.0759.

3-azido-3-(p-tolyl)indolin-2-one ***(83j)*****:**[113]

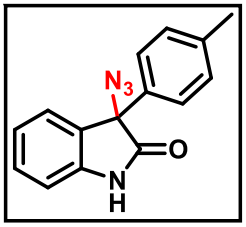

Prepared according to the general procedure (**A**), using 3-hydroxy-3-(p-tolyl)indolin-2-one (119.0 mg, 0.50 mmol) to afford 3-azido-3-(p-tolyl)indolin-2-one **83j** (120.0 mg, 91%) as a pale yellow solid after purification by column chromatography on silica gel (EtOAc:hexane = 5:95). Melting point: 310-312 °C. ^{1}H NMR (400 MHz, $CDCl_3$) δ 9.77 (s, 1H), 7.38 (m, 3H), 7.31 (d, *J* = 7.5 Hz, 1H), 7.25 (d, *J* = 8.1 Hz, 2H), 7.16 (td, *J* = 7.6, 0.8 Hz, 1H), 7.03 (d, *J* = 7.8 Hz, 1H), 2.39 (s, 3H). ^{13}C{^{1}H} NMR (100 MHz, $CDCl_3$) δ 176.9, 140.9, 138.9, 133.2, 130.5, 129.8, 129.1, 126.5, 125.3, 123.6, 111.4, 70.5, 21.2. IR (neat): 2098, 1725, 1619, 1471 cm^{-1}. HRMS (ESI-TOF) m/z: [M + Na]$^{+}$ calcd for $C_{15}H_{12}N_4ONa$: 287.0909; found: 287.0908.

3-azido-3-(4-methoxyphenyl)indolin-2-one ***(83k)*****:**[114]

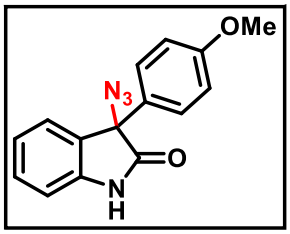

Prepared according to the general procedure (**A**), using 3-hydroxy-3-(4-methoxyphenyl)indolin-2-one (127.5 mg, 0.50 mmol) to afford 3-azido-3-(4-methoxyphenyl)indolin-2-one **83k** (138.5 mg, 99%) as a pale yellow liquid after purification by column chromatography on silica gel (EtOAc:hexane = 5:95). ^{1}H NMR (400 MHz, $CDCl_3$) δ 9.46 (s, 1H), 7.31 (m, 2H), 7.23 (m, 2H), 7.04 (td, *J* = 7.6, 0.8 Hz, 1H), 6.91 (d, *J* = 7.8 Hz, 1H), 6.83 (m, 2H), 3.71 (s, 3H). ^{13}C{^{1}H} NMR (100 MHz, $CDCl_3$) δ 176.7, 160.1, 140.9, 130.5, 128.9, 128.1, 125.4, 123.6, 114.4, 111.3, 70.2, 55.4. IR (neat): 2102, 1725, 1619, 1510 cm^{-1}. HRMS (ESI-TOF) m/z: [M + Na]$^{+}$ calcd for $C_{15}H_{12}N_4O_2Na$: 303.0858; found: 303.0851.

3-azido-3-benzylindolin-2-one ***(83l)*****:**

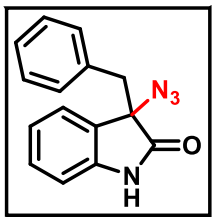

Batch condition: Prepared according to the general procedure (**A**), using 3-benzyl-3-hydroxyindolin-2-one (119.0 mg, 0.50 mmol) at 80 °C in dichloroethane to afford 3-azido-3-benzylindolin-2-one **83l** (112.0 mg, 85%) as a pale yellow semi solid after purification by column chromatography on silica gel (EtOAc:hexane = 5:95).

Flow condition: Prepared according to the general procedure **(B)**, a solution of 0.1 M 3-benzyl-3-hydroxyindolin-2-one (119.0 mg, 0.50 mmol) at 80 ^{o}C in 5 mL dichloroethane was flown through the packed bed of Amberlyst®-15 (bed height 6.0 cm) with 0-1 bar at 0.1 mL/min to afford 3-azido-3-benzylindolin-2-one **83l** (123.0 mg, 93%) as a pale yellow semi solid after purification by column chromatography on silica gel (EtOAc:hexane = 5:95). ^{1}H NMR (400 MHz, $CDCl_3$) δ 8.36 (s, 1H), 7.26 (m, 1H), 7.15 (m, 3H), 7.06 (m, 2H), 7.00 (m, 2H), 6.80 (d, *J* = 7.7 Hz, 1H), 3.36 (d, *J* = 13.1 Hz, 1H), 3.24 (d, *J* = 13.2 Hz, 1H). ^{13}C NMR (100 MHz, $CDCl_3$) δ 176.5, 140.5, 133.2, 130.5, 130.3, 128.1, 127.4, 126.5, 125.2, 123.0, 110.6, 68.0, 41.6. IR (neat): 2101, 1719, 1472 cm^{-1}. HRMS (ESI-TOF) m/z: $[M + Na]^+$ calcd for $C_{15}H_{12}N_4ONa$: 287.0909; found: 287.0909.

*3-azido-3-(3,4-dimethoxybenzyl)indolin-2-one **(83m)*:**

Batch condition: Prepared according to the general procedure (**A**), using 3-(3,4-dimethoxybenzyl)-3-hydroxyindolin-2-one (149.0 mg, 0.50 mmol) at 80 ^{o}C in dichloroethane to afford 3-azido-3-(3,4-dimethoxybenzyl)indolin-2-one **83m** (120.0 mg, 73%) as a pale yellow semisolid after purification by column chromatography on silica gel (EtOAc:hexane = 5:95).

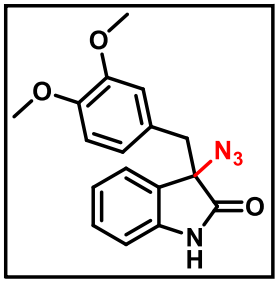

Flow condition: Prepared according to the general procedure **(B)**, a solution of 0.1 M 3-(3,4-dimethoxybenzyl)-3-hydroxyindolin-2-one (149.0 mg, 0.50 mmol) at 80 ^{o}C in 5 mL dichloroethane was flown through the packed bed of Amberlyst®-15 (bed height 6.0 cm) with 0-1 bar at 0.1 mL/min to afford 3-azido-3-(3,4-dimethoxybenzyl)indolin-2-one **83m** (98.0 mg, 60%) as a pale yellow semisolid after purification by column chromatography on silica gel (EtOAc:hexane = 5:95). ^{1}H NMR (400 MHz, $CDCl_3$) δ 8.65 (s, 1H), 7.24 (m, 1H), 7.14 (d, *J* = 7.1 Hz, 1H), 7.06 (m, 1H), 6.79 (d, *J* = 7.7 Hz, 1H), 6.59 (m, 2H), 6.39 (d, *J* = 2.0 Hz, 1H), 3.76 (s, 3H), 3.60 (s, 3H), 3.29 (d, *J* = 13.3 Hz, 1H), 3.19 (d, *J* = 13.1 Hz, 1H). ^{13}C NMR (100 MHz, $CDCl_3$) δ 176.4, 148.2, 140.9, 130.3, 126.8, 125.5, 125.1, 122.9, 122.8, 113.4, 110.8, 110.7, 68.1, 55.7, 55.6, 41.3. IR (neat): 2101, 1635 cm^{-1}. HRMS (ESI-TOF) m/z: $[M + Na]^+$ calcd for $C_{17}H_{16}N_4O_3Na$: 347.1120; found: 347.1118.

*3-azido-3-(4-bromobenzyl)indolin-2-one **(83n)**:*

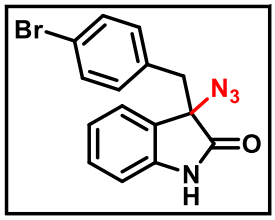

Prepared according to the general procedure **(A)**, using 3-(4-bromobenzyl)-3-hydroxyindolin-2-one (159.0 mg, 0.50 mmol) at 80 °C in dichloroethane to afford 3-azido-3-(4-bromobenzyl)indolin-2-one **83n** (171.0 mg, 70%) as a yellow solid after purification by column chromatography on silica gel (EtOAc:hexane = 5:95). ^{1}H NMR (400 MHz, $CDCl_3$) δ 7.93 (s, 1H), 7.27 (m, 3H), 7.09 (m, 2H), 6.86 (m, 2H), 6.79 (d, *J* = 7.8 Hz, 1H), 3.29 (d, *J* = 13.1 Hz, 1H), 3.21 (d, *J* = 13.1 Hz, 1H). ^{13}C NMR (100 MHz, $CDCl_3$) δ 175.6, 140.4, 132.2, 131.4, 130.5, 126.3, 125.1, 123.2, 121.7, 110.7, 67.7, 41.1. IR (neat): 2104, 1652 cm^{-1}.

*3-azido-3-benzyl-6-chloroindolin-2-one **(83o):***

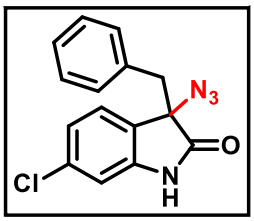

Prepared according to the general procedure **(A)**, using 3-benzyl-6-chloro-3-hydroxyindolin-2-one (137.0 mg, 0.50 mmol) at 80 °C in dichloroethane to afford 3-azido-3-benzyl-6-chloroindolin-2-one **83o** (104.0 mg, 70%) as a yellow white semisolid after purification by column chromatography on silica gel (EtOAc:hexane = 5:95). ^{1}H NMR (400 MHz, $CDCl_3$) δ 8.19 (s, 1H), 7.19 (m, 3H), 6.99 (m, 4H), 6.82 (t, *J* = 3.5 Hz, 1H), 3.35 (d, *J* = 13.2 Hz, 1H), 3.22 (d, *J* = 13.2 Hz, 1H). ^{13}C{^{1}H} NMR (100 MHz, $CDCl_3$) δ 176.1, 141.6, 136.1, 132.9, 130.6, 128.4, 127.7, 126.3, 125.0, 123.1, 111.4, 67.5, 41.5. IR (neat): 2114, 1725, 1614 cm^{-1}. HRMS (ESI-TOF) m/z: $[M + Na - N_2]^+$ calcd for $C_{15}H_{11}N_2OClNa$: 293.0458; found: 293.0386.

*3-azido-1,3-dibenzylindolin-2-one **(83p)*:**

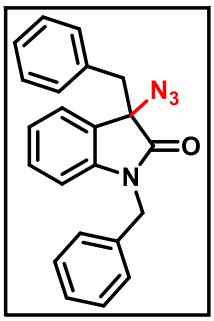

Prepared according to the general procedure **(A)**, using 1,3-dibenzyl-3-hydroxyindolin-2-one (165.0 mg, 0.50 mmol) at 80 °C in dichloroethane to afford 3-azido-1,3-dibenzylindolin-2-one **83p** (88.6 mg, 50%) as a yellow solid after purification by column chromatography on silica gel (EtOAc:hexane = 5:95). Melting point: 114-116 °C. ^{1}H NMR (400 MHz, $CDCl_3$) δ 7.29 (dd, *J* = 7.3, 1.2 Hz, 1H), 7.14 (m, 8H), 6.95 (d, *J* = 7.3 Hz, 2H), 6.71 (d, *J* = 6.6 Hz, 2H), 6.46 (d, *J* = 7.8 Hz, 1H), 5.00 (d, *J* = 16.0 Hz, 1H), 4.51 (d, *J* = 16.0 Hz, 1H), 3.43 (s, 2H).

$^{13}C\{^{1}H\}$ NMR (100 MHz, $CDCl_3$) δ 173.9, 142.7, 134.6, 133.1, 130.6, 130.2, 128.7, 128.2, 127.4, 127.3 126.7, 126.2, 124.5, 122.9, 109.9, 67.7, 43.8, 41.5. IR (neat): 2101, 1720, 1614, 1468 cm^{-1}. HRMS (ESI-TOF) m/z: $[M + Na]^+$ calcd for $C_{22}H_{18}N_4ONa$: 377.1379; found: 377.1378. Crystal preparation: The crystal is grown by the simple recrystallization method. The pure compound isolated after column chromatography is dissolved in dichloromethane and layered with hexane and kept at room temperature for 2 days to get the pure crystal.

5-(azidomethyl)benzo[d][1,3]dioxole ***(83q):***[111]

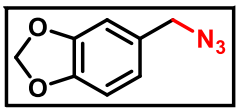

Prepared according to the general procedure **(B)**, a solution of 0.1 M benzo[d][1,3]dioxol-5-ylmethanol (76.0 mg, 0.50 mmol) in 5 mL dichloromethane was flown through the packed bed of Amberlyst®-15 (bed height 6.0 cm) with 0-1 bar at 0.1 mL/min to afford 5-(azidomethyl)benzo[*d*][1,3]dioxole **83q** (161.0 mg, 91%) as a colourless oil after purification by column chromatography on silica gel (EtOAc:hexane = 0:100). ^{1}H NMR (400 MHz, $CDCl_3$) δ 6.78 (m, 3H), 5.97 (s, 2H), 4.23 (s, 2H). ^{13}C NMR (100 MHz, $CDCl_3$) δ 148.1, 147.8, 129.1, 122.0, 108.8, 108.4, 101.3, 54.8. IR (neat): 2091, 1488, 1443 cm^{-1}.

5-(azidomethyl)-6-chlorobenzo[d][1,3]dioxole ***(83r):***[115]

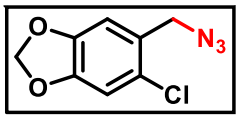

Prepared according to the general procedure **(B)**, a solution of 0.1 M (6-chlorobenzo[*d*][1,3]dioxol-5-yl)methanol (93.0 mg, 0.50 mmol) in 5 mL dichloromethane was flown through the packed bed of Amberlyst®-15 (bed height 6.0 cm) with 0-1 bar at 0.1 mL/min to afford 5-(azidomethyl)-6-chlorobenzo[*d*][1,3]dioxole **83r** (103.0 mg, 97%) as a colourless oil after purification by column chromatography on silica gel (EtOAc:hexane = 1:99). ^{1}H NMR (400 MHz, $CDCl_3$) δ 6.87 (s, 1H), 6.83 (s, 1H), 5.99 (s, 2H), 4.37 (s, 2H). ^{13}C NMR (100 MHz, $CDCl_3$) δ 148.3, 147.0, 126.3, 126.0, 110.1, 109.7, 102.1, 52.2. IR (neat): 2098, 1505, 1476, 1235 cm^{-1}. HRMS (ESI-TOF) m/z: $[M + H - N_2]^+$ calcd for $C_8H_7NO_2Cl$: 184.0165; found: 184.0163.

4-(azidomethyl)pyrene ***(83s)*****:**

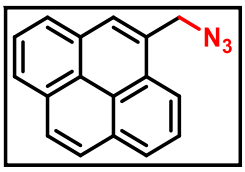

Batch condition: Prepared according to the general procedure **(A)**, using 1-Pyrenemethanol (116.0 mg, 0.50 mmol) to afford 4-(azidomethyl)pyrene **83s** (90.0 mg, 70%) as a pale yellow solid after purification by column chromatography on silica gel (EtOAc:hexane = 1:99).

Flow condition: Prepared according to the general procedure **(B)**, a solution of 0.1 M 1-Pyrenemethanol (116.0 mg, 0.50 mmol) in 5 mL dichloromethane was flown through the packed bed of Amberlyst®-15 (bed height 6.0 cm) with 0-1 bar at 0.1 mL/min to afford 4-(azidomethyl)pyrene **83s** (103.0 mg, 80%) as a pale yellow solid after purification by column chromatography on silica gel (EtOAc:hexane = 1:99). Melting point: 67-69 °C. ^{1}H NMR (400 MHz, $CDCl_3$) δ 8.09 (m, 9H), 4.99 (s, 2H). ^{13}C NMR (100 MHz, $CDCl_3$) δ 131.8, 131.3, 130.8, 129.3, 128.4, 128.3, 127.9, 127.5, 127.4, 126.3, 125.7, 125.6, 125.1, 124.7, 122.7, 53.2. IR (neat): 2031, 1508, 1291, 841 cm^{-1}. HRMS (ESI-TOF) m/z: $[M + H - N_2]^+$ calcd for $C_{17}H_{12}N$: 230.0970; found: 230.0970.

2-azido-2-benzyl-2H-benzo[b][1,4]oxazin-3(4H)-one ***(85a)*** **:**

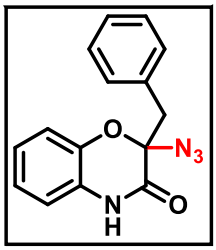

Prepared according to the general procedure **(C)**, a solution of 0.1 M 3-benzyl-3-(tert-butylperoxy)indolin-2-one (155.5 mg, 0.50 mmol) in 5 mL dichloromethane was flown through the packed bed of Amberlyst®-15 (bed height 6.0 cm) with 0-1 bar at 0.1 mL/min to afford 2-azido-2-benzyl-2*H*-benzo[*b*][1,4]oxazin-3(4*H*)-one **85a** (95.0 mg, 68%) as pale yellow solid after purification by column chromatography on silica gel (EtOAc:hexane = 8:92). Melting point: 79-81 °C. ^{1}H NMR (400 MHz, $CDCl_3$) δ 9.92 (s, 1H), 7.46 (m, 2H), 7.32 (m, 3H), 7.08 (m, 3H), 6.93 (m, 1H), 3.69 (d, *J* = 14.0 Hz, 1H), 3.50 (d, *J* = 14.0 Hz, 1H). ^{13}C NMR (100 MHz, $CDCl_3$) δ 162.5, 140.8, 133.1, 131.3, 128.3, 127.6, 125.6, 124.8, 123.9, 117.8, 115.9, 91.6, 40.4. IR (neat): 2111, 1607, 1501, 1210 cm^{-1}. HRMS (ESI-TOF) m/z: $[M + Na]^+$ calcd for $C_{15}H_{12}N_4O_2Na$: 303.0858; found: 303.0864.

*2-azido-2-methyl-2H-benzo[b][1,4]oxazin-3(4H)-one **(85b)**:*

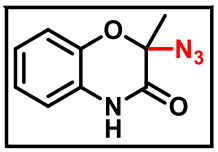

Prepared according to the general procedure **(C)**, a solution of 0.1 M 3-(tert-butylperoxy)-3-methylindolin-2-one (117.5 mg, 0.50 mmol) in 5 mL dichloromethane was flown through the packed bed of Amberlyst®-15 (bed height 6.0 cm) with 0-1 bar at 0.1 mL/min to afford 2-azido-2-methyl-2*H*-benzo[*b*][1,4]oxazin-3(4*H*)-one **85b** (96.0 mg, 94%) as pale yellow solid after purification by column chromatography on silica gel (EtOAc:hexane = 8:92). Melting point: 114-116 °C. ^{1}H NMR (400 MHz, $CDCl_3$) δ 9.29 (s, 1H), 7.06 (m, 3H), 6.93 (dd, *J* = 4.5, 2.4 Hz, 1H), 1.98 (s, 3H). ^{13}C NMR (100 MHz, $CDCl_3$) δ 163.0, 141.0, 126.1, 124.7, 123.9, 117.8, 116.0, 90.3, 20.7. IR (neat): 2118, 1699, 1506 cm^{-1}. HRMS (ESI-TOF) m/z: $[M + H - N_2]^+$ calcd for $C_9H_9N_2O_2$: 177.0664; found: 177.0668.

*2-azido-2-(4-methoxyphenyl)-2H-benzo[b][1,4]oxazin-3(4H)-one **(85c)**:*

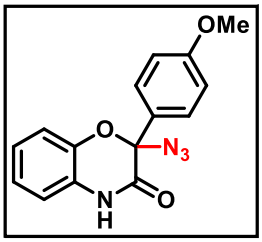

Prepared according to the general procedure **(C)**, a solution of 0.1 M 3-(tert-butylperoxy)-3-(4-methoxyphenyl)indolin-2-one (88.0 mg, 0.27 mmol) in 2.7 mL dichloromethane was flown through the packed bed of Amberlyst®-15 (bed height 6.0 cm) with 0-1 bar at 0.1 mL/min to afford 2-azido-2-(4-methoxyphenyl)-2*H*-benzo[*b*][1,4]oxazin-3(4*H*)-one **85c** (57.0 mg, 72%) as yellow semi solid after purification by column chromatography on silica gel (EtOAc:hexane = 8:92). ^{1}H NMR (400 MHz, $CDCl_3$) δ 8.26 (d, *J* = 8.2 Hz, 1H), 7.62 (m, 2H), 7.38 (d, *J* = 7.9 Hz, 1H), 7.20 (d, *J* = 7.8 Hz, 1H), 6.77 (s, 4H), 3.76 (s, 3H). ^{13}C NMR (100 MHz, $CDCl_3$) δ 154.5, 153.8, 149.7, 139.7, 134.5, 132.7, 124.7, 120.6, 116.1, 114.9, 102.2, 55.9. IR (neat): 2151, 1720, 1510, 1222 cm^{-1}. HRMS (ESI-TOF) m/z: $[M + H – N_2]^+$ calcd for $C_{15}H_{13}N_2O_3$: 269.0926; found: 269.0934.

*2-azido-2-(2-fluorobenzyl)-2H-benzo[b][1,4]oxazin-3(4H)-one **(85d)**:*

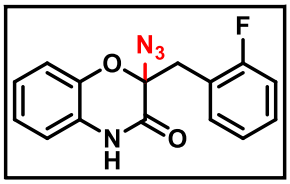

Prepared according to the general procedure **(C)**, a solution of 0.1 M 3-(tert-butylperoxy)-3-(2-fluorobenzyl)indolin-2-one (45.0 mg, 0.14 mmol) in 1.4 mL dichloromethane was flown through the packed bed of Amberlyst®-15 (bed height 6.0 cm) with 0-1 bar at 0.1 mL/min to afford 2-azido-2-methyl-2*H*-benzo[*b*][1,4]oxazin-3(4*H*)-one **85d** (20.7 mg, 51%) as pale yellow

solid after purification by column chromatography on silica gel (EtOAc:hexane = 8:92). Melting point: 126-128 °C. ^{1}H NMR (400 MHz, $CDCl_3$) δ 9.52 (s, 1H), 7.47 (m, 1H), 7.26 (m, 1H), 7.06 (m, 5H), 6.91 (m, 1H), 3.68 (d, *J* = 14.3 Hz, 1H), 3.61 (d, *J* = 14.4 Hz, 1H). ^{13}C{^{1}H} NMR (100 MHz, $CDCl_3$) δ 163.3, 162.5, 160.9, 140.7, 132.9 (d, *J* = 3.5 Hz), 129.6 (d, *J* = 8.2 Hz), 125.5, 124.8, 123.99 (d, *J* = 5.4 Hz), 120.5 (d, *J* = 15.2 Hz), 118.0, 116.0 , 115.6, 115.4, 91.5, 33.1 (d, *J* = 2.5 Hz). IR (neat): 2110, 1690, 1501, 750 cm^{-1}. HRMS (ESI-TOF) m/z: $[M + H - N_2]^+$ calcd for $C_{15}H_{12}N_2O_2F$: 271.0883; found: 271.0890.

*2-azido-2-(4-bromobenzyl)-2H-benzo[b][1,4]oxazin-3(4H)-one **(85e)*:**

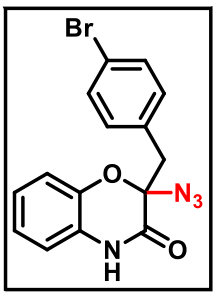

Prepared according to the general procedure **(C)**, a solution of 0.1 M 3-(4-bromobenzyl)-3-(tert-butylperoxy)indolin-2-one (116.7 mg, 0.30 mmol) in 3 mL dichloromethane was flown through the packed bed of Amberlyst®-15 (bed height 6.0 cm) with 0-1 bar at 0.1 mL/min to afford 2-azido-2-(4-bromobenzyl)-2*H*-benzo[*b*][1,4]oxazin-3(4*H*)-one **85e** (70.8 mg, 66%) as pale yellow solid after purification by column chromatography on silica gel (EtOAc:hexane = 8:92). Melting point: 141-143 °C. ^{1}H NMR (400 MHz, $CDCl_3$) δ 9.70 (s, 1H), 7.41 (d, *J* = 8.4 Hz, 2H), 7.31 (d, *J* = 8.4 Hz, 2H), 7.07 (m, 3H), 6.90 (m, 1H), 3.64 (d, *J* = 14.0 Hz, 1H), 3.41 (d, *J* = 14.0 Hz, 1H). ^{13}C NMR (100 MHz, $CDCl_3$) δ 162 .4, 140.6, 133.0, 132.1, 131.5, 125.4, 124.9, 124.0, 121.9, 117.8, 116.0, 91.4, 39.8. IR (neat): 2113, 1698, 1504, 751 cm^{-1}. HRMS (ESI-TOF) m/z: $[M + H - N_2]^+$ calcd for $C_{15}H_{12}BrN_2O_2$: 331.0082; found: 331.0081. Crystal preparation: The crystal is grown by the simple recrystallization method. The pure compound isolated after column chromatography is dissolved in dichloromethane and layered with hexane and kept at room temperature for 2 days to get the pure crystal.

*2-azido-2-benzyl-6-chloro-2H-benzo[b][1,4]oxazin-3(4H)-one **(85f)*:**

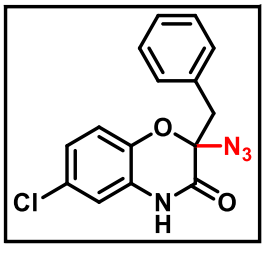

Prepared according to the general procedure **(C)**, a solution of 0.1 M 3-benzyl-3-(tert-butylperoxy)-6-chloroindolin-2-one (88.0 mg, 0.26 mmol) in 2.6 mL dichloromethane was flown through the packed bed of Amberlyst®-15 (bed height 6.0 cm) with 0-1 bar at 0.1 mL/min to afford 2-azido-2-benzyl-6-chloro-2*H*-benzo[*b*][1,4]oxazin-3(4*H*)-one **85f** (32.0 mg, 40%) as

white solid after purification by column chromatography on silica gel (EtOAc:hexane = 8:92). Melting point: 113-115 °C. ^{1}H NMR (400 MHz, $CDCl_3$) δ 8.45 (s, 1H), 7.34 (m, 5H), 6.99 (m, 2H), 6.82 (d, *J* = 1.7 Hz, 1H), 3.66 (d, *J* = 13.9 Hz, 1H), 3.45 (d, *J* = 13.9 Hz, 1H). ^{13}C NMR (100 MHz, $CDCl_3$) δ 161.7, 139.4, 132.8, 131.3, 128.9, 128.4, 127.7, 126.6, 124.5, 119.0, 115.6, 91.6, 40.3. IR (neat): 2114, 1699 cm^{-1}. HRMS (ESI-TOF) m/z: $[M + H - N_2]^+$ calcd for $C_{15}H_{12}ClN_2O_2$: 287.0587; found: 287.0581.

2-azido-2-(4-bromobenzyl)-6-chloro-2H-benzo[b][1,4]oxazin-3(4H)-one ***(85g)*****:**

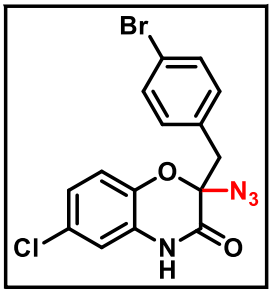

Prepared according to the general procedure **(C)**, a solution of 0.1 M 3-(4-bromobenzyl)-3-(tert-butylperoxy)-6-chloroindolin-2-one (103.0 mg, 0.24 mmol) in 2.4 mL dichloromethane was flown through the packed bed of Amberlyst®-15 (bed height 6.0 cm) with 0-1 bar at 0.1 mL/min to afford 2-azido-2-(4-bromobenzyl)-6-chloro-2*H*-benzo[*b*][1,4]oxazin-3(4*H*)-one **85g** (27.6 mg, 28%) as white semi solid after purification by column chromatography on silica gel (EtOAc:hexane = 8:92). ^{1}H NMR (400 MHz, $CDCl_3$) δ 9.28 (s, 1H), 7.42 (d, *J* = 8.4 Hz, 2H), 7.28 (d, *J* = 8.4 Hz, 2H), 7.02 (m, 2H), 6.87 (s, 1H), 3.62 (d, *J* = 13.9 Hz, 1H), 3.40 (d, *J* = 14.0 Hz, 1H). ^{13}C NMR (100 MHz, $CDCl_3$) δ 162.0, 139.2, 133.0, 131.8, 131.6, 129.1, 126.4, 124.7, 122.0, 119.0, 115.9, 91.3, 39.7. IR (neat): 2111, 1704 cm^{-1}. HRMS (ESI-TOF) m/z: $[M + H - N_2]^+$ calcd for $C_{15}H_{11}N_2O_2BrCl$: 364.9692; found: 364.9694.

2-azido-6-chloro-2-(4-methylbenzyl)-2H-benzo[b][1,4]oxazin-3(4H)-one ***(85h)*****:**

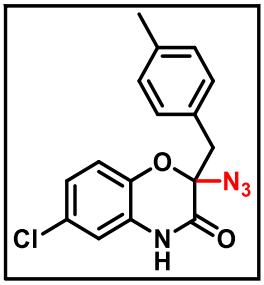

Prepared according to the general procedure **(C)**, a solution of 0.1 M 3-(tert-butylperoxy)-6-chloro-3-(4-methylbenzyl)indolin-2-one (64.0 mg, 0.18 mmol) in 1.8 mL dichloromethane was flown through the packed bed of Amberlyst®-15 (bed height 6.0 cm) with 0-1 bar at 0.1 mL/min to afford 2-azido-6-chloro-2-(4-methylbenzyl)-2*H*-benzo[*b*][1,4]oxazin-3(4*H*)-one **85h** (26.2 mg, 45%) as pale yellow solid after purification by column chromatography on silica gel (EtOAc:hexane = 8:92). Melting point: 130-132 °C^{1}H NMR (400 MHz, $CDCl_3$) δ 9.66 (s, 1H), 7.30 (d, *J* = 7.8 Hz, 2H), 7.11 (d, *J* = 7.7 Hz, 2H), 7.01 (s, 2H), 6.89 (s, 1H), 3.62 (d, *J* = 14.0 Hz, 1H), 3.43 (d, *J* = 14.1 Hz, 1H), 2.31 (s, 3H). ^{13}C{^{1}H} NMR (100

MHz, $CDCl_3$) δ 162.7, 139.5, 137.4, 131.1, 129.7, 129.1, 128.9, 126.6, 124.5, 118.9, 115.9, 91.6, 39.9, 21.2. IR (neat): 2117, 1698, 1645 cm^{-1}. HRMS (ESI-TOF) m/z: $[M + H - N_2]^+$ calcd for $C_{16}H_{14}N_2O_2Cl$: 301.0744; found: 301.0738.

*2-azido-2,4-dimethyl-2H-benzo[b][1,4]oxazin-3(4H)-one **(85i)**:*

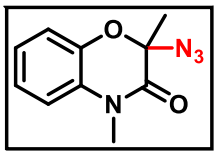

Prepared according to the general procedure **(C)**, a solution of 0.1 M 3-(tert-butylperoxy)-1,3-dimethylindolin-2-one (150.0 mg, 0.60 mmol) in 6.1 mL dichloromethane was flown through the packed bed of Amberlyst®-15 (bed height 6.0 cm) with 0-1 bar at 0.1 mL/min to afford 2-azido-2,4-dimethyl-2*H*-benzo[*b*][1,4]oxazin-3(4*H*)-one **85i** (85.0 mg, 65%) as white solid after purification by column chromatography on silica gel (EtOAc:hexane = 8:92). Melting point: 60-62 °C. ^1H NMR (400 MHz, $CDCl_3$) δ 7.12 (dq, *J* = 12.0, 4.2 Hz, 1H), 7.07 (d, *J* = 4.0 Hz, 2H), 7.00 (d, *J* = 7.8 Hz, 1H), 3.39 (s, 3H), 1.97 (s, 3H). $^{13}C\{^1H\}$ NMR (100 MHz, $CDCl_3$) δ 161.6, 141.5, 129.2 124.3, 123.9, 117.8, 114.7, 90.1, 29.0, 21.1. IR (neat): 2109, 1680, 1503, 1381 cm^{-1}. HRMS (ESI-TOF) m/z: $[M + H – N_2]^+$ calcd for $C_{10}H_{11}N_2O_2$: 191.0821; found: 191.0820.

*2-azido-4-benzyl-2-methyl-2H-benzo[b][1,4]oxazin-3(4H)-one **(85j)**:*

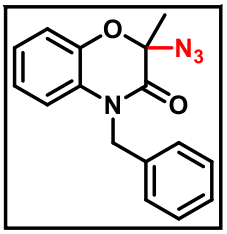

Prepared according to the general procedure **(C)**, a solution of 0.1 M 1-benzyl-3-(tert-butylperoxy)-3-methylindolin-2-one (56.2 mg, 0.17 mmol) in 1.7 mL dichloromethane was flown through the packed bed of Amberlyst®-15 (bed height 6.0 cm) with 0-1 bar at 0.1 mL/min to afford 2-azido-4-benzyl-2-methyl-2*H*-benzo[*b*][1,4]oxazin-3(4*H*)-one **85j** (23.0 mg, 46%) as white semi solid after purification by column chromatography on silica gel (EtOAc:hexane = 8:92). ^1H NMR (400 MHz, $CDCl_3$) δ 7.34 (m, 2H), 7.27 (m, 3H), 7.10 (dd, *J* = 7.7, 1.5 Hz, 1H), 7.04 (m, 1H), 6.99 (m, 1H), 6.89 (m, 1H), 5.48 (d, *J* = 16.1 Hz, 1H), 4.86 (d, *J* = 16.1 Hz, 1H), 2.06 (s, 3H). ^{13}C NMR (100 MHz, $CDCl_3$) δ 161.9, 141.7, 135.6, 129.1, 127.7, 126.4, 124.4, 123.9, 118.0, 115.5, 90.2, 45.8, 21.0. IR (neat): 2114, 1697, 1499, 1397 cm^{-1}. HRMS (ESI-TOF) m/z: $[M + H - N_2]^+$ calcd for $C_{16}H_{15}N_2O_2$: 267.1134; found: 267.1125.

diphenylmethanamine ***(87a)*****:**[116]

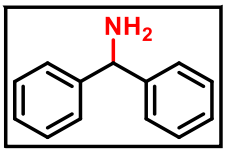

Prepared according to the general procedure **(E)**, using 3M (azidomethylene)dibenzene (627.0 mg, 3.0 mmol) in THF to afford diphenylmethanamine **87a** (320.0 mg, 58%) as a white solid after purification by column chromatography on silica gel (EtOAc:hexane = 20:80). Melting point: 293-294 °C. ^{1}H NMR (400 MHz, DMSO-d_6) δ 7.46 (d, *J* = 7.3 Hz, 4H), 7.32 (d, *J* = 8.9 Hz, 4H), 7.20 (m, 2H), 5.15 (s, 1H). ^{13}C NMR (100 MHz, DMSO-d_6) δ 146.8, 128.1, 126.7, 126.3, 59.3. IR (neat): 3853, 3741, 3302, 3059, 3030, 2926, 2855, 1746, 1558 cm^{-1}. HRMS (ESI-TOF) m/z: $[M + H]^+$ calcd for $C_{13}H_{14}N$: 184.1126; found: 184.1117.

1-benzhydryl-4-phenyl-1H-1,2,3-triazole ***(89a)****:*[117]

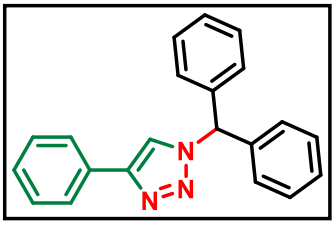

Prepared according to the general procedure (**F**), using (azidomethylene)dibenzene (124.5 mg, 0.59 mmol) to afford 1-benzhydryl-4-phenyl-1*H*-1,2,3-triazole **89a** (113.5 mg, 73%) as a white solid after purification by column chromatography on silica gel (EtOAc:hexane = 10:90). Melting point: 177-179 °C. ^{1}H NMR (400 MHz, $CDCl_3$) δ 7.81 (m, 2H), 7.61 (s, 1H), 7.40 (m, 8H), 7.33 (m, 1H), 7.17 (m, 5H). ^{13}C NMR (100 MHz, $CDCl_3$) δ 147.7, 138.3, 130.7, 129.1, 128.9, 128.8, 128.3, 128.2, 125.9, 119.7, 68.2. IR (neat): 3061, 3028, 1491, 1451, 1229, 1079 cm^{-1}. HRMS (ESI-TOF) m/z: $[M + H]^+$ calcd for $C_{21}H_{18}N_3$: 312.1501; found: 312.1492.

4-phenyl-1-(1-phenylethyl)-1H-1,2,3-triazole ***(89b)****:*[117]

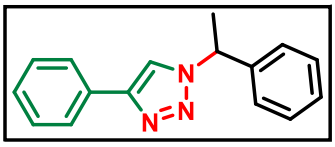

Prepared according to the general procedure (**F**), using (1-azidoethyl)benzene (88.2 mg, 0.59 mmol) to afford 4-phenyl-1-(1-phenylethyl)-1*H*-1,2,3-triazole **89b** (92.6 mg, 62%) as a white solid after purification by column chromatography on silica gel (EtOAc:hexane = 5:95). Melting point: 80-82 °C. ^{1}H NMR (400 MHz, $CDCl_3$) δ 7.80 (m, 2H), 7.63 (s, 1H), 7.35 (m, 8H), 5.87 (q, *J* = 7.1 Hz, 1H), 2.03 (d, *J* = 7.1 Hz, 3H). ^{13}C NMR (100 MHz, $CDCl_3$) δ 140.0, 130.8, 129.2, 128.9, 128.7,

128.2, 126.7, 125.8, 118.5, 60.4, 21.5. IR (neat): 2925, 2855, 1702, 1540 cm^{-1}. HRMS (ESI-TOF) m/z: $[M + H]^+$ calcd for $C_{16}H_{16}N_3$: 250.1346; found: 250.1345.

3-methylquinoxalin-2(1H)-one ***(90i):***[118]

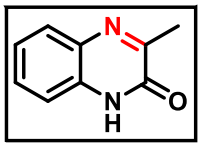

Prepared according to the general procedure (**G**), using 3-azido-3-methylindolin-2-one (56.5 mg, 0.30 mmol) to afford 3-methylquinoxalin-2(1*H*)-one **90i** (39.9 mg, 83%) as a white solid after purification by column chromatography on silica gel (EtOAc:hexane = 15:85). Melting point: 252-254 °C. ^{1}H NMR (400 MHz, DMSO-d_6) δ 12.30 (s, 1H), 7.67 (m, 1H), 7.44 (m, 1H), 7.24 (m, 2H), 2.39 (s, 3H). ^{13}C NMR (100 MHz, DMSO-d_6) δ 159.2, 154.9, 131.9, 131.7,129.3, 127.8, 123.0, 115.2, 20.6. IR (neat): 3392, 2376, 2355, 2318, 2259, 2135, 1651, 1021 cm^{-1}. HRMS (ESI-TOF) m/z: $[M + H]^+$ calcd for $C_9H_9N_2O$: 161.0715; found: 161.0710.

3-(p-tolyl)quinoxalin-2(1H)-one ***(90j):***[119]

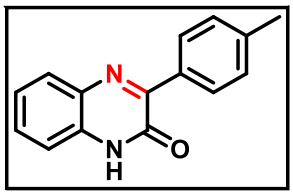

Prepared according to the general procedure (**G**), using 3-azido-3-(p-tolyl)indolin-2-one (79.9 mg, 0.30 mmol) to afford 3-(p-tolyl)quinoxalin-2(1*H*)-one **90j** (50.0 mg, 70%) as a yellow solid after purification by column chromatography on silica gel (EtOAc:hexane = 15:85). Melting point: 268-270 °C. ^{1}H NMR (400 MHz, DMSO-d_6) δ 12.46 (m, 1H), 8.26 (m, 2H), 7.82 (dd, *J* = 8.6, 1.3 Hz, 1H), 7.52 (m, 1H), 7.31 (m, 4H), 2.38 (s, 3H). ^{13}C NMR (100 MHz, DMSO-d_6) δ 154.7, 153.8, 140.1, 132.9, 131.9, 130.1, 129.2, 128.6, 123.4, 115.1, 21.1. IR (neat): 3392, 2376, 2352, 2320, 2259, 2135, 1648 cm^{-1}. HRMS (ESI-TOF) m/z: $[M + H]^+$ calcd for $C_{15}H_{13}N_2O$: 237.1028; found: 237.1019.

3-(4-methoxyphenyl)quinoxalin-2(1H)-one ***(90k):***[119]

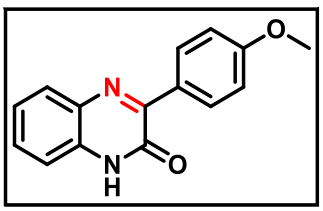

Prepared according to the general procedure (**G**), using 3-azido-3-(4-methoxyphenyl)indolin-2-one (84.0 mg, 0.30 mmol) to afford 3-(4-methoxyphenyl)quinoxalin-2(1*H*)-one **90k** (62.6 mg, 83%) as a pale yellow solid after purification by column chromatography on silica gel (EtOAc:hexane = 15:85). Melting point: 275-276 °C. ^{1}H NMR (400 MHz, DMSO-d_6) δ 12.52 (s,

1H), 8.39 (m, 2H), 7.80 (m, 1H), 7.50 (ddd, *J* = 8.3, 7.1, 1.4 Hz, 1H), 7.30 (dd, *J* = 11.8, 4.4 Hz, 2H), 7.03 (m, 2H), 3.83 (s, 3H). ^{13}C NMR (100 MHz, DMSO-d_6) δ 161.0, 154.7, 153.1, 132.1, 131.8, 131.0, 129.8, 128.5, 128.2, 123.4, 115.0, 113.4, 55.3 IR (neat): 3741, 2921, 2379, 2315, 1706, 1508 cm^{-1}. HRMS (ESI-TOF) m/z: $[M + H]^+$ calcd for $C_{15}H_{13}N_2O_2$: 253.0977; found: 253.0975.

3-benzylquinoxalin-2(1H)-one ***(90l)*****:**[120]

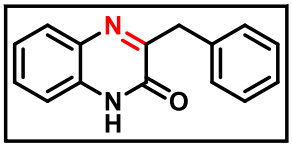

Prepared according to the general procedure (**G**), using 3-azido-3-benzylindolin-2-one (79.0 mg, 0.30 mmol) to afford 3-benzylquinoxalin-2(1*H*)-one **90l** (55.6 mg, 79%) as a white solid after purification by column chromatography on silica gel (EtOAc:hexane = 15:85). Melting point: 198-200 °C. ^{1}H NMR (400 MHz, $CDCl_3$) δ 11.78 (s, 1H), 7.84 (d, J = 7.7 Hz, 1H), 7.48 (m, 3H), 7.31 (m, 3H), 7.22 (m, 2H), 4.29 (s, 2H). ^{13}C NMR (100 MHz, $CDCl_3$) δ 159.94, 158.3, 156.3, 137.1, 132.9, 131.2, 130.1, 129.7, 129.2, 128.6, 126.8, 124.3, 115.6, 40.1. IR (neat): 3800, 2376, 2317, 1743, 1524 cm^{-1}. HRMS (ESI-TOF) m/z: $[M + H]^+$ calcd for $C_{15}H_{12}N_2O$: 237.1028; found: 237.1019.

3-(4-bromobenzyl)quinoxalin-2(1H)-one ***(90n)*****:**[112]

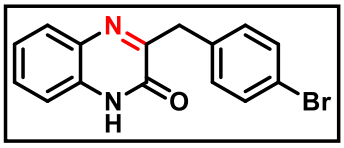

Prepared according to the general procedure (**G**), using 3-azido-3-(4-bromobenzyl)indolin-2-one (100.0 mg, 0.29 mmol) to afford 3-(4-bromobenzyl)quinoxalin-2(1*H*)-one **90n** (74.0 mg, 81%) as a white solid after purification by column chromatography on silica gel (EtOAc:hexane = 15:85). Melting point: 235-238 °C. ^{1}H NMR (400 MHz, DMSO-d_6) δ 12.42 (s, 1H), 7.70 (d, *J* = 7.9 Hz, 1H), 7.47 (d, *J* = 7.1 Hz, 3H), 7.28 (d, *J* = 8.2 Hz, 4H), 4.09 (s, 2H). ^{13}C NMR (100 MHz, DMSO-d_6) δ 159.9, 154.5, 136.9, 132.0, 131.6, 131.2, 129.9, 128.3, 123.2, 119.6, 115.3, 38.4. IR (neat): 2960, 1707, 1422, 1360, 1221, 1092, 979 cm^{-1}.

3.6.B. Copies of ^{1}H and ^{13}C NMR spectra of representative compounds

(azidomethylene)dibenzene (83a)

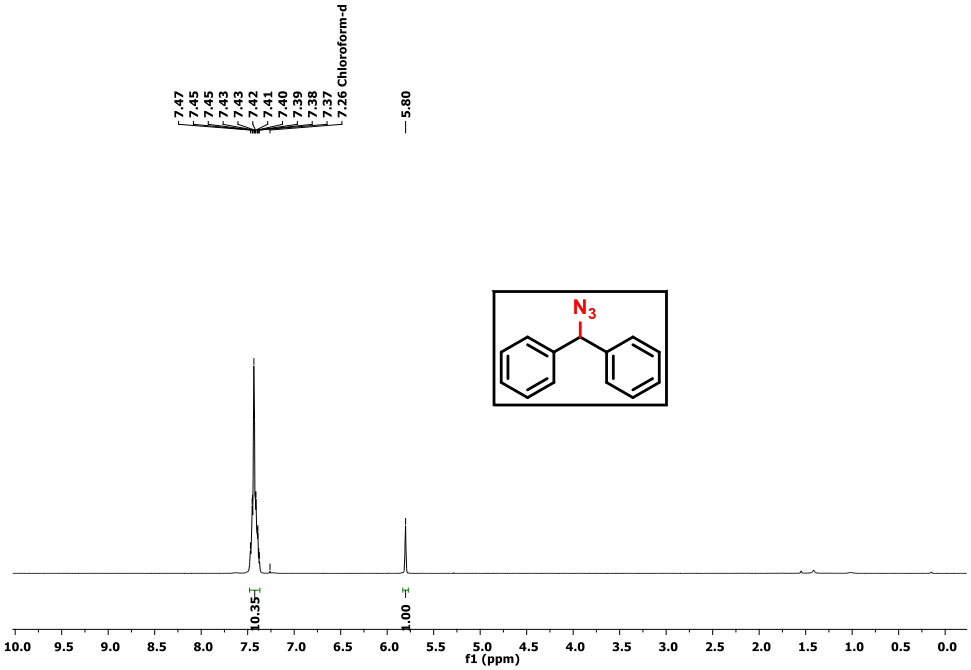

Figure 3.6.B.1: ^{1}H NMR of **83a**, 400 MHz, $CDCl_3$

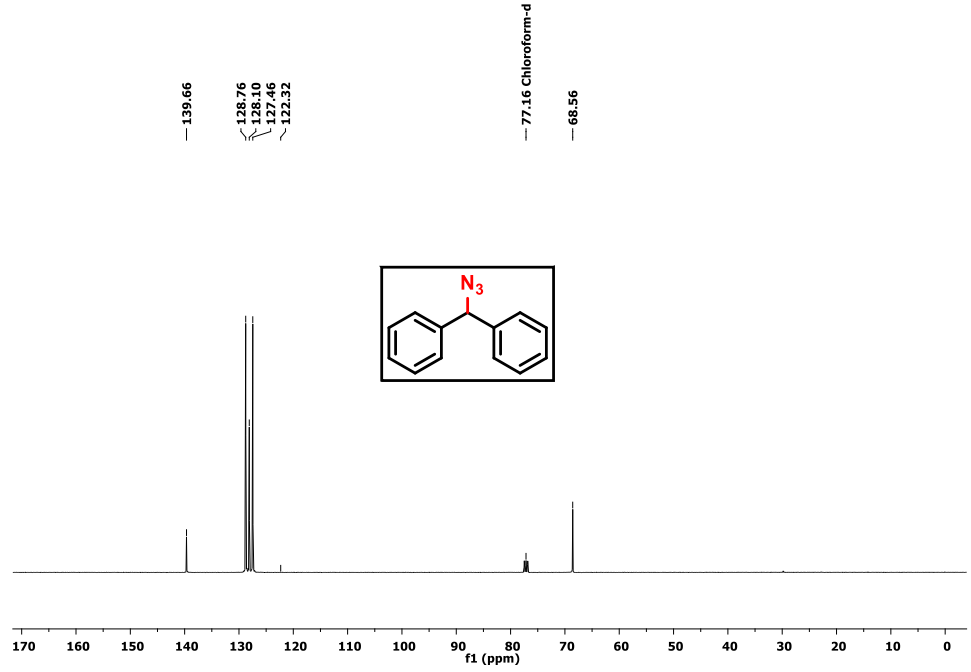

Figure 3.6.B.2: ^{13}C NMR of **83a**, 100 MHz, $CDCl_3$

(1-azidoethyl)benzene (83d)

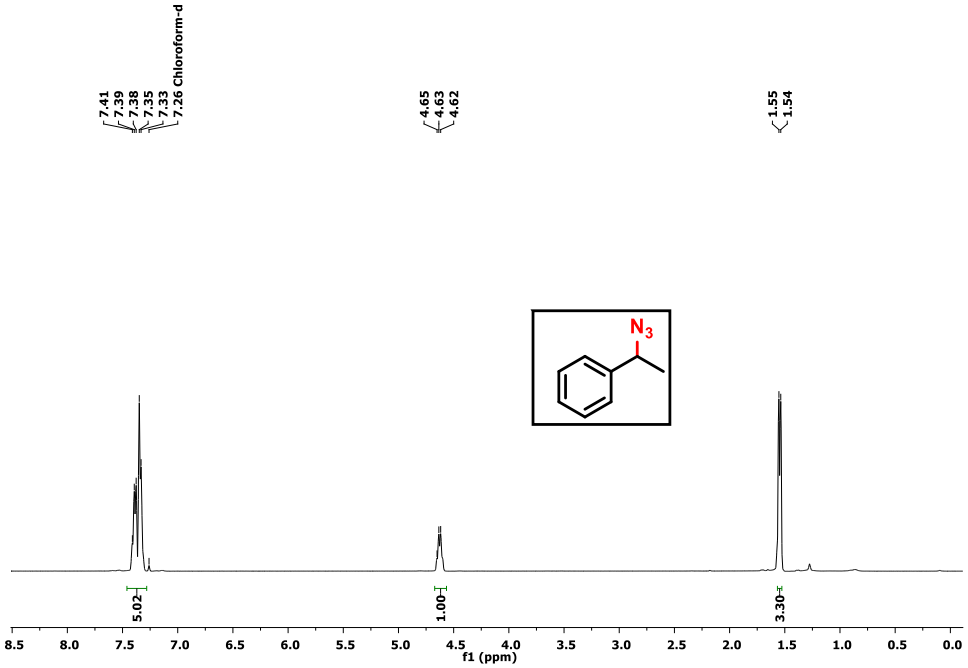

Figure 3.6.B.3: ^{1}H NMR of **83d**, 400 MHz, $CDCl_3$

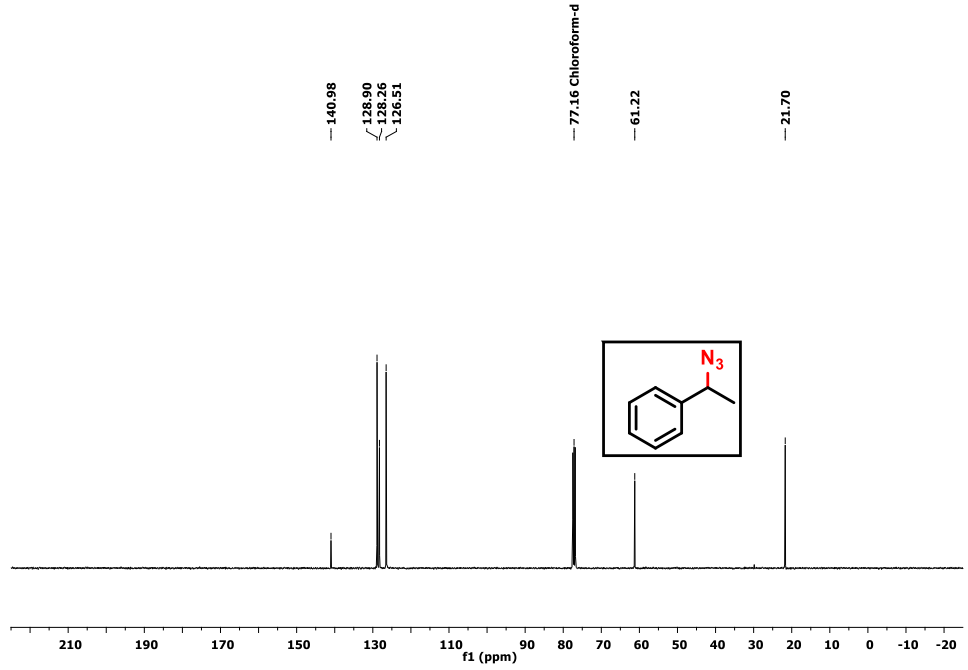

Figure 3.6.B.4: ^{13}C NMR of **83d**, 100 MHz, $CDCl_3$

(1-azidoethane-1,1-diyl)dibenzene (83f)

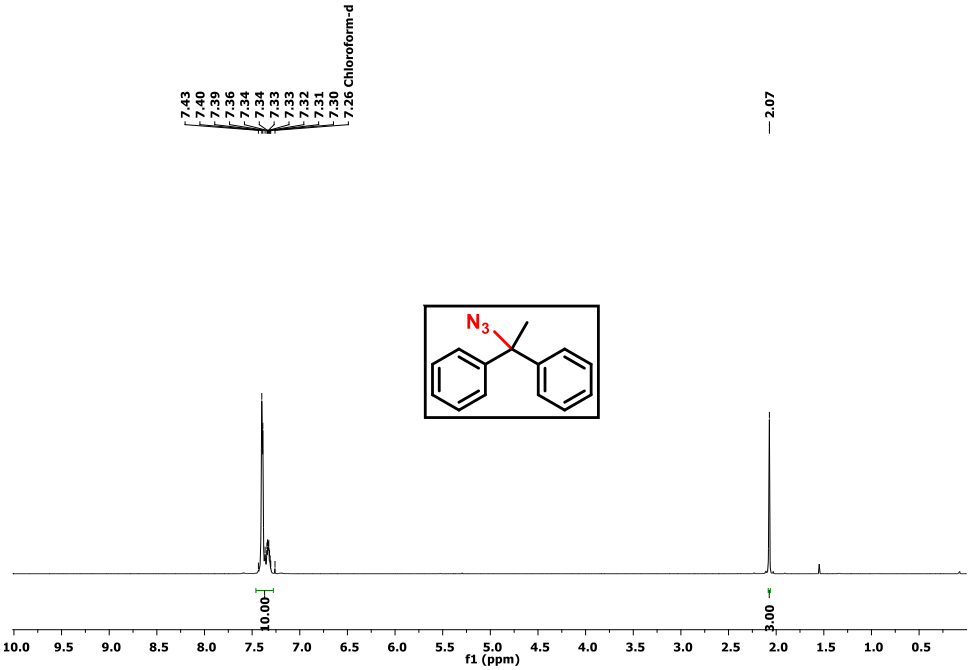

Figure 3.6.B.5: ^{1}H NMR of **83f**, 400 MHz, $CDCl_3$

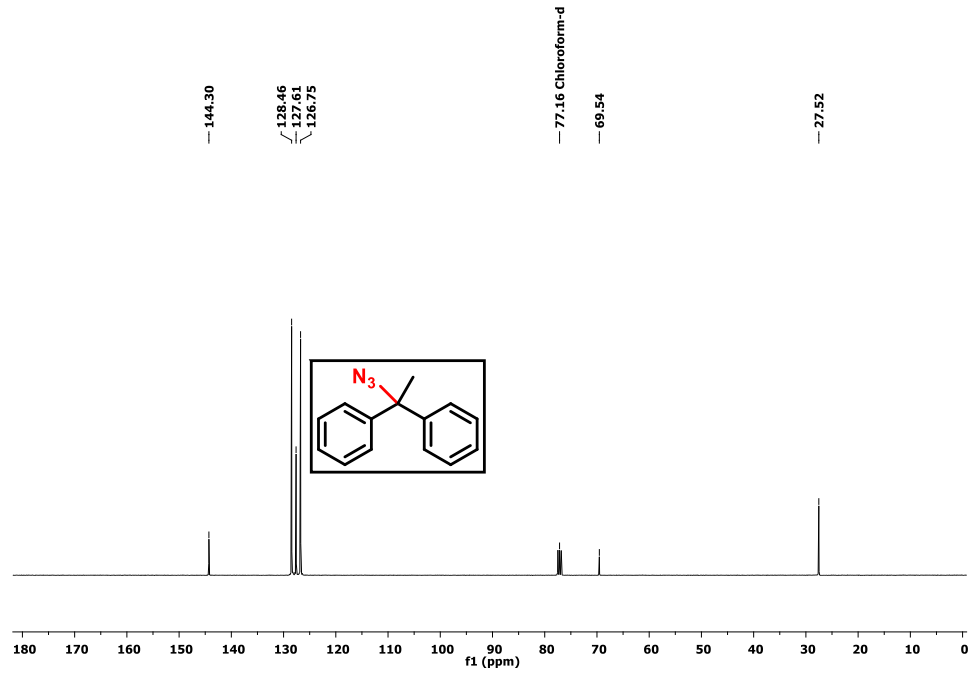

Figure 3.6.B.6: ^{13}C NMR of **83f**, 100 MHz, $CDCl_3$

3-azido-3-methylindolin-2-one (83h)

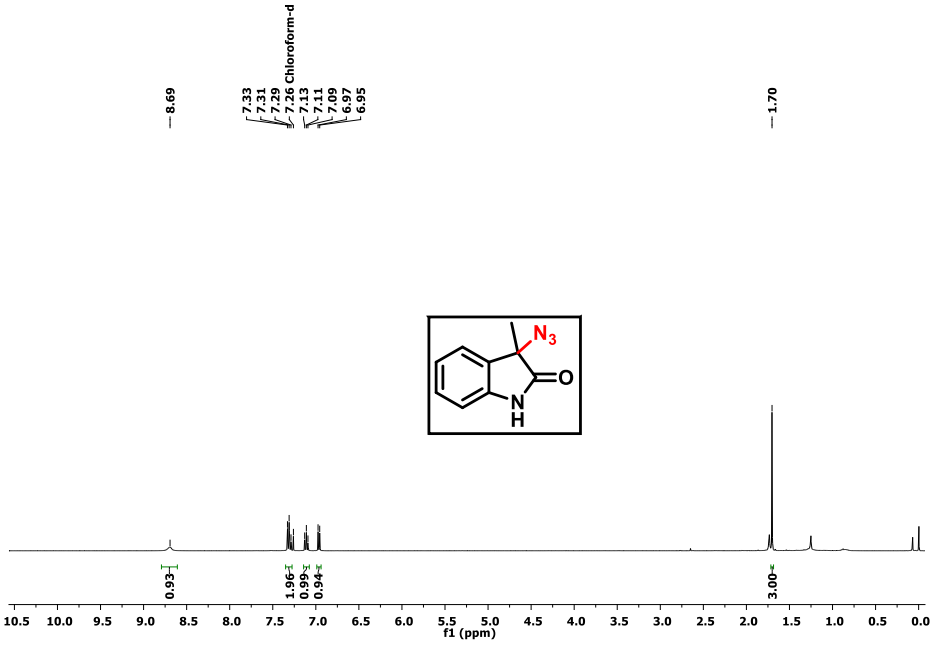

Figure 3.6.B.7: ^{1}H NMR of **83h**, 400 MHz, $CDCl_3$

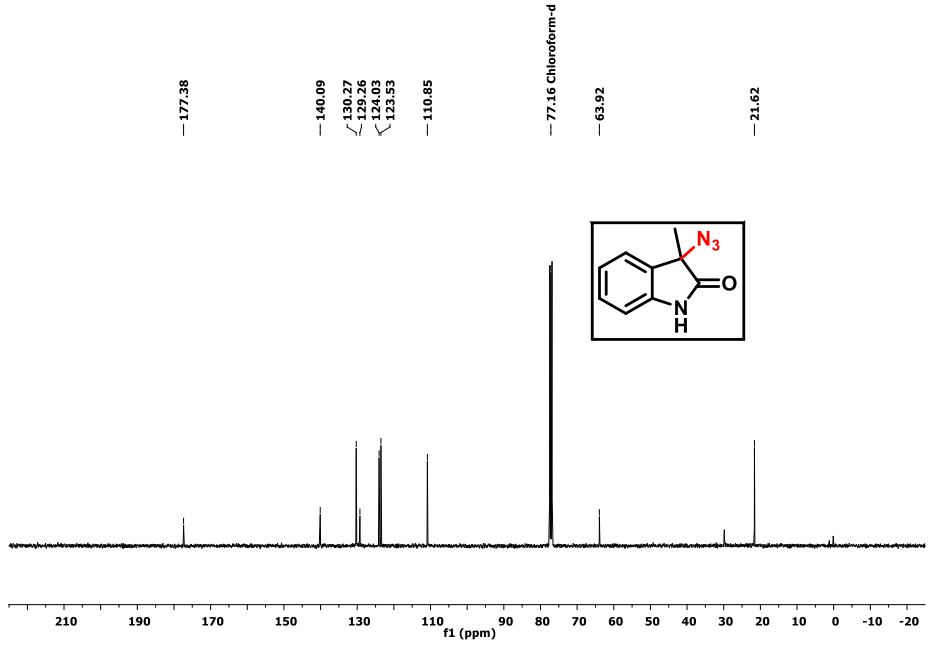

Figure 3.6.B.8: ^{13}C NMR of **83h**, 100 MHz, $CDCl_3$

3-azido-3-(4-bromobenzyl)indolin-2-one (83n)

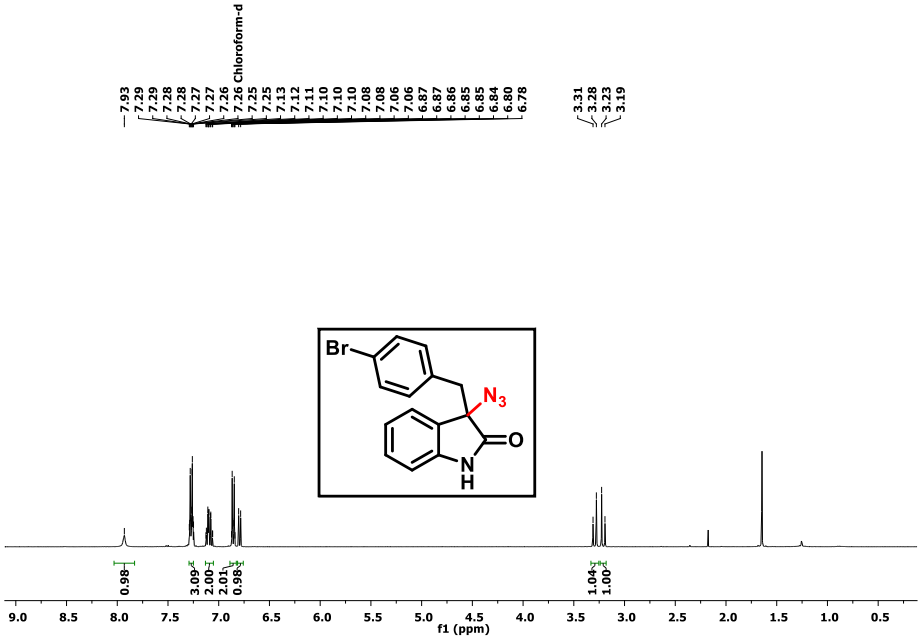

Figure 3.6.B.9: ^{1}H NMR of **83n**, 400 MHz, $CDCl_3$

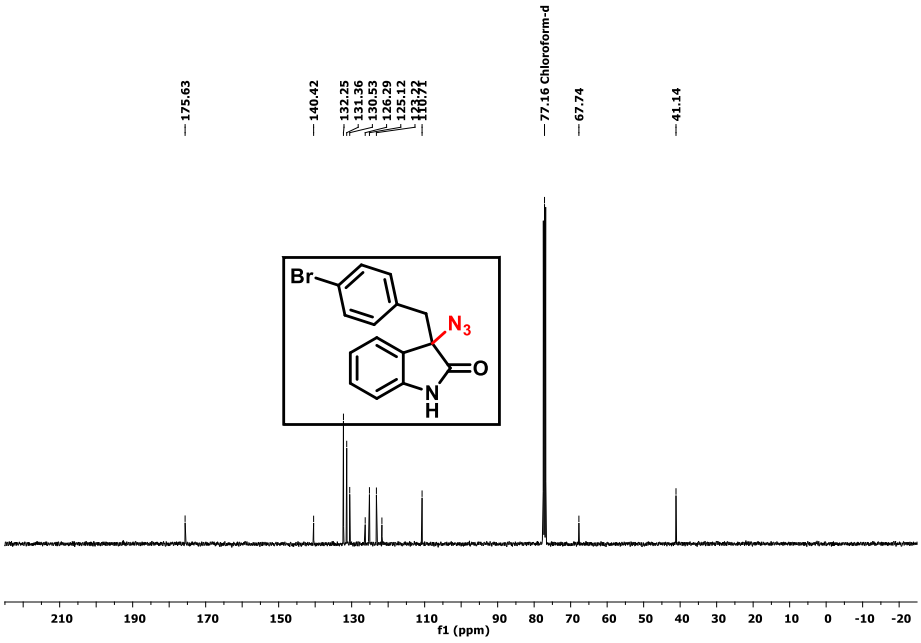

Figure 3.6.B.10: ^{13}C NMR of **83n**, 100 MHz, $CDCl_3$

5-(azidomethyl)benzo[d][1,3]dioxole (83q)

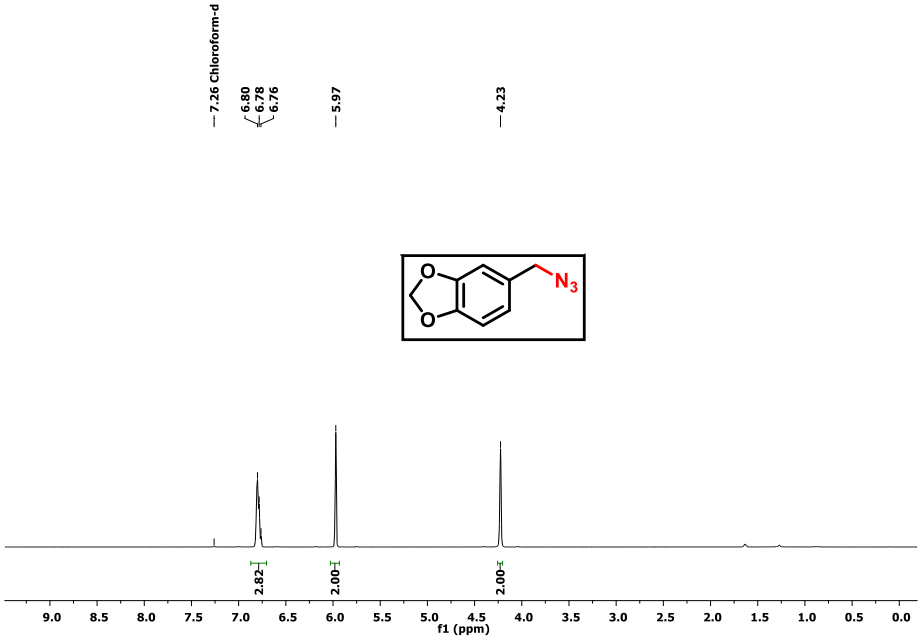

Figure 3.6.B.11: ^{1}H NMR of **83q**, 400 MHz, $CDCl_3$

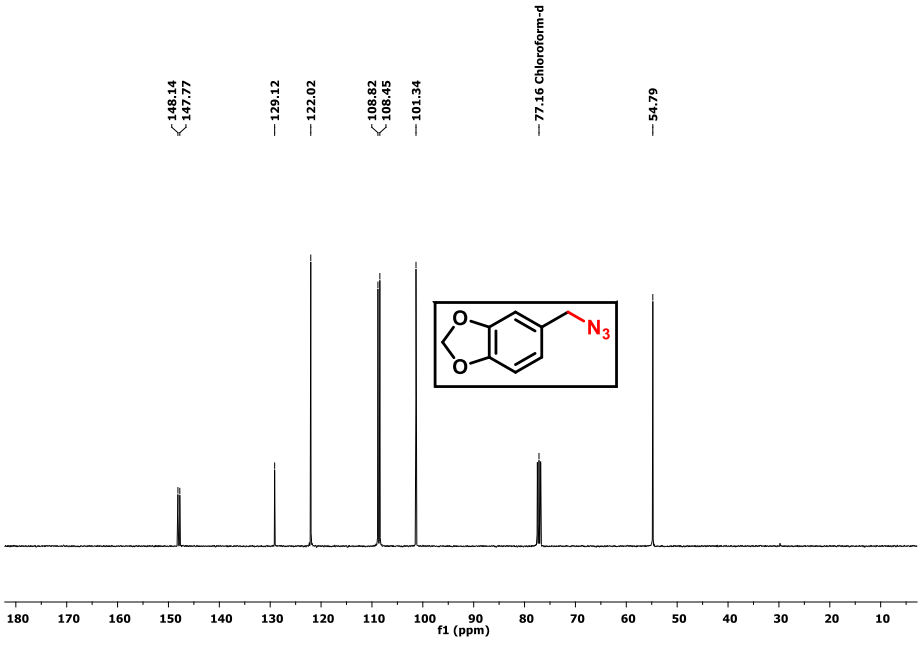

Figure 3.6.B.12: ^{13}C NMR of **83q**, 100 MHz, $CDCl_3$

4-(azidomethyl)pyrene (83s)

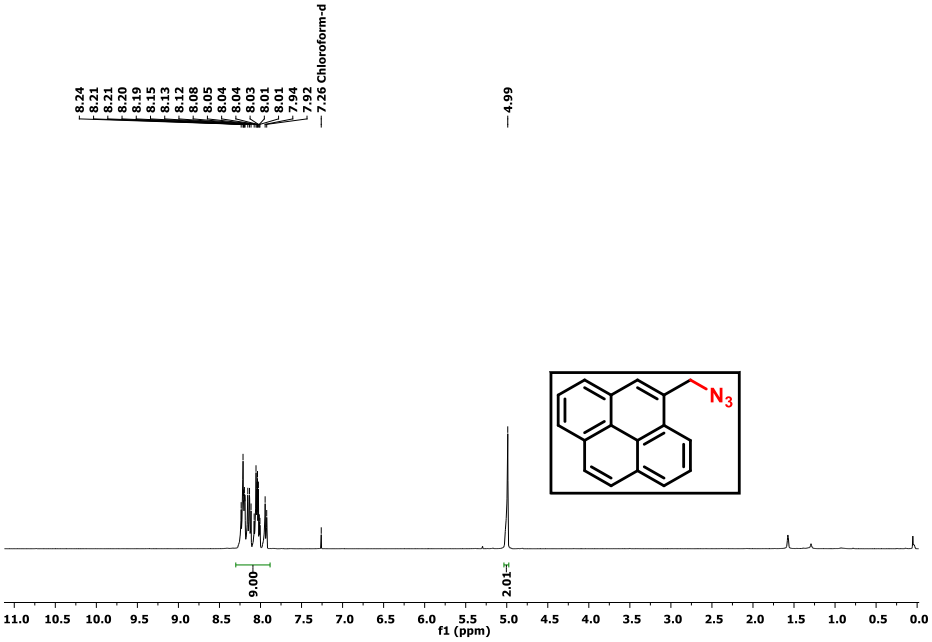

Figure 3.6.B.13: ^{1}H NMR of **83s**, 400 MHz, $CDCl_3$

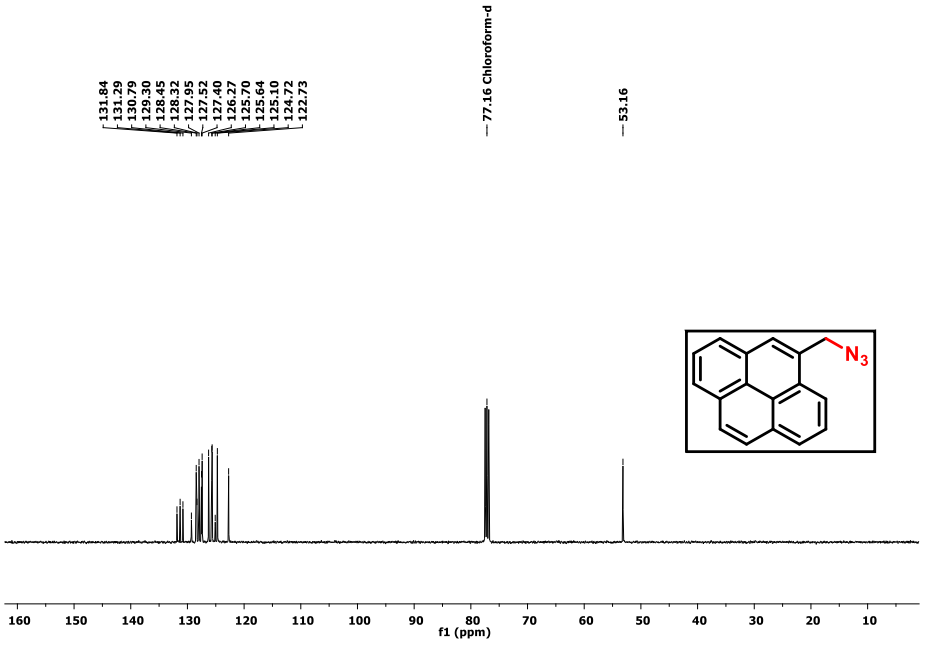

Figure 3.6.B.14: ^{13}C NMR of **83s**, 100 MHz, $CDCl_3$

2-azido-2-methyl-2*H*-benzo[b][1,4]oxazin-3(4*H*)-one (85b)

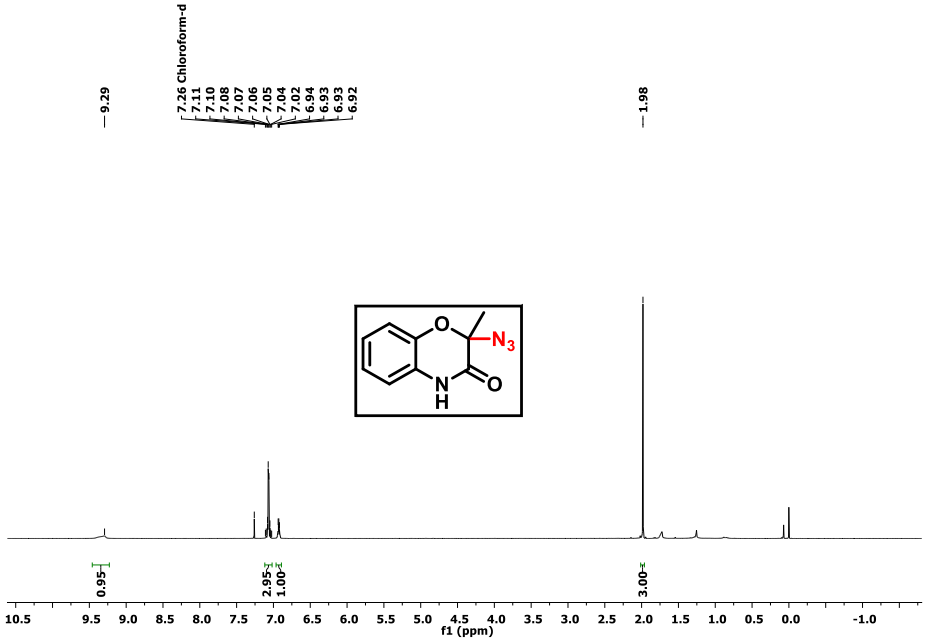

Figure 3.6.B.15: ^{1}H NMR of **85b**, 400 MHz, $CDCl_3$

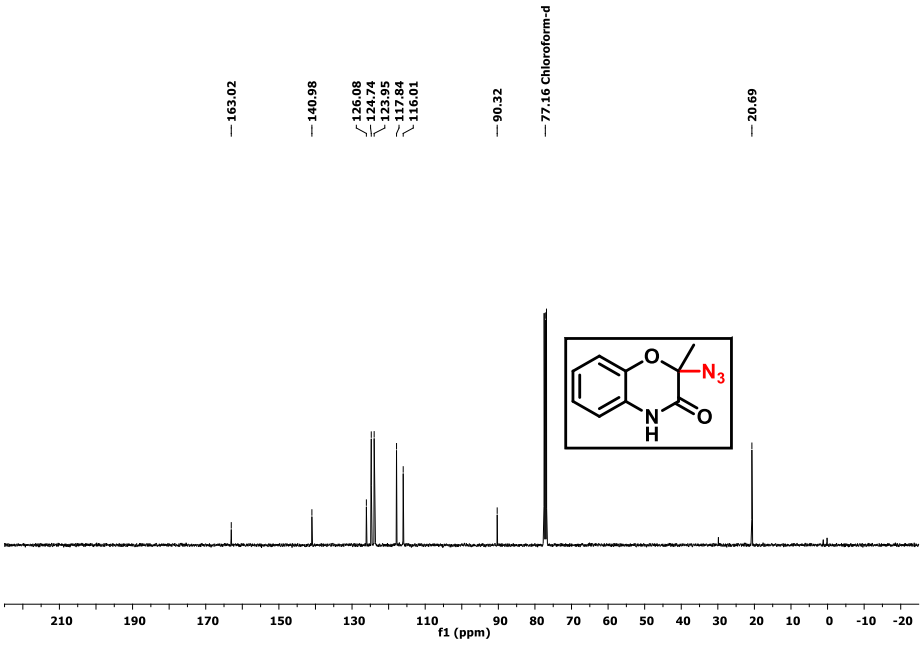

Figure 3.6.B.16: ^{13}C NMR of **85b**, 100 MHz, $CDCl_3$

2-azido-2-(4-bromobenzyl)-2*H*-benzo[b][1,4]oxazin-3(4*H*)-one (85e)

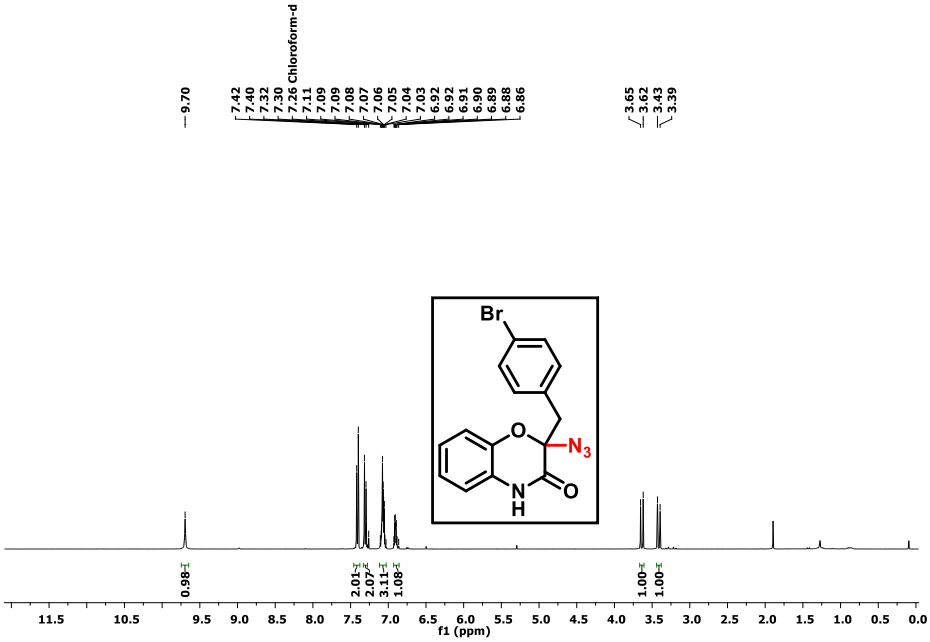

Figure 3.6.B.17: ^{1}H NMR of **85e**, 400 MHz, $CDCl_3$

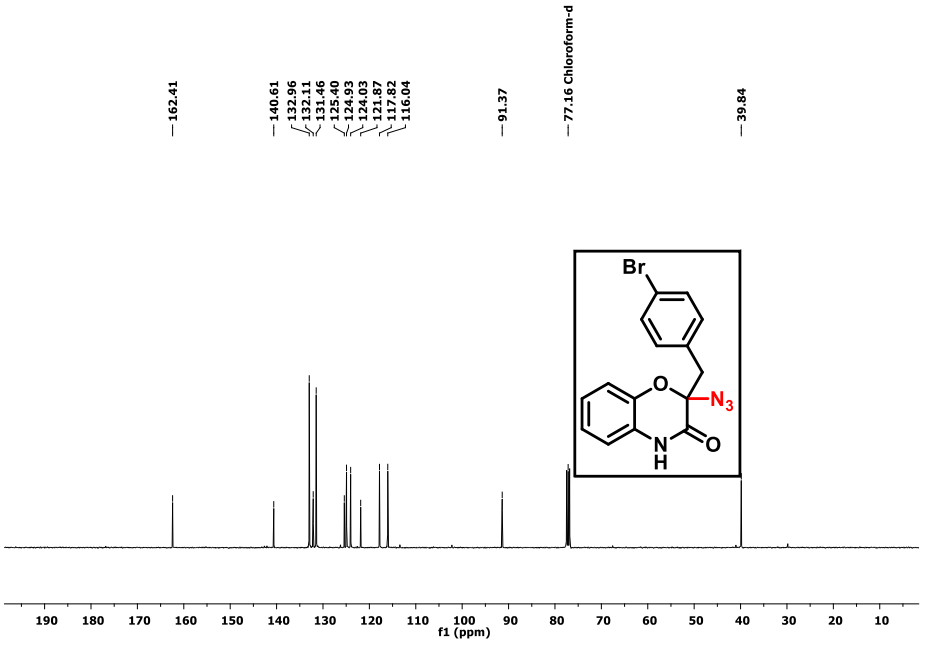

Figure 3.6.B.18: ^{13}C NMR of **85e**, 100 MHz, $CDCl_3$

2-azido-2-(4-bromobenzyl)-6-chloro-2*H*-benzo[b][1,4]oxazin-3(4*H*)-one (85g)

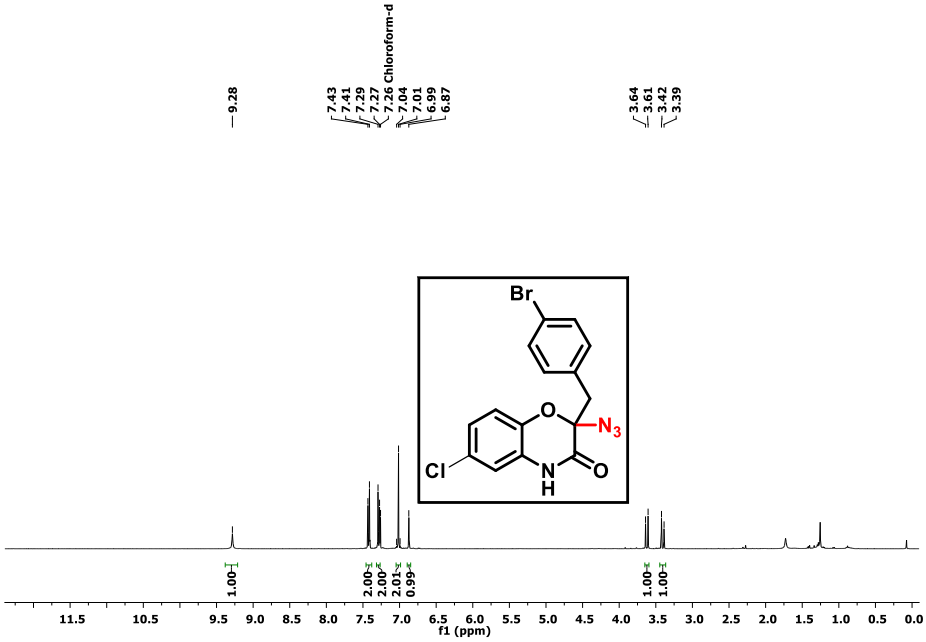

Figure 3.6.B.19: ^{1}H NMR of **85g**, 400 MHz, $CDCl_3$

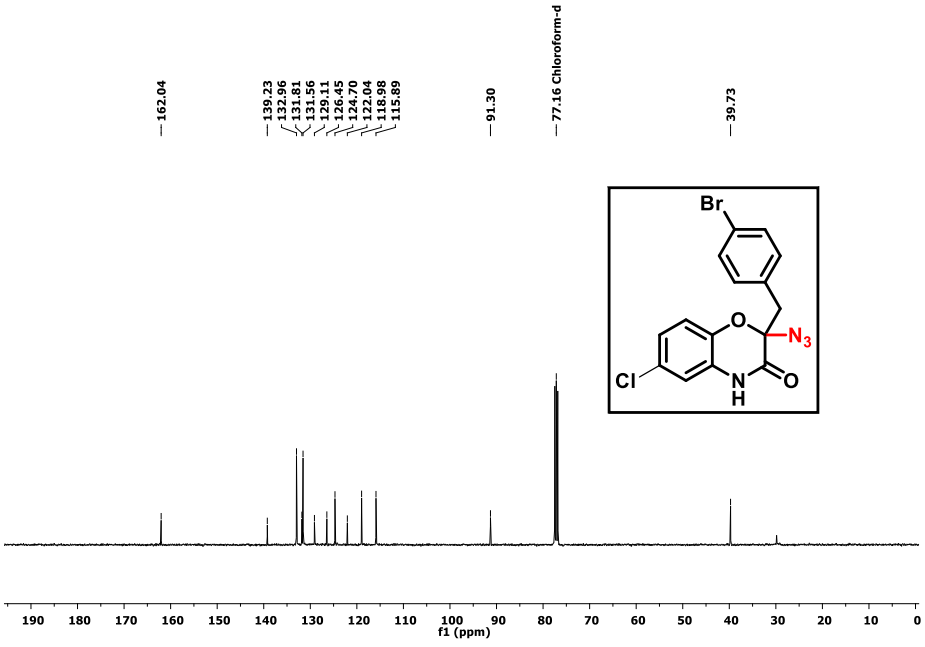

Figure 3.6.B.20: ^{13}C NMR of **85g**, 100 MHz, $CDCl_3$

2-azido-2,4-dimethyl-2*H*-benzo[b][1,4]oxazin-3(4*H*)-one (85i)

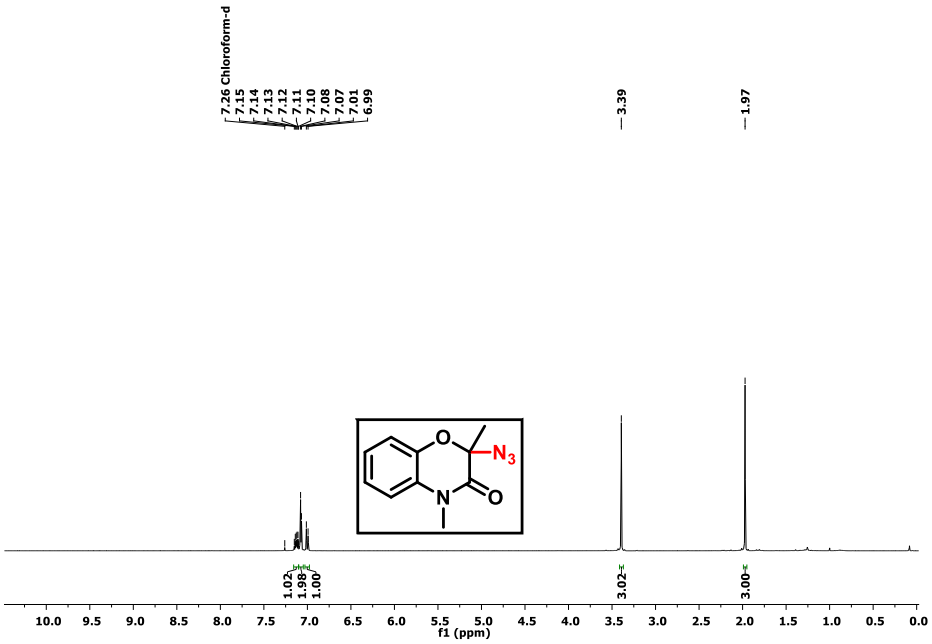

Figure 3.6.B.21: ^{1}H NMR of **85i**, 400 MHz, $CDCl_3$

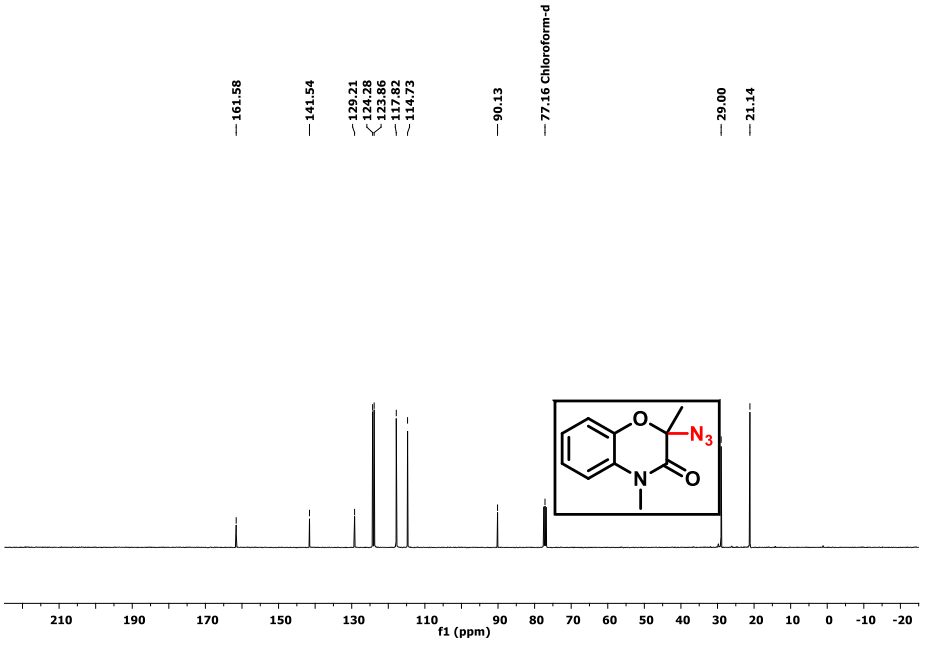

Figure 3.6.B.22: ^{13}C NMR of **85i**, 100 MHz, $CDCl_3$

3-methylquinoxalin-2(1*H*)-one (90i)

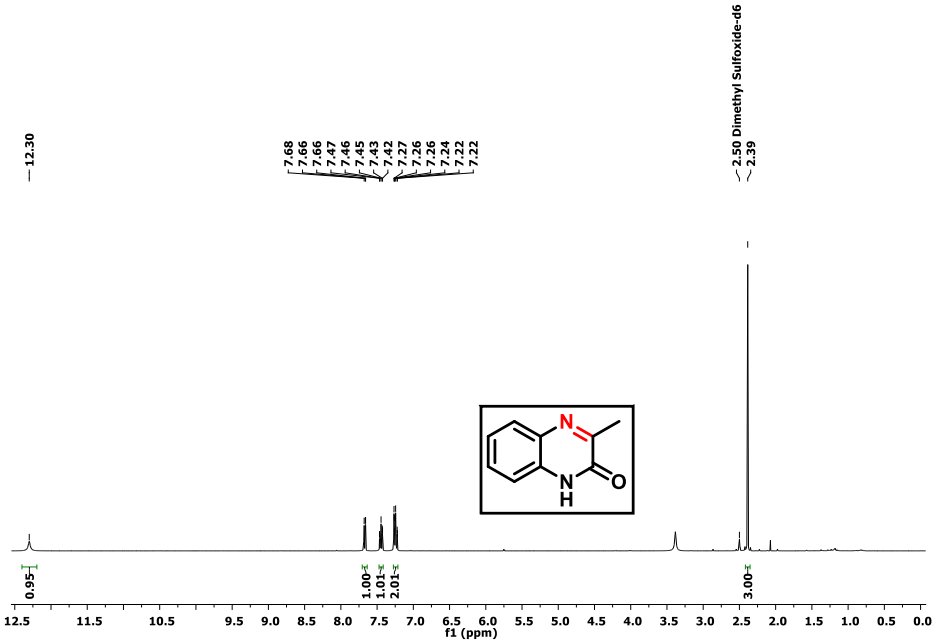

Figure 3.6.B.23: ^{1}H NMR of **90i**, 400 MHz, $CDCl_3$

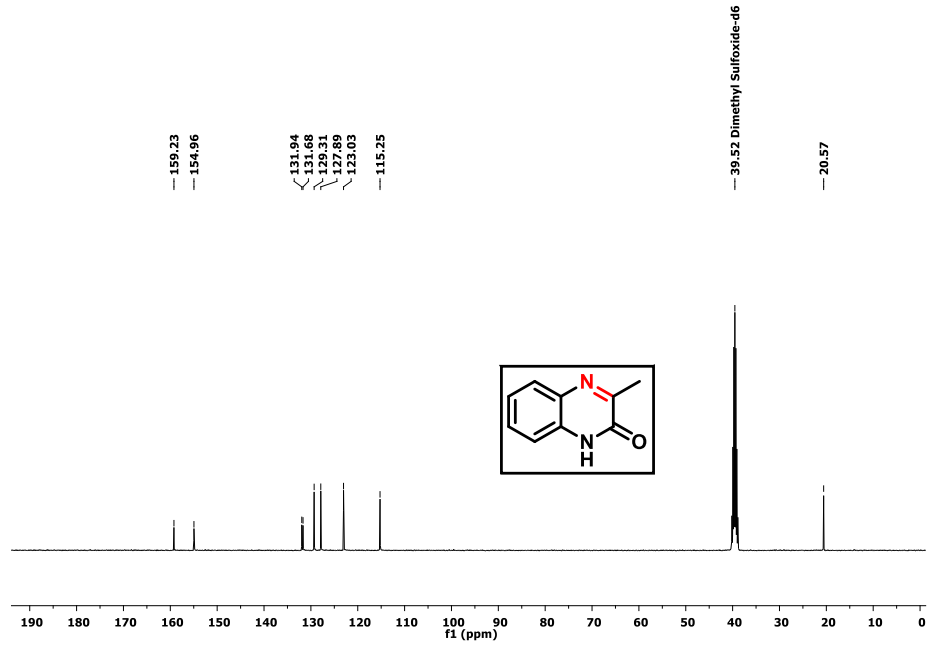

Figure 3.6.B.24: ^{13}C NMR of **90i**, 100 MHz, $CDCl_3$

3-(4-bromobenzyl)quinoxalin-2(1*H*)-one (90n)

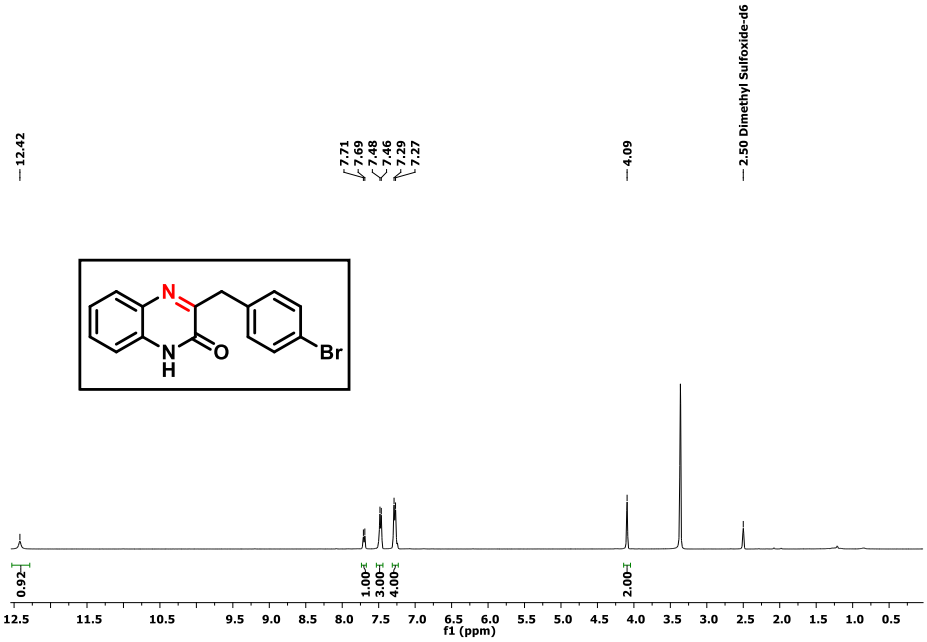

Figure 3.6.B.25: ^{1}H NMR of **90n**, 400 MHz, $CDCl_3$

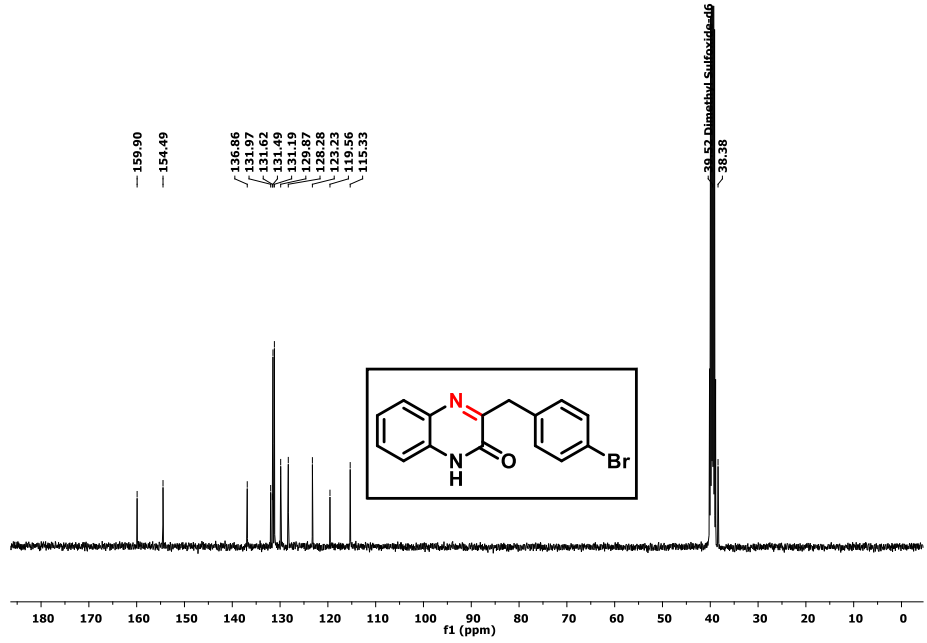

Figure 3.6.B.26: ^{13}C NMR of **90n**, 100 MHz, $CDCl_3$

3.7. ORTEP drawings of 83g, 83p, 85e showing thermal ellipsoids at the 50% probability level

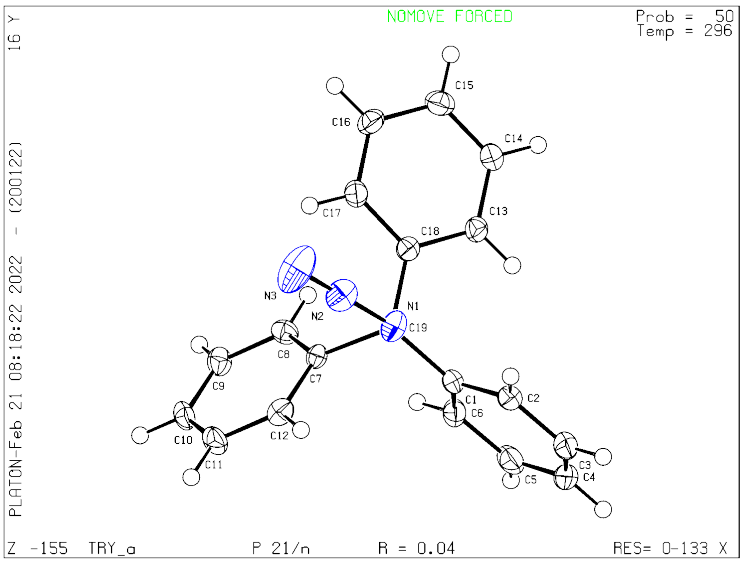

Figure 3.7.1: ORTEP drawing of **83g** showing thermal ellipsoids at the 50% probability level[3]

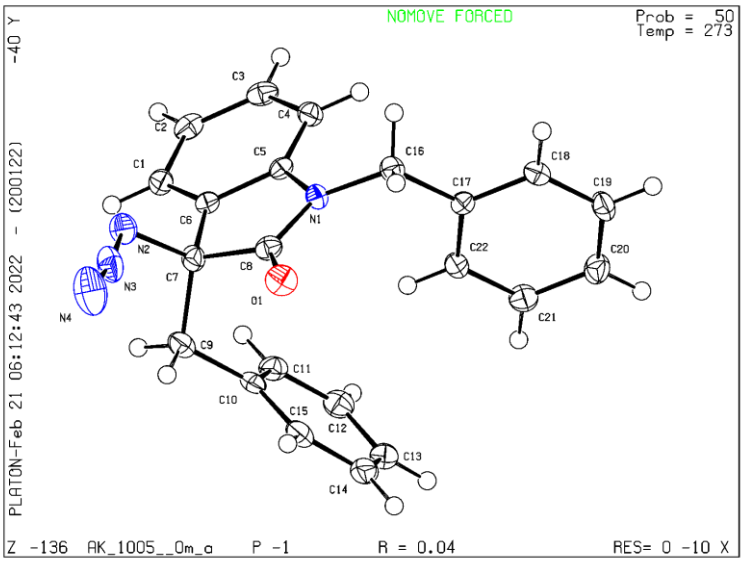

Figure 3.7.2: ORTEP drawing of **83p** showing thermal ellipsoids at the 50% probability level

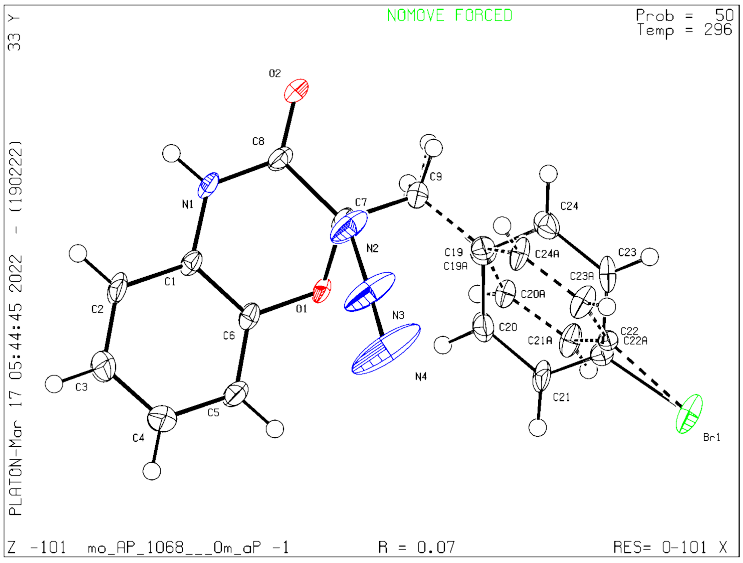

Figure 3.7.3: ORTEP drawing of **85e** showing thermal ellipsoids at the 50% probability level

3.8. Crystallographic parameters table for 83g, 83p, 85e

Parameters	**83g**	**83p**	**85e**
Emperical formula	$C_{19}H_{15}N_3$	$C_{22}H_{18}N_4O$	$C_{15}H_{11}BrN_4O_2$
Formula Mass/g mol^{-1}	285.35	354.40	359.18
Experimental crystal description	Rod	Rod	Rod
Colour	White	Yellow	White
Dcalcd/g cm^{-3}	1.282	1.309	1.647
Crystal system	Monoclinic	Triclinic	Triclinic
Space group	P 21/n	P -1	P -1
a/ Å	9.5337(6)	8.292(3)	6.0346(14)
b/ Å	16.3327(10)	10.211(3)	10.102(3)
c/ Å	10.1594(6)	11.100(4)	13.007(3)
α/ deg	90	79.076(10)	67.860(7)
β/ deg	110.914(2)	77.151(11)	84.761(8)
√/ deg	90	85.400(9)	80.567(8)
V/$Å^3$	1477.71(16)	899.0(5)	724.2(3)
Z	4	2	2
T / K	296(2)	273(2)	296
Diffraction Source	MoK\a	MoK\a	MoK\a
Diffraction radiation wavelength/ Å	0.71073	0.71073	0.71073
Diffraction reflection theta full	25.242	25.242	25.242
Reflection number total	3688	4542	3590
Reflection number gt	2350	2504	2915
μ/mm-1	0.078	0.083	2.851
F(000)	632	372	360
R1,wR2 [I>2σ(I)]	0.1040, 0.1511	0.0438, 0.0713	0.0736, 0.1758
R1,wR2(all data)	0.1831, 0.1782	0.0894, 0.0827	0.0892, 0.1956
GoF	1.168	0.804	1.068

Chapter IV: Skeletal Editing through Solid State Melt Rearrangement of Azides

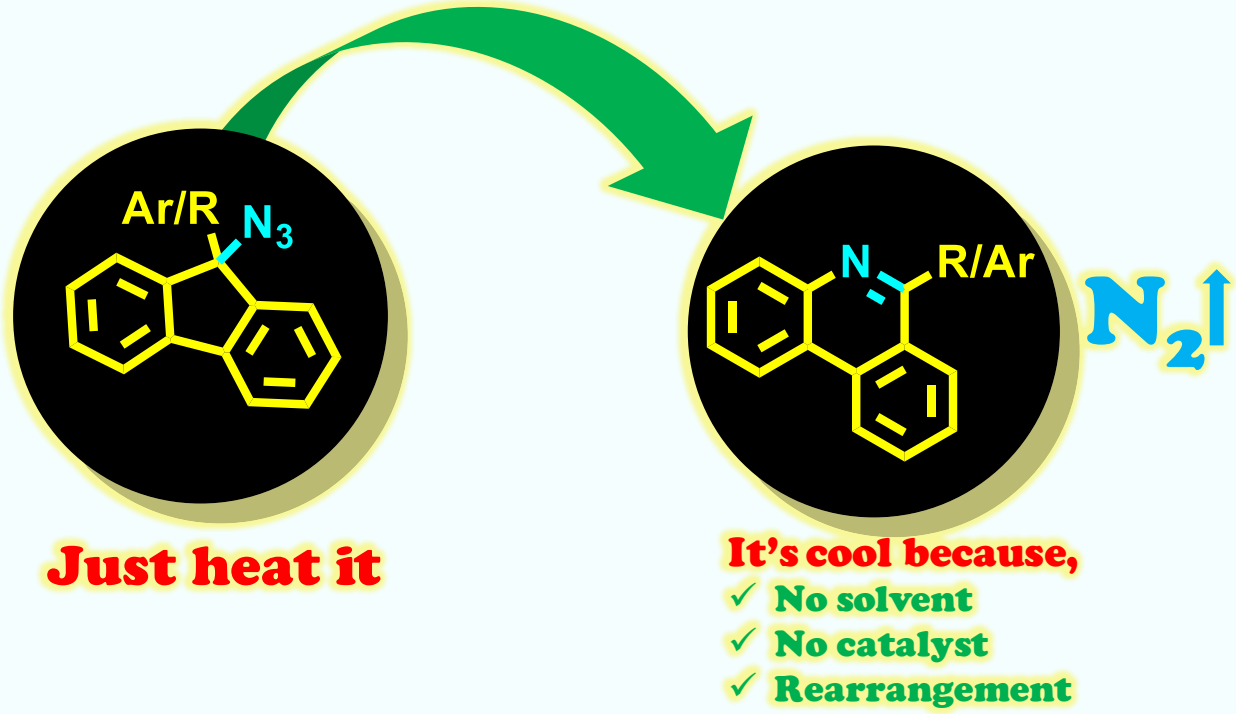

Skeletal Editing through Solid State Melt Rearrangement of Azides

4.1. Introduction to skeletal editing and solid-state melt rearrangement for *N*-heterocycle synthesis

Alkaloids are a group of natural products that usually comprise an *N*-heterocycle as a basic skeleton. Alkaloids show therapeutic properties for the treatment of cancer, tuberculosis, smoking cessation, etc.[121] Therefore, it has been exploited for pharmaceutical research and development.[121,122] Thus, the presence of a *N*-atom in a molecule can greatly impact its biological and physical properties.[123] Therefore, direct insertion of *N*-atom or rearrangement of the carbocyclic framework would be appealing to study the structure-activity relationship in the field of medicinal chemistry. The retrosynthetic analysis has been advantageous for revealing the synthetic equivalents for constructing target molecules. However, to synthesize derivative of that target molecule may necessitate the retrosynthetic approach to get new synthetic equivalents. Therefore, adding another atom directly to the target molecule may generate its library in one step. In this direction, skeletal editing shifts the new paradigm for core remodeling to streamline the discovery of new drug candidates from the parent framework in a single step. It allows the synthesis of structurally unique molecules from the existing active compounds (Figure 4.1.1).[124]

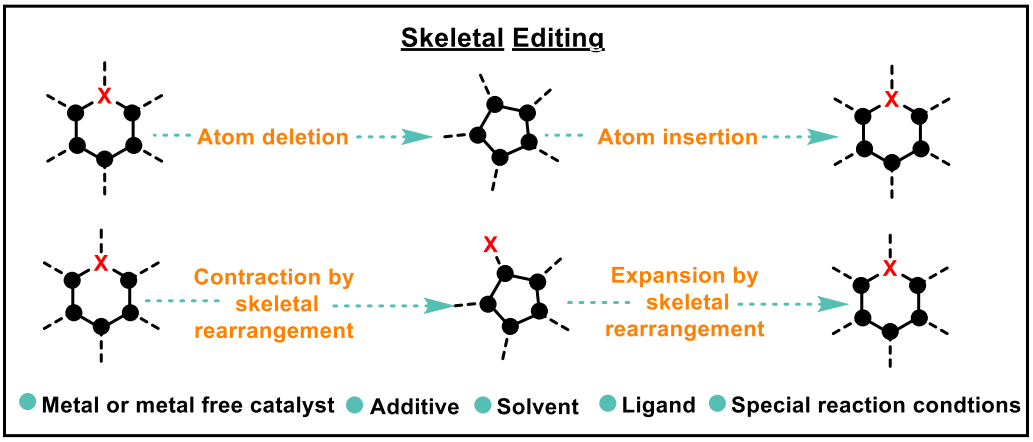

Figure 4.1.1: The concept of skeletal editing

The skeletal editing entails remodeling of the core for ring expansion by direct atom insertion or by rearrangement of the skeleton, whereas ring contraction is achieved by direct atom deletion or rearrangement of the skeleton. In addition, the direct insertion of *N*-atom or ring expansion through the rearrangement of the carbon skeleton will have multiple advantages such as atom/step economy, selectivity, and functional group (Fg) tolerance. Recent decades have witnessed the common practice of producing aromatic *N*-heterocycles using conventional condensation processes that employ preoxidized materials for *N*-heterocycles. For instance, early attempts to synthesize isoquinoline **92** from indene **91** required the oxidative cleavage of alkenes using ozone[125-126,] or OsO_4,[127] which tolerated a restricted functional group range[128] (Scheme 4.1.1).

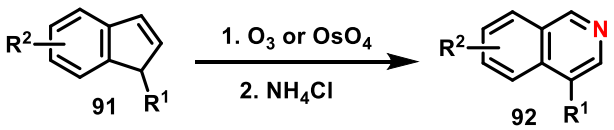

Scheme 4.1.1: Classical concept of nitrogen atom insertion

Additionally, the direct core modification can widen the scope toward exploring other chemical entities. However, the process is challenging because the cleavage of inert C-C bonds is quite difficult.[129] The skeletal editing through *N*-atom deletion has been recently disclosed. However, the insertion of a single nitrogen atom has limited reports despite its immense potential for synthesizing ubiquitous *N*-heterocycles.[130-131] The Schmidt rearrangement is one of the first reactions that fit this definition.[134] The more direct techniques have been made available to enable electrochemical nitrogen insertion by using gaseous ammonia by the Cheng group in 2022.[135] However, it show compatibility only with electron-rich indenes **91** bearing additional aryl and alkyl substitutions on the double bond (Scheme 4.1.2).

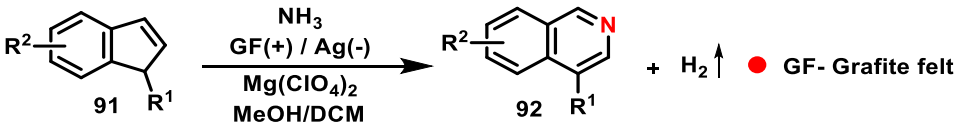

Scheme 4.1.2: Insertion of ammonia by electrochemical dehydrogenation of alkenes for aromatic *N*-heterocycles

Later, stoichiometric osmium nitride as a catalyst was exploited for *N*-atom insertion in 3-phenyl-1*H*-indenes **93** to achieve 1-phenylisoquinolines **94** subsequently (Scheme 4.1.3).[136] However, the need for a stoichiometric amount of metal salts limits its synthetic application. These difficulties emphasize the need for an efficient method for isoquinolines synthesis.[137]

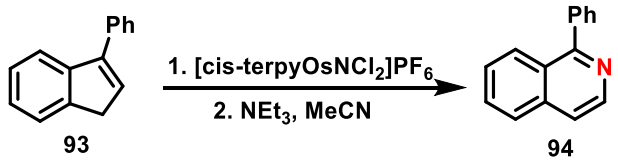

Scheme 4.1.3: Direct *N*-atom insertion from an osmium (VI) nitride for isoquinolines

The use of inexpensive cobalt-catalyzed *N*-atom insertion in arylcycloalkenes **91** with trimethylsilyl azide **95** as a source of nitrogen under an open-air condition with DME/H_2O as a green solvent is developed by Wei and group (Scheme 4.1.4).[137]

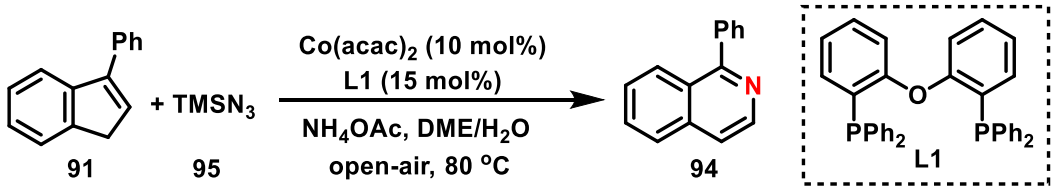

Scheme 4.1.4: Cobalt-catalyzed *N*-atom insertion in arylcycloalkenes

Recently, Morandi and coworkers reported operationally simple direct *N*-atom insertion into a broad range of indenes **96** and cyclopentadienes with commercially available (diacetoxyiodo)benzene (PIDA) as the oxidant and ammonium carbamate as the nitrogen source to access the library of isoquinolines **97** (Scheme 4.1.5).[138]

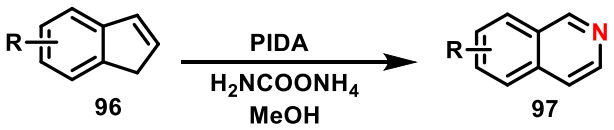

Scheme 4.1.5: PIDA and ammonium carbamate mediated isoquinolines synthesis

Morandi and coworkers have summarized the isoelectronic approach of indenes **96** to indoles **98** to access quinazolines **99**. However, unprotected indole nitrogen shows a direct reaction with the

electrophilic iodonitrene molecule. A labile isodiazene intermediate might be produced, which eventually facilitates the degradation of the underlying carbon skeleton.[139] However, with silyl-based group the reactivity of the nitrogen can be suppressed to deliver the desired product.[140] Additionally, the susceptibility of silyl group towards hydrolysis can be achieved by changing the substituents on the silicon atom[141] to afford either quinazolines or quinoxalines in a single step (Scheme 4.1.6).[142]

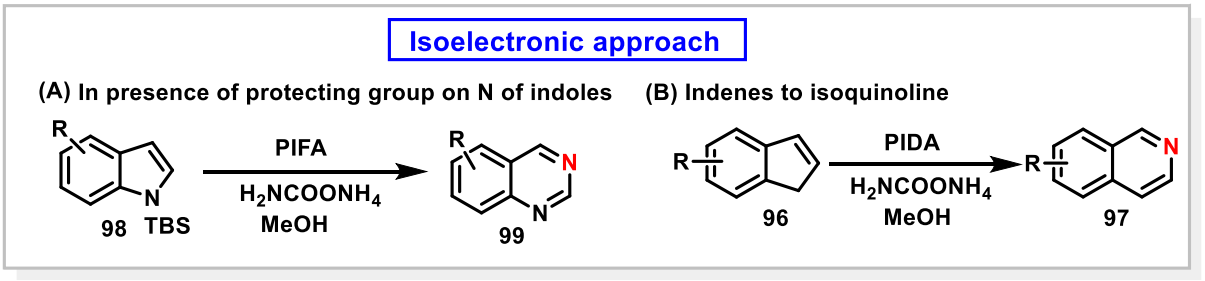

Scheme 4.1.6: Isoelectronic approach of nitrogen atom insertion; **A.** Skeletal editing of indoles with *N*-protection to access quinazolines or quinoxalines; **B.** Skeletal editing of indenes with PIDA and ammonium carbamate for isoquinolines

Moreover, isoquinoline and quinazoline synthesis in literature have been successfully demonstrated by skeletal editing through *N*-atom insertion. But this approach is limited for the synthesis of phenanthridines **100** that are basic scaffolds in natural products and staining agents (Figure 4.1.2).[143] Previous literature precedents revealed that these phenanthridines **100** can be accessed through various metal and metal-free approaches utilizing substituted biphenyl derivatives.[143]

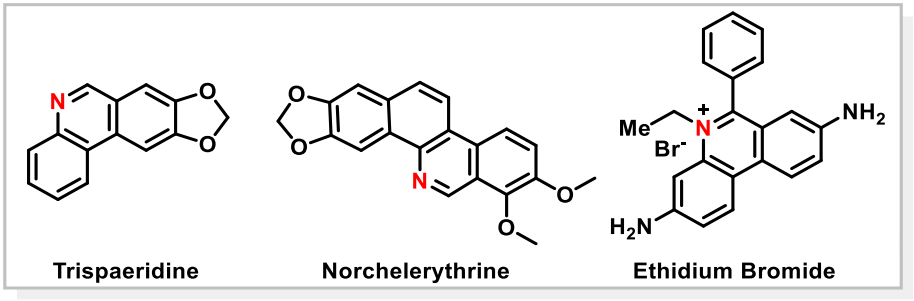

Figure 4.1.2: Phenanthridine core containing natural products and staining agent

The careful observation of these chemical operations suggests that these products could be achieved by taking metal or metal-free catalysts, specially designed starting materials, additives, bases, and extremely high temperatures for C-C, and C-N bond formation (Scheme 4.1.7).[143]

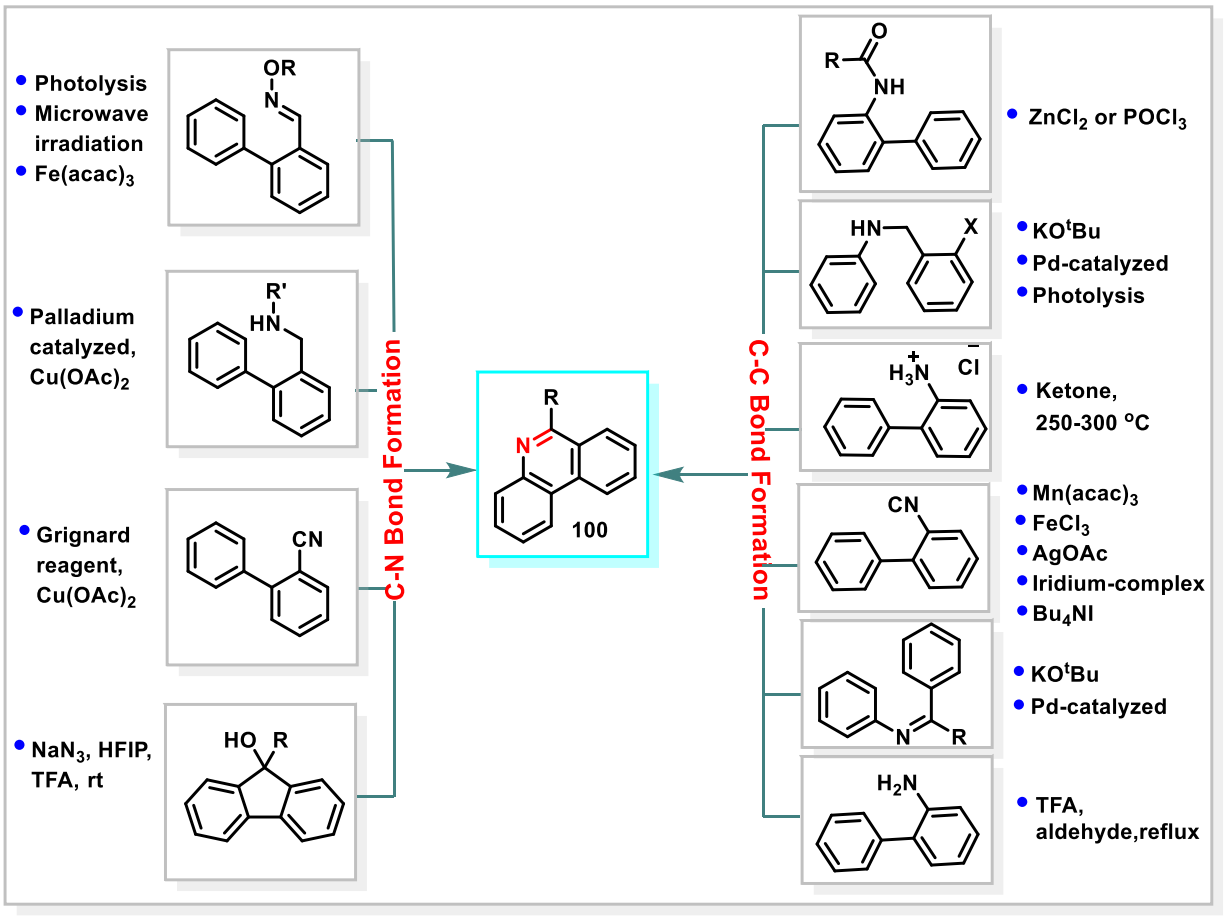

Scheme 4.1.7: Literature precedents of C-C and C-N bond to access phenanthridines

Such a procedure may end up with a certain amount of metal content or impurities from solvent or other additives, which is highly undesirable in the pharmaceutical industry. Hence, the demand for more efficient processes is still highly desirable. Therefore, this goal can be fulfilled with solid-state melt reactions (SSMR). The SSMR envisions strategy that can improve yield by eliminating the need for toxic solvents, protecting groups, metal salts and oxidants/reductants. An extensive amount of work has been done by Bakthadoss and coworkers for the synthesis of tetra and pentacyclic quinolinopyran tethered pyrazole/coumarin,[144(a)] and hybrid polycyclic quinolinobenzo[*a*]phenazinone, etc.[144(b)] Although several research groups have focused on solid-

state melt reactions to access numerous heterocycles but according to our knowledge, no report is available for azide rearrangement to access phenanthridines **100**. In this direction, we have envisioned solid-state melt rearrangement of 9-azido-9-alkyl/aryl-9*H*-fluorene **102** derivatives to access phenanthridines **100** by nitrogen expulsion under the heating condition without any catalyst and solvent.

4.2. The rationale of the present work

Azides as an indispensable organic scaffold have been widely used for creating various heterocycles exploiting metal or metal-free catalysts. Although the majority of chemical operations are conducted under mild conditions, a new synthetic approach is highly desired to attain the maximum possible sustainable and green parameters. Therefore, we envisioned to develop a solvent-free catalyst-free rearrangement reaction of azide to generate phenanthridine by the expulsion of N_2 gas. This approach is focused towards the prevention of waste and improving the atom economy.

4.3. Results and discussion

In order to study the solid-state melt rearrangement, "Just in Time" synthetic approach was utilized to access 9-azido-9-alkyl/aryl-9*H*-fluorenes **102** by following the azidation protocol developed in chapter III. The azidation of 9-alkyl/aryl-9*H*-fluorenols **101** with $TMSN_3$ **95** as an azidating source and Amberlyst®-15 as a Brønsted acid catalyst at room temperature in DCM solvent tolerated many functional groups such as electron-donating group and electron-withdrawing group on 9-substituted benzyl azide substrates (Scheme 4.3.1). The electron-donating groups such as Me- and OMe- resulted in 89% and 97% yield for **102b** and **102c**. Additionally, 4-phenyl substituted derivative was tolerant that furnished 92% of **102d.** Moreover, 9-hexyl-9*H*-fluorenol also gave excellent yield of 92% for **102e**. Further, bromo substituted fluorenols afforded good to excellent yields of **102f** to **102h.** Gratifyingly, 11-azido-11-(p-tolyl)-11*H*-benzo[*b*]fluorene **102i** was isolated in 88% yield from its respective starting material by following optimized reaction condition. However, 9-benzyl substituted fluorenols provided 9-azido-9-benzyl-9*H*-fluorene **102k**, 9-azido-9-(4-methoxybenzyl)-9*H*-fluorene **102l**, and 9-([1,1'-biphenyl]-4-ylmethyl)-9-azido-9*H*-fluorene **102m** in 71%, 83%, and 98% yields, respectively.

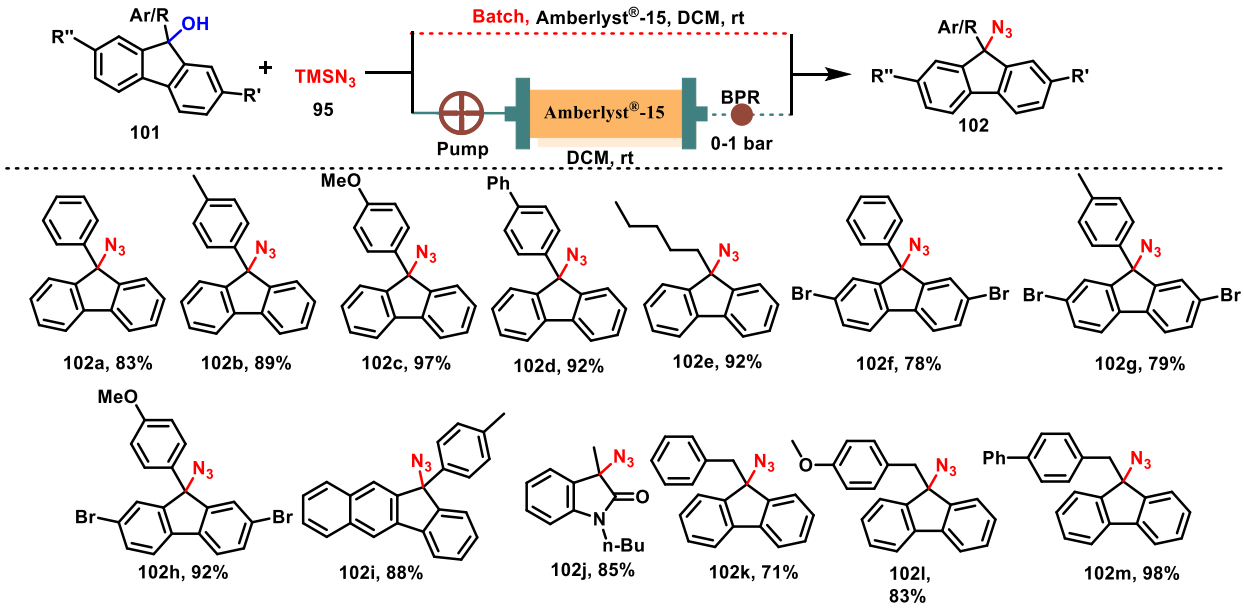

Scheme 4.3.1. Azidation of fluorenol derivatives under batch and continuous flow

After the successful synthesis of 9-azido-9-alkyl/aryl-9*H*-fluorenes **102**, we envisioned to study the rearrangement of azides. Initially, we have started optimization of reaction by taking **102c** as a starting material for TGA analysis. From the TGA, a gradual decrease in the mass of starting material by the expulsion of nitrogen from 80 ^{o}C onwards was observed. However, the sharp decrease in the peak is first observed at 160 ^{o}C (Figure 4.3.1). This further confirms the requirement of higher temperature for the skeletal editing by rearrangement of azides to accomplish phenanthridines **100**.

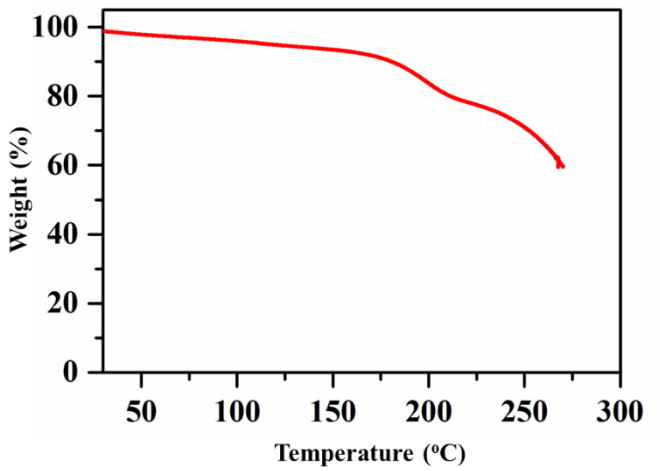

Figure 4.3.1: Thermogravimetric analysis of **102c**

Next, we have started screening of reaction condition with **102a**. Heating **102a** at 80 °C resulted in no reaction (Table 4.3.1, entry 1). Whereas traces of product formation were observed at 100 °C within 18 h of the reaction time (Table 4.3.1, entry 2). Further keeping time constant and increasing the temperatures at 120 °C, 140 °C, 160 °C, and 180 °C afforded **100a** in 40%, 54%, 84%, and 87% respectively (Table 4.3.1, entry 3-6). As there was no significant difference between the yield of product **100a** at 160 °C and 180 °C, we carried out time optimization at 160 °C.

Table 4.3.1: Optimization of reaction conditions for the skeletal editing of azides through rearrangement under batch conditions

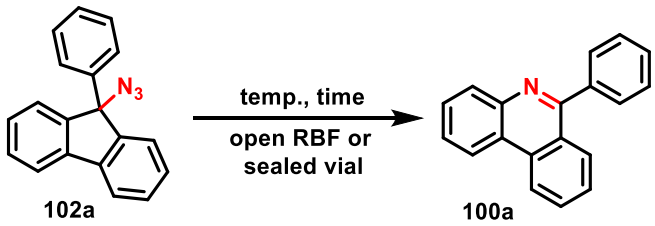

Entry	Temp (°C)	Time (h)	Yield (%)
1	80	18	n.d.
2	100	18	Traces
3	120	18	40
4	140	18	54
5	160	18	84
6	180	18	87
7	160	06	85

Reaction conditions: Compound **102a** (0.5 mmol) heated at the above-mentioned temperature and time (see table). The reported yields are isolated yields.

The time required for the completion of the reaction was studied with time-dependent IR spectroscopy (Figure 4.3.2). Time-dependent IR suggests an increase in time from 3 h to 6 h, the azide peak present at 2100 cm^{-1} is suppressed. This confirms the completion of the reaction within 6 h to furnish 85% of **100a** (Table 4.3.1, entry 7)**.**

Having established optimum reaction condition in hand, we have studied the substrate scope. Moreover, good to excellent yields of products **100a-m** were produced by altering the substitution on azidofluorenes moiety **102** at 160 ^{o}C.

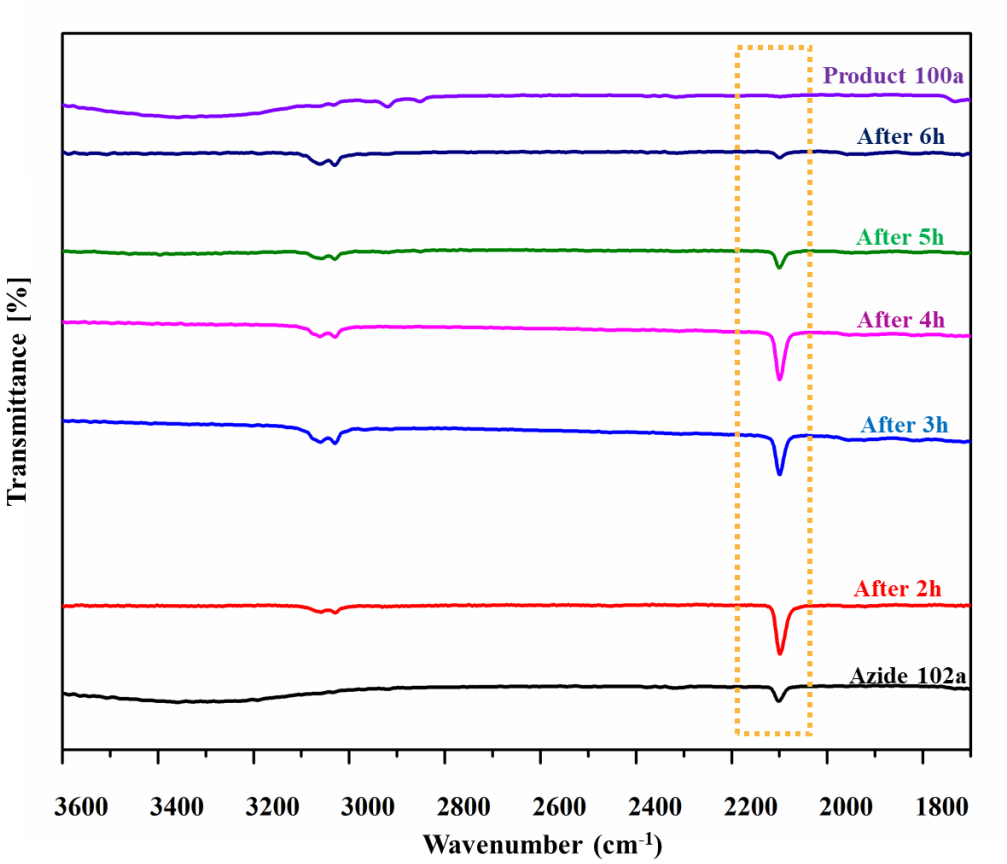

Figure 4.3.2: A gradual peak suppression of azides at 2100 cm^{-1} from time-dependent infrared spectroscopy

Various 9-azido-9-substitutedphenyl-9*H*-fluorenes **102** provided 6-phenylphenanthridine **100a**, 6-(p-tolyl)phenanthridine **100b**, 6-(4-methoxyphenyl)phenanthridine **100c**, and 6-([1,1'-biphenyl]-4-yl)phenanthridine **100d** in 85%, 90%, 77%, and 81% yields respectively (Scheme 4.3.2). This approach was also tolerant towards 9-azido-9-hexyl-9*H*-fluorene which gave a good yield of 81% to access 6-hexylphenanthridine **100e**.

With regard to the 9-aryl group in 9-azido-2,7-dibromophenyl-9*H*-fluorenes **102**, electron-donating groups were tolerated to give 82% and 80% yields of **100f** and **100g**. Whereas a slight

decrease in the yield of **100h** (77%) is observed when strong electron donating -OMe substituted **102h** was subjected under optimized condition. The unsymmetrical azide **102i** was also investigated to afford **100i** in 93% yield (Scheme 4.3.2). Additionally, 41% of **100j** is produced by heating 3-azido-1-butyl-3-methylindolin-2-one **102j** under solvent-free and catalyst-free condition. An interesting observation was obtained with substituted-9-benzyl on 9-azido-9*H*-fluorene **102** where after the ring expansion, oxidation takes place on benzyl sp3 C-H to afford phenanthridin-6-yl(substituted aryl)methanone derivatives **100k**, **100l**, and **100m** in 23%, 54%, and 41% yields respectively (Scheme 4.3.2).

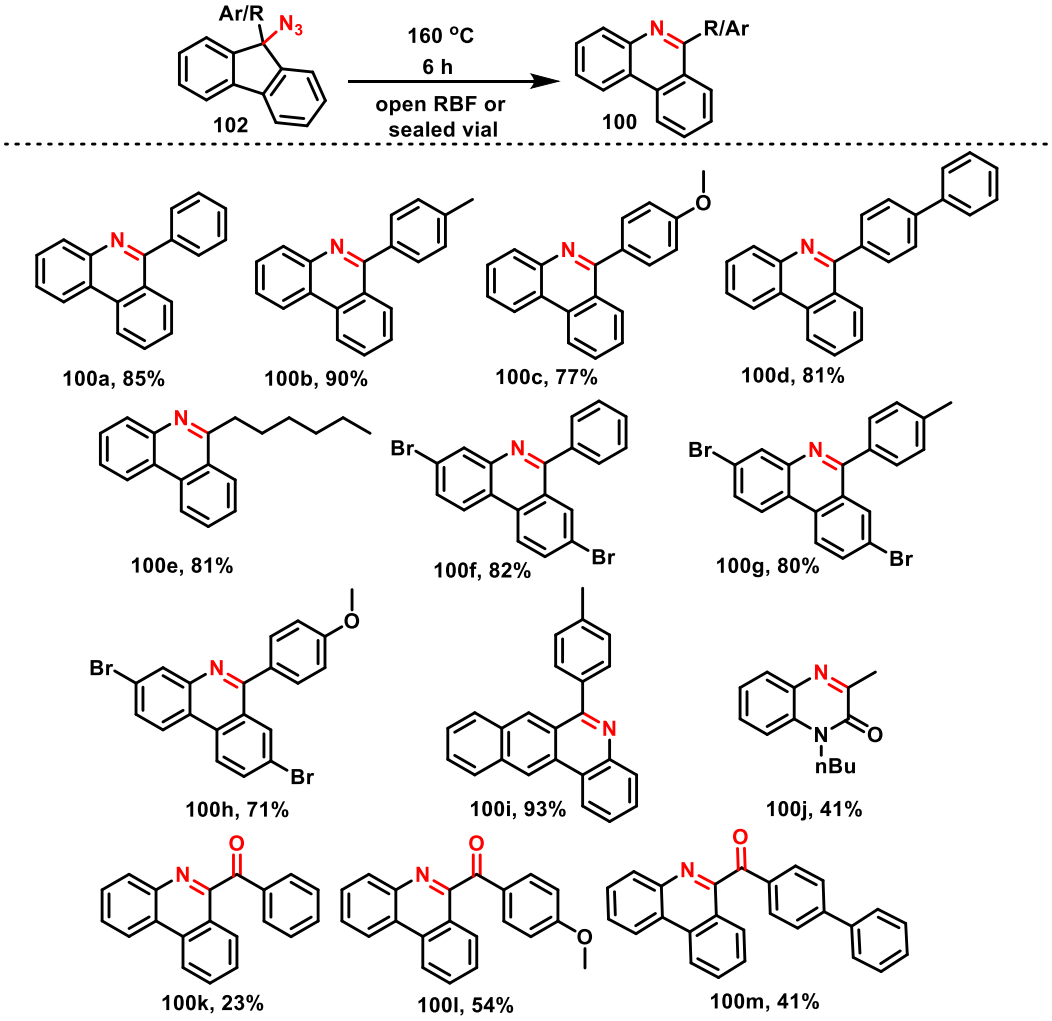

Reaction conditions: Compound **102** was heated at 160 °C in a resealable vial or open round bottom flask upto 6 h. The reported yields are the isolated yields.

Scheme 4.3.2: Substrate scope for the rearrangement of azides under batch

The skeletal editing by rearrangement of azide can be easily figured out from ^{13}C- NMR of azides **102b** and rearranged product (Figure 4.3.3). In azides, aliphatic quaternary peak appeared at 76.1 ppm, whereas no aliphatic quaternary peak is observed in the rearranged product **100b**. Along with that, a shift in methyl carbon peak is noted from 21.1 ppm to 21.5 ppm (Figure 4.3.3).

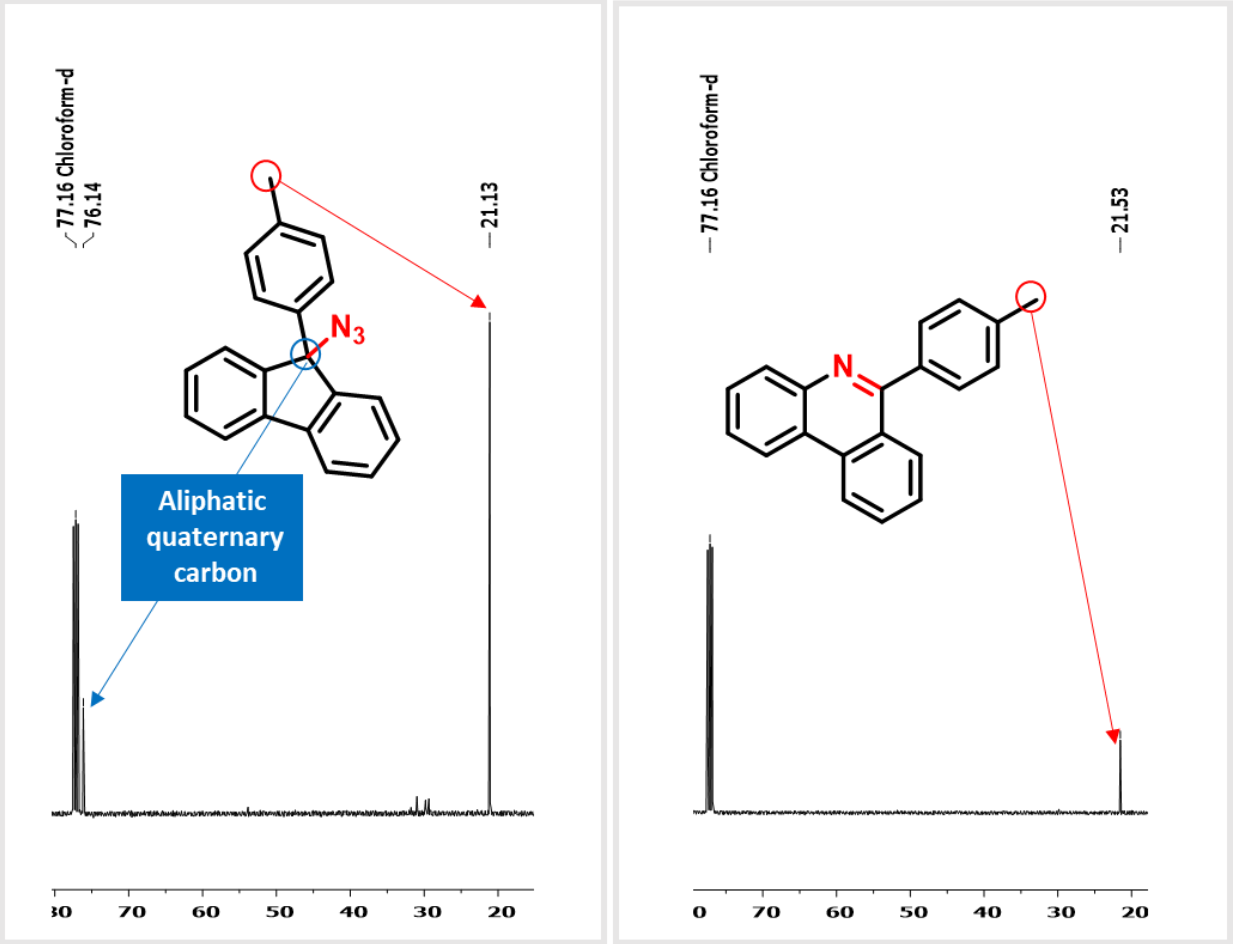

Figure 4.3.3: ^{13}C NMR of aliphatic quaternary carbon (blue colour); present in azides **102b** (left) and absent in phenanthridines **100b** (right)

The mechanistic pathway for the reaction involving azides has been known to follow thermal rearrangement in a concerted pathway.[145] Keeping that in mind, we proposed a plausible mechanism. The consecutive resonating structure leads to thermal decomposition of **II** by expulsion of N_2, to access phenanthridine **100** in a concerted pathway (Scheme 4.3.3).

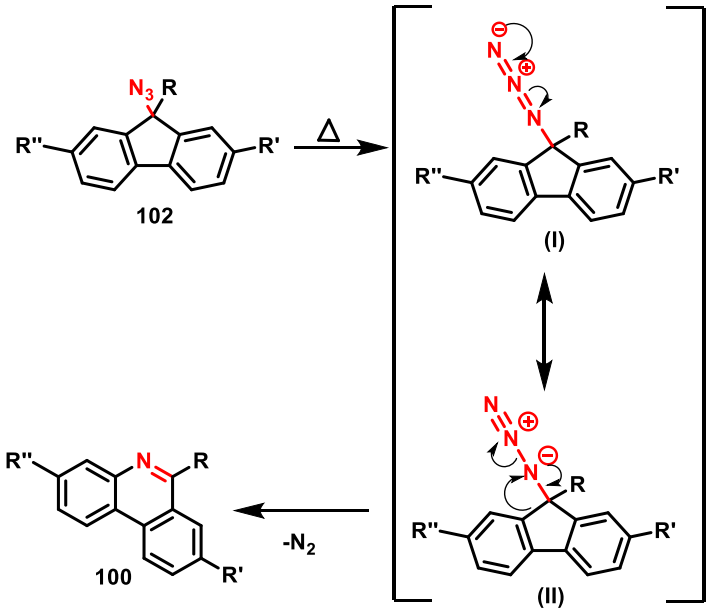

Scheme 4.3.3: A concerted thermal decomposition for skeletal editing of azides **102**

4.4. Conclusion

In conclusion, we have demonstrated skeletal editing through solid state melt rearrangement of azides **102** to generate library of phenanthridine derivatives **100** in good to excellent yields. Additionally, a detailed optimization study was carried out with thermogravimetric analysis and time-dependent infrared spectroscopy. The thermogravimetric analysis data confirmed nitrogen expulsion at 160 ^{o}C. Whereas, from time-dependent infrared spectroscopy minimization of azide peak **102a** was observed to afford **100a** in 6 h. The product formation was confirmed by ^{1}H NMR, ^{13}C NMR, HRMS and IR studies. Additionally, this direct core modification can expand the scope towards exploring other *N*-containing heterocycles. This work avoids the use of solvent, catalyst, and other additives. Hence, it follows sustainability parameter such as prevention of waste, achieving better atom economy for safer chemical synthesis.

4.5. Experimental sections

General information and data collection:

All the chemicals were purchased from Sigma-Aldrich and SD Fine Chemicals and used without further modification. All solvents were purchased from Rankem and Finar Chemicals. Deuterated

solvents were used as received. Column chromatographic separations were performed over 100−200 silica-gel. Visualization was accomplished with UV light. The ^{1}H and ^{13}C NMR spectra were recorded on 400 and 100 MHz, respectively, using Bruker or JEOL spectrometers. The chemical shift (δ) and coupling constant (*J*) values are given in parts per million and hertz, respectively. Abbreviations used in the NMR follow-up experiments: b, broad; s, singlet; d, doublet; t, triplet; q, quartet; td, dd doublet of triplet and double doublet; m, multiplet, tt, triplet of triplets and ddd, doublet of doublet of doublets. HRMS spectra were obtained with Waters-synapt G2 using electrospray ionization (ESI-TOF). Infrared spectra (ATIR) were obtained with a Bruker Alpha-E infrared spectrometer. Thermogravimetric analysis was recorded on a Perkin Elmer STA 6000, TGA analyzer under an air atmosphere with a heating rate of 5 °C/min.

A. General procedure for azidation of alcohols 101 in batch condition: To an oven-dried 20 mL resealable pressure tube (equipped with rubber septum) were added alcohols **101** (0.5 mmol), azidotrimethylsilane (1.5 mmol), and Amberlyst®-15 (w/w with respect to alcohols **101**) in dichloromethane (2 mL) with a magnetic bar and then the mixture was stirred at room temperature (25 ^{o}C) for 30 min to 1 h. The reaction progress was monitored through TLC until the completion of the reaction. The volatile solvents were removed using a vacuum, and the crude reaction mixture was directly purified by column chromatography on silica gel (EtOAc:hexane = 0:100 to 5:95).

B. General procedure for azidation of alcohols 101 in continuous-flow: In a typical procedure, the 0.1 M solution of alcohol derivatives **101** in dichloromethane and 3 equivalent of azidotrimethylsilane **95** was premixed and flown through Omnifit (6.6 x 150 mm) packed bed column packed with Amberlyst®-15 upto 5 cm (1.0 gm, swollen up to 6 cm after passing solvent) of bed at room temperature at 0-1 bar pressure at room temperature with 0.1 mL/min flow rate. After reaction completion, the catalyst bed was washed with dichloromethane. A volatile component was evaporated using a vacuum. The residue was directly purified by silica gel chromatography (EtOAc:hexane = 1:99 to 5:95). Amberlyst®-15 bed was recycled by washing with DCM and reused for the other substrates. **Note**: For preventive measurement, we have filtered the solution through a syringe filter before flowing it through pumps. (Filtration carried out using nylon syringe filter (0.22 µm)).

C. General procedure for the solid-state melt rearrangement of azides 102 to access phenanthridines 100: To an oven dried 20 mL resealable pressure tube (equipped with rubber septum) were added azides **102** (0.5 mmol) without a magnetic bar and then the mixture was heated at 160 ^{o}C for 6 h. The reaction progress was monitored through TLC until the completion of the reaction. The crude reaction mixture was directly purified by column chromatography on silica gel (EtOAc:hexane = 10:90 to 15:85).

4.6.A. Analytical data for product:

*9-azido-9-phenyl-9H-fluorene **(102a)*:**

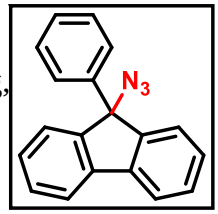

Prepared according to general procedure (**B**), using 9-phenyl-9*H*-fluoren-9-ol (750.0 mg, 2.9 mmol) to afford 9-azido-9-phenyl-9*H*-fluorene **102a** (682.0 mg, 83%) as a white solid after purification by column chromatography on silica gel (EtOAc:hexane = 1:99). Melting point: 70-72 ^{o}C. ^{1}H NMR (400 MHz, $CDCl_3$) δ 7.75 (dd, *J* = 7.6, 0.7 Hz, 2H), 7.44 (m, 2H), 7.31 (m, 9H). ^{13}C NMR (100 MHz, $CDCl_3$) δ 147.0, 140.6, 140.2, 129.6, 128.7, 128.6, 127.9, 126.1, 125.2, 120.4, 76.3. IR (neat): 2098 cm^{-1}. HRMS (ESI-TOF) m/z: $[M + H - N_2]^+$ calcd for $C_{19}H_{14}N$: 256.1126; found: 256.1125.

*9-azido-9-(p-tolyl)-9H-fluorene **(102b)*:**

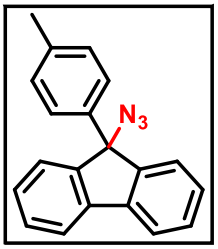

Prepared according to general procedure (**A**), using 9-(p-tolyl)-9*H*-fluoren-9-ol (440.0 mg, 1.62 mmol) to afford 9-azido-9-(p-tolyl)-9*H*-fluorene **102b** (428.0 mg, 89%) as a white solid after purification by column chromatography on silica gel (EtOAc:hexane = 1:99). Melting point: 77-79 ^{o}C. ^{1}H NMR (400 MHz, $CDCl_3$) δ 7.67 (m, 2H), 7.36 (m, 2H), 7.26 (m, 4H), 7.17 (m, 2H), 7.04 (d, *J* = 8.0 Hz, 2H), 2.25 (s, 3H). ^{13}C NMR (100 MHz, $CDCl_3$) δ 147.1, 140.1, 137.6, 137.5, 129.4, 129.3, 128.6, 126.0, 125.1, 120.4, 76.1, 21.1. IR (neat): 2095 cm^{-1}. HRMS (ESI-TOF) m/z: $[M + H - N_2]^+$ calcd for $C_{20}H_{16}N$: 270.1283; found: 270.1277.

9-azido-9-(4-methoxyphenyl)-9H-fluorene ***(102c)*****:**

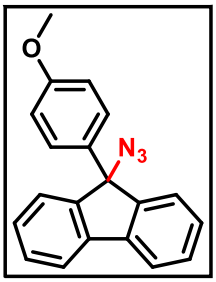

Prepared according to general procedure (**A**), using 9-(4-methoxyphenyl)-9*H*-fluoren-9-ol (800.0 mg, 2.774 mmol) to afford 9-azido-9-(4-methoxyphenyl)-9*H*-fluorene **102c** (843.0 mg, 97%) as a white solid after purification by column chromatography on silica gel (EtOAc:hexane = 1:99). Melting point: 109-111 °C. ^{1}H NMR (400 MHz, $CDCl_3$) δ 7.70 (d, *J* = 7.3 Hz, 2H), 7.31 (ddd, *J* = 23.4, 14.5, 6.9 Hz, 8H), 6.80 (d, *J* = 6.8 Hz, 2H), 3.74 (s, 3H). ^{13}C NMR (100 MHz, $CDCl_3$) δ 159.3, 147.2, 140.1, 132.5, 129.5, 129.0, 127.4, 125.1, 120.4, 114.0, 75.9, 55.4. IR (neat): 2092 cm^{-1}. HRMS (ESI-TOF) m/z: $[M + H - N_2]^+$ calcd for $C_{20}H_{16}NO$: 286.1232; found: 286.1230.

9-([1,1'-biphenyl]-4-yl)-9-azido-9H-fluorene ***(102d)*****:**

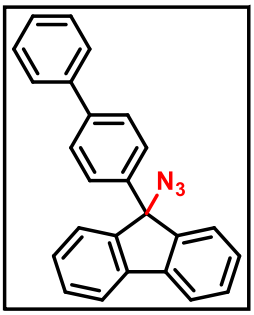

Prepared according to general procedure (**A**), using 9-([1,1'-biphenyl]-4-yl)-9*H*-fluoren-9-ol (384.5 mg, 1.15 mmol) to afford 9-([1,1'-biphenyl]-4-yl)-9-azido-9*H*-fluorene **102d** (380.0 mg, 92%) as a white solid after purification by column chromatography on silica gel (EtOAc:hexane = 1:99). Melting point: 112-114 °C. ^{1}H NMR (400 MHz, $CDCl_3$) δ 7.77 (d, *J* = 7.6 Hz, 2H), 7.54 (m, 4H), 7.39 (m, 11H). ^{13}C NMR (100 MHz, $CDCl_3$) δ 147.0, 140.8, 140.7, 140.2, 139.6, 129.7, 128.9, 128.7, 127.5, 127.4 127.2, 126.6, 125.2, 120.5, 76.2. IR (neat): 2097 cm^{-1}. HRMS (ESI-TOF) m/z: $[M + H - N_2]^+$ calcd for $C_{25}H_{18}N$: 332.1439; found: 332.1442.

9-azido-9-hexyl-9H-fluorene ***(102e)*****:**

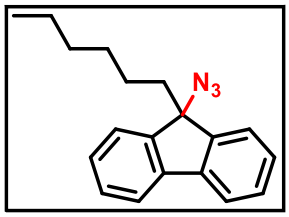

Prepared according to general procedure (**B**), using 9-hexyl-9*H*-fluoren-9-ol (266.0 mg, 1.0 mmol) to afford 9-azido-9-hexyl-9*H*-fluorene **102e** (268.4 mg, 92%) as a white semi-solid after purification by column chromatography on silica gel (EtOAc:hexane = 1:99). ^{1}H NMR (400 MHz, $CDCl_3$) δ 7.70 (dd, *J* = 7.4, 0.6 Hz, 2H), 7.53 (d, *J* = 7.0 Hz, 2H), 7.40 (m, 4H), 2.15 (m, 2H), 1.17 (m, 6H), 0.94 (m, 2H), 0.82 (t, *J* = 7.0 Hz, 3H). ^{13}C NMR (100 MHz, $CDCl_3$) δ 145.2, 140.4, 129.3, 128.2, 123.8, 120.3, 73.9, 38.3, 31.5, 29.4, 23.9, 22.6, 14.1. IR

(neat): 2090 cm^{-1}. HRMS (ESI-TOF) m/z: $[M + H - N_2]^+$ calcd for $C_{19}H_{22}N$: 264.1752; found: 264.1748.

*9-azido-2,7-dibromo-9-phenyl-9H-fluorene **(102f)**:*

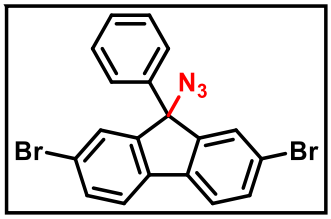

Prepared according to general procedure (**B**), using 2,7-dibromo-9-phenyl-9*H*-fluoren-9-ol (290.0 mg, 0.69 mmol) to afford 9-azido-2,7-dibromo-9-phenyl-9*H*-fluorene **102f** (240.0 mg, 78%) as a yellow solid after purification by column chromatography on silica gel (EtOAc:hexane = 1:99). Melting point: 134-136 °C. ^{1}H NMR (400 MHz, $CDCl_3$) δ 7.57 (s, 4H), 7.44 (m, 2H), 7.30 (m, 5H). ^{13}C NMR (100 MHz, $CDCl_3$) δ 148.8, 138.9, 138.1, 133.1, 129.0, 128.6, 128.5, 126.0, 122.8, 121.9, 75.8. IR (neat): 2098 cm^{-1}. HRMS (ESI-TOF) m/z: $[M + H - N_2]^+$ calcd for $C_{19}H_{12}Br_2N$: 411.9336; found: 411.9334.

*9-azido-2,7-dibromo-9-(p-tolyl)-9H-fluorene **(102g)**:*

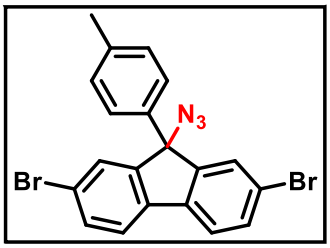

Prepared according to general procedure (**B**), using 2,7-dibromo-9-(p-tolyl)-9*H*-fluoren-9-ol (142.2 mg, 0.33 mmol) to afford 9-azido-2,7-dibromo-9-(p-tolyl)-9*H*-fluorene **102g** (118.2 mg, 79%) as a yellow solid after purification by column chromatography on silica gel (EtOAc:hexane = 1:99). Melting point: 160-162 °C. ^{1}H NMR (400 MHz, $CDCl_3$) δ 7.56 (s, 4H), 7.43 (s, 2H), 7.15 (m, 4H), 2.33 (s, 3H). ^{13}C NMR (100 MHz, $CDCl_3$) δ 148.9, 138.3, 138.1, 136.0, 133.0, 129.7, 128.6, 125.9, 122.8, 121.8, 75.7, 21.2. IR (neat): 2096 cm^{-1}. HRMS (ESI-TOF) m/z: $[M + H - N_2]^+$ calcd for $C_{20}H_{14}Br_2N$: 425.9493; found: 425.9487.

*9-azido-2,7-dibromo-9-(4-methoxyphenyl)-9H-fluorene **(102h)**:*

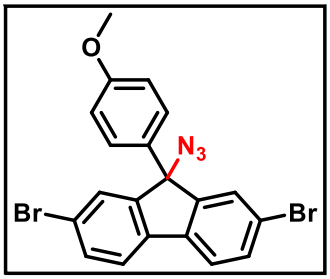

Prepared according to general procedure (**A**), using 2,7-dibromo-9-(4-methoxyphenyl)-9*H*-fluoren-9-ol (216.0 mg, 0.484 mmol) to afford 9-azido-2,7-dibromo-9-(4-methoxyphenyl)-9*H*-fluorene **102h** (209.0 mg, 92%) as a white solid after purification by column chromatography on silica gel (EtOAc:hexane = 1:99). Melting point: 112-114 °C. ^{1}H NMR (400 MHz, $CDCl_3$) δ 7.55 (d, *J* = 1.1 Hz, 4H), 7.43 (t, *J* = 1.1 Hz, 2H), 7.19

(m, 2H), 6.84 (m, 2H), 3.79 (s, 3H). ^{13}C NMR (100 MHz, $CDCl_3$) δ 159.7, 148.9, 138.0, 133.0, 130.8, 128.5, 127.3, 122.8, 121.9, 114.3, 75.5, 55.4. IR (neat): 2097 cm^{-1}. HRMS (ESI-TOF) m/z: $[M + H - N_2]^+$ calcd for $C_{20}H_{14}Br_2NO$: 441.9442; found: 441.9445.

*11-azido-11-(p-tolyl)-11H-benzo[b]fluorene **(102i)**:*

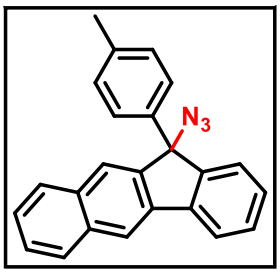

Prepared according to general procedure (**A**), using 11-(p-tolyl)-11*H*-benzo[*b*]fluoren-11-ol (364.6 mg, 1.13 mmol) to afford 11-azido-11-(p-tolyl)-11*H*-benzo[*b*]fluorene 1**02i** (344.0 mg, 88%) as a white solid after purification by column chromatography on silica gel (EtOAc:hexane = 1:99). Melting point: 134-136 °C. ^{1}H NMR (400 MHz, $CDCl_3$) δ 8.15 (s, 1H), 7.91 (dd, *J* = 14.5, 7.8 Hz, 2H), 7.78 (m, 2H), 7.49 (m, 3H), 7.36 (m, 2H), 7.26 (d, *J* = 8.0 Hz, 2H), 7.11 (d, *J* = 8.0 Hz, 2H), 2.32 (s, 3H). ^{13}C NMR (100 MHz, $CDCl_3$) δ 147.4, 145.2, 139.7, 138.4, 138.2, 137.6, 134.5, 133.8, 129.8, 129.4, 1239.3, 128.9, 128.4, 126.9, 126.3, 126.2, 125.5, 124.7, 120.9, 119.0, 76.0, 21.2. IR (neat): 2100 cm^{-1}. HRMS (ESI-TOF) m/z: $[M + H - N_2]^+$ calcd for $C_{24}H_{18}N$: 320.1439; found: 320.1437.

*3-azido-1-butyl-3-methylindolin-2-one **(102j)**:*

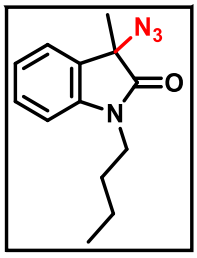

Prepared according to general procedure (**A**), using 1-butyl-3-hydroxy-3-methylindolin-2-one (200.0 mg, 0.91 mmol) to afford 3-azido-1-butyl-3-methylindolin-2-one 1**02j** (130.0 mg, 58%) as a white semi-solid after purification by column chromatography on silica gel (EtOAc:hexane = 1:99). ^{1}H NMR (400 MHz, $CDCl_3$) δ 7.33 (m, 2H), 7.10 (m, 1H), 6.88 (d, *J* = 7.7 Hz, 1H), 3.70 (t, *J* = 7.3 Hz, 2H), 1.68 (m, 5H), 1.38 (m, 2H), 0.95 (t, *J* = 7.4 Hz, 3H). ^{13}C NMR (100 MHz, $CDCl_3$) δ 174.9, 142.4, 130.1, 129.1, 123.8, 123.2, 109.2, 63.4, 40.1, 29.4, 21.6, 20.2, 13.8. IR (neat): 2099 cm^{-1}. HRMS (ESI-TOF) m/z: $[M + H - N_2]^+$ calcd for $C_{13}H_{17}N_2O$: 217.1341; found: 217.1331.

*9-azido-9-benzyl-9H-fluorene **(102k)**:*

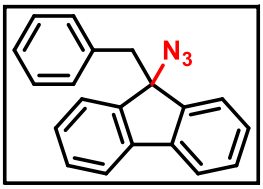

Prepared according to general procedure (**A**), using 9-benzyl-9*H*-fluoren-9-ol (285.0 mg, 1.04 mmol) to afford 9-azido-9-benzyl-9*H*-fluorene **102k** (222.0 mg, 71%) as a white semi-solid after purification by column

chromatography on silica gel (EtOAc:hexane = 1:99). ^{1}H NMR (400 MHz, $CDCl_3$) δ 7.61 (d, *J* = 7.5 Hz, 2H), 7.40 (m, 2H), 7.33 (m, 4H), 7.16 (m, 3H), 6.97 (d, *J* = 7.6 Hz, 2H), 3.29 (s, 2H). ^{13}C NMR (100 MHz, $CDCl_3$) δ 144.6, 140.1, 135.4, 130.9, 129.4, 127.8, 127.7, 126.9, 124.7, 120.3, 73.9, 44.7. IR (neat): 2093 cm^{-1}. HRMS (ESI-TOF) m/z: $[M + H - N_2]^+$ calcd for $C_{20}H_{16}N$: 270.1283; found: 270.1284.

9-azido-9-(4-methoxybenzyl)-9H-fluorene ***(102l)*****:**

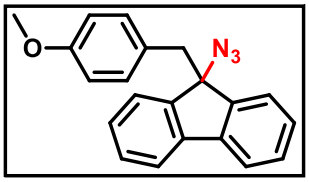

Prepared according to general procedure (**B**), using 9-(4-methoxybenzyl)-9*H*-fluoren-9-ol (1884.0 mg, 5.75 mmol) to afford 9-azido-9-(4-methoxybenzyl)-9*H*-fluorene **102l** (1700.0 mg, 83%) as a yellow solid after purification by column chromatography on silica gel (EtOAc:hexane = 1:99). Melting point: 49-51 ^{o}C. ^{1}H NMR (400 MHz, $CDCl_3$) δ 7.60 (d, *J* = 7.5 Hz, 2H), 7.36 (m, 6H), 6.86 (d, *J* = 8.5 Hz, 2H), 6.66 (d, *J* = 8.6 Hz, 2H), 3.73 (s, 3H), 3.20 (s, 2H). ^{13}C NMR (100 MHz, $CDCl_3$) δ 158.5, 144.7, 140.1, 131.8, 129.4, 127.8, 127.6, 124.7, 120.3, 113.1, 74.0, 55.2, 43.8. IR (neat): 2096 cm^{-1}. HRMS (ESI-TOF) m/z: $[M + H - N_2]^+$ calcd for $C_{21}H_{18}NO$: 300.1388; found: 300.1390.

9-([1,1'-biphenyl]-4-ylmethyl)-9-azido-9H-fluorene ***(102m)*****:**

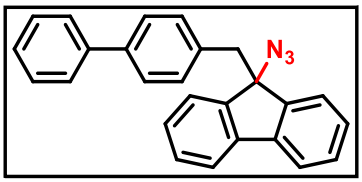

Prepared according to general procedure (**A**), using 9-([1,1'-biphenyl]-4-ylmethyl)-9*H*-fluoren-9-ol (188.8 mg, 0.542 mmol) to afford 9-([1,1'-biphenyl]-4-ylmethyl)-9-azido-9*H*-fluorene **102m** (198.4 mg, 98%) as a white semi-solid after purification by column chromatography on silica gel (EtOAc:hexane = 1:99). ^{1}H NMR (400 MHz, $CDCl_3$) δ 7.61 (d, *J* = 7.5 Hz, 2H), 7.56 (d, *J* = 1.3 Hz, 2H), 7.36 (m, 11H), 7.02 (d, *J* = 8.1 Hz, 2H), 3.29 (s, 2H). ^{13}C NMR (100 MHz, $CDCl_3$) δ 144.6, 140.8, 140.2, 139.6, 134.6, 131.3, 129.5, 128.9, 127.9, 127.3, 127.1, 126.3, 124.7, 120.4, 73.9, 44.4. IR (neat): 2093 cm^{-1}. HRMS (ESI-TOF) m/z: $[M + H - N_2]^+$ calcd for $C_{26}H_{20}N$: 346.1596; found: 346.1595.

6-phenylphenanthridine ***(100a)*****:**[146]

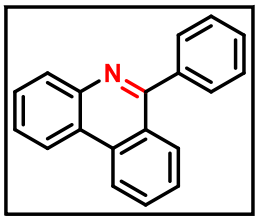

Prepared according to general procedure (**C**), using 9-azido-9-phenyl-9*H*-fluorene (51.1 mg, 0.17 mmol) to afford 6-phenylphenanthridine **100a** (37.0 mg, 85%) as a white solid after purification by column

chromatography on silica gel (EtOAc:hexane = 10:90. Melting point: 96-98 °C. ^{1}H NMR (400 MHz, $CDCl_3$) δ 8.64 (dd, *J* = 31.5, 8.2 Hz, 2H), 8.27 (d, *J* = 8.2 Hz, 1H), 8.11 (dd, *J* = 8.3, 0.5 Hz, 1H), 7.84 (t, *J* = 7.7 Hz, 1H), 7.76 (m, 3H), 7.68 (m, 1H), 7.57 (m, 4H). ^{13}C NMR (100 MHz, $CDCl_3$) δ 161.3, 143.8, 139.8, 133.5, 130.6, 130.4, 129.8, 129.0, 128.9, 128.8, 128.5, 127.2, 127.0, 125.3, 123.8, 122.3, 122.0. IR (neat): 1569, 1358 cm^{-1}. HRMS (ESI-TOF) m/z: $[M + H]^+$ calcd for $C_{19}H_{14}N$: 256.1126; found: 256.1127.

6-(p-tolyl)phenanthridine ***(100b):***[146]

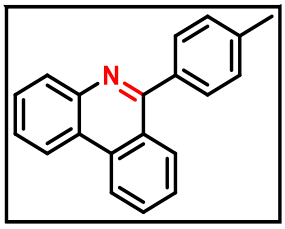

Prepared according to general procedure (**C**), using 9-azido-9-(p-tolyl)-9*H*-fluorene (64.0 mg, 0.22 mmol) to afford 6-(p-tolyl)phenanthridine **100b** (52.1 mg, 90%) as a white solid after purification by column chromatography on silica gel (EtOAc:hexane = 10:90). Melting point: 82-84 °C. ^{1}H NMR (400 MHz, $CDCl_3$) δ 8.65 (m, 2H), 8.20 (m, 2H), 7.85 (ddd, *J* = 8.3, 7.1, 1.3 Hz, 1H), 7.76 (ddd, *J* = 8.3, 7.1, 1.4 Hz, 1H), 7.64 (m, 4H), 7.38 (d, *J* = 7.8 Hz, 2H), 2.49 (s, 3H). ^{13}C NMR (100 MHz, $CDCl_3$) δ 161.5, 144.0, 138.7, 137.1, 133.6, 130.7, 130.5, 129.8, 129.2, 129.1, 128.9, 127.2, 126.9, 125.5, 123.8, 122.3, 122.1, 21.5. IR (neat): 1568, 1359 cm^{-1}. HRMS (ESI-TOF) m/z: $[M + H]^+$ calcd for $C_{20}H_{16}N$: 270.1283; found: 270.1280.

6-(4-methoxyphenyl)phenanthridine ***(100c):***[146]

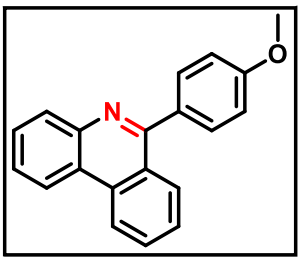

Prepared according to general procedure (**C**), using 9-azido-9-(4-methoxyphenyl)-9*H*-fluorene (150.0 mg, 0.48 mmol) to afford 6-(4-methoxyphenyl)phenanthridine **100c** (105.0 mg, 77%) as a white solid after purification by column chromatography on silica gel (EtOAc:hexane = 10:90). Melting point: 145-147 °C. ^{1}H NMR (400 MHz, $CDCl_3$) δ 8.69 (d, *J* = 8.3 Hz, 1H), 8.60 (d, *J* = 7.5 Hz, 1H), 8.20 (m, 2H), 7.84 (m, 1H), 7.68 (m, 5H), 7.10 (m, 2H), 3.92 (s, 3H). ^{13}C NMR (100 MHz, $CDCl_3$) δ 161.0, 160.3, 144.0, 133.6, 132.5, 131.3, 130.6, 130.4, 129.1, 128.9, 127.2, 126.8, 125.5, 123.8, 122.3, 122.0, 114.0, 55.6. IR (neat): 1512, 1245 cm^{-1}. HRMS (ESI-TOF) m/z: $[M + H]^+$ calcd for $C_{20}H_{16}NO$: 286.1232; found: 286.1242.

6-([1,1'-biphenyl]-4-yl)phenanthridine ***(100d)*****:**[146]

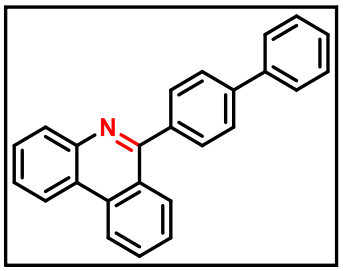

Prepared according to general procedure (**C**), using 9-([1,1'-biphenyl]-4-yl)-9-azido-9*H*-fluorene (110.0 mg, 0.31 mmol) to afford 6-([1,1'-biphenyl]-4-yl)phenanthridine **100d** (77.0 mg, 81%) as a white solid after purification by column chromatography on silica gel (EtOAc:hexane = 10:90). Melting point: 198-200 °C. ^{1}H NMR (400 MHz, $CDCl_3$) δ 8.71 (d, *J* = 8.1 Hz, 1H), 8.63 (d, *J* = 8.0 Hz, 1H), 8.30 (d, *J* = 7.8 Hz, 1H), 8.22 (d, *J* = 8.1 Hz, 1H), 7.83 (dd, *J* = 17.9, 6.9 Hz, 6H), 7.72 (d, *J* = 3.8 Hz, 3H), 7.64 (t, *J* = 7.4 Hz, 1H), 7.51 (t, *J* = 6.7 Hz, 2H), 7.42 (t, *J* = 6.5 Hz, 1H). ^{13}C NMR (100 MHz, $CDCl_3$) δ 161.0, 143.9, 141.7, 140.9, 138.8, 133.6, 130.7, 130.5, 130.4, 129.0, 127.7, 127.4, 127.3, 125.3, 123.8, 122.4, 122.1. IR (neat): 1642, 1361 cm^{-1}. HRMS (ESI-TOF) m/z: $[M + H]^+$ calcd for $C_{25}H_{18}N$: 332.1439; found: 332.1436.

6-hexylphenanthridine ***(100e)*****:**[147]

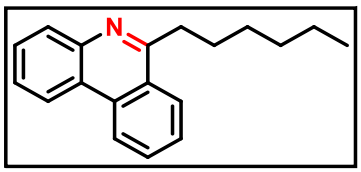

Prepared according to general procedure (**C**), using 9-azido-9-hexyl-9*H*-fluorene (116.5 mg, 0.40 mmol) to afford 6-hexylphenanthridine **100e** (85.0 mg, 81%) as a white solid after purification by column chromatography on silica gel (EtOAc:hexane = 10:90). Melting point: 69-71 °C. ^{1}H NMR (400 MHz, $CDCl_3$) δ 8.59 (dd, *J* = 40.3, 7.9 Hz, 2H), 8.19 (dd, *J* = 49.1, 7.9 Hz, 2H), 7.70 (m, 4H), 3.36 (m, 2H), 1.91 (d, *J* = 7.3 Hz, 2H), 1.53 (d, *J* = 6.1 Hz, 2H), 1.35 (s, 4H), 0.90 (d, *J* = 6.8 Hz, 3H). ^{13}C NMR (100 MHz, $CDCl_3$) δ 162.7, 143.9, 133.1, 130.4, 129.7, 128.7, 127.3, 126.5, 126.3, 125.4, 123.8, 122.6, 122.0, 36.6, 31.9, 29.8, 22.8, 14.3. IR (neat): 1577, 1454 cm^{-1}. HRMS (ESI-TOF) m/z: $[M + H]^+$ calcd for $C_{19}H_{22}N$: 264.1752; found: 264.1754.

3,8-dibromo-6-phenylphenanthridine ***(100f)*****:**[148]

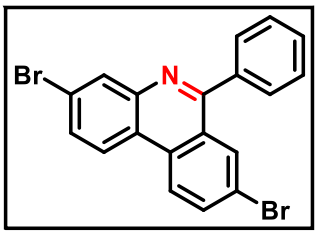

Prepared according to general procedure (**C**), using 9-azido-2,7-dibromo-9-phenyl-9*H*-fluorene (146.0 mg, 0.33 mmol) to afford 3,8-dibromo-6-phenylphenanthridine **100f** (111.7 mg, 82%) as a white

solid after purification by column chromatography on silica gel (EtOAc:hexane = 10:90). Melting point: 197-199 °C. ^{1}H NMR (400 MHz, $CDCl_3$) δ 8.51 (d, *J* = 8.8 Hz, 1H), 8.42 (m, 2H), 8.25 (d, *J* = 2.0 Hz, 1H), 7.96 (dd, *J* = 8.8, 2.0 Hz, 1H), 7.79 (dd, *J* = 8.8, 2.0 Hz, 1H), 7.71 (dd, *J* = 7.6, 1.7 Hz, 2H), 7.58 (m, 3H). ^{13}C NMR (100 MHz, $CDCl_3$) δ 161.4, 144.8, 138.9, 134.4, 133.1, 132.0, 131.5, 130.7, 129.8, 129.4, 128.9, 126.6, 124.2, 123.4, 123.1, 122.2, 121.8. IR (neat): 2918, 2851, 1586, 1450 cm^{-1}. HRMS (ESI-TOF) m/z: $[M + H]^+$ calcd for $C_{19}H_{12}Br_2N$: 411.9336; found: 411.9342.

3,8-dibromo-6-(p-tolyl)phenanthridine ***(100g):***[149]

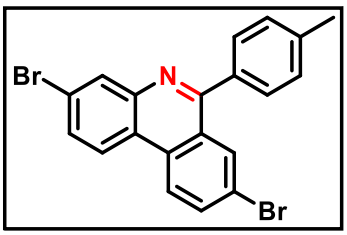

Prepared according to general procedure (**C**), using 9-azido-2,7-dibromo-9-(p-tolyl)-9*H*-fluorene (85.0 mg, 0.19 mmol) to afford 3,8-dibromo-6-(p-tolyl)phenanthridine **100g** (63.8 mg, 80%) as a white solid after purification by column chromatography on silica gel (EtOAc:hexane = 10:90). Melting point: 186-188 °C. ^{1}H NMR (400 MHz, $CDCl_3$) δ 8.49 (d, *J* = 8.8 Hz, 1H), 8.39 (dd, *J* = 5.4, 3.3 Hz, 2H), 8.28 (d, *J* = 2.0 Hz, 1H), 7.94 (dd, *J* = 8.8, 2.0 Hz, 1H), 7.76 (dd, *J* = 8.8, 2.0 Hz, 1H), 7.60 (d, *J* = 8.0 Hz, 2H), 7.39 (d, *J* = 7.8 Hz, 2H), 2.49 (s, 3H). ^{13}C NMR (100 MHz, $CDCl_3$) δ 161.4, 144.8, 139.5, 136.0, 134.3, 133.0, 132.0, 131.5, 130.5, 129.7, 129.5, 126.7, 124.1, 123.4, 123.1, 122.1, 121.7, 21.6. IR (neat): 1699, 1651, 1523, 1367 cm^{-1}. HRMS (ESI-TOF) m/z: $[M + H]^+$ calcd for $C_{20}H_{14}Br_2N$: 425.9493; found: 425.9497.

3,8-dibromo-6-(4-methoxyphenyl)phenanthridine ***(100h):***[150]

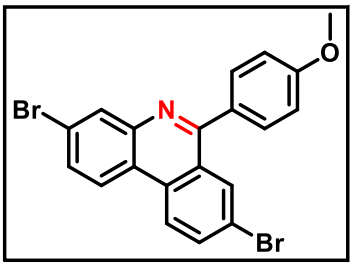

Prepared according to general procedure (**C**), using 9-azido-2,7-dibromo-9-(4-methoxyphenyl)-9*H*-fluorene (127.0 mg, 0.27 mmol) to afford 3,8-dibromo-6-(4-methoxyphenyl)phenanthridine **100h** (84.3 mg, 71%) as a white solid after purification by column chromatography on silica gel (EtOAc:hexane = 10:90). Melting point: 172-174 °C. ^{1}H NMR (400 MHz, $CDCl_3$) δ 8.49 (d, *J* = 8.8 Hz, 1H), 8.38 (dd, *J* = 5.4, 3.3 Hz, 2H), 8.30 (d, *J* = 2.0 Hz, 1H), 7.94 (dd, *J* = 8.8, 2.0 Hz, 1H), 7.71 (ddt, *J* = 11.5, 9.5, 2.4 Hz, 3H), 7.13 (m, 2H), 3.93 (s, 3H). ^{13}C NMR (100 MHz, $CDCl_3$) δ 161.0, 160.7, 144.9, 134.2, 132.9, 132.1, 131.5, 131.3, 130.5, 126.7, 124.2, 123.4, 123.1, 122.0, 121.7, 114.3, 55.6. IR (neat): 1700,

1511, 1426 cm^{-1}. HRMS (ESI-TOF) m/z: $[M + H]^+$ calcd for $C_{20}H_{14}Br_2NO$: 441.9442; found: 441.9446.

6-(p-tolyl)benzo[j]phenanthridine ***(100i)*****:**

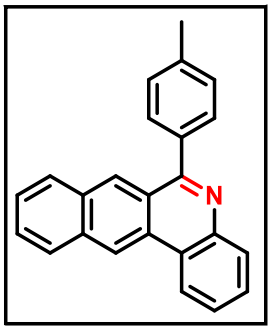

Prepared according to general procedure (**C**), using 11-azido-11-(p-tolyl)-11*H*-benzo[*b*]fluorene (208.0 mg, 0.60 mmol) to afford 5-(p-tolyl)benzo[*b*]phenanthridine **100i** (178.5 mg, 93%) as a yellow solid after purification by column chromatography on silica gel (EtOAc:hexane = 10:90). Melting point: 148-150 °C. ^{1}H NMR (400 MHz, $CDCl_3$) δ 9.07 (s, 1H), 8.83 (d, *J* = 8.2 Hz, 1H), 8.73 (s, 1H), 8.12 (dt, *J* = 9.8, 3.9 Hz, 3H), 7.87 (m, 1H), 7.69 (d, *J* = 8.0 Hz, 2H), 7.58 (m, 3H), 7.39 (d, *J* = 7.8 Hz, 2H), 2.50 (s, 3H). ^{13}C NMR (100 MHz, $CDCl_3$) δ 162.2, 141.6, 138.9, 137.0, 133.7, 133.6, 132.0, 130.8, 129.7, 129.4, 129.2, 128.4, 127.5, 126.2, 125.5, 123.0, 122.6, 121.1, 21.6. IR (neat): 3050, 1595, 1341, 1265 cm^{-1}. HRMS (ESI-TOF) m/z: $[M + H]^+$ calcd for $C_{24}H_{18}N$: 320.1439; found: 320.1442.

1-butyl-3-methylquinoxalin-2(1H)-one ***(100j)*****:**[151]

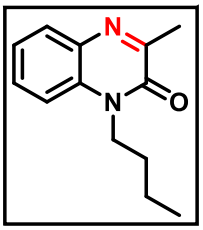

Prepared according to general procedure (**C**), using 3-azido-1-butyl-3-methylindolin-2-one (84.0 mg, 0.34 mmol) to afford 1-butyl-3-methylquinoxalin-2(1*H*)-one **100j** (30.0 mg, 41%) as a yellow solid after purification by column chromatography on silica gel (EtOAc:hexane = 30:70). Melting point: 142-144 °C. ^{1}H NMR (400 MHz, $CDCl_3$) δ 7.79 (d, *J* = 8.0 Hz, 1H), 7.49 (t, *J* = 7.8 Hz, 1H), 7.29 (m, 2H), 4.23 (m, 2H), 2.58 (s, 3H), 1.72 (m, 2H), 1.47 (m, 2H), 0.99 (t, *J* = 7.4 Hz, 3H). ^{13}C NMR (100 MHz, $CDCl_3$) δ 158.5, 155.0, 133.0, 132.5, 129.6, 129.7, 123.5, 113.7, 42.2, 29.4, 21.6, 20.4, 13.9. IR (neat): 2958, 1647, 1600, 1467 cm^{-1}. HRMS (ESI-TOF) m/z: $[M + H]^+$ calcd for $C_{13}H_{17}N_2O$: 217.1341; found: 217.1337.

phenanthridin-6-yl(phenyl)methanone ***(100k)*****:**[152]

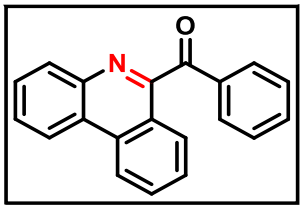

Prepared according to general procedure (**C**), using 9-azido-9-benzyl-9*H*-fluorene (68.0 mg, 0.23 mmol) to afford phenanthridin-6-yl(phenyl)methanone **100k** (15.0 mg, 23%) as a white solid after purification by column chromatography on silica gel (EtOAc:hexane = 15:85). Melting point: 142-144 °C. ^{1}H NMR (400 MHz, $CDCl_3$) δ 8.73 (d, *J* = 8.4 Hz, 1H), 8.66 (m, 1H), 8.23 (m, 1H), 8.15 (d, *J* = 8.2 Hz, 1H), 8.05 (dd, *J* = 8.4, 1.3 Hz, 2H), 7.90 (m, 1H), 7.78 (m, 2H), 7.65 (m, 2H), 7.48 (t, *J* = 7.8 Hz, 2H). ^{13}C NMR (100 MHz, $CDCl_3$) δ 194.9, 157.6, 142.8, 136.3, 134.1, 133.4, 131.4, 131.0, 130.7, 129.2, 128.7, 128.3, 127.9, 127.5, 124.6, 123.9, 122.5, 122.3. IR (neat): 3066, 1669, 1581, 1450, 1244 cm^{-1}. HRMS (ESI-TOF) m/z: $[M + H]^+$ calcd for $C_{20}H_{14}NO$: 284.1074; found: 284.1078.

(4-methoxyphenyl)(phenanthridin-6-yl)methanone ***(100l)*****:**[152]

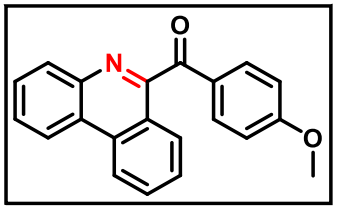

Prepared according to general procedure (**C**), using 9-azido-9-(4-methoxybenzyl)-9*H*-fluorene (29.0 mg, 0.08 mmol) to afford (4-methoxyphenyl)(phenanthridin-6-yl)methanone **100l** (15.0 mg, 54%) as a white solid after purification by column chromatography on silica gel (EtOAc:hexane = 10:90). Melting point: 160-162 °C. ^{1}H NMR (400 MHz, $CDCl_3$) δ 8.72 (d, *J* = 8.3 Hz, 1H), 8.65 (m, 1H), 8.22 (m, 1H), 8.12 (d, *J* = 7.8 Hz, 1H), 8.01 (m, 2H), 7.89 (m, 1H), 7.77 (m, 2H), 7.65 (m, 1H), 6.94 (m, 2H), 3.88 (s, 3H). ^{13}C NMR (100 MHz, $CDCl_3$) δ 193.6, 164.5, 158.2, 142.9, 133.4, 131.4, 130.7, 129.4, 129.2, 128.2, 127.9, 127.6, 124.6, 124.0, 122.4, 122.3, 114.1, 55.7. IR (neat): 2923, 1613, 1510, 1244 cm^{-1}. HRMS (ESI-TOF) m/z: $[M + H]^+$ calcd for $C_{21}H_{16}NO_2$: 314.1181; found: 314.1181.

[1,1'-biphenyl]-4-yl(phenanthridin-6-yl)methanone ***(100m)*****:**

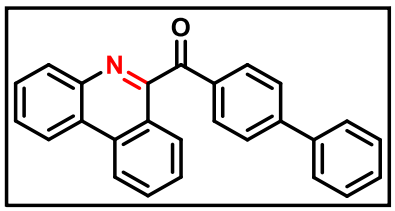

Prepared according to general procedure (**C**), using 9-([1,1'-biphenyl]-4-ylmethyl)-9-azido-9*H*-fluorene (158.0 mg, 0.42 mmol) to afford [1,1'-biphenyl]-4-yl(phenanthridin-6-yl)methanone **100m** (63.0 mg, 41%) as a white solid after purification by column chromatography on silica gel (EtOAc:hexane = 10:90). Melting point: 180-

182 °C. ^{1}H NMR (400 MHz, $CDCl_3$) δ 8.74 (d, *J* = 8.4 Hz, 1H), 8.67 (m, 1H), 8.25 (m, 1H), 8.20 (d, *J* = 7.8 Hz, 1H), 8.13 (d, *J* = 8.3 Hz, 2H), 7.91 (dd, *J* = 8.1, 7.4 Hz, 1H), 7.79 (m, 2H), 7.70 (m, 3H), 7.64 (dt, *J* = 3.3, 1.9 Hz, 2H), 7.47 (m, 2H), 7.41 (m, 1H). ^{13}C NMR (100 MHz, $CDCl_3$) δ 194.5, 157.7, 146.8, 142.8, 140.0, 135.1, 133.5, 131.5, 130.8, 129.3, 129.1, 128.5, 128.3, 128.0, 127.5, 127.4, 125.4, 124.7, 124.0, 122.5, 122.3. IR (neat): 3064, 1666, 1599, 1246 cm^{-1}. HRMS (ESI-TOF) m/z: $[M + H]^+$ calcd for $C_{26}H_{18}NO$: 360.1388; found: 360.1382.

4.6.B. Copies of ^{1}H and ^{13}C NMR spectra of representative compounds

9-azido-9-phenyl-9*H*-fluorene (102a):

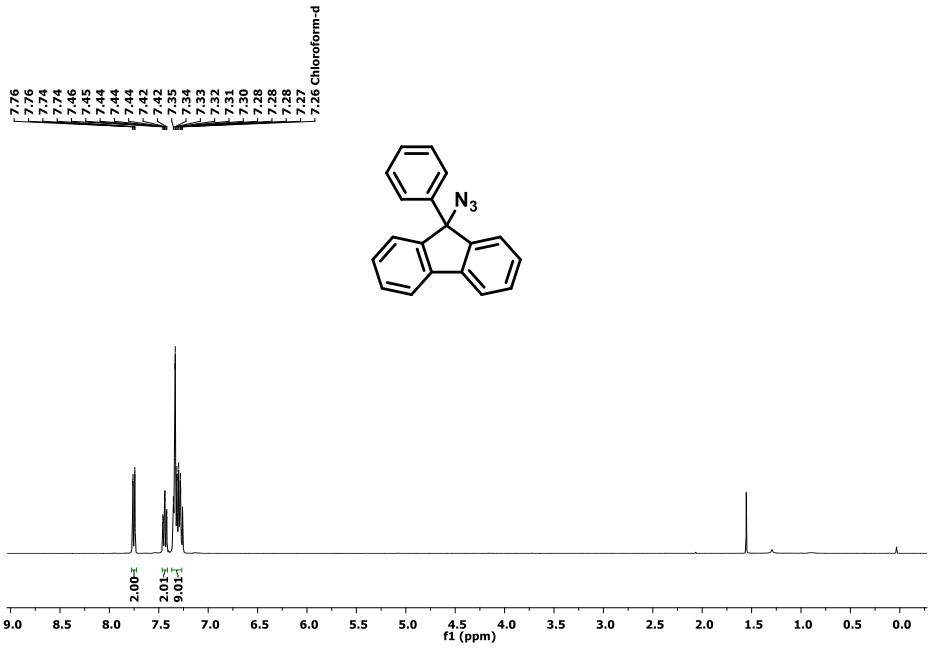

Figure 4.6.B.1: ^{1}H NMR of **102a**, 400 MHz, $CDCl_3$

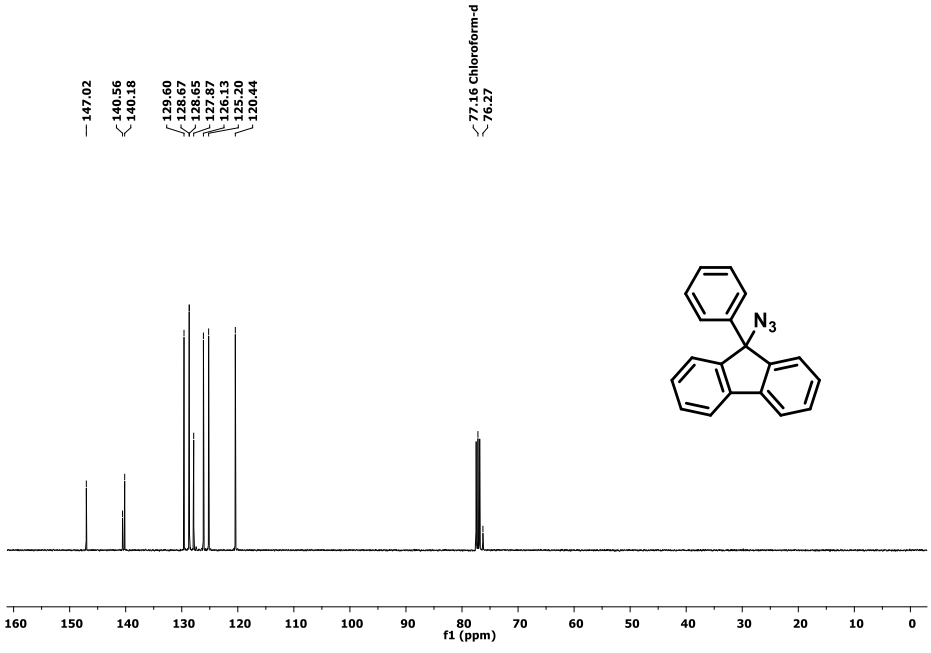

Figure 4.6.B.2: ^{13}C NMR of **102a**, 100 MHz, $CDCl_3$

9-([1,1'-biphenyl]-4-yl)-9-azido-9*H*-fluorene (102d):

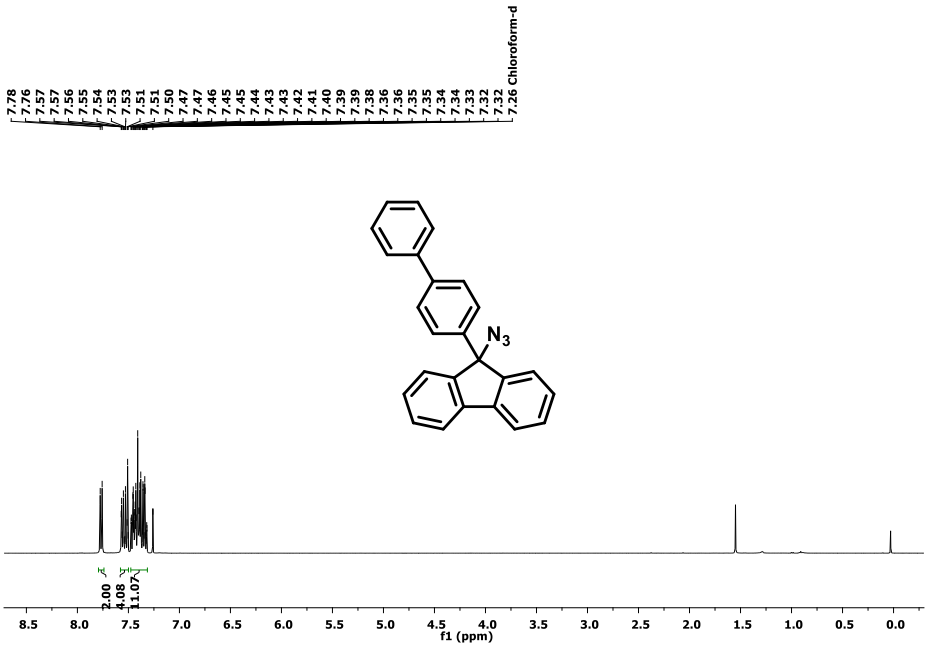

Figure 4.6.B.3: ^{1}H NMR of **102d**, 400 MHz, $CDCl_3$

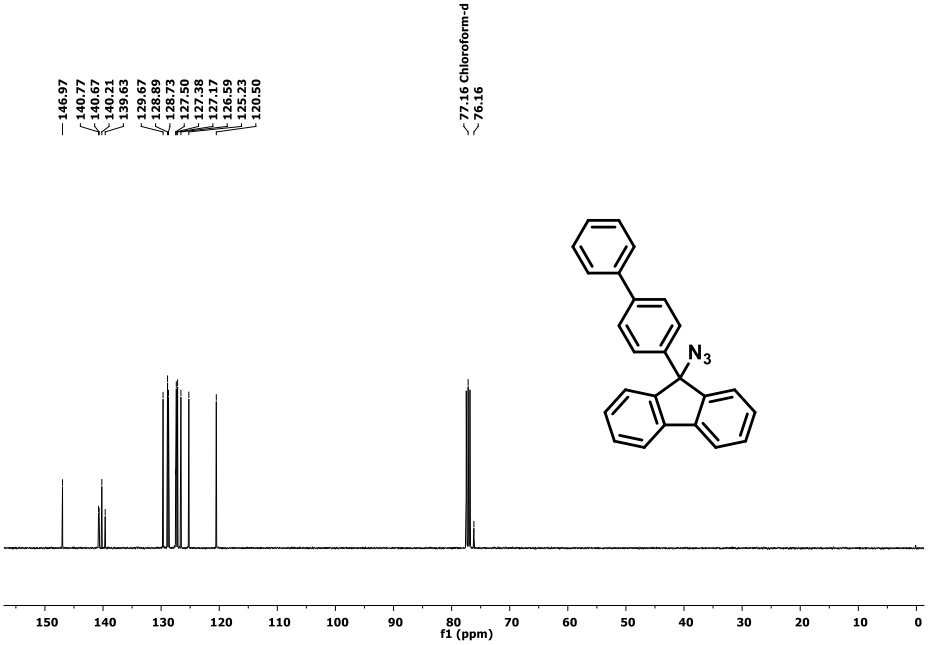

Figure 4.6.B.4: ^{13}C NMR of **102d**, 100 MHz, $CDCl_3$

9-azido-9-hexyl-9*H*-fluorene (102e):

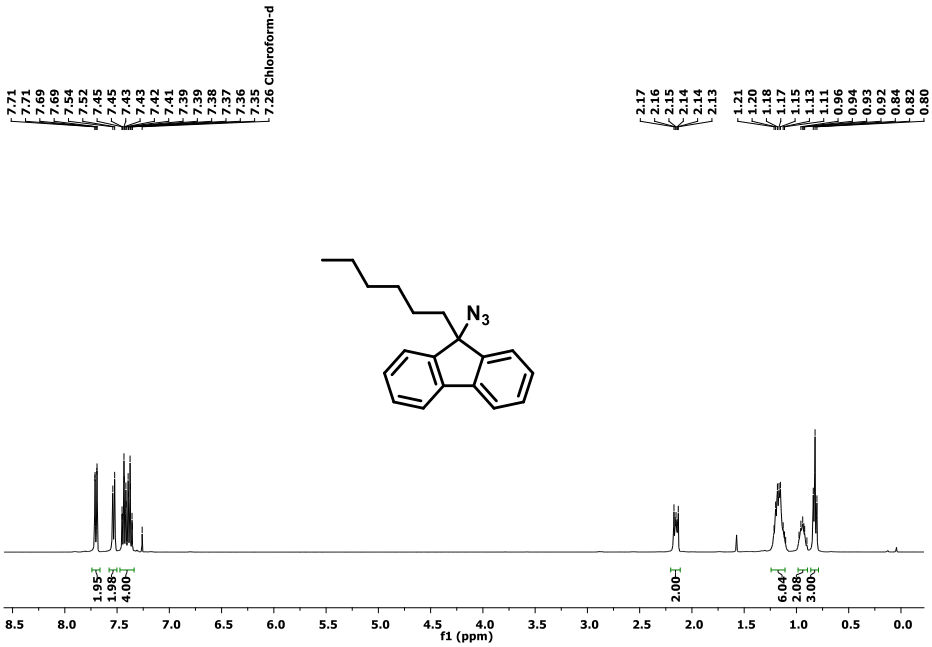

Figure 4.6.B.5: ^{1}H NMR of **102e**, 400 MHz, $CDCl_3$

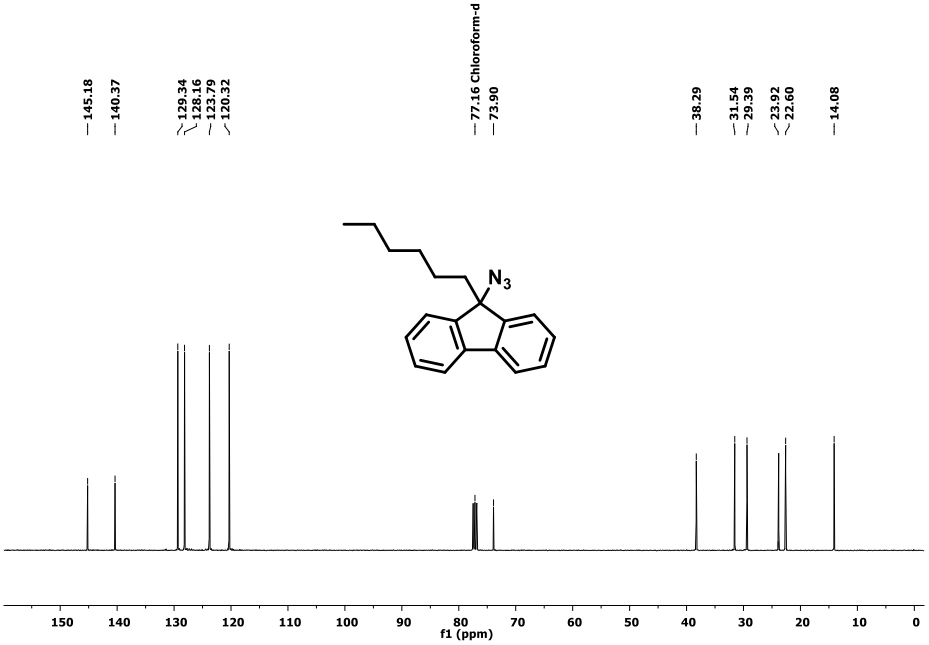

Figure 4.6.B.6: ^{13}C NMR of **102e**, 100 MHz, $CDCl_3$

9-azido-2,7-dibromo-9-(4-methoxyphenyl)-9*H*-fluorene (102h):

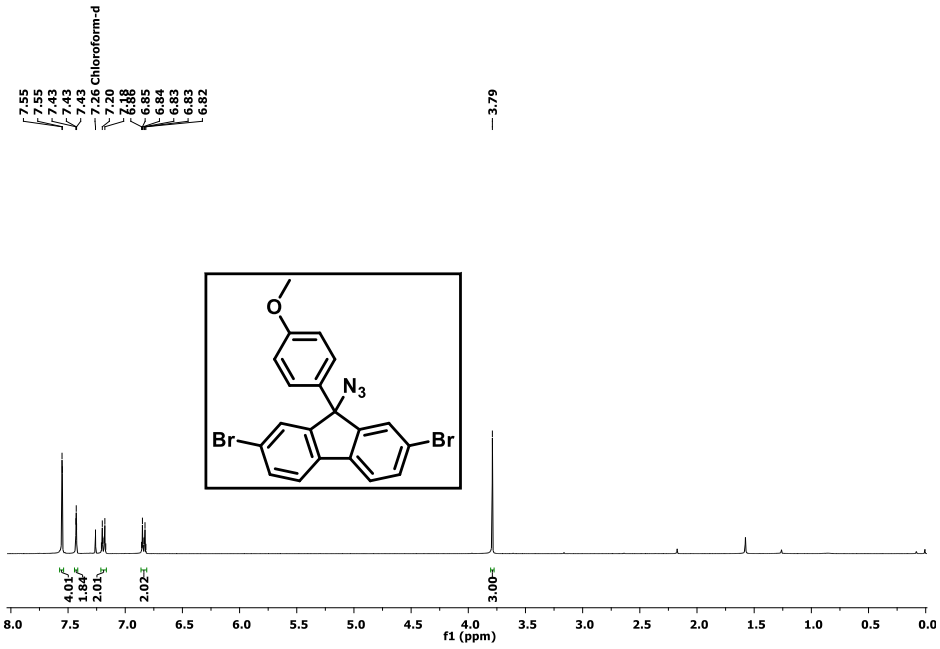

Figure 4.6.B.7: ^{1}H NMR of **102h**, 400 MHz, $CDCl_3$

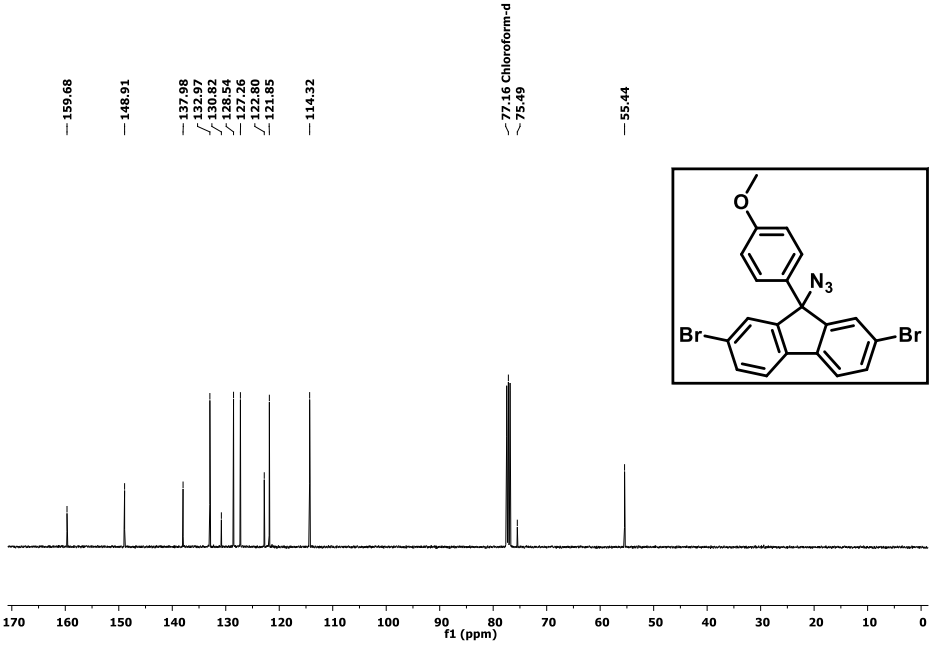

Figure 4.6.B.8: ^{13}C NMR of **102h**, 100 MHz, $CDCl_3$

9-azido-9-benzyl-9*H*-fluorene (102k):

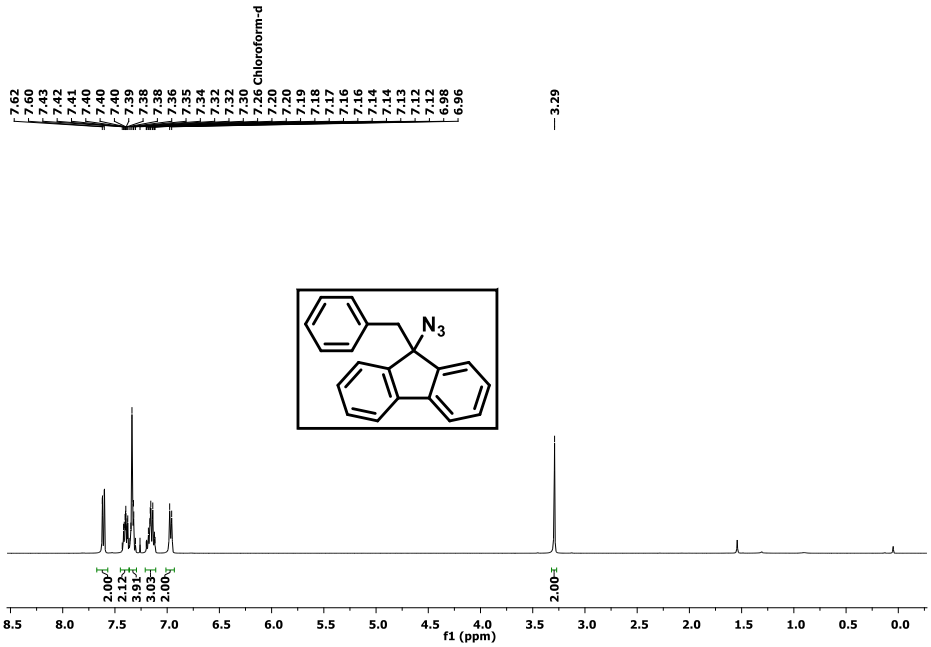

Figure 4.6.B.9: ^{1}H NMR of **102k**, 400 MHz, $CDCl_3$

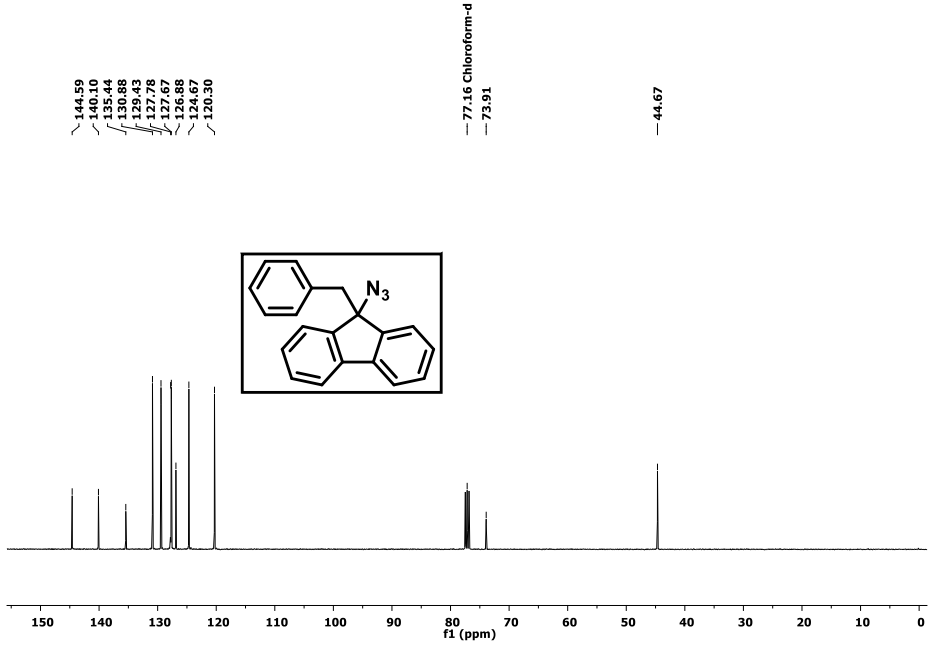

Figure 4.6.B.10: ^{13}C NMR of **102k**, 100 MHz, $CDCl_3$

6-hexylphenanthridine (100e):

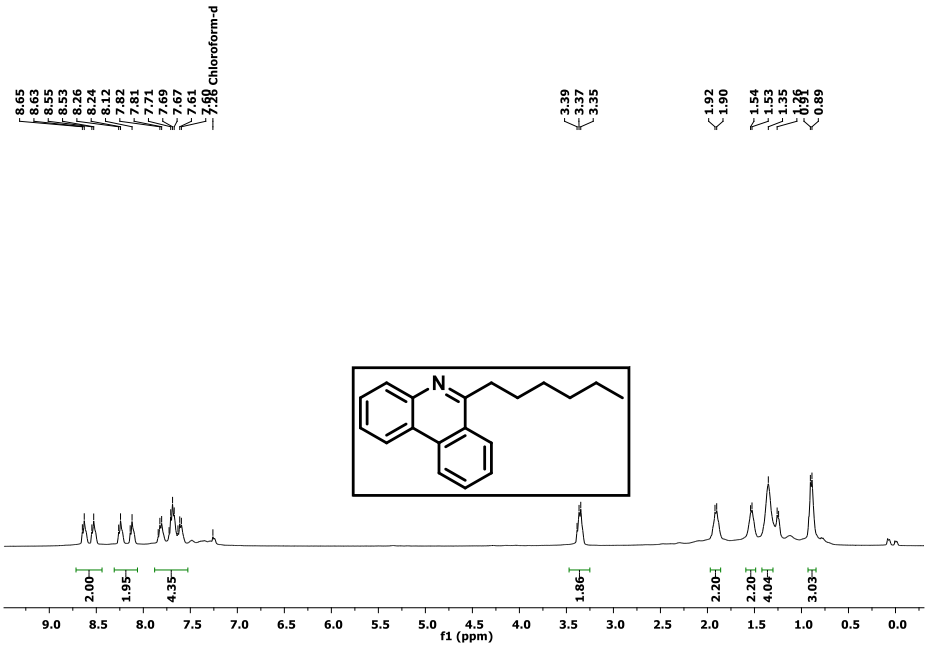

Figure 4.6.B.11: ^{1}H NMR of **100e**, 400 MHz, $CDCl_3$

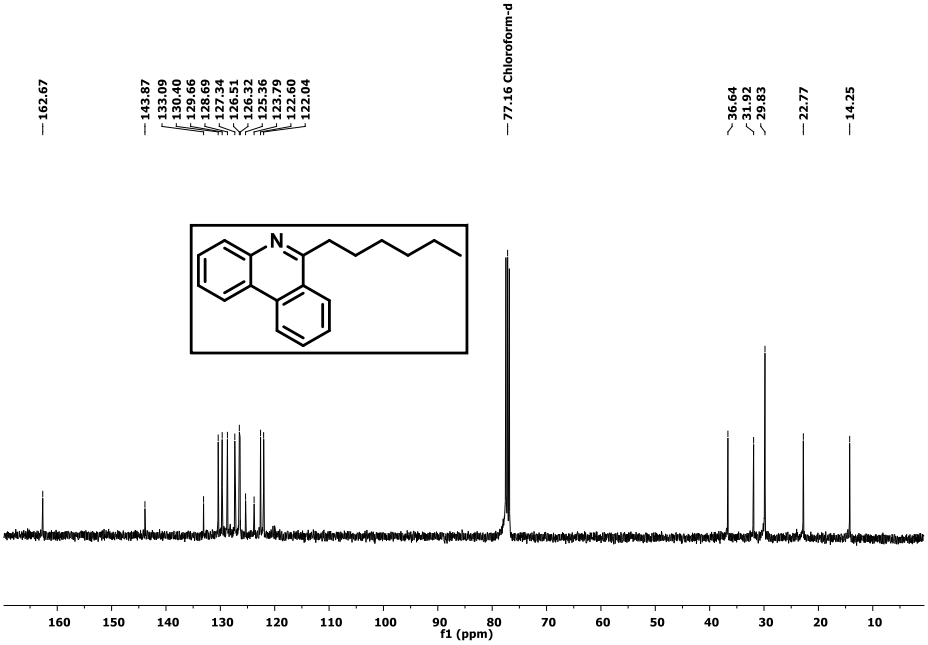

Figure 4.6.B.12: ^{13}C NMR of **100e**, 100 MHz, $CDCl_3$

6-(4-methoxyphenyl)phenanthridine (100c):

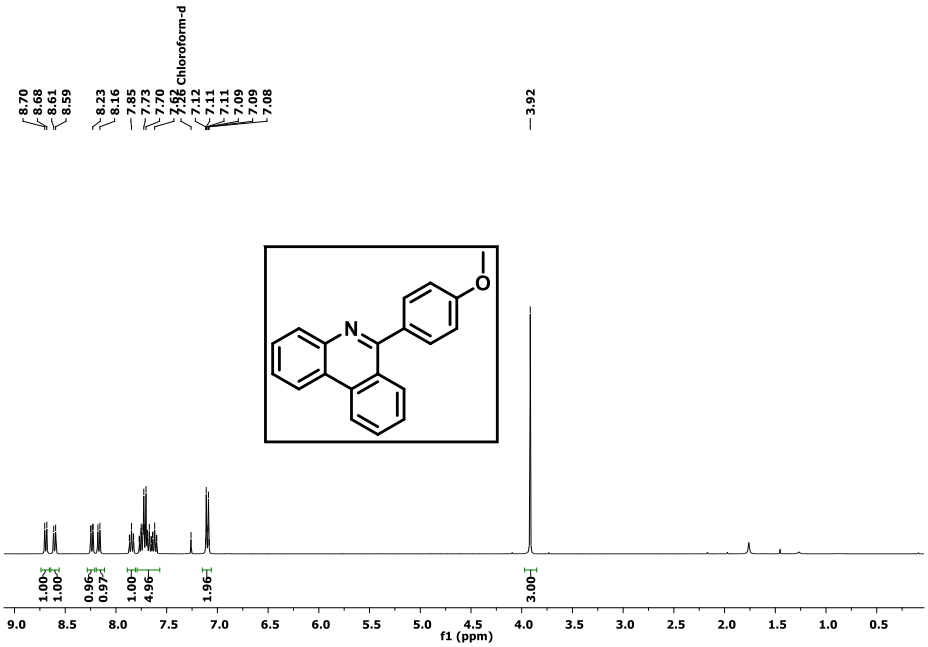

Figure 4.6.B.13: ^{1}H NMR of **100c**, 400 MHz, $CDCl_3$

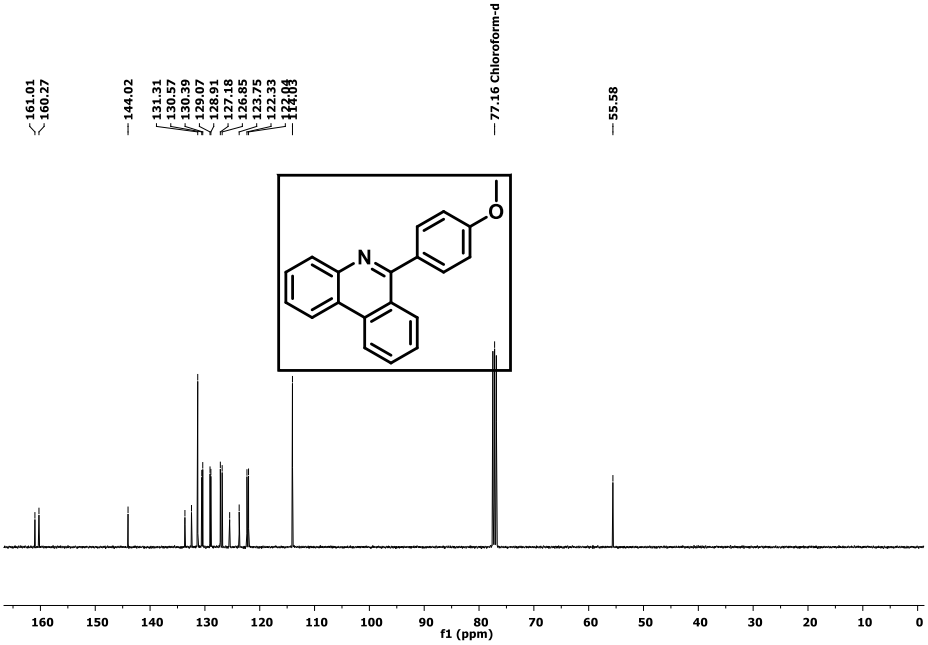

Figure 4.6.B.14: ^{13}C NMR of **100c**, 100 MHz, $CDCl_3$

3,8-dibromo-6-(4-methoxyphenyl)phenanthridine (100h):

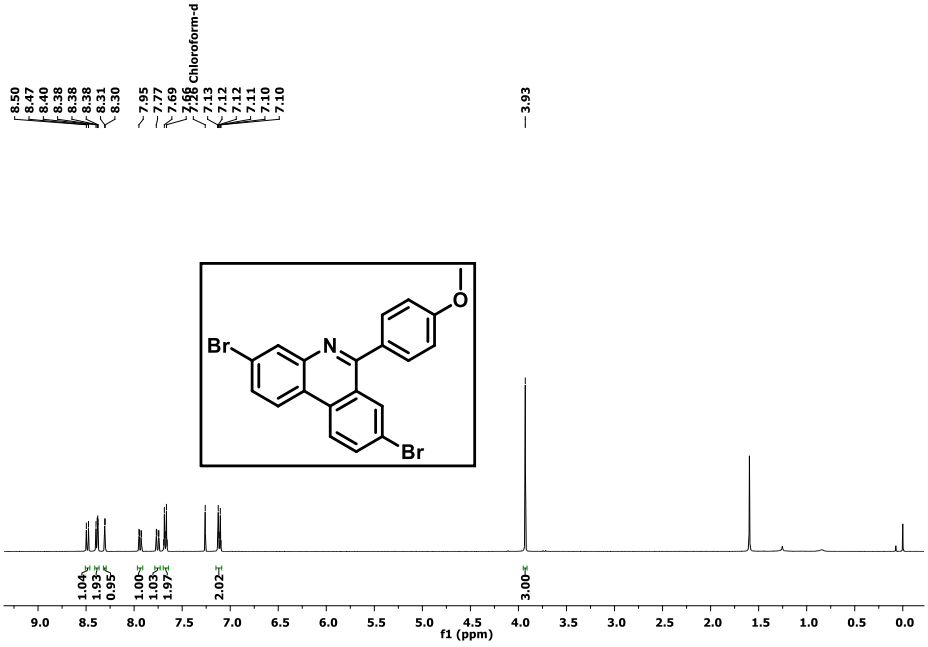

Figure 4.6.B.15: ^{1}H NMR of **100h**, 400 MHz, $CDCl_3$

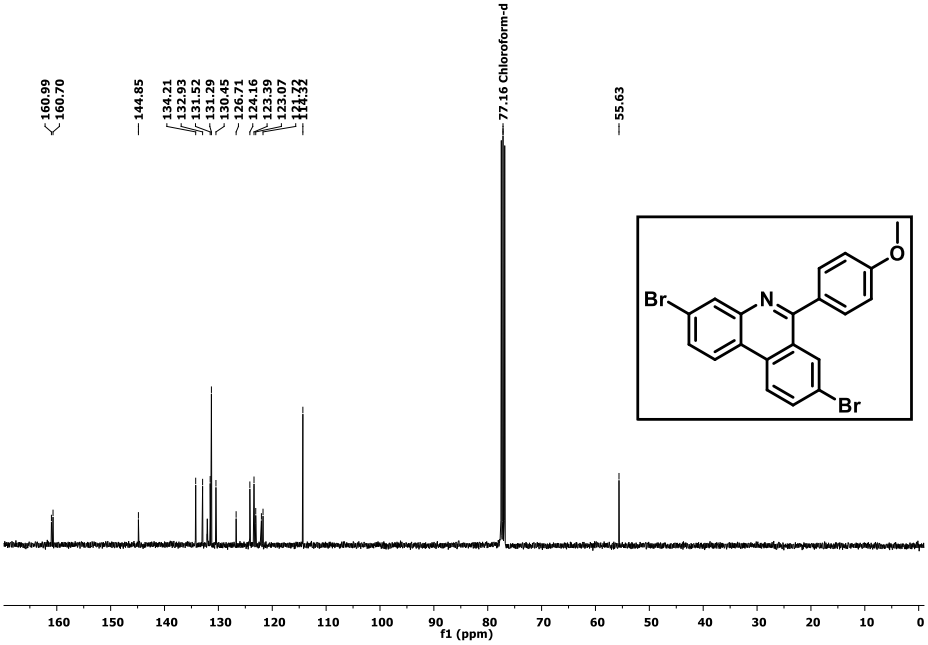

Figure 4.6.B.16: ^{13}C NMR of **100h**, 100 MHz, $CDCl_3$

(4-methoxyphenyl)(phenanthridin-6-yl)methanone (100l):

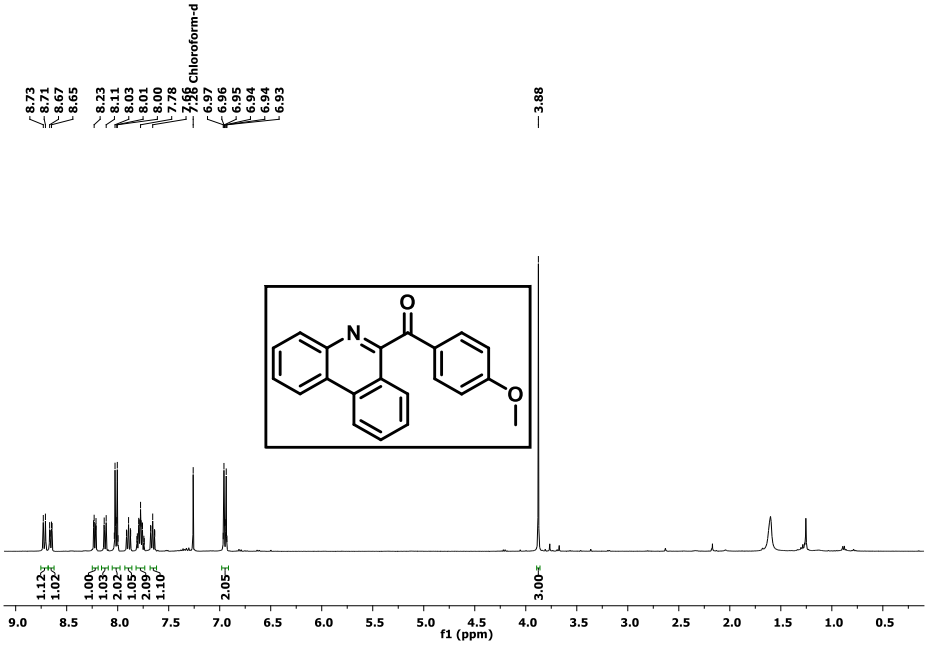

Figure 4.6.B.17: ^{1}H NMR of **100l**, 400 MHz, $CDCl_3$

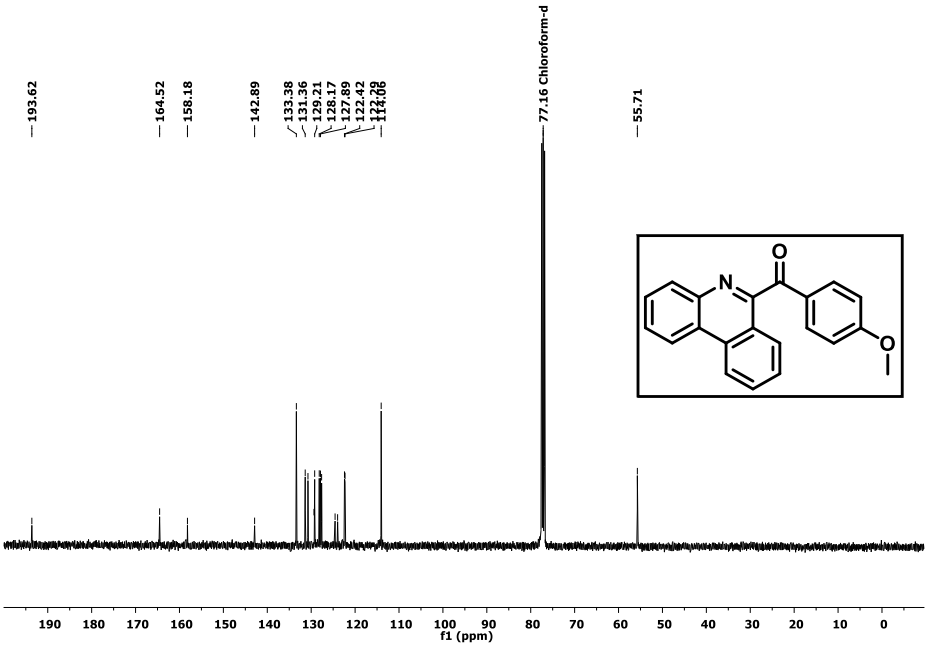

Figure 4.6.B.18: ^{13}C NMR of **100l**, 100 MHz, $CDCl_3$

Chapter V: Catalytic Acceptorless Dehydrogenation Strategy for Annulation under Neutral Conditions

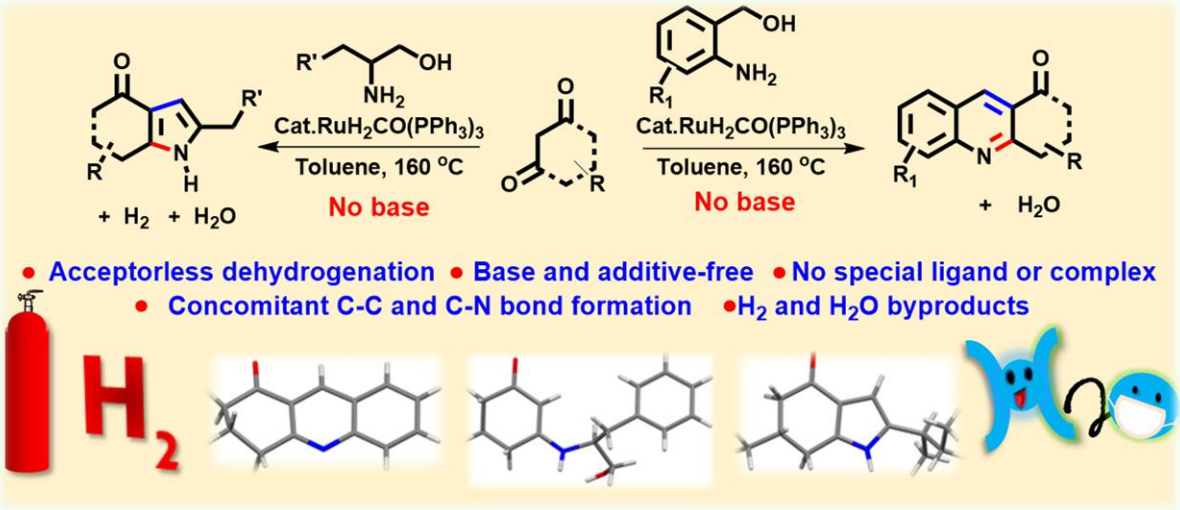

Catalytic Acceptorless Dehydrogenation Strategy for Annulation under Neutral Conditions

5.1. Catalytic acceptorless dehydrogenation and borrowing hydrogen method

Catalysis is one of the key aspects that involve transition-metal catalysts and shows a tremendous application in numerous synthetic transformations.[153] Moreover, heterocycles are the most diverse class of organic compounds known for their potential application in synthetic biology and materials science.[154] Additionally, the construction of a C-C or C-N bond is demanding synthetic organic transformation for heterocycles. In this context, environmentally benign alcohol serves as an excellent starting material to conduct such reactions. However, new bond construction using environmentally benign alcohol is challenging because hydroxy is a poor leaving group. Therefore, traditionally these alcohols **A** undergo functional group transformation in the presence of base and additives to make hydroxy as good leaving group. Next, incoming nucleophiles attacks on electrophilic center to give the desired product **B**. This process requires two or more than two steps and uses stoichiometric bases, metal salts, or additive. Further, it also generates a considerable amount of waste in a larger scale (Scheme 5.1.1).[155]

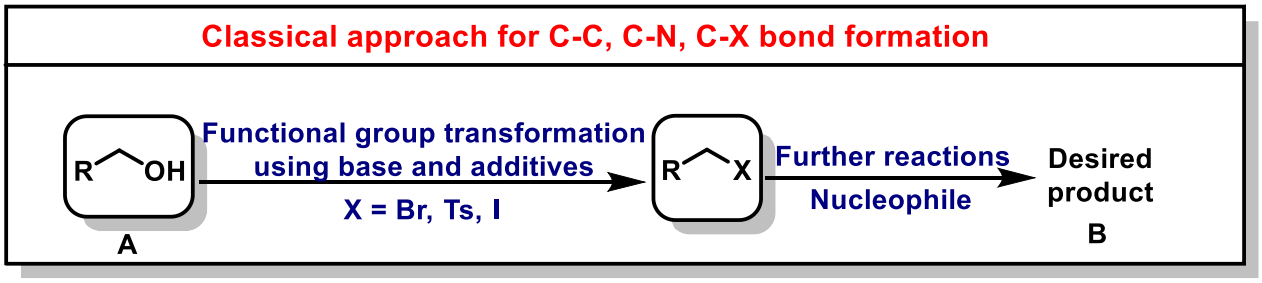

Scheme 5.1.1: Classical approach for C-C, C-N, and C-X bond formation

Therefore, a sustainable catalytic method emphasizing one-pot conditions that allows the assembly of many bond constructions with high atom economy and use inexpensive reactants is highly demanding in the current manufacturing procedures. In this regard, to move away from pitfalls associated with the classical approach, acceptorless dehydrogenation and borrowing

hydrogenation concepts have emerged as powerful tools to achieve sustainability goals.[155] In the modern chemical synthesis, the acceptorless dehydrogenation (AD) of alcohols has been extensively employed for chemical reactions due to several attractive features for C-C and C-X bond formation.[156]

Acceptorless dehydrogenation strategy is mainly based on the oxidation of an alcohol to give a carbonyl derivative with the liberation of hydrogen (Scheme 5.1.2). Subsequently, an attack of the nucleophile gives a condensation product with water as the byproduct. Notably, this process retains a high atom economy, which is a primary advantage in acceptorless dehydrogenation driven sustainable synthesis. Additionally, hydrogen gas is an essential high-energy clean fuel (Scheme 5.1.2).[153-154]

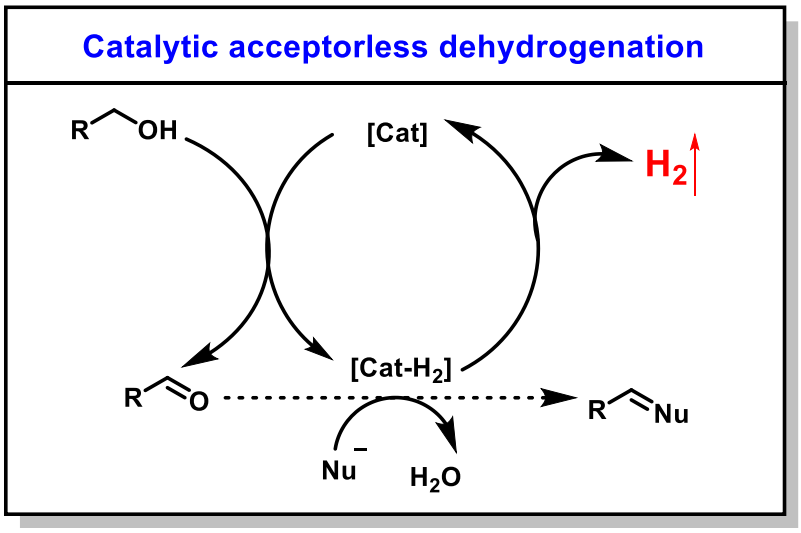

Scheme 5.1.2: General scheme for catalytic acceptorless dehydrogenation

In contrast, *Borrowing hydrogen* (BH) strategy follows the oxidation of an alcohol to give an aldehyde or ketone using a metal catalyst (Scheme 5.1.3). Later, the oxidized product is then attacked by nucleophiles to give an unsaturated intermediate. Further, the *in situ* generated H_2 can be used for the reduction of an unsaturated compound to afford the desired products such as an amine or α-alkylated carbonyl derivatives. Gratifyingly, water is the only by-product formed during the borrowing hydrogen process. Therefore, this process is atom economical and environmentally benign.[157]

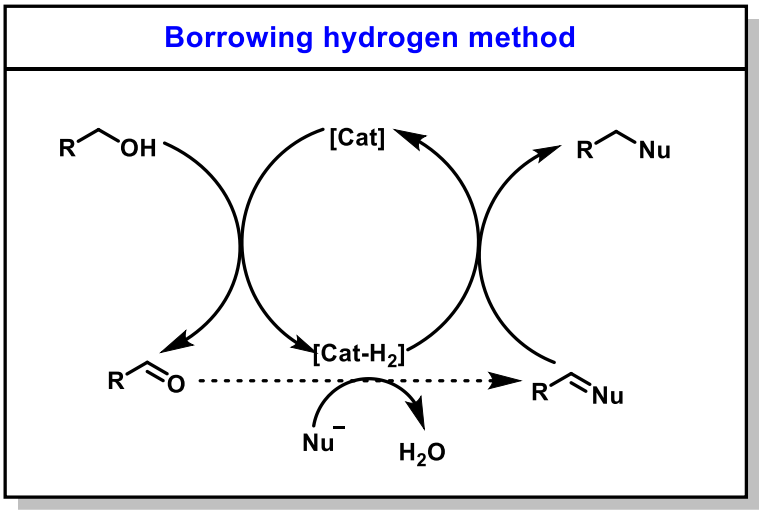

Scheme 5.1.3: General scheme for borrowing hydrogenation

Both the borrowing hydrogen and acceptorless dehydrogenation strategies have gained immense interest in the synthetic organic chemist because (i) it uses feedstock alcohol as alkylating agents, (ii) one pot operation enhances atom economy and step-economy, (iii) eliminates water and hydrogen gas as the byproducts. In the last few decades, several catalysts and catalytic reactions were reported using BH/AD strategy. Some selected reactions are described in the literature section.

5.2. Literature background on acceptorless dehydrogenation and borrowing hydrogen concept

A number of homogeneous and heterogeneous transition metal catalysts have been identified for AD and BH processes. The pioneering work on the BH process using alcohol as an alkylating reagent was done by Grigg, Watanabe, Murahashi and coworkers. In 1981, Grigg and coworkers performed *N*-alkylation of amines **103** using alcohol **104** as an alkylating agent in the presence of rhodium (Rh), iridium (Ir) or ruthenium (Ru) complexes at 100 ^{o}C (Scheme 5.2.1).[158]

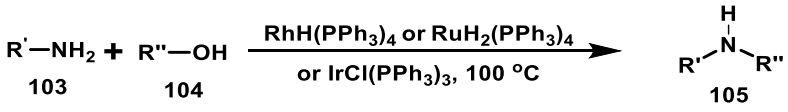

Scheme 5.2.1: *N*-alkylation of amines using alcohols

However, Watanabe and coworkers reported BH process for the *N*-alkylation of amines **103** using $RuCl_2(PPh_3)_3$ at 180 °C to access secondary amine **105** and tertiary amines **106** (Scheme 5.2.2).[159-160.]

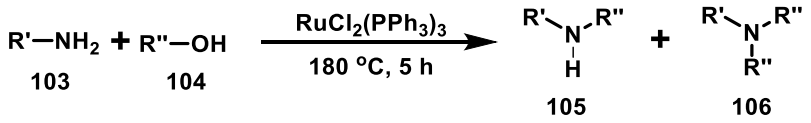

Scheme 5.2.2: Watanabe's approach for *N*-alkylation of amines

Next, Murahashi group reported the *N*-alkylation of amines using secondary alcohols **104** to get the secondary or tertiary amines facilitated by another variant of Ru-catalyst (Scheme 5.2.3).[161]

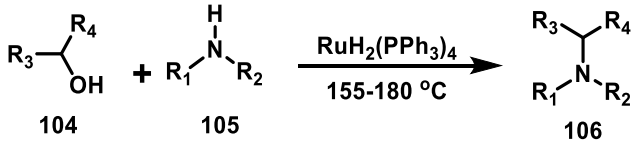

Scheme 5.2.3: Murahashi's work on *N*-alkylation of amines using alcohols

Milstein and coworkers reported the direct synthesis of imines **107** by following AD process using amine **103** and alcohol **104** in the presence of a Ru-PNP catalyst (Scheme 5.2.4).[162]

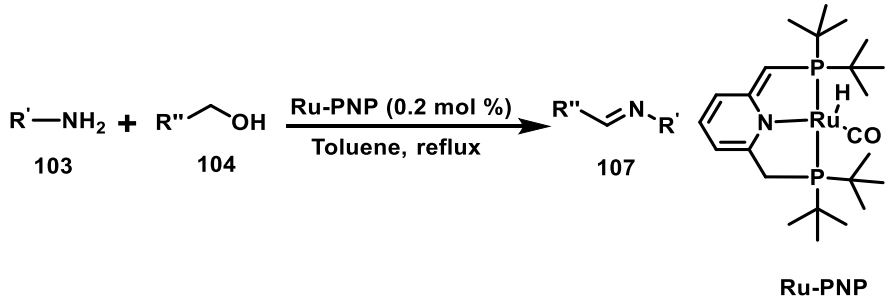

Scheme 5.2.4: Milstein's work on direct synthesis of imine using amine and alcohol

In 2011, Milstein group reported heterocycle synthesis from amino alcohols **108** with ruthenium pincer complexes has shown ligand-controlled selectivity to access pyrazines **109** and peptides **110** through extrusion of H_2 (Scheme 5.2.5).[163]

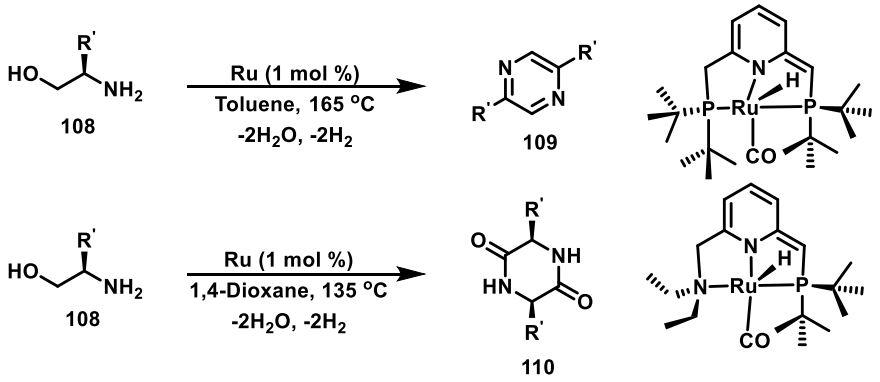

Scheme 5.2.5: Milstein's work to access pyrazines **109** and peptides **110**

Milstein group also reported a pathbreaking approach for the C-O and C-N bond to give amide derivative **111** by using alcohols and Ru-PNN catalyst (Scheme 5.2.6).[164]

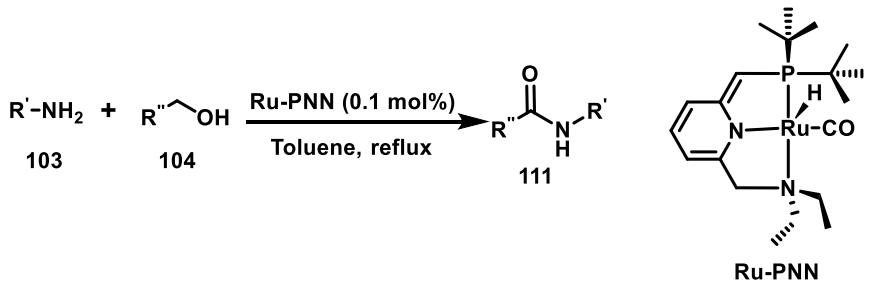

Scheme 5.2.6: Milstein's work on the direct synthesis of amides

However, the Srimani group synthesized a highly recyclable Ru-doped hydrotalcite catalyst for *N*-alkylation of benzamides with alcohols which followed the BH process (Scheme 5.2.7).[165] Additionally, the group has also demonstrated *N*-alkylation sulfonamides.

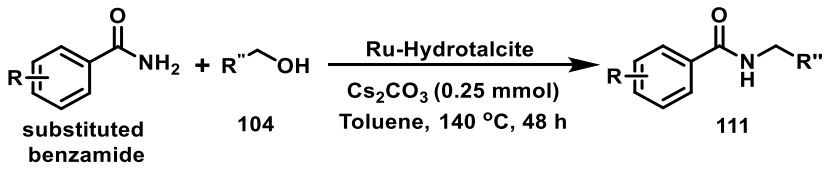

Scheme 5.2.7: Srimani's work on N-alkylation of benzamides

Oxidative cyclization of primary alcohols **104** with o-aminobenzamides **112** provided a new methodology for the construction of quinazolinones **113**, thus enabling a base-free, hydrogen-transfer process (Scheme 5.2.8).[166]

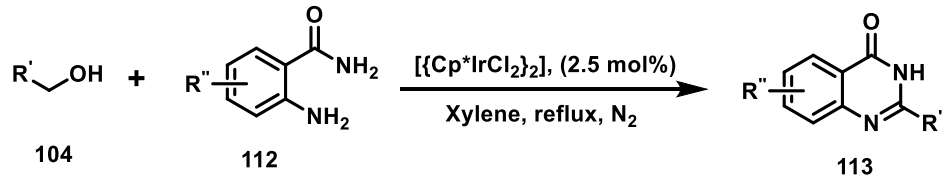

Scheme 5.2.8: Synthesis of quinazolinones via acceptorless dehydrogenation

Interestingly, Ryu group demonstrated C-C bond formation by α-alkylation of ketones **114** using $RuHCl(CO)(PPh_3)_3$ and alcohols as alkylating reagents (Scheme 5.2.9).[167]

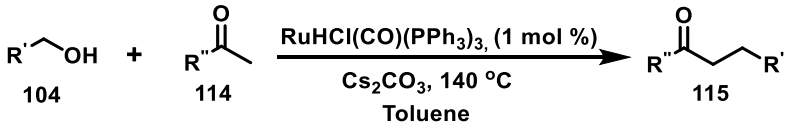

Scheme 5.2.9: Ryu's work on direct α-alkylation of ketones using alcohols

However, Gunanathan and coworkers performed ruthenium-catalyst mediated α-alkylation of ketones by utilizing secondary alcohols to furnish β-disubstituted ketones (Scheme 5.2.10).[168]

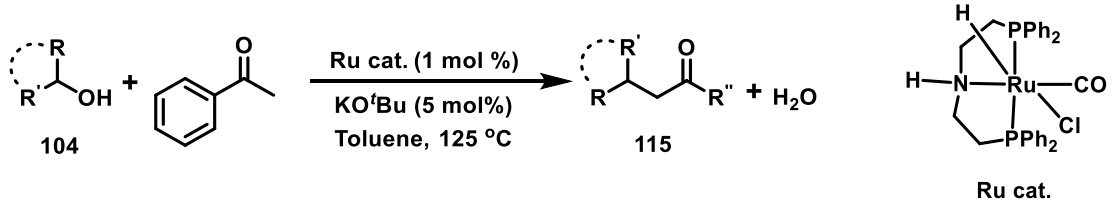

Scheme 5.2.10: Gunanathan's approach for α-alkylation of ketones using secondary alcohols

In 2022, Srimani group reported the synthesis and catalysis of sulfur-based Ni-SNS complexes.[169] The developed catalyst employed borrowing hydrogen strategy for C-alkylation of ketone enolates that tolerated many functional groups (Scheme 5.2.11). Additionally, this catalytic system also demonstrated the synthesis of quinoline moieties.

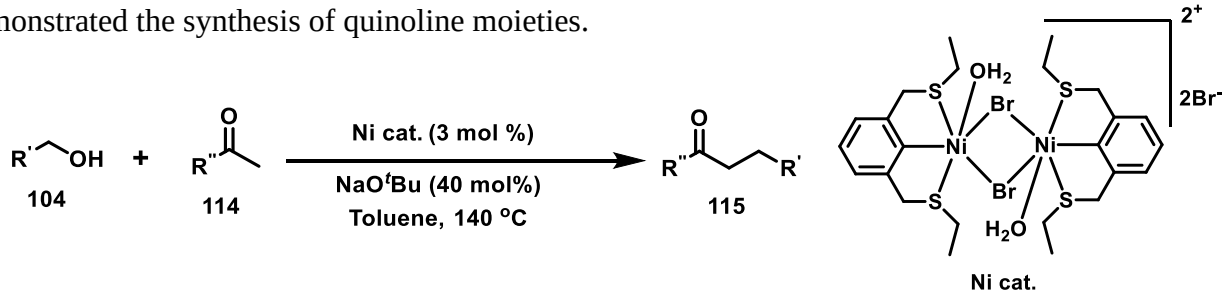

Scheme 5.2.11: Srimani's approach on Ni-SNS catalyzed α-alkylation of ketones

Next, Gnanaprakasam and coworkers reported Ru-NHC catalyzed α-alkylation of dimethylacetamide **116** (Scheme 5.2.12). Additionally, the *N*-acetyl derivatives of pyridine, pyrrolidine, and morpholine were also successful in giving alkylated product **117** by using benzyl alcohol in the presence of 1.0 mol % of Ru-NHC catalyst in a one pot condition under the borrowing hydrogen method.[170]

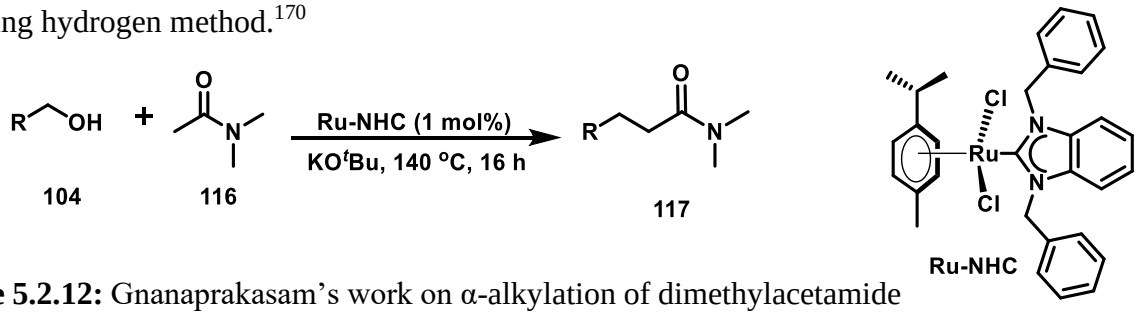

Scheme 5.2.12: Gnanaprakasam's work on α-alkylation of dimethylacetamide

Moreover, C-C bond formation to access the C3-alkylation of 2-oxindole **118** was reported using Ru,[171a-b] Rh,[171c] Pt/CeO2,[171d], and Pd/C[171e] catalyst (Scheme 5.2.13).

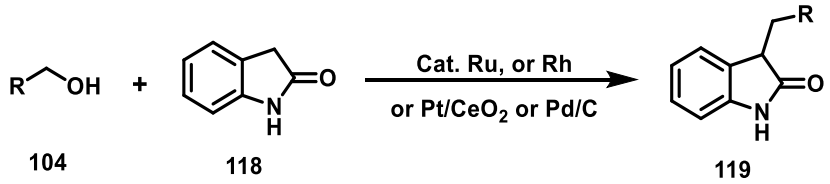

Scheme 5.2.13: Other approaches for direct C-alkylation of 2-oxindole **118** using alcohols

An efficient and simple acceptorless dehydrogenative approach for α-olefination of 2-oxindole **118** with diaryl methanol **120** by using an inexpensive Ru-NHC catalyst to synthesize a wide variety of arylidene-2-oxindole derivatives **121** were developed by Gnanaprakasam group (Scheme 5.2.14).[172]

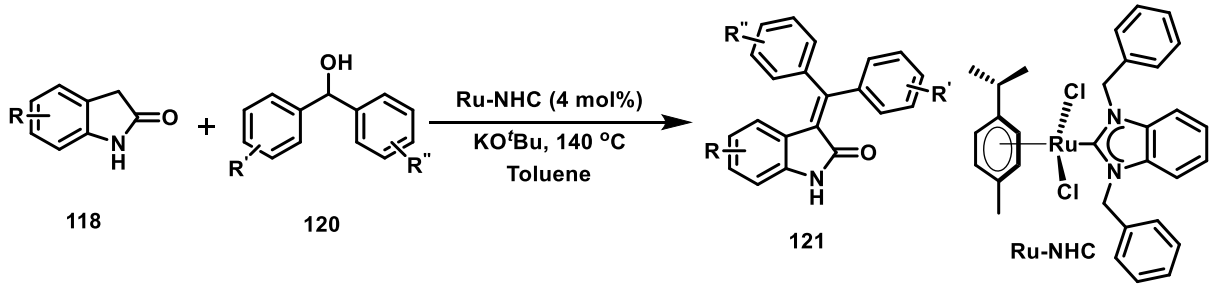

Scheme 5.2.14: Acceptorless dehydrogenative approach for α-olefination of 2-oxindole with diaryl methanol

The esterification of alcohols **104** using BH process is also explored using variety of Ru catalysts. In 2005, Milstein and coworkers reported the esterification of alcohol using a catalytic amount of Ru-pincer complex (Scheme 5.2.15).[173]

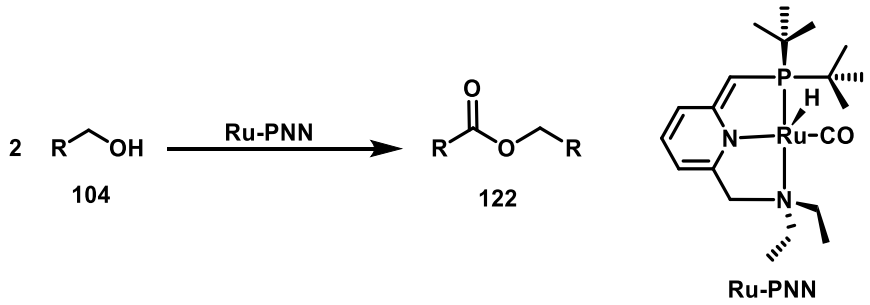

Scheme 5.2.15: Milstein's work on the synthesis of esters **122** from alcohols **104**

However, Ru-NHC catalyzed transformation was achieved by Madson and coworkers for C-O bond formation that gave desired ester product **122** (Scheme 5.2.16).[174]

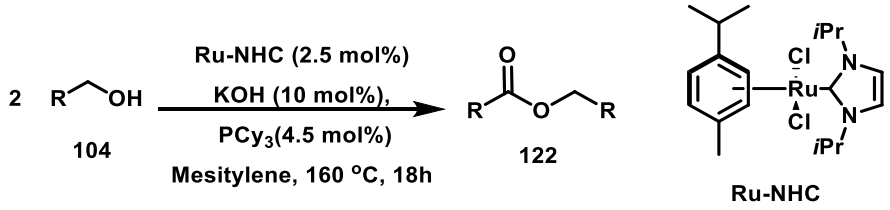

Scheme 5.2.16: Madson's work on the synthesis of esters from alcohols

Interestingly, with BH and AD approach, oxygen, sulphur, and nitrogen containing heterocycles could be easily achieved. The oxygen containing heterocycle synthesis was reported by Williams and coworkers (Scheme 5.2.17). They used readily available 1,4-alkynediols **123** in presence of $[Ru(PPh_3)_3(CO)H_2]$ catalytic system to access 2,5-substituted furans **124** by hydrogen-transfer isomerization at 130 °C.[175]

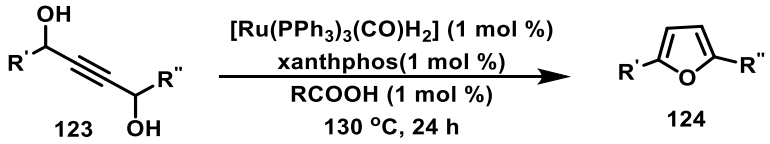

Scheme 5.2.17: Williams's work on synthesis furan **124** from alkynediols **123**

Hydrogen-transfer C-C bond-forming reactions of vicinal diols **125** with methyl acrylate **126**, using the $[Ru_3(CO)_{12}]$ and dppp were reported for the construction of lactones and spirolactones in good to excellent yields (Scheme 5.2.18). The report also incorporates mechanistic pathway for the formation of the lactone through C-C coupling and subsequent lactonization.[176]

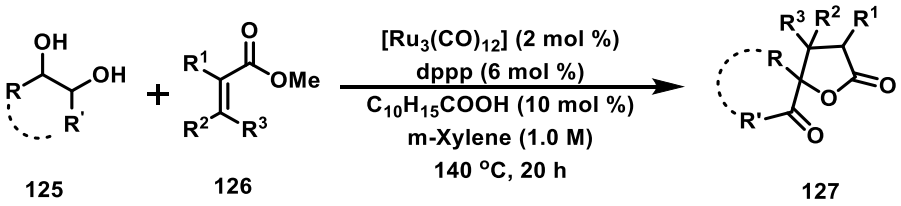

Scheme 5.2.18: Synthesis of lactones **127** from diols **125**

The oxygen and sulphur containing compounds such as, benzoxazoles **129a** and benzothiazoles **129b** was synthesized by reacting alcohols **104** with 2-aminophenols and thiophenols, respectively by using inexpensive and efficient catalyst iron(II) phthalocyanine (FePc) (Scheme 5.2.19).[177]

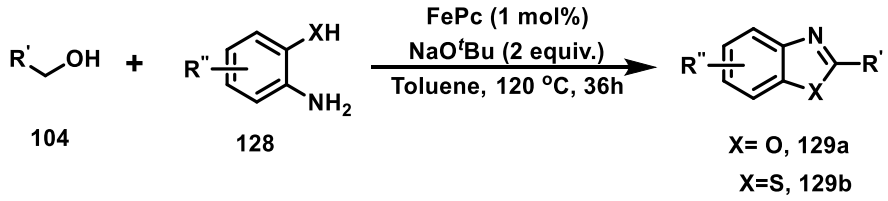

Scheme 5.2.19: Synthesis of benzoxazoles **129a** and benzothiazoles **129b**

In 2013, Beller group developed a straightforward $[Ru_3(CO)_{12}]$/Xantphos catalyst for three-component synthesis of tetrasubstituted pyrroles **131** from easily available benzylic ketones **114**, vicinal diols **125**, and ammonia **130** (Scheme 5.2.20).[178]

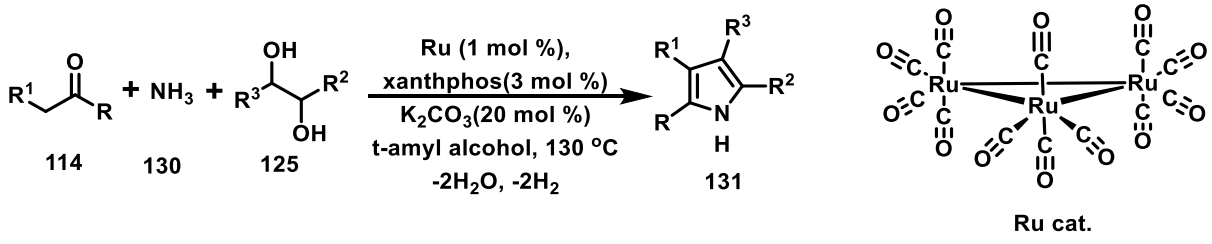

Scheme 5.2.20: Beller's work on three-component synthesis of pyrroles **131**

5.3. Literature reports on substituted pyrrole and pyridine derivatives using amino alcohols via AD/BH process

Aromatic heterocycles are the chemical entities that are most prevalent in a wide range of natural products, pharmaceutical agents, and agricultural products (Figure 5.3.1).[179] Several methods have been established for their synthesis that uses conventional metal and metal-free conditions.

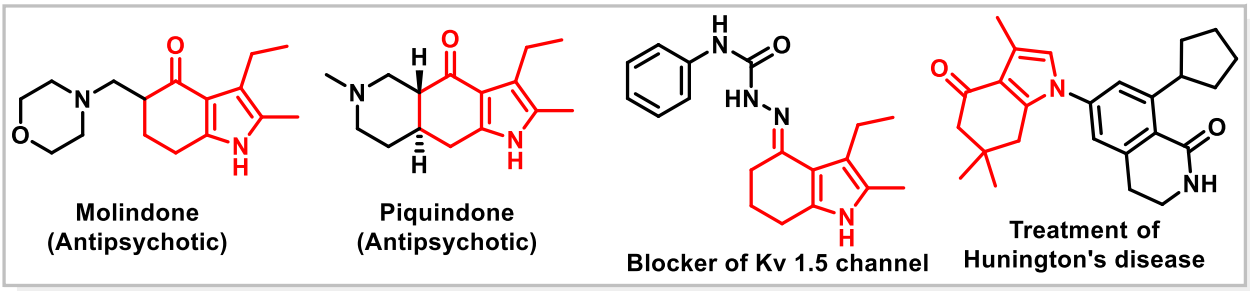

Figure 5.3.1: Biologically active compounds with a substituted pyrrole core

Although the classical technique offers exciting catalytic reaction steps and synthetically helpful approaches, its drawbacks include the generation of copious waste, multistep synthesis, and a lack of readily available feed-stock chemicals. Therefore, the chemical community is also interested in methods such as annulation, multicomponent, and tandem reactions.[180] However, the current AD manufacturing processes are extremely demanding for sustainable catalytic approach that concentrates on one-pot conditions that demand the assembly of many bond construction with high-atom economy and utilize affordable reactants. Due to a number of attractive features for the construction of C-C and C-X bonds in modern chemical syntheses, acceptorless dehydrogenation (AD) of alcohols has been widely used.[181] Notably, several research groups are now extensively exploiting the AD method to create diverse five- and six-membered aromatic *N*-heterocycles involving different transition metal complexes.[182] The amino alcohols are easily produced from their respective naturally occurring amino acids. Also, this has been a key chemical component in several dehydrogenative pyrrole derivative **133** synthesis.

In 2013, Kempe group introduced a iridium-catalyzed pyrrole **133** synthesis utilizing secondary alcohols **132** and amino alcohols **108** via the formation of C-N and C-C bond by the liberation of two equivalents of hydrogen gas (Scheme 5.3.1).[183]

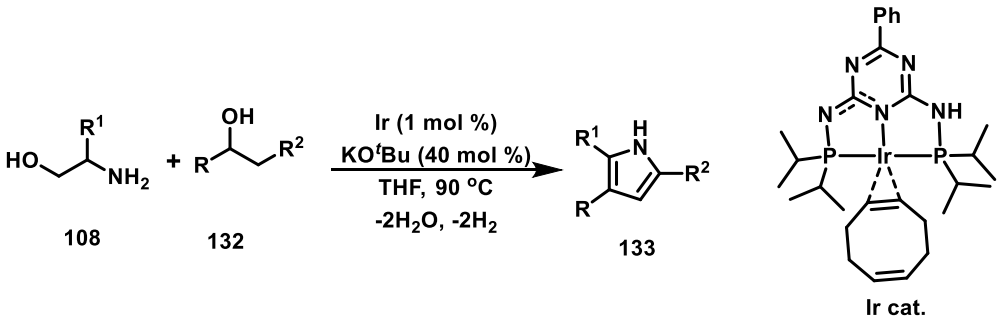

Scheme 5.3.1: Iridium catalyzed pyrrole **133** synthesis

Additionally, a regioselective pyridine synthesis was reported by Kempe group by Ir-catalyzed dehydrogenative condensation of alcohols **132** and 1,3-amino alcohol **134** (Scheme 5.3.2). This method gives access to unsymmetrically substituted pyridines **135** with a generation of three equivalents of H_2.[183]

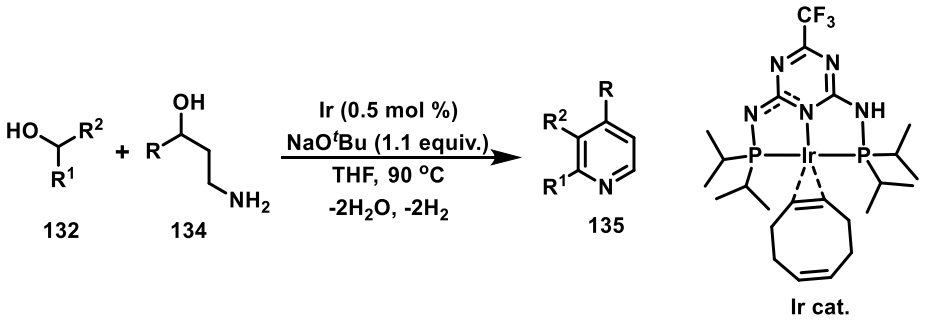

Scheme 5.3.2: Iridium catalyzed pyridine **135** synthesis

An environmentally benign dehydrogenative condensation protocol for pyrrole **133** synthesis was demonstrated by selective and successive C-N and C-C bond formations catalyzed by 0.5 mol% of Ru-PNN using readily available starting materials (Scheme 5.3.3).[184]

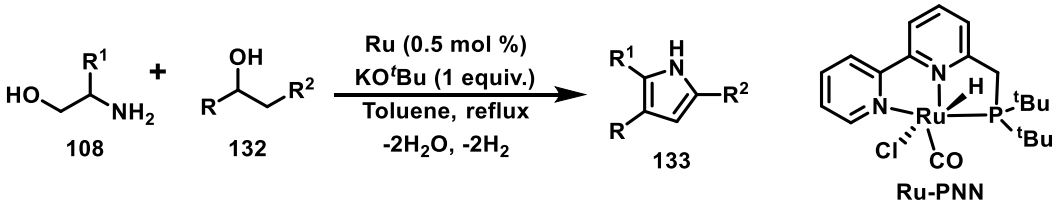

Scheme 5.3.3: Ru-PNN mediated pyrrole **133** synthesis

In the same year, another variant of Ru catalyst was developed by Saito group giving *N*-unsubstituted pyrroles **133** at 165 °C (Scheme 5.3.4).[185]

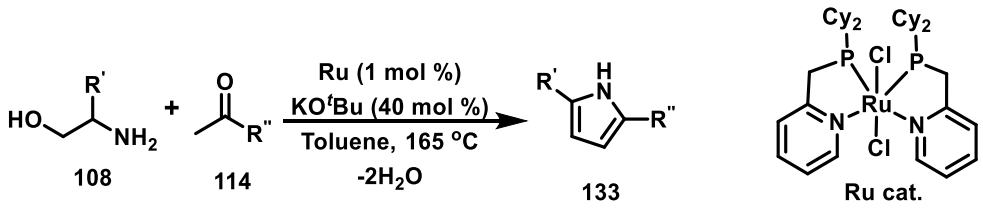

Scheme 5.3.4: Saito's approach for pyrrole synthesis

In 2016, Sun and coworkers reported cyclization of various aryl γ-amino alcohols **136** and secondary alcohols **137** with Ru-PNN catalyst furnished library of substituted pyridines **138** (Scheme 5.3.5).[186]

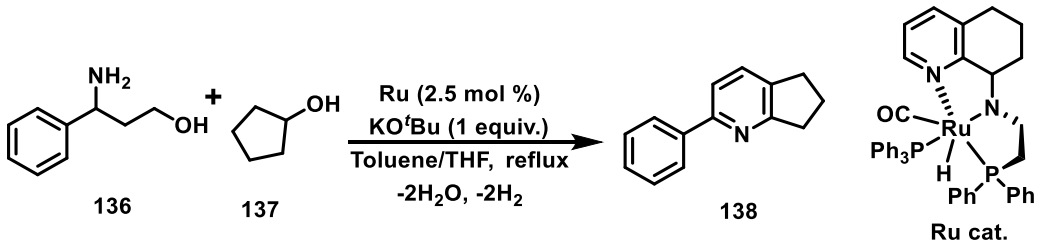

Scheme 5.3.5: Sun's work on pyridine **138** synthesis

Moreover, Kempe group developed Mn-catalyzed synthesis of pyrroles **133** by using secondary alcohols and aminoalcohols. Interestingly, it was first example of a base-metal-catalyzed version of this pyrrole synthesis (Scheme 5.3.6).[187]

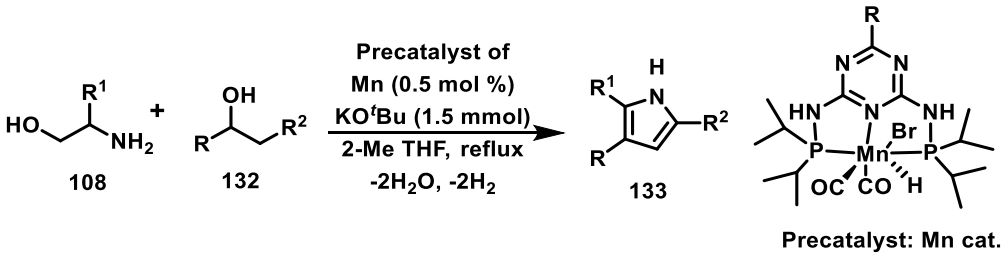

Scheme 5.3.6: Mn-catalyzed synthesis of pyrroles

In 2017, a versatile Ru(II)-PNN complex was synthesized and studied towards the construction of pyrroles and pyridines from secondary alcohols **132** and amino alcohols **108** (Scheme 5.3.7).[188]

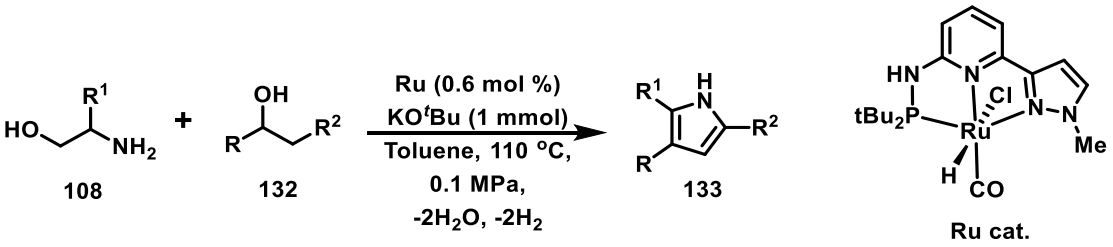

Scheme 5.3.7: Ru(II)-PNN complex for the synthesis of pyrroles

Moreover, Chen and coworkers reported Ru-NNN catalyzed acceptorless dehydrogenative condensation for the synthesis of pyridines, quinolines, and pyrroles (Scheme 5.3.8).[189]

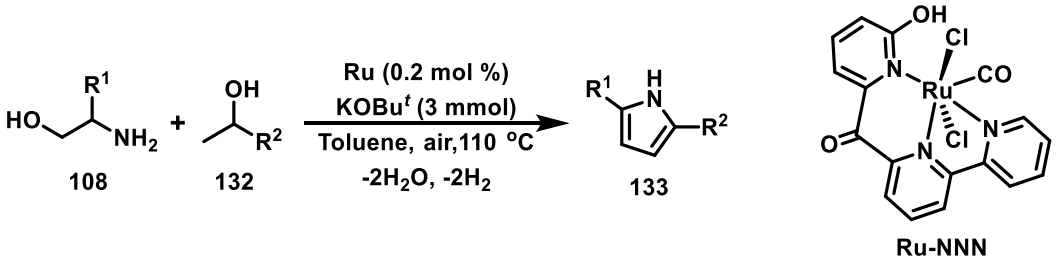

Scheme 5.3.8: Ru-NNN catalyzed synthesis of pyridines, quinolines, and pyrroles

Interestingly, Balaraman group was successful towards the synthesis of first example of molecularly defined SNS-cobalt(II)catalyst for the acceptorless dehydrogenative coupling (ADC) of unprotected amino alcohols **108** with secondary alcohols **132** to give pyrrole and pyridine derivatives (Scheme 5.3.9).[190]

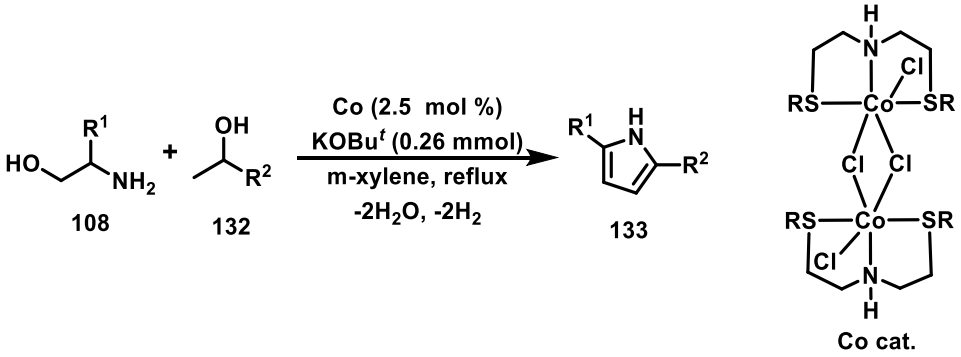

Scheme 5.3.9: Balaraman's approach for pyrrole and pyridine synthesis using SNS-cobalt (II) catalyst

Additionally, Banerjee group reported a nitrogen-ligated nickel catalyst to access five and six membered *N*-heterocycles by selective intermolecular cyclisation of β- and γ-amino alcohols (Scheme 5.3.10).[191]

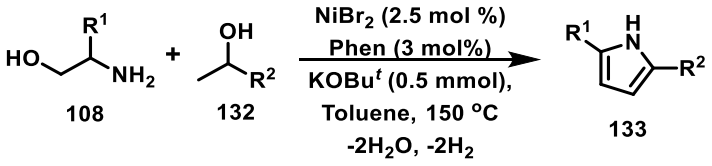

Scheme 5.3.10: Banerjee's work on nickel catalyzed pyrrole and pyridine synthesis

Besides, Ru, Mn, Co catalysts, a well-defined Re(I)PNP pincer complex was developed by Kircher group (Scheme 5.3.11). Further, the Re complex was utilized for an efficient synthesis of quinolines, pyrimidines, quinoxalines, pyrroles, and aminomethylated aromatic compounds by liberation of dihydrogen and elimination of water.[192]

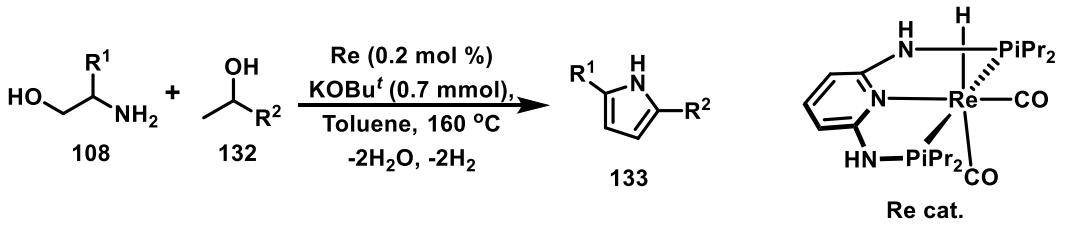

Scheme 5.3.11: Banerjee's work on nickel catalyzed pyrrole and pyridine synthesis

More recently, a Ru (II) complex bearing pyridyl-based benzimidazole-phosphine tridentate PNN ligand was synthesized and characterized by various spectroscopic techniques (Scheme 5.3.12). Finally, the complex was subjected for acceptorless dehydrogenation protocol for the synthesis of pyrroles.[192]

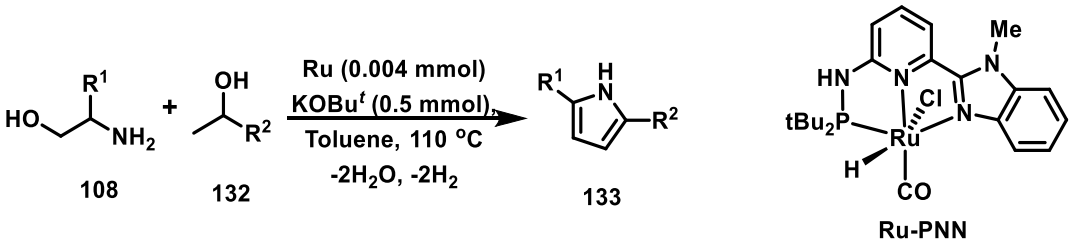

Scheme 5.3.12: Ma's work on ruthenium catalyzed pyrrole **133** synthesis

5.4. The rationale of the present work

Most of these reactions need a stoichiometric base for annulation and facilitated by specially designed complexes, which result in the generation of a large amount of waste, a decrease in the atom economy, and low sustainability. Base-free, efficient, and additive-free catalytic systems must be developed to synthesize other heterocycles, such as partially hydrogenated indole and an acridine system that are omnipresent in most therapeutic and natural products (Figure 5.3.1).[179,194,195]

Therefore, we envisioned an environmentally benign, acceptorless, and base-free condition for the annulation of cyclic-1,3-dicarbonyl compounds and amino alcohols for the synthesis of a variety of tetrahydro-4*H*-indol-4-one and 3,4-dihydroacridin-1(2*H*)-one using a readily available $RuH_2CO(PPh_3)_3$ catalyst. This method aims to synthesize a large variety of functionalized, cyclohexane-fused *N*-heterocycles with five and six members, where water and molecular hydrogen will be the by-products.

5.5. Results and discussion

We have started the investigation of the reaction conditions using 1,3-cyclohexanedione **139a** and (S)-2-amino-3-phenylpropan-1-ol **108a** as a model substrate (Table 5.5.1). At 160 °C, a control experiment was performed without a catalyst or base resulted no reaction. Then, to synthesize 2-benzyl-1,5,6,7-tetrahydro-4*H*-indol-4-one **140a**, we examined a variety of Ru catalysts (Table 5.5.1). With 5 mol% $RuCl_3$, the dehydrogenative annulation of **139a** and **108a** provided trace amount of product **140a** (Table 5.5.1, entry 1). A similar result was attained for dehydrogenative annulation with 5 mol% $RuHClCO(PPh_3)_3$ (Table 5.5.1, entry 2). A 70% yield of product **140a** was achieved using 5 mol% $RuH_2CO(PPh_3)_3$, with molecular hydrogen and water as a byproduct (Table 5.5.1, entry 3). Previously, dehydrogenation of alcohols to access ketone was reported by using $RuH_2CO(PPh_3)_3$.[196] However, there is no report available on annulation reaction with $RuH_2CO(PPh_3)_3$. Next, dichloro(p-cymene)ruthenium(II)dimer and dichloro(1,5-cyclooctadiene)ruthenium(II), polymer were used in the process gave poor yields (Table 5.5.1, entries 4-5). Whereas, product **140a** was obtained in 52% and 57% yield with Ru-PNN and Ru-MACHO catalysts, respectively (Table 5.5.1, entries 6-7). On the other hand, Ru-NHC and 5% Ru

on alumina gave 16% and traces of product, respectively (Table 5.5.1, entries 8-9). From the catalyst screening, we have observed that only 5 mol% $RuH_2CO(PPh_3)_3$ of the catalyst is required for this transformation (Table 5.5.1).

Table 5.5.1: Catalyst screening for AD annulation

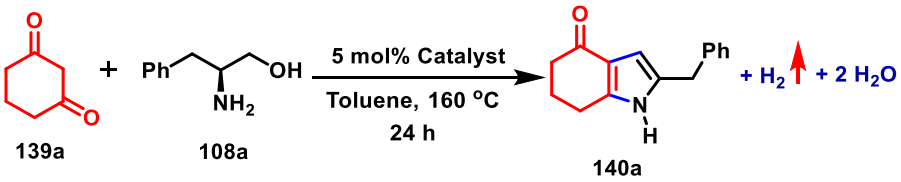

Entry	Catalyst	Yield (%) of 140a
1	$RuCl_3.H_2O$	Traces
2	$RuHClCO(PPh_3)_3$	Traces
3	$RuH_2CO(PPh_3)_3$	70
4	Dichloro(p-cymene)ruthenium(II)dimer	19
5	Dichloro(1,5-cyclooctadiene)ruthenium(II),polymer	25
6	Ru-PNN	52
7	Ru-MACHO	57
8	Ru-NHC	16
9	5% Ru on alumina	Traces

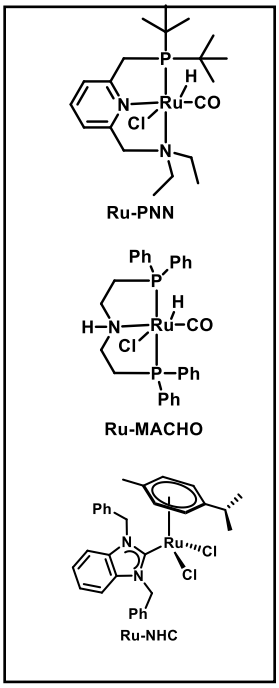

Reaction conditions: 139a (0.5 mmol), **108a** (0.5 mmol), catalyst (5 mol%), and toluene (2 mL) were heated at 160 °C for 24 h.

After the catalyst screening, we studied different concentration of catalyst for annulation reaction. With increasing catalyst amount from 0.5 mol% to 5 mol%, improvement in yield of desired product was observed. However, further increasing the mol% of catalyst has shown no improvement in product yield. Therefor, 5 mol% of $RuH_2CO(PPh_3)_3$ was considered as the optimum condition (Figure 5.5.1a). Later, temperature and time studies were carried out. At 80 ^oC, no reaction occurred. Whereas at 100 ^oC and 120 ^oC the reaction gave 25% and 28 % yield of desired product. However, 60% yield was observed when reaction was heated at 140 ^oC. Finally,

the best outcome was observed at 160 °C that delivered 70% yield of product (Figure 5.5.1b). Next, keeping optimum catalyst and temperature condition, we altered time interval required for this reaction. According to the product yields obtained at various intervals, heating reaction mixture for 24 h at 160 °C gave maximum yield (70%) (Figure 5.5.1c). Moreover, solvent studies suggested xylene, DMSO and 1,4-dioxane as less efficient for annulation. Interestingly, the yields were similar by using non polar solvent toluene and polar solvent DMF. However, we have chosen toluene in order to avoid the work up issues dealt by using DMF as a solvent (Figure 5.5.1d).

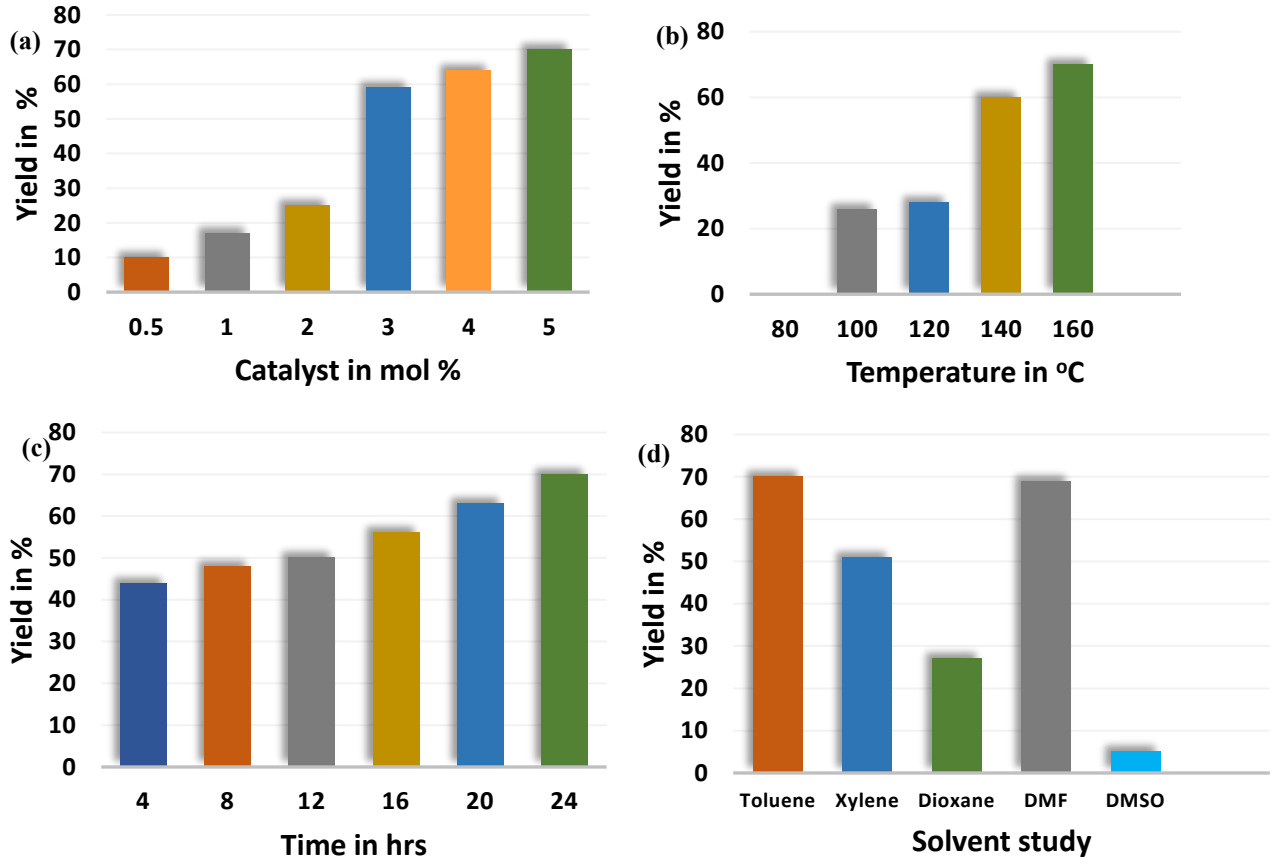

Figure 5.5.1: Optimization for catalyst concentration (a), temperature (b), time (c) and solvent study (d)

After getting best optimized condition, we explored the AD annulation reaction by altering various substitution on cyclic-1,3-diketone and amino alcohols. Consequently, the yields of product **140b-140e** from the reaction of cyclohexane-1,3-dione with various amino alcohols were 46-76% (Scheme 5.5.1). Additionally, this reaction was carried out using sulfur-containing amino alcohol

that gave **140f** in a 44% yield. Furthermore, regardless of substitution, this catalyst was successfully implemented in the dehydrogenative annulation of various dicarbonyl compounds to give the diverse derivatives **140g-y** in yields ranging from 25 to 95% (Scheme 5.5.1). In case of lower yields of product, starting materials were recovered. However, the reaction was also tolerant with 5-(4-(dimethylamino)phenyl)cyclohexane-1,3-dione derivative giving 49% yield. The tricyclic compounds **140aa** and **140ab** were synthesized in this reaction with prolinol with yields of 47% and 61%, respectively. However, product **140ac** was prepared from cyclopentane-1,3-dione provided 42% yield. With acyclic-1,3-dione, AD annulation was unsuccessful and the reaction stopped after the synthesis of the corresponding enaminone products **141a'**, **141b'**, and **141c'** (Scheme 5.5.1).

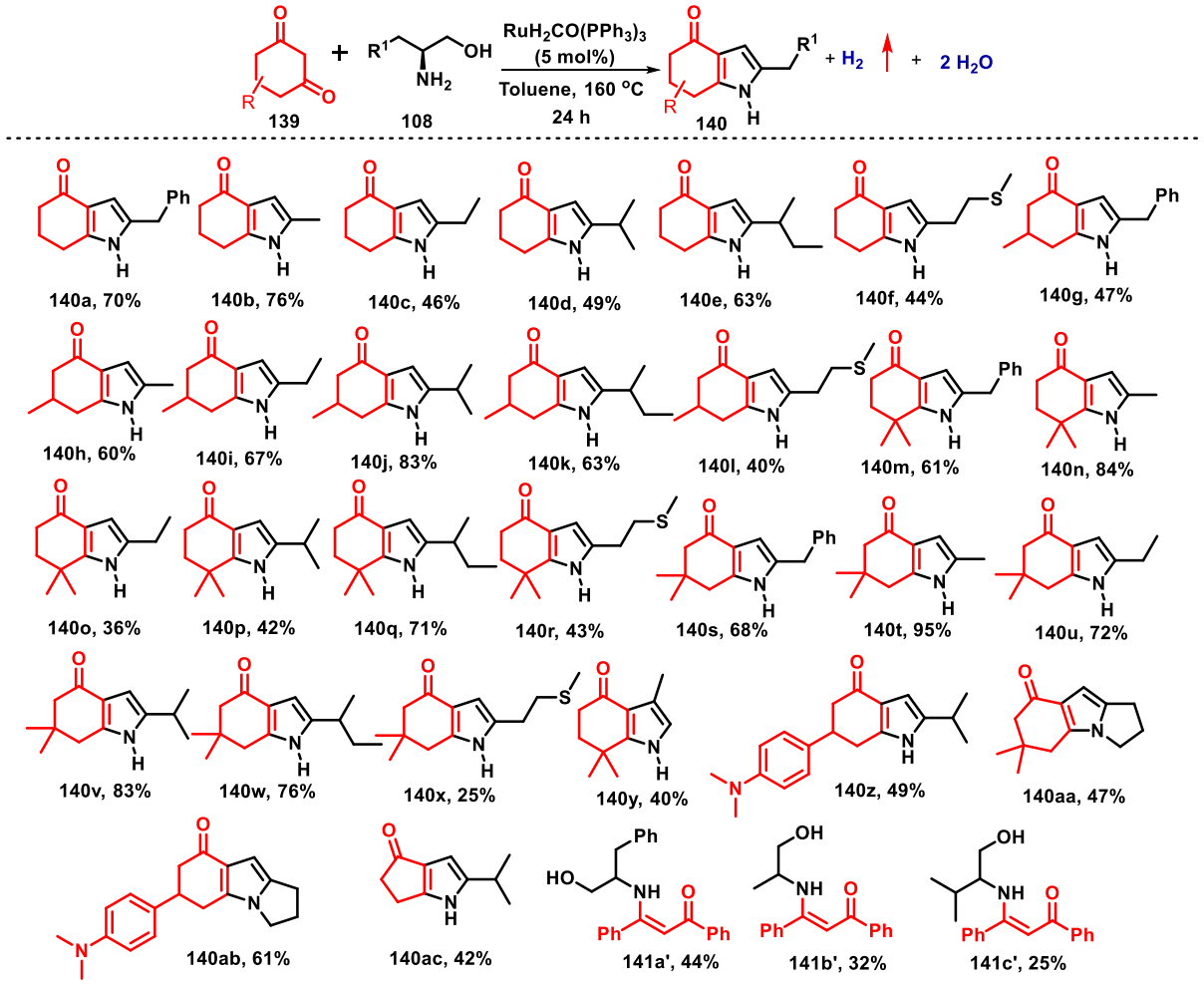

Scheme 5.5.1: Substrate scope for the intermolecular cyclisation of β-amino alcohol **108** with cyclic-1,3-diketone **139**

The base-free AD synthesis of derivatives of 3,4-dihydroacridin-1(2*H*)-one was also attempted. In order to get a 65% yield of the product **143a**, an equimolar concentration of cyclohexane-1,3-dione and 2-aminobenzyl alcohols in toluene was heated at 160 °C for 24 h in the presence of 5 mol% $RuH_2CO(PPh_3)_3$ (Scheme 5.5.2). The ideal temperature for intermolecular oxidative annulation was 160 °C. Moreover, other cyclic 1,3-dicarbonyl derivatives were effectively used for the annulation reaction. Having methyl and dimethyl substitution on 1,3-cyclohexanedione core, the reaction furnished 62%, 56%, and 67% yields of **143b**, **143c**, and **143d** respectively. Next, the reaction of 5-(4-(dimethylamino)phenyl)cyclohexane-1,3-dione, cyclopentane-1,3-dione, and 1,3-dimethylpyrimidine-2,4,6(1*H*,3*H*,5*H*)-trione with 2-amino alcohol provided **143e**, **143f**, and **143g** giving 62%, 44%, and 38% yields, respectively. Additionally, little decrease in the product formation was observed when 1-(2-aminophenyl)ethan-1-ol reacts with 1,3-cyclohexanedione and 5,5'-dimethyl-1,3-cyclohexanedione that delivered 42% and 34% of products **143h** and **143i**. Next, the reaction with (2-amino-3,5-dibromophenyl)methanol provided 68% and 34% of **143j** and **143k**, respectively. However, moderate yield of 47% was observed for the product **143l.**

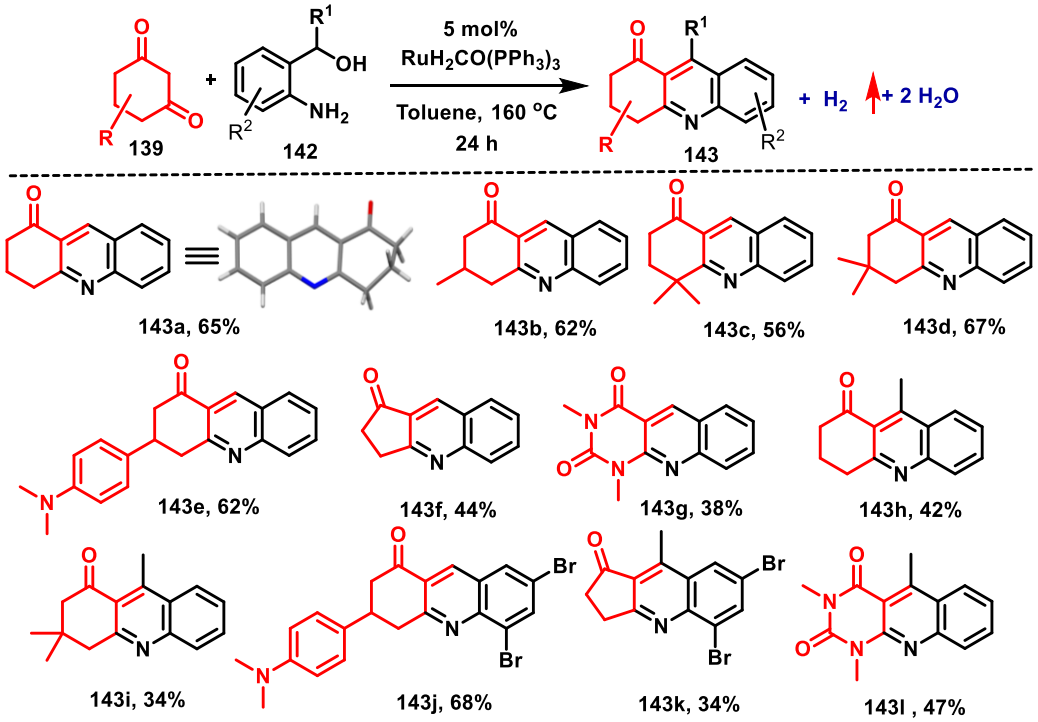

Scheme 5.5.2: Substrate scope for the intermolecular annulation of 2-aminobenzyl alcohol **142** with cyclic-1,3-diketone **139**

To understand the reactivity of 1,3-dione with amino alcohols in the AD annulation reaction, both intermediates of cyclic and acyclic 1,3-diketones were isolated and investigated. The X-ray analysis revealed that acyclic-1,3-dione led to the formation of a highly rigid structure Z-enaminone alcohol[197] (**141c'**), due to intramolecular hydrogen bonding (Figure 5.5.2). Thus, both the C nucleophile and alcohol are too far to react. Therefore, no AD annulation product was obtained (Figure 5.5.2). In the case of cyclic-1,3-dione (**141a**), both the C nucleophile and alcohol are in close proximity for the reaction. This might be due to the absence of a rigid structure for **141a**, which arises due to absence of intramolecular hydrogen bonding. Therefore, cyclic-1,3-dione easily underwent AD annulation.

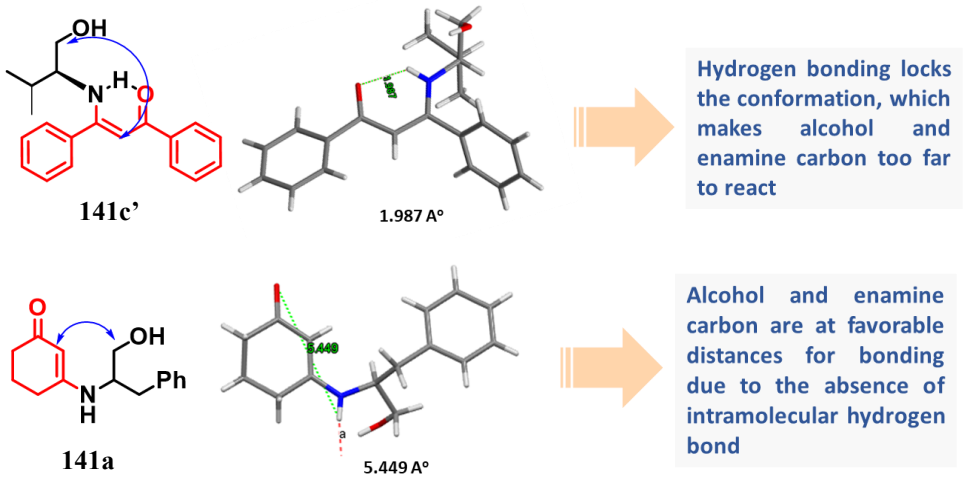

Figure 5.5.2: Favorable isomers for annulation

In literature, Pd-catalyst,[198] the stoichiometric quantity of K_2CO_3, and mesityl bromide is needed for the intramolecular enamine alcohol cyclization. To our knowledge, this is the only report from enaminone alcohol **141** to give tetrahydroindolones **140** (Scheme 5.5.3).

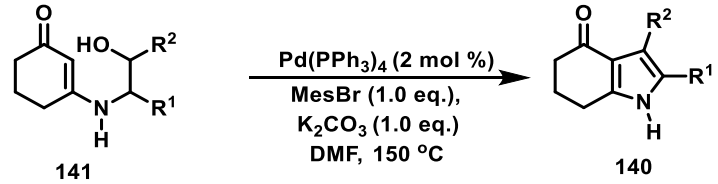

Scheme 5.5.3: Reported Pd- catalyzed intramolecular enaminone alcohol cyclization in literature

Therefore, we envisioned intramolecular dehydrogenative cyclization of various enaminone derivatives **141** using 5 mol % $RuH_2CO(PPh_3)_3$ catalyst (Scheme 5.5.4). The intramolecular

dehydrogenative cyclization of various enaminone derivatives **141** effectively delivered 1,5,6,7-tetrahydro-4*H*-indol-4-one derivatives **140** in high yields with the liberation of hydrogen and water (Scheme 5.5.4). All the enaminone alcohols delivered better yields than intermolecular reaction of cyclic-1,3-diketone and amino alcohols.

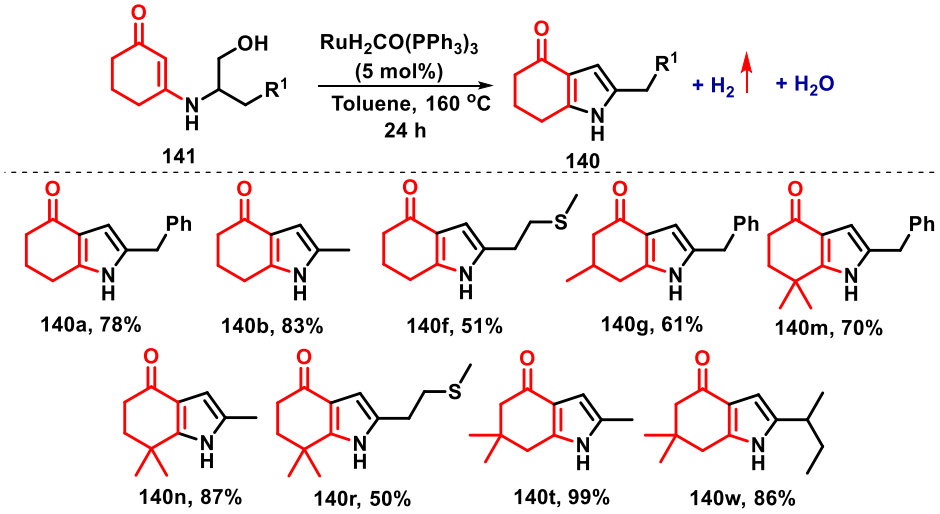

Scheme 5.5.4: Substrate scope for the intramolecular annulation of β-enaminone alcohol **141**

Next, in the presence of 5 mol% $RuH_2CO(PPh_3)_3$, several enaminone derivatives **144** underwent intramolecular dehydrogenative cyclization to furnish 3,4-dihydroacridin-1(2*H*)-one derivative **143** (Scheme 5.5.5). Moreover, we have achieved 3,4-dihydroacridin-1(2*H*)-one derivatives **143a**, **143b**, **143c**, and **143d** in 76%, 77%, 70%, and 88% yields, respectively by intramolecular annulation (Scheme 5.5.5).

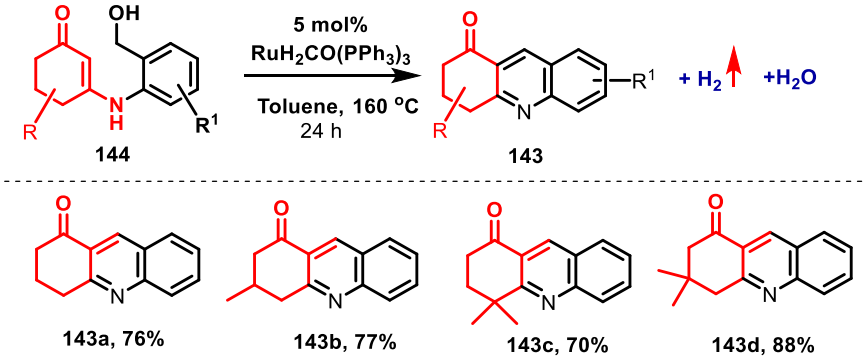

Scheme 5.5.5: Substrate scope for the intramolecular annulation using enaminone alcohols **144**

A gram-scale synthesis for **140v** has been carried out to demonstrate the scale-up application (Scheme 5.5.6). Interestingly, the gram-scale synthesis was carried out without the using any

solvent by heating the reaction mixture of 1,3-cyclohexane-1,3-dione and L-valinol for 24 h at 160 ^{o}C in the presence of 5 mol% of $RuH_2CO(PPh_3)_3$. A satisfactory yield of 78% (1.122 g) for **140v** was isolated after column chromatography.

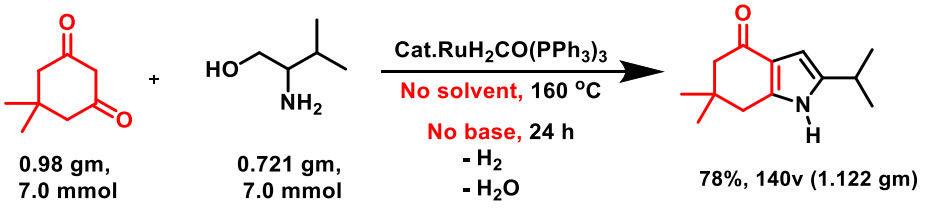

Scheme 5.5.6: Gram-scale AD annulation reaction

The synthetic applicability for this reaction was further demonstrated by environmentally benign alkylation of indolone derivatives with alcohols for the synthesis of Molindone intermediate (Scheme 5.5.7). Consequently, there was no reaction when heterocycle **140b** was taken with ethanol and heated in the presence of $RuH_2CO(PPh_3)_3$. The yield of product **145a** increased to 61% when Amberlyst®-15 was added to the process. With the established reaction conditions, **140** was alkylated by reacting with various alcohols in the presence of catalytic $RuH_2CO(PPh_3)_3$ and Amberlyst®-15, which produced **145b** and **145c** in yields of 48 and 40%, respectively (Scheme 5.5.7). Finally, intermediate **145a** can undergo the Mannich reaction that can directly deliver the molindone drug.[199]

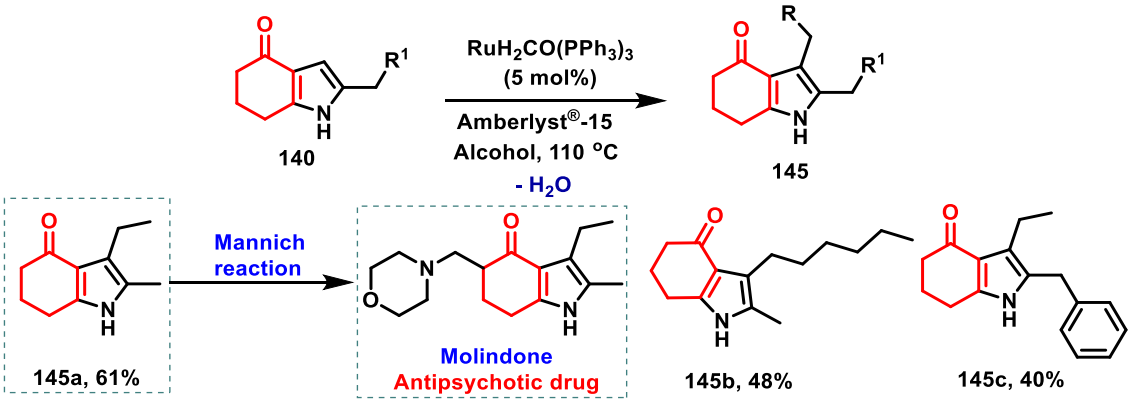

Scheme 5.5.7: AD synthesis of molindone drug intermediate

Subsequently, to investigate the reaction mechanism, we have performed several experiments. The formation of enaminone **141a** in the absence of catalyst indicated imine formation is the primary

step in pyrrole synthesis (Scheme 5.5.8, entry a). Imine formation as a key step was confirmed by Ru-catalyzed AD reaction of **141a** which gave 76% of **140a** (Scheme 5.5.8, entry b). Further, intramolecular C-C bond formation is observed to be more facile when enaminone alcohol and benzyl alcohol were subjected under standard reaction condition (Scheme 5.5.8, entry c). The reaction with cyclic-1,3-diketone, benzyl alcohol, and hexyl amine produced the corresponding enaminone products in the presence of a Ru catalyst that demonstrates the predominance of C-N bond formation to give enaminone over C- alkylation (Scheme 5.5.8, entry d). The cross over experiment involving cyclohexane-1,3-dione, (S)-phenyl alaninol, and 2-aminobenzyl alcohol in the presence of 5 mol% $RuH_2CO(PPh_3)_3$ produced **140a** (28%) and **143a** (24%), indicating no selectivity in the formation of five- and six-membered *N*-heterocycles (Scheme 5.5.8, entry e).

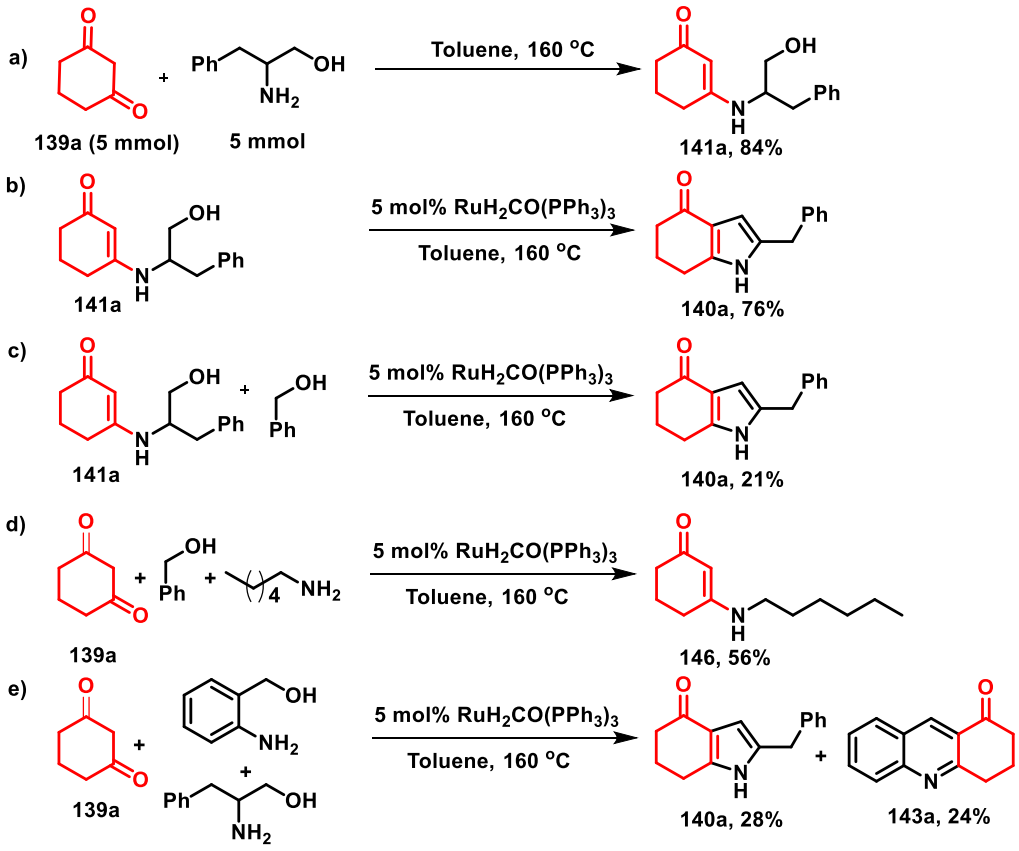

Scheme 5.5.8: Experiments for mechanistic investigation

Next, the liberation of molecular hydrogen was confirmed by analyzing the gas components from the reaction mixture by the GC analysis (Figure 5.5.3).

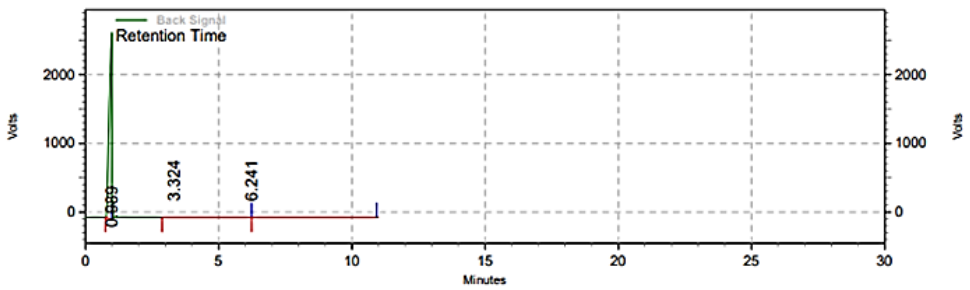

Figure 5.5.3: H_2 gas liberation through the GC analysis

In addition to GC analysis the liberation of hydrogen was also confirmed by HRMS analysis. Therefore, 1-phenyl-1-propyne was subjected for standard reaction condition by taking **139a** and **108a** in a resealable pressure tube. Next, the reaction mixture was subjected to HRMS analysis. The HRMS data suggested 1-phenyl-1-propyne acts as hydrogen acceptor and undergoes reduction to give prop-1-en-1-ylbenzene. The presence of 119.0861 peak confirms the exact mass of prop-1-en-1-ylbenzene formed by trapping of the released hydrogen (Figure 5.5.4).

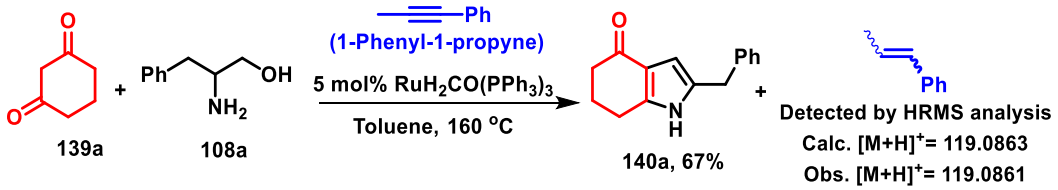

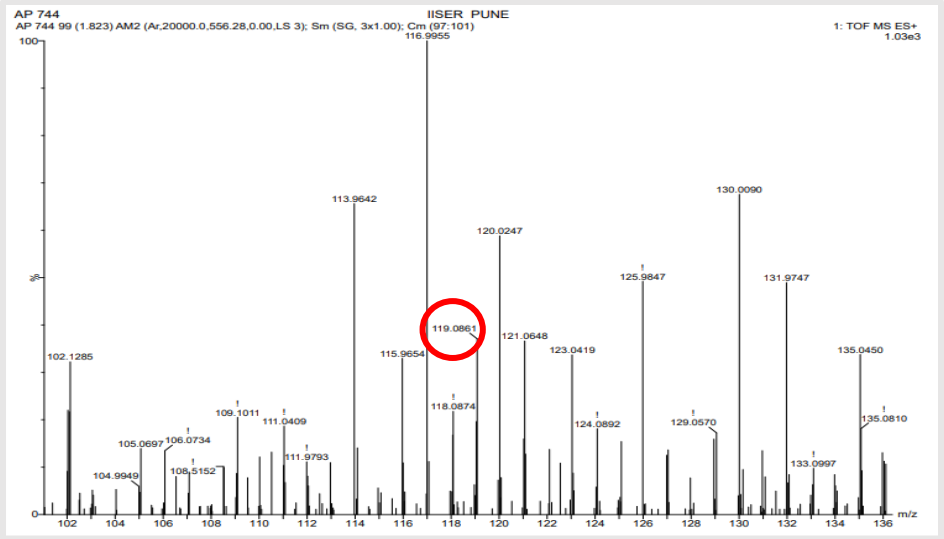

Figure 5.5.4: HRMS analysis for confirmation of H_2 liberation

With the experimental evidences and previous reports,[200] a plausible reaction mechanism is proposed for AD annulation (Scheme 5.5.9). Initially, the amino alcohols and carbonyl undergo a condensation reaction to form the enaminone alcohol **141a** intermediate. Then, **141a** reacts with $RuH_2CO(PPh_3)_3$ to give intermediate **A** via PPh_3 exchange. Further, intermediate **A** follows an O-H activation to give intermediate **B**.

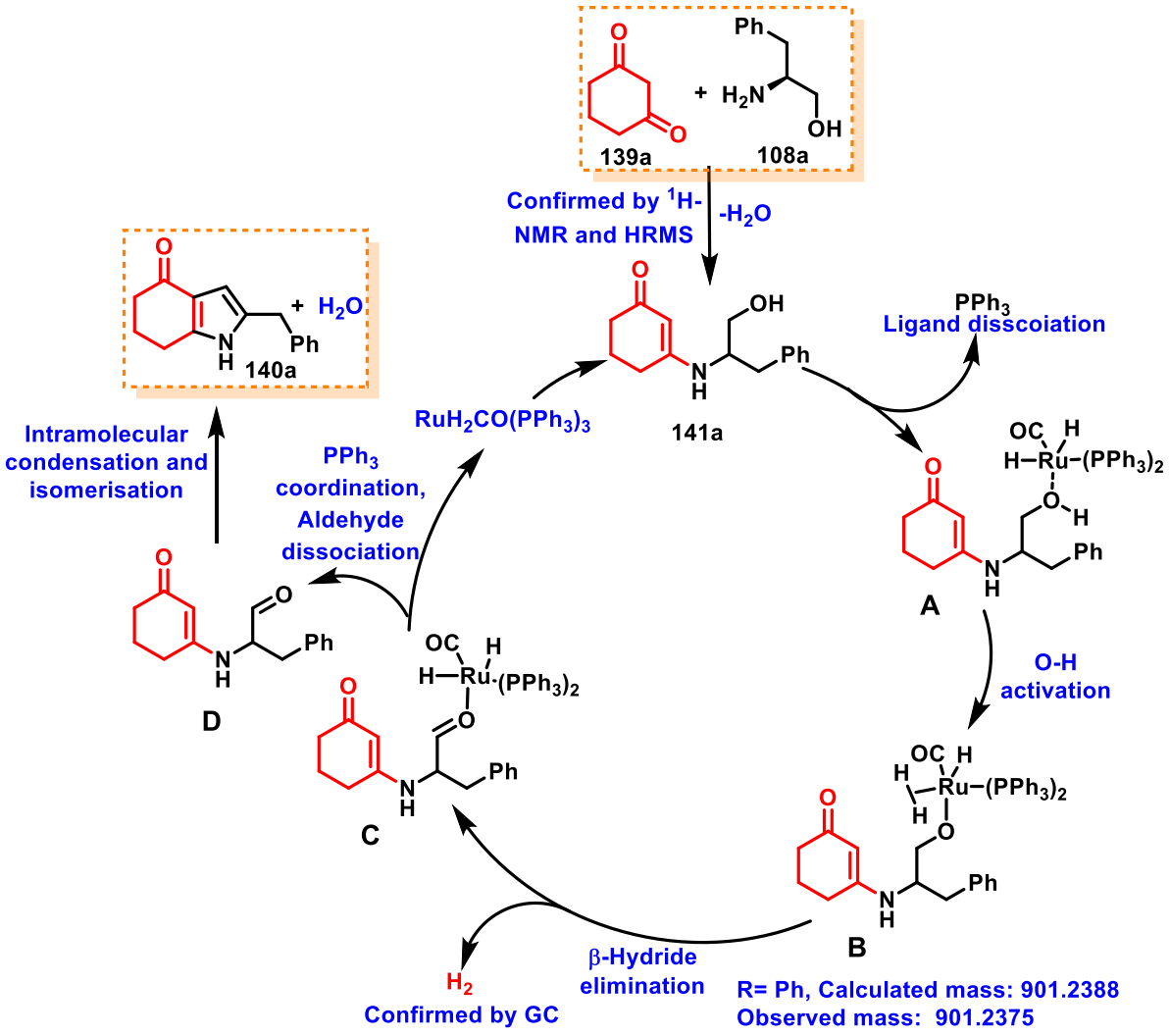

Scheme 5.5.9: A plausible reaction mechanism

The formation of intermediate **B** was confirmed by subjecting the reaction mixture for HRMS analysis which revealed the presence of molecular ion peak at 900.2303 (Figure 5.5.5).

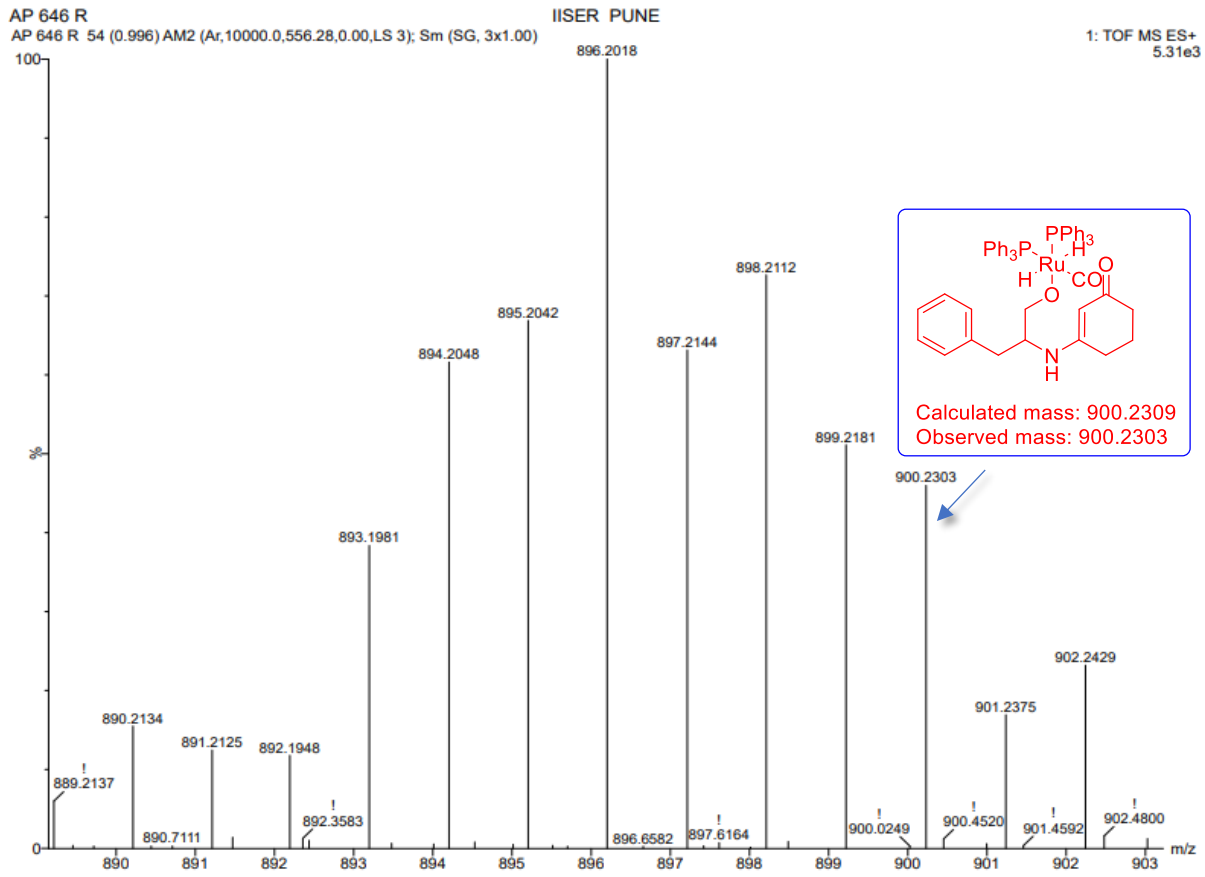

Figure 5.5.5: Detection of Intermediate **B** from HRMS

Next, the intermediate **C** was formed from **B** by the liberation of molecular H_2 (confirmed by the GC analysis: Figure 5.5.3) through β-hydride elimination. The original catalyst $RuH_2CO(PPh_3)_3$ was regenerated in the catalytic cycle by PPh_3 coordination and dissociation of aldehyde **D.** Moreover, ^{1}H-NMR analysis of the reaction mixture from the beginning and during course of the reaction suggested no changes in the Ru-H peak (Figure 5.5.6). The dissociated aldehyde proceeds through intramolecular condensation followed by isomerization to accomplish the desired product **140**. With the release of environmentally benign H_2 and water as byproducts, this catalytic method led to the formation of many *N*-containing aromatic molecules. The AD annulation proceeded by imination-dehydrogenation-condensation-isomerization. Furthermore, this method does not require the stoichiometric amounts of base or oxidant or the hydrogen acceptor for the formation of C-C bond.

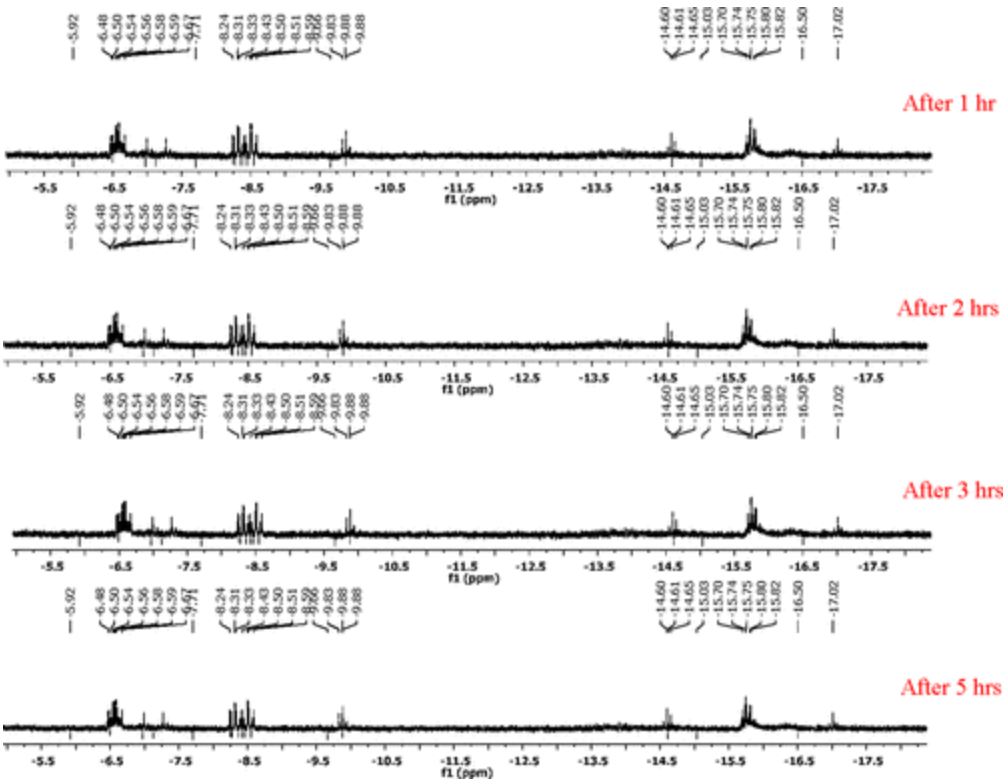

Figure 5.5.6: ^{1}H-NMR spectra of reaction mixture in toluene-d_8

5.6. Conclusion

In conclusion, a base-free acceptorless dehydrogenation method employing readily available $RuH_2CO(PPh_3)_3$ was developed for the synthesis of biologically inspired tetrahydroindole, and tetrahydroacridinone derivatives. With the release of H_2 and water as byproducts, this catalytic method resulted in the production of many *N*-containing aromatic compounds such as tetrahydroindoles, and tetrahydroacridinones. Additionally, intramolecular annulation of enaminone alcohols also successfully provided good to excellent yields of tetrahydroindoles, and tetrahydroacridinones. Moreover, alkylation of tetrahydroindolones demonstrated the synthesis of Molindone core derivative **145**. Overall, the AD annulation progressed by imination-dehydrogenation-condensation-isomerization in a domino manner. The plausible mechanism is proposed by performing cross over experiments and subjecting reaction mixture for HRMS, and GC analysis. The intermediate formation and molecular hydrogen trapping were confirmed by HRMS analysis. However, analysis of the gas component of reaction mixture through GC analysis

suggested liberation of molecular hydrogen. Further, the regeneration of $RuH_2CO(PPh_3)_3$ in catalytic cycle is studied by ^1H NMR analysis that revealed no changes in Ru-H peak. This method does not require stoichiometric quantities of base or oxidant for the synthesis of C-C bonds for the AD annulation and avoided solvent usage for gram scale synthesis of **140v**. The generated protocol was successful towards achieving few sustainability parameters such as, prevention of excess waste generation and avoiding the use of solvents.

5.7. Experimental sections

General information and data collection:

All the amino alcohols and cyclic-1,3-diketone derivatives were purchased from Sigma-Aldrich. Deuterated solvents were used as received. All the solvents used were dry grade and stored over 4 Å molecular sieves. Column chromatographic separation was performed over 100−200 mesh size silica-gel. Visualization was accomplished with UV light and iodine. The ^1H and ^{13}C NMR spectra were recorded on 400 and 100 MHz, respectively, using Bruker or JEOL spectrometers. The chemical shift (δ) and coupling constant (*J*) values are given in parts per million and hertz, respectively. Abbreviations used in the NMR follow-up experiments: b, broad; s, singlet; d, doublet; t, triplet; q, quartet; td, dd doublet of triplet and double doublet; m, multiplet, tt, triplet of triplets and ddd, doublet of doublet of doublets. HRMS spectra were obtained with Waters-synapt G2 using electrospray ionization (ESI-TOF). Infrared (ATIR) spectra were obtained with a Bruker Alpha-E infrared spectrometer. Single-crystal diffraction analysis data were collected at 100K with a BRUKER KAPPA APEX III CCD Duo diffractometer (operated at 1500 W power: 50 kV, 30 mA) using graphite monochromatic Mo Kα radiation and Cu-Kα radiation. More information on crystal structures can also be obtained from the Cambridge Crystallographic Data Centre (CCDC) with deposition numbers 2048644 (**140k**), 2048435 (**141a'**), 2048437 (**141c'**), 2048643 (**143a**).

A. General experimental procedure for the inter-molecular cyclisation of β-aminoalcohol 108 with cyclic-1,3-diketone 139: To an oven-dried 20 mL resealable pressure tube (equipped with rubber septum), cyclic-1,3-diketone (0.5 mmol), β-amino alcohol (0.5 mmol), and $RuH_2CO(PPh_3)_3$ (0.025 mmol) were added in toluene (2 ml) under a N_2 atmosphere using a N_2 balloon. Then, the tube was purged with N_2 and quickly removed septum and sealed with a cap using a crimper. The

reaction mixture was stirred at 160 °C for 24 h on a preheated oil bath. After cooling to room temperature, the reaction mixture was diluted by dichloromethane. After concentration under reduced pressure, the residue was purified by 100−200 mesh silica-gel column chromatography (EtOAc/hexane = 30:70 to 40:60).

B. General experimental procedure for the synthesis of enaminone alcohol 141/144: To an oven-dried 20 mL resealable pressure tube (equipped with rubber septum), cyclic-1,3-diketone (0.5 mmol), and amino alcohol (0.5 mmol) were charged in a 20 mL resealable pressure tube equipped with a stirring bar. Toluene (1 mL) was added and sealed with a cap using a crimper. The mixture was stirred at room temperature and 160 °C on a preheated oil bath for 24 h. After cooling down to room temperature, the reaction mixture was diluted by dichloromethane and MeOH. After concentration under reduced pressure, the residue was purified by 100−200 mesh silica-gel column chromatography (EtOAc/methanol = 99:1 to 90:10).

C. General experimental procedure for the intramolecular annulation of β-enaminone alcohol 141/144: To an oven-dried 20 mL resealable pressure tube (equipped with rubber septum), β-enaminone alcohol (0.5 mmol), and $RuH_2CO(PPh_3)_3$ (0.025 mmol) were added in toluene (1 ml) under a N_2 atmosphere using a N_2 balloon. Then, the tube was purged with N_2 and quickly removed septum and sealed with a cap using a crimper. The reaction mixture was stirred at 160 °C for 24 h in a preheated oil bath. After cooling to room temperature, the reaction mixture was diluted by dichloromethane and MeOH. After concentration under reduced pressure, the residue was purified by 100−200 mesh silica-gel column chromatography (EtOAc/hexane = 30:70 to 40:60).

D. General experimental procedure for the intermolecular annulation of 2-aminobenzyl alcohol 142 with 1,3-diketone 139: To an oven-dried 20 mL resealable pressure tube (equipped with rubber septum), cyclic-1,3-diketone (0.5 mmol), 2-aminobenzyl alcohol (0.5 mmol), and $RuH_2CO(PPh_3)_3$ (0.025 mmol) were added in toluene (2 ml) under a N_2 atmosphere using a N_2 balloon. Then, the tube was purged with N_2 and quickly removed septum and sealed with a cap using a crimper. The reaction mixture was stirred at 160 °C for 24 h in a preheated oil bath. After cooling to room temperature, the reaction mixture was diluted by dichloromethane. After

concentration under reduced pressure, the residue was purified by 100−200 mesh silica-gel column chromatography (EtOAc/hexane = 30:70 to 40:60).

E. General experimental procedure for the drug intermediate using acceptorless dehydrogenation reaction: To an oven-dried 20 mL resealable pressure tube (equipped with rubber septum), 2-substituted-1,5,6,7-tetrahydro-4*H*-indol-4-one (0.34 mmol), alcohol (excess), $RuH_2CO(PPh_3)_3$ (0.017 mmol) and 100 mg Amberlyst® 15 were added. Then, the tube was sealed with a cap using crimper. The reaction mixture was stirred at 110 °C for 24 h in a preheated oil bath. After cooling to room temperature, the reaction mixture was diluted by dichloromethane and MeOH. After concentration under reduced pressure, the residue was purified by 100−200 mesh silica-gel column chromatography (EtOAc/hexane = 30:70 to 40:60).

F. Detection of molecular hydrogen by reduction of prop-1-yn-1-ylbenzene:

To an oven-dried 20 mL resealable pressure tube (equipped with rubber septum), cyclohexane-1,3-dione (56 mg, 0.5 mmol), (S)-2-amino-3-phenylpropan-1-ol (76 mg, 0.50 mmol), prop-1-yn-1-ylbenzene (58 mg, 0.5mmol) and $RuH_2CO(PPh_3)_3$ (0.025 mmol) were added in toluene (2 ml) under a N_2 atmosphere using a N_2 balloon. Then, the tube was purged with N_2 and quickly removed septum and sealed with a cap using a crimper. The reaction mixture was stirred at 160 °C for 24 h in a preheated oil bath. After cooling to room temperature, the reaction mixture was diluted by dichloromethane. Further, the reaction mixture was concentrated under reduced pressure, the residue was purified by 100−200 mesh silica-gel column chromatography (EtOAc/hexane = 30:70 to 40:60) to afford 2-benzyl-1,5,6,7-tetrahydro-4*H*-indol-4-one **140a** in 67 % yield. The HRMS data of the reaction mixture confirmed the mass of reduced product Prop-1-en-1-ylbenzene with $(M+H)^+$ = 119.0861.

G. General experimental procedure for gram scale synthesis of 2-isopropyl-6,6-dimethyl-1,5,6,7-tetrahydro-*4H*-indol-4-one: To an oven-dried 20 mL round bottom flask, 5,5'-cyclohexane-1,3-dione (980 mg, 7.0 mmol), (S)-(+)-2-amino-3-methyl-1-butanol (721 mg, 7.0 mmol), and $RuH_2CO(PPh_3)_3$ (333 mg, 0.025 mmol) were added without maintaining any special conditions such as the inert atmosphere. The reaction mixture was stirred at 160 °C for 24 h on a preheated oil bath. After cooling to room temperature, the reaction mixture was diluted by

dichloromethane. After concentration under reduced pressure, the residue was purified by 100−200 mesh silica-gel column chromatography (EtOAc/hexane = 30:70 to 40:60) to obtain 1.122 gm (78 %) of 2-isopropyl-6,6-dimethyl-1,5,6,7-tetrahydro-*4H*-indol-4-one (**140v).**

H. Detection of H_2 gas using GC for the inter-molecular cyclisation of β-aminoalcohol with cyclic-1,3-diketone: In a 20 mL re-sealable vial (equipped with a rubber septum and N_2 balloon) was added $RuH_2CO(PPh_3)_3$ (24.2 mg, 5 mol %), toluene 2 mL, (S)-2-amino-3-phenylpropan-1-ol (76 mg, 0.50 mmol) and cyclohexane-1,3-dione (56 mg, 0.5 mmol). The tube was purged with N_2 and sealed with a cap using a crimper. The reaction mixture was heated at 160 ^oC using Radleys parallel reaction station for 6 h. After that, the gaseous component was taken using Gas tight syringe and injected into a GC instrument. The presence of a peak at a retention time of 0.88 corresponds to hydrogen gas.

I. Detection of intermediates with HRMS for the inter-molecular cyclisation of β-aminoalcohol with cyclic-1,3-diketone: In a 20 mL re-sealable vial (equipped with a rubber septum and N_2 balloon) was added $RuH_2CO(PPh_3)_3$ (24.2 mg, 5 mol %), toluene 2 mL, (S)-2-amino-3-phenylpropan-1-ol (76 mg, 0.50 mmol) and cyclohexane-1,3-dione (56 mg, 0.5 mmol). The tube was purged with N_2 and sealed with a cap using a crimper. The reaction mixture was heated at 160 ^oC using Radleys parallel reaction station for 4 hrs. After that, the reaction mixture was taken for HRMS to see desired mass.

J. Hydride detection for the inter-molecular cyclisation of β-aminoalcohol with cyclic-1,3-diketone using $RuH_2CO(PPh_3)_3$: In an NMR tube was added $RuH_2CO(PPh_3)_3$ (15.2 mg, 20 mol%), toluene-d_8 (0.6 mL), and cyclohexane-1,3-dione (8.9 mg, 0.08 mmol), (S)-2-amino-3-phenylpropan-1-ol (12.1 mg, 0.08 mmol). The tube was purged with N_2 and closed using an NMR tube cap. The reaction mixture was heated at 100 ^oC for 1, 2, 3, and 5 h. After 1 h NMR tube was cooled and subjected to ^1H-NMR. The notable peaks was observed due to the presence of Ru-H.

5.8.A. Analytical data for products:

2-Benzyl-1,5,6,7-tetrahydro-4H-indol-4-one ***(140a)***:[201]

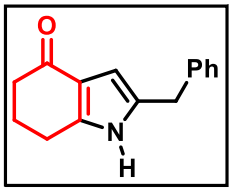

Prepared according to the general procedure (**A**), using (S)-2-amino-3-phenylpropan-1-ol (76.0 mg, 0.50 mmol) to afford 2-Benzyl-1,5,6,7-tetrahydro-4*H*-indol-4-one **140a** (70.0 mg, 62%) as a brown solid. Melting point: 131-136 °C. ^{1}H NMR (400 MHz, $CDCl_3$): δ 8.07 (s, 1H), 7.31 (m, 2H), 7.22 (m, 3H), 6.30 (s, 1H), 3.91 (s, 2H), 2.71 (t, *J* = 4.0 Hz, 2H), 2.43 (t, *J* = 8.0 Hz, 2H), 2.11 (m, 2H). ^{13}C NMR (100 MHz, $CDCl_3$): δ 194.8, 143.7, 138.8, 132.1, 129.1, 129.0, 127.0, 120.9, 103.9, 38.1, 34.1, 24.2, 23.1. IR (neat): 3227, 3154, 2924, 1623, 1480 cm^{-1}. HRMS (ESI-TOF) m/z: $[M + H]^+$ calcd for $C_{15}H_{16}NO$: 226.1232, found: 226.1234.

2-methyl-1,5,6,7-tetrahydro-4H-indol-4-one ***(140b)***: [202]

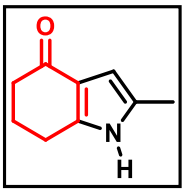

Prepared according to the general procedure (**A**), using (S)-2-aminopropan-1-ol (37.0 mg, 0.50 mmol) to afford 2-methyl-1,5,6,7-tetrahydro-4*H*-indol-4-one **140b** (56.0 mg, 76%) as a dark brown solid. Melting point: 115-120 °C. ^{1}H NMR (400 MHz, Methanol-d_4) δ 6.05 (s, 1H), 4.61 (s, 1H), 2.74 (t, *J* = 6.2 Hz, 2H), 2.38 (t, *J* = 6.0 Hz, 2H), 2.18 (s, 3H), 2.08. (m, 2H). ^{13}C NMR (100 MHz, Methanol-d_4) δ 197.6, 146.9, 130.6, 120.6, 103.2, 38.4, 25.2, 23.6, 12.3. IR (neat): 3220, 3162, 2934, 1618, 1476 cm^{-1}. HRMS (ESI-TOF) m/z: $[M + H]^+$ calcd for $C_9H_{12}NO$: 150.0919, found: 150.0917.

2-ethyl-1,5,6,7-tetrahydro-4H-indol-4-one ***(140c):***[203]

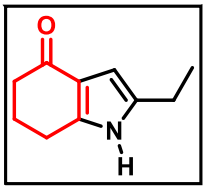

Prepared according to the general procedure (**A**), using (S)-2-aminobutan-1-ol (45.0 mg, 0.50 mmol) to afford 2-ethyl-1,5,6,7-tetrahydro-4*H*-indol-4-one **140c** (37.0 mg, 46%) as a brown solid. Melting point: 135-140 °C. ^{1}H NMR (400 MHz, $CDCl_3$) δ 8.43 (s, 1H), 6.22 (s, 1H), 2.77 (t, *J* = 6.2 Hz, 2H), 2.58 (q, *J* = 7.52 Hz, 2H), 2.45 (t, *J* = 6.1 Hz, 2H), 2.12 (dd, *J* = 12.5, 6.3 Hz, 2H), 1.23 (t, *J* = 7.7 Hz, 3H). ^{13}C NMR (100 MHz, $CDCl_3$) δ 194.7, 143.1, 135.5, 120.6, 101.4, 37.9, 24.2, 22.9, 20.8, 13.4. IR (neat): 3238, 3158, 2933, 1623, 1480 cm^{-1}. HRMS (ESI-TOF) m/z: $[M + H]^+$ calcd for $C_{10}H_{14}NO$: 164.1075, found: 164.1077.

2-isopropyl-1,5,6,7-tetrahydro-4H-indol-4-one ***(140d)*****:**[203]

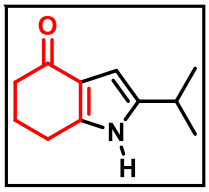

Prepared according to the general procedure (**A**), using (S)-2-amino-3-methylbutan-1-ol (52.0 mg, 0.50 mmol) to afford 2-isopropyl-1,5,6,7-tetrahydro-4*H*-indol-4-one **140d** (43.0 mg, 49%) as a brown solid. Melting point: 160-161 °C. ^{1}H NMR (400 MHz, $CDCl_3$) δ 8.76 (s, 1H), 6.20 (s, 1H), 2.88 (m, 1H), 2.78 (t, *J* = 4.0 Hz, 2H), 2.45 (t, *J* = 4.0 Hz, 2H), 2.13 (m, 2H), 1.24 (d, *J* =8.0 Hz, 6H). ^{13}C NMR (100 MHz, $CDCl_3$) δ 194.6, 143.2, 140.2, 120.1, 99.8, 37.8, 26.9, 24.0, 22.8, 22.3. IR (neat): 3237, 3156, 2952, 1625, 1481 cm^{-1}. HRMS (ESI-TOF) m/z: $[M + H]^+$ calcd for $C_{11}H_{16}NO$: 178.1232, found: 178.1231.

2-(sec-butyl)-1,5,6,7-tetrahydro-4H-indol-4-one ***(140e)*****:**

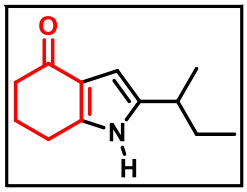

Prepared according to the general procedure (**A**), using (2S)-2-amino-3-methylpentan-1-ol (59.0 mg, 0.50 mmol) to afford 2-(sec-butyl)-1,5,6,7-tetrahydro-4*H*-indol-4-one **140e** (60.0 mg, 63%) as a brown solid. Melting point: 169-172 °C. ^{1}H NMR (400 MHz, $CDCl_3$) δ 8.37 (s, 1H), 6.22 (s, 1H), 2.77 (t, *J* = 8.0 Hz, 2H), 2.62 (m, 1H), 2.45 (t, *J* = 8.0 Hz, 2H), 2.13 (m, 2H), 1.57 (m, 2H), 1.22 (d, *J* = 8.0 Hz, 3H), 0.88 (t, *J* = 8.0 Hz, 3H). ^{13}C NMR (100 MHz, $CDCl_3$) δ 194.1, 142.4, 138.4, 119.9, 100.4, 37.4, 33.6, 29.4, 23.6, 22.5, 19.5, 11.3. IR (neat): 3244, 3160, 2958, 1625, 1482 cm^{-1}. HRMS (ESI-TOF) m/z: $[M + H]^+$ calcd for $C_{12}H_{18}NO$: 192.1388, found: 192.1388.

2-(2-(methylthio)ethyl)-1,5,6,7-tetrahydro-4H-indol-4-one ***(140f)*****:**

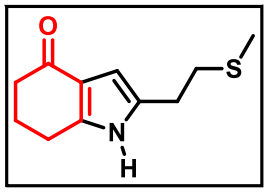

Prepared according to the general procedure (**A**), using (S)-(−)-2-Amino-4-methylthio-1-butanol (67.0 mg, 0.50 mmol) to afford 2-(2-(methylthio)ethyl)-1,5,6,7-tetrahydro-4*H*-indol-4-one **140f** (46.0 mg, 44%) as a blackish brown solid. Melting point: 134-139 °C. ^{1}H NMR (400 MHz, $CDCl_3$) δ 9.16 (s, 1H), 6.23 (s, 1H), 2.85 (t, *J* = 8.0 Hz, 2H), 2.76 (m, 4H), 2.45 (t, *J* = 8.0 Hz, 2H), 2.13 (m, 5H). ^{13}C NMR (100 MHz, $CDCl_3$) δ 195.5, 144.1, 132.9, 121.0, 103.1, 38.4, 34.7, 27.6, 24.6, 23.4, 16.1. IR (neat): 3290, 2939, 1623, 1482 cm^{-1}. HRMS (ESI-TOF) m/z: $[M + H]^+$ calcd for $C_{11}H_{16}NOS$: 210.0953, found: 210.0954.

2-benzyl-6-methyl-1,5,6,7-tetrahydro-4H-indol-4-one ***(140g)*****:**

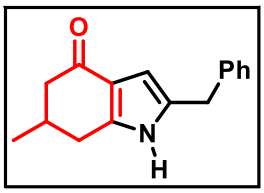

Prepared according to the general procedure (**A**), using (S)-2-amino-3-phenylpropan-1-ol (76.0 mg, 0.50 mmol) to afford 2-benzyl-6-methyl-1,5,6,7-tetrahydro-4*H*-indol-4-one **140g** (56.0 mg, 47%) as a brownish orange solid. Melting point: 175-180 °C. ^{1}H NMR (400 MHz, $CDCl_3$) δ 8.37 (s, 1H), 7.30 (m, 2H), 7.22 (m, 3H), 6.26 (s, 1H), 3.90 (s, 2H), 2.76 (m, 1H), 2.42 (m, 3H), 2.16 (m, 1H), 1.10 (d, *J* = 8.0 Hz, 3H). ^{13}C NMR (100 MHz, $CDCl_3$) δ 194.2, 143.5, 138.5, 132.1, 128.7, 126.7, 120.2, 103.5, 46.2, 34.0, 31.9, 31.0, 21.5. IR (neat): 3344, 2941, 1648, 1409 cm^{-1}. HRMS (ESI-TOF) m/z: $[M + H]^+$ calcd for $C_{16}H_{18}NO$: 240.1388, found: 240.1393.

2,6-dimethyl-1,5,6,7-tetrahydro-4H-indol-4-one ***(140h)*****:**

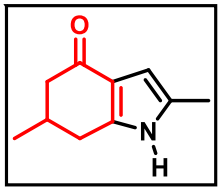

Prepared according to the general procedure (**A**), using (S)-2-aminopropan-1-ol (37.0 mg, 0.50 mmol) to afford 2,6-dimethyl-1,5,6,7-tetrahydro-4*H*-indol-4-one **140h** (49.0 mg, 60%) as a black solid. Melting point: 167-170 °C. ^{1}H NMR (400 MHz, $CDCl_3$) δ 9.22 (s, 1H), 6.13 (s, 1H), 2.82 (dd, *J* = 12.0 Hz,4.0 Hz, 1H), 2.41 (m, 3H), 2.19 (m, 4H), 1.12 (d, *J* = 4.0 Hz, 3H). ^{13}C NMR (100 MHz, $CDCl_3$) δ 194.8, 144.0, 129.7, 120.3, 102.7, 46.6, 32.3, 31.3, 21.6, 13.1. IR (neat): 3230, 3162, 2920, 1624, 1479 cm^{-1}. HRMS (ESI-TOF) m/z: $[M + H]^+$ calcd for $C_{10}H_{14}NO$: 164.1075, found: 164.1078.

2-ethyl-6-methyl-1,5,6,7-tetrahydro-4H-indol-4-one ***(140i)*****:**

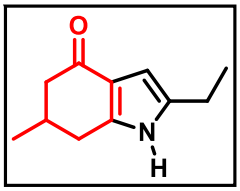

Prepared according to the general procedure (**A**), using (S)-2-aminobutan-1-ol (45.0 mg, 0.50 mmol) to afford 2-ethyl-6-methyl-1,5,6,7-tetrahydro-4*H*-indol-4-one **140i** (59.0 mg, 67%) as a brownish black solid. Melting point: 164-167 °C. ^{1}H NMR (400 MHz, $CDCl_3$) δ 9.25 (s, 1H), 6.17 (s, 1H), 2.83 (dd, *J* = 12.0 Hz, 4.0 Hz, 1H), 2.57 (q, *J* = 15.0 Hz, 7.5 Hz, 2H), 2.41 (m, 3H), 2.20 (dd, *J* = 16.0 Hz, 12.0 Hz, 1H), 1.22 (t, *J* = 8.0Hz, 3H), 1.12 (d, *J* =4.0Hz, 3H). ^{13}C NMR (100 MHz, $CDCl_3$) δ 194.4, 143.3, 135.8, 119.5, 100.7, 46.1, 31.8, 30.8, 21.1, 20.4, 13.0. IR (neat): 3227, 3158, 2959, 1625, 1480 cm^{-1}. HRMS (ESI-TOF) m/z: $[M + H]^+$ calcd for $C_{11}H_{16}NO$: 178.1232, found: 178.1234.

2-isopropyl-6-methyl-1,5,6,7-tetrahydro-4H-indol-4-one ***(140j)*****:**

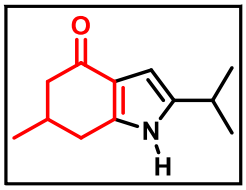

Prepared according to the general procedure (**A**), using (S)-2-amino-3-methylbutan-1-ol (52.0 mg, 0.50 mmol) to afford 2-isopropyl-6-methyl-1,5,6,7-tetrahydro-4*H*-indol-4-one **140j** (48.0 mg, 51%) as a brown solid. Melting point: 187-192 °C. ^{1}H NMR (400 MHz, $CDCl_3$) δ 9.27 (s, 1H), 6.17 (s, 1H), 2.87 (m, 2H), 2.41 (m, 3H), 2.19 (m, 1H), 1.23 (d, *J* = 8.0 Hz, 6H), 1.12 (d, *J* = 4.0 Hz, 3H). ^{13}C NMR (100 MHz, $CDCl_3$) δ 194.7, 143.5, 140.7, 120.1, 99.7, 46.4, 32.1, 31.1, 27.1, 22.4, 22.6, 21.4. IR (neat): 3226, 3159, 2955, 1624, 1484 cm^{-1}. HRMS (ESI-TOF) m/z: $[M + H]^+$ calcd for $C_{12}H_{18}NO$: 192.1388, found: 192.1391.

2-(sec-butyl)-6-methyl-1,5,6,7-tetrahydro-4H-indol-4-one ***(140k)*****:**

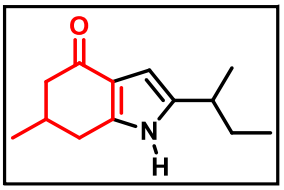

Prepared according to the general procedure (**A**), using (2S)-2-amino-3-methylpentan-1-ol (59.0 mg, 0.50 mmol) to afford 2-(sec-butyl)-6-methyl-1,5,6,7-tetrahydro-4*H*-indol-4-one **140k** (64.0 mg, 63%) as a brown solid. Melting point: 191-196 °C. ^{1}H NMR (400 MHz, $CDCl_3$) δ 8.85 (s, 1H), 6.17 (s, 1H), 2.83 (dd, *J* = 16.0 Hz, 4.0 Hz, 1H), 2.62 (m, 1H), 2.42 (m, 3H), 2.19 (dd, *J* =12.0 Hz, 16.0 Hz, 1H), 1.57 (m, 2H), 1.21 (d, *J* = 4.0 Hz, 3H), 1.12 (d, *J* = 8.0 Hz, 3H), 0.85 (t, *J* = 8.0 Hz, 3H). ^{13}C NMR (100 MHz, $CDCl_3$) δ 194.8, 143.2, 139.5, 120.1, 100.8, 46.6, 34.3, 32.3, 31.3, 29.9, 21.6, 20.1, 11.9. IR (neat): 3231, 3160, 2960, 1623, 1482 cm^{-1}. HRMS (ESI-TOF) m/z: $[M + H]^+$ calcd for $C_{13}H_{20}NO$: 206.1545, found: 206.1546. Crystal data: $C_{13}H_{19}NO$, M = 205, Monoclinic, space group P21 with a = 7.2804(13) Å, b = 7.7406(15) Å, c = 11.197(3) Å, α = 90°, β = 104.549(12)°, γ = 90°, V = 610.8(2), T = 100K, R1 = 0.0855, wR2 = 0.2298 on observed data, z = 2, F(000)= 224, Absorption coefficient = 0.543, λ= 1.54178 Å, 4950 reflections were collected on a Brucker APEX-III, 1574 observed reflections (I≥2σ (I)).

6-methyl-2-(2-(methylthio)ethyl)-1,5,6,7-tetrahydro-4H-indol-4-one ***(140l)*****:**

Prepared according to the general procedure (**A**), using (S)-(−)-2-amino-4-methylthio-1-butanol (67.0 mg, 0.50 mmol) to afford 6-methyl-2-(2-(methylthio)ethyl)-1,5,6,7-tetrahydro-4*H*-indol-4-one **140l** (44.0 mg, 40%) as a dark brown solid. Melting point: 115-120 °C. ^{1}H NMR (400 MHz, $CDCl_3$) δ 9.27 (s, 1H), 6.22 (s, 1H), 2.84 (m, 3H), 2.73 (t, *J* = 8.0 Hz, 2H), 2.48 (dd, *J* = 12.0 Hz, 8.0 Hz, 2H), 2.38 (m, 1H), 2.21 (m, 1H), 2.11 (s, 3H), 1.12 (d, *J* = 4.0 Hz, 3H). ^{13}C NMR (100 MHz, $CDCl_3$) δ 194.5, 143.4, 132.5, 120.0, 102.7, 46.4, 34.1, 32.1, 31.2, 27.2, 21.4, 15.6. IR (neat): 3222, 3154, 2920, 1623, 1480 cm^{-1}. HRMS (ESI-TOF) m/z: $[M + H]^+$ calcd for $C_{12}H_{18}NOS$: 224.1109, found: 224.1112.

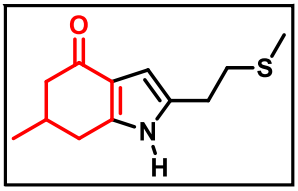

2-benzyl-7,7-dimethyl-1,5,6,7-tetrahydro-4H-indol-4-one ***(140m)*****:**

Prepared according to the general procedure (**A**), using (S)-2-amino-3-phenylpropan-1-ol (76.0 mg, 0.50 mmol) to afford 2-benzyl-7,7-dimethyl-1,5,6,7-tetrahydro-4*H*-indol-4-one **140m** (32.0 mg, 25%) as a dark brown solid. Melting point: 175-177 °C. ^{1}H NMR (400 MHz, $CDCl_3$) δ 8.02 (s, 1H), 7.28 (m, 2H), 7.20 (m, 3H), 6.24 (d, *J* = 1.8 Hz, 1H), 3.87 (s, 2H), 2.69 (t, *J* = 8.0 Hz, 2H), 1.91 (t, *J* = 8.0 Hz, 2H), 1.13 (s, 6H). ^{13}C NMR (100 MHz, $CDCl_3$) δ 199.3, 141.7, 138.6, 132.0, 128.8, 126.6, 119.1, 104.3, 41.4, 37.8, 34.0, 29.8, 24.6, 20.0. IR (neat): 3234, 3160, 2919, 1622, 1478 cm^{-1}. HRMS (ESI-TOF) m/z: $[M + H]^+$ calcd for $C_{17}H_{20}NO$: 254.1545, found: 254.1546.

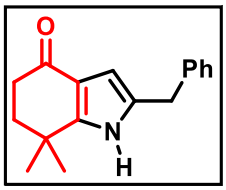

2,7,7-trimethyl-1,5,6,7-tetrahydro-4H-indol-4-one ***(140n)*****:**

Prepared according to the general procedure (**A**), using (S)-2-aminopropan-1-ol (37.0 mg, 0.50 mmol) to afford 2,7,7-trimethyl-1,5,6,7-tetrahydro-4*H*-indol-4-one **140n** (74.0 mg, 84%) as a dark brown solid. Melting point: 1181-183 °C. ^{1}H NMR (400 MHz, $CDCl_3$) δ 8.76 (s, 1H), 6.14 (s, 1H), 2.78 (t, *J* = 6.3 Hz, 2H), 2.22 (s, 3H), 1.96 (t, *J* = 6.3 Hz, 2H), 1.17 (s, 6H). ^{13}C NMR (100 MHz, $CDCl_3$) δ 199.8, 142.0, 129.6, 119.3, 103.7, 41.7, 38.2, 24.9, 20.3, 13.2. IR (neat): 3228, 3166, 2922, 1621, 1476 cm^{-1}. HRMS (ESI-TOF) m/z: $[M + H]^+$ calcd for $C_{11}H_{16}NO$: 178.1232, found: 178.1237.

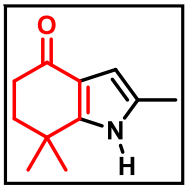

2-ethyl-7,7-dimethyl-1,5,6,7-tetrahydro-4H-indol-4-one ***(140o)*****:**

Prepared according to the general procedure (**A**), using (S)-2-aminobutan-1-ol (45.0 mg, 0.50 mmol) to afford 2-ethyl-7,7-dimethyl-1,5,6,7-tetrahydro-4*H*-indol-4-one **140o** (34.0 mg, 36%) as a brownish black solid. Melting point: 119-124 °C. ^{1}H NMR (400 MHz, $CDCl_3$) δ 9.05 (s, 1H), 6.16 (s, 1H), 2.79 (t, *J* = 6.2 Hz, 2H), 2.57 (q, *J* = 7.5 Hz, 15.1 Hz, 2H), 1.96 (t, *J* = 6.2 Hz, 2H), 1.22 (t, *J* = 7.6 Hz, 3H), 1.17 (s, 6H). ^{13}C NMR (100 MHz, $CDCl_3$) δ 200.0, 142.1, 136.3, 118.8, 101.8, 41.7, 38.2, 24.9, 21.0, 20.3, 13.5. IR (neat): 3242, 3168, 2962, 1623, 1476 cm^{-1}. HRMS (ESI-TOF) m/z: $[M + H]^+$ calcd for $C_{12}H_{18}NO$: 192.1388, found: 192.1392.

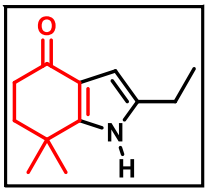

2-isopropyl-7,7-dimethyl-1,5,6,7-tetrahydro-4H-indol-4-one ***(140p)*****:**

Prepared according to the general procedure (**A**), using (S)-2-amino-3-methylbutan-1-ol (52.0 mg, 0.50 mmol) to afford 2-isopropyl-7,7-dimethyl-1,5,6,7-tetrahydro-4*H*-indol-4-one **140p** (43.0 mg, 42%) as a pale brown solid. Melting point: 191-196 °C. ^{1}H NMR (400 MHz, $CDCl_3$) δ 9.17 (s, 1H), 6.15 (s, 1H), 2.87 (m, 1H), 2.80 (t, *J* = 6.2 Hz, 2H), 1.97 (t, *J* = 6.2 Hz, 2H), 1.23 (d, *J* = 6.9 Hz, 6H), 1.18 (s, 6H). ^{13}C NMR (100 MHz, $CDCl_3$) δ 199.9, 141.9, 140.8, 118.5, 100.4, 41.5, 38.1, 27.2, 24.8, 22.4, 20.0. IR (neat): 3208, 3142, 2964, 1613, 1477 cm^{-1}. HRMS (ESI-TOF) m/z: $[M + H]^+$ calcd for $C_{13}H_{20}NO$: 206.1545, found: 206.1548.

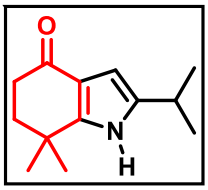

2-(sec-butyl)-7,7-dimethyl-1,5,6,7-tetrahydro-4H-indol-4-one ***(140q)*****:**

Prepared according to the general procedure (**A**), using (2S)-2-amino-3-methylpentan-1-ol (59.0 mg, 0.50 mmol) to afford 2-(sec-butyl)-6-methyl-1,5,6,7-tetrahydro-4*H*-indol-4-one **140q** (77.0 mg, 71%) as a yellowish brown solid. Melting point: 1154-160 °C. ^{1}H NMR (400 MHz, $CDCl_3$) δ 8.34 (s, 1H), 6.18 (s, 1H), 2.79 (t, *J* =6.24 Hz, 2H), 2.62 (m, 1H), 1.97 (t, *J* = 6.24 Hz, 2H), 1.57 (m, 2H), 1.22 (d, *J* = 6.9 Hz, 3H), 1.18 (s, 6H), 0.88 (t, *J* = 7.4 Hz, 3H). ^{13}C NMR (100 MHz, $CDCl_3$) δ 199.6, 141.1, 139.2, 118.9, 101.5, 41.5, 38.0, 34.2, 29.9, 24.8, 20.2, 19.9, 11.8. IR (neat): 3207, 3143, 2964, 1617, 1477 cm^{-1}. HRMS (ESI-TOF) m/z: $[M + H]^+$ calcd for $C_{14}H_{22}NO$: 220.1701, found: 220.1704.

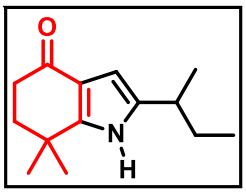

7,7-dimethyl-2-(2-(methylthio)ethyl)-1,5,6,7-tetrahydro-4H-indol-4-one ***(140r)*****:**

Prepared according to the general procedure (**A**), using (S)-(−)-2-Amino-4-methylthio-1-butanol (67.0 mg, 0.50 mmol) to afford 6-methyl-2-(2-(methylthio)ethyl)-1,5,6,7-tetrahydro-4*H*-indol-4-one **140r** (51.0 mg, 43%) as a brown solid. Melting point: 126-131 °C. ^{1}H NMR (400 MHz, $CDCl_3$) δ 8.82 (s, 1H), 6.23 (s, 1H), 2.80 (m, 6H), 2.14 (s, 3H), 1.97 (t, *J* = 6.1 Hz, 2H), 1.17 (s, 6H). ^{13}C NMR (100 MHz, $CDCl_3$) δ 199.7, 141.7, 132.5, 118.9, 103.6, 41.6, 37.9, 34.2, 29.8, 24.7, 20.2, 15.7. IR (neat): 3240, 3165, 2921, 1624, 1477 cm^{-1}. HRMS (ESI-TOF) m/z: $[M + H]^+$ calcd for $C_{13}H_{20}NOS$: 238.1266, found: 238.1270. .

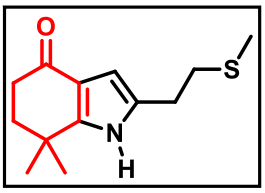

2-benzyl-6,6-dimethyl-1,5,6,7-tetrahydro-4H-indol-4-one ***(140s)*****:**

Prepared according to the general procedure (**A**), using (S)-2-amino-3-phenylpropan-1-ol (76.0 mg, 0.50 mmol) to 2-benzyl-6,6-dimethyl-1,5,6,7-tetrahydro-4*H*-indol-4-one **140s** (85.0 mg, 68%) as a dark brown solid. Melting point: 202-206 °C. ^{1}H NMR (400 MHz, $CDCl_3$) δ 8.00 (s, 1H), 7.31 (m, 3H), 7.21 (m, 2H), 6.29 (s, 1H), 3.91 (s, 2H), 2.56 (s, 2H), 2.31 (s, 2H), 1.08 (s, 6H). ^{13}C NMR (100 MHz, $CDCl_3$) δ 194.1, 142.6, 138.6, 132.1, 128.9, 126.9, 119.5, 103.6, 52.0, 36.9, 35.9, 34.1, 29.8, 28.8. IR (neat): 3234, 3162, 2925, 1627, 1479 cm^{-1}. HRMS (ESI-TOF) m/z: $[M + H]^+$ calcd for $C_{17}H_{20}NO$: 254.1545, found: 254.1552.

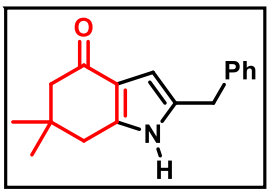

2,6,6-trimethyl-1,5,6,7-tetrahydro-4H-indol-4-one ***(140t)*****:**[204]

Prepared according to the general procedure (**A**), using (S)-2-aminopropan-1-ol (37.0 mg, 0.50 mmol) to 2,6,6-trimethyl-1,5,6,7-tetrahydro-4*H*-indol-4-one **140t** (84.0 mg, 95%) as a dark brown solid. Melting point: 184-187 °C. ^{1}H NMR (400 MHz, $CDCl_3$) δ 8.33 (s, 1H), 6.17 (s, 1H), 2.62 (s, 2H), 2.32 (s, 2H), 2.23 (s, 3H), 1.10 (s, 6H). ^{13}C NMR (100 MHz, $CDCl_3$) δ 194.2, 142.4, 129.3, 119.9, 103.1, 52.4, 37.3, 36.3, 29.1, 13.3. IR (neat): 3237, 3176, 2950, 1625, 1478 cm^{-1}. HRMS (ESI-TOF) m/z: $[M + H]^+$ calcd for $C_{11}H_{16}NO$: 178.1232, found: 178.1243.

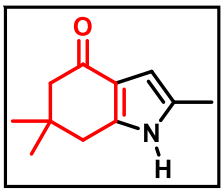

2-ethyl-6,6-dimethyl-1,5,6,7-tetrahydro-4H-indol-4-one ***(140u)*****:**

Prepared according to the general procedure (**A**), using (S)-2-aminobutan-1-ol (45.0 mg, 0.50 mmol) to afford 2-ethyl-6,6-dimethyl-1,5,6,7-tetrahydro-4*H*-indol-4-one **140u** (68.0 mg, 72%) as a brown solid. Melting point: 140-145 °C. ^{1}H NMR (400 MHz, $CDCl_3$) δ 8.51 (s, 1H), 6.20 (s, 1H), 2.63 (s, 2H), 2.57 (q, *J* = 7.5 Hz, 15.1 Hz, 2H), 2.32 (s, 2H), 1.23 (t, *J* = 7.5 Hz, 3H), 1.10 (s, 6H). ^{13}C NMR (100 MHz, $CDCl_3$) δ 194.1, 142.1, 135.8, 119.2, 101.1, 52.1, 36.9, 35.9, 28.8, 20.8, 13.2. IR (neat): 3232, 3161, 2960, 1625, 1479 cm^{-1}. HRMS (ESI-TOF) m/z: $[M + H]^+$ calcd for $C_{12}H_{18}NO$: 192.1388, found: 192.1398.

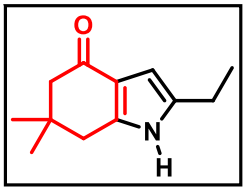

2-isopropyl-6,6-dimethyl-1,5,6,7-tetrahydro-4H-indol-4-one ***(140v)*****:**

Prepared according to the general procedure (**A**), using (S)-2-amino-3-methylbutan-1-ol (52.0 mg, 0.50 mmol) to afford 2-isopropyl-6,6-dimethyl-1,5,6,7-tetrahydro-4*H*-indol-4-one **140v** (85.0 mg, 83%) as a brown solid. Melting point: 176-178 °C. ^{1}H NMR (400 MHz, Methanol-d_4) δ 6.08 (s, 1H), 2.84 (hept, *J* = 6.8 Hz, 1H), 2.66 (s, 2H), 2.29 (s, 2H), 1.24 (s, 3H), 1.22 (s, 3H), 1.09 (s, 6H). ^{13}C NMR (100 MHz, Methanol-d_4) δ 196.9, 145.9, 142.5, 119.1, 100.1, 52.5, 37.3, 36.9, 28.7, 28.2, 22.7. IR (neat): 3239, 3160, 2958, 1627, 1481 cm^{-1}. HRMS (ESI-TOF) m/z: $[M + H]^+$ calcd for $C_{13}H_{20}NO$: 206.1545, found: 206.1554.

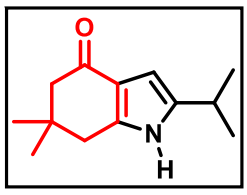

2-(sec-butyl)-6,6-dimethyl-1,5,6,7-tetrahydro-4H-indol-4-one ***(140w)*****:**

Prepared according to the general procedure (**A**), using (2S)-2-amino-3-methylpentan-1-ol (59.0 mg, 0.50 mmol) to afford2-(sec-butyl)-6,6-dimethyl-1,5,6,7-tetrahydro-4*H*-indol-4-one **140w** (85.0 mg, 76%) as a brown solid. Melting point: 145-151 °C. ^{1}H NMR (400 MHz, $CDCl_3$) δ 8.59 (s, 1H), 6.18 (s, 1H), 2.63 (m, 3H), 2.32 (s, 2H), 1.57 (m, 2H), 1.21 (d, *J* = 6.9 Hz, 3H), 1.10 (s, 6H), 0.86 (t, *J* = 7.4 Hz, 3H). ^{13}C NMR (100 MHz, $CDCl_3$) δ 194.2, 142.0, 139.1, 119.1, 100.6, 52.1, 36.9, 35.9, 34.1, 29.8, 28.8, 28.7. 19.8, 11.7. IR (neat): 3244, 3159, 2958, 1625, 1479 cm^{-1}. HRMS (ESI-TOF) m/z: $[M + H]^+$ calcd for $C_{14}H_{22}NO$: 220.1701, found: 220.1707.

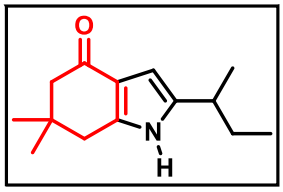

6,6-dimethyl-2-(2-(methylthio)ethyl)-1,5,6,7-tetrahydro-4H-indol-4-one ***(140x)*****:**

Prepared according to the general procedure (**A**), using (S)-(−)-2-Amino-4-methylthio-1-butanol (67.0 mg, 0.50 mmol) to afford 6-methyl-2-(2-(methylthio)ethyl)-1,5,6,7-tetrahydro-4*H*-indol-4-one **140x** (30.0 mg, 25 %) as a brown solid. Melting point: 153-158 °C. ^{1}H NMR (400 MHz, $CDCl_3$) δ 8.95 (s, 1H), 6.23 (s, 1H), 2.85 (t, *J* = 6.8 Hz, 2H), 2.74 (t, *J* = 6.9 Hz, 2H), 2.64 (s, 2H), 2.32 (s, 2H), 2.11 (s, 3H), 1.10 (s, 6H). ^{13}C NMR (100 MHz, $CDCl_3$) δ 194.1, 142.4 132.4, 119.2, 102.8, 52.1, 36.9, 35.9, 34.2, 28.8, 27.1, 15.7. IR (neat): 3240, 3155, 2926, 1624, 1479 cm^{-1}. HRMS (ESI-TOF) m/z: $[M + H]^+$ calcd for $C_{13}H_{20}NOS$: 238.1266, found: 238.1274.

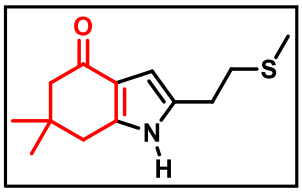

3,6,6-trimethyl-1,5,6,7-tetrahydro-4H-indol-4-one ***(140y)*****:**[205]

Prepared according to the general procedure (**A**), using (R)-(−)-1-amino-propanol (37.0 mg, 0.50 mmol) to afford 3,6,6-trimethyl-1,5,6,7-tetrahydro-4*H*-indol-4-one **140y** (35.0 mg, 40 %) as a white solid. Melting point: 149-153 °C. ^{1}H NMR (400 MHz, $CDCl_3$) δ 8.13 (s, 1H), 6.40 (s, 1H), 2.62 (s, 2H), 2.32 (s, 2H), 2.28 (s, 3H), 1.10 (s, 6H). ^{13}C NMR (100 MHz, $CDCl_3$) δ 194.6, 142.3, 119.1, 117.6, 115.9, 52.8, 37.2, 35.7, 28.6, 11.5. IR (neat): 3239, 2934, 1696, 1476 cm^{-1}. HRMS (ESI-TOF) m/z: $[M + H]^+$ calcd for $C_{11}H_{16}NO$: 178.1232, found: 178.1239.

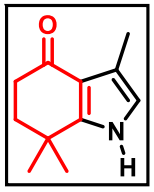

6-(4-(dimethylamino)phenyl)-2-isopropyl-1,5,6,7-tetrahydro-4H-indol-4-one ***(140z)*****:**

Prepared according to the general procedure **(A)**, using (S)-2-amino-3-methylbutan-1-ol (36.0 mg, 0.35 mmol) to afford 6-(4-(dimethylamino)phenyl)-2-isopropyl-1,5,6,7-tetrahydro-4*H*-indol-4-one **140z** (50.0 mg, 49%) as a blackish brown solid. Melting point: 120-124 °C. ^{1}H NMR (400 MHz, $CDCl_3$) δ 8.54 (s, 1H), 7.15 (d, *J* = 8.5 Hz, 2H), 6.73 (m, 2H), 6.25 (s, 1H), 3.42 (m, 1H), 2.98 (m, 1H), 2.93 (s, 6H), 2.87 (m, 2H), 2.68 (m, 2H), 1.25 (d, *J* = 6.9 Hz, 6H). ^{13}C NMR (100 MHz, $CDCl_3$) δ 193.9, 149.7, 142.6, 140.6, 131.7, 127.5, 120.2, 112.9, 100.1, 45.5, 41.9, 40.8, 31.2, 27.1, 22.5. IR (neat): 2961, 2926,1623, 1523, 1483 cm^{-1}. HRMS (ESI-TOF) m/z: $[M + H]^+$ calcd for $C_{19}H_{25}N_2O$: 297.1967, found: 297.1963.

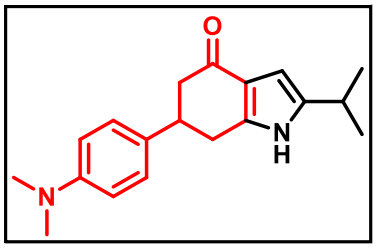

6,6-dimethyl-1,2,3,5,6,7-hexahydro-8H-pyrrolo[1,2-a]indol-8-one ***(140aa):***

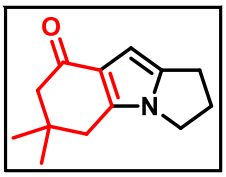

Prepared according to the general procedure **(A)**, using (S)-(+)-2-pyrrolidinemethanol (51.0 mg, 0.50 mmol) to afford 6,6-dimethyl-1,2,3,5,6,7-hexahydro-8*H*-pyrrolo[1,2-*a*]indol-8-one **140aa** (47.0 mg, 47%) as a blackish brown solid. Melting point: 124-128 °C. ^{1}H NMR (400 MHz, $CDCl_3$) δ 6.16 (s, 1H), 3.81 (m, 2H), 2.81 (t, *J* = 6.9 Hz, 2H), 2.57 (s, 2H), 2.51 (m, 2H), 2.31 (s, 2H), 1.11 (s, 6H). ^{13}C NMR (100 MHz, $CDCl_3$) δ 193.7, 138.1, 137.7, 123.3, 96.2, 52.2, 44.1, 36.3, 35.7, 28.9, 27.9, 23.7. IR (neat): 2954, 2868, 1645, 1464, 1369 cm^{-1}. HRMS (ESI-TOF) m/z: $[M + H]^+$ calcd for $C_{13}H_{18}NO$: 204.1388, found: 204.1384.

6-(4-(dimethylamino)phenyl)-1,2,3,5,6,7-hexahydro-8H-pyrrolo[1,2-a]indol-8-one ***(108ab):***

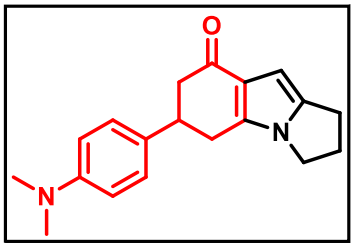

Prepared according to the general procedure **(A)**, using (S)-(+)-2-pyrrolidinemethanol (35.0 mg, 0.35 mmol) to afford 6-(4-(dimethylamino)phenyl)-1,2,3,5,6,7-hexahydro-8*H*-pyrrolo[1,2-*a*]indol-8-one **140ab** (62.0 mg, 61%) as a blackish brown solid. Melting point: 200-205 °C. ^{1}H NMR (400 MHz, $CDCl_3$) δ 7.17 (m, 2H), 6.73 (m, 2H), 6.21 (s, 1H), 3.83 (m, 2H), 3.42 (m, 1H), 2.94 (s, 6H), 2.84 (m, 4H), 2.69 (m, 2H), 2.51 (m, 2H). ^{13}C NMR (100 MHz, $CDCl_3$) δ 193.4, 149.6, 138.2, 131.6, 127.4, 124.1, 112.9, 96.3, 45.3, 44.1, 41.7, 40.7, 30.5, 27.8, 23.7. IR (neat): 2922, 2854, 1644, 1613, 1520, 1462 cm^{-1}. HRMS (ESI-TOF) m/z: $[M + H]^+$ calcd for $C_{19}H_{23}N_2O$: 295.1793, found: 295.1798.

2-isopropyl-5,6-dihydrocyclopenta[b]pyrrol-4(1H)-one ***(140ac):***

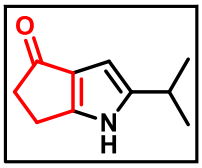

Prepared according to the general procedure **(A)**, using (S)-2-amino-3-methylbutan-1-ol (52.0 mg, 0.50 mmol) to afford 2-isopropyl-5,6-dihydrocyclopenta[*b*]pyrrol-4(1*H*)-one **140ac** (34 mg, 42%) as a brown solid. Melting point: 180-185 °C. ^{1}H NMR (400 MHz, $CDCl_3$) δ 9.30 (s, 1H), 5.96 (s, 1H), 2.88 (m, 5H), 1.25 (d, *J* = 6.9 Hz, 6H). ^{13}C NMR (100 MHz, $CDCl_3$) δ 193.9, 149.7, 142.6, 140.6, 131.7, 127.5, 120.2, 112.9, 100.1, 45.5, 41.9, 40.8, 31.2, 27.1, 22.5. IR (neat): 3237, 2961, 2925, 1659, 1576, 1487 cm^{-1}. HRMS (ESI-TOF) m/z: $[M + H]^+$ calcd for $C_{10}H_{14}NO$: 164.1075, found: 164.1070.

(Z)-3-((1-hydroxy-3-phenylpropan-2-yl)amino)-1,3-diphenylprop-2-en-1-one ***(141a‘):***

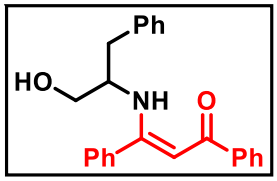

Prepared according to the general procedure **(A)**, using (S)-2-amino-3-phenylpropan-1-ol (76.0 mg, 0.50 mmol) to afford (Z)-3-((1-hydroxy-3-phenylpropan-2-yl)amino)-1,3-diphenylprop-2-en-1-one **141a‘** (78.0 mg, 44%) as a yellow semisolid. ^{1}H NMR (400 MHz, $CDCl_3$) δ 11.42 (d, *J* = 10.4 Hz, 1H), 7.86 (m, 2H), 7.35 (m, 9H), 7.05 (m, 2H), 6.81 (d, *J* = 7.3 Hz, 2H), 5.55 (s, 1H), 3.91 (s, 1H), 3.74 (m, 2H), 3.64 (m, 1H), 2.86 (m, 2H). ^{13}C NMR (100 MHz, $CDCl_3$) δ 188.6, 167.6, 140.6, 137.9, 135.8, 130.8, 129.8, 129.2, 128.6, 128.4, 128.3, 127.9, 127.5, 126.6, 94.3, 65.4, 59.0, 39.8. IR (neat): 3364, 3059, 3026, 2922, 1581, 1479, 1330 cm^{-1}. HRMS (ESI-TOF) m/z: $[M + H]^+$ calcd for $C_{24}H_{24}NO_2$: 358.1807, found: 358.1805.

(Z)-3-((1-hydroxypropan-2-yl)amino)-1,3-diphenylprop-2-en-1-one ***(141b‘):***

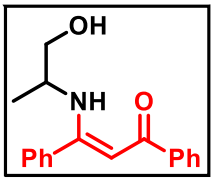

Prepared according to the general procedure **(A)**, using (S)-2-aminopropan-1-ol (37.0 mg, 0.50 mmol) to afford (Z)-3-((1-hydroxypropan-2-yl)amino)-1,3-diphenylprop-2-en-1-one **141b‘** (45.0 mg, 32%) as a yellowish brown semisolid. ^{1}H NMR (400 MHz, $CDCl_3$) δ 11.29 (d, *J* = 9.4 Hz, 1H), 7.86 (m, 2H), 7.40 (m, 8H), 5.72 (s, 1H), 3.65 (m, 1H), 3.59 (d, *J* = 3.6 Hz, 2H), 1.26 (s, 1H), 1.19 (d, *J* = 6.4 Hz, 3H). ^{13}C NMR (100 MHz, $CDCl_3$) δ 188.7, 167.2, 140.3, 135.9, 130.9, 129.6, 128.7, 128.4, 127.9, 127.2, 67.1, 52.3, 29.8, 18.8. IR (neat): 3358, 3058, 2926, 1561, 1480 cm^{-1}. HRMS (ESI-TOF) m/z: $[M + H]^+$ calcd for $C_{18}H_{20}NO_2$: 282.1494, found: 282.1499.

(Z)-3-((1-hydroxy-3-methylbutan-2-yl)amino)-1,3-diphenylprop-2-en-1-one ***(141c‘):***

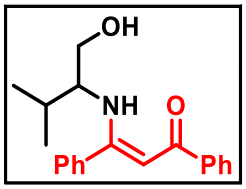

Prepared according to the general procedure **(A)**, using (S)-2-amino-3-methylbutan-1-ol (52.0 mg, 0.50 mmol) to afford (Z)-3-((1-hydroxy-3-methylbutan-2-yl)amino)-1,3-diphenylprop-2-en-1-one **141c‘** (39.0 mg, 25%) as a yellowish brown solid. Melting point: 99-101 °C. ^{1}H NMR (400 MHz, $CDCl_3$) δ 11.41 (d, *J* = 10.6 Hz, 1H), 7.87 (d, *J* = 7.6 Hz, 2H), 7.38 (m, 8H), 5.70 (s, 1H), 3.70 (m, 2H), 3.36 (m, 1H), 1.84 (m, 1H), 1.26 (s, 1H), 0.97 (d, *J* = 6.8 Hz, 3H), 0.86 (d, *J* = 6.8 Hz, 3H). ^{13}C NMR (100 MHz, $CDCl_3$) δ 188.4, 168.5, 140.2, 135.9, 130.9, 129.4, 128.9, 128.3,

128.2, 127.3, 64.4, 61.9 30.6, 19.8, 18.2. IR (neat): 3365, 3060, 2958, 1568, 1479 cm^{-1}. HRMS (ESI-TOF) m/z: $[M + H]^+$ calcd for $C_{20}H_{24}NO_2$: 310.1807, found: 310.1809. Crystal data: $C_{20}H_{23}NO_2$, M = 309, Monoclinic, space group C2 with a = 22.889(8) Å, b = 8.478(3) Å, c = 9.441(4) Å, α = 90°, β = 104.65(2)°, γ = 90°, V = 1772.5(12), T = 100K, R1 = 0.0563, wR2 = 0.1807 on observed data, z = 4, F(000)= 664, Absorption coefficient = 0.585, λ= 1.54178 Å, 9240 reflections were collected on a Brucker APEX-III, 2661 observed reflections (I≥2σ (I)).

3-((1-hydroxy-3-phenylpropan-2-yl)amino)cyclohex-2-en-1-one ***(141a)*****:**

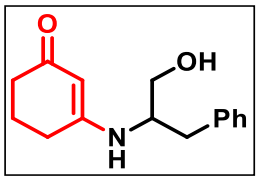

Prepared according to the general procedure (**B**), using (S)-2-amino-3-phenylpropan-1-ol (755.0 mg, 5 mmol) to afford 3-((1-hydroxy-3-phenylpropan-2-yl)amino)cyclohex-2-en-1-one **141a** (1029.0 mg, 84%) as a pale brown solid. Melting point: 128-133 °C. ^{1}H NMR (400 MHz, $CDCl_3$) δ 7.32 (m, 2H), 7.25 (m, 3H), 5.70 (s, 1H), 5.29 (s, 1H), 3.67 (m, 3H), 2.95 (d, *J* = 6.2 Hz, 2H), 2.34 (m, 4H), 1.95 (s, 2H). ^{13}C NMR (100 MHz, $CDCl_3$) δ 197.9, 164.9, 137.6, 129.4, 128.7, 126.8, 73.83, 61.7, 55.4, 36.3, 30.0, 21.9, 14.3. IR (neat): 3259, 3077, 2940, 1535, 1446 cm^{-1}. HRMS (ESI-TOF) m/z: $[M + H - N_2]^+$ calcd for $C_{15}H_{20}NO_2$: 246.1494, found: 246.1494.

Crystal data: $C_{15}H_{19}NO_2$, M = 245, Orthorhombic, space group P2(1)2(1)2(1) with a = 4.6957(2) Å, b = 12.4256(6) Å, c = 22.8195(10) Å, α = 90°, β = 90°, γ = 90°, V = 1331.45(10), T = 100K, R1 = 0.0341, wR2 = 0.1028 on observed data, z = 4, F(000)= 528, Absorption coefficient = 0.081, λ= 0.71073 Å, 24521 reflections were collected on a Brucker APEX-III, 3142 observed reflections (I≥2σ (I)).

3-((1-hydroxypropan-2-yl)amino)cyclohex-2-en-1-one ***(141b)*****:**[198]

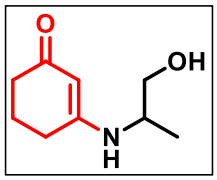

Prepared according to the general procedure (**B**), using (S)-2-aminopropan-1-ol (37 mg, 0.50 mmol) to afford 3-((1-hydroxypropan-2-yl)amino)cyclohex-2-en-1-one **141b** (80 mg, 95%) as a dark brown semisolid. ^{1}H NMR (400 MHz, DMSO-d_6) δ 6.81 (s, 1H), 4.84 (s, 1H), 3.25 (m, 2H), 2.88 (s, 1H), 2.72 (s, 1H), 2.29 (t, *J* = 6.0 Hz, 2H), 2.05 (t, *J* = 6.2 Hz, 2H), 1.76 (m, 2H), 1.06 (d, *J* = 6.3 Hz, 3H). ^{13}C NMR (100 MHz, DMSO-d_6) δ 194.5, 164.0, 94.7, 63.6, 49.5, 36.5,

28.8, 21.7, 16.6. IR (neat): 3253, 3093, 2941, 1518, 1379 cm^{-1}. HRMS (ESI-TOF) m/z: $[M + H]^+$ calcd for $C_9H_{16}NO_2$: 170.1181, found: 170.1187.

3-((1-hydroxy-4-(methylthio)butan-2-yl)amino)cyclohex-2-en-1-one ***(141f)*****:**

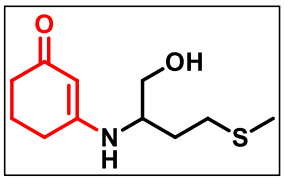

Prepared according to the general procedure (**B**), using (S)-(−)-2-Amino-4-methylthio-1-butanol (67.0 mg, 0.50 mmol) to afford 3-((1-hydroxy-4-(methylthio)butan-2-yl)amino)cyclohex-2-en-1-one **141f** (88.0 mg, 77%) as a brown semisolid. ^{1}H NMR (400 MHz, DMSO-d_6) δ 6.80 (d, *J* = 7.52 Hz, 1H), 4.89 (s, 1H), 4.85 (s, 1H), 3.33 (m, 4H), 2.41 (m, 2H), 2.31 (m, 2H), 2.06 (t, *J* = 6.12 Hz, 2H), 2.03 (s, 3H), 1.77 (m, 2H), 1.64 (m, 1H). ^{13}C NMR (100 MHz, DMSO-d_6) δ 194.6, 164.6, 94.7, 62.0, 52.9, 36.5, 30.2, 30.0, 28.8, 21.7, 14.7. IR (neat): 3353, 3058, 2926, 1650, 1012 cm^{-1}. HRMS (ESI-TOF) m/z: $[M + H]^+$ calcd for $C_{11}H_{20}NO_2S$: 230.1215, found: 230.1222.

3-((1-hydroxy-3-phenylpropan-2-yl)amino)-5-methylcyclohex-2-en-1-one ***(141g)*****:**

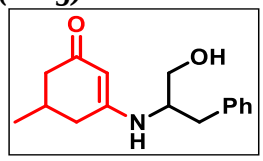

Prepared according to the general procedure (**B**), using (S)-2-amino-3-phenylpropan-1-ol (76.0 mg, 0.50 mmol) to afford 3-((1-hydroxy-3-phenylpropan-2-yl)amino)-5-methylcyclohex-2-en-1-one **141g** (49.0 mg, 37 %) as a dark brown solid. Melting point: 163-166 ºC. Diastereomer ratio % (major/minor): 58: 42. ^{1}H NMR (400 MHz, MeOH-d_4) δ 7.29 – 7.16 (m, 10.26 H), 3.78 – 3.69 (m, .9H), 3.64 – 3.51 (m, 3.64H), 2.96 (dd, *J* = 13.8, 5.8 Hz, 2H), 2.80 – 2.71 (m, 1.7H), 2.46 – 1.88 (m, 9.8H), diastereomer 2: 1.03 (d, *J* = 5.9 Hz, 2.19H), diastereomer 1: 1.00 (d, *J* = 6.0 Hz, 3H). ^{13}C NMR (100 MHz, MeOH-d_4) δ 199.6, 169.2, 139.3, 130.3, 129.5, 127.5, 95.3, 63.5, 57.4, 44.8, 38.3, 37.6, 30.1, 21.1. IR (neat): 3257, 3078, 2928, 1532, 1450 cm^{-1}. HRMS (ESI-TOF) m/z: $[M + H]^+$ calcd for $C_{16}H_{22}NO_2$: 260.1651, found: 260.1664.

3-((1-hydroxy-3-phenylpropan-2-yl)amino)-4,4-dimethylcyclohex-2-en-1-one ***(141m)*****:**

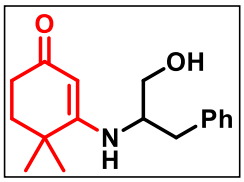

Prepared according to the general procedure (**B**), using (S)-2-amino-3-phenylpropan-1-ol (76.0 mg, 0.50 mmol) to afford 3-((1-hydroxy-3-phenylpropan-2-yl)amino)-4,4-dimethylcyclohex-2-en-1-one **141m** (92.0 mg, 67 %) as a yellowish brown solid. Melting point: 126-131 ºC. ^{1}H NMR

(400 MHz, $CDCl_3$) δ 7.28 (m, 2H), 7.21 (m, 3H), 5.13 (s, 1H), 3.63 (m, 3H), 2.92 (d, *J* = 7.0 Hz, 2H), 2.34 (s, 2H), 1.75 (s, 2H), 1.09 (s, 6H). ^{13}C NMR (100 MHz, DMSO-d_6) δ 195.6, 158.1, 129.9, 120.8, 119.9, 118.0, 85.1, 53.9, 47.8, 30.8, 28.3, 27.3, 17.7, 16.1. IR (neat): 3271, 2927, 1534, 1458 cm^{-1}. HRMS (ESI-TOF) m/z: $[M + H]^+$ calcd for $C_{17}H_{24}NO_2$: 274.1807, found: 274.1815.

3-((1-hydroxypropan-2-yl)amino)-4,4-dimethylcyclohex-2-en-1-one ***(141n)*****:**

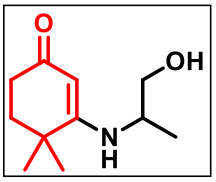

Prepared according to the general procedure (**B**), using (S)-2-aminopropan-1-ol (37.0 mg, 0.50 mmol) to afford 3-((1-hydroxypropan-2-yl)amino)-4,4-dimethylcyclohex-2-en-1-one **141n** (66.0 mg, 67%) as a brown solid. Melting point: 100-103 ºC. ^1H NMR (400 MHz, DMSO-d_6) δ 6.66 (s, 1H), 4.79 (s, 1H), 4.73 (s, 1H), 3.39 (m, 2H), 3.24 (m, 1H), 2.32 (t, *J* = 6.2 Hz, 2H), 1.64 (t, *J* = 6.2 Hz, 2H), 1.06 (d, *J* = 6.4 Hz, 3H), 0.95 (s, 6H). ^{13}C NMR (100 MHz, DMSO-d_6) δ 199.4, 162.5, 93.3, 63.8, 49.7, 35.5, 25.8, 25.3, 16.8. IR (neat): 3302, 2927, 1525, 1457 cm^{-1}. HRMS (ESI-TOF) m/z: $[M + H]^+$ calcd for $C_{11}H_{20}NO_2$: 198.1494, found: 198.1503.

3-((1-hydroxy-4-(methylthio)butan-2-yl)amino)-4,4-dimethylcyclohex-2-en-1-one ***(141r)*****:**

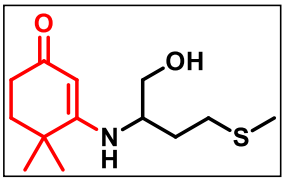

Prepared according to the general procedure (**B**), using (S)-(−)-2-Amino-4-methylthio-1-butanol (67.0 mg, 0.50 mmol) to afford 3-((1-hydroxy-4-(methylthio)butan-2-yl)amino)-4,4-dimethylcyclohex-2-en-1-one **141r** (105.0 mg, 82%) as a pale brown semisolid. ^1H NMR (400 MHz, DMSO-d_6) δ 6.66 (d, *J* = 7.0 Hz, 1H), 4.83 (s, 1H), 4.78 (s, 1H), 3.41 (d, *J* = 8.9 Hz, 2H), 3.30 (m, 2H), 2.39 (m, 4H), 2.02 (s, 3H), 1.87 (m, 1H), 1.64 (t, *J* = 6.2 Hz, 2H), 0.95 (s, 6H). ^{13}C NMR (100 MHz, DMSO-d_6) δ 199.4, 162.9, 93.2, 62.1, 52.9, 38.7, 35.4, 30.3, 30.0, 25.7, 25.1, 14.7. IR (neat): 3358, 2926, 1631, 1443 cm^{-1}. HRMS (ESI-TOF) m/z: $[M + H]^+$ calcd for $C_{13}H_{24}NO_2S$: 258.1528, found: 258.1235.

3-((1-hydroxypropan-2-yl)amino)-5,5-dimethylcyclohex-2-en-1-one ***(141t)*****:**

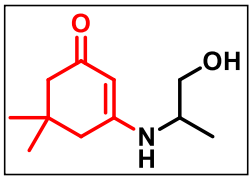

Prepared according to the general procedure (**B**), using (S)-2-aminopropan-1-ol (37.0 mg, 0.50 mmol) to 3-((1-hydroxypropan-2-yl)amino)-5,5-dimethylcyclohex-2-en-1-one **141t** (88.0 mg, 90%) as a yellowish brown solid. Melting point: 142-146 °C. ^{1}H NMR (400 MHz, DMSO-d_6) δ 6.70 (s, 1H), 4.84 (s, 1H), 4.75 (t, *J* = 4.8 Hz,1H), 3.39 (m, 2H), 3.24 (m, 1H), 2.16 (s, 2H), 1.94 (s, 2H), 1.07 (d, *J* = 6.2 Hz, 3H), 0.95 (s, 6H). ^{13}C NMR (100 MHz, DMSO-d_6) δ 193.8, 162.2, 93.4, 63.6, 50.3, 49.5, 42.3, 32.2, 28.0, 27.9, 16.6. IR (neat): 3251, 3076, 2940, 1521, 1376 cm^{-1}. HRMS (ESI-TOF) m/z: $[M + H]^+$ calcd for $C_{11}H_{20}NO_2$: 198.1494, found: 198.1502.

3,4-dihydroacridin-1(2H)-one ***(143a)*****:**[206]

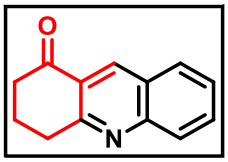

Prepared according to the general procedure (**D**), using (2-aminophenyl)methanol (61.0 mg, 0.50 mmol) to afford 3,4-dihydroacridin-1(2*H*)-one **143a** (56.0 mg, 57%) as a brown solid. Melting point: 96-101 °C. ^{1}H NMR (400 MHz, $CDCl_3$) δ 8.83 (s, 1H), 8.03 (d, *J* = 8.5 Hz, 1H), 7.91 (d, *J* = 7.4 Hz, 1H), 7.79 (t, *J* = 8.6 Hz, 1H), 7.53 (t, *J* = 7.0 Hz, 1H), 3.30 (t, *J* = 6.0 Hz, 2H), 2.79 (m, 2H), 2.26 (m, 2H). ^{13}C NMR (100 MHz, $CDCl_3$) δ 198.0, 162.1, 149.8, 137.2, 132.5, 129.9, 128.7, 126.9, 126.8, 126.4, 39.2, 33.6, 21.9. IR (neat): 2939, 1688, 1595, 1500, 755 cm^{-1}. HRMS (ESI-TOF) m/z: $[M + H]^+$ calcd for $C_{13}H_{12}NO$: 198.0919, found: 198.0924. Crystal data: $C_{13}H_{11}NO$, M = 197, Monoclinic, space group P 21/c with a = 8.1821(13) Å, b = 9.5096(18) Å, c = 12.598(2) Å, α = 90°, β = 99.337(5)°, γ = 90°, V = 967.2(3) , T = 100K, R1 = 0.0399, wR2 = 0.1157 on observed data, z = 4, F(000)= 416, Absorption coefficient = 0.086, λ= 0.71073 Å, 14102 reflections were collected on a Brucker APEX-III, 1591 observed reflections (I≥2σ (I)).

3-methyl-3,4-dihydroacridin-1(2H)-one ***(143b)*****:**

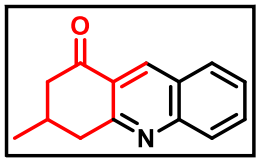

Prepared according to the general procedure (**D**), using (2-aminophenyl)methanol (61.0 mg, 0.50 mmol) to afford 3-methyl-3,4-dihydroacridin-1(2*H*)-one **143b** (65.0 mg, 62%) as a brown solid. Melting point: 94-99 °C. ^{1}H NMR (400 MHz, $CDCl_3$) δ 8.83 (s, 1H), 8.04 (d, *J* = 8.5 Hz, 1H), 7.93 (d, *J* =

8.2 Hz, 1H), 7.80 (m, 1H), 7.55 (t, *J* = 7.1 Hz, 1H), 3.39 (dd, *J* = 14.9, 3.2 Hz, 1H), 3.00 (dd, *J* = 16.8, 10.6 Hz, 1H), 2.87 (m, 1H), 2.48 (m, 2H), 1.23 (d, *J* = 6.2 Hz, 3H). ^{13}C NMR (100 MHz, $CDCl_3$) δ 198.1, 161.5, 149.9, 137.0, 132.4, 129.9, 128.7, 126.9, 125.9, 47.2, 41.8, 29.2, 21.4. IR (neat): 2947, 1689, 1599, 1506, 756 cm^{-1}. HRMS (ESI-TOF) m/z: $[M + H]^+$ calcd for $C_{14}H_{14}NO$: 212.1075, found: 212.1077.

4,4-dimethyl-3,4-dihydroacridin-1(2H)-one ***(143c)*****:**

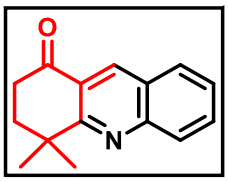

Prepared according to the general procedure (**D**), using (2-aminophenyl)methanol (61.0 mg, 0.50 mmol) to afford 4,4-dimethyl-3,4-dihydroacridin-1(2*H*)-one **143c** (63.0 mg, 56%) as a brown semisolid. ^{1}H NMR (400 MHz, $CDCl_3$) δ 8.84 (s, 1H), 8.02 (d, *J* = 8.5 Hz, 1H), 7.90 (d, *J* = 8.1 Hz, 1H), 7.77 (t, *J* = 8.2 Hz, 1H), 7.51 (t, *J* = 8.1 Hz, 1H), 3.31 (t, *J* = 6.3 Hz, 2H), 2.09 (t, *J* = 6.5 Hz, 2H), 1.27 (s, 6H). ^{13}C NMR (100 MHz, $CDCl_3$) δ 202.4, 161.3, 149.7, 138.1, 132.3, 129.7, 128.6, 126.9, 126.6, 125.3, 41.9, 35.3, 29.6, 24.4. IR (neat): 3057, 2925, 1687, 1590, 1495, 754 cm^{-1}. HRMS (ESI-TOF) m/z: $[M + H]^+$ calcd for $C_{15}H_{16}NO$: 226.1232, found: 226.1237.

3,3-dimethyl-3,4-dihydroacridin-1(2H)-one ***(143d)*****:**[206]

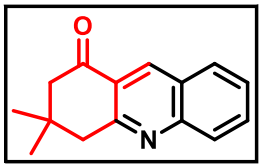

Prepared according to the general procedure (**D**), using (2-aminophenyl)methanol (61.0 mg, 0.50 mmol) to afford 3,3-dimethyl-3,4-dihydroacridin-1(2*H*)-one **143d** (75.0 mg, 67%) as a brown solid. Melting point: 105-110 °C. ^{1}H NMR (400 MHz, $CDCl_3$) δ 8.83 (s, 1H), 8.05 (d, *J* = 8.5 Hz, 1H), 7.94 (d, *J* = 8.1 Hz, 1H), 7.80 (t, *J* = 7.2 Hz, 1H), 7.55 (t, *J* = 7.1 Hz, 1H), 3.20 (s, 2H), 2.65 (s, 2H), 1.15 (s, 6H). ^{13}C NMR (100 MHz, $CDCl_3$) δ 198.1, 160.9, 150.2, 136.7, 132.4, 129.9, 128.7, 126.9, 125.4, 52.6, 47.6, 32.9, 28.5. IR (neat): 3050, 2947, 1689, 1513, 1409, 758 cm^{-1}. HRMS (ESI-TOF) m/z: $[M + H]^+$ calcd for $C_{15}H_{16}NO$: 226.1232, found: 226.1238.

3-(4-(dimethylamino)phenyl)-3,4-dihydroacridin-1(2H)-one ***(143e):***

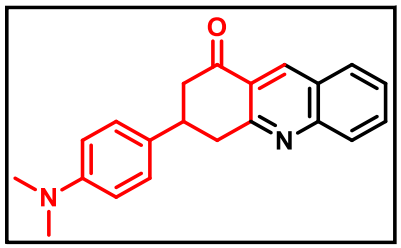

Prepared according to the general procedure **(D)**, using (2-aminophenyl)methanol (43.0 mg, 0.35 mmol) to afford 3-(4-(dimethylamino)phenyl)-3,4-dihydroacridin-1(2*H*)-one **143e** (68.0 mg, 62%) as a brown solid. Melting point: 185-190 °C. ^{1}H NMR (400 MHz, $CDCl_3$) δ 8.88 (s, 1H), 8.07 (d, *J* = 8.5 Hz, 1H), 7.96 (d, *J* = 8.1 Hz, 1H), 7.82 (t, *J* = 7.2 Hz, 1H), 7.57 (t, *J* = 7.5 Hz, 1H), 7.21 (d, *J* = 8.6 Hz, 2H), 6.75 (d, *J* = 8.7 Hz, 2H), 3.60 (m, 1H), 3.50 (m, 2H), 3.09 (m, 1H), 2.94 (s, 6H), 2.92 (m, 1H). ^{13}C NMR (100 MHz, $CDCl_3$) δ 197.9, 161.5, 150.1, 149.8, 137.1, 132.5, 130.7, 129.9, 128.8, 127.5, 126.9, 125.9, 113.0, 46.6, 41.5, 40.8, 38.6, 29.8. IR (neat): 3052, 1687, 1590, 1497 cm^{-1}. HRMS (ESI-TOF) m/z: $[M + H]^+$ calcd for $C_{21}H_{21}N_2O$: 317.1654, found: 317.1644.

2,3-dihydro-1H-cyclopenta[b]quinolin-1-one ***(143f):***[207]

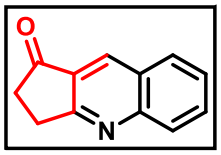

Prepared according to the general procedure **(D)**, using (2-aminophenyl)methanol (62.0 mg, 0.50 mmol) to afford 2,3-dihydro-1*H*-cyclopenta[*b*]quinolin-1-one **143f** (40.0 mg, 44%) as a black solid. Melting point: 145-147 °C. ^{1}H NMR (400 MHz, $CDCl_3$) δ 8.58 (s, 1H), 8.14 (d, *J* = 8.6 Hz, 1H), 7.98 (d, *J* = 8.2 Hz, 1H), 7.86 (t, *J* = 7.7 Hz, 1H), 7.60 (t, *J* = 7.6 Hz, 1H), 3.46 (t, *J* = 6 Hz, 2H), 2.91 (t, *J* = 6 Hz, 2H). ^{13}C NMR (100 MHz, $CDCl_3$) δ 205.0, 171.1, 151.8, 133.7, 132.9, 130.6, 129.1, 127.9, 127.0, 36.4, 29.0. IR (neat): 2922, 2852, 1700, 1623, 1585, 1493 cm^{-1}. HRMS (ESI-TOF) m/z: $[M + H]^+$ calcd for $C_{12}H_{10}NO$: 184.0762, found: 184.0761.

1,3-dimethylpyrimido[4,5-b]quinoline-2,4(1H,3H)-dione ***(143g):***[208]

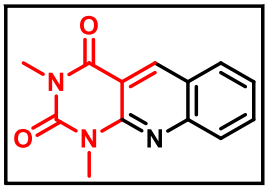

Prepared according to the general procedure **(D)**, using (2-aminophenyl)methanol (62.0 mg, 0.50 mmol) to afford 1,3-dimethylpyrimido[4,5-*b*]quinoline-2,4(1*H*,3*H*)-dione **143g** (45.0 mg, 38%) as a black solid. Melting point: 197-199 °C. ^{1}H NMR (400 MHz, $CDCl_3$) δ 8.96 (s, 1H), 7.94 (dd, *J* = 22.0, 8.4 Hz, 2H), 7.81 (m, 1H), 7.50(m, 1H), 3.80 (s, 3H), 3.51 (s, 3H). ^{13}C NMR (100 MHz, $CDCl_3$) δ 161.5, 151.7, 149.9, 148.5, 140.1, 133.2, 129.3, 128.2, 125.9,

124.8, 110.9, 29.7, 28.6. IR (neat): 3055, 2920, 1704, 1659, 1616, 1496, 1468, 1421 cm^{-1}. HRMS (ESI-TOF) m/z: $[M + H]^+$ calcd for $C_{13}H_{12}N_3O_2$: 242.0930, found: 242.0937.

9-methyl-3,4-dihydroacridin-1(2H)-one ***(143h):***[209]

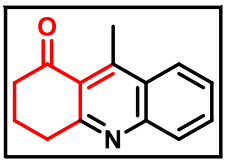

Prepared according to the general procedure **(D)**, using 1-(2-aminophenyl)ethan-1-ol (68.0 mg, 0.50 mmol) to afford 9-methyl-3,4-dihydroacridin-1(2*H*)-one **143h** (45.0 mg, 42%) as a brown semisolid. ^1H NMR (400 MHz, $CDCl_3$) δ 8.19 (d, *J* = 8.5 Hz, 1H), 8.01 (d, *J* = 8.4 Hz, 1H), 7.76 (m, 1H), 7.55 (m, 1H), 3.27 (m, 2H), 3.03 (s, 3H), 2.79 (t, *J* = 6.6 Hz, 2H), 2.19 (m, 2H). ^{13}C NMR (100 MHz, $CDCl_3$) δ 200.7, 162.2, 131.7, 129.1, 127.8, 126.5, 125.6, 116.7, 41.2, 34.7, 21.4, 16.2. IR (neat): 2930, 2853, 1679, 1613, 1563 cm^{-1}. HRMS (ESI-TOF) m/z: $[M + H]^+$ calcd for $C_{14}H_{14}NO$: 212.1075, found: 212.1081.

3,3,9-trimethyl-3,4-dihydroacridin-1(2H)-one ***(143i):***[209]

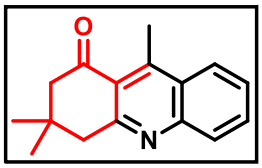

Prepared according to the general procedure **(D)**, using 1-(2-aminophenyl)ethan-1-ol (68.0 mg, 0.50 mmol) to afford 3,3,9-trimethyl-3,4-dihydroacridin-1(2*H*)-one **143i** (40.0 mg, 34%) as a yellow solid. Melting point: 88-90 °C. ^1H NMR (400 MHz, $CDCl_3$) δ 8.22 (d, *J* = 8.5 Hz, 1H), 8.02 (d, *J* = 8.4 Hz, 1H), 7.77 (t, *J* = 7.6 Hz, 1H), 7.57 (t, *J* = 7.8 Hz, 1H), 3.19 (s, 2H), 3.07 (s, 3H), 2.67 (s, 2H), 1.14 (s, 6H). ^{13}C NMR (100 MHz, $CDCl_3$) δ 200.7, 161.2, 131.7, 129.2, 127.8, 126.6, 125.7, 124.3, 54.9, 48.6, 32.3, 28.4, 16.2. IR (neat): 2928, 2866, 1680, 1562, 1371 cm^{-1}. HRMS (ESI-TOF) m/z: $[M + H]^+$ calcd for $C_{16}H_{18}NO$: 240.1388, found: 240.1398.

6,8-dibromo-3-(4-(dimethylamino)phenyl)-3,4-dihydroacridin-1(2H)-one ***(143j):***

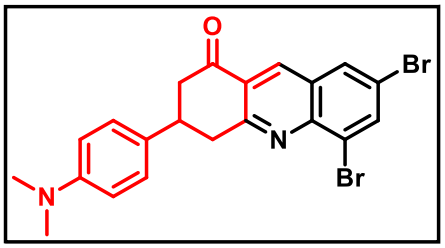

Prepared according to the general procedure **(D)**, using (2-amino-3,5-dibromophenyl)methanol (40.0 mg, 0.14 mmol) to afford 6,8-dibromo-3-(4-(dimethylamino)phenyl)-3,4-dihydroacridin-1(2*H*)-one **143j** (58.0 mg, 68%) as a yellow solid. Melting point: 196-201 °C. ^1H NMR (400 MHz, $CDCl_3$) δ 8.74 (s, 1H), 8.23 (d, *J* = 1.8 Hz, 1H), 8.07 (d, *J* = 2.0 Hz, 1H), 7.19 (t, *J* = 5.8 Hz, 2H),

6.76 (d, *J* = 8.1 Hz, 2H), 3.71 (m, 1H), 3.52 (m, 2H), 3.11 (m, 1H), 2.95 (s, 6H), 2.94 (s, 1H). ^{13}C NMR (100 MHz, $CDCl_3$) δ 197.2, 162.9, 138.4, 136.4, 131.4, 128.7, 127.4, 126.9, 125.4, 119.9, 113.0, 46.5, 41.5, 40.8, 38.3. IR (neat): 2952, 2800, 1692, 1600, 1582, 1522, 1458 cm^{-1}. HRMS (ESI-TOF) m/z: $[M + H]^+$ calcd for $C_{21}H_{19}Br_2N_2O$: 472.9864, found: 472.9856.

6,8-dibromo-9-methyl-2,3-dihydro-1H-cyclopenta[b]quinolin-1-one ***(143k):***

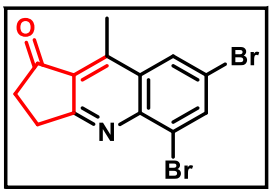

Prepared according to the general procedure **(D)**, using 1-(2-amino-4,6-dibromophenyl)ethan-1-ol (146.0 mg, 0.5 mmol) to afford 6,8-dibromo-9-methyl-2,3-dihydro-1*H*-cyclopenta[*b*]quinolin-1-one **143j** (60.0 mg, 34%) as a light purple solid. Melting point: 219-220 °C. ^{1}H NMR (400 MHz, $CDCl_3$) δ 8.30 (d, *J* = 2.1 Hz, 1H), 8.25 (d, *J* = 2.1 Hz, 1H), 3.43 (m, 2H), 3.05 (s, 3H), 2.89 (m, 2H). ^{13}C NMR (100 MHz, $CDCl_3$) δ 205.9, 172.2, 147.6, 138.2, 134.6, 130.6, 129.5, 127.8, 126.0, 119.8, 36.8, 28.6, 12.8. IR (neat): 2921, 2851, 1600 cm^{-1}. HRMS (ESI-TOF) m/z: $[M + H]^+$ calcd for $C_{13}H_{10}Br_2NO$: 353.9129, found: 353.9130.

1,3,5-trimethylpyrimido[4,5-b]quinoline-2,4(1H,3H)-dione ***(143l):***[209]

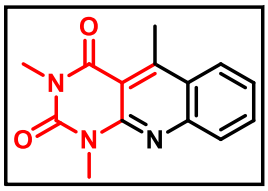

Prepared according to the general procedure **(D)**, using 1-(2-aminophenyl)ethan-1-ol (68 mg, 0.50 mmol) to afford 1,3,5-trimethylpyrimido[4,5-*b*]quinoline-2,4(1*H*,3*H*)-dione **143j** (60 mg, 47%) as a white solid. Melting point: 221-223 °C. ^{1}H NMR (400 MHz, $CDCl_3$) δ 8.15 (s, 1H), 7.91 (s, 1H), 7.76 (t, *J* = 7.5 Hz, 1H), 7.50 (t, *J* = 7.5 Hz, 1H), 3.78 (s, 3H), 3.47 (s, 3H), 3.23 (s, 3H). ^{13}C NMR δ 162.3, 153.9, 151.3, 148.6, 148.1, 132.5, 128.7, 125.3, 108.7, 30.0, 28.5, 16.1. IR (neat): 2923, 2852, 1661, 1579 cm^{-1}. HRMS (ESI-TOF) m/z: $[M + H]^+$ calcd for $C_{14}H_{14}N_3O_2$: 256.1086, found: 256.1087.

3-((2-(hydroxymethyl)phenyl)amino)cyclohex-2-en-1-one ***(144a)*****:**

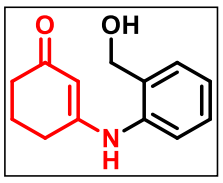

Prepared according to the general procedure (**B**), using (2-aminophenyl)methanol (61.0 mg, 0.50 mmol) to afford 3-((2-(hydroxymethyl)phenyl)amino)cyclohex-2-en-1-one **144a** (101.0 mg, 92%) as a yellow solid. Melting point: 163-167 °C. ^{1}H NMR (400 MHz, MeOH-d_4) δ 7.55

(m, 1H), 7.34 (m, 2H), 7.21 (m, 1H), 4.98 (s, 1H), 4.57 (s, 2H), 2.63 (t, *J* = 6.2 Hz, 2H), 2.32 (t, *J* = 6.4 Hz, 2H), 2.01 (m, 2H). ^{13}C NMR (100 MHz, MeOH-d_4) δ 200.8, 169.3, 138.9, 136.8, 129.5, 129.3, 128.6, 128.1, 98.3, 61.4, 36.8, 29.7, 22.9. IR (neat): 3841, 3741, 3613, 1696, 1520 cm^{-1}. HRMS (ESI-TOF) m/z: $[M + H]^+$ calcd for $C_{13}H_{16}NO_2$: 218.1181, found: 218.1184.

3-((2-(hydroxymethyl)phenyl)amino)-5-methylcyclohex-2-en-1-one ***(144b)*****:**

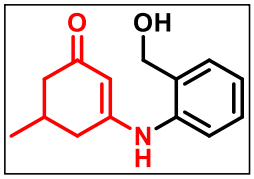

Prepared according to the general procedure (**B**), using (2-aminophenyl)methanol (61.0 mg, 0.50 mmol) to afford 3-((2-(hydroxymethyl)phenyl)amino)-5-methylcyclohex-2-en-1-one **144b** (94.0 mg, 82%) as a yellow solid. Melting point: 168-170 °C. ^{1}H NMR (400 MHz, MeOH-d_4) δ 7.54 (m, 1H), 7.33 (m, 2H), 7.21 (m, 1H), 4.97 (s, 1H), 4.57 (s, 2H), 2.61 (m, 1H), 2.36 (m, 2H), 2.24 (m, 1H), 2.07 (m, 1H), 1.12 (d, *J* = 6.5 Hz, 3H). ^{13}C NMR (100 MHz, MeOH-d_4) δ 200.6, 168.7, 138.8, 136.8, 129.5, 129.3, 128.6, 128.0, 97.9, 61.4, 45.0, 37.7, 30.7, 21.1. IR (neat): 3843, 3741, 3615, 1690, 1525 cm^{-1}. HRMS (ESI-TOF) m/z: $[M + H]^+$ calcd for $C_{14}H_{18}NO_2$: 232.1338, found: 232.1345.

3-((2-(hydroxymethyl)phenyl)amino)-4,4-dimethylcyclohex-2-en-1-one ***(144c)*****:**

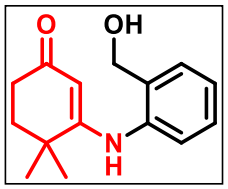

Prepared according to the general procedure (**B**), using (2-aminophenyl)methanol (61.0 mg, 0.50 mmol) to afford 3-((2-(hydroxymethyl)phenyl)amino)-4,4-dimethylcyclohex-2-en-1-one **144c** (98.0 mg, 80%) as a white solid. Melting point: 128-132 °C.^{1}H NMR (400 MHz, MeOH-d_4) δ 7.53 (dd, *J* = 8.1, 5.6 Hz, 1H), 7.32 (m, 2H), 7.22 (m, 1H), 4.57 (s, 2H), 2.65 (t, *J* = 6.3 Hz, 2H), 1.88 (t, *J* = 6.3 Hz, 2H), 1.12 (s, 6H). ^{13}C NMR (100 MHz, MeOH-d_4) δ 205.9, 166.9, 138.7, 137.1, 129.5, 129.3, 128.3, 127.9, 97.1, 61.5, 40.5, 36.8, 26.7, 25.4. IR (neat): 3841, 3739, 3614, 1694, 1523 cm^{-1}. HRMS (ESI-TOF) m/z: $[M + H]^+$ calcd for $C_{15}H_{20}NO_2$: 246.1494, found: 246.1497.

3-((2-(hydroxymethyl)phenyl)amino)-5,5-dimethylcyclohex-2-en-1-one ***(144d)*****:**

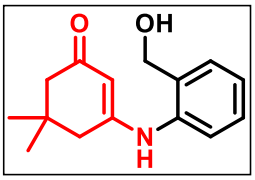

Prepared according to the general procedure (**B**), using (2-aminophenyl)methanol (61.0 mg, 0.50 mmol) to afford 3-((2-(hydroxymethyl)phenyl)amino)-5,5-dimethylcyclohex-2-en-1-one **144d** (104.0 mg, 85%) as a yellow solid. Melting point: 177-182 ºC. ^{1}H NMR (400 MHz, MeOH-d_4) δ 7.56 (m, 1H), 7.35 (m, 2H), 7.20 (m, 1H), 4.95 (s, 1H), 4.58 (s, 2H), 2.49 (s, 2H), 2.20 (s, 2H), 1.13 (s, 6H). ^{13}C NMR (100 MHz, MeOH-d_4) δ 198.7, 166.4, 137.5, 135.4, 127.9, 127.3, 126.7, 95.7, 59.9, 49.2, 41.9, 32.5, 26.9. IR (neat): 3842, 3740, 3615, 1694, 1523 cm^{-1}. HRMS (ESI-TOF) m/z: $[M + H]^+$ calcd for $C_{15}H_{20}NO_2$: 246.1494, found: 246.1496.

3-ethyl-2-methyl-1,5,6,7-tetrahydro-4H-indol-4-one ***(145a)*****:**[210]

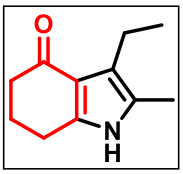

Prepared according to the general procedure (**F**), using 2-methyl-1,5,6,7-tetrahydro-4*H*-indol-4-one (25.0 mg, 0.17 mmol) to afford 3-ethyl-2-methyl-1,5,6,7-tetrahydro-4*H*-indol-4-one **145a** (18.0 mg, 61%) as a white solid. Melting point: 191-196 ºC. ^{1}H NMR (400 MHz, $CDCl_3$) δ 8.53 (s, 1H), 2.74 (t, *J* = 6.2 Hz, 2H), 2.65 (q, *J* = 14.9, 7.4 Hz, 2H), 2.43 (t, *J* = 5.9 Hz, 2H), 2.15 (s, 3H), 2.09 (m, 2H), 1.12 (t, *J* = 7.4 Hz, 3H). ^{13}C NMR (100 MHz, $CDCl_3$) δ 195.1, 142.3, 123.9, 120.8, 118.4, 38.9, 24.1, 23.1, 18.2, 15.6, 10.4. IR (neat): 3227, 3187, 2956, 2854, 1623, 1469 cm^{-1}. HRMS (ESI-TOF) m/z: $[M + H]^+$ calcd for $C_{11}H_{16}NO$: 178.1232, found: 178.1236.

3-hexyl-2-methyl-1,5,6,7-tetrahydro-4H-indol-4-one ***(145b)*****:**

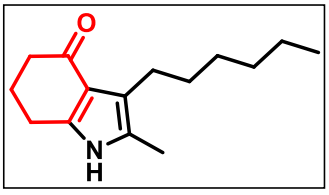

Prepared according to the general procedure (**E**), using 2-methyl-1,5,6,7-tetrahydro-4*H*-indol-4-one (50.0 mg, 0.34 mmol) to afford 3-hexyl-2-methyl-1,5,6,7-tetrahydro-4*H*-indol-4-one **145b** (37.0 mg, 48%) as a white solid. Melting point: 93-98 ºC. ^{1}H NMR (400 MHz, $CDCl_3$) δ 7.88 (s, 1H), 2.73 (t, *J* = 6.2 Hz, 2H), 2.60 (t, *J* = 7.5 Hz, 2H), 2.42 (t, *J* = 5.9 Hz, 2H), 2.13 (s, 3H), 2.09 (m, 2H), 1.61 (s, 2H), 1.50 (m, 2H), 1.29 (m, 4H), 0.86 (t, *J* = 6.7 Hz, 3H). ^{13}C NMR (100 MHz, $CDCl_3$) δ 194.6, 141.7, 123.8, 119.5, 118.7, 38.7, 31.8, 30.9, 29.3, 24.8, 23.9, 23.1, 22.8, 14.2, 10.5. IR (neat): 3222, 3185, 2923, 2853, 1620, 1467 cm^{-1}. HRMS (ESI-TOF) m/z: $[M + H]^+$ calcd for $C_{15}H_{24}NO$: 234.1858, found: 234.1861.

2-benzyl-3-ethyl-1,5,6,7-tetrahydro-4H-indol-4-one ***(145c)*****:**

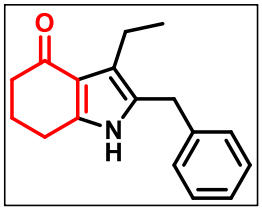

Prepared according to the general procedure (**E**), using 2-benzyl-1,5,6,7-tetrahydro-4*H*-indol-4-one (32.0 mg, 0.14 mmol) to afford 2-benzyl-3-ethyl-1,5,6,7-tetrahydro-4*H*-indol-4-one **145c** (14.0 mg, 40%) as a white solid. Melting point: 150-152 ^{o}C. ^{1}H NMR (400 MHz, $CDCl_3$) δ 7.77 (s, 1H), 7.32 (m, 2H), 7.21 (m, 3H), 3.88 (s, 2H), 2.74 (q, *J* = 14.8, 7.4 Hz, 2H), 2.67 (t, *J* = 6.2 Hz, 2H), 2.42 (t, *J* = 6.9 Hz, 2H), 2.08 (m, 2H), 1.17 (t, *J* = 7.4 Hz, 3H). ^{13}C NMR (100 MHz, $CDCl_3$) δ 194.9, 142.7, 139.2, 128.9, 128.7, 126.8, 126.4, 121.8, 118.6, 38.8, 31.3, 24.0, 23.2, 18.3, 15.9. IR (neat): 3843, 3740, 2926, 1629,1525, 1469 cm^{-1}. HRMS (ESI-TOF) m/z: $[M + H]^+$ calcd for $C_{17}H_{20}NO$: 254.1545, found: 254.1551.

3-(hexylamino)cyclohex-2-en-1-one ***(146)*****:**

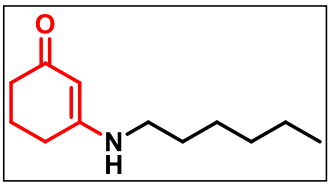

Prepared according to the general procedure (**A**), using hexan-1-amine (54.0 mg, 0.50 mmol) to afford 3-(hexylamino)cyclohex-2-en-1-one **146** (52.0 mg, 53%) as a black semisolid. ^{1}H NMR (400 MHz, $CDCl_3$) δ 5.11 (s, 1H), 4.86 (s, 1H), 3.04 (dd, *J* = 12.4, 6.4 Hz, 2H), 2.31 (m, 4H), 1.93 (m, 2H), 1.56 (m, 2H), 1.31 (m, 6H), 0.87 (t, *J* = 6.3 Hz, 3H). ^{13}C NMR (100 MHz, $CDCl_3$) δ 197.5, 164.9, 96.7, 43.1, 36.4, 31.6, 29.8, 28.6, 26.7, 22.4, 21.7, 14.1. IR (neat): 3842, 3741, 2932, 1696, 1538 cm^{-1}. HRMS (ESI-TOF) m/z: $[M + H]^+$ calcd for $C_{12}H_{22}NO$: 196.1701; found: 196.1703.

5.8.B. Copies of ^{1}H and ^{13}C NMR spectra of representative compound

2-Benzyl-1,5,6,7-tetrahydro-4*H*-indol-4-one (140a)

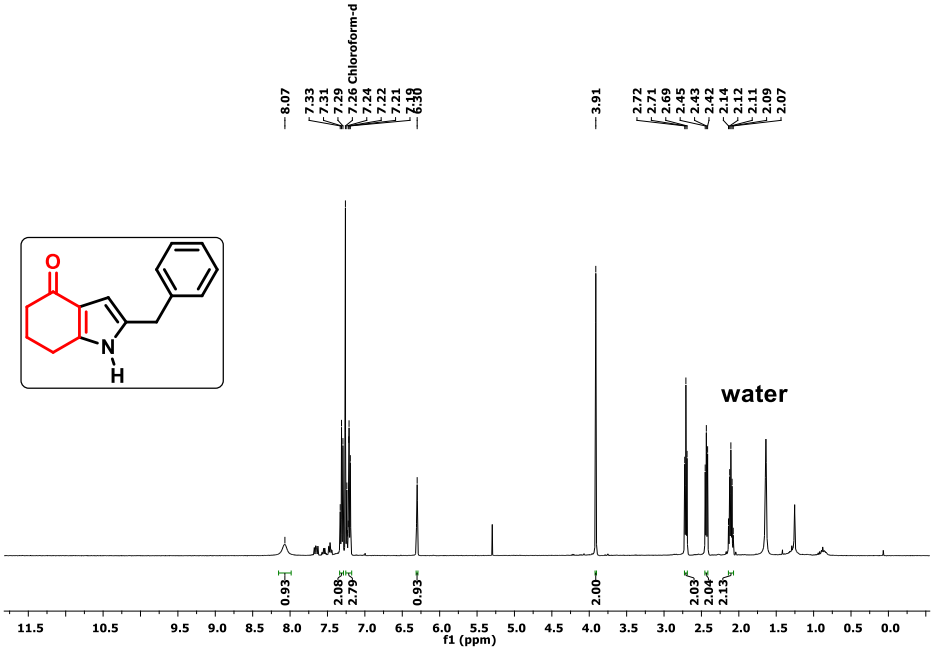

Figure 5.8.B.1: ^{1}H NMR of **140a**, 400 MHz, $CDCl_3$

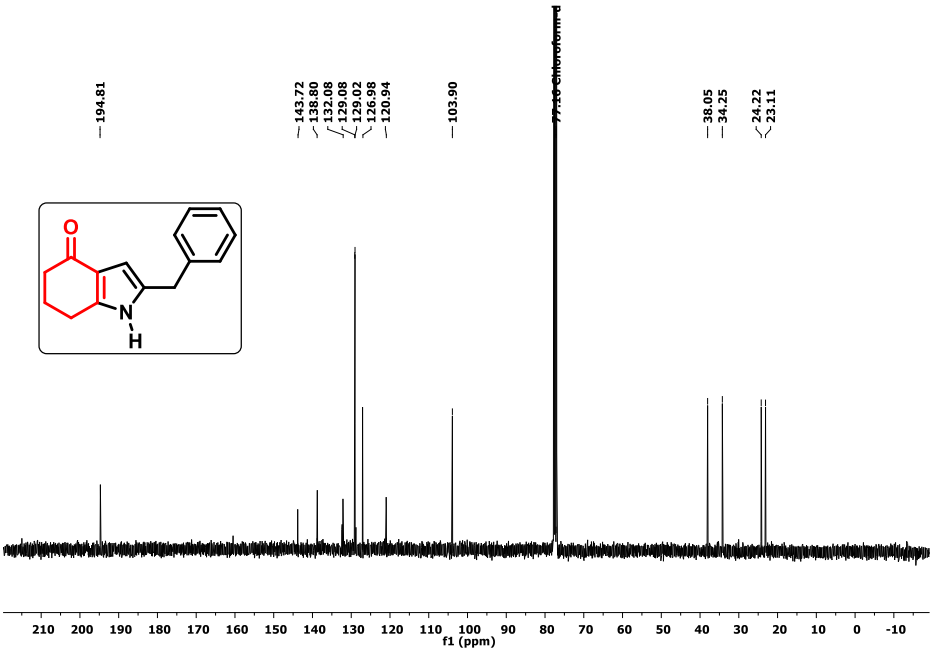

Figure 5.8.B.2: ^{13}C NMR of **140a**, 100 MHz, $CDCl_3$

2-methyl-1,5,6,7-tetrahydro-4*H*-indol-4-one (140b)

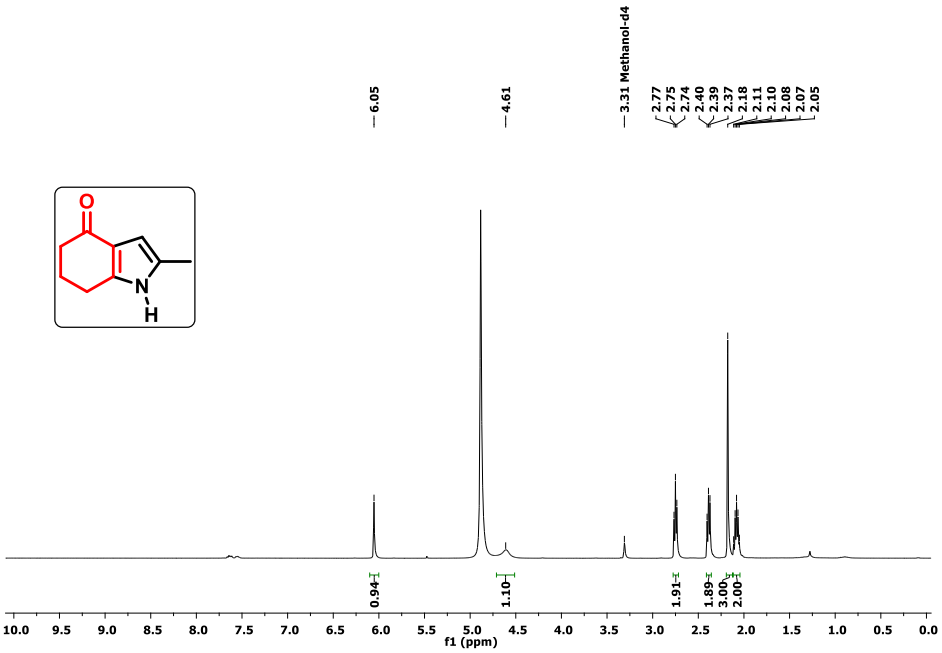

Figure 5.8.B.3: ^{1}H NMR of **140b**, 400 MHz, $CDCl_3$

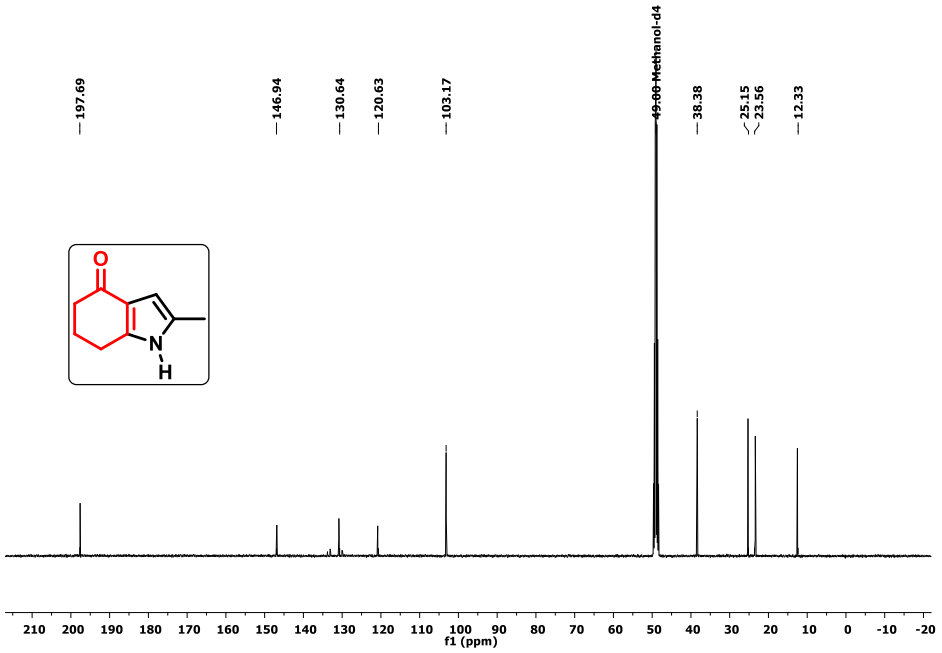

Figure 5.8.B.4: ^{13}C NMR of **140b**, 100 MHz, $CDCl_3$

2-(sec-butyl)-1,5,6,7-tetrahydro-4*H*-indol-4-one (140e)

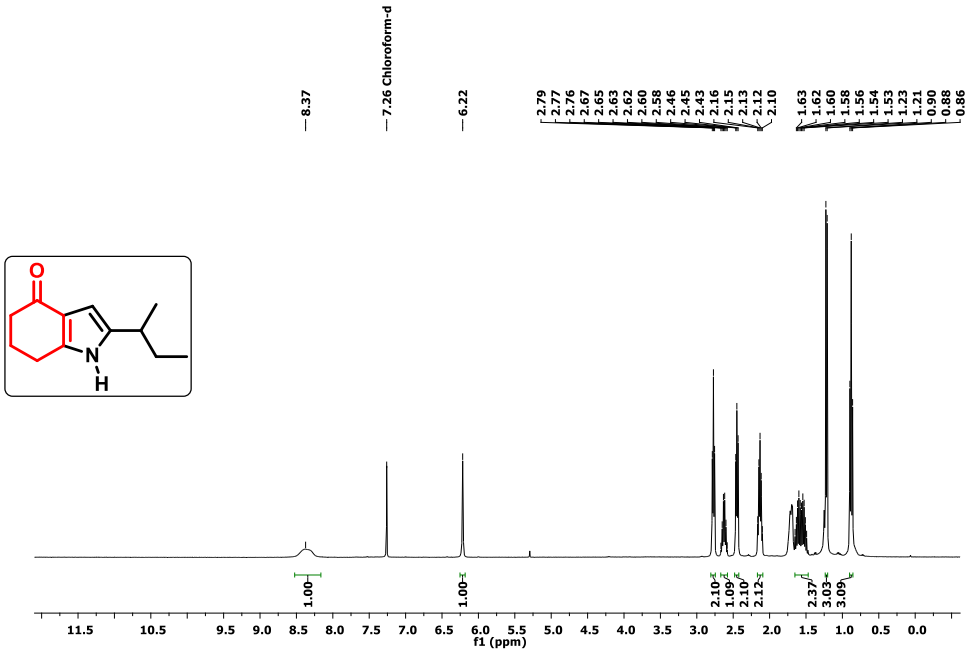

Figure 5.8.B.5: ^{1}H NMR of **140e**, 400 MHz, $CDCl_3$

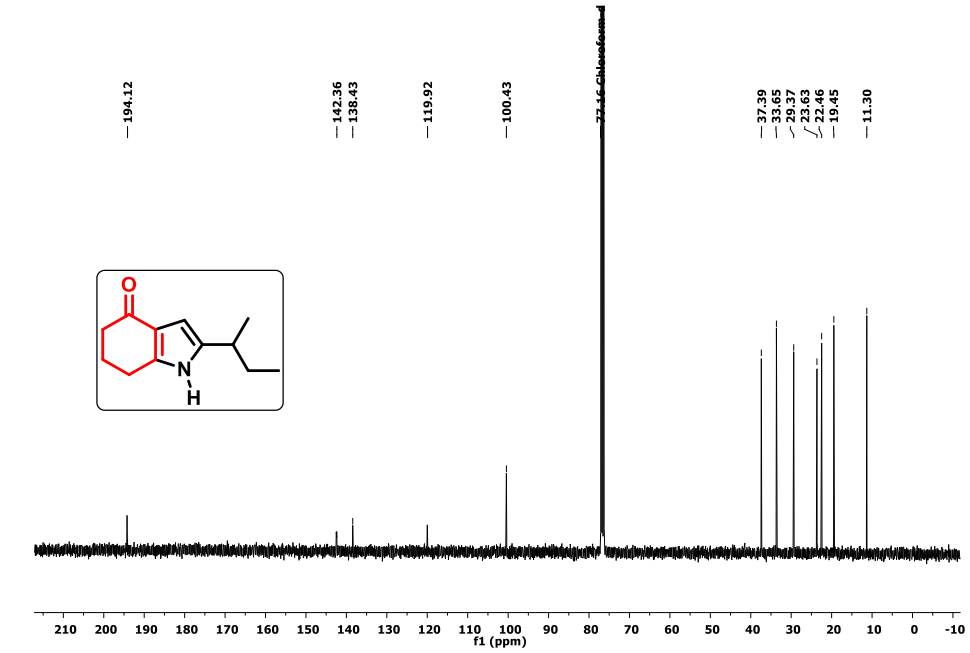

Figure 5.8.B.6: ^{13}C NMR of **140e**, 100 MHz, $CDCl_3$

2-(sec-butyl)-7,7-dimethyl-1,5,6,7-tetrahydro-4*H*-indol-4-one (140q)

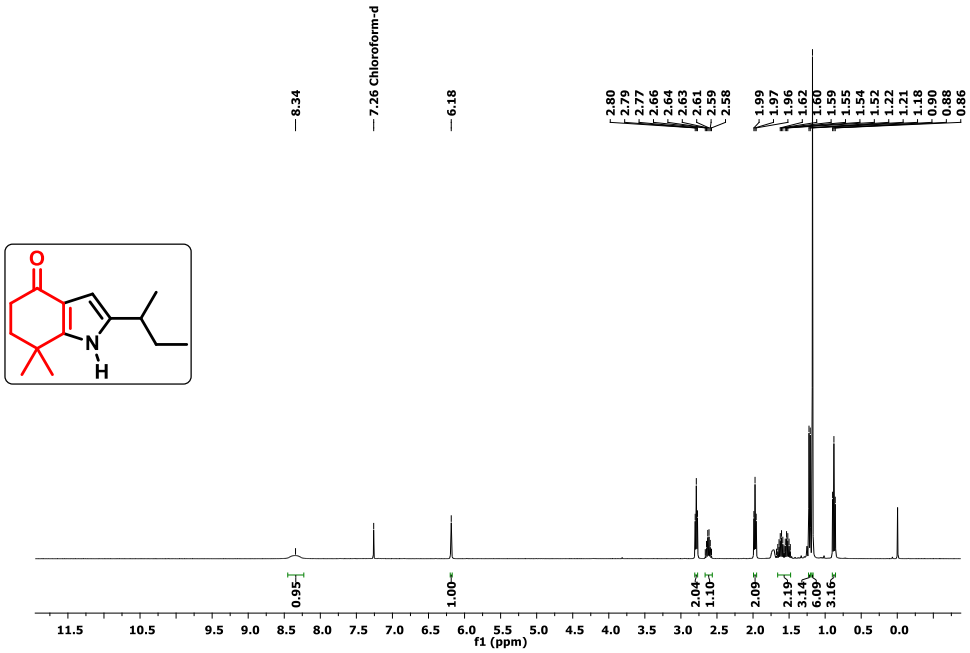

Figure 5.8.B.7: ^{1}H NMR of **140q**, 400 MHz, $CDCl_3$

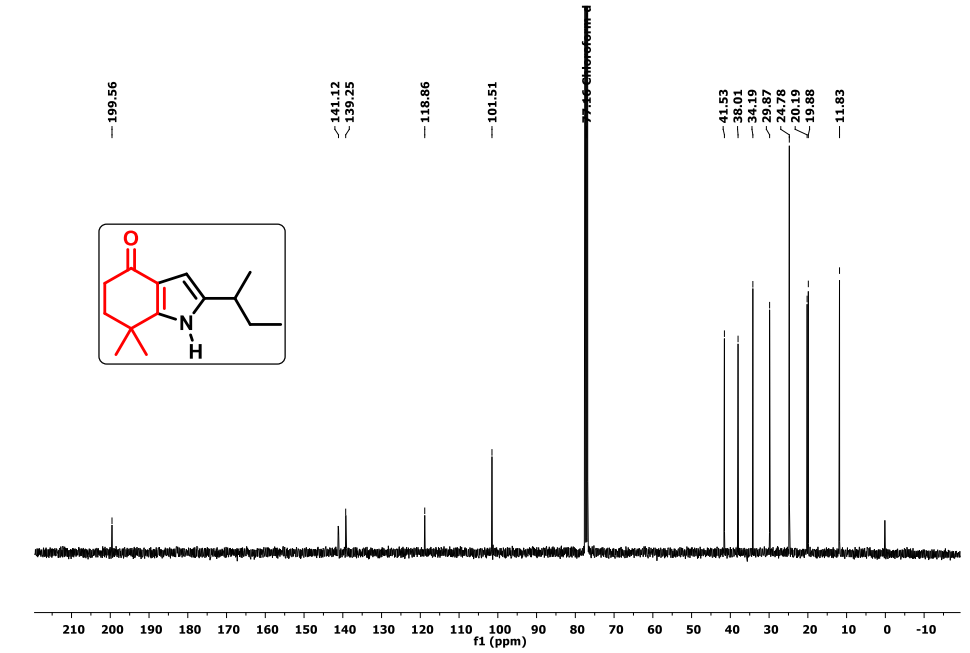

Figure 5.8.B.8: ^{13}C NMR of **140q**, 100 MHz, $CDCl_3$

2-isopropyl-6,6-dimethyl-1,5,6,7-tetrahydro-4*H*-indol-4-one (140v)

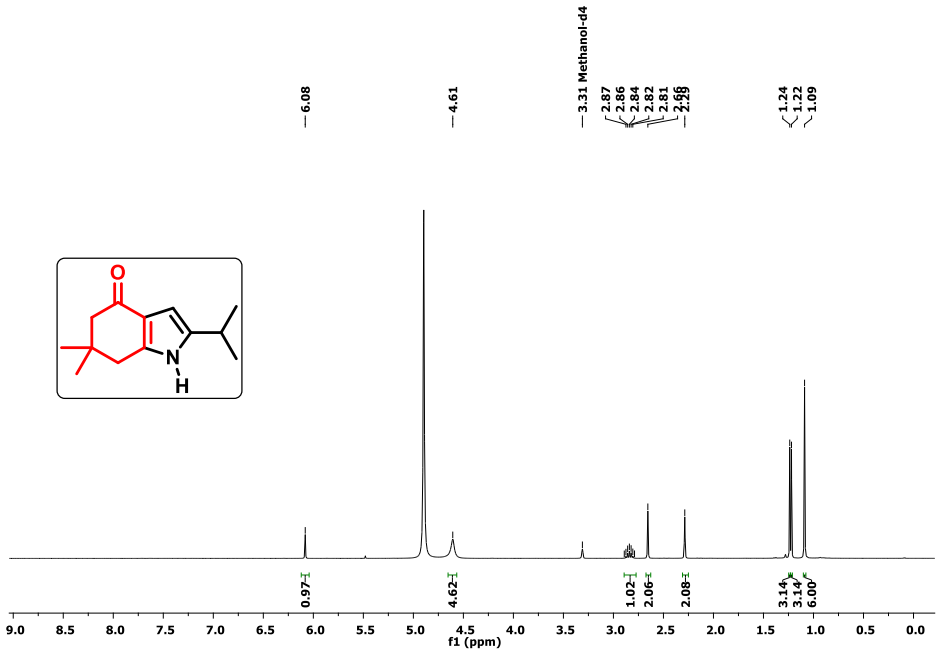

Figure 5.8.B.9: ^{1}H NMR of **140v**, 400 MHz, Methanol-d_4

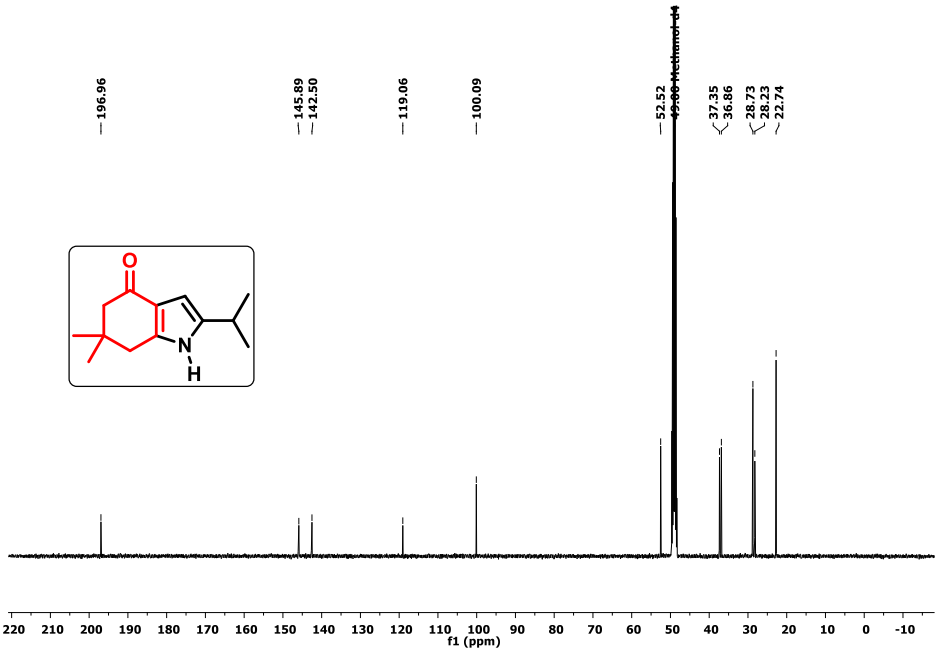

Figure 5.8.B.10: ^{13}C NMR of **140v**, 100 MHz, Methanol-d_4

6,6-dimethyl-1,2,3,5,6,7-hexahydro-8*H*-pyrrolo[1,2-a]indol-8-one (140aa)

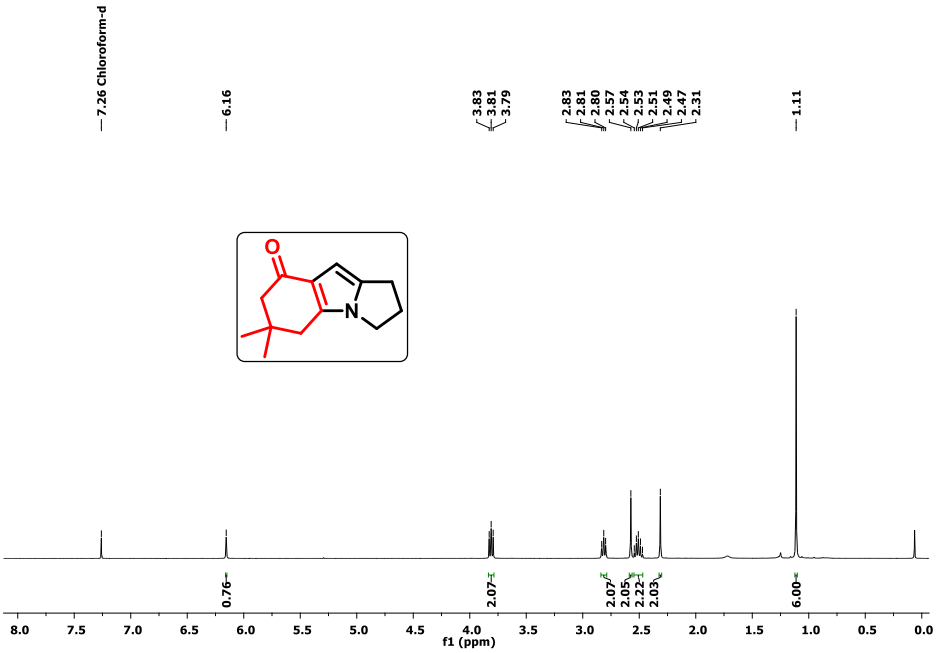

Figure 5.8.B.11: ^{1}H NMR of **140aa**, 400 MHz, $CDCl_3$

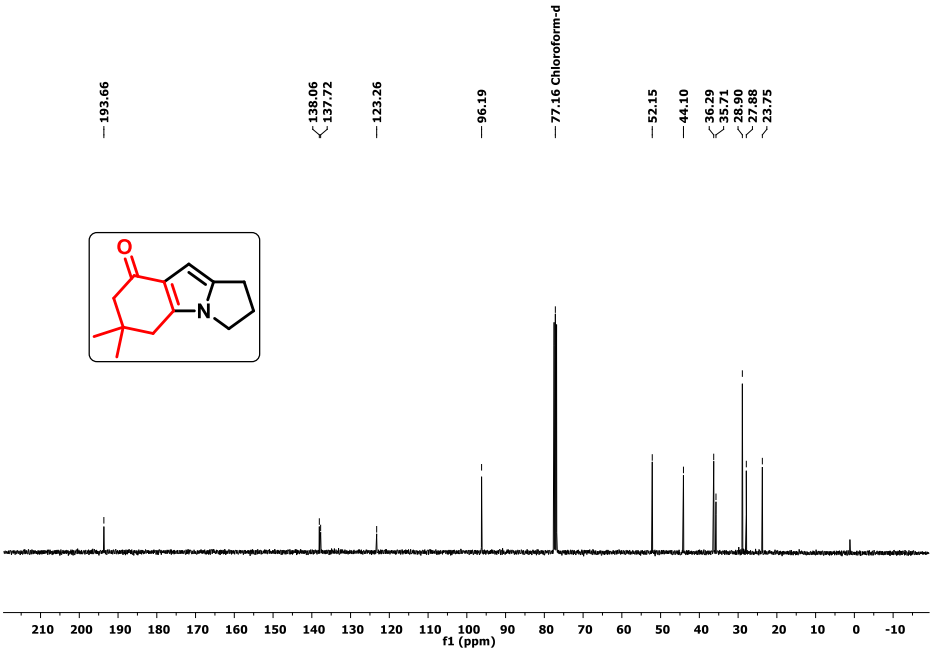

Figure 5.8.B.12: ^{13}C NMR of **140aa**, 100 MHz, $CDCl_3$

(Z)-3-((1-hydroxy-3-methylbutan-2-yl)amino)-1,3-diphenylprop-2-en-1-one (141c')

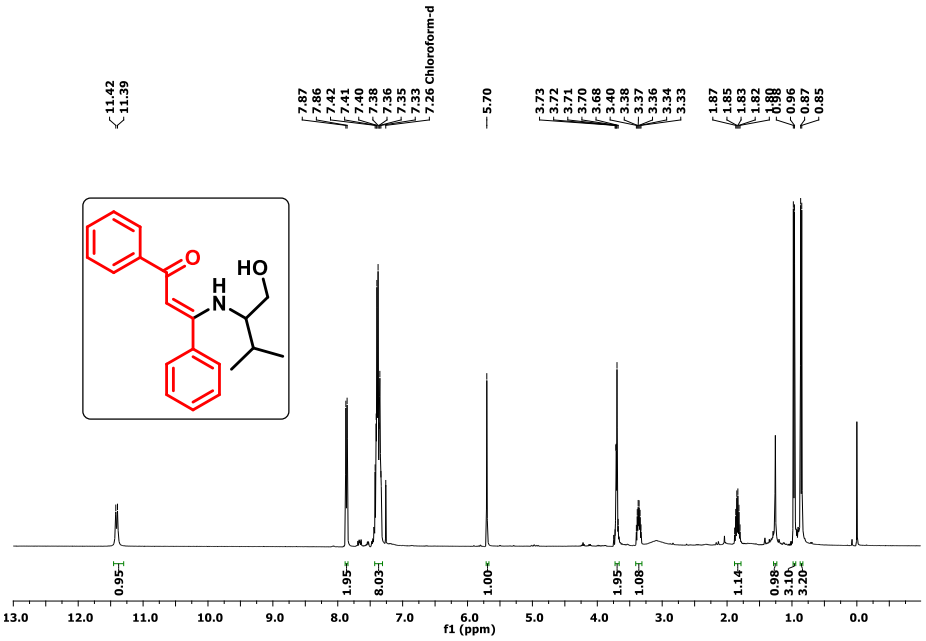

Figure 5.8.B.13: ^{1}H NMR of **141c'**, 400 MHz, $CDCl_3$

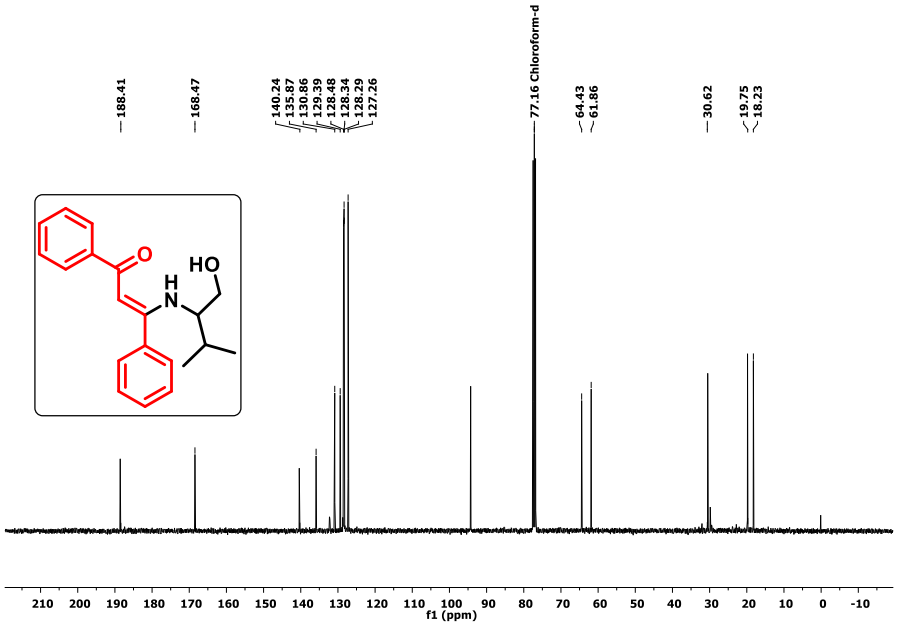

Figure 5.8.B.14: ^{13}C NMR of **141c'**, 100 MHz, $CDCl_3$

3-((1-hydroxypropan-2-yl)amino)-5,5-dimethylcyclohex-2-en-1-one (141t)

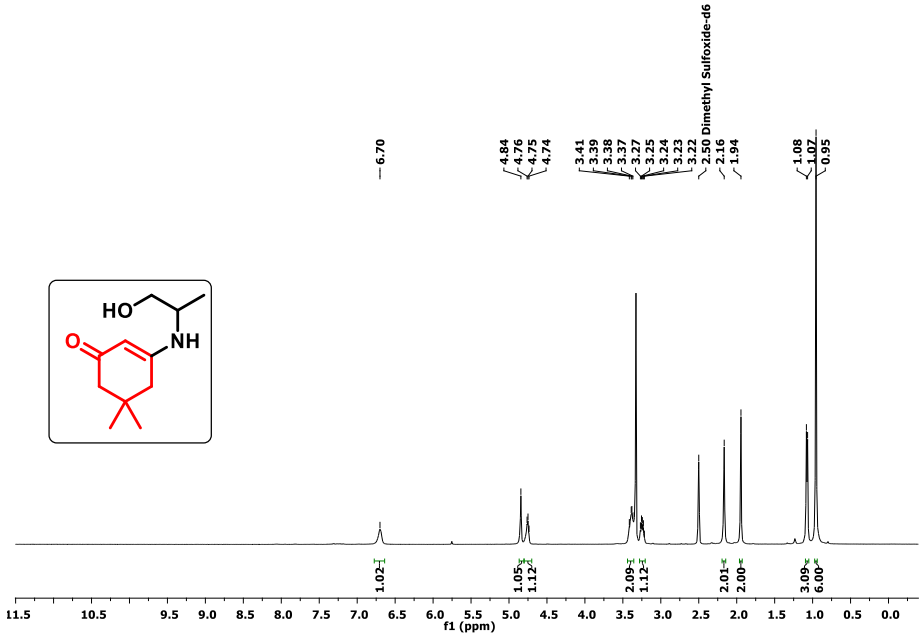

Figure 5.8.B.15: ^{1}H NMR of **141t**, 400 MHz, DMSO-d_6

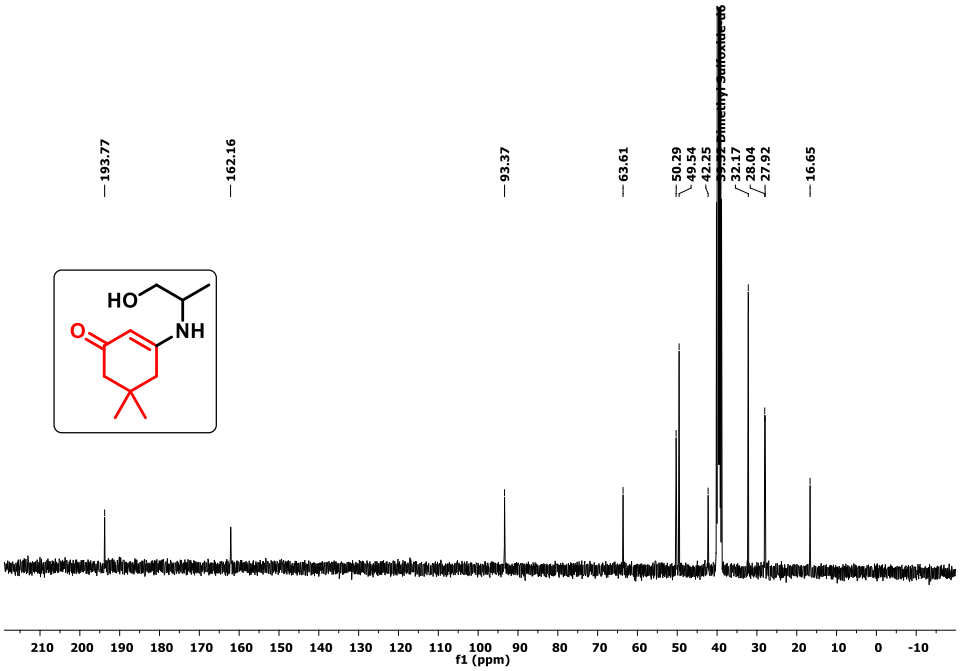

Figure 5.8.B.16: ^{13}C NMR of **141t**, 100 MHz, DMSO-d_6

3,3-dimethyl-3,4-dihydroacridin-1(2*H*)-one (143d)

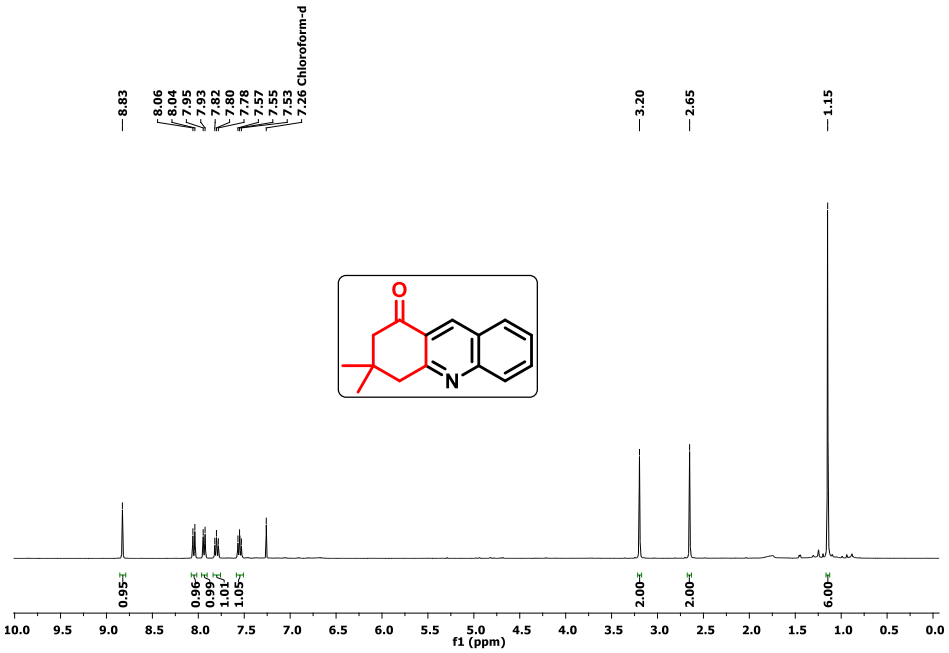

Figure 5.8.B.17: ^{1}H NMR of **143d**, 400 MHz, $CDCl_3$

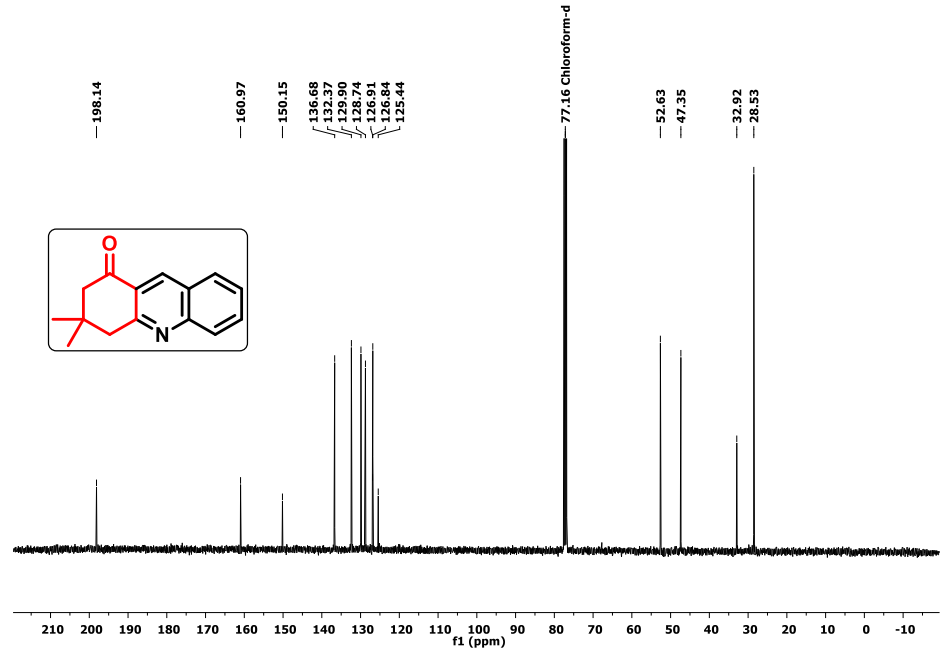

Figure 5.8.B.18: ^{13}C NMR of **143d**, 100 MHz, $CDCl_3$

2,3-dihydro-1*H*-cyclopenta[b]quinolin-1-one (143f)

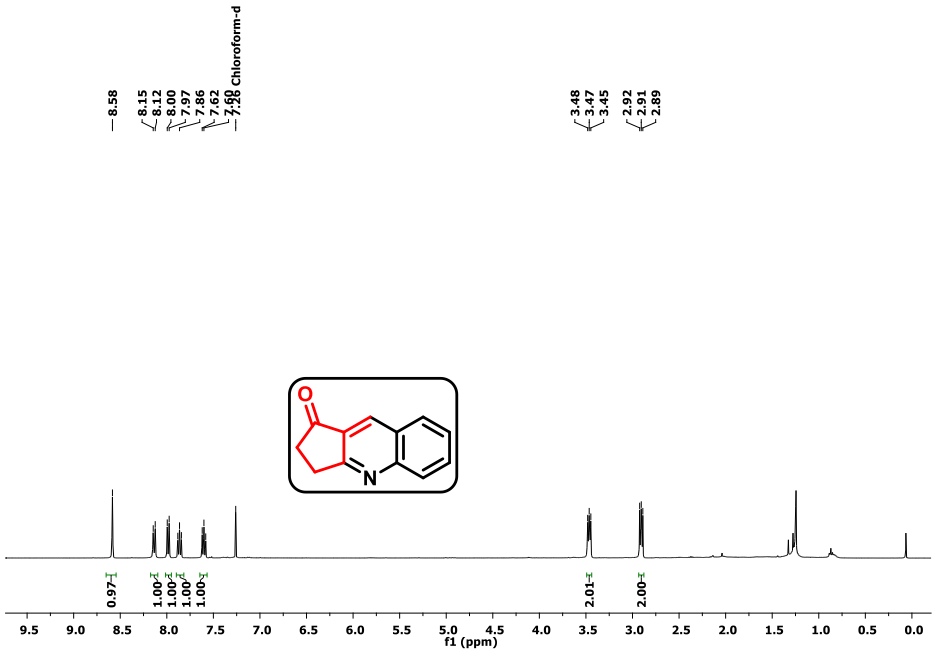

Figure 5.8.B.19: ^{1}H NMR of **143f**, 400 MHz, $CDCl_3$

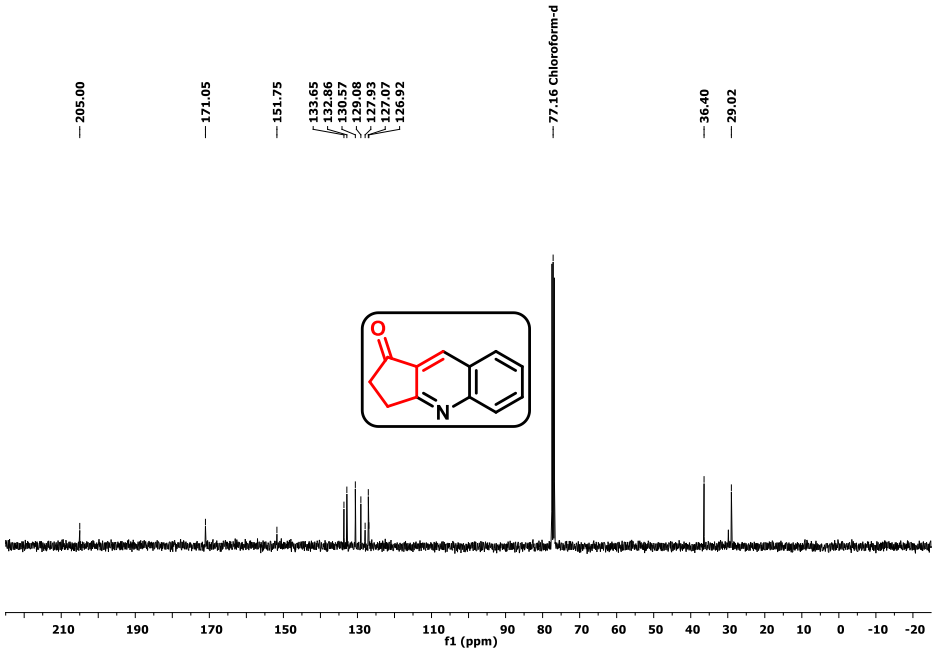

Figure 5.8.B.20: ^{13}C NMR of **143f**, 100 MHz, $CDCl_3$

1,3,5-trimethylpyrimido[4,5-b]quinoline-2,4(1*H*,3*H*)-dione (143l)

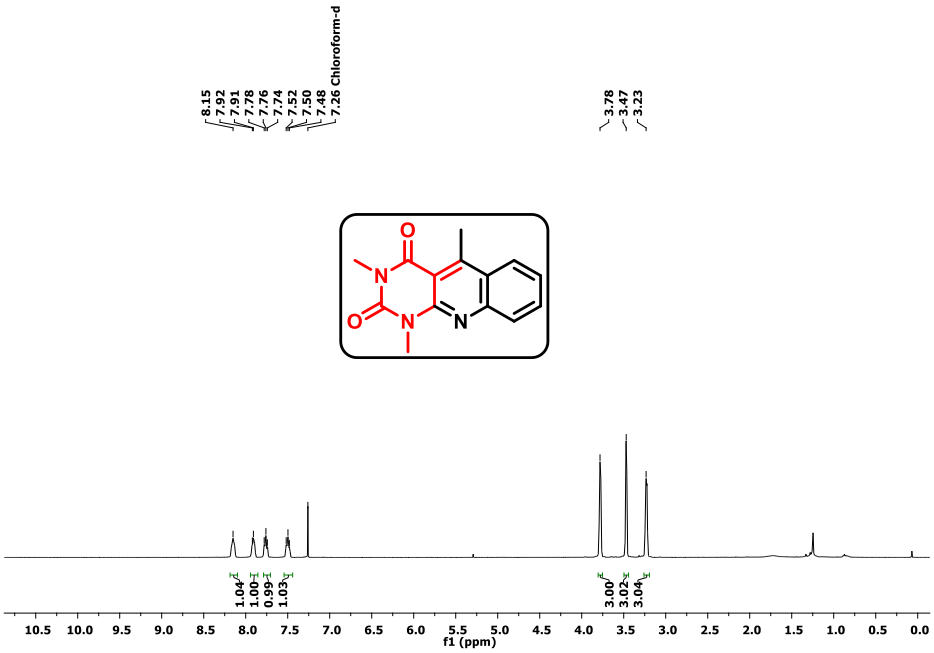

Figure 5.8.B.21: ^{1}H NMR of **143l**, 400 MHz, $CDCl_3$

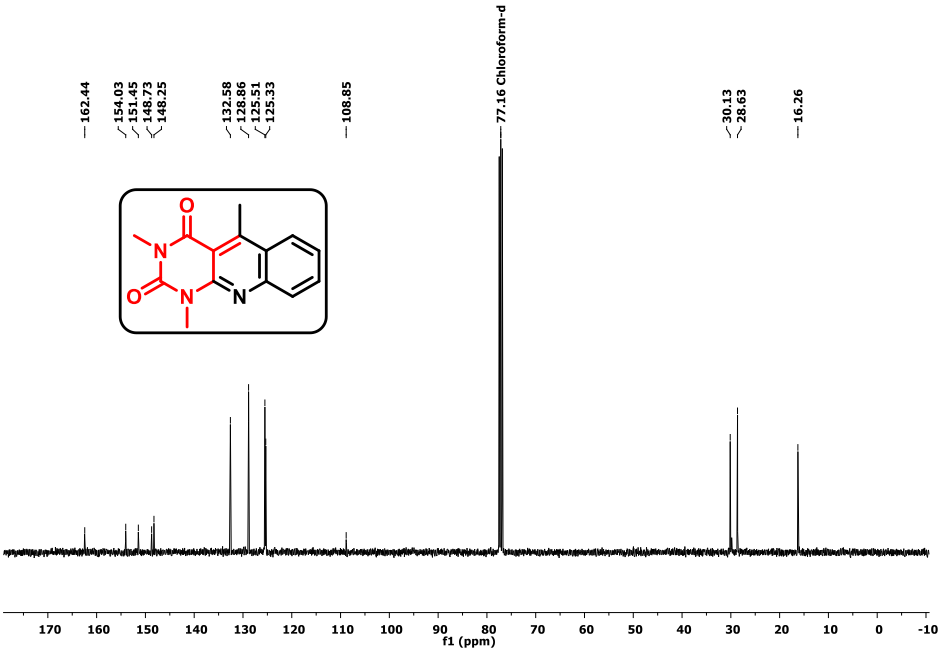

Figure 5.8.B.22: ^{13}C NMR of **143l**, 100 MHz, $CDCl_3$

3-((2-(hydroxymethyl)phenyl)amino)-4,4-dimethylcyclohex-2-en-1-one (144c)

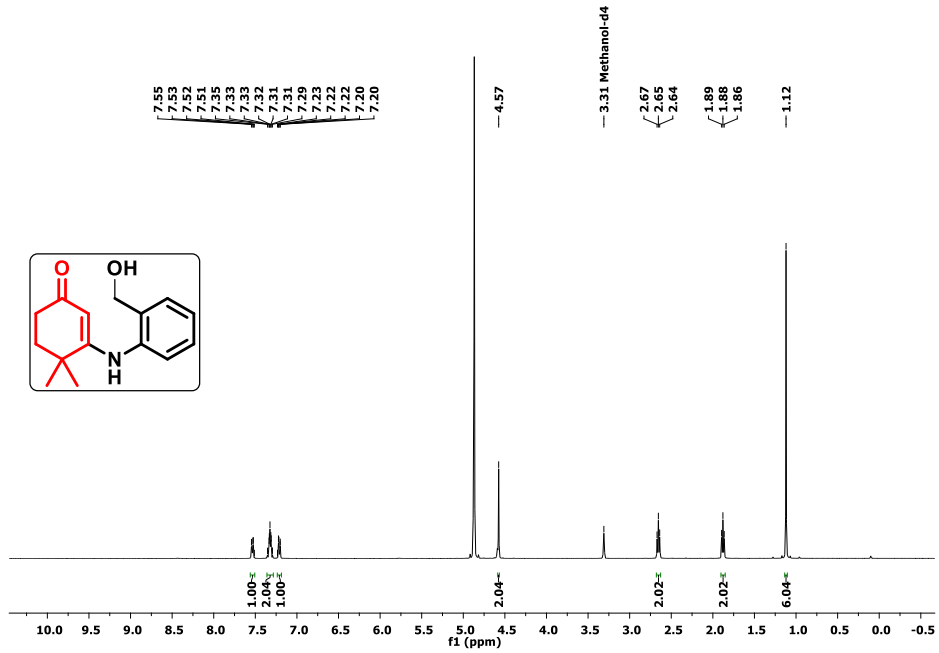

Figure 5.8.B.23: ^{1}H NMR of **144c**, 400 MHz, MeOH-d_4

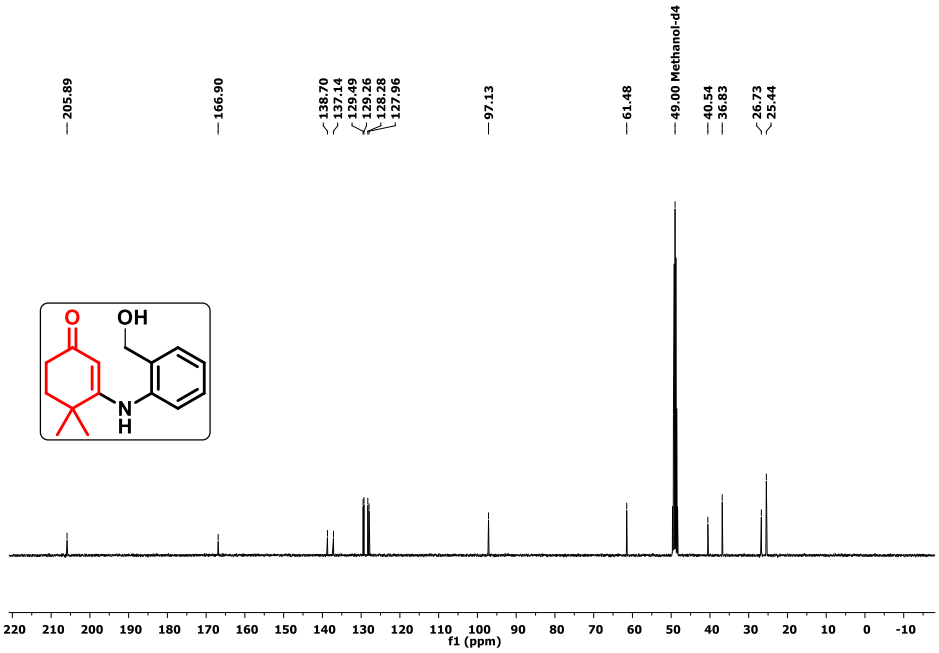

Figure 5.8.B.24: ^{13}C NMR of **144c**, 100 MHz, MeOH-d

3-ethyl-2-methyl-1,5,6,7-tetrahydro-4*H*-indol-4-one (145a)

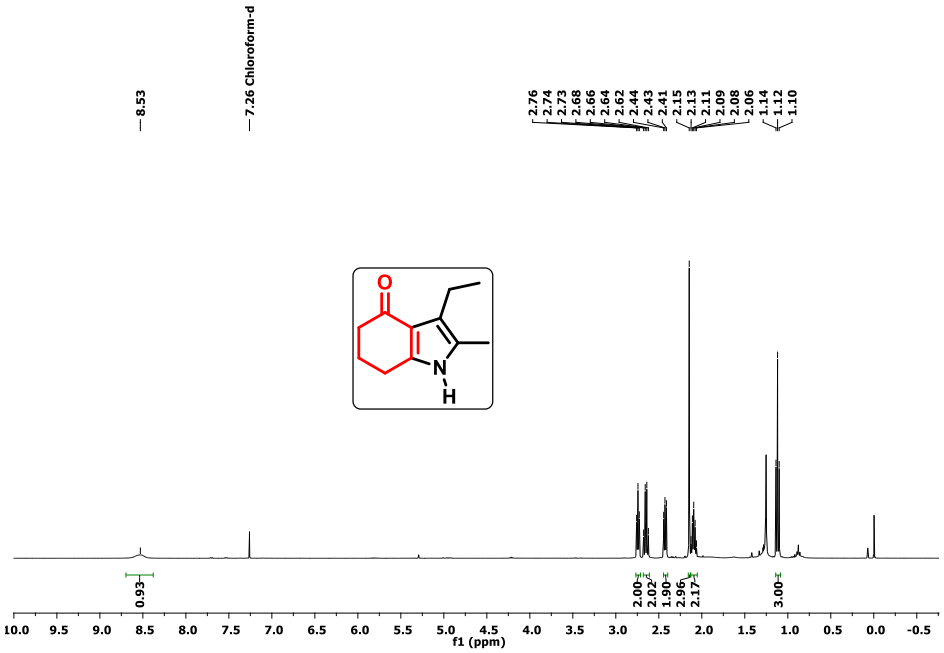

Figure 5.8.B.25: ^{1}H NMR of **145a**, 400 MHz, $CDCl_3$

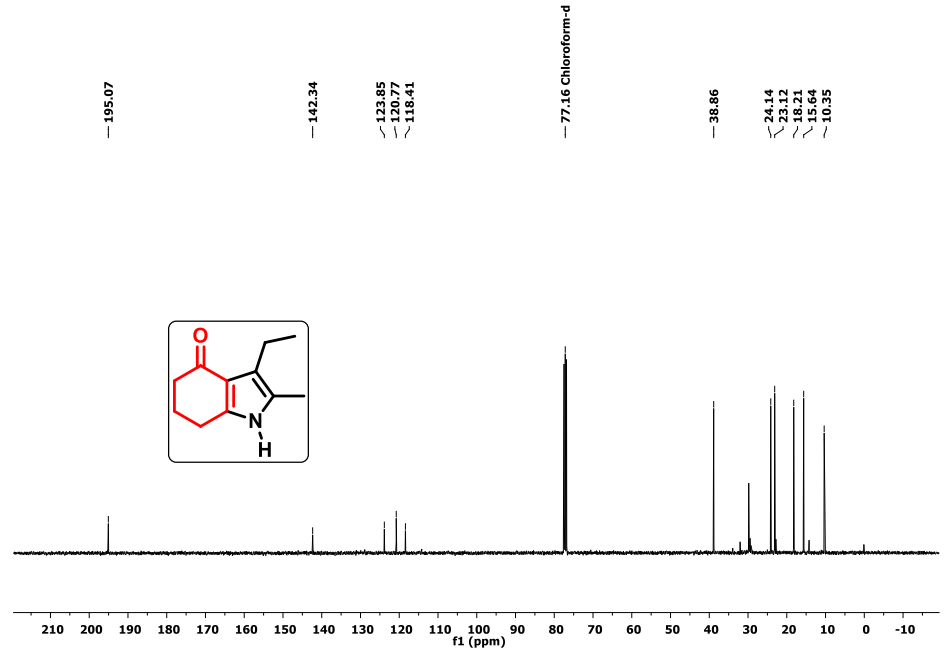

Figure 5.8.B.26: ^{13}C NMR of **145a**, 400 MHz, $CDCl_3$

3-hexyl-2-methyl-1,5,6,7-tetrahydro-4*H*-indol-4-one (145b)

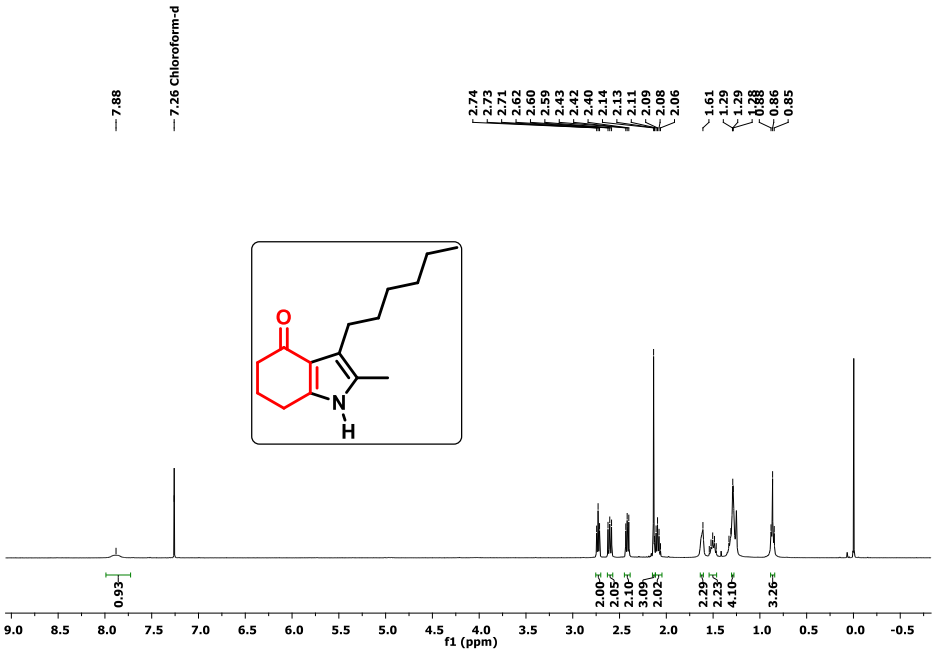

Figure 5.8.B.27: ^{1}H NMR of **145b**, 400 MHz, $CDCl_3$

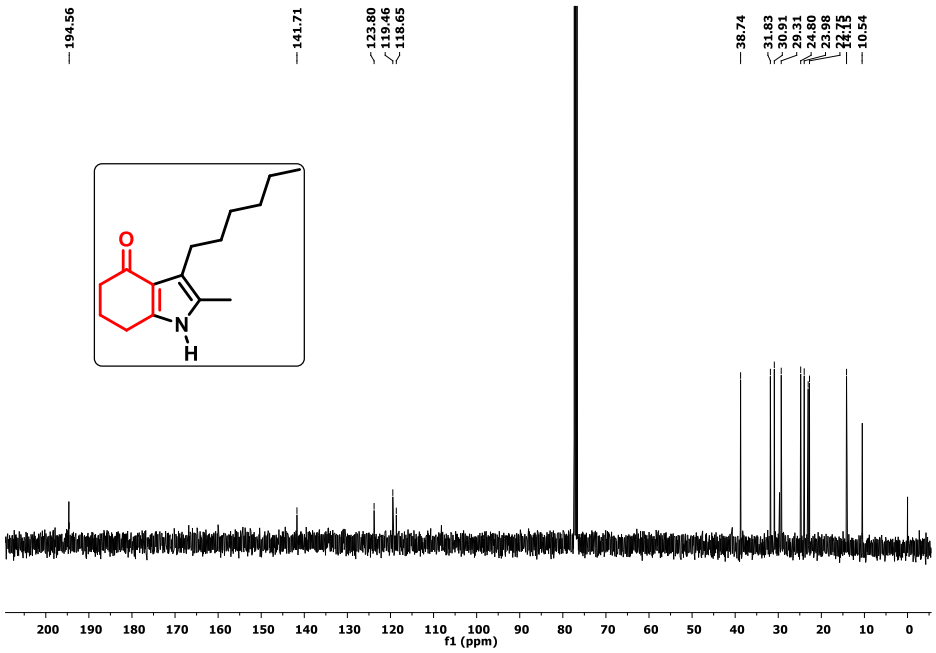

Figure 5.8.B.28: ^{13}C NMR of **145b**, 400 MHz, $CDCl_3$

5.9. ORTEP drawings of 140k, 141a, 141c' and 143a showing thermal ellipsoids at the 50% probability level

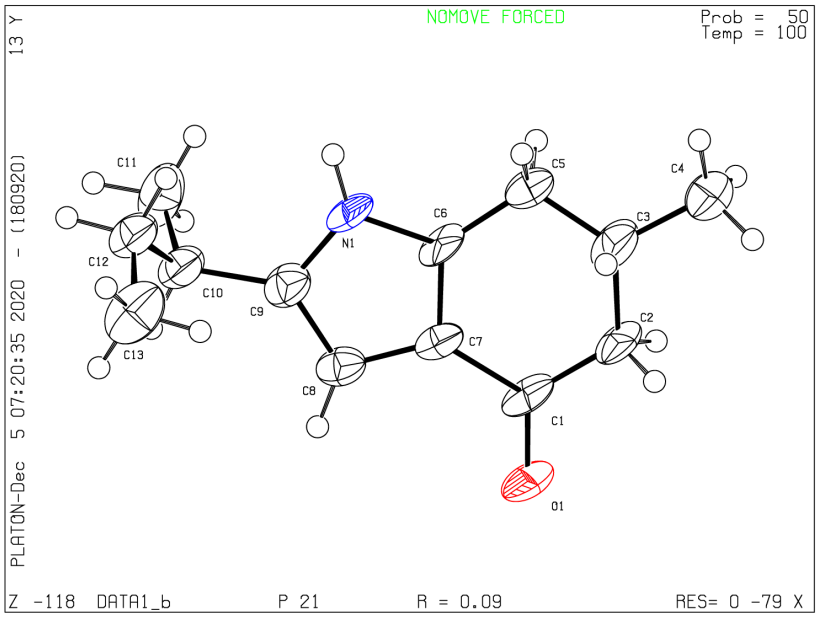

Figure 5.9.1: Crystal structure of compound **140k, CCDC Number: 2048644**

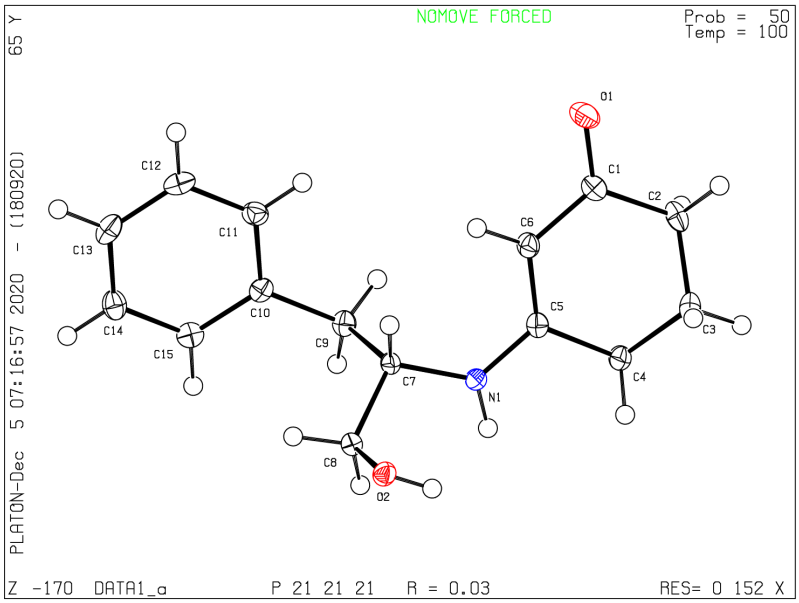

Figure 5.9.2: Crystal structure of compound **141a, CCDC Number: 2048435**

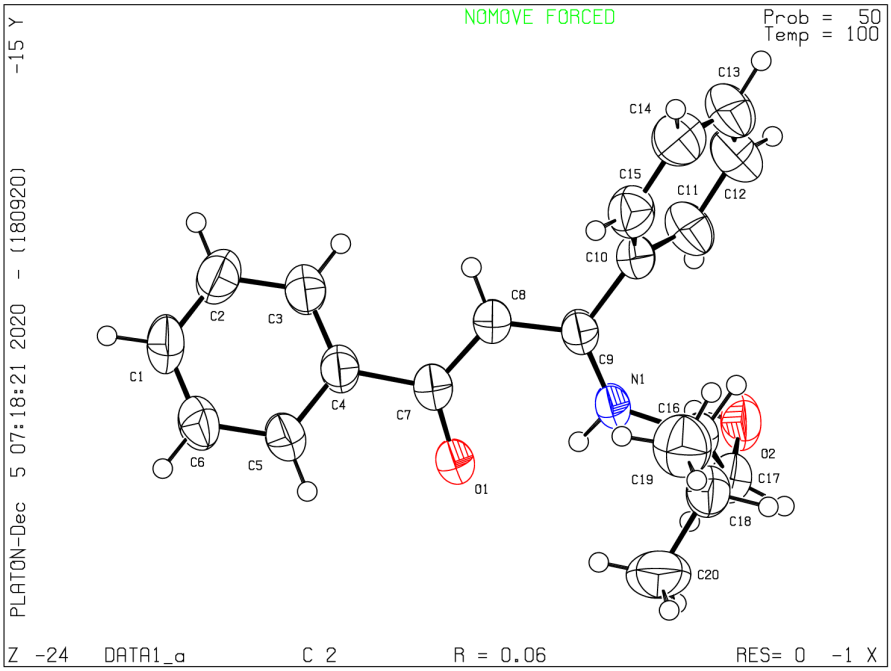

Figure 5.9.3: Crystal structure of compound **141c', CCDC Number: 2048437**

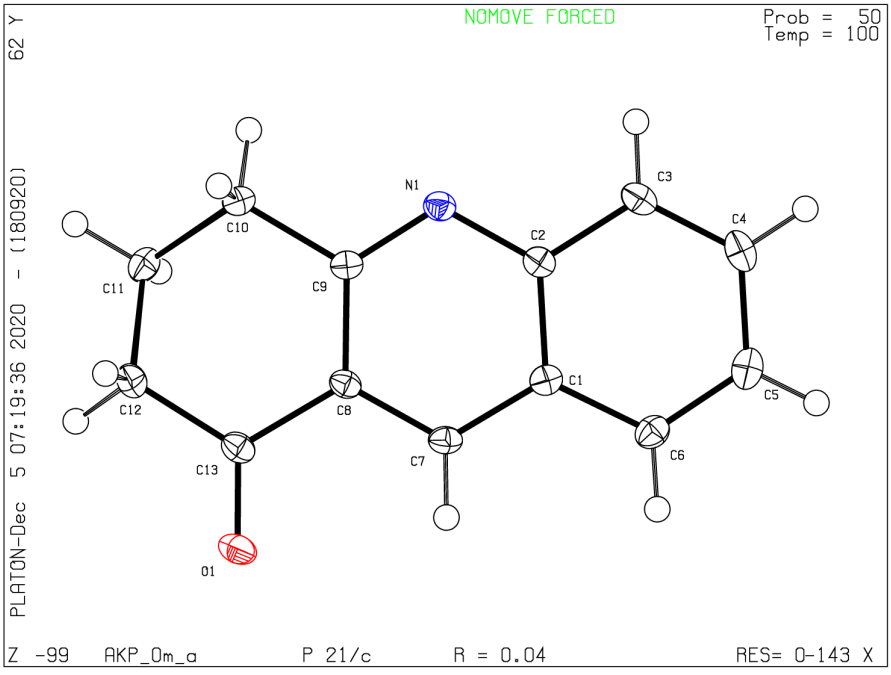

Figure 5.9.4: Crystal structure of compound **143a, CCDC Number: 2048643**

REFERENCES

(1) Meadows, D. H.; Meadows, D. L.; Randers, J. *The Limits to Growth; Universe Books: New York*, **1972**.

(2) Catling, D. C.; Zahnle, K. J. *The Planetary Air Leak. As Earth's atmosphere slowly trickles away into space, will our planet come to look like Venus? Sci. Am.* **2009**, *300*, 36-43.

(3) *World Commission on Environment and Development Our Common Future; Oxford University Press: Oxford*, **1987**.

(4) Csefalvay, E.; Akien, G. R.; Qi, L.; Horva´th, I. T. *Catal. Today*. **2015**, *239*, 50-55.

(5) Horva´th, I. T. *Chem. Rev.* **2018**, *118*, 369-371.

(6) Menges, N. *The Role of Green Solvents and Catalysts at the Future of Drug Design and of Synthesis.* **2017**, Ed. by Saleh, H.; Koller, M. London: IntechOpen, **2017**. 10.5772/intechopen.71018.

(7) *Green Chemistry: An Introductory Text By Mike Lancaster. Royal Society of Chemistry: Cambridge, UK*. **2002**, *310*, ISBN 0-85404-620-8

(8) Isaacs, N. S.; Keating, N. *J. Chem. Soc. Chem. Commun.* **1992**, 876.

(9) Gaikwad, V.V.; Bhanage, B. M. *Appl. Organomet. Chem.* **2019**, *33*, e4741.

(10) Hock, H.; Lang, S. *Ber. Dtsch. Chem. Ges. B.* **1944**, *77*, 257-264.

(11) (a) Kaneda, K.; Mizugaki, T. *Energy Environ. Sci.* **2009**, *2*, 655-673. (b) Zhang, W. *Green Chem.* **2009**, *11*, 911-920. (c) Candeias, N. R.; Branco, L. S. C.; Gois, P. M. P.; Afonso, C. A. M.; Trindade, A. F. *Chem. Rev.* **2009**, *109*, 2703-2802.

(12) (a) Posner, G. H. *Angew. Chem., Int. Ed. Engl.* **1978**, *17*, 487-496. (b) Kabalka, G. W.; Pagni, R. M. *Tetrahedron* **1997**, *53*, 7999-8065. (c) Ranu, B. C.; Bhar, S.; Chakraborty, R.; Das, A. R.; Saha, M.; Sarkar, A.; Chakraborti, R.; Sarkar, D. C. *J. Indian Inst. Sci.* **1994**, *74*, 15-33. (d) Ley, S. V.; Baxendale, I. R.; Bream, R. N.; Jackson, P. S.; Leach, A. G.; Longbottom, D. A.; Nesi, M.; Scott, J. S.; Storer, R. I.; Taylor, S. J. *J. Chem. Soc., Perkin Trans.* **2000**, *1*, 3815-4195. (e) Früchtel, J. S.; Jung, G. *Angew. Chem., Int. Ed. Engl.* **1996**, *35*, 17-42.

(13) (a) Gawande, M. B.; Bonifμcio, V. D. B.; Luque, R.; Branco, P. S.; Varma, R. S. *ChemSusChem* **2014**, *7*, 24-44. (b) Polshettiwar, V.; Varma, R.S. *Tetrahedron Lett*. **2008**, *49*, 7165-7167.

(14) Crisenza, G. E. M.; Melchiorre, P. *Nat. Commun.* **2020**, *11*, 803.

(15) Hoffmann, N. *Chem. Rev.* **2008**, *108*, 1052-1103.

(16) Douglas, J. J.; Sevrin, M. J.; Stephenson, C. R. J. *Org. Process Res. Dev.* **2016**, *20*, 1134-1147.

(17) Ischay, M. A.; Anzovino, M. E.; Du, J.; Yoon, T. P. *J. Am. Chem. Soc.* **2008**, *130*, 12886-12887.

(18) Hari, D. P.; Hering, T.; König, B. *Org. Lett.* **2012**, *14*, 5334-5337.

(19) Chu, L.; Lipshultz, J. M.; MacMillan, D. W. C. *Angew. Chem., Int. Ed.* **2015**, *54*, 7929-7933.

(20) Gambacorta, G.; Sharley, J. S.; Baxendale, I. R. *Beilstein J. Org. Chem.* **2021**, *17*, 1181-1312.

(21) Baumann, M.; Moody, T. S.; Smyth, M.; Wharry, S.; *Org. Process Res. Dev.* **2020**, *24*, *10*, 1802-1813.

(22) Filippo, M. D.; Baumann, M. *Molecules* **2021**, *26*, 22, 6992.

(23) Porta, R.; Benaglia, Maurizio.; Puglisi, Alessandra. *Org. Process Res. Dev.* **2016**, *20*, *1*, 2-25.

(24) Cambié, D.; Bottecchia, C.; Straathof, N. J. W.; Hessel, V.; Noël, T. *Chem. Rev.* **2016**, *116*, *17*, 10276-10341.

(25) Mohanta, N.; Nair, K.; Sutar, D. V.; Gnanaprakasam, B. *React. Chem. Eng.* **2020**, ***5***, 1501-1508.

(26) Silva-Brenes, D.V.; Emmanuel, N.; Mejías, V. L.; Duconge, J.; Vlaar, C.; Stelzer, T.; Monbaliu, J. C. *Green Chem.* **2022**, *24*, 2094-2103.

(27) Wiles, C.; Watts, P. *Green Chem.* **2012**, *14*, 38-54.

(28) Ley, S. V. *Chem. Rec*. **2012**, *12*, 378-390.

(29) Yoshida, J.-i.; Kim, H.; Nagaki, A. *ChemSusChem* **2011**, *4*, 331-340.

(30) Jiménez-González, C.; Poechlauer, P.; Broxterman, Q. B.; Yang, B.-S.; Ende, D. am; Baird, J.; Bertsch, C.; Hannah, R. E.; Dell'Orco, P.; Noorman, H.; Yee, S.; Reintjens, R.; Wells, A.; Massonneau, V.; Manley J. *Org. Process Res. Dev.* **2011**, *15*, 900-911.

(31) (a) Xu, L.-M.; Li, B.-J.; Yang, Z.; Shi, Z.-J. *Chem. Soc. Rev.* **2010**, *39*, 712-733. (b) Lyons, T. W.; Sanford, M. S. *Chem. Rev.* **2010**, *110*, 1147-1169. (c) Colby, D. A.; Bergman, R. G.; Ellman, J. A. *Chem. Rev.* **2010**, *110*, 624-655. (d) Chen, X.; Engle, K. M.; Wang, D.-H.; Yu, J.-Q. *Angew. Chem., Int. Ed.* **2009**, *48*, 5094-5115. (e) Wang, D. H.; Engle, K. M.; Shi, B.-F.; Yu, J.-Q. *Science* **2010**, *327*, 315-319. (f) Li, Z.-P.; Li, C.-J. *J. Am. Chem. Soc.* **2005**, *127*, 3672-3673.

(32) Giri, R.; Shi, B.-F.; Engle, K. M.; Maugel, N.; Yu, J.- Q. *Chem. Soc. Rev.* **2009**, *38*, 3242-3272.

(33) Punniyamurthy, T.; Velusamy, S.; Iqbal, J. *Chem. Rev.* **2005**, *105*, 2329-2363.

(34) (a) Haines, A. H. Academic Press, London, **1985**. (b) Haines, A. H. Academic Press, London, **1988**.

(35) Cr-catalyzed oxidations: (a) Pearson, A. J.; Han, G. R. *J. Org. Chem.* **1985**, *50*, 2791-2801. (b) Muzart, J. *Tetrahedron Lett*. **1986**, *27*, 3139-3142. (c) Muzart, J.; Ajjou, A. N. A. *J. Mol. Catal.* **1991**, *66*, 155-161. (d) Choudary, B. M.; Prasad, A. D.; Bhuma, V.; Swapna, V. *J. Org. Chem.* **1992**, *57*, 5841-5844. (e) Das, T. K.; Chaudhari, K.; Nandanan, E.; Chandwadkar, A. J.; Sudalai, A.; Ravindranathan, T.; Sivasanker, S. *Tetrahedron Lett*. **1997**, *38*, 3631-3634. (f) Rothenberg, G.; Wiener, H.; Sasson, Y. *J. Mol. Catal. A: Chem.* **1998**, *136*, 253-262. (g) Mohapatra, S. K.; Selvam, P. *J. Catal*. **2007**, *249*, 394-396.

(36) Mn-catalyzed oxidations: (a) Lee, N. H.; Lee, C. S.; Jung, D. S. *Tetrahedron Lett.* **1998**, *39*, 1385-1388. (b) Pan, J. F.; Chen, K. *J. Mol. Catal. A: Chem.* **2001**, *176*, 19-22. (c) Blay, G.; Fern´andez, I.; Gim´enez, T.; Pedro, J. R.; Ruiz, R.; Pardo, E.; Lloret, F.; Mu˜noz, M. C. *Chem. Commun.* **2001**, 2102-2103.

(37) Co-catalyzed oxidations: (a) Li, P.; Alper, H. *J. Mol. Catal. A: Chem.* **1990**, *61*, 51-54. (b) Jurado-Gonzalez, M.; Sullvian, A. C.; Wilson, J. R. H. *Tetrahedron Lett*. **2003**, *44*, 4283-4286. (c) Modica, E.; Bombieri, G.; Colombo, D.; Marchini, N.; Ronchetti, F.; Scala, A.; Toma, L. Eur. *J. Org. Chem.* **2003**, 2964-2971. (d) Li, X. G.; Wang, J.; He, R. *Chin. Chem. Lett.* **2007**, *18*, 1053-1056.

(38) Ru-catalyzed oxidations: (a) Murahashi, S.; Oda, Y.; Naota, T.; Kuwabara, T. *Tetrahedron Lett.* **1993**, *34*, 1299-1302. (b) Nikalje, M. D.; Sudalai, A. *Tetrahedron* **1999**, *55*, 5903-5908. (c) Murahashi, S.; Komiya, N.; Oda, Y.; Kuwabara, T.; Naota, T. *J. Org. Chem.* **2000**, *65*, 9186-9193.

(39) Rh-catalyzed oxidations: Catino, A. J.; Nichols, J. M.; Choi, H.; Gottipamula, S.; Doyle, M. P. *Org. Lett.* **2005**, *7*, 5167-5170.

(40) Fe-catalyzed oxidations: (a) Barton, D. H. R.; Doller, D. *Acc. Chem. Res*. **1992**, *25*, 504-512. (b) Barton, D. H. R.; Chavasiri, W. *Tetrahedron* **1994**, *50*, 19-30. (c) Evans, S.; Smith, J. R. L. *J. Chem. Soc., Perkin Trans.* **2000**, *2*, 1541-1551. (d) Stavropoulos, P.; Celenligil-Cetin, R.; Tapper, A. E. *Acc. Chem. Res.* **2001**, *34*, 745-752. (e) Kim, S. S.; Sar, S. K.; Tamrakar, P. *Bull. Korean Chem. Soc.* **2002**, *23*, 937-938. (f) Pavan, C.; Legros, J.; Bolm, C. *Adv. Synth. Catal.* **2005**, *347*, 703-705. (g) Nakanishi, M.; Bolm, C. *Adv. Synth. Catal.* **2007**, *349*, 861-864. (h) Nagano, T.; Kobayashi, S. *Chem. Lett.* **2008**, *37*, 1042-1045. (i) Gonzalez-de-Castro, A.; Robertson, C. M.; Xiao, J. *J. Am. Chem. Soc.* **2014**, *136*, 8350-8360.

(41) Peng, H.; Lin, A.; Zhang, Y.; Jiang, H.; Zhou, J.; Cheng, Y.; Zhu, C.; Hu, H. *ACS Catal.* **2012**, *21*, 163-167.

(42) Bi-catalyzed oxidations: (a) Bonvin, Y.; Callens, E.; Larrosa, I.; Henderson, D. A.; Oldham, J.; Burton, A. J.; Barrett, A. G. M. *Org. Lett.* **2005**, *7*, 4549-4552. (b) Callens, E.; Burton, A. J.; White, A. J. P.; Barrett, A. G. M. *Tetrahedron Lett.* **2008**, *49*, 3709-3712.

(43) (a) Liu, Y.-J.; Xu, H.; Kong, W.-J.; Shang, M.; Dai, H.-X.; Yu, J.-Q. *Nature* **2014**, *515*, 389-393. (b) Shaabani, A.; Hezarkhani, Z.; Badali, E. *RSC Adv.* **2015**, *5*, 61759-61767. (c) Garcia-Bosch, I.; Siegler, M. A. *Angew. Chem., Int. Ed.* **2016**, *55*, 12873-12876. (d) Peng, H.; Lin, A.; Zhang, Y.; Jiang, H.; Zhou, J.; Cheng, Y.; Zhu, C.; Hu, H. *ACS Catal.* **2012**, *2*, 163-167. (e) Nakamura, A.; Nakada, M. *Synthesis* **2013**, 1421. (f) Zhong, Y.-L.; Gauthier, D. R.;

Shi, Y.-J.; McLaughlin, M.; Chung, J. Y. L.; Dagneau, P.; Yasuda, N. *J. Org. Chem.* **2012**, *77*, 3297-3310.

(44) Zhang, Z.; Gao, Y.; Liu, Y.; Li, J.; Xie, H.; Li, H.; Wang, W. *Org. Lett.* **2015**, *17*, 5492-5495.

(45) Tan, J.; Zheng, T.; Yu, Y.; Xu, K. *RSC Adv.* **2017**, *7*, 15176-15180.

(46) Carrillo, A. I.; Schmidt, L. C.; Marin, M. L.; Scaiano, J. C. *Catal. Sci. Technol.* **2014**, *4*, 435-440.

(47) Aksoylu, A. E.; Madalena, M.; Freitas, A.; Pereira, M. F. R.; Figueiredo, J. *Carbon* **2001**, *39*, 175-185.

(48) Klemm, D.; Heublein, B.; Fink, H. P.; Bohn, A. *Angew. Chem., Int. Ed.* **2005**, *44*, 3358-3393.

(49) Lengke, M. F.; Fleet, M. E.; Southam, G. *Langmuir* **2007**, *23*, 8982-8987.

(50) (a) Visuvamithiran, P.; Shanthi, K.; Palanichamy, M.; Murugesan, V. *Catal. Sci. Technol.* **2013**, *3*, 2340-2348. (b) Wu, H.; Song, J.; Xie, C.; Hu, Y.; Liu, S.; Han, B. *ACS Sustain. Chem. Eng.* **2018**, *6*, *11*, 13670-13675. (c) Saha, R.; Sekar, G. *Applied Catalysis B: Environmental* **2019**, *250*, 325-336.

(51) Montazeri, H.; Amani, A.; Shahverdi, H. R.; Haratifar, E.; Shahverdi, A. R.; *J. Nanostruct. Chem.* **2013**, *3*, 25-31.

(52) (a) Nasir Baig, R. B.; Rajender, S. V. *Chem. Commun.* **2013**, *49*, 752-770. (b) Ricciardi, R.; Huskens, J.; Verboom, W. *ChemSusChem* **2015**, *8*, 2586-2605.

(53) (a) Yin, L.; Liebscher, J. *Chem. Rev.* 2007, *107*, 133-173. (b) Phan, N. T. S.; Sluys, M. V. D.; Jones, C. W. *Adv. Synth. Catal.* 2006, *348*, 609-679. (c) Moreno-Mañas, M.; Pleixats, R. *Acc. Chem. Res.* 2003, *36*, 638-643.

(54) Zarghani, M.; Akhlaghinia, B. *RSC Adv.* 2016, *6*, 38592-38601.

(55) (a) Fatiadi, A. J. *Synthesis* 1976, 65-104. (b) Soldatenkov, A. T.; Poly- anskii, K. B.; Kolyadina, N. M.; Soldatova, S. A. *Chem. Heterocycl. Compd.* 2009, *45*, 633-657. (c) Taylor, R. J. K.; Reid, M.; Foot, J.; Raw, S. A. *Acc. Chem. Res.* 2005, *38*, 851-869.

(56) Lv, X. M.; Kong, L. J.; Lin, Q.; Liu, X. F.; Zhou, Y. M.; Yu, J.; *Synth. Commun.* **2011**, *41*, *21*, 3215-3222.

(57) Gutmann, B.; Elsner, P.; Roberge, D.; Kappe, C. O. *ACS Catal*. **2013**, *3*, 2669-2676.

(58) (a) Niu, F.; Zhang, L.; Luo, S.-Z.; Song, W.-G. *Chem. Commun.* 2010, *46*, 1109-1111. b) Arefi, M.; Saberi, D.; Karime, M.; Heydari, A. *ACS Comb. Sci.* **2015**, *17*, 341 -345.

(59) Guo, F.; Li, H.; Zhang, Z.; Meng, S.; Li, D. *Mater. Sci. Eng. B.* 2009, *163*, 134-137.

(60) Liu, Z.; Ma, R.; Ebina, Y.; Takada, K.; Sasaki, T. *Chem. Mater.* 2007, *19*, 6504-6512.

(61) Zhu, C.; Guo, S.; Fang, Y.; Han, L.; Wang, S. *Nano Res.* 2011, *4*, 648-657.

(62) Li, X. C.; Zhang, L.; He, G. H. *Carbon* 2016, *99*, 514-522.

(63) Wang, J.; Fan, S.; Luan, Y.; Tang, J.; Jin, Z.; Yang, M.; Lu, Y. *RSC Adv.* 2015, *5*, 2405-2410.

(64) (a) Rothenberg, G.; Wiener, H.; Sasson, Y. *J. Mol. Catal. A* 1998, *136*, 253-259. (b) Dhakshinamoorthy, A.; Alvaro, M.; Garcia, H. *J. Catal.* 2009, *267*, 1-4.

(65) Zhang, L.; Zhang, J. Y. *J. Comb. Chem.* **2006**, *8*, 361-367.

(66) Phakhodee, W.; Duangkamol, C.; Pattarawarapan, M. *Tetrahedron Lett.* 2016, *57*, 2087-2089.

(67) Gautam, P.; Kathe, P.; Bhanage, B. M. *Green Chem.* **2017**, *19*, 823-830.

(68) Subramanian, K.; Yedage, S. L.; Bhanage, B. M. *J. Org. Chem.* **2017**, *82*, 10025-10032.

(69) Arzumanyan, A. V. *Tetrahedron Lett.* **2017**, *58*, 4667-4671.

(70) Chun, S.; Chung, Y. K. *Org. Lett*. **2017**, *19*, 3787-3790.

(71) Sai Prathima, P.; Bikshapathi, R.; Rao, V. J. *Tetrahedron Lett.* **2015**, *56*, *46*, 6385-6388.

(72) Reviews of Reactive Intermediate Chemistry (M. Platz, R. Moss, M. Jones Jr.), Wiley, Germany, **2007**.

(73) (a) The Chemistry of the Azido Group (Ed.: S. Patai), Wiley, New York, **1971.** (b) The Chemistry of Halides, Pseudo-halides and Azides, Supplement D, (Eds.: S. Patai, Z.

Rappoport), Wiley, Chichester, **1983.** (c) Chemistry of Halides, Pseudo-Halides and Azides, Part 1(Ed.: S. Patai), Wiley, Chichester, **1995.** (d) Chemistry of Halides, Pseudo-Halides and Azides, Part 2 (Ed.: S. Patai), Wiley, Chichester,**1995**.

(74) Monograph: Azides and Nitrenes Reactivity and Utility (Ed.: E. F. V. Scriven), Academic Press, New York, **1984**.

(75) Jang, S.; Sachin, K.; Lee, H.; Wook Kim, D.; Soo Lee, H. *Bioconjugate Chem.* **2012**, *23*, 2256-2261.

(76) Brase, S.; Gil, C.; Knepper, K.; Zimmermann, V. *Angew. Chem., Int. Ed.* **2005**, *44*, 5188-5240.

(77) Padwa, A. Aziridines and Azirines: Monocyclic. In Comprehensive Heterocyclic Chemistry III; Katritzky, A. R., Ramsden, C. A., Scriven, E. F. V., Taylor, R. J. K., Eds.; Elsevier Science: Oxford, **2008**; Vol. 1, Chapter 1.01.6.2, pp 50-64.

(78) Gololobov, Y. G.; Kasukhin, L. F. *Tetrahedron* **1992**, *48*, 1353-1406.

(79) Li, Y. L.; Combs, A. P. Int. Patent Appl.WO2015191677A1, Dec 17, **2015**.

(80) Kim, M. S.; Yoo, M. H.; Rhee, J. K.; Kim, Y. J.; Park, S. J.; Choi, J. H.; Sung, S. Y.; Lim, H. G.; Cha, D. W. Int. Patent Appl. WO2009084827A2, July 9, **2009**.

(81) Bathula, S.N.V.P.; Vadla, R. *Asian J. Pharm. Clin. Res.* **2011**, *4*, 66-67.

(82) Aganda, K. C.; Hong, B.; Lee, A. *Adv. Synth. Catal.* **2021**, *363*, 1443-1448.

(83) Brase, S.; Banert, K., Eds. Organic Azides: Syntheses and Applications; John Wiley & Sons, Ltd.: Chichester, U.K., **2010**.

(84) Li, J.; Cao, J.; Wei, J.; Shi, X.; Zhang, L.; Feng, J.; Chen, Z. *Eur. J.Org. Chem.* **2011**, *2011*, 229-233.

(85) Denk, C.; Wilkovitsch, M.; Skrinjar, P.; Svatunek, D.; Mairinger, S.; Kuntner, C.; Filip, T.; Fröhlich, J.; Wanek, T.; Mikula, H. *Org. Biomol. Chem.* **2017**, *15*, 5976-5982.

(86) Kurosawa, W.; Kan, T.; Fukuyama, T. *J. Am. Chem. Soc.* **2003**, *125*, 8112-8113.

(87) Besset, C.; Chambert, S.; Fenet, B.; Queneau, Y. *Tetrahedron Lett.* **2009**, *50*, 7043-7047.

(88) Terrasson, V.; Marque, S.; Georgy, M.; Campagne, J. M.; Prim, D. *Adv. Synth.Catal.* **2006**, *348*, 2063-2067.

(89) Khedar, P.; Pericherla, K.; Kumar, A. *Synlett* **2014**, *25*, 515-518.

(90) Rueping, M.; Vila, C.; Uria, U. *Org. Lett.* **2012**, *14*, 768-771.

(91) Sawama, Y.; Nagata, S.; Yabe, Y.; Morita, K.; Monguchi, Y.; Sajiki, H. *Chem. Eur. J.* **2012**, *18*, 16608-16611.

(92) Reddy, C. R.; Madhavi, P. P.; Reddy, A. S. *Tetrahedron Lett.* **2007**, *48*, 7169-7172.

(93) Kumar, A.; Sharma, R. K.; Singh, T. V.; Venugopalan, P. *Tetrahedron* **2013**, *69*, 10724-10732.

(94) Tummatorn, J.; Thongsornkleeb, C.; Ruchirawata, S.; Thongarama, P.; Kaewmee, B. *Synthesis* **2015**, *47*, 323-329.

(95) Hajipour, A. R.; Rajaei, A.; Ruoho, A. E. *Tetrahedron Lett.* **2009**, *50*, 708-711.

(96) Tandiary, M. A.; Masui, Y.; Onaka, M. *RSC Adv.* **2015**, *5*, 15736-15739.

(97) Kamble, S.; More, S.; Rode, C. *New J. Chem.* **2016**, *40*, 10240-10245.

(98) Yin, X. P.; Zhu, L.; Zhou, J. *Adv. Synth. Catal.* **2018**, *360*, 1116-1122.

(99) Regier, J.; Maillet, R.; Bolshan, Y. *Eur. J. Org. Chem*. **2019**, 2390-2396.

(100) Dallingera, D.; Kappe, C. O. *Curr. Opin. Green Sustain. Chem.* **2017**, *7*, 6-12.

(101) Delvillea, M.; Nieuwland, P.; Janssena, P.; Koch, K.; Van Hest, J.; Rutjes, F. *Chem. Eng. J.* **2011**, *167*, 556-559.

(102) Donnelly, A.; Zhang, H.; Baumann, M. *Molecules* **2019**, *24*, 3658.

(103) Baxendale, I.; Deeley, J.; Griffiths-Jones, C.; Ley, S.; Saaby, S.; Tranmer, G. *Chem. Commun.* **2006**, 2566-2568.

(104) Sagandira, C.; Watts, P. *Beilstein J. Org. Chem.* **2019**, *15*, 2577-2589.

(105) Sampath, G.; Kannan, S. *Catal. Commun.* **2013**, *37*, 41-44.

(106) Findley, T. J. K.; Sucunza, D.; Miller, L. C.; Davies, D. T.; Procter, D. J. *Chem. Eur. J.* **2008**, *14*, 6862-6865.

(107) Yarlagadda, B.; Devunuri, N.; Mandava, VBR. *J. Heterocycl. Chem*. **2017**, *54*, *2*, 864-870.

(108) Chaudhari, M. B.; Mohanta, N.; Pandey, A. M.; Vandana, M.; Karmodiya, K.; Gnanaprakasam, B. *React. Chem. Eng.* **2019**, *4*, 1277-1283.

(109) Qin, X.; Hao, X.; Han, H.; Zhu, S.; Yang, Y.; Wu, B.; Hussain, S.; Parveen, S.; Jing, C.; Ma, B.; Zhu, C. *J. Med. Chem.* **2015**, *58*, *3*, 1254-1267.

(110) Khedar, P.; Pericherla, K.; Kumar, A. *Synlett* **2014**, *25*, 515-518.

(111) Vaněk, V.; Pícha, J.; Fabre, B.; Buděšínský, M.; Lepšík, M.; Jiráček, J. *Eur. J. Org. Chem.* **2015**, 3689-3701.

(112) Mamedov, V.; Zhukova, A.; Syakaev, V.; Beschastnova, T.; Kadyrova, M.; Isaeva, A.; Mamedova, S.; Gavrilova, E.; Latypov, S.; Sinyashin, O. *J. Heterocyclic Chem.* **2019,** *56*, 2221-2234.

(113) Bao, W.; Gao, L.; Ying, W.; Chen, W.; Chen, G.; Wei, W.; Liu, Y.; Li, Q. *Synlett* **2018**, *30*, 109-113.

(114) Pastor, M.; Vayer, M.; Weinstabl, H.; Maulide, N. *J. Org. Chem.* **2022**, *87*, 606-612.

(115) Kulkarni, S. S.; Hu, X.; Manetsch, R. *Chem. Commun.* **2013**, *49*, 1193-1195.

(116) Årstad, E.; Barrett, A. G. M.; Hopkins, B. T.; Köbberling, J. *Org. Lett.* **2002**, *4*, 1975-1977.

(117) Rao, C. S.; Sait, S. S.; Cherukuri, J.; Ramadevi, B.; Reddy, C. V. R. *Asian J. Chem.* **2016**, *28*, *12*, 2579-2581.

(118) da Costa, E. P.; Coelho, S. E.; de Oliveira, A. H.; Araújo, R. M.; Cavalcanti, L. N.; Domingos, J. B.; Menezes, F. G. *Tetrahedron Lett.* **2018**, *59*, *44*, 3961-3964.

(119) Huang, J.; Chen, W.; Liang, J.; Yang, Q.; Fan, Y.; Chen, M. W.; Peng, Y. *J. Org. Chem.* **2021**, *86*, *21*, 14866-14882.

(120) Mamedov, V. A.; Zhukova, N. A.; Syakaev, V. V.; Beschastnova, T. N.; Kadyrova, M. S.; Isaeva, A. O.; Mamedova, S. V.; Gavrilova, E. L.; Latypov, S. K.; Sinyashina, O. G. *J. Heterocycl. Chem.* **2019**, doi:10.1002/jhet.3616.

(121) Vitaku, E.; Smith, D. T.; Njardarson, J. T. *J. Med. Chem.* **2014**, *57*, 10257-10274.

(122) (a) Taylor, R. D.; MacCoss, M.; Lawson, A. D. *J. Med. Chem.* **2014**, *57*, 5845-5859. (b) Pennington, L. D.; Moustakas, D. T. *J. Med. Chem.* **2017**, *60*, 3552-3579. (c) Kittakoop, P.; Mahidol, C.; Ruchirawat, S. *Curr. Top. Med. Chem.* **2014**, *14*, *2*, 239-252.

(123) (a) Roque, J. B.; Kuroda, Y.; Göttemann, L. T.; Sarpong, R. *Nature* **2018**, *564*, 244-248. (b) Dherange, B. D.; Kelly, P. Q.; Liles, J. P.; Sigman, M. S.; Levin, M. D. *J. Am. Chem. Soc.* **2021**, *143*, 11337-11344. (c) Jurczyk, J.; Lux, M. C.; Adpressa, D.; Kim, S. F.; Lam, Y.- H.; Yeung, C. S.; Sarpong, R. *Science* **2021**, *373*, 1004-1012. (d) Woo, J.; Christian, A. H.; Burgess, S. A.; Jiang, Y.; Mansoor, U. F.; Levin, M. D. *Science* **2022**, *376*, 527-532. (e) Jurczyk, J.; Woo, J.; Kim, S. F.; Dherange, B. D.; Sarpong, R.; Levin, M. D. *Nat. Synth.* **2022**, *1*, 352-364.

(124) Joule, J. A. *In Adv. Heterocycl. Chem.* 119 (eds Eric F. V. Scriven & Christopher A. Ramsden) 81-106 (Academic Press, **2016**).

(125) Fremery, M. I.; Fields, E. K. *J. Org. Chem.* **1964**, *29*, 2240-2243.

(126) Miller, R. B.; Frincke, J. M. *J. Org. Chem.* **1980**, *45*, 5312-5315.

(127) Dime, D. S.; McLean, S. *J. Org. Chem.* **1981**, *46*, 4999-5000.

(128) Quin, L. D.; Tyrell, J. A. Fundamentals of Heterocyclic Chemistry: Importance in Nature and in the Synthesis of Pharmaceuticals. *344* (John Wiley & Sons, Inc, **2010**).

(129) a) Chen, F.; Wang, T.; Jiao, N. *Chem. Rev.* **2014**, *114*, 8613-8661. (b) Xia, Y.; Lu, G.; Liu, P.; Dong, G. *Nature* **2016**, 539, 546-550. (c) Chen, P.; Billett, B. A.; Tsukamoto, T.; Dong, G. *ACS Catal.* **2017**, *7*, 1340-1360. (d) Smaligo, A. J.; Swain, M.; Quintana, J. C.; Tan, M. F.; Kim, D. A.; Kwon, O. *Science* **2019**, *364*, 681-685. (e) Xia, Y.; Ochi, S.; Dong, G. *J. Am. Chem. Soc.* **2019**, *141*, 13038-13042. (f) Lyu, H.; Kevlishvili, I.; Yu, X.; Liu, P.; Dong, G. *Science* **2021**, *372*, 175-182.

(130) Qin, H.; Cai, W.; Wang, S.; Guo, T.; Li, G.; Lu, H. *Angew. Chem. Int. Ed.* **2021**, *60*, 20678-20683.

(131) Kennedy, S. H. ; Dherange, B. D.; Berger, K. J.; Levin, M. D. *Nature* **2021**, *593*, 223-227.

(132) Hui, C.; Brieger, L.; Strohmann, C.; Antonchick, A. P. *J. Am. Chem. Soc.* **2021**, *143*, 18864-18870.

(133) Im, J. K.; Jeong, I.; Yang, B.; Moon, H.; Choi, J.; Chung. W. *Synthesis* **2021**, *53*, 1760-1770.

(134) (a) Smith, P. A. S. In Molecular Rearrangements; de Mayo, P., Ed.; Wiley: New York, **1963**; Vol. 1, Chapter 8. (b) Lang, S.; Murphy, J. A. *Chem. Soc. Rev.* **2006**, *35*, 146-156 (c) Wrobleski, A.; Coombs, T. C.; Huh, C. W.; Li, S.-W.; Aubé, J. *Org. React.* **2012**, *78*, 1-320.

(135) Liu, S.; Cheng, X.; *Nat. Commun.* **2022**, *13*, 425.

(136) Kelly, P. Q.; Filatov, A. S.; Levin, M. D. *Angew. Chem. Int. Ed.* **2022**, *61*, e202213041.

(137) Wang, J.; Lu, H.; He, Y.; Jing, C.; Wei, H. *J. Am. Chem. Soc.* **2022**, *144*, 22433-22439.

(138) Finkelstein, P.; Reisenbauer, J. C.; Green, O.; Botlik, B.; Florin, A.; Morandi, B. (ChemRxiv)

(139) Li, C.-J. *Acc. Chem. Res.* **2009**, *42*, 335-344.

(140) Wesenberg, L. J.; Diehl, E.; Zähringer, T. J. B.; Dörr, C.; Schollmeyer, D.; Shimizu, A.; Yoshida, J.; Hellmich, U. A.; Waldvogel, S. *Chem. Eur. J.* **2020**, *26*, 17574-17580.

(141) Zhang, L.; Liardet, L.; Luo, J.; Ren, D.; Grätzel, M.; Hu, X. *Nat. Catal.* **2019**, *2*, 366-373.

(142) Reisenbauer, C.; Green, O.; Franchino, A.; Finkelstein, P.; Morandi, B. *Science* **2022**, *377*, 1104-1109.

(143) (a) Talukdar, V.; Vijayan, A.; Katari, N. K.; Radhakrishnan, K. V.; Das, P. *Adv. Synth.Catal.* **2021**, *363*, 1202-1245. (b) Feng, J.; Wang, L.; Xue, X.; Chao, Z.; Hong, B.; Gu, Z. *Org. Lett.* **2021**, *23*, *20*, 8056-8061.

(144) (a) Bakthadoss, M.; Kannan, D. RSC Adv. **2014**, *4*, 11723-11731. (b) Bakthadoss, M.; Vinayagam, V. *Mol. Divers.* **2021**, *25*, 2447-2458.

(145) Ghosh, A.; Sarkara, A.; Brindisi, M. *Org. Biomol. Chem.* **2018**, *16*, *12*, 2006-2027.

(146) Jaiswal, Y.; Kumar, Y.; Pal, J.; Subramanian, R.; Kumar, A. *Chem. Commun.* **2018**, *54*, 7207-7210.

(147) Mehta, B. K.; Yanagisawa, K.; Shiro, M.; Kotsuki, H. *Org. Lett*. **2003**, *5*, *10*, 1605-1608.

(148) Emmerling, S. T.; Schuldt, R.; Bette, S.; Yao, L.; Dinnebier, R. E.; Kästner, J.; Lotsch, B. V. *J. Am. Chem. Soc.* **2021**, *143*, 15711-15722.

(149) Chen, Y.; Li, F.; Bo, Z. *Macromolecules* **2010**, *43*, 1349-1355.

(150) Emmerling, S. T.; Ziegler, F.; Fischer, F. R.; Schoch, R.; Bauer, M.; Plietker, B.; Buchmeiser, M. R.; Lotsch, B. V. *Chem. Eur. J*. **2022**, 28, e2021041.

(151) Xinya, L.; Zhuangzhuang, G.; Yanpeng, L.; Xiaoyu, C.; Jingya, L.; Dapeng, Z.; Yangjie, W.; Yusheng, W. *Org. Biomol. Chem.* **2022**, *20*, 1391-1395.

(152) Bao, L.; Wang, Z. X.; Chen, X. Y. *Org. Lett*. **2023**, *25*, *3*, 565-568.

(153) Subaramanian, M.; Sivakumar, G.; Balaraman, E. *Chem. Rec.* **2021**, *21*, 3839-3871.

(154) Properzi, R.; Marcantoni, E. *Chem. Soc. Rev.* **2014**, *43*, 779-791.

(155) Gunanathan, C.; Milstein, D. *Science* **2013**, *341*, 1229712.

(156) (a) Crabtree, R. H. *Chem. Rev.* **2017**, *117*, 9228-9246. (b) Filonenko, G. A.; van Putten, R.; Hensen, E. J. M.; Pidko, E. A. *Chem. Soc. Rev.* **2018**, *47*, 1459-1483.

(157) Reed-Berendt, B. G.; Latham, D. E.; Dambatta, M. B.; Morrill, L. C. *ACS Cent. Sci.* **2021**, *7*, *4*, 570-585.

(158) Grigg, R.; Mitchell, T. R. B.; Sutthivaiyakit, S.; Tongpenyai, N. *J. Chem. Soc. Chem. Commun.* **1981**, 611-612.

(159) Watanabe, Y.; Tsuji, Y.; Ohsugi, Y. *Tetrahedron Lett*. **1981**, *22*, 2667-2670.

(160) Watanabe, Y.; Tsuji, Y.; Ige, H.; Ohsugi, Y.; Ohta, T. *J. Org. Chem*. **1984**, *49*, 3359-3363.

(161) Murahashi, S.; Rondo, R.; Hakata, T. *Tetrahedron Lett*. **1982**, *23*, 229-232.

(162) Gnanaprakasam, B.; Zhang, J.; Milstein, D. *Angew. Chem. Int. Ed.* **2010**, *49*, 1468-1471.

(163) Gnanaprakasam, B.; Balaraman, E.; Ben-David, Y.; Milstein, D. *Angew. Chem.* **2011**, *123*, 12448-12452.

(164) Gunanathan, C.; Ben-David, Y.; Milstien, D. *Science* **2007**, *317*, 790-792.

(165) Sardar, B.; Jamatia, R.; Samanta, A.; Srimani, D. *J. Org. Chem.* **2022**, *87*, 5556-5567.

(166) Zhou, J.; Fang, J. *J. Org. Chem.* **2011**, *76*, 7730-7736.

(167) Kuwahara, T.; Fukuyama, T.; Ryu, I. *Org. Lett*. **2012**, *14*, 4703-4705.

(168) Thiyagarajan, S.; Sankar, R. V.; Gunanathan, C. *Org. Lett*. **2020**, *22*, 7879-7884.

(169) Sharma, R.; Mondal, A.; Samanta, A.; Biswas, N.; Das, B.; Srimani, D. *Adv. Synth. Catal.* **2022**, *364*, 2429–2437.

(170) Bisht, G. S.; Chaudhari, M. B.; Gupte, V. S.; Gnanaprakasam, B. *ACS Omega* **2017**, *2*, 8234-8252.

(171) (a) Jensen, T.; Madsen, R. *J. Org. Chem.* **2009,** *74*, 3990-3992. (b) Chaudhari, M. B.; Bisht, G. S.; Kumari, P.; Gnanaprakasam, B. *Org. Biomol. Chem.* **2016**, *14*, 9215-9220. (c) Jin, H.; Xie, J.; Pan, C.; Zhu, Z.; Cheng, Y.; Zhu, C. *ACS Catal.* **2013**, *3*, 2195-2198. (d) Chaudhari, C.; Siddiki, S. M. A. H.; Kon, K.; Tomita, A.; Tai, Y.; Shimizu, K-I. *Catal. Sci. Technol.* **2014**, *4*, 1064-1069. (e) Putra, A. E.; Oe, Y.; Ohta, T. *Eur. J. Org. Chem.* **2015**, 7799-7805.

(172) Bisht, G. S.; Pandey, A. M.; Chaudhari, M. B.; Agalave, S. G.; Kanyal, A.; Karmodiya, K.; Gnanaprakasam, B. *Org. Biomol. Chem.* **2018, *16***, 7223-7229.

(173) Zhang, J.; Leitus, G.; Ben-David, Y.; Milstein, D. *J. Am. Chem. Soc.* **2005**, 127, 10840-10841.

(174) Sølvhøj, A.; Madson, R. *Organometallics* **2011**, *30*, 6044.

(175) Pridmore, S. J.; Slatford, P. A.; Williams, J. M. J.; *Tetrahedron Lett.* **2007**, *48*, 5111-5114.

(176) McInturff, E. L.; Mowat, J.; Waldeck, A. R.; Krische, M. J.; *J. Am. Chem. Soc.* **2013**, *135*, 17230-17235.

(177) Bala, M.; Verma, P. K.; Sharma, U.; Kumar, N.; Singh, B. *Green Chem.* **2013**, *15*, 1687-1693.

(178) Zhang, M.; Neumann, H.; Beller, M. *Angew. Chem. Int., Ed.* **2013**, *52*, 597-601.

(179) (a) Keller, P. A. In Comprehensive Heterocyclic Chemistry III; Katritzky, A. R., Ramsden, C. A., Scriven, E. F. V., Taylor, R. J. K., Eds.; Elsevier: Oxford, U.K., **2008**, *7*, 217-308. (b) The Alkaloids: Chemistry and Biology; Cordell, G. A., Ed.; Academic Press: San Diego, CA, **2000**, *54*. (c) Pharmaceuticals: Classes, Therapeutic Agents, Areas of Application; McGuire, J. L., Ed.; Wiley−VCH: Weinheim, Germany, **2000**, 1-4. (d) Brown, B. R. The Organic Chemistry of Aliphatic Nitrogen Compounds; Cambridge University Press: Cambridge, U.K., **2004**. (e) Joule, J. A.; Mills, K. Heterocyclic Chemistry, 5th Edition; Wiley: Chichester, U.K., **2010**.

(180) (a) Allais, C.; Grassot, J. M.; Rodriguez, J.; Constantieux, T. *Chem. Rev.* **2014**, *114*, 10829-10868. (b) Hill, M. D. *Chem. Eur. J.* **2010**, *16*, 12052-12062. (c) Broere, D. L. J.; Ruijter, E. *Synthesis* **2012**, *44*, 2639-2672.

(181) (a) Crabtree, R. H. *Chem. Rev.* **2017**, *117*, 9228-9246. (b) Filonenko, G. A.; Van Putten, R.; Hensen, E. J. M.; Pidko, E. A. *Chem. Soc. Rev.* **2018**, *47*, 1459-1483.

(182) (a) Nandakumar, A.; Midya, S. B.; Landge, V. G.; Balaraman, E. *Angew.Chem. Int. Ed.* **2015**, *54*, 11022-11034. (b) Huang, F.; Liu, Z.; Yu, Z. *Angew. Chem. Int. Ed.* **2016**, *55*, 862-875.

(183) (a) Michlik, S.; Kempe, R. *Nat. Chem.* **2013,** *5*, 140-144. (b) Michlik, S.; Kempe, R. *Angew. Chem. Int., Ed.* **2013**, *52*, 6326-6329.

(184) Srimani, D.; Ben-David, Y.; Milstein, D. *Angew. Chem. Int., Ed.* **2013**, *52*, 4012 -4015.

(185) Iida, K.; Miura, T.; Ando, J.; Saito, S. *Org. Lett.* **2013**, *15*, 1436-1439.

(186) Pan, B.; Liu, B.; Yue, E.; Liu, Q.; Yang, Z.; Wang, Z.; Sun, W. *ACS Catal.* **2016**, *6*, 1247-1253.

(187) Kallmeier, F.; Dudziec, B.; Irrgang, T.; Kempe, R. *Angew. Chem. Int., Ed.* **2017**, *56*, 7261-7265.

(188) Chai, H.; Wang, L.; Liu, T.; Yu, Z. *Organometallics* **2017**, *36*, 4936-4942.

(189) Deng, D.; Hu, B.; Yang, M.; Chen, D. *Organometallics* **2018**, *37*, 2386-2394.

(190) Midya, S.; Landge, V.; Sahoo, M.; Rana, J.; Balaraman, E. *Chem. Commun.* **2018**, *54*, 90-93.

(191) (a) Singh, K.; Vellakkaran, M.; Banerjee, D. *Green Chem.* **2018**, *20*, 2250. (b) Alanthadka, A.; Bera, S.; Vellakkaran, M.; Banerjee, D**.** *J. Org. Chem.* **2019**, *84*, 13557-13564.

(192) Mastalir, M.; Glatz, M.; Pittenauer, E.; Allmaier, G.; Kirchner, K. *Org. Lett*. **2019**, *21*, 1116-1120.

(193) Chai, H.; Zhang, G.; Tan, W.; Ma, J. A. *Appl. Organomet. Chem.* **2020**, *34*, e5367.

(194) (a) Gholap, S. S. *Eur. J. Med. Chem.* **2016**, *110*, 13-31. (b) Rigby, J. H.; Cavezza, A.; Heeg, M. J. *J. Am. Chem. Soc.* **1998,** *120*, 3664-3670. (c) Li, W.; Usman, M.; Wu, L. -Y.; Liu, W. -B. *J. Org. Chem.* **2019**, *84*, 15754-15763.

(195) (a) Patil, S. A.; Patil, R.; Pfeffer, L. M.; Miller, D. D**.** *Future Med. Chem.* **2013**, *5*, 1647-1660. (b) Shaheen, F.; Ahmad, M.; Nahar, K. S.; Samreen, H. S.; Anjum, S.; Tashkhodjaev, B.; Turgunov, K.; Sultankhodzhaev, M. N.; Choudhary, M. I.; Ahmad, M.; Attaur, R. *Eur. J. Org. Chem.* **2006**, 2371-2377. (c) Morkunas, M.; Dube, L.; Götz, F.; Maier, M. E. *Tetrahedron Lett*. **2013**, *69*, 8559-8563. (d) Cottiglia, F.; Dhanapal, B.; Stcher, O.; Heilmann, J. *J. Nat. Prod.* **2004**, *67*, 537-541.

(196) Muthaiah, S.; Hong, S. H. *Adv. Synth. Catal.* **2012**, *354*, 3045-3053.

(197) Stanovnik, B. *Eur. J. Org. Chem.* **2019**, 5120-5132.

(198) Aoyagi, Y.; Mizusaki, T.; Shishikura, M.; Komine, T.; Yoshinaga, T.; Inaba, H.; Ohta, A.; Takeya, K. *Tetrahedron*, **2006**, *62*, 8533-8538.

(199) Hanbauer, M.; Nazir, Z.; Hildebrand, P.; Figini, A.; Liang, L.; Fumagalli, T. US 2014/0081020 A1.

(200) (a) Zbieg, J. R.; Yamaguchi, E.; McInturff, E. L.; Krische, M. J. *Science* **2012**, *332*, 324-327. (b) Murahashi, S-I.; Naota, T.; Ito, K.; Maeda, Y.; Taki, H. *J. Org. Chem.* **1987**, *52*, 4319-4327. (c) Xie, X.; Huynh, H. V. *ACS Catal*. **2015**, *5*, 4143-4151. (d) Dam, J. H.; Osztrovszky, G.; Nordstrøm, L. U. Madsen, R. *Chem. Eur. J*. **2010**, *16*, 6820-6827. (e) Kuwahara, T.; Fukuyama, T.; I. Ryu. *RSC Adv*. **2013**, *3*, 13702-13704.

(201) Reddy, C. R.; Reddy, M. D.; Srikanth, B. *Org. Biomol. Chem*. **2012**, *10*, 4280-4288.

(202) Luo, J.; Lu, D.; Peng, Y.; Tang, Q. *Asian J. Org. Chem.* **2017**, *6*, 1546-1550.

(203) Hu, L.; Luo, J.; Lu, D.; Tang, Q. *Tetrahedron Lett*. **2018**, *59*, 1698-1701.

(204) Huy, Q.; Yong, T.; Leea, R.; Kim, S. H. *Tetrahedron* **2014**, *70*, 8108-8113.

(205) Huang, K.; Veal, J. M.; Fadden, R. P.; Rice, J.W.; Eaves, J.; Strachan, J. P.; Barabasz, A. F.; Foley, B. E.; Barta, T. E.; Ma, W.; Silinski, M. A.; Hu, M.; Partridge, J, M.; Scott, A.; DuBois, L. G.; Freed, T.; Steed, P. M.; Ommen, A. J.; Smith, E. D.; Hughes, P. F.; Woodward, A. R.; Hanson, G. J.; McCall, W. S.; Markworth, C. J.; Hinkley, L.; Jenks, M.; Geng, L.; Lewis, M.; Bert Pronk, J. O.; Verleysen, K.; Hall, S. E. *J. Med. Chem.* **2009**, *52*, 4288-4305.

(206) Sridharan, V.; Ribelles, P.; Ramos, M. T.; Menéndez. J. C. *J. Org. Chem*. **2009**, *74*, 5715-5718.

(207) Cini, E.; Petricci, E.; Truglio, G. I.; Vecchio, M.; Taddei, M. *RSC Adv*. **2016**, *6*, 31386-31390.

(208) Panday, A. K.; Mishra, R.; Jana, A.; Parvin, T.; Choudhury, L. *J. Org. Chem*. **2018**, *83*, 3624-3632.

(209) Na, J. E.; Lee, K. Y.; Park, D. Y.; Kim. J. N. *Bull. Korean Chem. Soc*. **2005**, *26*, 323-326.

(210) Fukada, N.; Trudell, M. L.; Johnson, B.; Cook, J. H. *Tetrahedron Lett*. **1985,** *2*, 2139-2142.

LIST OF PUBLICATIONS

1. **Pandey, A. M**.; Mondal, Shankhajit.; Andotra, P.; Gnanaprakasam, B. Skeletal Editing through Solid-State Melt Rearrangement of Azidofluorenes for the Synthesis of Phenanthridine Derivatives. (Manuscript under preparation)
2. **Pandey, A. M**.; Mondal, S.; Gnanaprakasam, B. Continuous Flow Direct Azidation of Alcohols and Peroxides for the Synthesis of Quinoxalinones, Benzooxazinone and Triazole Derivatives. *J. Org. Chem.*, **2022**, *87*, 15, 9926–9939. (**Highlighted as a useful chemistry in Organic Chemistry Portal**)
3. "A Continuous Flow Process for Synthesis of Organic Azides" Indian Patent No. **IN202221031963** dated March 06, 2022.
4. "A Continuous Flow Process for Synthesis of Organic Azides" US Patent No. **PCT/IB2023/055692** filed June 02, 2023.
5. **Pandey, A. M**.; Digrawal, N; Mohanta, N.; Jamdade, A.; Chaudhari, M. B.; Bisht, G. S.; Gnanaprakasam, B. Catalytic Acceptorless Dehydrogenation of Amino Alcohols and 2-Hydroxybenzyl Alcohols for Annulation Reaction under Neutral Condition. *J. Org. Chem.*, 2021, *86*, 13, 8805–8828.
6. **Pandey, A. M**.; Agalave, S. G.; Gnanaprakasam, B. MnO_2@Fe_3O_4 Magnetic Nanoparticles as Efficient and Recyclable Heterogeneous Catalyst for Benzylic sp^3 C-H Oxidation. *Chem. Asian J*., **2019**, *14*, 3414 –3423.
7. Mondal, S.; **Pandey, A. M**.; Gnanaprakasam, B. Continuous-Flow Fe-Zeolite Catalyzed Temperature Directed Synthesis of Bioactive Tetraketones and Xanthenes using Epoxide and Cyclic-1,3-diketone via Meinwald Rearrangement. *React. Chem. Eng.*, **2023**, 8, 855-862.
8. Mohanta, N.; **Pandey, A. M**.; Mondal, S.; Mondal, S.; Gnanaprakasam, B. Catalyst Assisted Selective Vinylation and Methylallylation of Quaternary Carbon Centre by using tert-Butyl Acetate. (Just accepted in *J. Org. Chem.*,)
9. Chaudhari, M. B.; Mohanta, **Pandey, A. M**.; Vandana, M.; Karmodiya, K.; Gnanaprakasam, B. Peroxidation of 2-oxindole and Barbituric Acid Derivatives under Batch and Continuous Flow using an Eco-friendly Ethyl Acetate Solvent. *React. Chem. Eng*., **2019**, 4, 1277-1283.

10. Bisht, G. S.; **Pandey, A. M**.; Chaudhari, M. B.; Agalave, S. G.; Kanyal, A.; Karmodiya, K.; Gnanaprakasam, B. Ru-Catalyzed Dehydrogenative Synthesis of Antimalarial Arylidene Oxindoles. *Org. Biomol. Chem*., **2018**, *16*, 7223-7229.

ACES Asian Chemical Editorial Society

DOI: 10.1002/asia.201900810

CHEMISTRY AN ASIAN JOURNAL Full Paper

MnO_2@Fe_3O_4 Magnetic Nanoparticles as Efficient and Recyclable Heterogeneous Catalyst for Benzylic sp^3 C–H Oxidation

Akanksha M. Pandey,[a] Sandip G. Agalave,[a] Chathakudath P. Vinod,[b] and Boopathy Gnanaprakasam*[a]

Abstract: Herein, we report a highly chemoselective and efficient heterogeneous MnO_2@Fe_3O_4 MNP catalyst for the oxidation of benzylic sp^3 C–H group of ethers using TBHP as a green oxidant to afford ester derivatives in high yield under batch/continuous flow module. This catalyst was also effective for the benzylic sp^3 C–H group of methylene derivatives to furnish the ketone in high yield which can be easily integrated into continuous flow condition for scale up. The catalyst is fully characterized by spectroscopic techniques and it was found that 0.424% MnO_2@Fe_3O_4 catalyzes the reaction; the magnetic nanoparticles of this catalyst could be easily recovered from the reaction mixture. The recovered catalyst was recycled for twelve cycles without any loss of the catalytic activity. The advantages of MnO_2@Fe_3O_4 MNP are its catalytic activity, easy preparation, recovery, and recyclability, gram scale synthesis with a TOF of up to 14.93 h^{-1} and low metal leaching during the reaction.

Introduction

Designing a sustainable chemical process for the functional group transformation is one of the formidable challenges in organic synthesis.[1] Metal-catalyzed direct conversion of the C–H bond to carbonyl compounds using oxidant is greatly increased in the last few decades among the synthetic chemist due to the molecular economy and reaction greenness. Hence, oxidation of a saturated sp^3 C–H bond can rapidly install an oxygen atom on a carbon atom and have attracted considerable attention, given that most of the recognized drugs and natural products are oxygen-containing compounds.[2] In recent years, a plethora of methodologies have been developed for direct benzylic sp^3 C–H bond oxyfunctionalization.[3] However, most of the commonly employed conditions include stoichiometric quantities of transition metal salts which pose problems in terms of cost, toxicity and atom economy.[4] Selective benzylic oxidation using catalytic amount of transition metals such as Cr,[5] Mn,[6] Co,[7] Ru,[8] Rh,[9] Fe,[10] Re,[11] etc and post-transition metal Bi[12] has been reported. The reported homogeneous transition metal catalysts for the direct transformation of activated methylene group have several advantages to afford the ketone in moderate to good yield. However, in spite of the advances, there are limitations exist in this transformation such as the decomposition of the metal catalysts, the lack of regio- and stereoselectivity, exothermic reactions, the problems of catalyst extraction and recycling as well as product purification make them less ideal for the synthesis of fine chemicals where product contamination with heavy metal is highly undesirable which led to environmental and economic concern in large scale synthesis.[13] Thus, there is ongoing interest in finding more sustainable catalysts that assist catalytic transformation to take place under more realistic and environmentally benign conditions. Also, there is a report for transition metal free benzylic sp^3 C–H bond oxidation of activated methylene group to form ketone or ester which requires external additives $NaNO_2$ and HCl.[14] Recently, J. Tan and co-workers[15] showed *tert*-butyl hydrogen peroxide (TBHP) mediated direct oxidation reaction of benzylic sp^3 C–H bonds to ketones, but there is no such report on the continuous flow benzylic sp^3 C–H bond oxidation of ether to ester.

Heterogenization of the presented homogeneous catalysts, particularly expensive and/or toxic heavy metal complexes could resolve these problems. From these perspectives various materials such as mesoporous silica,[16] activated carbon,[17] polymers,[18] biomass,[19] etc. have been used as a support to generate a heterogeneous catalytic system. Recently, Sekar, et al. reported the oxidation of alkylarene using binaphthyl stabilized Pt nanoparticles (Pt-BNP) as a catalyst.[20]Advantageously, these supported catalyst systems can be effectively recycled and reused with the inherent catalytic activity.

Magnetic nanomaterials are found to be more selective and effective than conventional heterogeneous materials as a robust, readily available, extremely small size and large surface area of heterogeneous catalyst support. Further, it has more volume ratio which allows more reactions to occur at the same time and consequently speed up the reaction process.[21,22] Advantageously, they are magnetically separable, which eliminates the requirement of catalyst filteration or centrifugation

[a] A. M. Pandey, Dr. S. G. Agalave, Dr. B. Gnanaprakasam
Department of Chemistry
Indian Institute of Science Education and Research
Pune-411008 (India)
E-mail: gnanaprakasam@iiserpune.ac.in

[b] Dr. C. P. Vinod
CSIR-NCL Catalysis and Inorganic Chemistry Division
Pune (India)

Supporting information and the ORCID identification number(s) for the author(s) of this article can be found under:
https://doi.org/10.1002/asia.201900810.

after completion of the reaction. The Fe_3O_4 MNPs, due to their unique physicochemical properties becoming increasingly significant in the field of catalysis, imaging, photonics, nanoelectronics, sensors, biomaterials, and biomedicine.[23] In literature, these Fe_3O_4 nanoparticles are used for the selective oxidation of benzylic and allylic C–H bonds to carbonyl compounds using TBHP as an oxidant.[24] Manganese-based catalyst has attracted considerable research interest because of its nanostructures have a large surface area and high catalytic activity as well as it is cheap, mild and nontoxic oxidative reagent used for the selective oxidation of various functional groups.[25] Thus, developing Mn supported on Fe_3O_4 MNPs for benzylic sp^3 C–H oxidation of ether and methylene compounds are highly attractive and desirable approach in terms of the green chemistry points of view; which will also allow finding a more economical and environmentally benign procedure.

Herein, we wish to disclose a facile and atom-economical methodology for the direct oxidation of benzylic sp^3 C–H bond using $MnO_2@Fe_3O_4$ as an MNP supported catalyst for the oxidative esterification of benzylic ethers to form various ester derivatives (Scheme 1).

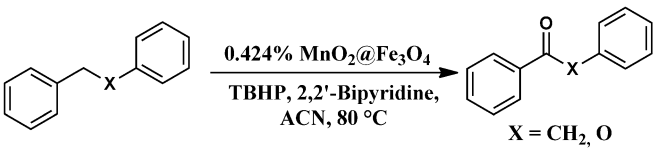

Scheme 1. General protocol for the benzylic sp^3 C–H oxidation using $MnO_2@Fe_3O_4$ MNP catalyst.

The newly developed catalytic system proceeds with high selectivity and broad substrate scope under mild reaction conditions with TBHP as the environmentally benign terminal oxidant. It is also found that the present catalytic system was effective and versatile for the oxidative benzylic sp^3 C–H group to form various ketone derivatives. This novel and chemoselective methodology work well in batch and continuous flow module. To date, to the best of our knowledge, $MnO_2@Fe_3O_4$ MNP catalyzed benzylic sp^3 C–H group oxidation of ethers and methylene derivatives using TBHP as an oxidant have not been reported.

Results and Discussion

The synthesis of nano-sized $MnO_2@Fe_3O_4$ was achieved by the procedure reported for $Fe(OH)_3@Fe_3O_4$.[26] The % of Mn on Fe_3O_4 support was analyzed by Microwave Plasma Atomic Emission Spectroscopy (MP-AES) analysis which showed that catalyst contains 0.424% of Mn.

Figure 1 represents the XRD pattern of 0.424% $MnO_2@Fe_3O_4$ nanocomposites, showing that the peaks of both Fe_3O_4 and MnO_2 appear along with enhanced peak intensity which is caused by overlapping of both the peaks. As revealed, diffraction peaks are completely corresponding to the standard pattern characteristic peaks of the magnetite cubic inverse spinel structure (JCPDS 01-074-2435).

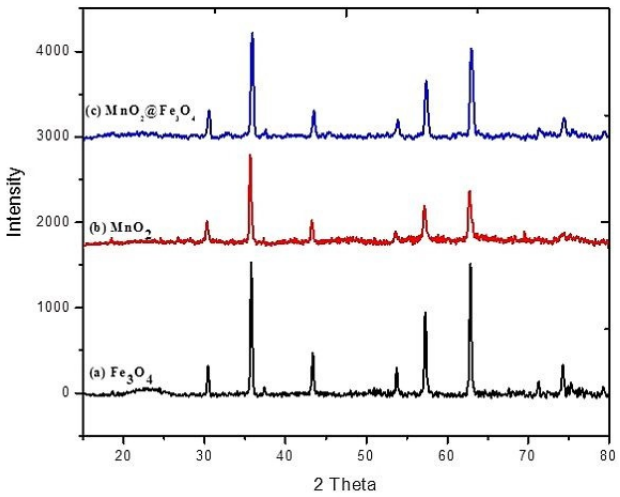

Figure 1. PXRD data of (a) Fe_3O_4; (b) MnO_2; (c) $MnO_2@Fe_3O_4$.

The morphology of the fresh and used $MnO_2@Fe_3O_4$ catalyst was evaluated by TEM analysis (Figure 2). From TEM analysis it is found that, the average particle size of fresh catalyst is 10.48 nm, whereas average particle size of used catalyst is 12.34 nm.

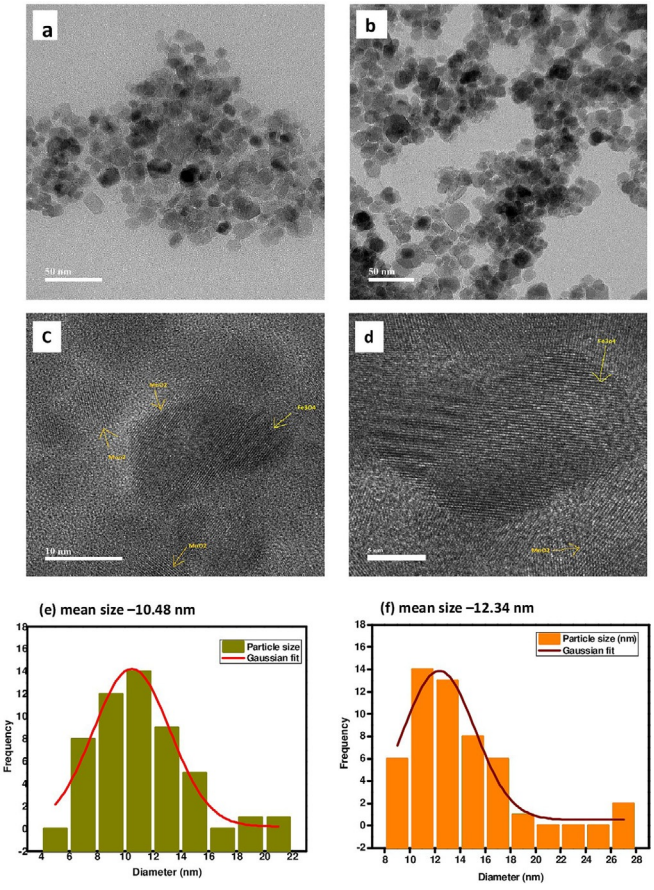

Figure 2. TEM images of $MnO_2@Fe_3O_4$ catalyst (a) Fresh catalyst, (b) used catalyst; Lattice fringes for (c) fresh catalyst, (d) used catalyst; Histograms generated for (e) fresh, (f) used $MnO_2@Fe_3O_4$ catalyst.

The N_2 adsorption-desorption isotherms and pore size distribution of fresh MnO_2@Fe_3O_4 catalyst is shown in Figure 3. From Figure 3, it is clear that pure MnO_2@Fe_3O_4 catalyst exhibited isotherm of type IV, which is a typical characteristic of the mesoporous material.[27] Specific surface area (SBET) was calcu-

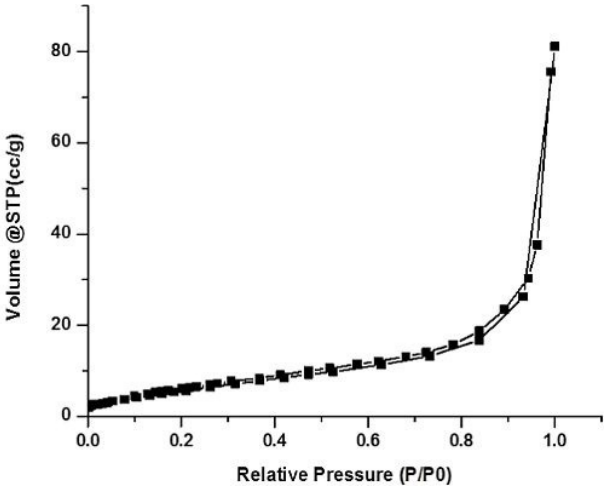

Figure 3. BET isotherm of MnO_2@Fe_3O_4 catalyst.

lated by employing the Brunauer-Emmett-Teller (BET) method and the pore size distribution is obtained by means of Barrett-Joyner-Halenda (BJH) method equation using the adsorption isotherm branch. Figure 3 shows that the volume adsorbed increases with increasing relative pressures for all isotherms which are due to the volume filling of micropores in Fe_3O_4 membrane. The BET specific surface area and the pore diameter of MnO_2@Fe_3O_4 were found to be 13.19 $m^2 g^{-1}$ and 0.059 $cm^3 g^{-1}$, respectively.

Thermal gravimetric analysis (TGA) of the MnO_2@Fe_3O_4 composite nanoparticles were also performed at the range of 25 to 800 °C, with a temperature ramp rate of 10 °C min^{-1} under a nitrogen atmosphere (Figure 4). As shown in Figure 4, the first weight loss stage (below 150 °C) can be attributed to the evaporation of water and solvent molecules onto the surface of the

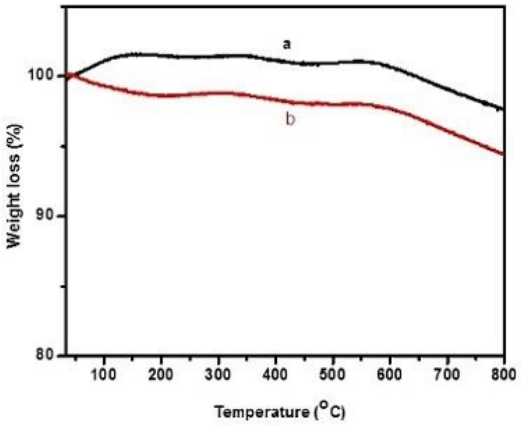

Figure 4. Thermogravimetric analysis of (a) Fe_3O_4; (b) MnO_2@Fe_3O_4 catalyst.

catalyst. The weight loss of nanocomposites is about 3.3% at 300–550 °C, corresponding to the thermal decomposition of the crystal phase transformation of Fe_3O_4 to γ-Fe_2O_3. Thus, the results indicate that MnO_2@Fe_3O_4 catalyst has excellent stability at temperatures as high as 800 °C. Surface morphology of fresh MnO_2@Fe_3O_4 nanocomposite was determined by FESEM (Figure 5). The FESEM image of MnO_2@Fe_3O_4 showing the formation of spherical particles with an average size 14–23 nm range. The EDAX analysis reveals that Fe, O, and Mn are the main elements present with Fe being the most abundant in the selected field.

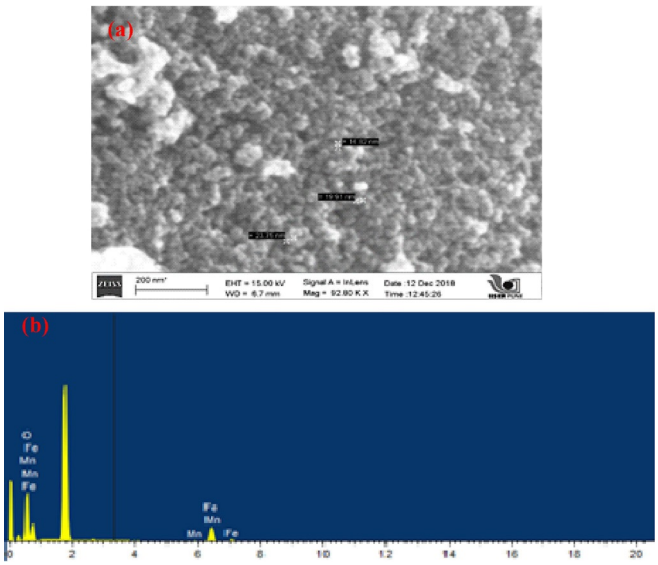

Figure 5. (a) FESEM images of MnO_2@Fe_3O_4 catalyst; (b) EDAX of MnO_2@Fe_3O_4 catalyst.

To confirm the XRD results, the compositions and the valence states of fresh MnO_2@Fe_3O_4 MNP were further characterized with XPS and the results are shown in Figure 6. The Mn peak is analyzed in Figure 6a, which shows that each broad peak can be classified into two parts at 641.52 and 643.06 eV for $Mn2p_{3/2}$ and 653.58 and 656.34 for $Mn2p_{1/2}$. The peaks at 641.52 and 643.06 eV are the characteristics of Mn^{3+} while those at 653.58 and 656.34 eV are the characteristics of Mn^{4+}.[28,29] Moreover, the Fe spectrum is depicted in Figure 6b, and two dominant peaks located at 711.0 and 724.23 eV are in good accordance with Fe $2p_{3/2}$ and Fe $2p_{1/2}$ spin orbit peaks along with other peaks which are consistent with the standard Fe_3O_4 XPS spectrum in which Fe is present in the form of Fe^{2+} and Fe^{3+}. For the O1s XPS spectrum (Figure 6c), the spectrum contains three main peaks located at 530.09, 530.70, and 531.98 eV.[30] The XPS results for used MnO_2@Fe_3O_4 MNP is in ESI.

Catalytic studies

Initially, the conversion of (benzyloxy)benzene **1a** into phenyl benzoate **2a** was chosen as a model reaction using 7 mmol of TBHP (5–6 M in decane) as an oxidant in acetonitrile (ACN) solvent at room temperature for 24 hrs. To identify the impor-

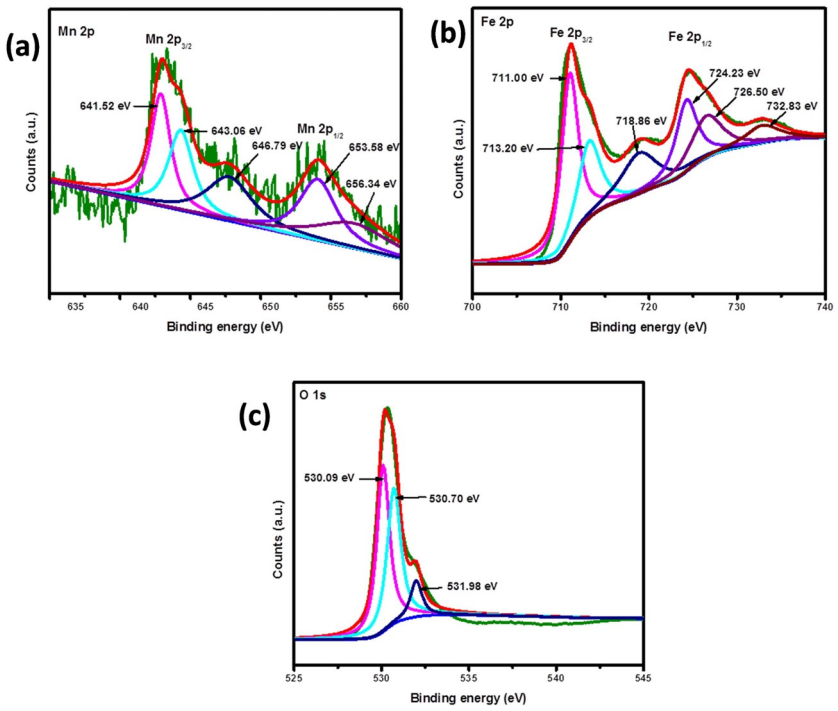

Figure 6. XPS for fresh MnO_2@Fe_3O_4 MNP catalyst of (a) Mn $2p_{3/2}$ and $2p_{1/2}$; (b) Fe $2p_{3/2}$ and $2p_{1/2;}$ (c) O 1s.

tance of the catalyst for the oxidation of (benzyloxy)benzene **1a**, a blank control experiment was performed (Table 1, entry 1), and no phenyl benzoate **2a** was detected. Heating of **1a** in ACN by using 5 mol% $Mn(OAc)_3.2H_2O$ gave 23% of phenyl benzoate **2a** along with the recovery of starting material (Table 1, entry 2). In another control experiment only with Fe_3O_4, 33% yield of phenyl benzoate **2a** was observed when the reaction carried out at 80 °C (Table 1, entry 3).

Table 1. Optimization of the reaction conditions (solvent) for the benzylic sp^3 C–H group.

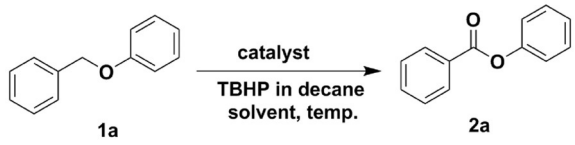

entry	catalyst (50 mg)	solvent	*T* [°C]	yield [%]
1	–	ACN	80	nd
2	$Mn(OAc)_3.2H_2O$	ACN	80	23
3	Fe_3O_4	ACN	80	33
4	MnO_2@Fe_3O_4	ACN	rt	38
5	MnO_2@Fe_3O_4	ACN	80	55
6	MnO_2@Fe_3O_4	ACN	100	55
7	MnO_2@Fe_3O_4	DCE	80	48
8	MnO_2@Fe_3O_4	DCM	80	30
9	MnO_2@Fe_3O_4	Chlorobenzene	80	50
10	MnO_2@Fe_3O_4	DEC	80	50
11	MnO_2@Fe_3O_4	DMSO	80	55
12	MnO_2@Fe_3O_4	1,4-Dioxane	80	nd
13	MnO_2@Fe_3O_4	DME	80	nd
14	MnO_2@Fe_3O_4	Acetone	80	nd

Reaction conditions: (benzyloxy)benzene **1a** (1 mmol), TBHP in decane (7 mmol), and 50 mg of catalyst were stirred at various temperature (see table 1) for 24 hrs.

Whereas 0.424% MnO_2@Fe_3O_4 catalyst at room temperature condition afforded **1a** in 38% yield (Table 1, entry 4). Further, heating of **1a** in ACN solvent using 50 mg of 0.424% MnO_2@Fe_3O_4 MNP afforded 55% of **2a** (Table 1, entry 5). Increasing the temperature up to 100 °C has no influence on the outcome of the reaction (Table 1, entry 6). Performing this reaction with other solvents such as dichloroethane (DCE), dichloromethane (DCM), chlorobenzene, diethyl carbonate (DEC) and dimethylsulfoxide (DMSO) has not improved the yield (Table 1, entry 7–11). However, no phenyl benzoate was detected when 1,4-dioxane, dimethoxyethane (DME) and acetone were employed as a solvent (Table 1, entry 12–14).

Furthermore, we have also optimized the effect of various oxidants and additives for the oxidation reaction. Oxidants such as 4-methyl pyridine-*N*-oxide, $K_2S_2O_8$, TEMPO, and NHPI are failed to deliver or giving less yield of phenyl benzoate **2a** (Table 2, entries 2–5). Based on the previous studies,[9,31] the role of the nitrogen-containing ligand was pivotal in the benzylic sp^3 C–H oxidation reaction. This is because that nitrogen-containing ligand such as triethylamine, pyridine, 2,2′-bipyridine could behave as a hydrogen bond acceptor with TBHP to speed up the formation of *t*-butoxyl radical. This radical could abstract the hydrogen from a benzylic carbon atom of the substrate.[32]There is no (benzyloxy)benzene **2a** formation when triethylamine was used as a additive (Table 2, entry-6). Moreover, the good conversion of about 66% was obtained when 10 mol% of pyridine used as a additive (Table 2, entry 7). Other oxidants were not effective for this transformation (Table 2, entries 8–10). The reactions proceeded smoothly when the reaction carried out by using TBHP as the oxidizing agent and 2,2′-bipyridine as an additive in ACN as the solvent, afforded the desired (benzyloxy)benzene **2a** in 80% yield (Table 2, entry 12).

Table 2. Optimization of the reaction conditions (oxidant/additive) for the benzylic sp^3 C–H group.[a]

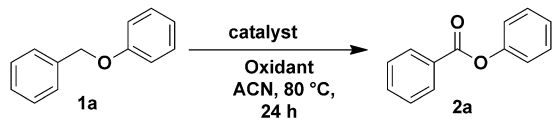

entry	catalyst (50 mg)	oxidant	Additive /ligand	yield [%]
1	$MnO_2@Fe_3O_4$	TBHP	–	55
2	$MnO_2@Fe_3O_4$	4-Methyl pyridine-*N*-oxide	–	–
3	$MnO_2@Fe_3O_4$	$K_2S_2O_8$	–	–
4	$MnO_2@Fe_3O_4$	TEMPO	–	–
5	$MnO_2@Fe_3O_4$	NHPI	–	30
6	$MnO_2@Fe_3O_4$	TBHP	NEt_3	–
7	$MnO_2@Fe_3O_4$	TBHP	Pyridine	66
8	$MnO_2@Fe_3O_4$	4-Methyl pyridine-*N*-oxide	Pyridine	–
9	$MnO_2@Fe_3O_4$	$K_2S_2O_8$	Pyridine	–
10	$MnO_2@Fe_3O_4$	TEMPO	Pyridine	–
11	$MnO_2@Fe_3O_4$	NHPI	Pyridine	60
12	$MnO_2@Fe_3O_4$	TBHP	2,2′-bipyridine	80
13	$Mn@Al_2O_3$	TBHP	2,2′-bipyridine	75
14	$Ru@Fe_3O_4$	TBHP	2,2′-bipyridine	72

[a] **Reaction conditions:** (benzyloxy)benzene **1a** (1 mmol), oxidant (7 mmol), additive (10 mol%) and 50 mg of catalyst were stirred at 80 °C (see Table 1) for 24 h.

Furthermore, other supported catalysts such as $Mn@Al_2O_3$ and $Ru@Fe_3O_4$ under similar reaction conditions are also afforded esters **2a** in good yield (Table 2, entries 13–14). From the results of optimization, the best reaction condition was obtained by reacting (benzyloxy)benzene **1a** (1 mmol), 50 mg of 0.424% $MnO_2@Fe_3O_4$ MNP as a catalyst, 10 mol% 2,2′-bipyridine as an additive and 5–6 M TBHP in decane (7 mmol) as an oxidant in ACN solvent (2.0 mL) at 80 °C for 24 h.

After the optimal conditions established, the scope of this reaction was investigated with various benzylic ethers and the results are summarized in Scheme 2. This oxidative reaction is well tolerated with various electron donating substrates (**2b**–**2d**). It is noteworthy that, the reaction conditions were compatible with the presence of halogenated groups which can extend the possibility for further functionalization. Interestingly, reaction with benzylic aliphatic ether **1k**–**n** is smoothly converted into corresponding ester **2k**–**n** in excellent yield. This reaction is highly chemoselective for benzylic ethers giving corresponding esters in excellent yields; however, there is no ester formation with alkylated phenol **1o** and allylic ether **1p**.

In order to demonstrate the general utility of this synthetic strategy, we carried out gram scale reactions in batch conditions (Scheme 2). Two representative benzyloxy benzene, one with a methyl substituted **1b** and the other with a halogen-substituted **1g**, were chosen to react with TBHP in presence of supported $MnO_2@Fe_3O_4$ MNP catalyst under optimized reaction condition. The reactions were performed in 10 mmol scales using 0.500 g of $MnO_2@Fe_3O_4$ at 80 °C for 24 h to afford **2b** and **2g** in 86% and 80% yields, with TON = 358.33; TOF = 14.93 h^{-1} and TON = 335.7; TOF = 13.98 h^{-1} respectively.

To expand this reaction for sustainable continuous flow process, the optimized batch reaction condition was transferred to a continuous flow reactor. In continuous flow, the reaction and

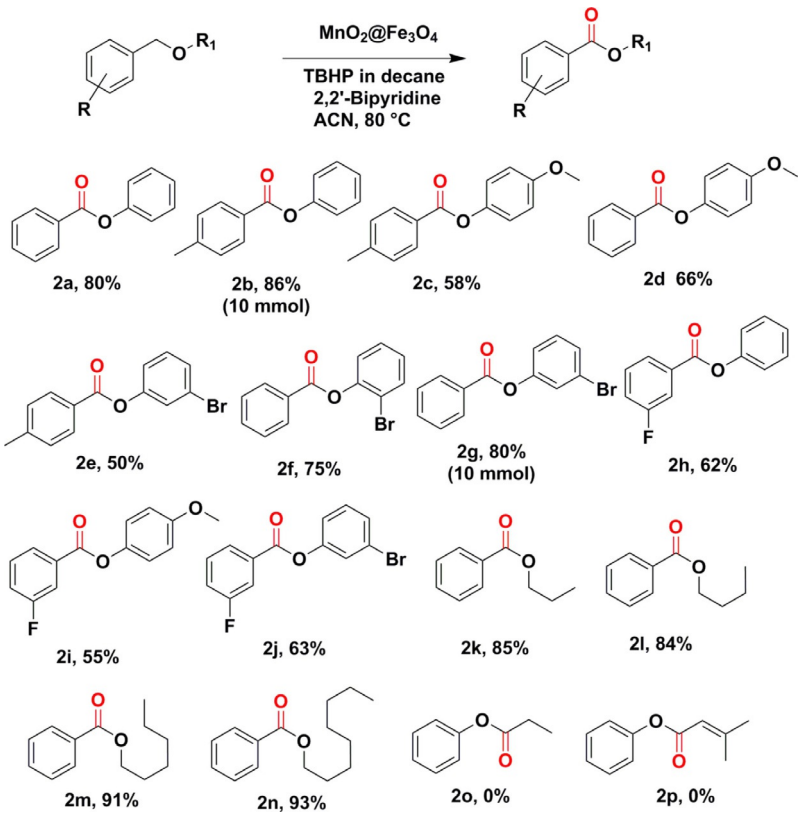

Scheme 2. Substrate scope for ester synthesis in batch condition.

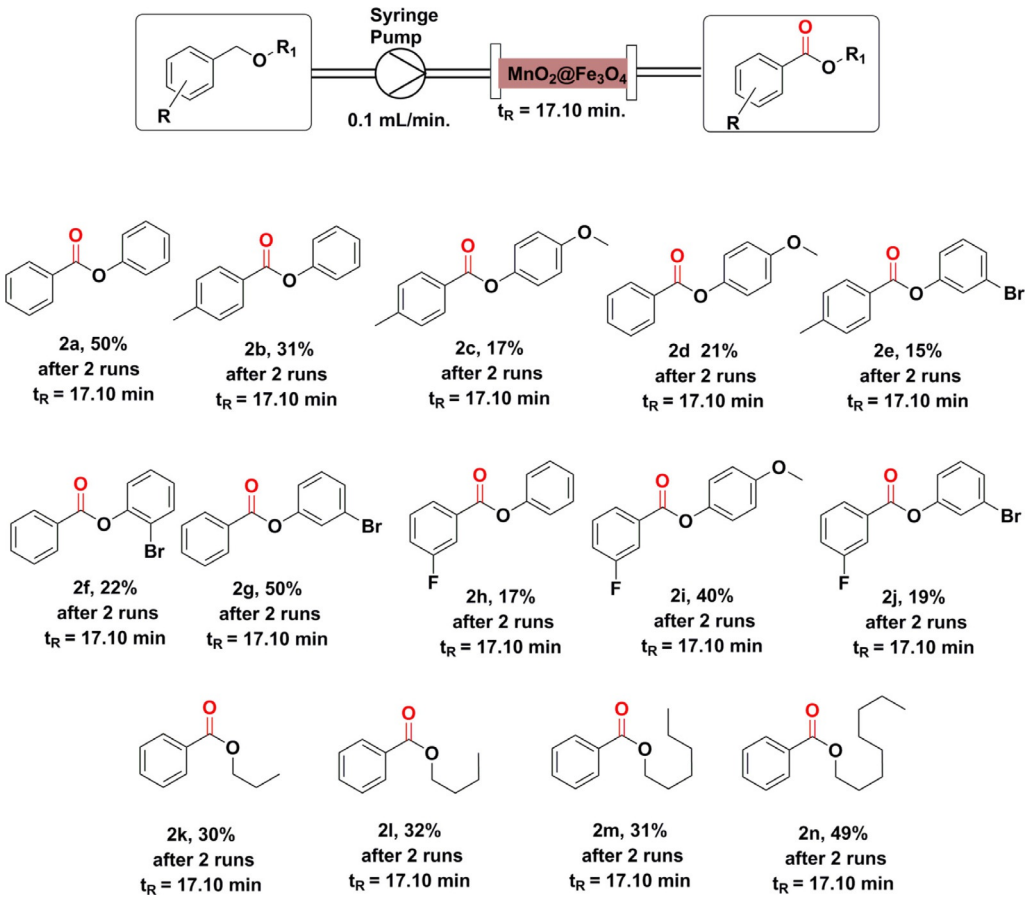

Scheme 3. Continuous flow setup and substrate scope for ester synthesis.

separation of the MnO_2@Fe_3O_4 MNP can be performed simultaneously which avoid the mechanical degradation of the supported catalyst. Developing a continuous flow process for sp^3 C–H oxidation reaction using 0.424% MnO_2@Fe_3O_4 MNP catalyst can improve efficiency and safety for the TBHP mediated reaction. Hence, continuous flow reactions were performed using Holmarc syringe pump (Model no.-HO-SPLF-2D) and by preparing the catalyst bed in the Omnifit column reactor (Scheme 3).

For our initial study, we chose (benzyloxy)benzene **1a** as a model substrate and a set of reaction conditions was attempted (Table 3). Initially, 0.05:0.25 M solution of **1a**:TBHP in presence of 0.10 mmol of 2,2′-bipyridine as a ligand in acetonitrile solvent was reacted by flowing it through the Omnifit fixed bed reactor containing 0.424% MnO_2@Fe_3O_4 catalyst (1.0 g; void volume 1.7 mL; flow rate 0.1 mL min^{-1}) at room temperature it furnished 10% of product **2a** after one cycle (Table 3, entry 1). Increase in the molar concentration of TBHP up to 0.35 does not improve the outcome of the reaction (Table 3, entry 2). Effect of temperature has a great influence on the esterification of ether **1a**. A best-optimized condition was obtained by increasing temperature up to 80 °C, to afford the product **2a** in 50% yield after two cycles (Table 3, entry 3). This reaction required only 17.10 min. to afford the final product of ester **2a**. Further increase in the temperature and molar concentration of TBHP has no effect on the formation of product **2a** (Table 3, entries 4 and 5).

Table 3. Optimization of the reaction conditions for the benzylic sp^3 C–H group in continuous flow.[a]

entry	catalyst/ additive[b]	substrate (**1a**): TBHP	flow rate [mL min^{-1}]	*T* [°C]	t_R [min]/ cycle	yield [%][c]
1	MnO_2@Fe_3O_4	0.05:0.25	0.1	rt	17.10/1	10
2	MnO_2@Fe_3O_4	0.05:0.35	0.1	rt	17.10/1	10
3	MnO_2@Fe_3O_4	0.05:0.35	0.1	80	17.10/2	50
4	MnO_2@Fe_3O_4	0.05:0.35	0.1	100	17.10/2	50
5	MnO_2@Fe_3O_4	0.05:0.45	0.1	80	17.10/2	50

[a] **Reaction conditions:** 0.05 M solution of **1a** + 0.25–0.45 M solution of TBHP (5.0–6.0 M in decane) prepared from in 20 mL ACN and flown on 0.424% MnO_2@Fe_3O_4 catalyst loaded bed reactor with the help of 1.7 mL syringe pump (Model no.-HO-SPLF-2D). [b] 0.1 mmol of 2,2′-bipyridine ligand used, t_R = residence time. [c] Isolated yields.

Having established the optimal reaction conditions, various benzylic ethers (**1a**–**n**) were tested in a continuous flow to explore the generality of this oxidative transformation. By screening different substrate in a continuous flow, and we found that the present catalytic system was not compatible in a continuous flow and afforded considerable yields (15 to 50%) of the ester product after 2 runs (Scheme 3).

The catalytic selective oxidation of benzylic sp^3 C–H group to the corresponding carbonyl compounds is one of the mainly significant reactions in the synthesis of fine chemicals

and pharmaceutically important ingredients.[1] We also investigated the catalytic activity of MnO_2@Fe_3O_4 catalyst in batch as well as in continuous flow reactor for ketone synthesis using ethylbenzene **3a** as a model substrate and using TBHP as an oxidant Table 4. In batch, the oxidation of ethylbenzene (1 mmol) **3a** for the generation of acetophenone **4a** was carried out using 5 mmol of TBHP (5–6 M in decane) in 2.0 mL acetonitrile at 80 °C for 7 h (Table 4). Control catalytic experiments of ethylbenzene **3a** were performed on $Mn(OAc)_3.2H_2O$ and Fe_3O_4 (Table 4, entries 1–2) and under the same reaction conditions.

The conversions were 72% and 48% when using $Mn(OAc)_3.2H_2O$ and Fe_3O_4 respectively. 0.424% MnO_2@Fe_3O_4 was found to be superior to the others and produced the desired product acetophenone **4a** in 83% in isolated yield. The present catalytic system has been optimized again in a continuous flow to acclimatize the benzylic sp3 C–H oxidation reaction of ethylbenzene **3a**. The reaction solvents such as toluene and methanol led poor yield of desired product **4a**. The best-optimized condition was obtained by a flowing mixture of a 0.05 M solution of ethylbenzene **3a** and 0.25 M solution of TBHP (5–6 M in decane) by keeping a flow rate of 0.1 mL min^{-1} affording 95% of desired product **4a** in residence time of t_R = 17.10 min (Table 5).

Table 5. Continuous flow setup and optimization of the reaction conditions for benzylic sp^3 C–H oxidation of ethyl benzene.[a]

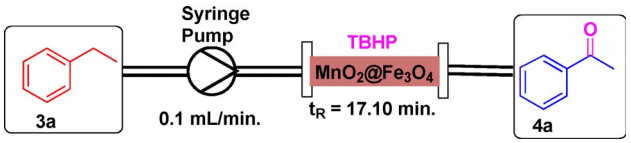

entry	catalyst	substrate (**3a**):TBHP	solvent	T [°C]	flow rate [mL min^{-1}]	t_R [min]/ cycle	Yield of **4a** [%]
1	MnO_2@Fe_3O_4	0.05:0.25	toluene	rt	0.1	17.10/1	20
2	MnO_2@Fe_3O_4	0.05:0.25	toluene	80	0.1	17.10/1	55
3	MnO_2@Fe_3O_4	0.05:0.25	methanol	80	0.1	17.10/1	nd
4	MnO_2@Fe_3O_4	0.05:0.25	ACN	80	0.1	17.10/1	95
5	MnO_2@Fe_3O_4	0.05:0.25	ACN	100	0.1	17.10/1	95

[a] **Reaction conditions:** 0.05 M solution of **3a** + 0.25 M solution of TBHP (5.0–6.0 M in decane) was flown on 0.424% MnO_2@Fe_3O_4 catalyst loaded on Omnifit fixed bed reactor with the help of 1.7 mL syringe pump (Model no.-HO-SPLF-2D).

Table 4. Optimization table for sp^3 benzylic oxidation of ethyl benzene.[a]

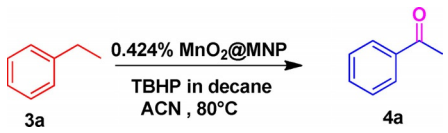

entry	catalyst	solvent	T [°C]	t [h]	yield [%]
1[b]	$Mn(OAc)_3.2H_2O$	ACN	80	7	72
2	Fe_3O_4	ACN	80	7	48
3	0.424% Mn@Fe_3O_4	ACN	80	7	83

Reaction conditions: [a] Ethylbenzene **3a** (1 mmol), TBHP in decane (5 mmol), and 50 mg of catalyst were stirred at 80 °C (see Table 4) for 7 h. [b] 5 mol% catalyst was used.

Having established the optimal reaction conditions in batch and in a continuous flow, a series of substrates were used to examine the generality of substrates and the catalytic activity of the MnO_2@Fe_3O_4 MNP catalyst (Scheme 4). The reactions proceeded smoothly in acetonitrile as the solvent and using TBHP as the oxidizing agent afforded the desired oxidative product **4a** in excellent yields in both batch and continuous flow.The yields were generally comparable to the batch reaction, but reactions are completed in a shorter duration of time in continuous flow (17.10 minutes) as compared to the batch condition (7 h).Besides model substrate, other substrates such as 9*H*-xanthene, diphenylmethane, 1,2,3,4-tetrahydronaphthalene, 2,3-dihydro-1*H*-indene, 9H-fluorene, and 2-ethylnaphthalene afforded the desired ketones (**4b**–**g**) in good to excellent yield under batch and continuous flow module. Substituted ethylbenzene containing an electron-donating functional group also afforded respective ketone products (**4h**,**i**) in good to excellent yield (72–90%). On the other hand, methylene groups adjacent to a heterocyclic ring in 1*H*-oxindole, and 1-methyl oxindole were also converted into the corresponding ketones (**4j**,**k**) in excellent yield.

To check the stability and productivity of the heterogeneous MnO_2@Fe_3O_4 MNP catalyst, we have performed a long time experiment in continuous flow. For this, substrate **3a** was chosen as a model substrate. For instance, 11 mmol of **3a** was pumped continuously for 12 h with a flow rate of 0.1 mL min^{-1} to afford 10.43 mmol of product **4a**. The progress of product **4a** formation was monitored by using ^{1}H-NMR which clearly indicates that the present catalyst is highly efficient and productive.

Recyclability of the catalyst

The recyclability of a heterogeneous catalyst is an important application in industry. The reusability and recyclability of the MnO_2@Fe_3O_4 MNP catalyst were studied for the benzylic oxidation of compound **1b** (Figure 7) and **3b** (Figure 8) for the ten and twelve catalytic cycles, respectively in batch condition. Furthermore, this catalyst is still active for the further oxidation reaction. After completion of each cycle, the catalyst was separated from the reaction mixture simply with the help of a magnetic needle retriever, washed with acetonitrile and ethyl acetate three times, dried at 100 °C for 2 h and then the catalyst was used directly for the next cycle without any additional treatment. The yield of the product remained the same without any extension of reaction time. This result clearly indicates the efficiency of the catalyst which was not lost over a prolonged reaction.

Hot filtration test

In order to check the heterogeneity of the catalyst, a hot filtration test was performed for the benzylic sp^3 C–H oxidation of

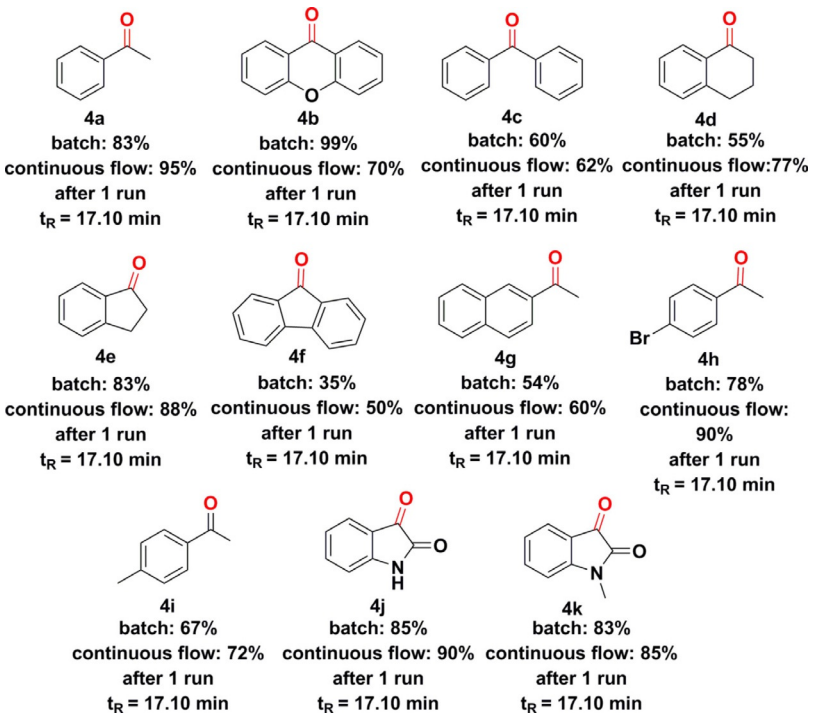

Scheme 4. Substrate scope for ketone synthesis in a batch as well as in a continuous flow module.

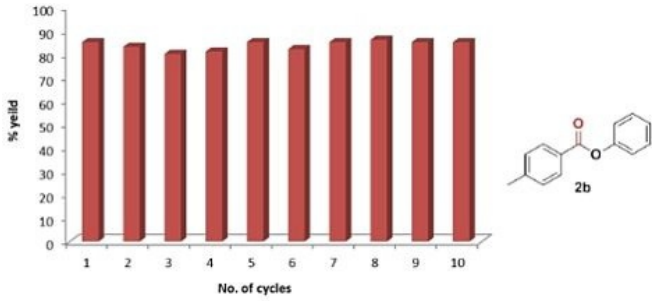

Figure 7. Recyclability of MnO_2@Fe_3O_4 MNP for the synthesis of phenyl 4-methylbenzoate (**2b**).

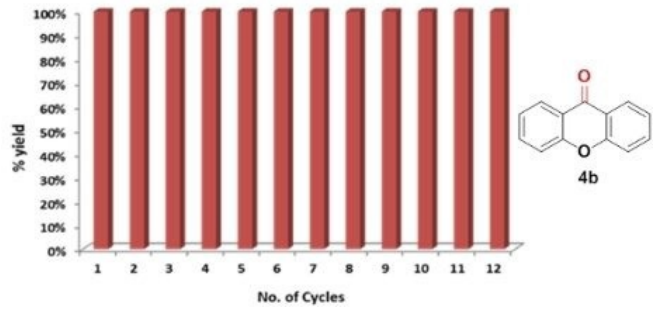

Figure 8. Recyclability of MnO_2@Fe_3O_4 MNP for the synthesis of 9H-xanthen-9-one (**4b**).

1a to investigate whether the reaction proceeded in a heterogeneous or a homogeneous approach. After continuing the reaction for 16 h, the catalyst was separated by magnetic retriever and found that 60% of the product **2a**. No further enhancement in the product **2a** formation was observed after the separation of the MNP catalyst. Moreover, Microwave Plasma Atomic Emission Spectroscopy measurement of the filtrate showed the absence of Mn in the supernatant solution of the reaction mixture. This study clearly shows that Mn was intact to a great extent with the heterogeneous support and no leaching occurred during the catalytic reaction.

Conclusions

In summary, we demonstrated that MnO_2@Fe_3O_4 MNP is an efficient heterogeneous catalyst for the direct benzylic sp^3 C–H oxidation of ethers by using TBHP as an oxidant to afford the ester in high yield. This process was also applicable to benzylic sp^3 C–H oxidation of methylene compounds to furnish ketone derivatives under batch and continuous flow modules in high yield. The main advantages of this procedure are mild reaction conditions, a demonstration in batch as well as in continuous flow modules, scalable synthesis, easy and quick isolation of products, and recyclability of catalyst for more than 12 cycles. Hence, we believe that the present catalyst will find a wide range of applications in organic synthesis as well as in industry.

Experimental Section

Materials and characterization: All the chemicals were purchased from Sigma Aldrich or Alfa-Aesar. Deuterated solvents were used as received. All the solvents used were dry grade. Column chromatographic separations performed over 100–200 Silica-gel. Visualization was accomplished with UV light and phosphomolybdic acid (PMA), Ceric ammonium molybdate (CAM) stain followed by heating. The iron (III) chloride (product number: 44939) was purchased

from Sigma Aldrich. All the experiments were carried out without maintaining the inert condition. The flow chemistry experiments were carried on Holmarc syringe pump (Model no.-HO-SPLF-2D) and for heating Vapourtec R-series was used. ^{1}H and ^{13}C NMR spectra were recorded on 400 and 100 MHz, respectively, using a Bruker 400 MHz or JEOL 400 MHz spectrometers. Abbreviations used in the NMR follow-up experiments: b, broad; s, singlet; d, doublet; t, triplet; q, quartet; m, multiplet. High-resolution mass spectra were recorded with Waters-synapt G2 using electrospray ionization (ESI-TOF). Fourier-transform infrared (FTIR) spectra were obtained with a Bruker Alpha-E Fourier transform infrared spectrometer. Powder X-ray diffraction (PXRD)patterns were measured on Bruker D8 Advanced X-ray diffractometer at room temperature using $Cu_{K\alpha}$ radiation ($\lambda = 1.5406$ Å) with a scan speed of 0.5° min^{-1} and a step size of 0.01° in 2θ. BET was recorded on Quantachrome Instruments. Thermogravimetric analysis was recorded on a PerkinElmer STA 6000, TGA analyzer under air atmosphere with a heating rate of 10 °C min^{-1}. The Hi-Resolution Transmission Electron Microscopy (HRTEM) imaging was performed using Jeol JEM2200FS (200 kV) HRTEM instrument. The XPS was collected using Thermo Scientific Kalpha+ spectrometer using a monochromated $Al_{K\alpha}$ (1486.6 eV) source. The base pressure of the spectrometer was always better than 5×10^{-9} mbar. The electron flood gun was on during acquisition for charge neutralization. The wide area spectrum was collected using 200 eV pass energy and individual core-levels at 50 eV.

1. General procedure for the synthesis MnO_2@Fe_3O_4 MNP catalyst

A mixture of $FeCl_3.6H_2O$ (4.32 g, 16 mmol) and $FeCl_2.4H_2O$ (1.60 g, 8 mmol) was dissolved in 40 mL deionized water. The resultant solution was left to be stirred for 30 min at 80° C. Then ammonia solution (25% (w/w)) was added in a drop-wise manner over 5 min to the stirring mixture to maintain the reaction pH about 11. The resulting black dispersion was stirred vigorously for 1 h at room temperature and then was refluxed for 1 h. The black magnetite Fe_3O_4 nanoparticles were isolated by magnetic decantation, washed several times with deionized water and then dried at 80 °C for 4 h. To introduce reactive Mn on the surface of the magnetic nanoparticle (MNP), 0.6 g of dried Fe_3O_4 nanoparticles were suspended in a mixture of 50 mL ethanol and then, 0.6 g of $Mn(OAc)_3.2H_2O$ was ultrasonically dispersed. After complete dissolution and dispersion, the nanoparticles were separated from the ethanol solution by magnetic decantation and dried at 80 °C for 4 h. MnO_2@Fe_3O_4 magnetic nanoparticles were obtained by drop-wise addition of aqueous ammonia (25% (w/w)) to the dried brown nanoparticles under vigorous stirring. Finally, the MnO_2@Fe_3O_4 MNP were magnetically separated, washed with water, and dried in an oven at 100 °C for overnight.

2. General procedure for the synthesis of the esters from sp^3-CH oxidation of (benzyloxy)benzene derivatives in batch

In a 20 mL glass seal tube, catalyst (25 mg), (benzyloxy)benzene derivatives (0.5 mmol, 1 equiv) in ACN (2 mL) were added TBHP (5–6 M in decane, 3.5 mmol, 7 equiv), 0.05 mmol of 2,2′-bipyridine and the tube was sealed by using a crimper. The mixture was stirred at 80 °C for 24 h. After completion, the reaction mixture was allowed to cool to room temperature. It was then diluted with EtOAc and the catalyst was separated with an external magnet and washing twice with EtOAc. The volatiles were removed under reduced pressure, and the crude product was purified by column chromatography to afford the ester products. All of the esters were identified by spectral comparison with literature data.

3. General procedure for the synthesis of the esters from sp^3-CH oxidation of (benzyloxy)benzene derivatives in a continuous flow

0.05 M solution of the substrate and 0.35 M of 5.0–6.0 M TBHP in decane and 0.1 mmol of 2,2′-bipyridine in 20 mL of ACN solvent was pumped using syringe pump through packed bed containing 1.5 g of 0.424% MnO_2@Fe_3O_4 (up to 5 cm) and preheated at 80 °C with the flow rate of 0.1 mL min^{-1}. A 3.5 to 3.8 psi back pressure was maintained in the reaction. The collected organic layer was concentrated under reduced pressure and the crude product was purified by column chromatography using ethyl acetate: hexane as an eluent to afford the ketone product.

4. General procedure for oxidation of benzylic sp^3 C–H group of methylene derivatives to the ketone in batch

In a 20 mL glass seal tube, catalyst (50 mg), alkyl benzene (1 mmol, 1 equiv) in ACN (2 mL) was added *t*BuOOH (5–6 M in decane, 5 mmol, 5 equiv) and the tube was sealed by using a crimper. The mixture was stirred at 80 °C for 7 h. After completion, the reaction mixture was allowed to cool to room temperature. It was then diluted with EtOAc and the catalyst was separated with an external magnet and washing twice with EtOAc. The volatiles was removed under reduced pressure, and the crude product was purified by column chromatography to afford the desired product.

5. General procedure for oxidation of benzylic sp^3 C–H group of methylene derivatives to the ketone in a continuous flow

0.05 M solution of the substrate and 0.25 M of 5.0–6.0 M TBHP in decane in 20 mL of ACN solvent was pumped using syringe pump through packed bed containing 1.5 g of 0.424% MnO_2@Fe_3O_4 (up to 5 cm) and preheated at 80 °C with the flow rate of 0.1 mL min^{-1}. A 3.5 to 3.8 psi back pressure was maintained in the reaction. The collected organic layer was concentrated under reduced pressure and the crude product was purified by column chromatography using ethyl acetate: hexane as an eluent to afford the desired product.

6. Study of lifetime of the catalyst and gram scale synthesis of benzylic sp^3 C–H group of methylene derivatives to the ketone in a continuous flow

0.05 M solution of the substrate **3a** (1.166 g, 10.99 mmol) and 0.25 M of TBHP (5.0–6.0 M in decane, 7.08 g, 54.99 mmol) in 110 mL of ACN solvent was pumped using syringe pump through packed bed containing 1.3 g of 0.424% MnO_2@Fe_3O_4 (up to 3 cm) and preheated at 80 °C with the flow rate of 0.1 mL min^{-1} at 3.5 bar pressure for 12 h. The reaction mixture was monitored at regular intervals by ^{1}H NMR analysis. The entire reaction fraction was concentrated in a rotary evaporator to afford 1.25 gm of acetophenone **4b** as yellowish oil.

7. General procedure for catalyst recovery for the synthesis of the esters from (benzyloxy)benzene derivatives in batch

In a 20 mL glass seal tube, catalyst (25 mg), (benzyloxy)benzene derivatives (0.5 mmol, 1 equiv) in ACN (2 mL) were added TBHP (5–

6 M in decane, 3.5 mmol, 7 equiv), 0.05 mmol of 2,2′-bipyridine and the tube was sealed by using a crimper. The mixture was stirred at 80 °C for 24 h. After completion, the reaction mixture was allowed to cool to room temperature; the supported catalyst was separated by an external magnet and washed with acetonitrile and ethyl acetate for three times, then dried and directly used in the next run.

Acknowledgements

This research was supported by the Council of Scientific and Industrial Research [02(0296/17/EMR-II)], India. A. P. thanks, IISER-Pune for the research support. S.G.A. thanks SERB-NPDF (PDF/2017/001286) for the research fellowship. B. G. thanks CSIR for the research support.

Conflict of interest

The authors declare no conflict of interest.

Keywords: Benzylic sp^3 C–H Oxidation · Carbonyl Compounds · Continuous flow · Heterogeneous Catalysis · Magnetic Nanoparticles · *tert*-Butyl Hydroperoxide

[1] a) L.-M. Xu, B.-J. Li, Z. Yang, Z.-J. Shi, *Chem. Soc. Rev.* **2010**, *39*, 712–733; b) T. W. Lyons, M. S. Sanford, *Chem. Rev.* **2010**, *110*, 1147–1169; c) D. A. Colby, R. G. Bergman, J. A. Ellman, *Chem. Rev.* **2010**, *110*, 624–655; d) X. Chen, K. M. Engle, D.-H. Wang, J.-Q. Yu, *Angew. Chem. Int. Ed.* **2009**, *48*, 5094–5115; *Angew. Chem.* **2009**, *121*, 5196–5217; e) D. H. Wang, K. M. Engle, B.-F. Shi, J.-Q. Yu, *Science* **2010**, *327*, 315–319; f) Z.-P. Li, C.-J. Li, *J. Am. Chem. Soc.* **2005**, *127*, 3672–3673.

[2] R. Giri, B.-F. Shi, K. M. Engle, N. Maugel, J.-Q. Yu, *Chem. Soc. Rev.* **2009**, *38*, 3242.

[3] T. Punniyamurthy, S. Velusamy, J. Iqbal, *Chem. Rev.* **2005**, *105*, 2329–2363.

[4] a) A. H. Haines, Methods for the Oxidation of Organic Compounds. Alkanes, Alkenes, Alkynes and Arenes, Academic Press, London, **1985**; b) A. H. Haines, Methods for the Oxidation of Organic Compounds-Alcohols, alcohols derivatives, Alkyl halides, Nitroalkanes, Alkyl Azides, Carbonyl compounds, Hydroxyarenes and Aminoarenes, Academic Press, London, **1988**.

[5] Cr-catalyzed oxidations: a) A. J. Pearson, G. R. Han, *J. Org. Chem.* **1985**, *50*, 2791–2801; b) J. Muzart, *Tetrahedron Lett.* **1986**, *27*, 3139–3142; c) J. Muzart, A. N. A. Ajjou, *J. Mol. Catal.* **1991**, *66*, 155–161; d) B. M. Choudary, A. D. Prasad, V. Bhuma, V. Swapna, *J. Org. Chem.* **1992**, *57*, 5841–5844; e) T. K. Das, K. Chaudhari, E. Nandanan, A. J. Chandwadkar, A. Sudalai, T. Ravindranathan, S. Sivasanker, *Tetrahedron Lett.* **1997**, *38*, 3631; f) G. Rothenberg, H. Wiener, Y. Sasson, *J. Mol. Catal. A* **1998**, *136*, 253–262; g) S. K. Mohapatra, P. Selvam, *J. Catal.* **2007**, *249*, 394–396.

[6] Mn-catalyzed oxidations: a) N. H. Lee, C. S. Lee, D. S. Jung, *Tetrahedron Lett.* **1998**, *39*, 1385–1388; b) J. F. Pan, K. Chen, *J. Mol. Catal. A* **2001**, *176*, 19–22; c) G. Blay, I. Fernández, T. Giménez, J. R. Pedro, R. Ruiz, E. Pardo, F. Lloret, M. C. Muñoz, *Chem. Commun.* **2001**, 2102–2103; d) W. Wang, D. Xu, Q. Sun, W. Sun, *Chem. Asian J.* **2018**, *13*, 2458–2464.

[7] Co-catalyzed oxidations: a) P. Li, H. Alper, *J. Mol. Catal.* **1990**, *61*, 51–54; b) M. Jurado-Gonzalez, A. C. Sullvian, J. R. H. Wilson, *Tetrahedron Lett.* **2003**, *44*, 4283–4286; c) E. Modica, G. Bombieri, D. Colombo, N. Marchini, F. Ronchetti, A. Scala, L. Toma, *Eur. J. Org. Chem.* **2003**, 2964–2971; d) X. G. Li, J. Wang, R. He, *Chin. Chem. Lett.* **2007**, *18*, 1053–1056.

[8] Ru-catalyzed oxidations: a) S. Murahashi, Y. Oda, T. Naota, T. Kuwabara, *Tetrahedron Lett.* **1993**, *34*, 1299–1302; b) M. D. Nikalje, A. Sudalai, *Tetrahedron* **1999**, *55*, 5903–5908; c) S. Murahashi, N. Komiya, Y. Oda, T. Kuwabara, T. Naota, *J. Org. Chem.* **2000**, *65*, 9186–9193.

[9] Rh-catalyzed oxidations: A. J. Catino, J. M. Nichols, H. Choi, S. Gottipamula, M. P. Doyle, *Org. Lett.* **2005**, *7*, 5167–5170.

[10] Fe-catalyzed oxidations: a) D. H. R. Barton, D. Doller, *Acc. Chem. Res.* **1992**, *25*, 504–512; b) D. H. R. Barton, W. Chavasiri, *Tetrahedron* **1994**, *50*, 19–30; c) S. Evans, J. R. L. Smith, *J. Chem. Soc. Perkin Trans. 2* **2000**, 1541–1551; d) P. Stavropoulos, R. Celenligil-Cetin, A. E. Tapper, *Acc. Chem. Res.* **2001**, *34*, 745–752; e) S. S. Kim, S. K. Sar, P. Tamrakar, *Bull. Korean Chem. Soc.* **2002**, *23*, 937–938; f) C. Pavan, J. Legros, C. Bolm, *Adv. Synth. Catal.* **2005**, *347*, 703–705; g) M. Nakanishi, C. Bolm, *Adv. Synth. Catal.* **2007**, *349*, 861–864; h) T. Nagano, S. Kobayashi, *Chem. Lett.* **2008**, *37*, 1042–1045; i) A. Gonzalez-de-Castro, C. M. Robertson, J. Xiao, *J. Am. Chem. Soc.* **2014**, *136*, 8350–8360; j) C. Miao, H. Zhao, Q. Zhao, C. Xiaa, W. Sun, *Catal. Sci. Technol.* **2016**, *6*, 1378–1383.

[11] H. Peng, A. Lin, Y. Zhang, H. Jiang, J. Zhou, Y. Cheng, C. Zhu, H. Hu, *ACS Catal.* **2012**, *21*, 163–167.

[12] Bi-catalyzed oxidations: a) Y. Bonvin, E. Callens, I. Larrosa, D. A. Henderson, J. Oldham, A. J. Burton, A. G. M. Barrett, *Org. Lett.* **2005**, *7*, 4549–4552; b) E. Callens, A. J. Burton, A. J. P. White, A. G. M. Barrett, *Tetrahedron Lett.* **2008**, *49*, 3709–3712.

[13] a) Y.-J. Liu, H. Xu, W.-J. Kong, M. Shang, H.-X. Dai, J.-Q. Yu, *Nature* **2014**, *515*, 389–393; b) A. Shaabani, Z. Hezarkhani, E. Badali, *RSC Adv.* **2015**, *5*, 61759–61767; c) I. Garcia-Bosch, M. A. Siegler, *Angew. Chem. Int. Ed.* **2016**, *55*, 12873–12876; *Angew. Chem.* **2016**, *128*, 13065–13068; d) H. Peng, A. Lin, Y. Zhang, H. Jiang, J. Zhou, Y. Cheng, C. Zhu, H. Hu, *ACS Catal.* **2012**, *2*, 163–167; e) A. Nakamura, M. Nakada, *Synthesis* **2013**, *45*, 1421–1451; f) Y.-L. Zhong, D. R. Gauthier, Y.-J. Shi, M. McLaughlin, J. Y. L. Chung, P. Dagneau, N. Yasuda, *J. Org. Chem.* **2012**, *77*, 3297–3310.

[14] Z. Zhang, Y. Gao, Y. Liu, J. Li, H. Xie, H. Li, W. Wang, *Org. Lett.* **2015**, *17*, 5492–5495.

[15] J. Tan, T. Zheng, Y. Yu, K. Xu, *RSC Adv.* **2017**, *7*, 15176–15180.

[16] A. I. Carrillo, L. C. Schmidt, M. L. Marin, J. C. Scaiano, *Catal. Sci. Technol.* **2014**, *4*, 435–440.

[17] A. E. Aksoylu, M. Madalena, A. Freitas, M. F. R. Pereira, J. Figueiredo, *Carbon* **2001**, *39*, 175–185.

[18] D. Klemm, B. Heublein, H. P. Fink, A. Bohn, *Angew. Chem. Int. Ed.* **2005**, *44*, 3358–3393; *Angew. Chem.* **2005**, *117*, 3422–3458.

[19] M. F. Lengke, M. E. Fleet, G. Southam, *Langmuir* **2007**, *23*, 8982–8987.

[20] R. Saha, G. Sekar, *Appl. Catal. B* **2019**, *250*, 325–336.

[21] H. Montazeri, A. Amani, H. R. Shahverdi, E. Haratifar, A. R. Shahverdi, *J. Nanostruct. Chem.* **2013**, *3*, 25–31.

[22] a) R. B. Nasir Baig, S. V. Rajender, *Chem. Commun.* **2013**, *49*, 752–770; b) R. Ricciardi, J. Huskens, W. Verboom, *ChemSusChem* **2015**, *8*, 2586–2605.

[23] a) L. Yin, J. Liebscher, *Chem. Rev.* **2007**, *107*, 133–173; b) N. T. S. Phan, M. V. D. Sluys, C. W. Jones, *Adv. Synth. Catal.* **2006**, *348*, 609–679; c) M. Moreno-Mañas, R. Pleixats, *Acc. Chem. Res.* **2003**, *36*, 638–643.

[24] M. Zarghani, B. Akhlaghinia, *RSC Adv.* **2016**, *6*, 38592–38601.

[25] a) A. J. Fatiadi, *Synthesis* **1976**, 65–104; b) A. T. Soldatenkov, K. B. Polyanskii, N. M. Kolyadina, S. A. Soldatova, *Chem. Heterocycl. Compd.* **2009**, *45*, 633–657; c) R. J. K. Taylor, M. Reid, J. Foot, S. A. Raw, *Acc. Chem. Res.* **2005**, *38*, 851–869.

[26] a) F. Niu, L. Zhang, S.-Z. Luo, W.-G. Song, *Chem. Commun.* **2010**, *46*, 1109–1111; b) M. Arefi, D. Saberi, M. Karime, A. Heydari, *ACS Comb. Sci.* **2015**, *17*, 341–345.

[27] F. Guo, H. Li, Z. Zhang, S. Meng, D. Li, *Mater. Sci. Eng. B* **2009**, *163*, 134–137.

[28] Z. Liu, R. Ma, Y. Ebina, K. Takada, T. Sasaki, *Chem. Mater.* **2007**, *19*, 6504–6512.

[29] C. Zhu, S. Guo, Y. Fang, L. Han, S. Wang, *Nano Res.* **2011**, *4*, 648–657.

[30] X. C. Li, L. Zhang, G. H. He, *Carbon* **2016**, *99*, 514–522.

[31] J. Wang, S. Fan, Y. Luan, J. Tang, Z. Jin, M. Yang, Y. Lu, *RSC Adv.* **2015**, *5*, 2405–2410.

[32] a) G. Rothenberg, H. Wiener, Y. Sasson, *J. Mol. Catal. A* **1998**, *136*, 253–259; b) A. Dhakshinamoorthy, M. Alvaro, H. Garcia, *J. Catal.* **2009**, *267*, 1–4.

Manuscript received: June 15, 2019
Revised manuscript received: August 1, 2019
Accepted manuscript online: August 16, 2019
Version of record online: September 18, 2019

JOC The Journal of Organic Chemistry

pubs.acs.org/joc Article

Continuous-Flow Direct Azidation of Alcohols and Peroxides for the Synthesis of Quinoxalinone, Benzooxazinone, and Triazole Derivatives

Akanksha M. Pandey, Shankhajit Mondal, and Boopathy Gnanaprakasam*

Cite This: J. Org. Chem. 2022, 87, 9926−9939 Read Online

ACCESS | Metrics & More | Article Recommendations | Supporting Information

ABSTRACT: Continuous-flow reactors provide an ideal tool for the synthesis of potentially explosive but synthetically useful organic substances like organic azides due to their intrinsically small volume leading to very effective collision and highly controlled reaction conditions. Herein, we report the continuous-flow direct azidation of various alcohols by using $TMSN_3$ as an azide transfer reagent in the presence of Amberlyst-15 as a recyclable catalyst. Numerous 3-hydroxy-2-oxindoles effectively undergo azide transfer to afford azide-functionalized quaternary stereocenters in a continuous-flow module. Interestingly, peroxyoxindole undergoes sequential skeletal rearrangement to generate a carbocation followed by nucleophilic azidation to afford a library of substituted 2-azido-2*H*-benzo[*b*][1,4]oxazin-3(4*H*)-one derivatives under continuous flow. Furthermore, a continuous-flow Cu-catalyzed click reaction afforded triazole-functionalized deivatives. Next, reduction of azide in the presence of PPh_3 affords the amine derivatives in good yields. The continuous-flow application was extended further for the thermolytic skeletal rearrangement of 3-azide-2-oxindole for the synthesis of biologically important quinoxalin-2(1*H*)-ones without any reagents. Furthermore, this continuous-flow direct azidation reaction is scaled up to 6.144 g of azides with a turnover number of 9.24 under safer conditions.

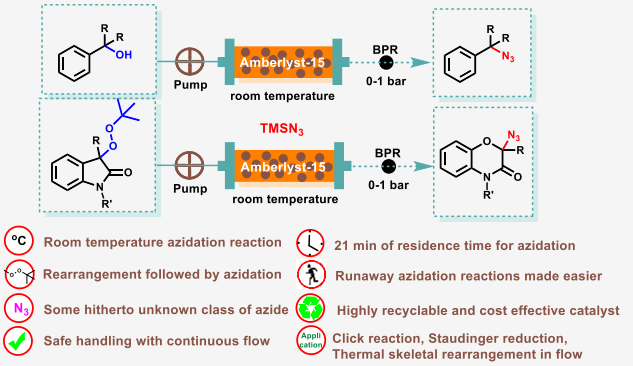

INTRODUCTION

Nitrogen-containing heterocyclic compounds have shown widespread utility in pharmaceutical applications. For instance, 1,2,3-triazoles have been known for their applications in various organic syntheses, drug development, chemical biology, and materials science. Other heterocycles such as 2*H*-1,4-benzoxazin-3(4*H*)-one and quinoxalin-2(1*H*)-ones were also proven to have applications in medicinal chemistry. In addition to their usefulness, many 1,2,3- or 1,2-nitrogen-enriched heterocycles were synthesized from organic azides or hydrazides through click reactions or condensation chemistry. Many organic intermediates have shown intriguing reactions to generate the respective products with greater molecular complexity.[1]

In the 19th century, azides as an indispensable tool for performing various chemical operations have witnessed an impressive library of powerful named reactions.[2,3] These energy rich intermediates are building blocks for the bioconjugation of proteins.[4] They are readily converted into N-heterocycles[5,6] and known as effective ammonia surrogates[7] (Figure 1). Moreover, organic azides were also used for (3+2) cycloaddition with alkynes and nitriles to generate triazole and tetrazole moieties to access important bioactive molecules such as anticancer and antimicrobial drugs and as an aldose reductase inhibitor (Figure 1).[8−11] Although these azides have extensive applications, there are severe safety concerns because of their explosive nature in the large-scale manufacturing process. Moreover, azides with a C/N ratio of ≥3 are generally stable to handle.[12] Hence, a process technology requires the augmentation of the safety concerns of azide synthesis and relevant associated chemical transformations.

In addition, for the synthesis of alkyl azides, the traditional batch methods involve the activation of the -OH group, which requires two steps: (i) conversion to a good leaving group and (ii) substitution with NaN_3. After activation of the -OH group, it can be converted into genotoxic alkyl halide,[13] sulfonates,[14] or acetates,[15] which upon reaction with NaN_3 affords azide. In addition, it can also be accessed using other precursors such as amines, hydrazines, etc.[5,12] In addition, tedious workup and safety concerns in scaling up the reaction become substantial challenges. Hence, developing a direct azidation approach from alcohol is the best way to avoid the generation of waste and to

Received: April 21, 2022
Published: July 22, 2022

https://doi.org/10.1021/acs.joc.2c00941
J. Org. Chem. 2022, 87, 9926−9939

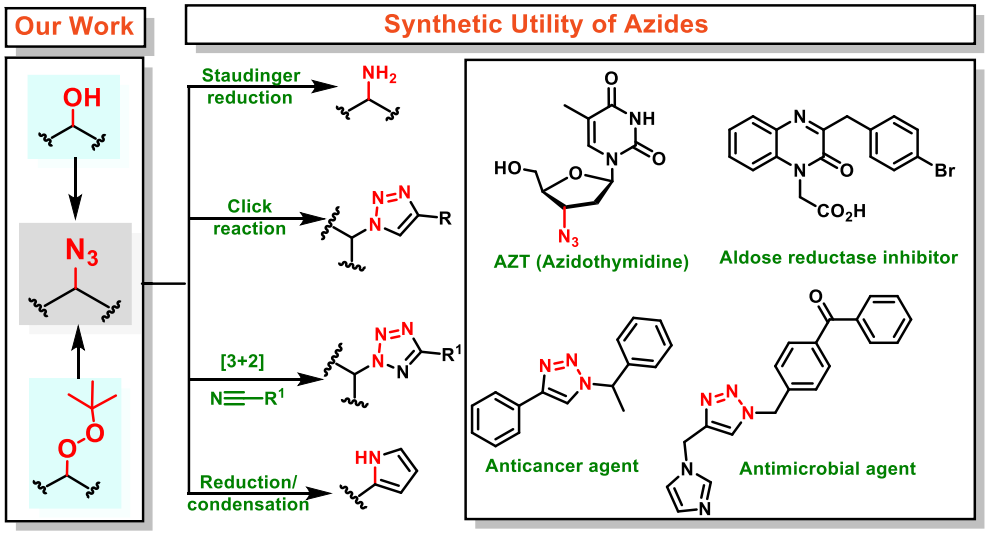

Figure 1. Synthetic utility of azides under continuous flow.

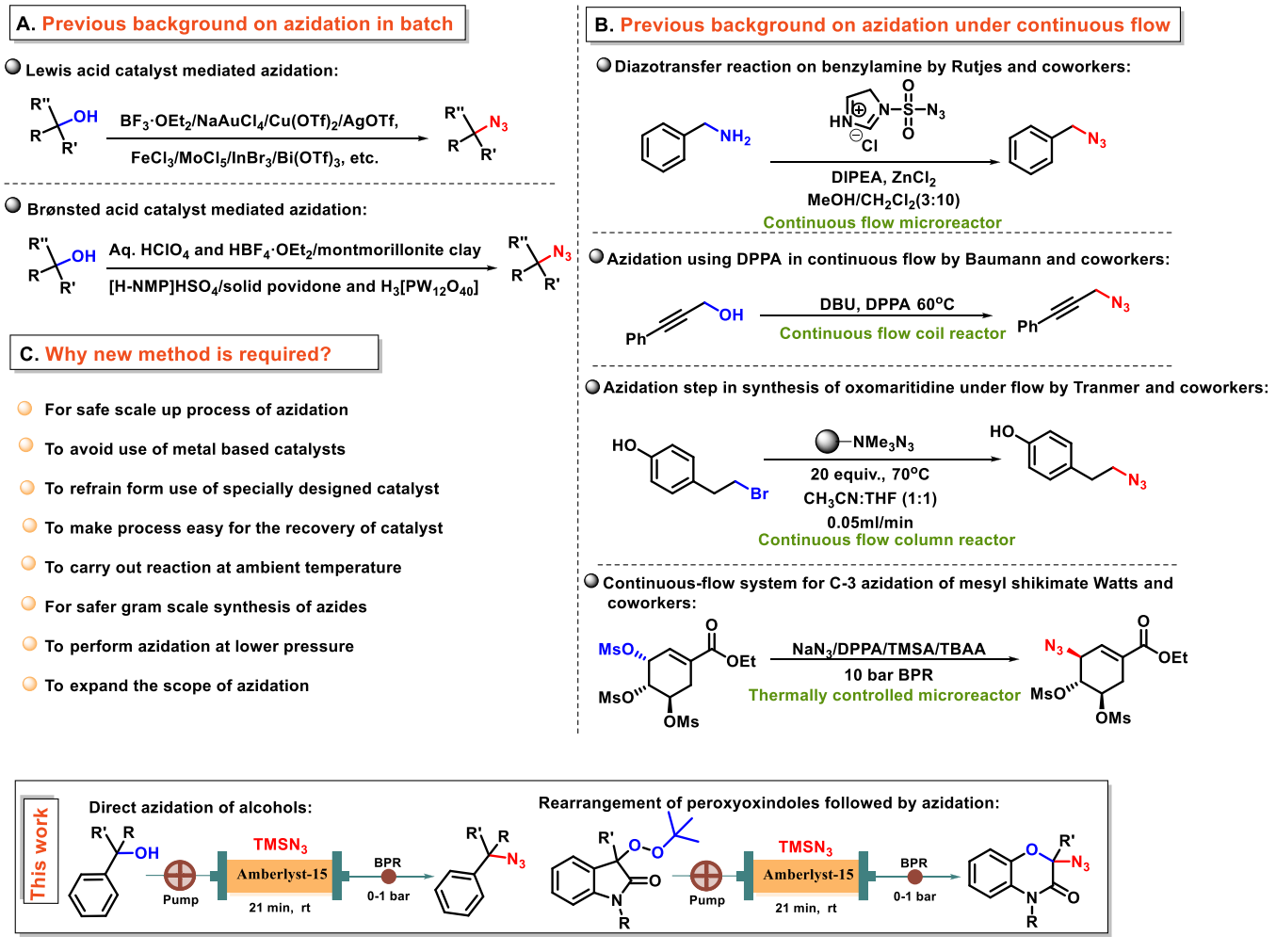

Figure 2. Literature precedents and this work.

minimize the synthetic steps. With this in mind, the Mitsunobu reaction shows direct substitution of the hydroxyl group to attain azides using hydrazoic acid.[16]

In view of potential safety concerns related to genotoxic sodium azide and hydrazoic acid, $TMSN_3$ was found to be a commercially available, safe, and practical azide source for investigating new methodologies. To perform this chemical operation, various Lewis acid catalysts such as $BF_3{\cdot}OEt_2$,[17] $NaAuCl_4$,[17] $Cu(OTf)_2$,[18] AgOTf,[19] $FeCl_3$,[20] $MoCl_5$,[21] $InBr_3$,[22] and $Bi(OTf)_3$,[23] which facilitate the substitution by the

https://doi.org/10.1021/acs.joc.2c00941
J. Org. Chem. 2022, 87, 9926−9939

activation of the hydroxyl group, have been studied. However, contrary to Lewis acid-mediated azidation reactions, fewer approaches have been realized for this transformation using a Brønsted acid catalyst. Hajipour used acidic ionic liquid [H-NMP]HSO_4 for this transformation using alcohols and sodium azide,[24] whereas Onaka demonstrated a combination of TMSCl and $TMSN_3$ with montmorillonite clay to obtain azides.[25] Similarly, Rode accomplished it with the use of a solid povidone and phosphotungstic acid hybrid as a catalyst for heterogeneous azidation of alcohols.[26] More recently, Zhou and Regier achieved it with aqueous perchloric acid[27] and $HBF_4{\cdot}OEt_2$,[28] respectively (Figure 2). Although numerous methods for azidation exist, a more convenient method for the safer generation of azide is highly desired.

To minimize the safety hazards associated with reaction scale-up of these explosive and high-energy molecules that decompose with heat, light, and shock under batch conditions, we opted to develop a continuous-flow protocol that would enable and streamline the assembly and delivery of these entities by mitigating any safety concerns associated with it. The advent of continuous flow as a green tool manifests enhanced heat and mass transfer, precise residence time control, shorter process times, increased safety, reproducibility, better product quality, and easy scalability. These advantages have led to more frequent implementation of continuous processes not only in academia but also in the fine chemical manufacturing sector.[29] The potential of continuous flow for azidation has been explored further by using imidazole-1-sulfonyl azide hydrochloride as a diazo transfer reagent for benzyl amine to azide transfer[30] and aqueous sodium azide for C-3 azidation of mesyl shikimate.[31] Furthermore, azidation with azide exchange resin was a crucial step in the total synthesis of oxomaritidine.[32] Moreover, a telescoped-flow process was also established to obtain propargyl amine using DPPA.[33] However, these methods used NaN_3 or heating. Henceforth, an efficient method for the broad substrates with mild and safer reaction conditions for the large-scale synthesis under continuous flow are still highly desirable.

Herein, we report continuous-flow direct azidation of various alcohols and peroxides in the presence of environmentally and industrially beneficial Amberlyst-15 as a catalyst. This method delivers a wide array of compounds, including the quaternary stereocenter. In the case of peroxide, it affords sequential skeletal rearrangement and azidation under flow conditions. Further application of the azide was demonstrated toward the click reaction to generate a quaternary stereocenter with a triazole moiety. We have also developed the rearrangement of azides to generate quinoxalinone derivatives under continuous-flow heating conditions. In addition, this quaternary azide can be reduced to generate a quaternary amine stereocenter efficiently in a continuous-flow module. We have also demonstrated the application of azides toward Staudinger reduction, click reaction, and ring expansion reactions.

RESULTS AND DISCUSSION

As outlined in Table 1, direct azidation was optimized under batch conditions by using diphenylmethanol and azidotrimethylsilane was used as an azide transfer reagent. A control experiment was carried out at room temperature and 60 °C in the absence of a catalyst, which resulted in no reaction (Table 1, entries 1 and 2, respectively). Next, we screened homogeneous and heterogeneous Lewis and Bronstead catalysts for azidation to synthesize (azidomethylene)dibenzene (**3a**). Azidation of **2a**

Table 1. Optimization of the Reaction Conditions for the Azidation of Alcohols under Batch Conditions[a]

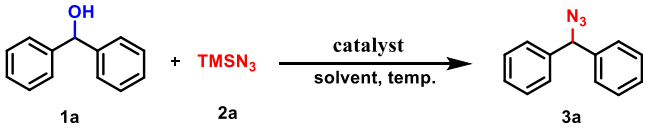

entry	equiv (**1a**:**2a**)	catalyst	temp (°C)	yield of **3a** (%)
1	1:3	–	rt	–
2	1:3	–	60	–
3[b]	1:3	$Bi(NO_3)_3$	rt	95
4[b]	1:3	$In(OTf)_3$	rt	73
5	1:3	Amberlyst-15	rt	98
6	1:2	Amberlyst-15	rt	69
7	1:1	Amberlyst-15	rt	50
8[c]	1:3	Amberlyst-15	rt	98

[a]For the reactions, **1a** (0.5 mmol), $TMSN_3$ (see the table), Amberlyst-15 (w/w with respect to **1a**), and DCM (2 mL) were stirred at room temperature for 12 h. The reported yields are isolated yields. [b]With 5 mol % catalyst. [c]For 30 min.

with 5 mol % $Bi(NO_3)_3$ led to 95% yields, whereas azidation with 5 mol % $In(OTf)_3$ stirred at rt for 12 h afforded 73% product **3a** (Table 1, entries 3 and 4, respectively).

To develop azidation under metal-free conditions, this reaction was examined with Amberlyst-15, and a 98% yield was achieved (Table 1, entry 5). Amberlyst-15 can serve as an excellent source of acid and can be recovered and reused several times. When 1:2 and 1:1 **1a**:**2a** ratios (equivalents) were used at rt with Amberlyst-15 (w/w) with respect to **1a**, the reaction afforded 69% and 50% yields of **3a**, respectively (Table 1, entries 6 and 7, respectively). In addition, this reaction afforded 98% **3a** in 30 min when 3 equiv of $TMSN_3$ was used (Table 1, entry 8).

Having batch-optimized conditions in hand, we investigated this strategy for the other substrates. The wide variation of substrate scope assures the reliability and tolerance of the safer azidation method for various differently substituted alcohols. Thus, the reaction of various alcohols such as primary, secondary, and tertiary alcohols with $TMSN_3$ provided 50–99% yields of products **3a**–**p** (Scheme 1). This method was tolerant to both electron-withdrawing groups and electron-donating groups containing alcohols to afford the respective azide via direct nucleophilic substitution. Furthermore, more sterically hindered tertiary alcohols were successfully azidated to afford (1-azidoethane-1,1-diyl)dibenzene **3f** and (azidomethanetriyl)tribenzene **3g** in 86% and 80% yields, respectively. The structure of **3g** was further confirmed by X-ray analysis (see Figure S2). Quaternary 3-hydroxy-2-oxindole derivatives smoothly underwent the azidation reaction affording the respective azides **3h**–**p** in very good yields. The structure of **3p** was confirmed by X-ray analysis (see Figure S3).

To overcome the safety hazards under batch conditions, we integrated this reaction under continuous flow to provide a rapid and safer synthesis of various azide derivatives. Henceforth, we filled the Omnifit column with Amberlyst-15 and connected it to the Vaportec R-series pump. Various concentrations of azide and alcohol in DCM were passed through the Amberlyst-15 at various flow rates to obtain the optimized reaction condition. Initially, 0.025 M **1a** and 0.075 M **2a** in a DCM solvent at room temperature were passed through the catalyst at a flow rate of 0.1 mL/min, and each afforded a 96% isolated yield of product **3a** (Table 2, entry 1).

https://doi.org/10.1021/acs.joc.2c00941
J. Org. Chem. 2022, 87, 9926–9939

Scheme 1. Substrate Scope for the Azidation of Alcohols under Batch Conditions[a]

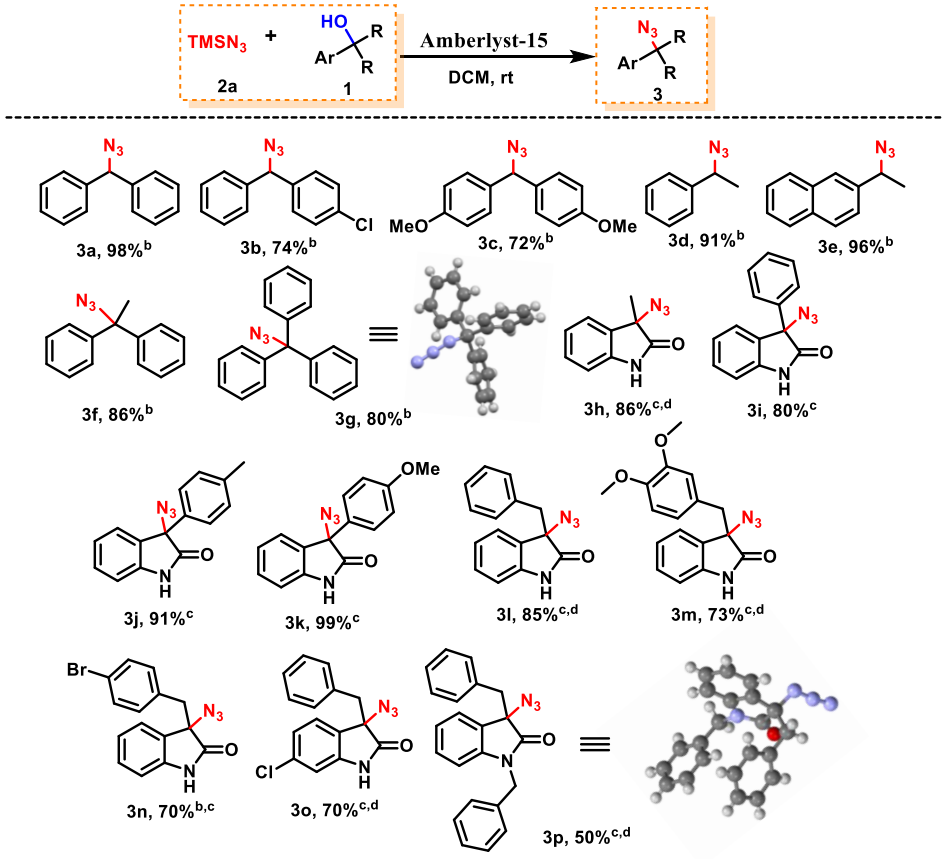

[a]For the reactions, **1** (0.5 mmol), **2a** (1.5 mmol), Amberlyst-15 (w/w with respect to **1**), and DCM (2 mL) were stirred at rt. The reported yields are the isolated yields. [b]For 30 min. [c]For 1 h. [d]At 80 °C in DCE.

Table 2. Continuous-Flow Optimization of the Reaction Conditions for the Azidation of Alcohols[a]

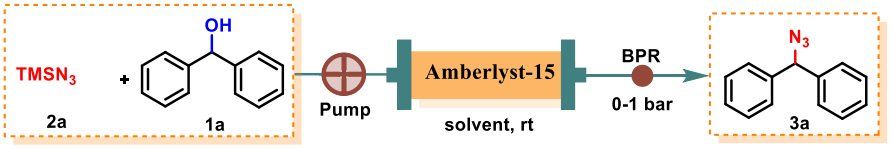

entry	substrate concentrations (M) (**1a**:**2a**)	flow rate (mL/min)	solvent	t_R (min)/no. of runs	yield (%)
1	0.025:0.075	0.1	DCM	21/1	96
2	0.025:0.075	0.1	EtOAc	21/1	nd
3	0.025:0.075	0.1	acetone	21/1	trace
4	0.025:0.075	0.1	THF	21/1	nd
5	0.025:0.075	0.1	ACN	21/1	trace
6	0.025:0.075	0.1	MeOH	21/1	nd
7	0.025:0.075	0.1	1,4-dioxane	21/1	nd
8	0.025:0.075	0.3	DCM	07/1	89
9	0.025:0.075	0.5	DCM	04/1	83
10	0.1:0.3	0.1	DCM	21/1	99
11	0.3:0.9	0.1	DCM	21/1	90

[a]For the reactions, a 0.1 M solution of **1a** and a solution of **2a** were prepared and passed through the 6.6 mm × 150 mm Omnifit packed bed reactor (1.00 g of Amberlyst-15, 6 cm bed height) (Vaportec R-series) at a specified temperature. t_R is the residence time. The mentioned yields are isolated yields.

To check the effect of solvent, flow rate, and concentration, various experiments were performed, and the results are summarized in Table 2 (entries 2−11). For instance, EtOAc, acetone, THF, ACN, MeOH, and 1,4-dioxane with 0.025 M **1a** and 0.075 M **2a** at a flow rate of 0.1 mL/min failed to give product **3a** (Table 2, entries 2−7, respectively). Hence, DCM became the optimum solvent, and we pursued further flow rate optimization. At 0.3 and 0.5 mL/min flow rates of **1a**, comparatively lower yields of **3a** were observed (Table 2, entries 8 and 9, respectively). Finally, this reaction was studied at

https://doi.org/10.1021/acs.joc.2c00941
J. Org. Chem. 2022, 87, 9926−9939

Scheme 2. Substrate Scope for the Azidation of Alcohols under Flow Conditions[a]

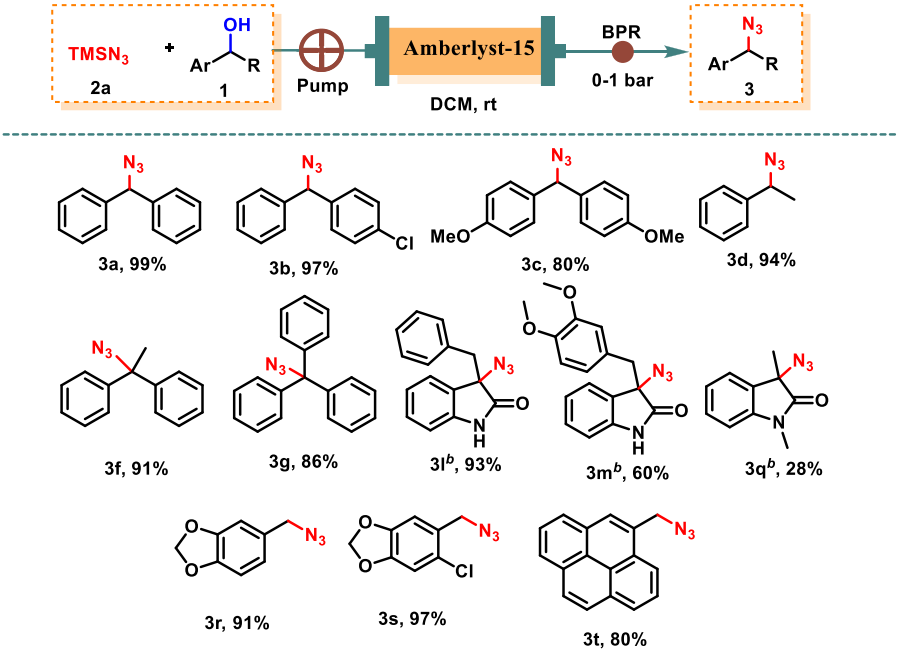

[a]For the reactions, a 0.1 M solution of **1** and a 0.3 M solution of $TMSN_3$ in DCM were prepared and passed through the 6.6 mm × 150 mm Omnifit packed bed reactor (1 g of Amberlyst-15, 6 cm bed height) (Vaportec R-series) with a flow rate of 0.1 mL/min at a specified temperature. t_R = 21 min; [b]80 °C in DCE. The mentioned yields are isolated yields.

Table 3. Optimization of the Reaction Conditions for the Azidation of Peroxides under Flow[a]

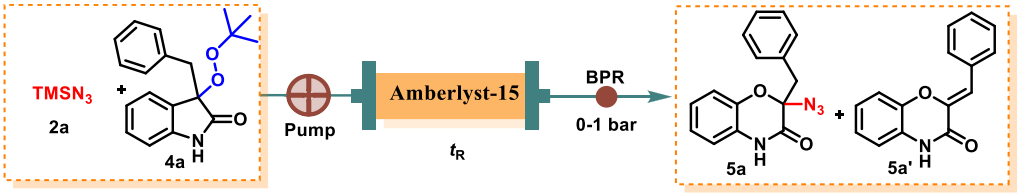

entry	substrate concentrations (M) (**4a**:**2a**)	flow rate (mL/min)	t_R (min)/no. of runs	yield (%) of **5a**
1	0.05:0.15	0.1	21/1	38
2	0.1:0.3	0.1	21/1	60
3	0.1:0.5	0.1	21/1	61
4	0.3:0.9	0.1	21/1	40
5[b]	0.1:0.3	0.1	21/1	–
6[c]	0.1:0.3	0.1	10/1	63
7[c]	0.1:0.3	0.2	05/1	68
8[d]	0.1:0.3	0.1	03/1	38

[a]For the reactions, a solution of **4a** and a solution of $TMSN_3$ **2a** in DCM were prepared and passed through the 6.6 mm × 150 mm Omnifit packed bed reactor (1g of Amberlyst-15, 6 cm bed height) (Vaportec R-series) at a specified temperature. t_R is the residence time. The mentioned yields are isolated yields. [b]At 60 °C. [c]With 0.5 g of Amberlyst-15, 3 cm bed height. [d]With 0.2 g of Amberlyst-15, 1 cm bed height.

different concentrations of 0.1 M **1a** and 0.3 M **2a** and 0.3 M **1a** and 0.9 M **2a**, which gave 98% and 90% yields of **3a**, respectively (Table 2, entries 10 and 11, respectively).

Next, the optimized flow condition was used for various alcohols. Thus, implementation of the optimum condition, which used 0.1 M **1a**, 0.3 M **2a**, and a flow rate of 0.1 mL at room temperature, for different alcohols improved the yields of azide products **3a**–**d**, **3f**, and **3g** (80–99%) (Scheme 2). Benzyl-substituted 3-hydroxy-2-oxindoles led to azide **3l** in 93% yield upon being heated at 80 °C in a DCE solvent, whereas a decrease in the yield was observed in the case of *N*-methyl-protected 3-methyl-3-hydroxy-2-oxindoles with a 28% yield of **3q**. Next, primary alcohols such as piperonyl alcohol, 6-chloropiperonyl alcohol, and pyrene methanol gave 91%, 97%, and 80% yields of **3r**–**t**, respectively.

Next we studied this azidation with peroxyoxindole for the skeletal rearrangement and subsequent azidation reactions. The optimized condition was established with model peroxide **4a** and flowing various concentrations of **4a**, which directly impact the yield of product **5a**. Thus, increasing the molar concentration of **4a** from 0.05 to 0.1 M improved the yield of **5a** from 38% to 60% (Table 3, entries 1 and 2), while 0.1 M **4a** with 0.5 M **2a** and 0.3 M **4a** with 0.9 M **2a** gave 61% and 40% yields of **5a**, respectively. As there was not much difference in product yield (Table 3, entries 2 and 3), 0.1 and 0.3 M were considered the ideal concentrations. Heating the reaction

https://doi.org/10.1021/acs.joc.2c00941
J. Org. Chem. 2022, 87, 9926–9939

Scheme 3. Substrate Scope for the Azidation of Peroxides under Flow[a]

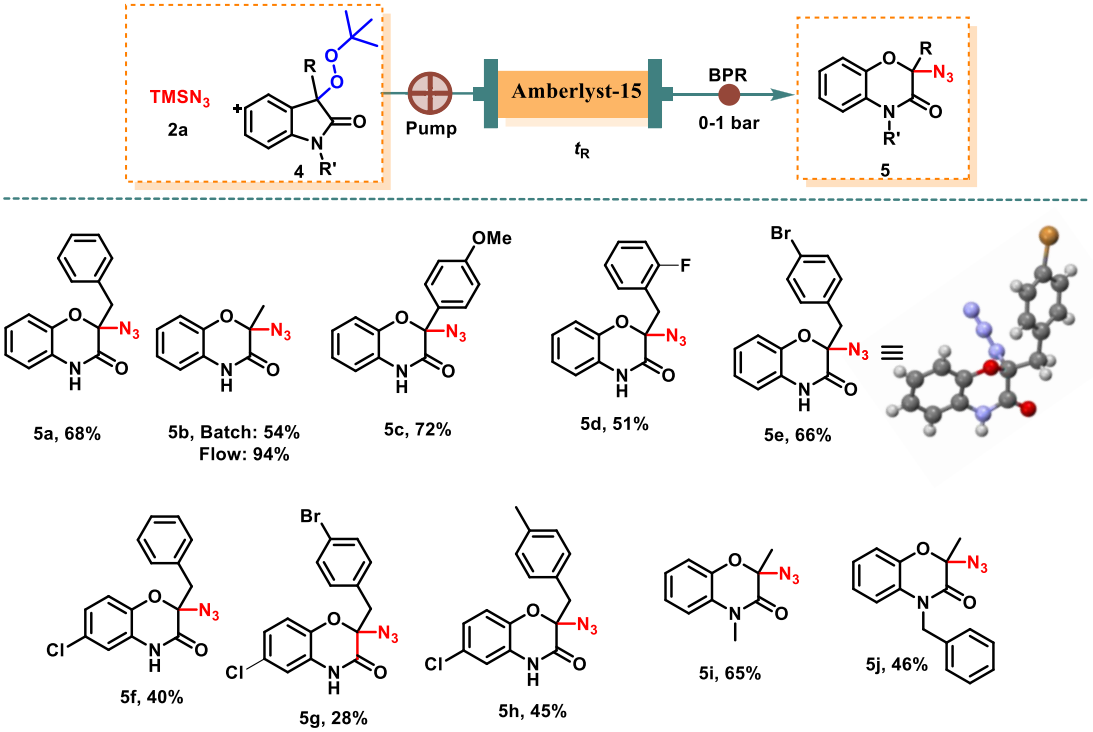

[a]For the reactions, a 0.1 M solution of peroxide **4** and a 0.3 M solution of $TMSN_3$ in DCM were prepared and passed through the 6.6 mm × 150 mm Omnifit packed bed reactor (1g of Amberlyst-15, 6 cm bed height) (Vaportec R-series) with a flow rate of 0.1 mL/min at room temperature. t_R = 21 min. The mentioned yields are isolated yields.

Scheme 4. Gram Scale and Catalyst Lifetime

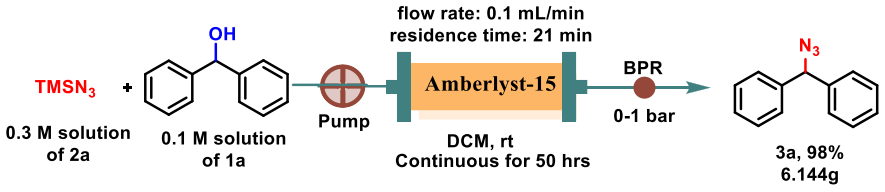

mixture at 60 °C gave only rearranged product **5a′** and no azidation product **5a**. To improve the outcome of the reaction, the bed height and flow rate were varied, which revealed entry 7 as the optimum condition with a 68% yield of **5a**. Competing product **5a′** was minimized by controlling the flow.

With these investigations, the generality of the reaction was explored with a variety of peroxides to generate a library of 2*H*-1,4-benzoxazin-3(4*H*)-one quaternary azide derivatives (Scheme 3). Notably, this sequential rearrangement−azidation reaction proceeded smoothly with 3-methyl-3-peroxyoxindoles to afford a 94% yield of **5b** (54% under batch conditions). Various other C3-substituted peroxides have also been subjected to these tandem reactions and afforded the corresponding products **5c−e** in moderate yields (Scheme 3). However, a decrease in yield was observed with chloro-substituted peroxyoxindole to afford the respective heterocyclic quaternary azides **5f−h** in moderate yields. Similarly, N-substituted peroxyoxindoles also afforded rearranged azides **5i** and **5j** in 65% and 46% yields, respectively (Scheme 3).

To demonstrate the feasibility of our protocol with respect to upscaling and to show the stability and efficiency of Amberlyst-15, we have demonstrated a long-duration experiment under continuous flow. Substrate **1a** and $TMSN_3$ were chosen as model substrates for this purpose. For instance, 30.0 mmol of reactant was pumped continuously for 50 h with a flow rate of 0.1 mL/min to afford 29.38 mmol of product with a TON (turnover number) of 9.24 and a TOF (turnover frequency) of 0.185 h^{-1} (Scheme 4). Product **3a** was isolated after continuous-flow synthesis for 50 h, leading to compound **3a** (6.144 g) in 98% yield. Although we have stopped the reaction after 50 h, the catalyst was still active for further reaction. Although it is known that there is a significant loss of activity of Amberlyst-15 for the other chemical transformation,[34,35] we found a negligible loss of activity over a longer period of the reaction.

The appeal of the azidation reactions in Schemes 1−3 is augmented by opportunities for further exploiting the azide unit in synthetic applications. A Staudinger reduction of azide **3a** facilitated the production of diphenylmethanamine **6a** in 58% yield under continuous flow (Scheme 5A). Next, [3+2] copper-catalyzed alkyne−azide cycloaddition was performed for **3a** and **3d** with ethynylbenzene using continuous flow to obtain new structural motif 1-benzhydryl-4-phenyl-1*H*-1,2,3-triazole **7a** and 4-phenyl-1-(1-phenylethyl)-1*H*-1,2,3-triazole **7b** (Scheme 5B).[36]

In addition, the synthetic utility of 3-azide **3** has been demonstrated by using a 0.1 M solution of **3** at 180 °C in a

https://doi.org/10.1021/acs.joc.2c00941
J. Org. Chem. 2022, 87, 9926−9939

Scheme 5. Synthetic Utility of Azides for Staudinger Reduction and Click Reaction under Flow

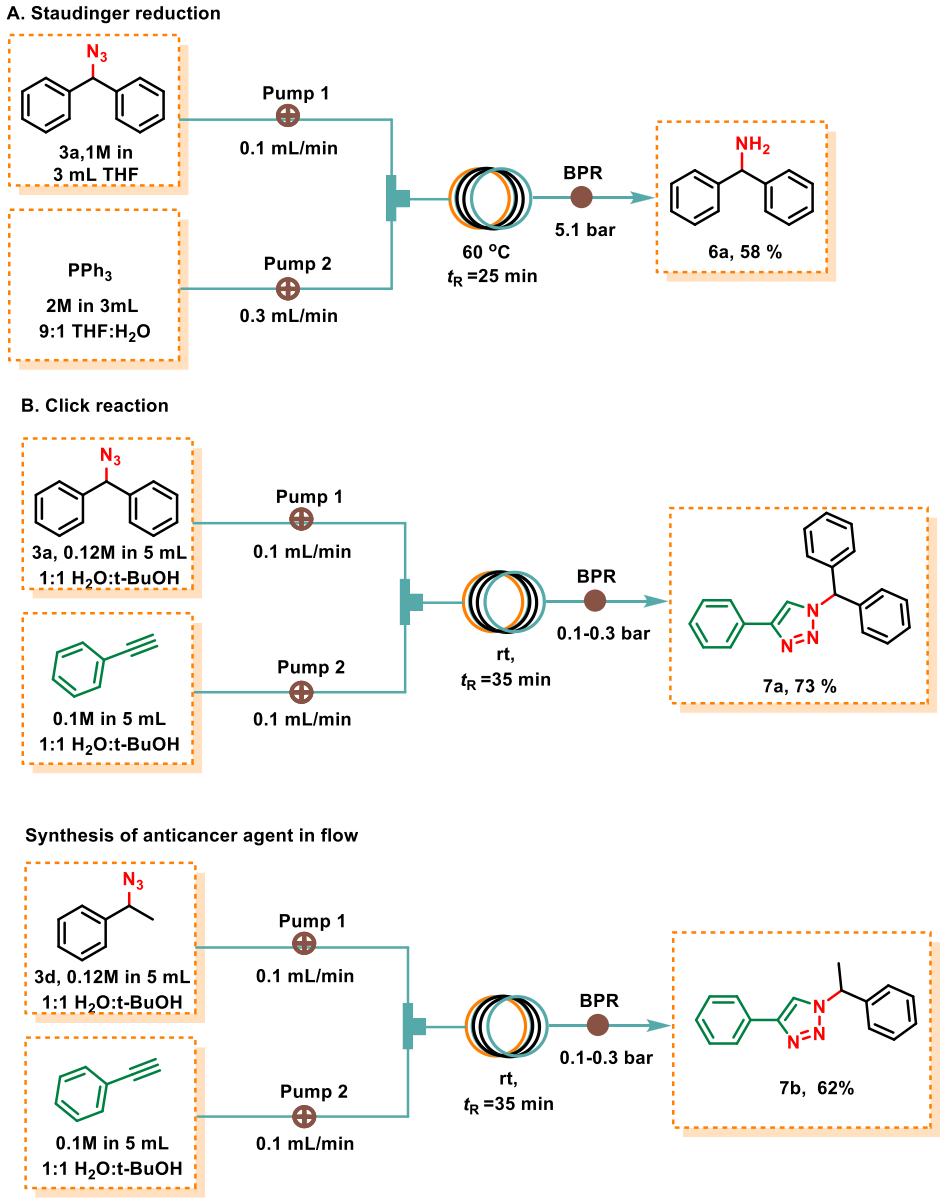

Vaportec HT reactor to give quinoxalin-2(1*H*)-one derivatives in 100 min. For instance, 3-benzyl- and 3-methyl-substituted 3-azide-2-oxindoles afforded **8l** and **8i** in 79% and 83% yields, respectively. In the case of -Me- and -OMe-substituted 3-phenyl-3-azide-2-oxindoles, 70% and 83% yields of **8j** and **8k**, respectively, were observed (Scheme 6). Next, **8n** having a bromo substitution on the C-3 benzyl core of **3n** was isolated in 81% yield. In addition, **8n** can be converted into the aldose reductase inhibitor in a single step.[38]

To shed light on the mechanism, Amberlyst protonates the hydroxyl group of **1a** to make it a better leaving group. Subsequent attack by N_3^- followed by expulsion of a water molecule gives rise to the desired azide **3a**. It should be noted that the nucleophilic attack can proceed via the S_N1 pathway. On the contrary, in the case of the azidation of peroxyoxindoles, at first Amberlyst-15 leads to the deprotection of **4** to give **A**.[37] In the next step, the distant oxygen atom of **A** coordinates to TMS because of the high affinity of oxygen for silicon, thereby making N_3^- free nucleophile. Then, positively charged species **B** facilitates ring expansion, generating in situ carbocationic species **C** that is attacked by N_3^- to afford azide **5** (Scheme 7).

CONCLUSION

In conclusion, we demonstrated safer azidation of various alcohols and peroxides using $TMSN_3$ as a reagent for azidation in the presence of Amberlyst-15 under batch and continuous-flow conditions. A process for the scale-up under continuous-flow azidation was demonstrated on a gram scale (6.14 g) with a 98% yield. Furthermore, continuous-flow azidation of quaternary hydroxy oxindole generates a wide array of quaternary azides in very good yields. The azidation of peroxides proceeded via a sequential deprotection−bond migration−nucleophilic substitution process to afford ring expansion followed by the transfer of azide, which afforded several substituted 2-azido-2*H*-benzo[*b*][1,4]oxazin-3(4*H*)-ones. In a continuous flow, expedient syntheses of rearranged azide products were observed in 21 min of residence time. This method was tolerant to functional groups and exhibited a broad substrate scope and a good yield. It

https://doi.org/10.1021/acs.joc.2c00941
J. Org. Chem. 2022, 87, 9926−9939

Scheme 6. Thermal Skeletal Rearrangement of Azides to Quinoxalin-2(1*H*)-one Derivatives under Flow[a]

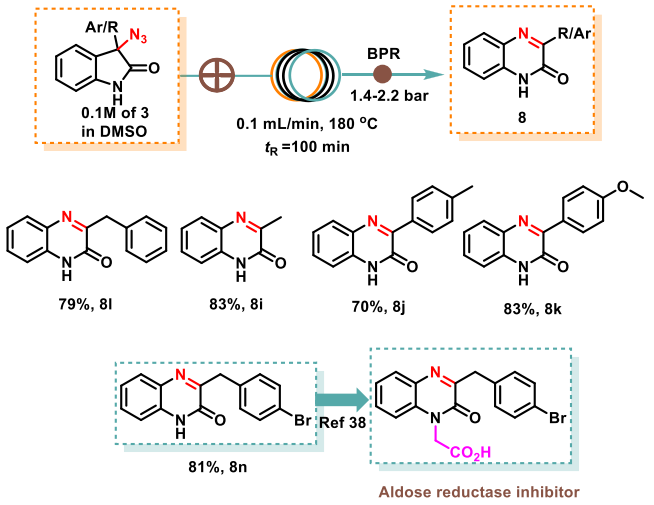

[a]For the reactions, a 0.1 M solution of azide **3** in DMSO was prepared and passed through the SS coil reactor with a volume of 10 mL (Vaportec R-series) with a flow rate of 0.1 mL/min at 180 °C. t_R = 100 min. The mentioned yields are isolated yields.

Scheme 7. Plausible Mechanism for the Azidation of Peroxyoxyindoles via In Situ Ring Expansion

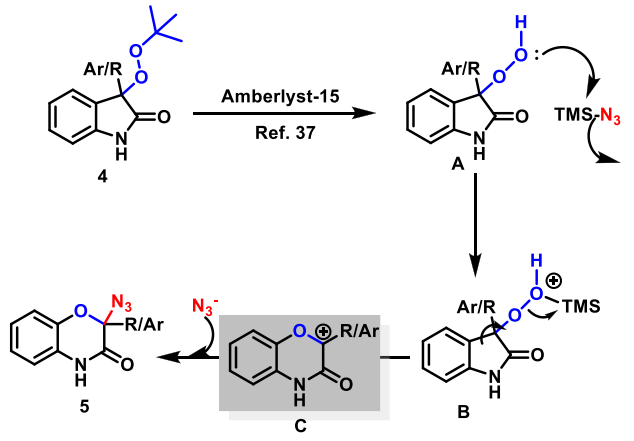

is a safer process for the longer and scale-up operation. The usefulness of azides was shown in the continuous-flow click reaction utilizing alkyne and azide to generate a biologically important triazole scaffold. In addition, this (azidomethylene)-dibenzene was reduced under continuous flow to generate the diphenylmethanamine efficiently. Thermolytic rearrangement of quaternary oxindole azide was developed in the continuous-flow module to generate a wide array of 2*H*-1,4-benzoxazin-3(4*H*)-one derivatives in very good yields in 100 min by using an SS coil reactor.

EXPERIMENTAL SECTION

General Information and Collection of Data. All of the chemicals were purchased from Sigma-Aldrich and SD Fine Chemicals and used without further modification. All solvents were purchased from Rankem and Finar Chemicals. Deuterated solvents were used as received. Column chromatographic separations were performed over 100−200 silica gel. Visualization was accomplished with UV light. The flow chemistry experiments were carried out on a Vaportec R-series instrument with a glass column (Omntifit, 6.6 mm × 150 mm). The ^{1}H and ^{13}C{^{1}H} NMR spectra were recorded at 400 and 100 MHz, respectively, using Bruker or JEOL spectrometers. The following abbreviations were used in the NMR follow-up experiments: b, broad; s, singlet; d, doublet; t, triplet; q, quartet; td and dd, doublet of triplets and doublet of doublets, respectively; m, multiplet; tt, triplet of triplets; and ddd, doublet of doublet of doublets. The flow chemistry experiments were carried out on a Vaportec R-series instrument with a glass column (Omntifit, 6.6 mm × 150 mm) and a Vaportec R-series instrument with an SS coil reactor (10 mL). HRMS spectra were recorded with Waters-synapt G2 using electrospray ionization (ESI-TOF). Infrared (ATIR) spectra were recorded with a Bruker Alpha-E infrared spectrometer. Single-crystal diffraction analysis data were collected at 100 K with a BRUKER KAPPA APEX III CCD Duo diffractometer (operated at 1500 W power; 50 kV, 30 mA) using graphite monochromatic Mo Kα radiation and Cu Kα radiation.

Caution should be exercised when using azides. Both organic and inorganic azides can be heat- and shock-sensitive and can explosively decompose with little input of external energy.

A small amount of $TMSN_3$ should be used when performing batch reaction. To evaluate the stability of azide, a (^{N}carbon + ^{N}oxygen)/^{N}nitrogen ratio of ≥3 should be used.

Experimental Procedure A for a Long-Duration Experiment of Azidation of Diphenylmethanol under Continuous Flow. Diphenylmethanol (30 mmol, 5.52 g) in 300 mL of dichloromethane and 3 equiv of azidotrimethylsilane (90 mmol, 10.35 g) was premixed and passed through the Omnifit (6.6 mm × 150 mm) packed bed column (1 g of Amberlyst-15, bed height of 5 cm, swollen to 6 cm) at room temperature with a flow rate of 0.1 mL/min with 0−2 bar pressure for 50 h. The conversion was monitored by TLC and NMR. After 50 h, the reaction was stopped and the mixture was concentrated under vacuum and then subjected to column chromatography on silica gel (hexane). Product **3a** was isolated (6.144 g) in 98% yield with a TON of 9.24 and a TOF of 0.185 h^{-1}

General Procedure B for the Azidation of Alcohols under Batch Conditions. To an oven-dried 20 mL resealable pressure tube (equipped with a rubber septum) were added alcohols (0.5 mmol), azidotrimethylsilane (1.5 mmol), and Amberlyst-15 (w/w with respect to alcohols) in dichloromethane (2 mL) with a magnetic bar, and then the mixture was stirred at room temperature (25 °C) for 30 min to 1 h. The progress of the reaction was monitored by TLC until the reaction had reached completion. The volatile solvents were removed using vacuum, and the crude reaction mixture was directly purified by column chromatography on silica gel directly (from 0:100 to 5:95 EtOAc:hexane).

General Procedure C for the Azidation of Alcohols under Continuous Flow. In a typical procedure, the 0.1 M solution of alcohol derivatives in dichloromethane and 3 equiv of azidotrimethylsilane was premixed and passed through the Omnifit (6.6 mm × 150 mm) packed bed column packed with Amberlyst-15 up to 5 cm (1.0 g, swollen up to 6 cm after passing solvent) at room temperature at 0−1 bar pressure with a flow rate of 0.1 mL/min. After the reaction had reached completion, the catalyst bed was washed with dichloromethane. A volatile component was evaporated using a vacuum. The residue was directly purified by silica gel chromatography (from 1:99 to 5:95 EtOAc:hexane). The Amberlyst-15 bed was recycled by being washed with DCM and reused for the other substrates.

For preventive measurement, we have filtered the solution through a syringe filter before pumping it through pumps [filtration carried out using a nylon syringe filter (0.22 μm)]. The time mentioned under flow is the residence time (t_R); the residence time can be calculated as (reactor volume)/(flow rate).

General Procedure D for the Azidation of Peroxides under Continuous Flow. The 0.1 M solution of peroxide derivatives in dichloromethane and 3 equiv of azidotrimethylsilane was premixed and passed through the Omnifit (6.6 mm × 150 mm) packed bed column packed with Amberlyst-15 up to 5 cm (1.0 g, swollen up to 6 cm after passing solvent) at room temperature at 0−1 bar pressure with a flow rate of 0.1 mL/min. After the reaction had reached completion, the catalyst bed was washed with dichloromethane. A volatile component

https://doi.org/10.1021/acs.joc.2c00941
J. Org. Chem. 2022, 87, 9926−9939

was evaporated using a vacuum. The residue was directly purified by silica gel chromatography (10:90 EtOAc:hexane).

General Procedure E for the Synthesis of Diphenylmethanamine.[33] To perform the Staudinger reduction step in a flow process, the stream of a 1.0 M solution of (azidomethylene)dibenzene **3a** was combined in a T-piece with a stream of triphenylphosphine (2 equiv) in aqueous THF (9:1 THF:water) at flow rates of 0.1 mL/min for **3a** and 0.3 mL/min for triphenylphosphine. The resulting mixture was then allowed to react in a Vaportec R-series SS coil reactor (10 mL, 60 °C, residence time of 25 min) before being passed through a back-pressure regulator and collected in a flask. The volatile component of the crude mixture was evaporated using a vacuum and extracted with DCM. The residue was directly purified by silica gel chromatography (40:60 EtOAc:hexane).

General Procedure F for the Click Reaction under Flow. Azides **3** (0.12 M, 5 mL of *t*-BuOH/H_2O) and phenylacetylene (0.1 M, 5 mL of *t*-BuOH/H_2O) were passed through pump 1 and pump 2, respectively, with a flow rate of 0.1 mL/min each through PTFE tubing (7 mL) at room temperature at 0.1−0.3 bar pressure. The reaction mixture was collected continuously after 35 min. The reaction mixture was extracted with EtOAc (3 × 10 mL). The solvent was evaporated under vacuum, and the residue was subjected to column chromatography purification using EtOAc/*n*-hexane (20:80) to afford the corresponding 1,2,3-triazole derivatives in good yields.

General Procedure G for Ring Expansion of Quaternary 2-Oxindole Azides in Batch Mode. The tertiary azide of 2-oxindole (0.1 M, 5 mL of DMSO) was passed through a Vaportec R-series 10 mL SS coil reactor with a flow rate of 0.1 mL/min at 180 °C and 1.4−2.2 bar pressure. The reaction mixture was collected continuously after 100 min. To the reaction mixture were added 50 mL of water and 2 mL of EtOAc, and the mixture was left to precipitate overnight. Next, the formed precipitate was filtered, washed with water several times, dissolved in methanol, and passed through a bed of sodium sulfate to afford the corresponding quinoxalin-2(1*H*)-one derivatives in excellent yields.

Analytical Data for the Products. *(Azidomethylene)dibenzene (**3a**). Batch Condition.* The title compound was prepared according to general procedure B, using diphenyl methanol (184 mg, 1.0 mmol) to afford (azidomethylene)dibenzene **3a** (204.8 mg, 98%) as a colorless oil after purification by column chromatography on silica gel directly (hexane).

Flow Condition. The title compound was prepared according to general procedure A. A solution of 0.1 M diphenyl methanol (5520.0 mg, 30 mmol) in 300 mL of dichloromethane was passed through the packed bed of Amberlyst-15 (6.0 cm bed height) at 0−1 bar and a flow rate of 0.1 mL/min to afford (azidomethylene)dibenzene **3a** (6144.0 mg, 98% yield) as a colorless oil after purification by column chromatography on silica gel directly (hexane): ^{1}H NMR (400 MHz, $CDCl_3$) δ 7.40 (m, 10H), 5.79 (s, 1H); $^{13}C\{^1H\}$ NMR (100 MHz, $CDCl_3$) δ 139.7, 128.8, 128.1, 127.5, 68.6; IR (neat) 2096, 1455, 1238 cm^{-1}; HRMS (ESI-TOF) m/z $[M + H - N_2]^+$ calcd for $C_{13}H_{12}N$ 182.0970, found 182.0966.

*1-[Azido(phenyl)methyl]-4-chlorobenzene (**3b**). Batch Condition.* The title compound was prepared according to general procedure B, using (4-chlorophenyl)(phenyl)methanol (109 mg, 0.50 mmol) to afford 1-[azido(phenyl)methyl]-4-chlorobenzene **3b** (89.9 mg, 74%) as a pale yellow oil after purification by column chromatography on silica gel directly (1:99 EtOAc:hexane).

Flow Condition. The title compound was prepared according to general procedure C. A solution of 0.1 M (4-chlorophenyl)(phenyl)-methanol (109.0 mg, 0.50 mmol) in 5 mL of dichloromethane was passed through a packed bed of Amberlyst-15 (6.0 cm bed height) at 0−1 bar and a flow rate of 0.1 mL/min to afford 1-[azido(phenyl)methyl]-4-chlorobenzene **3b** (117.8 mg, 97% yield) as a pale yellow oil after purification by column chromatography on silica gel directly (1:99 EtOAc:hexane): ^{1}H NMR (400 MHz, $CDCl_3$) δ 7.26 (m, 9H), 5.63 (s, 1H); $^{13}C\{^1H\}$ NMR (100 MHz, $CDCl_3$) δ 139.2, 138.3, 134.0, 128.9, 128.4, 127.5, 67.9; IR (neat) 2098, 1659, 1495, 1087, 703 cm^{-1}; HRMS (ESI-TOF) m/z $[M + H - N_2]^+$ calcd for $C_{13}H_{11}ClN$ 216.0580, found 216.0571.

*4,4′-(Azidomethylene)bis(methoxybenzene) (**3c**). Batch Condition.* The title compound was prepared according to general procedure B, using bis(4-methoxyphenyl)methanol (122 mg, 0.50 mmol) to afford 4,4′-(azidomethylene)bis(methoxybenzene) **3c** (96.8 mg, 72%) as a pale yellow oil after purification by column chromatography on silica gel directly (1:99 EtOAc:hexane).

Flow Condition. The title compound was prepared according to general procedure C. A solution of 0.1 M bis(4-methoxyphenyl)-methanol (122 mg, 0.50 mmol) in 5 mL of dichloromethane was passed through a packed bed of Amberlyst-15 (6.0 cm bed height) at 0−1 bar and a flow rate of 0.1 mL/min to afford 4,4′-(azidomethylene)bis-(methoxybenzene) **3c** (107.6 mg, 80% yield) as a pale yellow oil after purification by column chromatography on silica gel directly (1:99 EtOAc:hexane): ^{1}H NMR (400 MHz, $CDCl_3$) δ 8.51 (s, 1H), 6.20 (s, 1H), 2.63 (s, 2H), 2.57 (q, J = 7.5, 15.1 Hz, 2H), 2.32 (s, 2H), 1.23 (t, J = 7.5 Hz, 3H), 1.10 (s, 6H); $^{13}C\{^1H\}$ NMR (100 MHz, $CDCl_3$) δ 194.1, 142.1, 135.8, 119.2, 101.1, 52.1, 36.9, 35.9, 28.8, 20.8, 13.2; IR (neat) 2092, 1611, 1508, 1243 cm^{-1}; HRMS (ESI-TOF) m/z $[M + H - N_2]^+$ calcd for $C_{15}H_{16}NO_2$ 242.1181, found 242.1174.

*(1-Azidoethyl)benzene (**3d**).*[39] The title compound was prepared according to general procedure B, using 1-phenylethan-1-ol (61 mg, 0.50 mmol) to afford (1-azidoethyl)benzene **3d** (133.2 mg, 91%) as a colorless oil after purification by column chromatography on silica gel directly (hexane).

Flow Condition. The title compound was prepared according to general procedure C. A solution of 0.1 M 1-phenylethan-1-ol (61 mg, 0.50 mmol) in 5 mL of dichloromethane was passed through a packed bed of Amberlyst-15 (6.0 cm bed height) at 0−1 bar and a flow rate of 0.1 mL/min to afford (1-azidoethyl)benzene **3d** (138.0 mg, 94% yield) as a colorless oil after purification by column chromatography on silica gel directly (hexane): ^{1}H NMR (400 MHz, $CDCl_3$) δ 7.37 (m, 15H), 4.63 (m, 1H), 1.54 (d, J = 6.7 Hz, 3H); $^{13}C\{^1H\}$ NMR (100 MHz, $CDCl_3$) δ 141.0, 128.9, 128.5, 126.5, 61.2, 21.7; IR (neat) 2099, 1246 cm^{-1}.

*2-(1-Azidoethyl)naphthalene (**3e**).* The title compound was prepared according to general procedure B, using 1-(naphthalen-2-yl)ethan-1-ol (86 mg, 0.50 mmol) to afford 2-(1-azidoethyl)-naphthalene **3e** (97.6 mg, 99%) as a colorless oil after purification by column chromatography on silica gel directly (0:100 EtOAc:hexane) as a colorless oil after purification by column chromatography on silica gel directly (hexane): ^{1}H NMR (400 MHz, $CDCl_3$) δ 8.16 (dd, J = 8.2, 3.4 Hz, 1H), 7.92 (ddd, J = 11.2, 8.0, 2.7 Hz, 2H), 7.59 (m, 4H), 5.40 (m, 1H), 1.78 (dd, J = 6.8, 2.8 Hz, 3H); $^{13}C\{^1H\}$ NMR (100 MHz, $CDCl_3$) δ 136.2, 134.0, 130.6, 129.1, 128.8, 126.5, 125.9, 125.4, 123.6, 123.1, 57.6, 20.7; IR (neat) 2009, 1508, 1241 cm^{-1}; HRMS (ESI-TOF) m/z $[M + H - N_2]^+$ calcd for $C_{12}H_{12}N$ 170.0970, found 170.0968.

*(1-Azidoethane-1,1-diyl)dibenzene (**3f**). Batch Condition.* The title compound was prepared according to general procedure B, using 1,1-diphenylethan-1-ol (198 mg, 1.0 mmol) to afford (1-azidoethane-1,1-diyl)dibenzene **3f** (191.8 mg, 86%) as a pale yellow oil after purification by column chromatography on silica gel directly (hexane).

Flow Condition. The title compound was prepared according to general procedure C. A solution of 0.1 M 1,1-diphenylethan-1-ol (198 mg, 1.0 mmol) in 10 mL of dichloromethane was passed through a packed bed of Amberlyst-15 (6.0 cm bed height) at 0−1 bar and a flow rate of 0.1 mL/min to afford (1-azidoethane-1,1-diyl)dibenzene **3f** (203.0 mg, 91% yield) as a pale yellow oil after purification by column chromatography on silica gel directly (hexane): ^{1}H NMR (400 MHz, $CDCl_3$) δ 7.35 (m, 10H), 2.07 (s, 3H); $^{13}C\{^1H\}$ NMR (100 MHz, $CDCl_3$) δ 144.3, 128.5, 127.6, 126.7, 69.5, 27.5; IR (neat) 2087, 1492, 1444, 1238 cm^{-1}; HRMS (ESI-TOF) m/z $[M + H - N_2]^+$ calcd for $C_{14}H_{14}N$ 196.1126, found 196.1129.

*(Azidomethanetriyl)tribenzene (**3g**). Batch Condition.* The title compound was prepared according to general procedure B, using triphenylmethanol (130 mg, 0.5 mmol) to afford (azidomethanetriyl)-tribenzene **3g** (114.0 mg, 80%) as a white solid after purification by column chromatography on silica gel directly (hexane).

Flow Condition. The title compound was prepared according to general procedure C. A solution of 0.1 M triphenylmethanol (130 mg, 0.5 mmol) in 5 mL of dichloromethane was passed through a packed

https://doi.org/10.1021/acs.joc.2c00941
J. Org. Chem. 2022, 87, 9926−9939

bed of Amberlyst-15 (6.0 cm bed height) at 0−1 bar and a flow rate of 0.1 mL/min to afford (azidomethanetriyl)tribenzene **3g** (122.5 mg, 86% yield) as a white solid after purification by column chromatography on silica gel directly (hexane): mp 67−69 °C; ^{1}H NMR (400 MHz, $CDCl_3$) δ 7.32 (m, 15H); $^{13}C\{^1H\}$ NMR (100 MHz, $CDCl_3$) δ 143.3, 128.6, 128.3, 127.8; IR (neat) 2096, 1455, 1238 cm^{-1}; HRMS (ESI-TOF) m/z $[M + H - N_2]^+$ calcd for $C_{19}H_{16}N$ 258.1283, found 258.1290. The crystal was grown by a simple recrystallization method. The pure compound isolated after column chromatography was dissolved in dichloromethane, layered with hexane, and kept at room temperature for 2 days to obtain the pure crystal.[42]

*3-Azido-3-methylindolin-2-one (**3h**).* The title compound was prepared according to general procedure B, using 3-hydroxy-3-methylindolin-2-one (81.5 mg, 0.5 mmol) at 80 °C in dichloroethane to afford 3-azido-3-methylindolin-2-one **3h** (80.5 mg, 86%) as a yellow solid after purification by column chromatography on silica gel directly (5:95 EtOAc:hexane): mp 94−96 °C; ^{1}H NMR (400 MHz, $CDCl_3$) δ 8.69 (s, 1H), 7.31 (t, J = 8.2 Hz, 2H), 7.11 (t, J = 7.6 Hz, 1H), 6.96 (d, J = 7.7 Hz, 1H), 1.70 (s, 3H); $^{13}C\{^1H\}$ NMR (100 MHz, $CDCl_3$) δ 177.4, 140.1, 130.3, 129.3, 124.0, 123.5, 110.8, 63.9, 21.6; IR (neat) 2089, 1716, 1620, 1472, 1201 cm^{-1}; HRMS (ESI-TOF) m/z $[M + H - N_2]^+$ calcd for $C_9H_9N_2O$ 161.0715, found 161.0709.

*3-Azido-3-phenylindolin-2-one (**3i**).* The title compound was prepared according to general procedure B, using 3-hydroxy-3-phenylindolin-2-one (45 mg, 0.5 mmol) to afford 3-azido-3-phenylindolin-2-one **3i** (40 mg, 80%) as a pale yelow solid after purification by column chromatography on silica gel directly (5:95 EtOAc:hexane): mp 328−330 °C; ^{1}H NMR (400 MHz, $CDCl_3$) δ 8.77 (s, 1H), 7.39 (m, 6H), 7.26 (m, 1H), 7.12 (td, J = 7.6 Hz, 1H), 7.00 (d, J = 7.8 Hz, 1H); $^{13}C\{^1H\}$ NMR (100 MHz, $CDCl_3$) δ 176.0, 140.7, 136.3, 130.6, 129.1, 129.0, 128.9, 126.6, 125.6, 123.8, 111.1, 70.4; IR (neat) 3249, 2101, 1730, 1717, 1622, 1476 cm^{-1}; HRMS (ESI-TOF) m/z $[M + Na]^+$ calcd for $C_{14}H_{10}N_4ONa$ 273.0752, found 273.0759.

*3-Azido-3-(p-tolyl)indolin-2-one (**3j**).* The title compound was prepared according to general procedure B, using 3-hydroxy-3-(*p*-tolyl)indolin-2-one (119.0 mg, 0.50 mmol) to afford 3-azido-3-(*p*-tolyl)indolin-2-one **3j** (120.0 mg, 91%) as a pale yellow solid after purification by column chromatography on silica gel directly (5:95 EtOAc:hexane): mp 310−312 °C; ^{1}H NMR (400 MHz, DMSO-d_6) δ 6.81 (s, 1H), 4.84 (s, 1H), 3.25 (m, 2H), 2.88 (s, 1H), 2.72 (s, 1H), 2.29 (t, J = 6.0 Hz, 2H), 2.05 (t, J = 6.2 Hz, 2H), 1.76 (m, 2H), 1.06 (d, J = 6.3 Hz, 3H); $^{13}C\{^1H\}$ NMR (100 MHz, DMSO-d_6) δ 194.5, 164.0, 94.7, 63.6, 49.5, 36.5, 28.8, 21.7, 16.6; IR (neat) 2098, 1725, 1619, 1471 cm^{-1}; HRMS (ESI-TOF) m/z $[M + Na]^+$ calcd for $C_{15}H_{12}N_4ONa$ 287.0909, found 287.0908.

*3-Azido-3-(4-methoxyphenyl)indolin-2-one (**3k**).* The title compound was prepared according to general procedure B, using 3-hydroxy-3-(4-methoxyphenyl)indolin-2-one (127.5 mg, 0.50 mmol) to afford 3-azido-3-(4-methoxyphenyl)indolin-2-one **3k** (138.5 mg, 99%) as a pale yellow liquid after purification by column chromatography on silica gel directly (5:95 EtOAc:hexane): ^{1}H NMR (400 MHz, DMSO-d_6) δ 6.80 (d, J = 7.52 Hz, 1H), 4.89 (s, 1H), 4.85 (s, 1H), 3.33 (m, 4H), 2.41 (m, 2H), 2.31 (m, 2H), 2.06 (t, J = 6.12 Hz, 2H), 2.03 (s, 3H), 1.77 (m, 2H), 1.64 (m, 1H); $^{13}C\{^1H\}$ NMR (100 MHz, DMSO-d_6) δ 194.6, 164.6, 94.7, 62.0, 52.9, 36.5, 30.2, 30.0, 28.8, 21.7, 14.7; IR (neat) 2102, 1725, 1619, 1510 cm^{-1}; HRMS (ESI-TOF) m/z $[M + Na]^+$ calcd for $C_{15}H_{12}N_4O_2Na$ 303.0858, found 303.0851.

*3-Azido-3-benzylindolin-2-one (**3l**). Batch Condition.* The title compound was prepared according to general procedure A, using 3-benzyl-3-hydroxyindolin-2-one (119 mg, 0.50 mmol) at 80 °C in dichloroethane to afford 3-azido-3-benzylindolin-2-one **3l** (112 mg, 85%) as a pale yellow semisolid after purification by column chromatography on silica gel directly (5:95 EtOAc:hexane).

Flow Condition. The title compound was prepared according to general procedure C. A solution of 0.1 M 3-benzyl-3-hydroxyindolin-2-one (119 mg, 0.50 mmol) at 80 °C in 5 mL of dichloroethane was passed through a packed bed of Amberlyst-15 (6.0 cm bed height) at 0−1 bar and a flow rate of 0.1 mL/min to afford 3-azido-3-benzylindolin-2-one **3l** (123.0 mg, 93%) as a pale yellow semisolid after purification by column chromatography on silica gel directly (5:95 EtOAc:hexane): ^{1}H NMR (400 MHz, $CDCl_3$) δ 8.36 (s, 1H), 7.26 (m, 1H), 7.15 (m, 3H), 7.06 (m, 2H), 7.00 (m, 2H), 6.80 (d, J = 7.7 Hz, 1H), 3.36 (d, J = 13.1 Hz, 1H), 3.24 (d, J = 13.2 Hz, 1H); $^{13}C\{^1H\}$ NMR (100 MHz, $CDCl_3$) δ 176.5, 140.5, 133.2, 130.5, 130.3, 128.1, 127.4, 126.5, 125.2, 123.0, 110.6, 68.0, 41.6; IR (neat) 2101, 1719, 1472 cm^{-1}; HRMS (ESI-TOF) m/z $[M + Na]^+$ calcd for $C_{15}H_{12}N_4ONa$ 287.0909, found 287.0909.

*3-Azido-3-(3,4-dimethoxybenzyl)indolin-2-one (**3m**). Batch Condition.* The title compound was prepared according to general procedure A, using 3-(3,4-dimethoxybenzyl)-3-hydroxyindolin-2-one (149 mg, 0.50 mmol) at 80 °C in dichloroethane to afford 3-azido-3-(3,4-dimethoxybenzyl)indolin-2-one **3m** (120.0 mg, 73%) as a pale yellow semisolid after purification by column chromatography on silica gel directly (5:95 EtOAc:hexane).

Flow Condition. The title compound was prepared according to general procedure C. A solution of 0.1 M 3-(3,4-dimethoxybenzyl)-3-hydroxyindolin-2-one (149 mg, 0.50 mmol) at 80 °C in 5 mL of dichloroethane was passed through a packed bed of Amberlyst-15 (6.0 cm bed height) at 0−1 bar and a flow rate of 0.1 mL/min to afford 3-azido-3-(3,4-dimethoxybenzyl)indolin-2-one **3m** (98.0 mg, 60%) as a pale yellow semisolid after purification by column chromatography on silica gel directly (5:95 EtOAc:hexane): ^{1}H NMR (400 MHz, $CDCl_3$) δ 8.65 (s, 1H), 7.24 (m, 1H), 7.14 (d, J = 7.1 Hz, 1H), 7.06 (m, 1H), 6.79 (d, J = 7.7 Hz, 1H), 6.59 (m, 2H), 6.39 (d, J = 2.0 Hz, 1H), 3.76 (s, 3H), 3.60 (s, 3H), 3.29 (d, J = 13.3 Hz, 1H), 3.19 (d, J = 13.1 Hz, 1H); $^{13}C\{^1H\}$ NMR (100 MHz, $CDCl_3$) δ 176.4, 148.2, 140.9, 130.3, 126.8, 125.5, 125.1, 122.9, 122.8, 113.4, 110.8, 110.7, 68.1, 55.7, 55.6, 41.3; IR (neat) 2101, 1635 cm^{-1}; HRMS (ESI-TOF) m/z $[M + Na]^+$ calcd for $C_{17}H_{16}N_4O_3Na$ 347.1120, found 347.1118.

*3-Azido-3-(4-bromobenzyl)indolin-2-one (**3n**).* The title compound was prepared according to general procedure B, using 3-(4-bromobenzyl)-3-hydroxyindolin-2-one (159.0 mg, 0.50 mmol) at 80 °C in dichloroethane to afford 3-azido-3-(4-bromobenzyl)indolin-2-one **3n** (171.0 mg, 70%) as a yellow solid after purification by column chromatography on silica gel directly (5:95 EtOAc:hexane): ^{1}H NMR (400 MHz, $CDCl_3$) δ 7.93 (s, 1H), 7.27 (m, 3H), 7.09 (m, 2H), 6.86 (m, 2H), 6.79 (d, J = 7.8 Hz, 1H), 3.29 (d, J = 13.1 Hz, 1H), 3.21 (d, J = 13.1 Hz, 1H); $^{13}C\{^1H\}$ NMR (100 MHz, $CDCl_3$) δ 175.6, 140.4, 132.2, 131.4, 130.5, 126.3, 125.1, 123.2, 121.7, 110.7, 67.7, 41.1; IR (neat) 2104, 1652 cm^{-1}.

*3-Azido-3-benzyl-6-chloroindolin-2-one (**3o**).* The title compound was prepared according to general procedure B, using 3-benzyl-6-chloro-3-hydroxyindolin-2-one (137.0 mg, 0.50 mmol) at 80 °C in dichloroethane to afford 3-azido-3-benzyl-6-chloroindolin-2-one **3o** (104.0 mg, 70%) as a yellow-white semisolid after purification by column chromatography on silica gel directly (5:95 EtOAc:hexane): ^{1}H NMR (400 MHz, $CDCl_3$) δ 11.42 (d, J = 10.4 Hz, 1H), 7.86 (m, 2H), 7.35 (m, 9H), 7.05 (m, 2H), 6.81 (d, J = 7.3 Hz, 2H), 5.55 (s, 1H), 3.91 (s, 1H), 3.74 (m, 2H), 3.64 (m, 1H), 2.86 (m, 2H); $^{13}C\{^1H\}$ NMR (100 MHz, $CDCl_3$) δ 188.6, 167.6, 140.6, 137.9, 135.8, 130.8, 129.8, 129.2, 128.6, 128.4, 128.3, 127.9, 127.5, 126.6, 94.3, 65.4, 59.0, 39.8; IR (neat) 2114, 1725, 1614 cm^{-1}; HRMS (ESI-TOF) m/z $[M + Na]^+$ calcd for $C_{15}H_{11}N_4OClNa$ 321.0519, found 321.0514.

*3-Azido-1,3-dibenzylindolin-2-one (**3p**).* The title compound was prepared according to general procedure B, using 1,3-dibenzyl-3-hydroxyindolin-2-one (165.0 mg, 0.50 mmol) at 80 °C in dichloroethane to afford 3-azido-1,3-dibenzylindolin-2-one **3p** (88.6 mg, 50%) as a yellow-white solid after purification by column chromatography on silica gel directly (5:95 EtOAc:hexane): mp 114−116 °C; ^{1}H NMR (400 MHz, $CDCl_3$) δ 7.86 (dd, J = 8.3, 1.3 Hz, 1H), 7.49 (d, J = 7.5 Hz, 2H), 7.39 (m, 1H), 7.30 (m, 5H), 7.22 (m, 5H), 5.46 (s, 2H), 4.33 (s, 2H); $^{13}C\{^1H\}$ NMR (100 MHz, $CDCl_3$) δ 159.6, 155.0, 137.2, 135.4, 133.2, 132.8, 130.1, 130.0, 129.7, 129.0, 128.6, 127.8, 127.0, 126.7, 123.8, 114.5, 46.1, 40.9; IR (neat) 2101, 1720, 1614, 1468 cm^{-1}; HRMS (ESI-TOF) m/z $[M + Na]^+$ calcd for $C_{22}H_{18}N_4ONa$ 377.1378, found 377.1378. The crystal was grown by simple recrystallization. The pure compound isolated after column chromatography was dissolved in dichloromethane, layered with hexane, and kept at room temperature for 2 days to obtain the pure crystal.

*3-Azido-1,3-dimethylindolin-2-one (**3q**).* The title compound was prepared according to general procedure C. A solution of 0.1 M 3-

https://doi.org/10.1021/acs.joc.2c00941
J. Org. Chem. 2022, 87, 9926−9939

hydroxy-1,3-dimethylindolin-2-one (89 mg, 0.50 mmol) in 5 mL of dichloromethane was passed through the packed bed of Amberlyst-15 (6.0 cm bed height) at 0−1 bar and a flow rate of 0.1 mL/min to afford 3-azido-1,3-dimethylindolin-2-one **3q** (28.3 mg, 28%) as a colorless oil after purification by column chromatography on silica gel directly (5:95 EtOAc:hexane): ^{1}H NMR (400 MHz, $CDCl_3$) δ 11.41 (d, J = 10.6 Hz, 1H), 7.87 (d, J = 7.6 Hz, 2H), 7.38 (m, 8H), 5.70 (s, 1H), 3.70 (m, 2H), 3.36 (m, 1H), 1.84 (m, 1H), 1.26 (s, 1H), 0.97 (d, J = 6.8 Hz, 3H), 0.86 (d, J = 6.8 Hz, 3H); ^{13}C{^{1}H} NMR (100 MHz, $CDCl_3$) δ 188.4, 168.5, 140.2, 135.9, 130.9, 129.4, 128.9, 128.3, 128.2, 127.3, 64.4, 61.9 30.6, 19.8, 18.2; IR (neat) 2098, 1720, 1616, 1471 cm^{-1}; HRMS (ESI-TOF) m/z [M + H − N_2]$^+$ calcd for $C_{10}H_{11}N_2O$ 175.0871, found 175.0862.

*5-(Azidomethyl)benzo[d][1,3]dioxole (**3r**).*[40] The title compound was prepared according to general procedure C. A solution of 0.1 M benzo[d][1,3]dioxol-5-ylmethanol (76 mg, 0.50 mmol) in 5 mL of dichloromethane was passed through a packed bed of Amberlyst-15 (6.0 cm bed height) at 0−1 bar and a flow rate of 0.1 mL/min to afford 5-(azidomethyl)benzo[d][1,3]dioxole **3r** (161 mg, 91%) as a colorless oil after purification by column chromatography on silica gel directly (0:100 EtOAc:hexane): ^{1}H NMR (400 MHz, $CDCl_3$) δ 6.78 (m, 3H), 5.97 (s, 2H), 4.23 (s, 2H); ^{13}C{^{1}H} NMR (100 MHz, $CDCl_3$) δ 148.1, 147.8, 129.1, 122.0, 108.8, 108.4, 101.3, 54.8; IR (neat) 2091, 1488, 1443 cm^{-1}.

*5-(Azidomethyl)-6-chlorobenzo[d][1,3]dioxole (**3s**).* The title compound was prepared according to general procedure C. A solution of 0.1 M (6-chlorobenzo[d][1,3]dioxol-5-yl)methanol (93 mg, 0.50 mmol) in 5 mL of dichloromethane was passed through a packed bed of Amberlyst-15 (6.0 cm bed height) at 0−1 bar and a flow rate of 0.1 mL/min to afford 5-(azidomethyl)-6-chlorobenzo[d][1,3]dioxole **3s** (103 mg, 97%) as a colorless oil after purification by column chromatography on silica gel directly (1:99 EtOAc:hexane): ^{1}H NMR (400 MHz, $CDCl_3$) δ 6.87 (s, 1H), 6.83 (s, 1H), 5.99 (s, 2H), 4.37 (s, 2H); ^{13}C{^{1}H} NMR (100 MHz, $CDCl_3$) δ 148.3, 147.0, 126.3, 126.0, 110.1, 109.7, 102.1, 52.2; IR (neat) 2098, 1505, 1476, 1235 cm^{-1}; HRMS (ESI-TOF) m/z [M + H − N_2]$^+$ calcd for $C_8H_7NO_2Cl$ 184.0165, found 184.0163.

*4-(Azidomethyl)pyrene (**3t**). Batch Condition.* The title compound was prepared according to general procedure B, using 1-pyrenemethanol (116 mg, 0.50 mmol) to afford 4-(azidomethyl)pyrene **3t** (90.0 mg, 70%) as a pale yellow solid after purification by column chromatography on silica gel directly (1:99 EtOAc:hexane).

Flow Condition. The title compound was prepared according to general procedure C. A solution of 0.1 M 1-pyrenemethanol (116 mg, 0.50 mmol) in 5 mL of dichloromethane was passed through a packed bed of Amberlyst-15 (6.0 cm bed height) at 0−1 bar and a flow rate of 0.1 mL/min to afford 4-(azidomethyl)pyrene **3t** (103.0 mg, 80% yield) as a pale yellow solid after purification by column chromatography on silica gel directly (1:99 EtOAc:hexane): mp 67−69 °C; ^{1}H NMR (400 MHz, $CDCl_3$) δ 8.09 (m, 9H), 4.99 (s, 2H); ^{13}C{^{1}H} NMR (100 MHz, $CDCl_3$) δ 131.8, 131.3, 130.8, 129.3, 128.4, 128.3, 127.9, 127.5, 127.4, 126.3, 125.7, 125.6, 125.1, 124.7, 122.7, 53.2; IR (neat) 2031, 1508, 1291, 841 cm^{-1}; HRMS (ESI-TOF) m/z [M + H − N_2]$^+$ calcd for $C_{17}H_{12}N$ 230.0970, found 230.0970.

*2-Azido-2-benzyl-2H-benzo[b][1,4]oxazin-3(4H)-one (**5a**).* The title compound was prepared according to general procedure C. A solution of 0.1 M 3-benzyl-3-(*tert*-butylperoxy)indolin-2-one (155.5 mg, 0.50 mmol) in 5 mL of dichloromethane was passed through a packed bed of Amberlyst-15 (6.0 cm bed height) at 0−1 bar and a flow rate of 0.1 mL/min to afford 2-azido-2-benzyl-2H-benzo[b][1,4]-oxazin-3(4H)-one (95.0 mg, 68%) as a pale yellow solid after purification by column chromatography on silica gel directly (8:92 EtOAc:hexane): mp 79−81 °C; ^{1}H NMR (400 MHz, $CDCl_3$) δ 9.92 (s, 1H), 7.46 (m, 2H), 7.32 (m, 3H), 7.08 (m, 3H), 6.93 (m, 1H), 3.69 (d, J = 14.0 Hz, 1H), 3.50 (d, J = 14.0 Hz, 1H); ^{13}C{^{1}H} NMR (100 MHz, $CDCl_3$) δ 162.5, 140.8, 133.1, 131.3, 128.3, 127.6, 125.6, 124.8, 123.9, 117.8, 115.9, 91.6, 40.4; IR (neat) 2111, 1607, 1501, 1210 cm^{-1}; HRMS (ESI-TOF) m/z [M + Na]$^+$ calcd for $C_{15}H_{12}N_4O_2Na$ 303.0858, found 303.0864.

*2-Azido-2-methyl-2H-benzo[b][1,4]oxazin-3(4H)-one (**5b**).* The title compound was prepared according to general procedure C. A solution of 0.1 M 3-(*tert*-butylperoxy)-3-methylindolin-2-one (117.5 mg, 0.50 mmol) in 5 mL of dichloromethane was passed through a packed bed of Amberlyst-15 (6.0 cm bed height) at 0−1 bar and a flow rate of 0.1 mL/min to afford 2-azido-2-methyl-2H-benzo[b][1,4]-oxazin-3(4H)-one (96.0 mg, 94%) as a pale yellow solid after purification by column chromatography on silica gel directly (8:92 EtOAc:hexane): mp 114−116 °C; ^{1}H NMR (400 MHz, $CDCl_3$) δ 9.29 (s, 1H), 7.06 (m, 3H), 6.93 (dd, J = 4.5, 2.4 Hz, 1H), 1.98 (s, 3H); ^{13}C{^{1}H} NMR (100 MHz, $CDCl_3$) δ 163.0, 141.0, 126.1, 124.7, 123.9, 117.8, 116.0, 90.3, 20.7; IR (neat) 2118, 1699, 1506 cm^{-1}; HRMS (ESI-TOF) m/z [M + H − N_2]$^+$ calcd for $C_9H_9N_2O_2$ 177.0664, found 177.0668.

*2-Azido-2-(4-methoxyphenyl)-2H-benzo[b][1,4]oxazin-3(4H)-one (**5c**).* The title compound was prepared according to general procedure C. A solution of 0.1 M 3-(*tert*-butylperoxy)-3-(4-methoxyphenyl)indolin-2-one (88.0 mg, 0.27 mmol) in 2.7 mL of dichloromethane was passed through a packed bed of Amberlyst-15 (6.0 cm bed height) at 0−1 bar and a flow rate of 0.1 mL/min to afford 2-azido-2-(4-methoxyphenyl)-2H-benzo[b][1,4]oxazin-3(4H)-one (57.0 mg, 72%) as a yellow semisolid after purification by column chromatography on silica gel directly (8:92 EtOAc:hexane): ^{1}H NMR (400 MHz, $CDCl_3$) δ 8.26 (d, J = 8.2 Hz, 1H), 7.62 (m, 2H), 7.38 (d, J = 7.9 Hz, 1H), 7.20 (d, J = 7.8 Hz, 1H), 6.77 (s, 4H), 3.76 (s, 3H); ^{13}C{^{1}H} NMR (100 MHz, $CDCl_3$) δ 154.5, 153.8, 149.7, 139.7, 134.5, 132.7, 124.7, 120.6, 116.1, 114.9, 102.2, 55.9; IR (neat) 2151, 1720, 1510, 1222 cm^{-1}; HRMS (ESI-TOF) m/z [M + H − N_2]$^+$ calcd for $C_{15}H_{13}N_2O_3$ 269.0926, found 269.0934.

*2-Azido-2-(2-fluorobenzyl)-2H-benzo[b][1,4]oxazin-3(4H)-one (**5d**).* The title compound was prepared according to general procedure C. A solution of 0.1 M 3-(*tert*-butylperoxy)-3-(2-fluorobenzyl)indolin-2-one (45.0 mg, 0.14 mmol) in 1.4 mL of dichloromethane was passed through a packed bed of Amberlyst-15 (6.0 cm bed height) at 0−1 bar and a flow rate of 0.1 mL/min to afford 2-azido-2-methyl-2H-benzo[b][1,4]oxazin-3(4H)-one (20.7 mg, 51%) as a pale yellow solid after purification by column chromatography on silica gel directly (8:92 EtOAc:hexane): mp 126−128 °C; ^{1}H NMR (400 MHz, $CDCl_3$) δ 9.52 (s, 1H), 7.47 (m, 3H), 7.26 (m, 1H), 7.06 (m, 5H), 6.91 (m, 1H), 3.68 (d, J = 14.3 Hz, 1H), 3.61 (d, J = 14.4 Hz, 1H); ^{13}C{^{1}H} NMR (100 MHz, $CDCl_3$) δ 163.3, 162.5, 160.9, 140.7, 132.9 (d, J = 3.5 Hz), 129.6 (d, J = 8.2 Hz), 125.5, 124.8, 123.99 (d, J = 5.4 Hz), 120.5 (d, J = 15.2 Hz), 118.0, 116.0, 115.6, 115.4, 91.5, 33.1 (d, J = 2.5 Hz); IR (neat) 2110, 1690, 1501, 750 cm^{-1}; HRMS (ESI-TOF) m/z [M + H − N_2]$^+$ calcd for $C_{15}H_{12}N_2O_2F$ 271.0883, found 271.0890.

*2-Azido-2-(4-bromobenzyl)-2H-benzo[b][1,4]oxazin-3(4H)-one (**5e**).* The title compound was prepared according to general procedure C. A solution of 0.1 M 3-(4-bromobenzyl)-3-(*tert*-butylperoxy)indolin-2-one (116.7 mg, 0.30 mmol) in 3 mL of dichloromethane was passed through a packed bed of Amberlyst-15 (6.0 cm bed height) at 0−1 bar and a flow rate of 0.1 mL/min to afford 2-azido-2-(4-bromobenzyl)-2H-benzo[b][1,4]oxazin-3(4H)-one (70.8 mg, 66%) as a pale yellow solid after purification by column chromatography on silica gel directly (8:92 EtOAc:hexane): mp 141−143 °C; ^{1}H NMR (400 MHz, $CDCl_3$) δ 9.70 (s, 1H), 7.41 (d, J = 8.4 Hz, 2H), 7.31 (d, J = 8.4 Hz, 2H), 7.07 (m, 3H), 6.90 (m, 1H), 3.64 (d, J = 14.0 Hz, 1H), 3.41 (d, J = 14.0 Hz, 1H); ^{13}C{^{1}H} NMR (100 MHz, $CDCl_3$) δ 162. 4, 140.6, 133.0, 132.1, 131.5, 125.4, 124.9, 124.0, 121.9, 117.8, 116.0, 91.4, 39.8; IR (neat) 2113, 1698, 1504, 751 cm^{-1}; HRMS (ESI-TOF) m/z [M + H − N_2]$^+$ calcd for $C_{15}H_{12}BrN_2O_2$ 331.0082, found 331.0081. The crystal was grown by a simple recrystallization method. The pure compound isolated after column chromatography was dissolved in dichloromethane, layered with hexane, and kept at room temperature for 2 days to obtain the pure crystal.

*2-Azido-2-benzyl-6-chloro-2H-benzo[b][1,4]oxazin-3(4H)-one (**5f**).* The title compound was prepared according to general procedure C. A solution of 0.1 M 3-benzyl-3-(*tert*-butylperoxy)-6-chloroindolin-2-one (88.0 mg, 0.26 mmol) in 2.6 mL of dichloromethane was passed through a packed bed of Amberlyst-15 (6.0 cm bed height) at 0−1 bar and a flow rate of 0.1 mL/min to afford 2-azido-2-benzyl-6-chloro-2H-benzo[b][1,4]oxazin-3(4H)-one (32.0 mg, 40%) as a white solid after purification by column chromatography on silica gel directly (8:92

https://doi.org/10.1021/acs.joc.2c00941
J. Org. Chem. 2022, 87, 9926−9939

EtOAc:hexane): mp 113−115 °C; ^{1}H NMR (400 MHz, $CDCl_3$) δ 8.45 (s, 1H), 7.34 (m, 5H), 6.99 (m, 2H), 6.82 (d, J = 1.7 Hz, 1H), 3.66 (d, J = 13.9 Hz, 1H), 3.45 (d, J = 13.9 Hz, 1H); ^{13}C{^{1}H} NMR (100 MHz, $CDCl_3$) δ 161.7, 139.4, 132.8, 131.3, 128.9, 128.4, 127.7, 126.6, 124.5, 119.0, 115.6, 91.6, 40.3; IR (neat) 2114, 1699 cm^{-1}; HRMS (ESI-TOF) m/z [M + H − N_2]$^+$ calcd for $C_{15}H_{12}ClN_2O_2$ 287.0587, found 287.0581.

*2-Azido-2-(4-bromobenzyl)-6-chloro-2H-benzo[b][1,4]oxazin-3(4H)-one (**5g**).* The title compound was prepared according to general procedure C. A solution of 0.1 M 3-(4-bromobenzyl)-3-(*tert*-butylperoxy)-6-chloroindolin-2-one (103.0 mg, 0.24 mmol) in 2.4 mL of dichloromethane was passed through a packed bed of Amberlyst-15 (6.0 cm bed height) at 0−1 bar and a flow rate of 0.1 mL/min to afford 2-azido-2-(4-bromobenzyl)-6-chloro-2*H*-benzo[*b*][1,4]oxazin-3(4*H*)-one (27.6 mg, 28%) as a white semisolid after purification by column chromatography on silica gel directly (8:92 EtOAc:hexane): ^{1}H NMR (400 MHz, $CDCl_3$) δ 9.28 (s, 1H), 7.42 (d, J = 8.4 Hz, 2H), 7.28 (d, J = 8.4 Hz, 2H), 7.02 (m, 2H), 6.87 (s, 1H), 3.62 (d, J = 13.9 Hz, 1H), 3.40 (d, J = 14.0 Hz, 1H); ^{13}C{^{1}H} NMR (100 MHz, $CDCl_3$) δ 162.0, 139.2, 133.0, 131.8, 131.6, 129.1, 126.4, 124.7, 122.0, 119.0, 115.9, 91.3, 39.7; IR (neat) 2111, 1704 cm^{-1}; HRMS (ESI-TOF) m/z [M + H − N_2]$^+$ calcd for $C_{15}H_{11}N_2O_2BrCl$ 364.9692, found 364.9694.

*2-Azido-6-chloro-2-(4-methylbenzyl)-2H-benzo[b][1,4]oxazin-3(4H)-one (**5h**).* The title compound was prepared according to general procedure C. A solution of 0.1 M 3-(*tert*-butylperoxy)-6-chloro-3-(4-methylbenzyl)indolin-2-one (64.0 mg, 0.18 mmol) in 1.8 mL of dichloromethane was passed through a packed bed of Amberlyst-15 (6.0 cm bed height) at 0−1 bar and a flow rate of 0.1 mL/min to afford 2-azido-6-chloro-2-(4-methylbenzyl)-2*H*-benzo[*b*][1,4]oxazin-3(4*H*)-one (26.2 mg, 45%) as a pale yellow solid after purification by column chromatography on silica gel directly (8:92 EtOAc:hexane): mp 130−132 °C; ^{1}H NMR (400 MHz, $CDCl_3$) δ 9.22 (s, 1H), 6.13 (s, 1H), 2.82 (dd, J = 12.0, 4.0 Hz, 1H), 2.41 (m, 3H), 2.19 (m, 4H), 1.12 (d, J = 4.0 Hz, 3H); ^{13}C{^{1}H} NMR (100 MHz, $CDCl_3$) δ 194.8, 144.0, 129.7, 120.3, 102.7, 46.6, 32.3, 31.3, 21.6, 13.1; IR (neat) 2117, 1698, 1645 cm^{-1}; HRMS (ESI-TOF) m/z [M + H − N_2]$^+$ calcd for $C_{16}H_{14}N_2O_2Cl$ 301.0744, found 301.0738.

*2-Azido-2,4-dimethyl-2H-benzo[b][1,4]oxazin-3(4H)-one (**5i**).* The title compound was prepared according to general procedure C. A solution of 0.1 M 3-(*tert*-butylperoxy)-1,3-dimethylindolin-2-one (150.0 mg, 0.60 mmol) in 6.1 mL of dichloromethane was passed through a packed bed of Amberlyst-15 (6.0 cm bed height) at 0−1 bar and a flow rate of 0.1 mL/min to afford 2-azido-2,4-dimethyl-2*H*-benzo[*b*][1,4]oxazin-3(4*H*)-one (85.0 mg, 65%) as a white solid after purification by column chromatography on silica gel directly (8:92 EtOAc:hexane): mp 60−62 °C; ^{1}H NMR (400 MHz, $CDCl_3$) δ 9.27 (s, 1H), 6.22 (s, 1H), 2.84 (m, 3H), 2.73 (t, J = 8.0 Hz, 2H), 2.48 (dd, J = 12.0, 8.0 Hz, 2H), 2.38 (m, 1H), 2.21 (m, 1H), 2.11 (s, 3H), 1.12 (d, J = 4.0 Hz, 3H); ^{13}C{^{1}H} NMR (100 MHz, $CDCl_3$) δ 194.5, 143.4, 132.5, 120.0, 102.7, 46.4, 34.1, 32.1, 31.2, 27.2, 21.4, 15.6; IR (neat) 2109, 1680, 1503, 1381 cm^{-1}; HRMS (ESI-TOF) m/z [M + H − N_2]$^+$ calcd for $C_{10}H_{11}N_2O_2$ 191.0821, found 191.0820.

*2-Azido-4-benzyl-2-methyl-2H-benzo[b][1,4]oxazin-3(4H)-one (**5j**).* The title compound was prepared according to general procedure C. A solution of 0.1 M 1-benzyl-3-(*tert*-butylperoxy)-3-methylindolin-2-one (56.2 mg, 0.17 mmol) in 1.7 mL of dichloromethane was passed through a packed bed of Amberlyst-15 (6.0 cm bed height) at 0−1 bar and a flow rate of 0.1 mL/min to afford 2-azido-4-benzyl-2-methyl-2*H*-benzo[*b*][1,4]oxazin-3(4*H*)-one (23.0 mg, 46%) as a white semisolid after purification by column chromatography on silica gel directly (8:92 EtOAc:hexane): ^{1}H NMR (400 MHz, $CDCl_3$) δ 7.34 (m, 2H), 7.27 (m, 3H), 7.10 (dd, J = 7.7, 1.5 Hz, 1H), 7.04 (m, 1H), 6.99 (m, 1H), 6.89 (m, 1H), 5.48 (d, J = 16.1 Hz, 1H), 4.86 (d, J = 16.1 Hz, 1H), 2.06 (s, 3H); ^{13}C{^{1}H} NMR (100 MHz, $CDCl_3$) δ 161.9, 141.7, 135.6, 129.1, 127.7, 126.4, 124.4, 123.9, 118.0, 115.5, 90.2, 45.8, 21.0; IR (neat) 2114, 1697, 1499, 1397 cm^{-1}; HRMS (ESI-TOF) m/z [M + H − N_2]$^+$ calcd for $C_{16}H_{15}N_2O_2$ 267.1134, found 267.1125.

*Diphenylmethanamine (**6a**).* The title compound was prepared according to general procedure E, using 3 M (azidomethylene)-dibenzene (627 mg, 3.0 mmol) in THF to afford diphenylmethanamine **6a** (320 mg, 58%) as a white solid after purification by column chromatography on silica gel directly (20:80 EtOAc:hexane): mp: 293−294 °C; ^{1}H NMR (400 MHz, DMSO-d_6) δ 7.46 (d, J = 7.3 Hz, 4H), 7.32 (d, J = 8.9 Hz, 4H), 7.20 (m, 2H), 5.15 (s, 1H); ^{13}C{^{1}H} NMR (100 MHz, DMSO-d_6) δ 146.8, 128.1, 126.7, 126.3, 59.3; IR (neat) 3853, 3741, 3302, 3059, 3030, 2926, 2855, 1746, 1558 cm^{-1}; HRMS (ESI-TOF) m/z [M + H]$^+$ calcd for $C_{13}H_{14}N$ 184.1126, found 184.1117.

*1-Benzhydryl-4-phenyl-1H-1,2,3-triazole (**7a**).* The title compound was prepared according to general procedure F, using (azidomethylene)dibenzene (124.5 mg, 0.59 mmol) to afford 1-benzhydryl-4-phenyl-1*H*-1,2,3-triazole **7a** (113.5 mg, 73%) as a white solid after purification by column chromatography on silica gel directly (10:90 EtOAc:hexane): mp 177−179 °C; ^{1}H NMR (400 MHz, $CDCl_3$) δ 7.81 (m, 2H), 7.61 (s, 1H), 7.40 (m, 8H), 7.33 (m, 1H), 7.17 (m, 5H); ^{13}C{^{1}H} NMR (100 MHz, $CDCl_3$) δ 147.7, 138.3, 130.7, 129.1, 128.9, 128.8, 128.3, 128.2, 125.9, 119.7, 68.2; IR (neat) 3061, 3028, 1491, 1451, 1229, 1079 cm^{-1}; HRMS (ESI-TOF) m/z [M + H]$^+$ calcd for $C_{21}H_{18}N_3$ 312.1501, found 312.1492.

*4-Phenyl-1-(1-phenylethyl)-1H-1,2,3-triazole (**7b**).* The title compound was prepared according to general procedure F, using (1-azidoethyl)benzene (88.2 mg, 0.59 mmol) to afford 4-phenyl-1-(1-phenylethyl)-1*H*-1,2,3-triazole **7b** (92.6 mg, 62%) as a white solid after purification by column chromatography on silica gel directly (5:95 EtOAc:hexane): mp 80−82 °C; ^{1}H NMR (400 MHz, $CDCl_3$) δ 7.80 (m, 2H), 7.63 (s, 1H), 7.35 (m, 8H), 5.87 (q, J = 7.1 Hz, 1H), 2.03 (d, J = 7.1 Hz, 3H); ^{13}C{^{1}H} NMR (100 MHz, $CDCl_3$) δ 140.0, 130.8, 129.2, 128.9, 128.7, 128.2, 126.7, 125.8, 118.5, 60.4, 21.5; IR (neat) 2925, 2855, 1702, 1540 cm^{-1}; HRMS (ESI-TOF) m/z [M + H]$^+$ calcd for $C_{16}H_{16}N_3$ 250.1346, found 250.1345.

*3-Benzylquinoxalin-2(1H)-one (**8l**).* The title compound was prepared according to general procedure G, using 3-azido-3-benzylindolin-2-one (79.0 mg, 0.30 mmol) to afford 3-benzylquinoxalin-2(1*H*)-one **8l** (55.6 mg, 79%) as a white solid after purification by column chromatography on silica gel directly (15:85 EtOAc:hexane): mp 198−200 °C; ^{1}H NMR (400 MHz, $CDCl_3$) δ 11.78 (s, 1H), 7.84 (d, J = 7.7 Hz, 1H), 7.48 (m, 3H), 7.31 (m, 3H), 7.22 (m, 2H), 4.29 (s, 2H); ^{13}C{^{1}H} NMR (100 MHz, $CDCl_3$) δ 159.94, 158.3, 156.3, 137.1, 132.9, 131.2, 130.1, 129.7, 129.2, 128.6, 126.8, 124.3, 115.6, 40.1; IR (neat) 3800, 2376, 2317, 1743, 1524 cm^{-1}; HRMS (ESI-TOF) m/z [M + H]$^+$ calcd for $C_{15}H_{12}N_2O$ 237.1028, found 237.1019.

*3-Methylquinoxalin-2(1H)-one (**8i**).* The title compound was prepared according to general procedure G, using 3-azido-3-methylindolin-2-one (56.5 mg, 0.30 mmol) to afford 3-methylquinoxalin-2(1*H*)-one **8i** (39.9 mg, 83%) as a white solid after purification by column chromatography on silica gel directly (15:85 EtOAc:hexane): mp 252−254 °C; ^{1}H NMR (400 MHz, DMSO-d_6) δ 12.30 (s, 1H), 7.67 (m, 1H), 7.44 (m, 1H), 7.24 (m, 2H), 2.39 (s, 3H); ^{13}C{^{1}H} NMR (100 MHz, DMSO-d_6) δ 159.2, 154.9, 131.9, 131.7,129.3, 127.8, 123.0, 115.2, 20.6; IR (neat) 3392, 2376, 2355, 2318, 2259, 2135, 1651, 1021 cm^{-1}; HRMS (ESI-TOF) m/z [M + H]$^+$ calcd for $C_9H_9N_2O$ 161.0715, found 161.0710.

*3-(p-Tolyl)quinoxalin-2(1H)-one (**8j**).* The title compound was prepared according to general procedure G, using 3-azido-3-(*p*-tolyl)indolin-2-one (79.9 mg, 0.30 mmol) to afford 3-(*p*-tolyl)-quinoxalin-2(1*H*)-one **8j** (50.0 mg, 70%) as a yellow solid after purification by column chromatography on silica gel directly (15:85 EtOAc:hexane): mp 268−270 °C; ^{1}H NMR (400 MHz, DMSO-d_6) δ 12.46 (m, 1H), 8.26 (m, 2H), 7.82 (dd, J = 8.6, 1.3 Hz, 1H), 7.52 (m, 1H), 7.31 (m, 4H), 2.38 (s, 3H); ^{13}C{^{1}H} NMR (100 MHz, DMSO-d_6) δ 154.7, 153.8, 140.1, 132.9, 131.9, 130.1, 129.2, 128.6, 123.4, 115.1, 21.1; IR (neat) 3392, 2376, 2352, 2320, 2259, 2135, 1648 cm^{-1}; HRMS (ESI-TOF) m/z [M + H]$^+$ calcd for $C_{15}H_{13}N_2O$ 237.1028, found 237.1019.

*3-(4-Methoxyphenyl)quinoxalin-2(1H)-one (**8k**).* The title compound was prepared according to general procedure G, using 3-azido-3-(4-methoxyphenyl)indolin-2-one (84.0 mg, 0.30 mmol) to afford 3-(4-methoxyphenyl)quinoxalin-2(1*H*)-one **8k** (62.6 mg, 83%) as a pale yellow solid after purification by column chromatography on silica gel directly (15:85 EtOAc:hexane): mp 275−276 °C; ^{1}H NMR (400 MHz,

https://doi.org/10.1021/acs.joc.2c00941
J. Org. Chem. 2022, 87, 9926−9939

DMSO-d_6) δ 12.52 (s, 1H), 8.39 (m, 2H), 7.80 (m, 1H), 7.50 (ddd, J = 8.3, 7.1, 1.4 Hz, 1H), 7.30 (dd, J = 11.8, 4.4 Hz, 2H), 7.03 (m, 2H), 3.83 (s, 3H); $^{13}C\{^1H\}$ NMR (100 MHz, DMSO-d_6) δ 161.0, 154.7, 153.1, 132.1, 131.8, 131.0, 129.8, 128.5, 128.2, 123.4, 115.0, 113.4, 55.3; IR (neat) 3741, 2921, 2379, 2315, 1706, 1508 cm^{-1}; HRMS (ESI-TOF) m/z $[M + H]^+$ calcd for $C_{15}H_{13}N_2O_2$ 253.0977, found 253.0975.

*3-(4-Bromobenzyl)quinoxalin-2(1H)-one (**8n**).*[41] The title compound was prepared according to general procedure G, using 3-azido-3-(4-bromobenzyl)indolin-2-one (100.0 mg, 0.29 mmol) to afford 3-(4-bromobenzyl)quinoxalin-2(1*H*)-one **8n** (74.0 mg, 81%) as a white solid after purification by column chromatography on silica gel directly (15:85 EtOAc:hexane): mp 235−238 °C; ^1H NMR (400 MHz, DMSO-d_6) δ 12.42 (s, 1H), 7.70 (d, J = 7.9 Hz, 1H), 7.47 (d, J = 7.1 Hz, 3H), 7.28 (d, J = 8.2 Hz, 4H), 4.09 (s, 2H); $^{13}C\{^1H\}$ NMR (100 MHz, DMSO-d_6) δ 159.9, 154.5, 136.9, 132.0, 131.6, 131.2, 129.9, 128.3, 123.2, 119.6, 115.3, 38.4; IR (neat) 2960, 1707, 1422, 1360, 1221, 1092, 979 cm^{-1}.

■ ASSOCIATED CONTENT

Supporting Information

The Supporting Information is available free of charge at https://pubs.acs.org/doi/10.1021/acs.joc.2c00941.

Experimental procedures, characterization data, and copies of NMR spectra for the compounds (PDF)

FAIR data, including the primary NMR FID files, for compounds **3a−t**, **5a−j**, **6a**, **7a**, **7b**, **8i−l**, and **8n** (ZIP)

Accession Codes

CCDC 2162372−2162374 contain the supplementary crystallographic data for this paper. These data can be obtained free of charge via www.ccdc.cam.ac.uk/data_request/cif, or by emailing data_request@ccdc.cam.ac.uk, or by contacting The Cambridge Crystallographic Data Centre, 12 Union Road, Cambridge CB2 1EZ, UK; fax: +44 1223 336033.

■ AUTHOR INFORMATION

Corresponding Author

Boopathy Gnanaprakasam − *Department of Chemistry, Indian Institute of Science Education and Research, Pune 411008, India*; orcid.org/0000-0002-3047-9636; Email: gnanaprakasam@iiserpune.ac.in

Authors

Akanksha M. Pandey − *Department of Chemistry, Indian Institute of Science Education and Research, Pune 411008, India*

Shankhajit Mondal − *Department of Chemistry, Indian Institute of Science Education and Research, Pune 411008, India*

Complete contact information is available at: https://pubs.acs.org/10.1021/acs.joc.2c00941

Notes

The authors declare no competing financial interest.

■ ACKNOWLEDGMENTS

This research was supported by the SERB (CRG/2018/003935). A.M.P. thanks IISER-Pune for the research fellowship and "IISER Pune -Trimurti Fabricators Pvt. Ltd. and Twenty Twenty Interior Design Software India Pvt Ltd Research Grant" for Grant AY 2021-22. B.G. thanks SERB, Venbiotech, and IISER-Pune for the financial support.

■ REFERENCES

(1) Platz, M., Moss, R., Jones, M., Jr., Eds. *Reviews of Reactive Intermediate Chemistry*; Wiley, 2007.

(2) (a) Patai, S., Ed. *The Chemistry of the Azido Group*; Wiley: New York, 1971. (b) Patai, S., Rappoport, Z., Eds. *The Chemistry of Halides, Pseudo-halides and Azides, Supplement D*; Wiley: Chichester, U.K., 1983. (c) Patai, S., Ed. *Chemistry of Halides, Pseudo-Halides and Azides, Part 1*; Wiley: Chichester, U.K., 1995. (d) Patai, S., Ed. *Chemistry of Halides, Pseudo-Halides and Azides, Part 2*; Wiley: Chichester, U.K., 1995.

(3) Scriven, E. F. V., Ed. *Monograph: Azides and Nitrenes Reactivity and Utility*; Academic Press: New York, 1984.

(4) Jang, S.; Sachin, K.; Lee, H.; Kim, D. W.; Lee, H. S. Development of a Simple Method for Protein Conjugation by Copper-Free Click Reaction and Its Application to Antibody-Free Western Blot Analysis. *Bioconjugate Chem.* **2012**, *23*, 2256−2261.

(5) Brase, S.; Gil, C.; Knepper, K.; Zimmermann, V. Organic Azides: An Exploding Diversity of a Unique Class of Compounds. *Angew. Chem., Int. Ed.* **2005**, *44*, 5188−5240.

(6) Padwa, A. Aziridines and Azirines: Monocyclic. In *Comprehensive Heterocyclic Chemistry III*; Katritzky, A. R., Ramsden, C. A., Scriven, E. F. V., Taylor, R. J. K., Eds.; Elsevier Science: Oxford, U.K., 2008; Vol. *1*, Chapter 1.01.6.2, pp 50−64.

(7) Gololobov, Y. G.; Kasukhin, L. F. Recent Advances in the Staudinger Reaction. *Tetrahedron* **1992**, *48*, 1353−1406.

(8) Li, Y. L.; Combs, A. P. Bicyclic Heteroaryl amino alkyl Phenyl Derivatives as PI3K Inhibitors. Int. Patent Appl. WO2015191677A1, 2015.

(9) Kim, M. S.; Yoo, M. H.; Rhee, J. K.; Kim, Y. J.; Park, S. J.; Choi, J. H.; Sung, S. Y.; Lim, H. G.; Cha, D. W. Synthetic Intermediates, Process for Preparing Pyrrolylheptanoic Acid Derivatives Therefrom. Int. Patent Appl. WO2009084827A2, 2009.

(10) Bathula, S. N. V. P.; Vadla, R. Bioactivity of 1, 4-disubstituted 1, 2, 3-triazoles as Cytotoxic Agents Against the Various Human Cell Lines. *Asian J. Pharm. Clin. Res.* **2011**, *4*, 66−67.

(11) Aganda, K. C.; Hong, B.; Lee, A. Visible-Light-Promoted Switchable Synthesis of C-3- Functionalized Quinoxalin-2(1*H*)-ones. *Adv. Synth. Catal.* **2021**, *363*, 1443−1448.

(12) Brase, S., Banert, K., Eds. *Organic Azides: Syntheses and Applications*; John Wiley & Sons, Ltd.: Chichester, U.K., 2010.

(13) Li, J.; Cao, J.; Wei, J.; Shi, X.; Zhang, L.; Feng, J.; Chen, Z. Ionic Liquid Brush as a Highly Efficient and Reusable Catalyst for On-Water Nucleophilic Substitutions. *Eur. J. Org. Chem.* **2011**, *2011*, 229−233.

(14) Denk, C.; Wilkovitsch, M.; Skrinjar, P.; Svatunek, D.; Mairinger, S.; Kuntner, C.; Filip, T.; Fröhlich, J.; Wanek, T.; Mikula, H. [18F] Fluoroalkyl Azides for Rapid Radiolabeling and (Re)investigation of their Potential Towards *in vivo* Click Chemistry. *Org. Biomol. Chem.* **2017**, *15*, 5976−5982.

(15) Kurosawa, W.; Kan, T.; Fukuyama, T. Stereocontrolled Total Synthesis of (−)-Ephedradine A (Orantine). *J. Am. Chem. Soc.* **2003**, *125*, 8112−8113.

(16) Besset, C.; Chambert, S.; Fenet, B.; Queneau, Y. Direct Azidation of Unprotected Carbohydrates under Mitsunobu Conditions using Hydrazoic Acid. *Tetrahedron Lett.* **2009**, *50*, 7043−7047.

(17) Terrasson, V.; Marque, S.; Georgy, M.; Campagne, J. M.; Prim, D. Lewis Acid-Catalyzed Direct Amination of Benzhydryl Alcohols. *Adv. Synth.Catal.* **2006**, *348*, 2063−2067.

(18) Khedar, P.; Pericherla, K.; Kumar, A. Copper Triflate: An Efficient Catalyst for Direct Conversion of Secondary Alcohols into Azides. *Synlett* **2014**, *25*, 515−518.

(19) Rueping, M.; Vila, C.; Uria, U. Direct Catalytic Azidation of Allylic Alcohols. *Org. Lett.* **2012**, *14*, 768−771.

(20) Sawama, Y.; Nagata, S.; Yabe, Y.; Morita, K.; Monguchi, Y.; Sajiki, H. Iron-Catalyzed Chemoselective Azidation of Benzylic Silyl Ethers. *Chem. - Eur. J.* **2012**, *18*, 16608−16611.

(21) Reddy, C. R.; Madhavi, P. P.; Reddy, A. S. Molybdenum (V) Chloride-Catalyzed Amidation of Secondary Benzyl Alcohols with Sulfonamides and Carbamates. *Tetrahedron Lett.* **2007**, *48*, 7169−7172.

(22) Kumar, A.; Sharma, R. K.; Singh, T. V.; Venugopalan, P. Indium (III) Bromide Catalyzed Direct Azidation of α-hydroxyketones using $TMSN_3$. *Tetrahedron* **2013**, *69*, 10724−10732.
(23) Tummatorn, J.; Thongsornkleeb, C.; Ruchirawat, S.; Thongaram, P.; Kaewmee, B. Convenient and Direct Azidation of Sec-Benzyl Alcohols by Trimethylsilyl Azide with Bismuth (III) Triflate Catalyst. *Synthesis* **2015**, *47*, 323−329.
(24) Hajipour, A. R.; Rajaei, A.; Ruoho, A. E. A Mild and Efficient Method for Preparation of Azides from Alcohols using Acidic Ionic Liquid [H-NMP] HSO_4. *Tetrahedron Lett.* **2009**, *50*, 708−711.
(25) Tandiary, M. A.; Masui, Y.; Onaka, M. A Combination of Trimethylsilyl Chloride and Hydrous Natural Montmorillonite Clay: An Efficient Solid Acid Catalyst for the Azidation of Benzylic and Allylic Alcohols with Trimethylsilyl Azide. *RSC Adv.* **2015**, *5*, 15736−15739.
(26) Kamble, S.; More, S.; Rode, C. Highly Selective Direct Azidation of Alcohols Over a Heterogeneous Povidone-Phosphotungstic Solid Acid Catalyst. *New J. Chem.* **2016**, *40*, 10240−10245.
(27) Yin, X. P.; Zhu, L.; Zhou, J. Metal-Free Azidation of α-Hydroxy Esters and α-Hydroxy Ketones Using Azidotrimethylsilane. *Adv. Synth. Catal.* **2018**, *360*, 1116−1122.
(28) Regier, J.; Maillet, R.; Bolshan, Y. A Direct Brønsted Acid Catalyzed Azidation of Benzhydrols and Carbohydrates. *Eur. J. Org. Chem.* **2019**, *2019*, 2390−2396.
(29) Dallinger, D.; Kappe, C. O. Why Flow Means Green − Evaluating the Merits of Continuous Processing in the Context of Sustainability. *Curr. Opin. Green Sustainable Chem.* **2017**, *7*, 6−12.
(30) Delville, M.; Nieuwland, P.; Janssen, P.; Koch, K.; Van Hest, J.; Rutjes, F. Continuous Flow Azide Formation: Optimization and Scale-up. *Chem. Eng. J.* **2011**, *167*, 556−559.
(31) Sagandira, C.; Watts, P. Safe and Highly Efficient Adaptation of Potentially Explosive Azide Chemistry Involved in the Synthesis of Tamiflu Using Continuous-Flow Technology. *Beilstein J. Org. Chem.* **2019**, *15*, 2577−2589.
(32) Baxendale, I.; Deeley, J.; Griffiths-Jones, C.; Ley, S.; Saaby, S.; Tranmer, G. A Flow Process for the Multi-Step Synthesis of the Alkaloid Natural Product Oxomaritidine: A New Paradigm for Molecular Assembly. *Chem. Commun.* **2006**, 2566−2568.
(33) Donnelly, A.; Zhang, H.; Baumann, M. Development of a Telescoped Flow Process for the Safe and Effective Generation of Propargylic Amines. *Molecules* **2019**, *24*, 3658.
(34) Sampath, G.; Kannan, S. Fructose Dehydration to 5-hydroxymethylfurfural: Remarkable Solvent Influence on Recyclability of Amberlyst-15 Catalyst and Regeneration Studies. *Catal. Commun.* **2013**, *37*, 41−44.
(35) Findley, T. J. K.; Sucunza, D.; Miller, L. C.; Davies, D. T.; Procter, D. J. A Flexible, Stereoselective Approach to the Decorated cis-Hydrindane Skeleton: Synthesis of the Proposed Structure of Faurinone. *Chem. - Eur. J.* **2008**, *14*, 6862−6865.
(36) Yarlagadda, B.; Devunuri, N.; Mandava, V. B. R. Facile Synthesis of n-(benzyl-1h-1,2,3-triazol-5-yl) methyl)-4-(6-methoxybenzo [d] thiazol-2-yl)-2-nitrobenzamides via Click Chemistry. *J. Heterocycl. Chem.* **2017**, *54* (2), 864−870.
(37) Chaudhari, M. B.; Mohanta, N.; Pandey, A. M.; Vandana, M.; Karmodiya, K.; Gnanaprakasam, B. Peroxidation of 2-oxindole and Barbituric Acid Derivatives Under Batch and Continuous Flow Using an Eco-friendly Ethyl Acetate Solvent. *React. Chem. Eng.* **2019**, *4*, 1277.
(38) Qin, X.; Hao, X.; Han, H.; Zhu, S.; Yang, Y.; Wu, B.; Hussain, S.; Parveen, S.; Jing, C.; Ma, B.; Zhu, C. Design and Synthesis of Potent and Multifunctional Aldose Reductase Inhibitors Based on Quinoxalinones. *J. Med. Chem.* **2015**, *58* (3), 1254−1267.
(39) Khedar, P.; Pericherla, K.; Kumar, A. Copper Triflate: An Efficient Catalyst for Direct Conversion of Secondary Alcohols into Azides. *Synlett* **2014**, *25*, 515−518.
(40) Vaněk, V.; Pícha, J.; Fabre, B.; Buděšínský, M.; Lepšík, M.; Jiráček, J. The Development of a Versatile Trifunctional Scaffold for Biological Applications. *Eur. J. Org. Chem.* **2015**, *2015*, 3689−3701.
(41) Mamedov, V.; Zhukova, A.; Syakaev, V.; Beschastnova, T.; Kadyrova, M.; Isaeva, A.; Mamedova, S.; Gavrilova, E.; Latypov, S.; Sinyashin, O. 3-(α-Chlorobenzyl)quinoxalin-2(1*H*)-ones as Versatile Reagents for the Synthesis of 3-Benzylquinoxalin-2(1*H*)-ones and Thiazolo[3,4-a]quinoxalin-4(5*H*)-ones. *J. Heterocyclic Chem.* **2019**, *56*, 2221.
(42) Hinz, A.; Labbow, R.; Reiß, F.; Schulz, A.; Sievert, K.; Villinger, A. Synthesis and Structure of Tritylium Salts. *Struct. Chem.* **2015**, *26*, 1641−1650.

https://doi.org/10.1021/acs.joc.2c00941
J. Org. Chem. 2022, 87, 9926−9939

JOC The Journal of Organic Chemistry

pubs.acs.org/joc Article

Catalytic Acceptorless Dehydrogenation of Amino Alcohols and 2-Hydroxybenzyl Alcohols for Annulation Reaction under Neutral Conditions

Akanksha M. Pandey, Naveen Kumar Digrawal, Nirmala Mohanta, Akash Bandu Jamdade, Moreshwar B. Chaudhari, Girish Singh Bisht, and Boopathy Gnanaprakasam*

Cite This: J. Org. Chem. 2021, 86, 8805−8828 Read Online

ABSTRACT: A base-free and acceptorless Ru-catalyzed dehydrogenative approach has been developed for the synthesis of *N*-heterocycles by using 1,3-dicarbonyls and amino alcohols through a domino sequential enamine formation and intramolecular oxidative cyclization strategy. This unified approach is also applicable for the synthesis of O-heterocycles involving 2-hydroxybenzyl alcohol as a coupling reactant via consecutive C-alkylation and intramolecular cyclization steps. The present protocol is general for the synthesis of varieties of biologically important scaffolds, such as tetrahydro-4*H*-indol-4-one, 3,4-dihydroacridin-1(2*H*)-one, and tetrahydro-1*H*-xanthen-1-ones derivatives using a single catalytic system, viz. $RuH_2CO(PPh_3)_3$. Environmentally benign H_2O and H_2 are the only byproducts in this domino process. Moreover, $RuH_2CO(PPh_3)_3$-catalyzed C3-alkylation of tetrahydro-4*H*-indol-4-one using alcohol as a alkylating partner is also described in this report. For the first time, a solvent-free gram-scale reaction for the acceptorless dehydrogenative annulation has been demonstrated. A plausible mechanism for the Ru-catalyzed base-free and acceptorless dehydrogenative annulation of amino alcohols or 2-hydroxybenzyl alcohols has been provided with several experimental investigations and spectroscopic evidence.

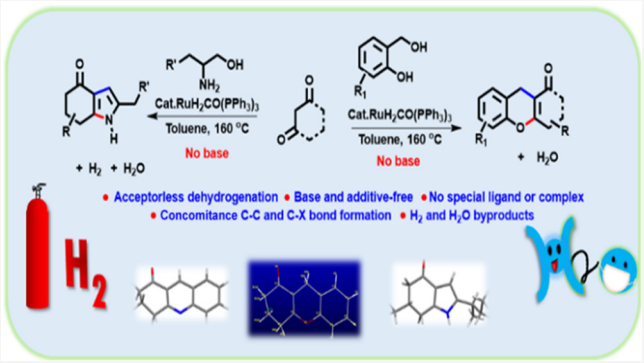

INTRODUCTION

Aromatic heterocycles are the prevalent chemical entities found in various natural products, pharmaceutical ingredients, and agricultural products (Figure 1).[1] Several approaches developed for its synthesis involve traditional metal and metal-free conditions. These methods involve reactions, such as annulation reactions, multicomponent reactions, and tandem reactions, and have received attention from the chemical community.[2] Although these methods provide interesting catalytic reaction steps and synthetically useful approaches, the formation of associated copious waste, multistep synthesis, and limited feedstock chemicals are disadvantages of the traditional approach. A sustainable catalytic method emphasizing one-pot conditions that allow the assembly of many bond constructions with high-atom economy and use inexpensive reactants is highly demanding in the current manufacturing procedures. In the modern era, the acceptorless dehydrogenation (AD) of alcohols has been extensively employed for chemical syntheses due to several attractive features for C−C and C−X bond formation in modern chemical syntheses.[3] Notably, the formation of water and value-added byproducts such as molecular hydrogen involves readily available alcohols and retains high atom economy, which are primary advantages in AD-driven sustainable synthesis. In recent years, this strategy is most frequently used for the formation of C−C or C−N bonds involving enolates or amines as nucleophiles in the presence of transition metals as a catalyst through redox reaction, which is popularly known as "borrowing hydrogen catalysis" (BHC).[4] In general, this reaction proceeds through sequential dehydrogenation−condensation−hydrogenation steps,[5] and its synthetic applications are extended to the α-alkylation of various carbonyl derivatives.

Currently, several research groups are extensively employing the AD strategy for the annulation reactions to synthesize various five- and six-membered aromatic N-heterocycles involving the various transition metals complexes.[6]

The amino alcohols are easily synthesized from the respective naturally occurring amino acids. These are an important

Received: March 26, 2021
Published: June 21, 2021

https://doi.org/10.1021/acs.joc.1c00714
J. Org. Chem. 2021, 86, 8805−8828

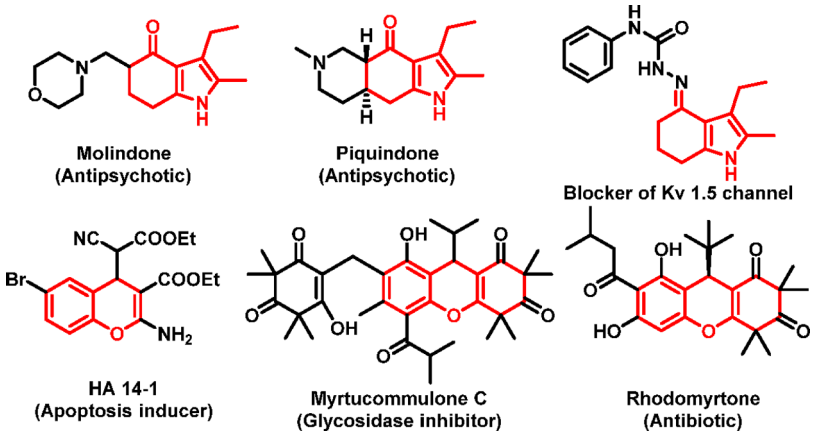

Figure 1. Biologically active compounds with a pyrrole and 4*H*-chromene core.

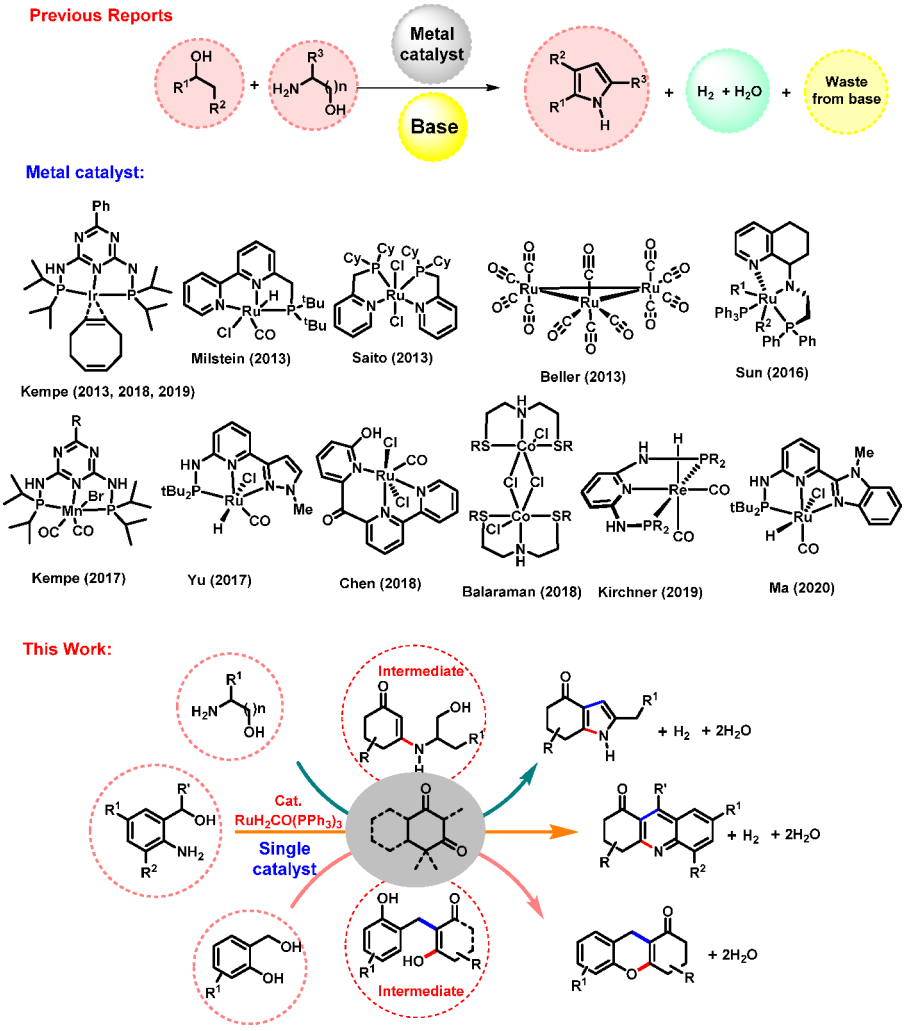

Figure 2. State of the art for the present work.

chemical entity in various dehydrogenative synthesis of pyrrole derivatives. In 2013, the research groups of Kempe,[7] Milstein,[8] Saito,[9] and Beller[10] have reported several well-defined homogeneous Ir and Ru catalysts for the AD synthesis of pyrrole, which involves acyclic secondary alcohols, amino alcohols, and a base (Figure 2). In 2016, the Sun group reported the same reaction strategy catalyzed using another variant of the Ru catalyst.[11] In 2017, inspired from Kempe,[12] Yu,[13] and Chen,[14] a study reported the pyrrole synthesis by using specially designed Mn and Ru catalysts. In 2018, Balaraman et al.[15] and Banerjee et al.[16] have reported a Co-based dimeric complex and Ni catalyst for pyrrole synthesis under similar reaction conditions.

Recently, Kirchner et al.[17] and Ma et al.[18] have reported the assorted Mn and Ru catalysts for preparing pyrrole heterocycles. Most of these reactions are catalyzed through a specially

https://doi.org/10.1021/acs.joc.1c00714
J. Org. Chem. 2021, 86, 8805−8828

Scheme 1. Catalyst Screening for AD Annulation[a]

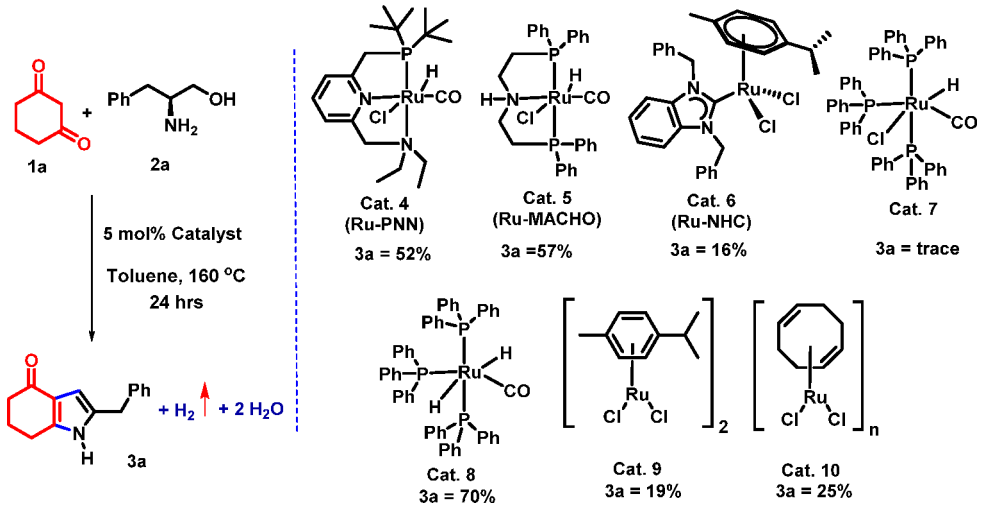

[a]Reaction conditions: **1** (0.5 mmol), **2** (0.5 mmol), catalyst (5 mol %), and toluene (2 mL) were heated at 160 °C for 24 h.

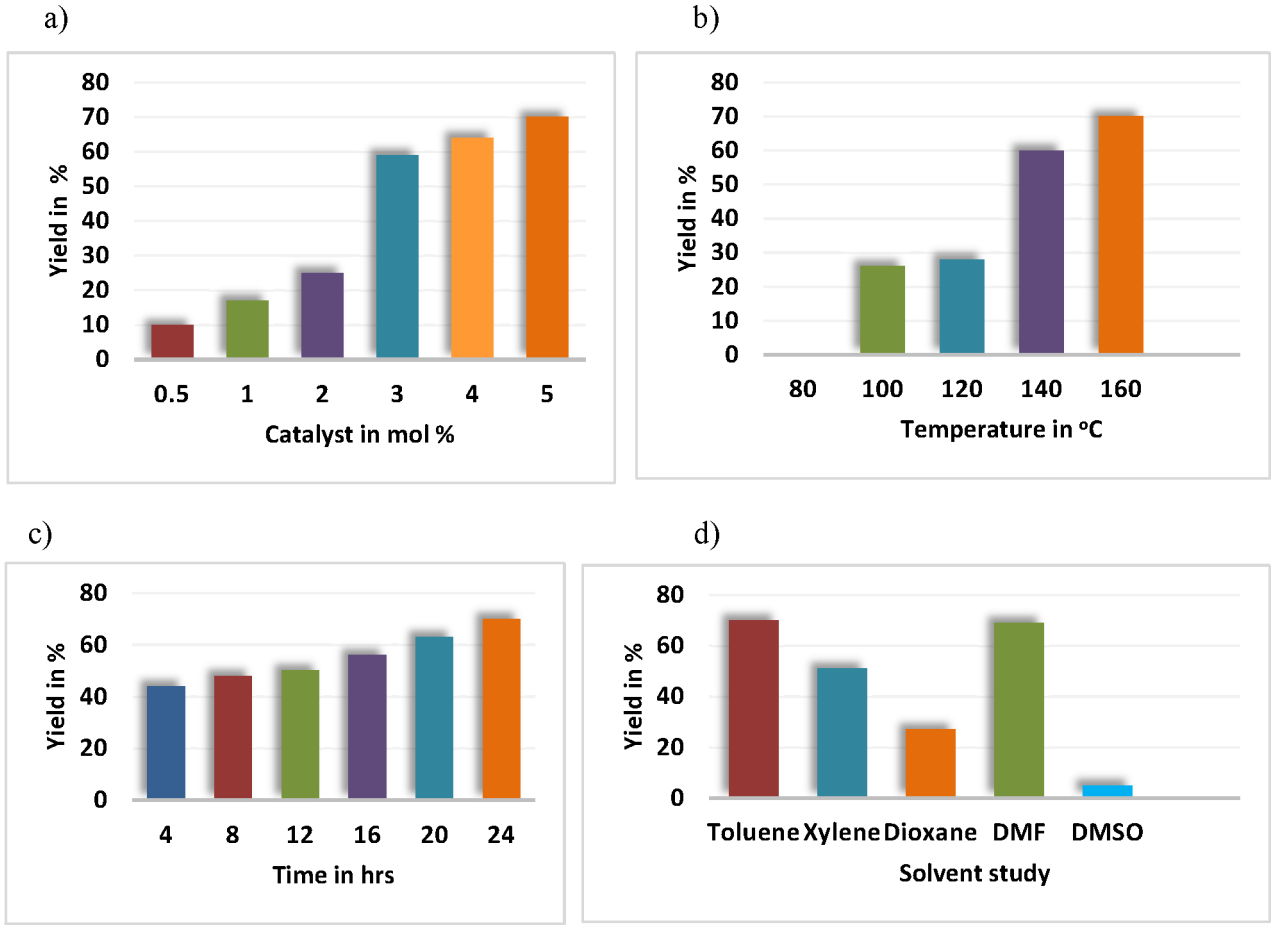

Figure 3. Optimization for catalyst concentration (a), temperature (b), time (c), and solvent (d).

designed complex and require a stoichiometric base for annulation, which leads to the generation of copious waste, a decrease in the atom economy, and low sustainability. By contrast, existing AD annulation is limited to a few simple N-heterocycles, requires a stoichiometric base for annulation, and is catalyzed using specially designed complexes, necessitating the development of base-free, efficient, and ligand-free catalytic systems for the synthesis of other heterocycles, containing oxygen and partially hydrogenated indole and an acridine system, because of their omnipresence in most therapeutic and natural products (Figure 1).[1,19,20]

Herein, we report an environmentally benign, acceptorless, and base-free condition for the annulation of cyclic 1,3-dicarbonyl compounds and amino alcohols for the synthesis of

https://doi.org/10.1021/acs.joc.1c00714
J. Org. Chem. 2021, 86, 8805−8828

Scheme 2. Substrate Scope for the Intermolecular Cyclization of β-Amino Alcohol with β-Diketone

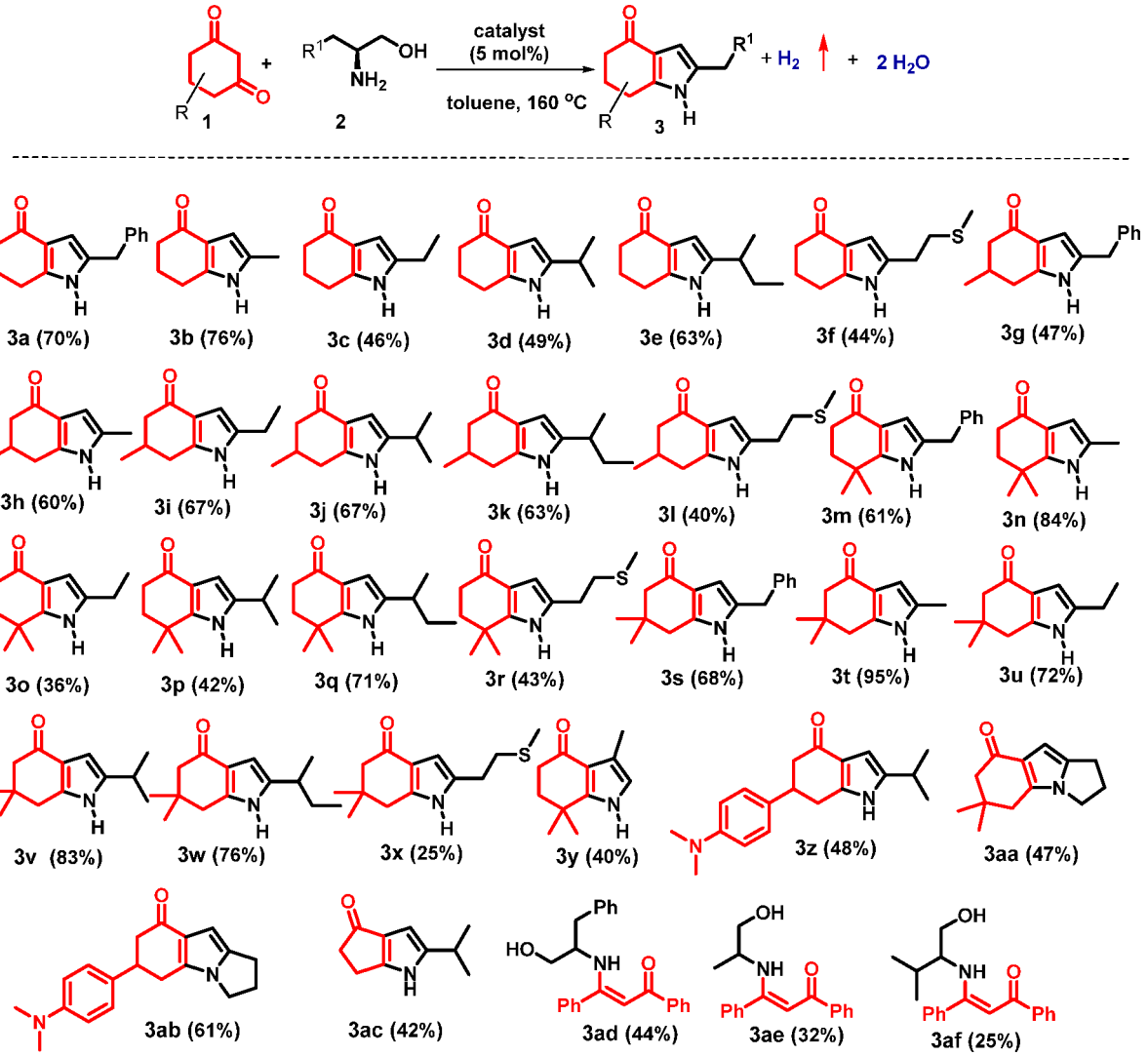

diversified tetrahydro-4*H*-indol-4-one, 3,4-dihydroacridin-1(2*H*)-one and tetrahydro-1*H*-xanthen-1-ones derivatives by using easily accessible 5 mol % $RuH_2CO(PPh_3)_3$ as a catalyst (Figure 2). In this process, the formation of water and useful value-added molecular hydrogen as byproducts led to the synthesis of wide arrays of five- and six-membered, functionalized, cyclohexane-fused N- and O-heterocycles.

RESULTS AND DISCUSSION

Initially, we examined reaction conditions by using 1,3-cyclohexanedione and (*S*)-2-amino-3-phenylpropan-1-ol as a model substrate (Scheme 1). A control experiment was conducted at 160 °C in the absence of catalyst and base, which resulted in no reaction. Next, we screened various Ru catalysts for annulation to synthesize 2-benzyl-1,5,6,7-tetrahydro-4*H*-indol-4-one (**3a**). Dehydrogenative annulation of **1a** and **2a** with 5 mol % $RuCl_3$ led to the trace yields of product **3a**. A similar result was obtained for dehydrogenative annulation with 5 mol % $RuHClCO(PPh_3)_3$. With 5 mol % $RuH_2CO(PPh_3)_3$, 70% yield of the product **3a** was obtained and molecular hydrogen and water were formed as byproducts. Previously, dehydrogenation of alcohols to afford ketone were reported[21] by using $RuH_2CO(PPh_3)_3$. However, there is no annulation reaction using this catalyst. A poor yield was obtained for the reaction with $Ru(p\text{-cymene})_2Cl_2$ and $Ru(COD)Cl_2$. Milstein (**4**) and MACHO (**5**) catalyst afforded 52% and 57% yield of product **3a**. Catalyst screening indicated 5 mol % $RuH_2CO(PPh_3)_3$ as the optimum catalyst among all the catalytic systems (Scheme 1). A study on the catalyst concentration indicated that 5 mol % catalyst is required for maximum conversion and increased yields (Figure 3a). A similar result was observed for the reactions at 160 °C, which provided high yields. The product yields monitored at different temperatures and various time intervals showed that heating for 24 h at 160 °C led to 70% yield (Figure 3b and 3c). The solvent study (Figure 3d) reveals that this reaction is efficient when toluene used as a solvent. This reaction in DMF (69%) afforded slightly lower yield. Other solvents such as xylene (51%), dioxane (27%), and DMSO (5%) were less efficient for this reaction.

By using the optimized reaction conditions, we investigated this strategy for other the substrates. Thus, the reaction of cyclohexane-1,3-dione with various amino alcohols provided 46−76% yields of products **3b−e**, respectively (Scheme 2). Moreover, this reaction was conducted using sulfur-containing amino alcohol to obtain 44% yield of product **3f**. Furthermore,

https://doi.org/10.1021/acs.joc.1c00714
J. Org. Chem. 2021, 86, 8805−8828

Scheme 3. Substrate Scope for the Intramolecular Annulation of β-Enaminone Alcohol

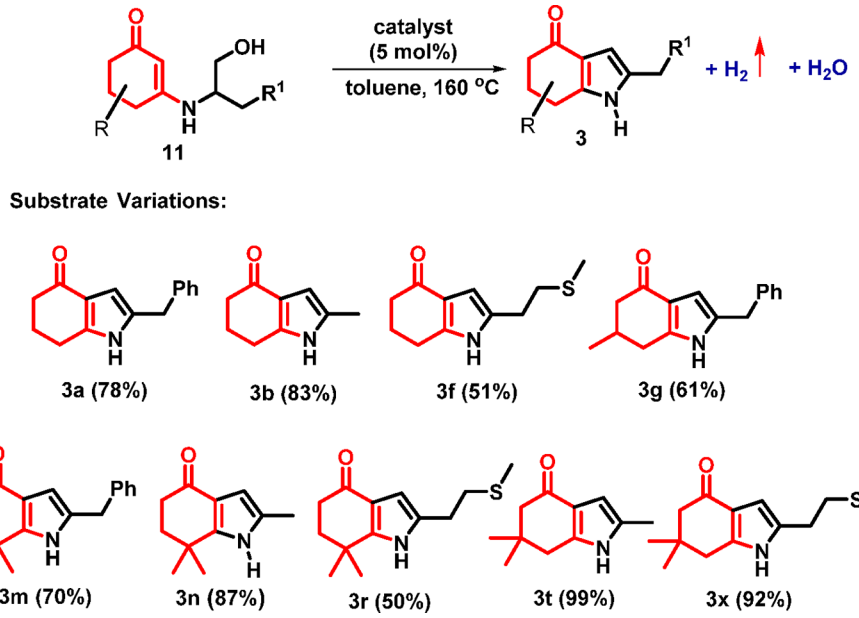

Scheme 4. Substrate Scope for the Intermolecular Annulation of 2-Aminobenzyl Alcohol with β-Diketone[a]

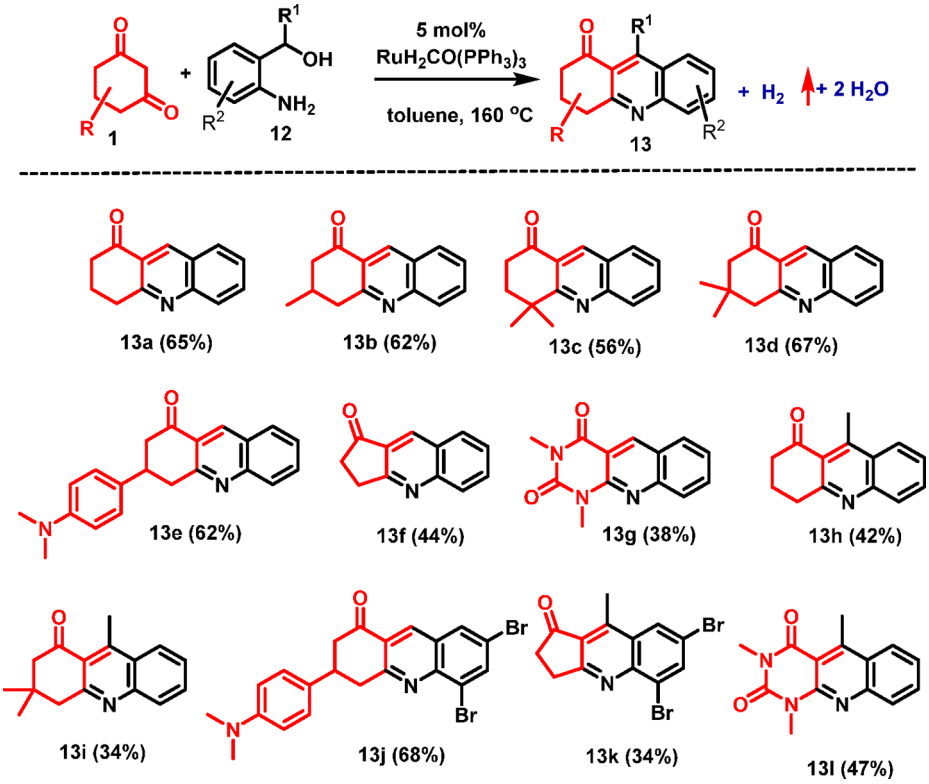

[a]Reaction conditions: **1** (0.5 mmol), **12** (0.5 mmol), $RuH_2CO(PPh_3)_3$ (5 mol %), and toluene (2 mL) were heated at 160 °C for 24 h; the reported yields are the isolated yields.

irrespective of substitution, this catalyst was efficiently used in dehydrogenative annulation with other dicarbonyl compounds to afford the diversified derivatives **3g–z** in 40 to 95% yield (Scheme 2). This reaction with prolinol afforded the tricyclic products **3aa** and **3ab** in 47% and 61% yield, respectively. With cyclopentane-1,3-dione, product **3ac** was obtained in 42% yield. However, AD annulation was not successful with acyclic-1,3-dione and led to the formation of respective enaminone products **3ad**, **3ae**, and **3af**.

Next, intramolecular dehydrogenative cyclization of various enaminone derivatives **11** (Scheme 3) was performed in the presence of 5 mol % $RuH_2CO(PPh_3)_3$. For the intramolecular enamine alcohol cyclization, Pd catalyst[22] along with a stoichiometric amount of K_2CO_3 and mesityl bromide is required. To avoid the stoichiometric base and additives, we

https://doi.org/10.1021/acs.joc.1c00714
J. Org. Chem. 2021, 86, 8805–8828

Scheme 5. Substrate Scope for the Intramolecular Annulation Using Enaminone Alcohols[a]

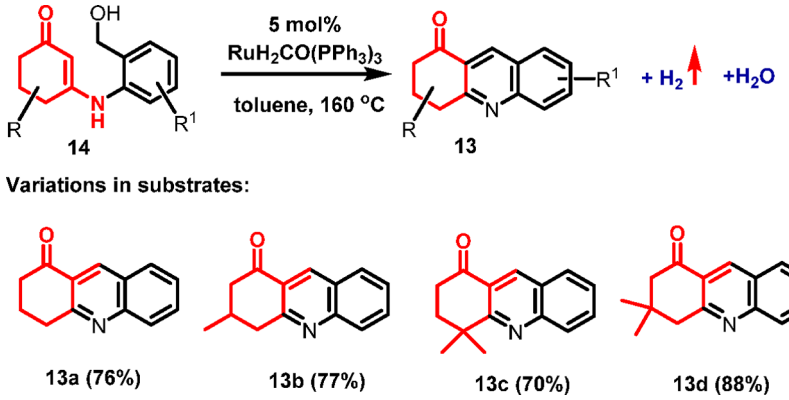

[a]Reaction conditions: **1** (0.5 mmol), **2** (0.5 mmol), $RuH_2CO(PPh_3)_3$ (5 mol %), and toluene (2 mL) were heated at 160 °C for 24 h; the reported yields are the isolated yields.

Scheme 6. Base-Free Acceptorless Dehydrogenative Synthesis of Xanthenone Core with Various Catalysts[a]

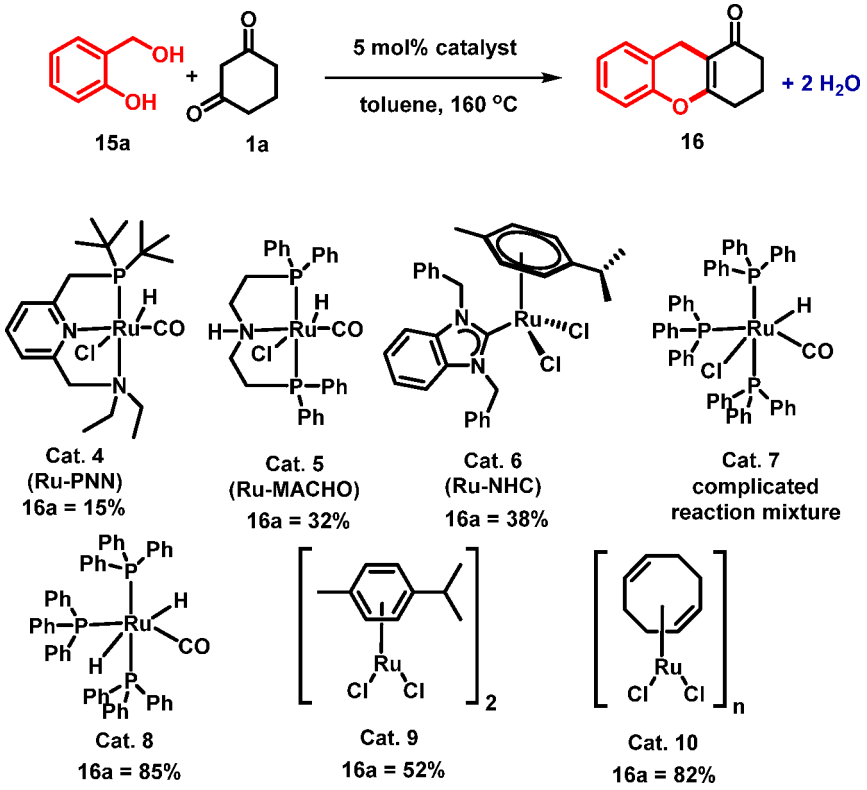

[a]Reaction conditions: **1a** (1 mmol), **15a** (0.5 mmol), cat. (5 mol %), and toluene (2 mL) were heated at 160 °C for 24 h; the reported yields are the isolated yields.

envisioned the additive-free dehydrogenative enamine−alcohol cyclization in the presence of 5 mol % $RuH_2CO(PPh_3)_3$. At the outset, this cyclization efficiently proceeds with the liberation of hydrogen and water to produce 1,5,6,7-tetrahydro-4*H*-indol-4-one derivatives in a considerably high yield (Scheme 3).

Similarly, the base-free AD synthesis of 3,4-dihydroacridin-1(2*H*)-one derivatives was attempted. Thus, an equimolar concentration of cyclohexane-1,3-dione and 2-aminobenzyl alcohols in toluene was heated at 160 °C for 24 h in the presence of 5 mol % $RuH_2CO(PPh_3)_3$ in the closed system, which led to 65% yield of the product **13a** (Scheme 4). For intermolecular oxidative annulation, the optimal temperature was 160 °C. A decrease in temperature resulted in lower conversion and yields. This type of cyclization was successfully conducted with other cyclic 1,3-dicarbonyl derivatives to obtain 34−68% yields of the respective polycyclic heteroaromatic compounds **13b−l** (Scheme 4).

Close monitoring of the reaction revealed that enaminone formation was the primary reaction, and enaminone then underwent Ru-catalyzed dehydrogenation to generate the corresponding aldehyde. The intramolecular condensation of enamine carbon nucleophile with the aldehyde resulted in the formation of 3,4-dihydroacridin-1(2*H*)-one derivatives. Furthermore, we evaluated this AD strategy through the intramolecular reaction of enaminone alcohols in the presence of 5 mol % $RuH_2CO(PPh_3)_3$ and observed considerably high yields

https://doi.org/10.1021/acs.joc.1c00714
J. Org. Chem. 2021, 86, 8805−8828

Scheme 7. Substrate Scope for Product 16

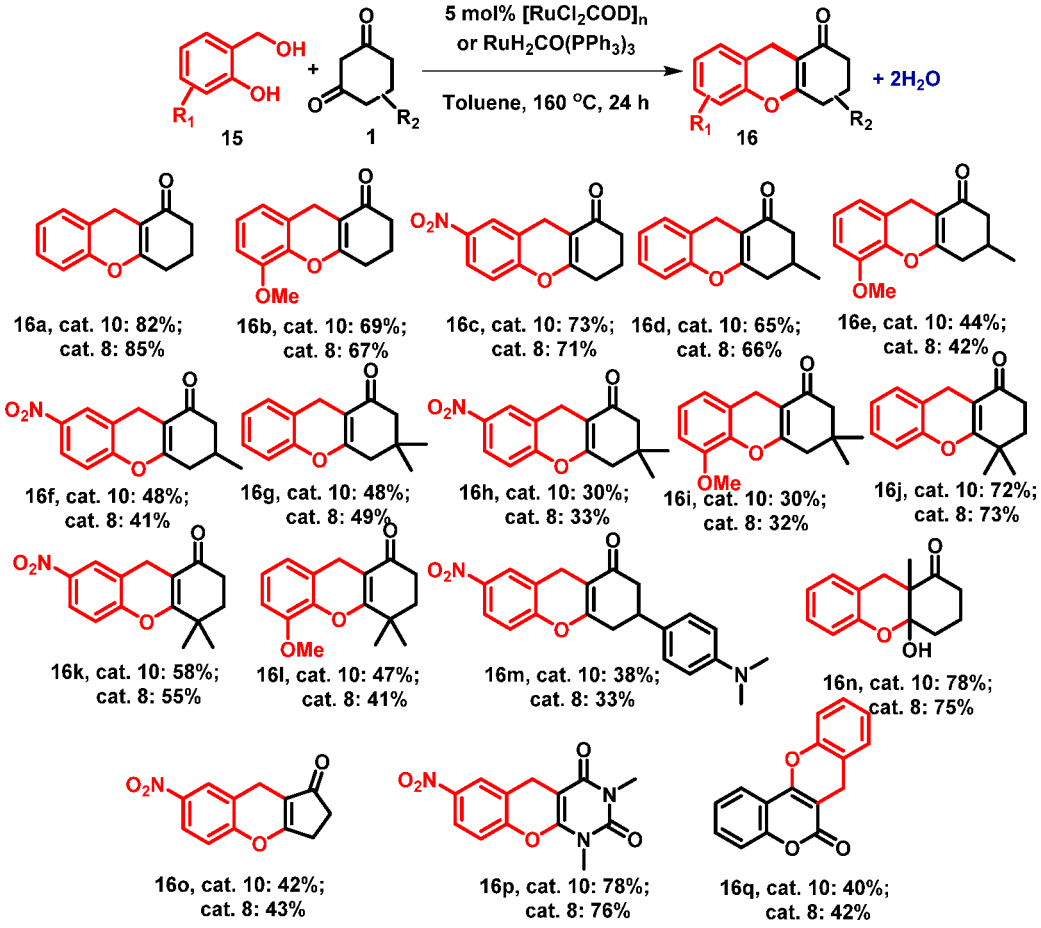

[a]Reaction conditions: **1** (1 mmol), **2** (0.5 mmol), $[RuCl_2COD]_n$ or $RuH_2CO(PPh_3)_3$ (5 mol %) and toluene (2 mL) were heated at 160 °C for 24 h; the reported yields are the isolated yields.

of the 3,4-dihydroacridin-1(2*H*)-one derivatives **13a−d** in 70−88% yield (Scheme 5).

Nitrogen- and oxygen-containing aromatic compounds have the utmost importance in organic syntheses because of their omnipresence in most therapeutics. In particular, 4*H*-chromene derivatives are a discrete class of natural products and drugs that exhibit promising biological activities.[20] The conventional synthesis of functionalized 2,3,4,9-tetrahydro-1*H*-xanthen-1-one derivatives[23] involves requirement for mutagenic halogenated starting materials, limited substrate scope, prefunctionalization, and use of additives and which encouraged us to develop an environmentally benign, practical, and efficient catalytic approach.

Cyclohexane-1,3-dione and 2-hydroxybenzyl alcohol were selected as model substrates for catalyst optimization (see the Supporting Information). After optimization, the 1:0.5 mmol ratio of 2-hydroxybenzyl alcohol (**15a**) and cyclohexane-1,3-dione (**1a**) with 5 mol % of $[Ru\text{-}COD)Cl_2]_n$ in toluene at 160 °C led to 82% yield of 2,3,4,9-tetrahydro-1*H*-xanthen-1-one (**16**), while decreasing the temperature to 140 °C led to a decrease in the yield. A slight increase yield (85%) was obtained when 5 mol % $RuH_2CO(PPh_3)_3$ was used (Scheme 6). The use of 5 mol % $Ru(p\text{-cymene})_2Cl_2$ led to 52% yield (Scheme 6). This reaction with pincer catalysts **4** and **5** afforded only 15% and 30% of product **16a** (Scheme 6). For Ru-NHC (**6**), only 38% yield was observed. Other catalysts such as a $RuHCl(CO)(PPh_3)_3$ and $Ru(PPh_3)_3Cl_2$ provided decomposed or complicated reaction mixtures (Scheme 6).

With catalyst optimization, we explored the acceptorless dehydrogenative strategy for the substrate scope in AD alkylation/cyclization. Various salicyl alcohols were treated with cyclohexane-1,3-dione. $[RuCl_2COD]_n$ or $RuH_2CO(PPh_3)_3$ was effective for this transformation to afford the product **16** with the same yield. Thus, the reaction of electron-neutral 2-hydroxybenzyl alcohol led to an 82% isolated yield of 2,3,4,9-tetrahydro-1*H*-xanthen-1-one **16a** (Scheme 7). The reaction of electron-donating 2-(hydroxymethyl)-6-methoxyphenol and electron-withdrawing 2-(hydroxymethyl)-4-nitrophenol with cyclohexane-1,3-dione provided 69% and 73% yields, respectively, of 5-methoxy-2,3,4,9-tetrahydro-1*H*-xanthen-1-one **16b** and 7-nitro-2,3,4,9-tetrahydro-1*H*-xanthen-1-one **16c**, respectively (Scheme 7). Subsequently, 5-methylcyclohexane-1,3-dione reacted smoothly with 2-hydroxybenzyl alcohol, 2-(hydroxymethyl)-6-methoxyphenol, and 2-(hydroxymethyl)-4-nitrophenol to produce good to moderate yields of compounds **16d−f**, respectively (Scheme 7). The reaction of 5,5-dimethylcyclohexane-1,3-dione with substituted hydroxy benzyl alcohols provided 48%, 30%, and 30% yields of 3,3-dimethyl-2,3,4,9-tetrahydro-1*H*-xanthen-1-one (**16g**), 3,3-dimethyl-7-nitro-2,3,4,9-tetrahydro-1*H*-xanthen-1-one (**16h**), and 5-methoxy-3,3-dimethyl-2,3,4,9-tetrahydro-1*H*-xanthen-1-one (**16i**), respectively. Furthermore, we extended our substrate scope

https://doi.org/10.1021/acs.joc.1c00714
J. Org. Chem. 2021, 86, 8805−8828

Scheme 8. Gram-Scale AD Annulation Reaction

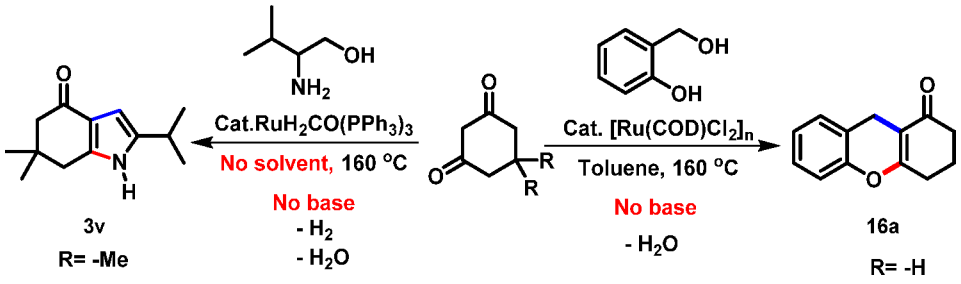

Scheme 9. AD Synthesis of Molindone Drug Intermediate

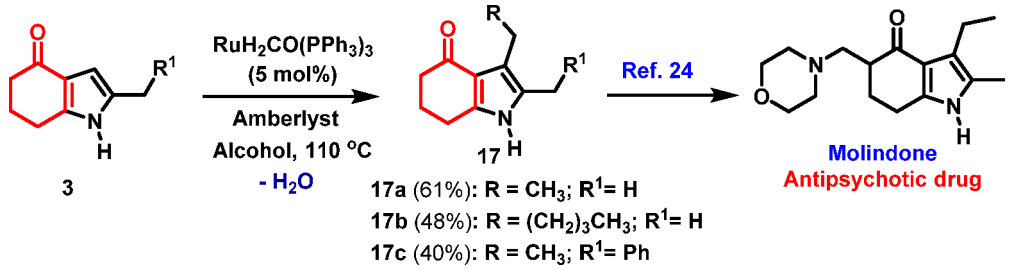

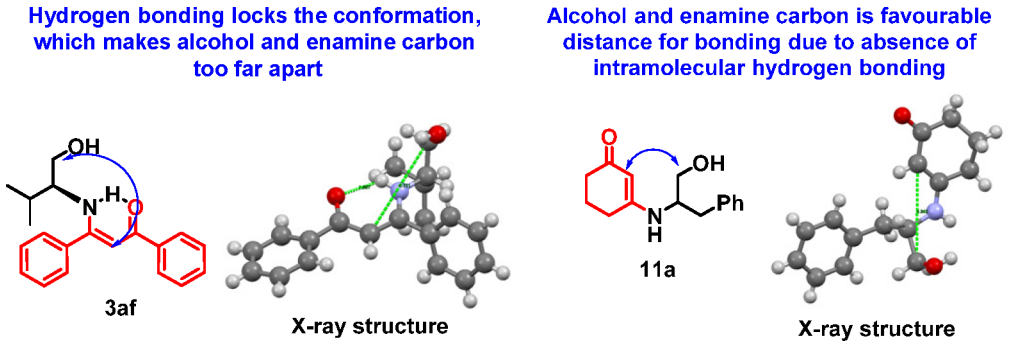

Figure 4. Favorable isomers for annulation.

investigation to the reaction of 4,4-dimethylcyclohexane-1,3-dione with 2-hydroxybenzyl alcohol, 2-(hydroxymethyl)-6-methoxyphenol, and 2-(hydroxymethyl)-4-nitrophenol to obtain 72%, 58%, and 47% isolated yields of **16j**, **16k**, and **16l**, respectively (Scheme 7). Further substrate scope with other cyclohexane-1,3-dione and 2-(hydroxymethyl)-4-nitrophenol provided the respective products **16m** in 38% yield (Scheme 7). 2-Methylcyclohexane-1,3-dione afforded the product **16n** as a diastereomeric mixture. Other dicarbonyls, cyclopentane-1,3-dione, dimethylbarbituric acid, and 4-hydroxycoumarin afforded the respective annulated products **16o−q** in 40−78% yield (Scheme 7).

To demonstrate scale-up application, gram-scale syntheses for **3v** and **16a** have been performed (Scheme 8). To avoid the consumption of a large volume of the solvent, gram-scale synthesis was performed under solvent-free conditions by heating the reaction mixture that contains 1,3-cyclohexane-1,3-dione and L-valinol in the presence 5 mol % of $RuH_2CO(PPh_3)_3$ at 160 °C for 24 h. The product **3v** was isolated in 78% (1.122 g) yield. Similarly, a solvent-free gram-scale reaction was explored for the synthesis of **16a** using $[Ru(COD)Cl_2]_n$ and furnished a poor yield (32%). The same reaction in toluene solvent afforded 67% (1.82 g) yield. The rationale for the use of $[Ru(COD)Cl_2]_n$ as a catalyst for this scale-up is recovery and reuse. After the reaction, $[RuCl_2COD]_n$ was filtered, washed with toluene, and dried at 100 °C for 4 h. Recovered catalyst was tested for the reaction, and we found that a decrease in catalytic activity afforded the product **16a** in 56% (1.0 g) yield.

To synthesize molindone intermediates, we established the sustainable alkylation of indolone derivatives by using alcohols. Hence, a reaction of heterocycle **3b** with ethanol in the presence of $RuH_2CO(PPh_3)_3$ resulted in no reaction. The addition of Amberlyst-15 to this reaction led to 61% yield of product **17a**. Having the optimized condition on hand, alkylation of **3** was performed by using various alcohols in the presence of catalytic $RuH_2CO(PPh_3)_3$, and Amberlyst-15 afforded **17b,c** in 48 and 40% yield, respectively (Scheme 9). Finally, the intermediate **17a** was subjected to the Mannich reaction that led to molindone drug formation.[24]

To understand the reactivity of 1,3-dione with amino alcohols in the AD reaction, both intermediates from the cyclic and acyclic compounds were isolated and investigated. The X-ray analysis evidenced that acyclic 1,3-dione led to the formation of a highly rigid structure, *Z*-enaminone alcohol[25] (**3af**), because of intramolecular hydrogen bonding (Figure 4). Thus, both the C nucleophile and alcohol are too far away to react, and no AD annulation product was obtained (Figure 4). In the case of cyclic-1,3-dione (**11a**), both the C nucleophile and alcohol are in close proximity for reaction. This might be due to the absence of a rigid structure for **11a**, which arises from the intramolecular

https://doi.org/10.1021/acs.joc.1c00714
J. Org. Chem. 2021, 86, 8805−8828

Scheme 10. Crossover Experiments

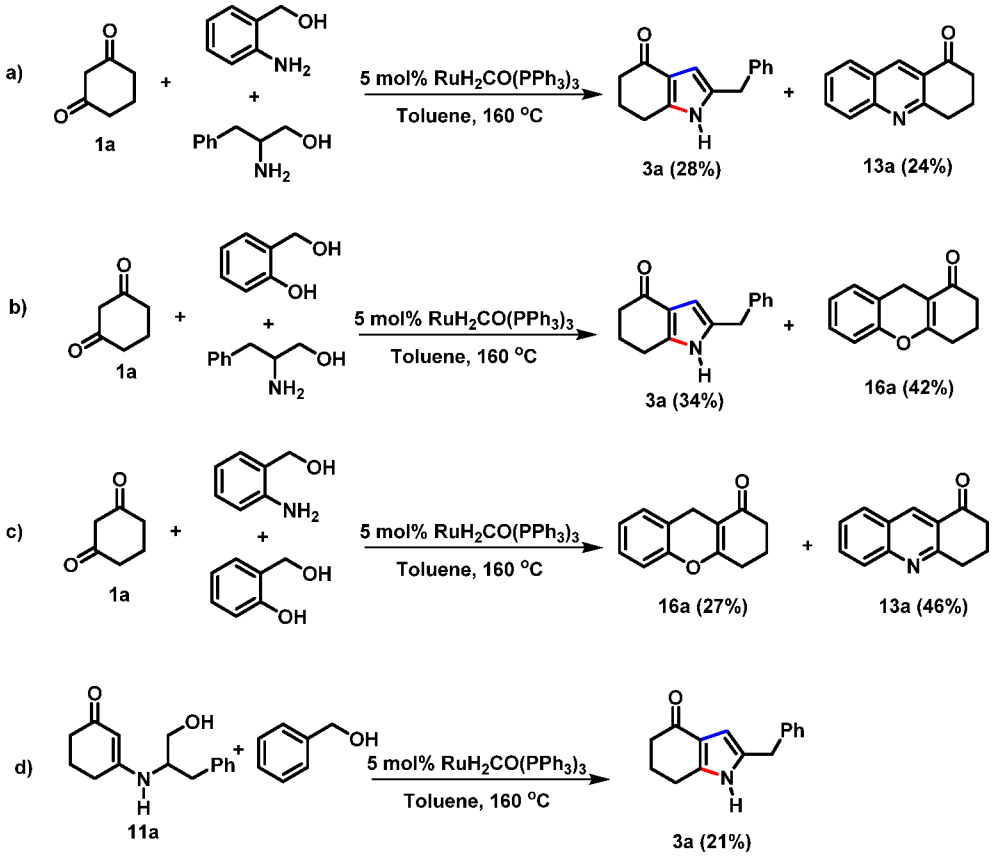

hydrogen bonding. Thus, cyclic-1,3-dione easily underwent AD annulation.

To further understand the reactivity of 1,3-dicarbonyl in annulation, several crossover experiments were performed (Scheme 10). To understand the selectivity in heterocycle formation, several reactions involving cyclohexane-1,3-dione, (*S*)-phenyl alaninol, 2-hydroxybenzyl alcohol, and 2-aminobenzyl alcohol were performed. The reactions of cyclohexane-1,3-dione, (*S*)-phenyl alaninol, and 2-aminobenzyl alcohol in the presence of 5 mol % $RuH_2CO(PPh_3)_3$ afforded **3a** (28%) and **13a** (24%), which indicated no selectivity in the formation of five- and six-membered N-heterocycle (Scheme 10, entry a). A similar reaction involving (*S*)-phenylalaninol and 2-hydroxy benzyl alcohol afforded comparable yields of product **3a** and **16a** (Scheme 10, entry b). Subsequently, the competence of six-membered N- versus O-heterocycle formation was studied using dione **1a**, 2-aminobenzyl alcohol, and 2-hydroxybenzyl alcohol (Scheme 10, entry c). This reaction indicated that nitrogen heterocycle **13a** and O-heterocycle **16a** were obtained as the major and minor products, respectively. To study the competence of inter- and intramolecular reactions, the treatment of intermediate **11a** with benzyl or 2-hydroxybenzyl alcohol afforded exclusively intramolecular cyclization product **3a** (Scheme 10, entry d).

To investigate the reaction mechanism, we have performed several experiments. In the absence of catalyst, the formation of enaminone **11a** in the reaction of cyclohexane-1,3-dione and amino alcohols indicated that imine formation is the primary step in pyrrole ring generation (Scheme 11, entry a). The Ru-catalyzed AD reaction of **11a** afforded pyrrole **3a** (76%), which further confirms imine formation as a key step (Scheme 11, entry b). Molecular hydrogen was detected through GC in this reaction (Scheme 11, entry c), and trapping of the liberated hydrogen with alkyne (Scheme 11, entry d) supported dehydrogenation. The reaction with 1,3-dione, benzyl alcohol, and hexylamine in the presence of Ru catalyst provided the respective enaminone products, which confirms that enaminone formation **11** is more predominant than C alkylation with 1,3-dicarbonyl (Scheme 11, entry e). The reaction of 1,3-cyclohexanedione with 2-hydroxy-3-methoxybenzyl alcohol resulted the product **19**, which supports the necessity of phenolic O−H for the formation of product **17**.

On the basis of the experimental evidence and previous reports,[26] a plausible reaction mechanism for the AD annulation is proposed (Scheme 12). The initial condensation reaction of amines and carbonyl results in the formation of the enaminone alcohol **11** intermediate. The O−H activation of intermediate **11** in the presence of $RuH_2CO(PPh_3)_3$ via PPh_3 exchange resulted in the formation of intermediates **A** and **B**. The intermediate **C** was formed through the liberation of molecular H_2 (confirmed by the GC analysis) and β-hydride elimination.

Finally, PPh_3 coordination and dissociation of aldehyde **D** resulted in the recovery of original catalyst $RuH_2CO(PPh_3)_3$, which was confirmed by ^{1}H NMR analysis. The ^{1}H NMR spectra indicated no changes in the Ru−H peak at the beginning and during the reaction course (Figure 5). The dissociated aldehyde undergoes intramolecular condensation followed by isomerization, which results in the formation of the desired product **3**.

To obtain mechanistic insights into domino alkylation/cyclization for tetrahydroxanthenenone (**16**) formation, gas liberation was studied. The control experiments conducted for

https://doi.org/10.1021/acs.joc.1c00714
J. Org. Chem. 2021, 86, 8805−8828

Scheme 11. Mechanistic Studies

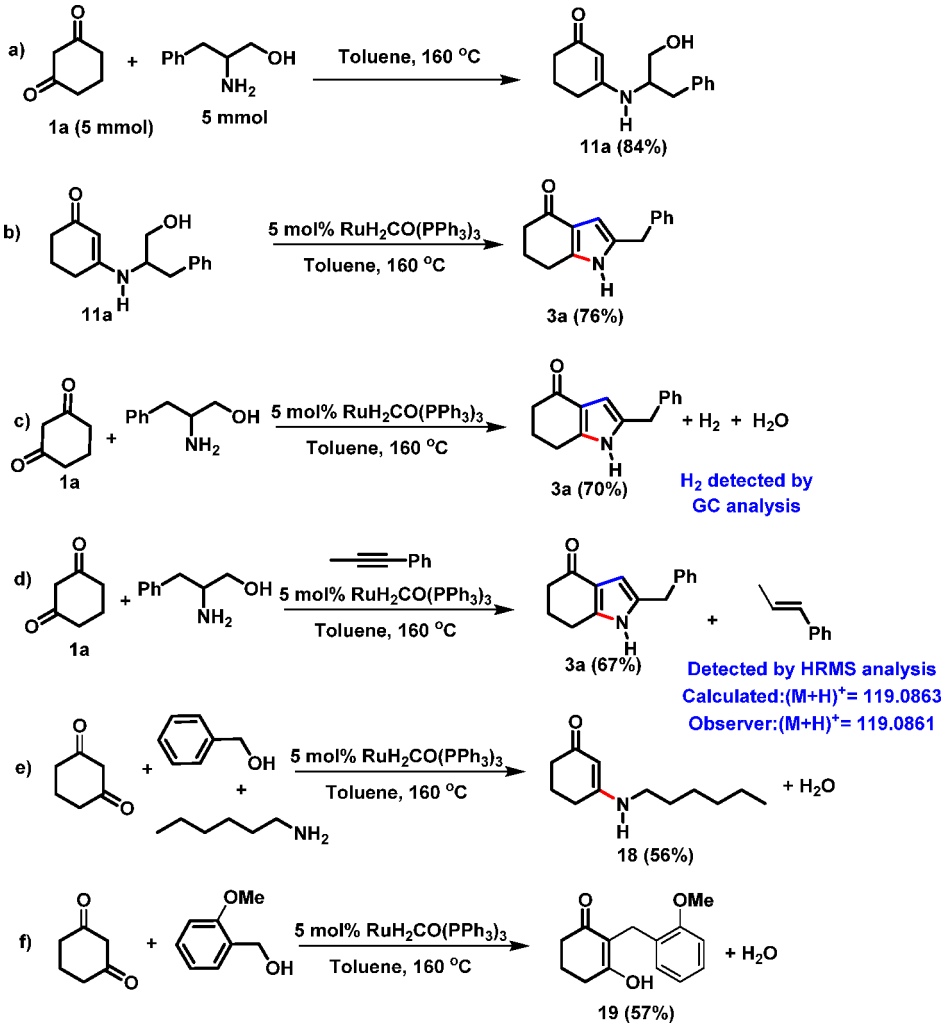

the hydroxyl benzyl alcohol and cyclohexane-1,3-dione showed no reaction and no enol ether formation. To analyze molecular hydrogen liberation, a gaseous component was taken using a gastight syringe from the reaction mixture and was directly injected into the GC instrument. The presence of a strong peak at a retention time of 0.88 confirmed the liberation of molecular hydrogen (Figure 6).

To prove the involvement of metal hydrides in the reaction, we conducted the reaction of cyclohexane-1,3-dione **2** with 2-hydroxybenzyl alcohol **15** in benzene-d_6 (0.6 mL) in the presence of $[RuCl_2COD]_n$ in an NMR tube and recorded the ^1H NMR spectra. Consequently, the appearance of a ^1H NMR signal on the negative scale at −20 suggested the formation of the Ru−H species (Figure 7).

On the basis of experimental investigations and the literature,[26] we proposed a plausible mechanism for acceptorless domino alkylation/cyclization (Scheme 13). Initially, the alcohol **15** binds with the metal catalyst **10** to produce complex **E**. Oxidation occurs through β-hydride elimination to provide Ru−H (**F**) (the presence of Ru−H was confirmed through ^1H NMR spectroscopy) and aromatic aldehyde **G**. Subsequently, aldol-type condensation between compound **1** and aldehyde **G** afforded the condensed product **H**. The coordination of Ru−H with unsaturated compound leads to the formation of compound **I**, which finally undergoes saturation in the presence of 2-hydroxy benzyl alcohol to produce intermediate **J**. Finally, intermediate **J** undergoes intramolecular addition with carbonyl followed by dehydration to provide the desired product **16**.

CONCLUSION

In summary, a base-free acceptorless dehydrogenation strategy was developed for biologically inspired tetrahydroindole, tetrahydroacridinone, and tetrahydroxanthenone derivatives by using easily accessible $RuH_2CO(PPh_3)_3$. This catalytic approach led to the generation of several N- and O-containing aromatic compounds with the liberation of environmentally benign H_2 and water as byproducts. AD annulation proceeded through imination−dehydrogenation−condensation−isomerization in a domino manner. In the case of tetrahydroxanthenone, AD annulation proceeded under the one-pot conditions involving alkylation−cyclization reactions by following tandem dehydrogenation−condensation−hydrogenation−condensation steps. A crucial intermediate enaminone was isolated, and the first base-free intramolecular AD annulation reactions using the Ru catalyst were proposed. Furthermore, in this approach, stoichiometric amounts of base and oxidant for C−C bond formation and hydrogen acceptor, respectively, are not required. Preliminary experiments and crossover experiments were performed to support reaction coordinates for the formation of tetrahydroindole and tetrahydroxanthenone derivatives.

https://doi.org/10.1021/acs.joc.1c00714
J. Org. Chem. 2021, 86, 8805−8828

Scheme 12. Plausible Mechanism for Acceptorless Dehydrogenative Annulation with Amino Alcohols

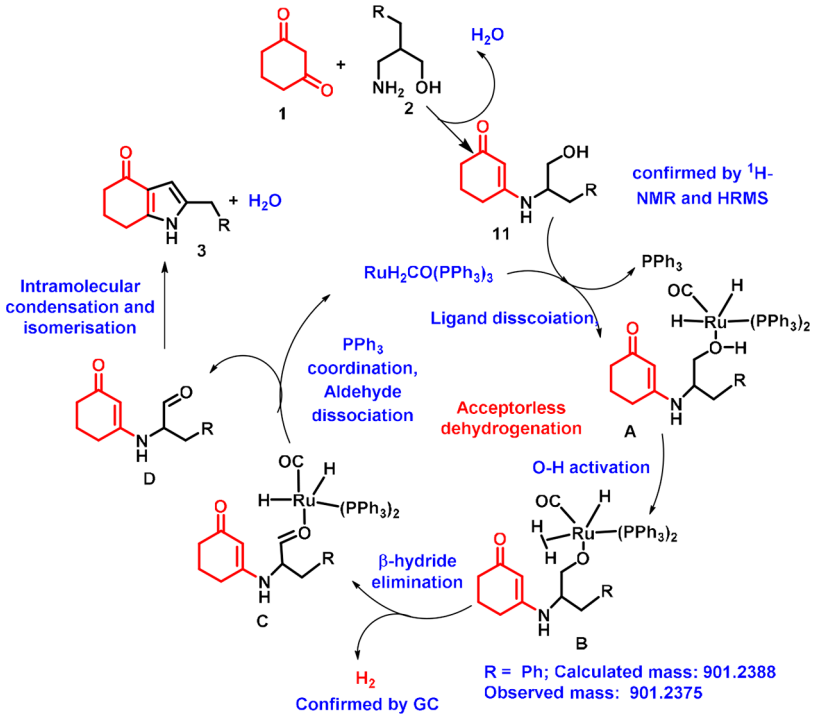

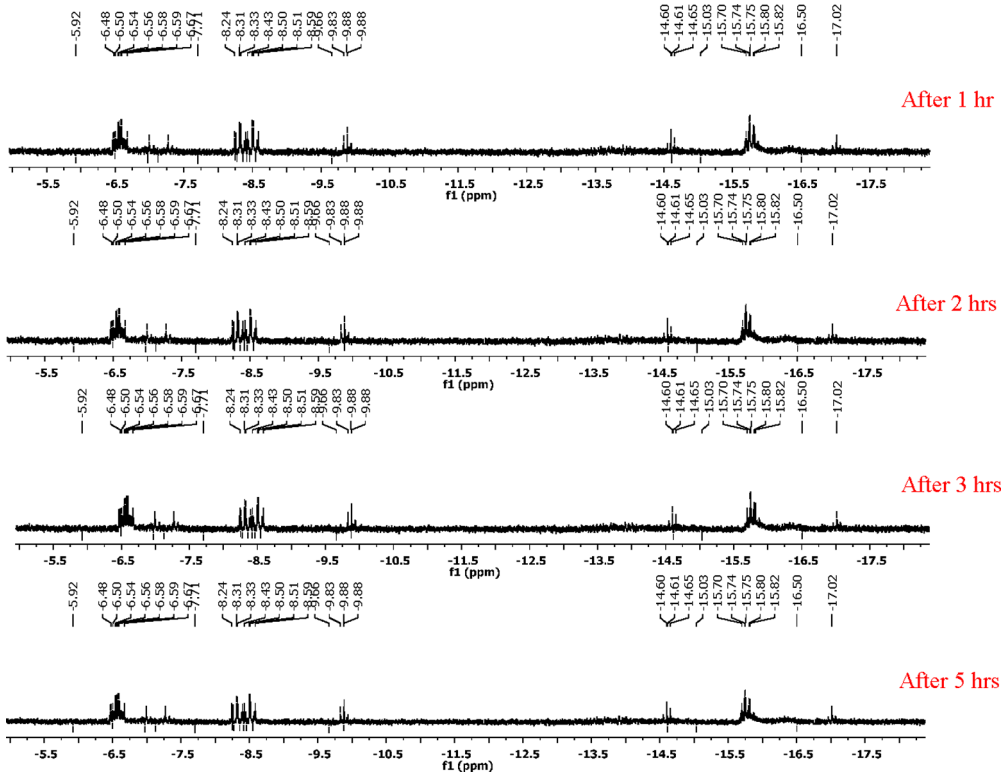

Figure 5. ^{1}H NMR spectra of reaction mixture in toluene-d_8.

EXPERIMENTAL SECTION

General Information and Data Collection. The amino alcohols and diketone derivatives were purchased from Sigma-Aldrich. Deuterated solvents were used as received. The solvents used were dry grade and stored over 4 Å molecular sieves. Column chromatographic separation was performed over 100−200 mesh size silica gel. Visualization was accomplished with UV light and iodine. The ^{1}H and ^{13}C{^{1}H} NMR spectra were recorded at 400 and 100 MHz, respectively using Bruker or JEOL spectrometers. Abbreviations used in the NMR follow-up experiments: b, broad; s, singlet; d, doublet; t, triplet; q, quartet; td, dd doublet of triplet and double doublet; m, multiplet, tt, triplet of triplets and ddd, doublet of doublet of doublets. HRMS spectra were obtained with a Waters-synapt G2 using electrospray ionization (ESI-TOF). Infrared (ATIR) spectra were obtained with a Bruker Alpha-E infrared spectrometer. Single-crystal diffraction analysis

https://doi.org/10.1021/acs.joc.1c00714
J. Org. Chem. 2021, 86, 8805−8828

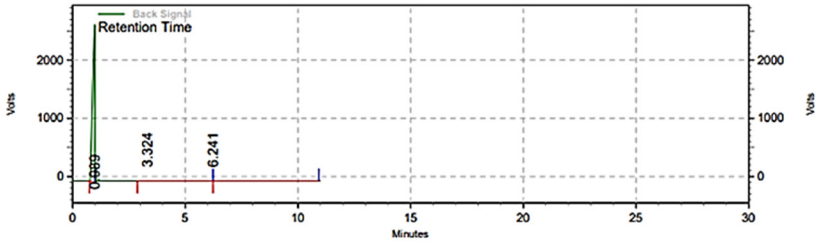

Figure 6. H_2 gas liberation through the GC analysis.

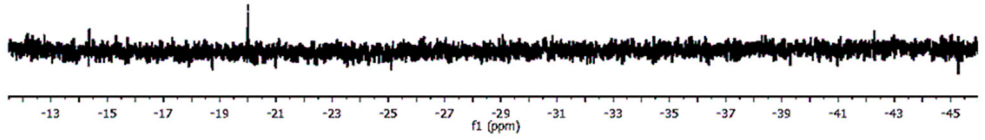

Figure 7. ^1H NMR spectra of reaction mixture in benzene-d_6 showing Ru−H at −20.0 ppm

Scheme 13. Plausible Mechanism for Acceptorless Dehydrogenative Annulation with 2-Hydroxybenzyl Alcohol

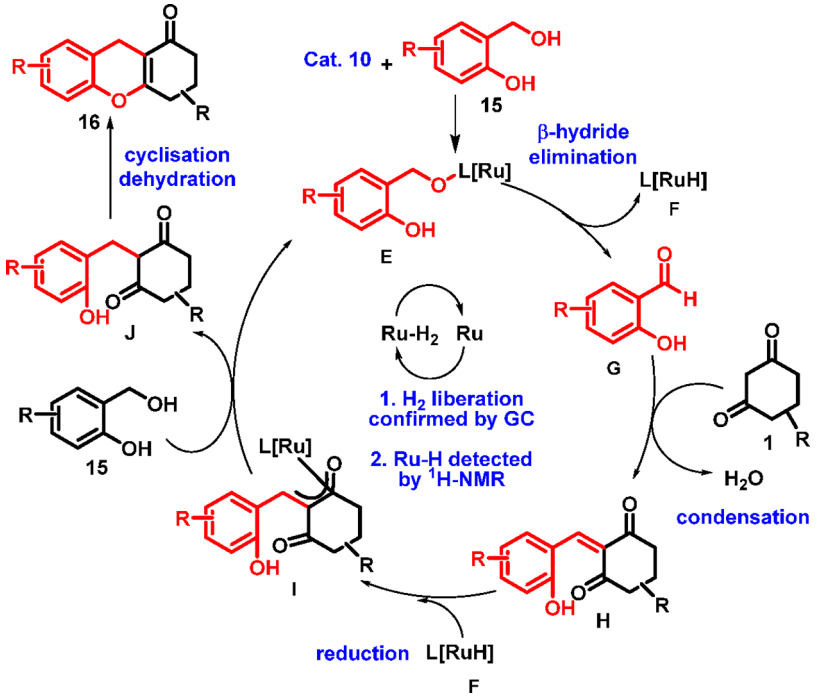

data were collected at 100 K with a Bruker Kappa Apex III CCD Duo diffractometer (operated at 1500 W power: 50 kV, 30 mA) using graphite monochromatic Mo Kα radiation and Cu Kα radiation. More information on crystal structures can also be obtained from the Cambridge Crystallographic Data Centre (CCDC) with deposition numbers 2048644 (**3k**), 2048437 (**3af**), 2048435 (**11a**), 2048643 (**13a**), 2051625 (**16a**), and 2064954 (**16n**).

A. General Experimental Procedure for the Intermolecular Cyclization of β-Amino Alcohol with β-Diketone. To an oven-dried 20 mL resealable pressure tube (equipped with rubber septum) were added β-diketone (0.5 mmol), β-amino alcohol (0.5 mmol), and $RuH_2CO(PPh_3)_3$ (0.025 mmol) in toluene (2 mL) under a N_2 atmosphere using a N_2 balloon. Then the tube was purged with N_2, the septum was quickly removed, and the tube was sealed with a cap using a crimper. The reaction mixture was stirred at 160 °C for 24 h on a preheated oil bath. After being cooled to room temperature, the reaction mixture was diluted by dichloromethane. After concentration under reduced pressure, the residue was purified by 100−200 mesh silica gel column chromatography (EtOAc/hexane = 30:70 to 40:60).

https://doi.org/10.1021/acs.joc.1c00714
J. Org. Chem. 2021, 86, 8805−8828

B. General Experimental Procedure for Enaminone Alcohol Synthesis. To an oven-dried 20 mL resealable pressure tube (equipped with rubber septum) were charged β-diketone (0.5 mmol) and amino alcohol (0.5 mmol) in a 20 mL resealable pressure tube equipped with a stirring bar. Toluene (1 mL) was added and the tube sealed with a cap using a crimper. The mixture was stirred at room temperature and 160 °C on a preheated oil bath for 24 h. After being cooled to room temperature, the reaction mixture was diluted with dichloromethane and MeOH. After concentration under reduced pressure, the residue was purified by 100−200 mesh silica gel column chromatography (EtOAc/methanol = 99:1 to 90:10).

C. General Experimental Procedure for the Intramolecular Annulation of β-Enaminone Alcohol. To an oven-dried 20 mL resealable pressure tube (equipped with rubber septum) were added β-enaminone alcohol (0.5 mmol) and $RuH_2CO(PPh_3)_3$ (0.025 mmol) in toluene (1 mL) under a N_2 atmosphere using a N_2 balloon. Then the tube was purged with N_2, the septum was quickly removed, and the tube was sealed with a cap using a crimper. The reaction mixture was stirred at 160 °C for 24 h on a preheated oil bath. After being cooled to room temperature, the reaction mixture was diluted by dichloromethane and MeOH. After concentration under reduced pressure, the residue was purified by 100−200 mesh silica gel column chromatography (EtOAc/hexane = 30:70 to 40:60).

D. General Experimental Procedure for the Intermolecular Annulation of 2-Aminobenzyl Alcohol with β-Diketone. To an oven-dried 20 mL resealable pressure tube (equipped with rubber septum) were added β-diketone (0.5 mmol), 2-aminobenzyl alcohol (0.5 mmol), and $RuH_2CO(PPh_3)_3$ (0.025 mmol) in toluene (2 mL) under a N_2 atmosphere using a N_2 balloon. Then the tube was purged with N_2, the septum was quickly removed, and the tube was sealed with a cap using a crimper. The reaction mixture was stirred at 160 °C for 24 h on a preheated oil bath. After being cooled to room temperature, the reaction mixture was diluted by dichloromethane. After concentration under reduced pressure, the residue was purified by 100−200 mesh silica gel column chromatography (EtOAc/hexane = 30:70 to 40:60).

E. General Experimental Procedure for the Intramolecular Annulation Using Enaminone Alcohols. To an oven-dried 20 mL resealable pressure tube (equipped with rubber septum) were added enaminone alcohol (0.5 mmol) and $RuH_2CO(PPh_3)_3$ (0.025 mmol) in toluene (1 mL) under a N_2 atmosphere using a N_2 balloon. Then the tube was purged with N_2, the septum was quickly removed, and the tube was sealed with a cap using a crimper. The reaction mixture was stirred at 160 °C for 24 h on a preheated oil bath. After being cooled to room temperature, the reaction mixture was diluted by dichloromethane. After concentration under reduced pressure, the residue was purified by 100−200 mesh silica gel column chromatography (EtOAc/hexane = 30:70 to 40:60).

F. General Experimental Procedure for the Synthesis of 2,3,4,9-Tetrahydro-1*H*-xanthen-1-one Derivatives. To a 20 mL resealable vial (equipped with rubber septum and N_2 balloon) were added catalyst **8**, i.e., $RuH_2CO(PPh_3)_3$ (0.025 mmol), or catalyst **10**, i.e., $[RuCl_2(COD)]_n$ (15 mg), toluene (2 mL), salicyl alcohol (1 mmol), and β-diketone (0.5 mmol). The tube was purged with N_2 and sealed with a cap using a crimper. The reaction mixture was heated at 160 °C using Radley's parallel reaction station for 24 h. After reaction completion, the mixture was allowed to cool at room temperature, and without any workup, the filtration was done using cotton and rinsing the vial with DCM and methanol. The volatile solvent was evaporated under vacuum, and product was purified by column chromatography (EtOAc/hexane = 10:90) on silica gel to afford the desired products in pure form.

G. General Experimental Procedure for the Drug Intermediate Using Acceptorless Dehydrogenation Reaction. To an oven-dried 20 mL resealable pressure tube (equipped with rubber septum) were added 2-substituted 1,5,6,7-tetrahydro-4*H*-indol-4-one (0.34 mmol), alcohol (excess), $RuH_2CO(PPh_3)_3$ (0.017 mmol), and 100 mg Amberlyst 15. Then the tube was sealed with a cap using a crimper. The reaction mixture was stirred at 110 °C for 24 h on a preheated oil bath. After being cooled to room temperature, the reaction mixture was diluted by dichloromethane and MeOH. After concentration under reduced pressure, the residue was purified by 100−200 mesh silica gel column chromatography (EtOAc/hexane = 30:70−50:50).

H. Detection of Molecular Hydrogen by Reduction of Prop-1-yn-1-ylbenzene. To an oven-dried 20 mL resealable pressure tube (equipped with rubber septum) were added cyclohexane-1,3-dione (56 mg, 0.5 mmol), (*S*)-2-amino-3-phenylpropan-1-ol (76 mg, 0.50 mmol), prop-1-yn-1-ylbenzene (58 mg, 0.5 mmol), and $RuH_2CO(PPh_3)_3$ (0.025 mmol) in toluene (2 mL) under a N_2 atmosphere using a N_2 balloon. Then the tube was purged with N_2, the septum was quickly removed, and the tube was sealed with a cap using a crimper. The reaction mixture was stirred at 160 °C for 24 h on a preheated oil bath. After being cooled to room temperature, the reaction mixture was diluted by dichloromethane. The reaction mixture was concentrated under reduced pressure, and the residue was purified by 100−200 mesh silica gel column chromatography (EtOAc/hexane = 30:70 to 40:60) to afford 2-benzyl-1,5,6,7-tetrahydro-4*H*-indol-4-one **3a** in 67% yield. The HRMS data of reaction mixture confirmed the mass of reduced product prop-1-en-1-ylbenzene with $(M + H)^+ = 119.0861$.

I. General Experimental Procedure for the Gram-Scale Synthesis of 2-Isopropyl-6,6-dimethyl-1,5,6,7-tetrahydro-4*H*-indol-4-one. To an oven-dried 20 mL round-bottom flask were added 5,5′-cyclohexane-1,3-dione (980 mg, 7.0 mmol), (*S*)-(+)-2-amino-3-methyl-1-butanol (721 mg, 7.0 mmol), and $RuH_2CO(PPh_3)_3$ (333 mg, 0.025 mmol) without maintaining any special conditions such as inert atmosphere. The reaction mixture was stirred at 160 °C for 24 h on a preheated oil bath. After being cooled to room temperature, the reaction mixture was diluted by dichloromethane. After concentration under reduced pressure, the residue was purified by 100−200 mesh silica gel column chromatography (EtOAc/hexane = 30:70 to 40:60) to obtain 1.122 g (78%) of 2-isopropyl-6,6-dimethyl-1,5,6,7-tetrahydro-4*H*-indol-4-one (**3v**).

J. General Experimental Procedure for the Gram-Scale Synthesis of 2,3,4,9-Tetrahydro-1*H*-xanthen-1-one. To a 20 mL resealable vial were added $[RuCl_2(COD)]_n$ (0.393 g, 5 mol %), salicyl alcohol (3.321g, 26.8 mmol), and cyclohexane-1,3-dione (1.5 g, 13.4 mmol) in 10 mL of toluene. The tube was sealed with a cap using a crimper under N_2 atmosphere. The reaction mixture was heated at 160 °C using Radley's parallel reaction station for 24 h. After reaction completion, the mixture was allowed to cool at room temperature, and without any workup, the filtration was done by using cotton with rinsing the vial with DCM and methanol. The volatile solvent was evaporated under vacuum and product was purified by column chromatography (petroleum ether: ethyl acetate = 75:25) on silica gel to furnish **16a** in 67% (1.82 g) yield. Further, catalyst was filtered, washed with toluene and dried at 100 °C for 4 h. With 0.3 g of recovered $[RuCl_2(COD)]_n$ catalyst, salicyl alcohol (2.534 g, 20.44 mmol), and cyclohexane-1,3-dione (1.145 g, 10.44 mmol) the reaction afforded **16a** in 56% (1.0 g) yield.

K. Detection of H_2 Gas Using GC for the Intermolecular Cyclization of β-Amino Alcohol with β-Diketone. To a 20 mL resealable vial (equipped with rubber septum and N_2 balloon) were added $RuH_2CO(PPh_3)_3$ (24.2 mg, 5 mol %), toluene 2 mL, and (*S*)-2-amino-3-phenylpropan-1-ol (76 mg, 0.50 mmol). The tube was purged with N_2 and sealed with a cap using a crimper. The reaction mixture was heated at 160 °C using Radley's parallel reaction station for 6 h. After that, the gaseous component was taken using a gas-tight syringe and injected into a GC instrument. The presence of a peak at retention time 0.88 corresponds to hydrogen gas.

L. Detection of Intermediates with HRMS for the Intermolecular Cyclization of β-Amino Alcohol with β-Diketone. To a 20 mL resealable vial (equipped with rubber septum and N_2 balloon) were added $RuH_2CO(PPh_3)_3$ (24.2 mg, 5 mol %), toluene 2 mL, and (*S*)-2-amino-3-phenylpropan-1-ol (76 mg, 0.50 mmol). The tube was purged with N_2 and sealed with a cap using a crimper. The reaction mixture was heated at 160 °C using Radley's parallel reaction station for 4 h. After that, the reaction mixture was taken for HRMS to determine the desired mass.

M. Hydride Detection for the Intermolecular Cyclization of β-Amino Alcohol with β-Diketone Using $RuH_2CO(PPh_3)_3$. To an

https://doi.org/10.1021/acs.joc.1c00714
J. Org. Chem. 2021, 86, 8805−8828

NMR tube were added $RuH_2CO(PPh_3)_3$ (15.2 mg, 20 mol %), toluene-d_8 (0.6 mL), cyclohexane-1,3-dione (8.9 mg, 0.08 mmol), and (*S*)-2-amino-3-phenylpropan-1-ol (12.1 mg, 0.08 mmol). The tube was purged with N_2 and closed using NMR tube cap. The reaction mixture was heated at 100 °C on a preheated oil bath for 1, 2, 3, and 5 h. After 1 h, the NMR tube was cooled and subjected to ^{1}H NMR. The notable peaks was observed due to the presence of Ru−H.

N. Detection of H_2 Gas Using GC for the Synthesis of 2,3,4,9-Tetrahydro-1*H*-xanthen-1-one Derivatives. To a 20 mL resealable vial (equipped with rubber septum and N_2 balloon) were added dichloro(1,5-cyclooctadiene)ruthenium(II), polymer (15 mg, 5 mol %), toluene 2 mL, salicyl alcohol (1 mmol), and diketo compound (0.5 mmol). The tube was purged with N_2 and sealed with a cap using a crimper. The reaction mixture was heated at 160 °C using Radley's parallel reaction station for 24 h. After reaction completion, the gaseous component was taken using a gas-tight syringe and injected into a GC instrument. The presence of a peak at retention time 0.88 corresponds to hydrogen gas.

O. Hydride Detection for the Synthesis of 2,3,4,9-Tetrahydro-1*H*-xanthen-1-one Derivatives. In a NMR tube were added dichloro(1,5-cyclooctadiene)ruthenium(II), polymer (4.2 mg, 10 mol %), benzene-d_6 (0.6 mL), cyclohexane-1,3-dione (16.8 mg, 0.15 mmol), and 2-hydroxybenzyl alcohol (18.6 mg, 0.15 mmol). The tube was purged with N_2 and closed using NMR tube cap. The reaction mixture was heated at 80 °C on a preheated oil bath for 30 min. After 30 min, the NMR tube was cooled and subjected to ^{1}H NMR. The notable peak was observed at −20.0 due to the presence of Ru−H.

P. Experimental Procedure for the Synthesis of Intermedate to 6-Methoxy-3,3-dimethyl-2,3,4,9-tetrahydro-1*H*-xanthen-1-one. To a 20 mL resealable vial (equipped with rubber septum and N_2 balloon) were added $RuH_2CO(PPh_3)_3$ (0.025 mmol) or $[RuCl_2(COD)]_n$ (15 mg) in toluene (2 mL) and 3-hydroxy-2-(2-hydroxy-4-methoxybenzyl)-5,5-dimethylcyclohex-2-en-1-one (0.5 mmol) prepared according to procedure A. The tube was purged with N_2 and sealed with a cap using a crimper. The reaction mixture was heated at 160 °C using Radley's parallel reaction station for 8 h. After reaction completion, the mixture was allowed to cool to room temperature and further extracted with DCM and methanol. The volatile solvent was evaporated under vacuum and product was purified by column chromatography (petroleum ether/ethyl acetate = 80:20) on silica gel to afford the desired products in pure form.

Q. Analytical Data for the Product. *2-Benzyl-1,5,6,7-tetrahydro-4H-indol-4-one (**3a**).*[27] Prepared according to procedure A. The tube was purged with N_2 and sealed with a cap using a crimper. The reaction used (*S*)-2-amino-3-phenylpropan-1-ol (76 mg, 0.50 mmol) and 1,3-cyclohexanedione (56 mg, 0.50 mmol), and the residue was purified by 100−200 mesh silica gel column chromatography (EtOAc/hexane = 35:65) to afford 2-benzyl-1,5,6,7-tetrahydro-4*H*-indol-4-one **3a** (78 mg, 70%) as a brown solid. Melting point: 131−136 °C. ^{1}H NMR (400 MHz, $CDCl_3$): δ 8.07 (s, 1H), 7.31 (m, 2H), 7.22 (m, 3H), 6.30 (s, 1H), 3.91 (s, 2H), 2.71 (t, J = 4.0 Hz, 2H), 2.43 (t, J = 8.0 Hz, 2H), 2.11 (m, 2H). ^{13}C{^{1}H} NMR (100 MHz, $CDCl_3$): δ 194.8, 143.7, 138.8, 132.1, 129.1, 129.0, 127.0, 120.9, 103.9, 38.1, 34.1, 24.2, 23.1. IR (neat): 3227, 3154, 2924, 1623, 1480 cm^{-1}. HRMS (ESI-TOF) m/z: $[M + H]^+$ calcd for $C_{15}H_{16}NO$ 226.1232; Found 226.1234.

*2-Methyl-1,5,6,7-tetrahydro-4H-indol-4-one (**3b**).*[28] Prepared according to procedure A using (*S*)-2-aminopropan-1-ol (37 mg, 0.50 mmol) and 1,3-cyclohexanedione (56 mg, 0.50 mmol), and the residue was purified by 100−200 mesh silica gel column chromatography (EtOAc/hexane = 45:65) to afford 2-methyl-1,5,6,7-tetrahydro-4*H*-indol-4-one **3b** (56 mg, 76%) as a dark brown solid. Melting point: 115−120 °C. ^{1}H NMR (400 MHz, methanol-d_4) δ 6.05 (s, 1H), 4.61 (s, 1H), 2.74 (t, J = 6.2 Hz, 2H), 2.38 (t, J = 6.0 Hz, 2H), 2.18 (s, 3H), 2.08. (m, 2H). ^{13}C{^{1}H} NMR (100 MHz, methanol-d_4) δ 197.6, 146.9, 130.6, 120.6, 103.2, 38.4, 25.2, 23.6, 12.3. IR (neat): 3220, 3162, 2934, 1618, 1476 cm^{-1}. HRMS (ESI-TOF) m/z: $[M + H]^+$ calcd for $C_9H_{12}NO$ 150.0919; Found 150.0917.

*2-Ethyl-1,5,6,7-tetrahydro-4H-indol-4-one (**3c**).*[29] Prepared according to procedure A using (*S*)-2-aminobutan-1-ol (45 mg, 0.50 mmol) and 1,3-cyclohexanedione (56 mg, 0.50 mmol), and the residue was purified by 100−200 mesh silica gel column chromatography (EtOAc/hexane = 40:60) to afford 2-ethyl-1,5,6,7-tetrahydro-4*H*-indol-4-one **3c** (37 mg, 46%) as a brown solid. Melting point: 135−140 °C. ^{1}H NMR (400 MHz, $CDCl_3$) δ 8.43 (s, 1H), 6.22 (s, 1H), 2.77 (t, J = 6.2 Hz, 2H), 2.58 (q, J = 7.52 Hz, 2H), 2.45 (t, J = 6.1 Hz, 2H), 2.12 (dd, J = 12.5, 6.3 Hz, 2H), 1.23 (t, J = 7.7 Hz, 3H). ^{13}C{^{1}H} NMR (100 MHz, $CDCl_3$) δ 194.7, 143.1, 135.5, 120.6, 101.4, 37.9, 24.2, 22.9, 20.8, 13.4. IR (neat): 3238, 3158, 2933, 1623, 1480 cm^{-1}. HRMS (ESI-TOF) m/z: $[M + H]^+$ calcd for $C_{10}H_{14}NO$ 164.1075; Found 164.1077.

*2-Isopropyl-1,5,6,7-tetrahydro-4H-indol-4-one (**3d**).*[29] Prepared according to procedure A using (*S*)-2-amino-3-methylbutan-1-ol (52 mg, 0.50 mmol) and 1,3-cyclohexanedione (56 mg, 0.50 mmol), and the residue was purified by 100−200 mesh silica gel column chromatography (EtOAc/hexane = 40:60) to afford 2-isopropyl-1,5,6,7-tetrahydro-4*H*-indol-4-one **3d** (43 mg, 49%) as a brown solid. Melting point: 160−161 °C. ^{1}H NMR (400 MHz, $CDCl_3$) δ 8.76 (s, 1H), 6.20 (s, 1H), 2.88 (m, 1H), 2.78 (t, J = 4.0 Hz, 2H), 2.45 (t, J = 4.0 Hz, 2H), 2.13 (m, 2H), 1.24 (d, J = 8.0 Hz, 6H). ^{13}C{^{1}H} NMR (100 MHz, $CDCl_3$) δ 194.6, 143.2, 140.2, 120.1, 99.8, 37.8, 26.9, 24.0, 22.8, 22.3. IR (neat): 3237, 3156, 2952, 1625, 1481 cm^{-1}. HRMS (ESI-TOF) m/z: $[M + H]^+$ calcd for $C_{11}H_{16}NO$ 178.1232; Found 178.1231.

*2-sec-Butyl-1,5,6,7-tetrahydro-4H-indol-4-one (**3e**).* Prepared according to procedure A using (2*S*)-2-amino-3-methylpentan-1-ol (59 mg, 0.50 mmol) and 1,3-cyclohexanedione (56 mg, 0.50 mmol), and the residue was purified by 100−200 mesh silica gel column chromatography (EtOAc/hexane = 40:60) to afford 2-(sec-butyl)-1,5,6,7-tetrahydro-4*H*-indol-4-one **3e** (60 mg, 63%) as a brown solid. Melting point: 169−172 °C. ^{1}H NMR (400 MHz, $CDCl_3$) δ 8.37 (s, 1H), 6.22 (s, 1H), 2.77 (t, J = 8.0 Hz, 2H), 2.62 (m, 1H), 2.45 (t, J = 8.0 Hz, 2H), 2.13 (m, 2H), 1.57 (m, 2H), 1.22 (d, J = 8.0 Hz, 3H), 0.88 (t, J = 8.0 Hz, 3H). ^{13}C{^{1}H} NMR (100 MHz, $CDCl_3$) δ 194.1, 142.4, 138.4, 119.9, 100.4, 37.4, 33.6, 29.4, 23.6, 22.5, 19.5, 11.3. IR (neat): 3244, 3160, 2958, 1625, 1482 cm^{-1}. HRMS (ESI-TOF) m/z: $[M + H]^+$ calcd for $C_{12}H_{18}NO$ 192.1388; Found 192.1388.

*2-(2-(Methylthio)ethyl)-1,5,6,7-tetrahydro-4H-indol-4-one (**3f**).* Prepared according to procedure A using (*S*)-(−)-2-amino-4-methylthio-1-butanol (67 mg, 0.50 mmol) and 1,3-cyclohexanedione (56 mg, 0.50 mmol), and the residue was purified by 100−200 mesh silica gel column chromatography (EtOAc/hexane = 40:60) to afford 2-(2-(methylthio)ethyl)-1,5,6,7-tetrahydro-4*H*-indol-4-one **3f** (46 mg, 44%) as a blackish brown solid. Melting point: 134−139 °C. ^{1}H NMR (400 MHz, $CDCl_3$) δ 9.16 (s, 1H), 6.23 (s, 1H), 2.85 (t, J = 8.0 Hz, 2H), 2.76 (m, 4H), 2.45 (t, J = 8.0 Hz, 2H), 2.13 (m, 5H). ^{13}C{^{1}H} NMR (100 MHz, $CDCl_3$) δ 195.5, 144.1, 132.9, 121.0, 103.1, 38.4, 34.7, 27.6, 24.6, 23.4, 16.1. IR (neat): 3290, 2939, 1623, 1482 cm^{-1}. HRMS (ESI-TOF) m/z: $[M + H]^+$ calcd for $C_{11}H_{16}NOS$ 210.0953; Found 210.0954.

*2-Benzyl-6-methyl-1,5,6,7-tetrahydro-4H-indol-4-one (**3g**).* Prepared according to procedure A using (*S*)-2-amino-3-phenylpropan-1-ol (76 mg, 0.50 mmol) and 5-methyl-1,3-cyclohexanedione (63 mg, 0.50 mmol), and the residue was purified by 100−200 mesh silica gel column chromatography (EtOAc/hexane = 35:65) to afford 2-benzyl-6-methyl-1,5,6,7-tetrahydro-4*H*-indol-4-one **3g** (56 mg, 47%) as a brownish orange solid. Melting point: 175−180 °C. ^{1}H NMR (400 MHz, $CDCl_3$) δ 8.37 (s, 1H), 7.30 (m, 2H), 7.22 (m, 3H), 6.26 (s, 1H), 3.90 (s, 2H), 2.76 (m, 1H), 2.42 (m, 3H), 2.16 (m, 1H), 1.10 (d, J = 8.0 Hz, 3H). ^{13}C{^{1}H} NMR (100 MHz, $CDCl_3$) δ 194.2, 143.5, 138.5, 132.1, 128.7, 126.7, 120.2, 103.5, 46.2, 34.0, 31.9, 31.0, 21.5. IR (neat): 3344, 2941, 1648, 1409 cm^{-1}. HRMS (ESI-TOF) m/z: $[M + H]^+$ calcd for $C_{16}H_{18}NO$ 240.1388; Found 240.1393.

*2,6-Dimethyl-1,5,6,7-tetrahydro-4H-indol-4-one (**3h**).* Prepared according to procedure A using (*S*)-2-aminopropan-1-ol (37 mg, 0.50 mmol) and 5-methyl-1,3-cyclohexanedione (63 mg, 0.50 mmol), and the residue was purified by 100−200 mesh silica gel column chromatography (EtOAc/hexane = 40:60) to afford 2,6-dimethyl-1,5,6,7-tetrahydro-4*H*-indol-4-one **3h** (49 mg, 60%) as a black solid. Melting point: 167−170 °C. ^{1}H NMR (400 MHz, $CDCl_3$) δ 9.22 (s, 1H), 6.13 (s, 1H), 2.82 (dd, J = 12.0 Hz, 4.0 Hz, 1H), 2.41 (m, 3H), 2.19 (m, 4H), 1.12 (d, J = 4.0 Hz, 3H). ^{13}C{^{1}H} NMR (100 MHz, $CDCl_3$) δ 194.8, 144.0, 129.7, 120.3, 102.7, 46.6, 32.3, 31.3, 21.6, 13.1.

https://doi.org/10.1021/acs.joc.1c00714
J. Org. Chem. 2021, 86, 8805−8828

IR (neat): 3230, 3162, 2920, 1624, 1479 cm^{-1}. HRMS (ESI-TOF) m/z: $[M + H]^+$ calcd for $C_{10}H_{14}NO$ 164.1075; Found 164.1078.

*2-Ethyl-6-methyl-1,5,6,7-tetrahydro-4H-indol-4-one (**3i**).* Prepared according to procedure A using (*S*)-2-aminobutan-1-ol (45 mg, 0.50 mmol) and 5-methyl-1,3-cyclohexanedione (63 mg, 0.50 mmol), and the residue was purified by 100−200 mesh silica gel column chromatography (EtOAc/hexane = 40:60) to afford 2-ethyl-6-methyl-1,5,6,7-tetrahydro-4*H*-indol-4-one **3i** (59 mg, 67%) as a brownish black solid. Melting point: 164−167 °C. ^1H NMR (400 MHz, $CDCl_3$) δ 9.25 (s, 1H), 6.17 (s, 1H), 2.83 (dd, J = 12.0 Hz, 4.0 Hz, 1H), 2.57 (q, J = 15.0 Hz, 7.5 Hz, 2H), 2.41 (m, 3H), 2.20 (dd, J = 16.0 Hz, 12.0 Hz, 1H), 1.22 (t, J = 8.0 Hz, 3H), 1.12 (d, J = 4.0 Hz, 3H). $^{13}C\{^1H\}$ NMR (100 MHz, $CDCl_3$) δ 194.4, 143.3, 135.8, 119.5, 100.7, 46.1, 31.8, 30.8, 21.1, 20.4, 13.0. IR (neat): 3227, 3158, 2959, 1625, 1480 cm^{-1}. HRMS (ESI-TOF) m/z: $[M + H]^+$ calcd for $C_{11}H_{16}NO$ 178.1232; Found 178.1234.

*2-Isopropyl-6-methyl-1,5,6,7-tetrahydro-4H-indol-4-one (**3j**).* Prepared according to procedure A using (*S*)-2-amino-3-methylbutan-1-ol (52 mg, 0.50 mmol) and 5-methyl-1,3-cyclohexanedione (63 mg, 0.50 mmol), and the residue was purified by 100−200 mesh silica gel column chromatography (EtOAc/hexane = 40:60) to afford 2-isopropyl-6-methyl-1,5,6,7-tetrahydro-4*H*-indol-4-one **3j** (64 mg, 67%) as a brown solid. Melting point: 187−192 °C. ^1H NMR (400 MHz, $CDCl_3$) δ 9.27 (s, 1H), 6.17 (s, 1H), 2.87 (m, 2H), 2.41 (m, 3H), 2.19 (m, 1H), 1.23 (d, J = 8.0 Hz, 6H), 1.12 (d, J = 4.0 Hz, 3H). $^{13}C\{^1H\}$ NMR (100 MHz, $CDCl_3$) δ 194.7, 143.5, 140.7, 120.1, 99.7, 46.4, 32.1, 31.1, 27.1, 22.4, 22.6, 21.4. IR (neat): 3226, 3159, 2955, 1624, 1484 cm^{-1}. HRMS (ESI-TOF) m/z: $[M + H]^+$ calcd for $C_{12}H_{18}NO$ 192.1388; Found 192.1391.

*2-sec-Butyl-6-methyl-1,5,6,7-tetrahydro-4H-indol-4-one (**3k**).* Prepared according to procedure A using (2S)-2-amino-3-methylpentan-1-ol (59 mg, 0.50 mmol) and 5-methyl-1,3-cyclohexanedione (63 mg, 0.50 mmol), and the residue was purified by 100−200 mesh silica gel column chromatography (EtOAc/hexane = 40:60) to afford 2-(sec-butyl)-6-methyl-1,5,6,7-tetrahydro-4*H*-indol-4-one **3k** (64 mg, 63%) as a brown solid. Melting point: 191−196 °C. ^1H NMR (400 MHz, $CDCl_3$) δ 8.85 (s, 1H), 6.17 (s, 1H), 2.83 (dd, J = 16.0 Hz, 4.0 Hz, 1H), 2.62 (m, 1H), 2.42 (m, 3H), 2.19 (dd, J = 12.0 Hz, 16.0 Hz, 1H), 1.57 (m, 2H), 1.21 (d, J = 4.0 Hz, 3H), 1.12 (d, J = 8.0 Hz, 3H), 0.85 (t, J = 8.0 Hz, 3H). $^{13}C\{^1H\}$ NMR (100 MHz, $CDCl_3$) δ 194.8, 143.2, 139.5, 120.1, 100.8, 46.6, 34.3, 32.3, 31.3, 29.9, 21.6, 20.1, 11.9. IR (neat): 3231, 3160, 2960, 1623, 1482 cm^{-1}. HRMS (ESI-TOF) m/z: $[M + H]^+$ calcd for $C_{13}H_{20}NO$ 206.1545; Found 206.1546. Crystal preparation: The crystal is grown by simple recrystallization method. The pure compound isolated after column chromatography is dissolved in dichloromethane and layered with hexane and kept at room temperature for 2 days to get pure crystal. Crystal data: $C_{13}H_{19}NO$, M = 205, monoclinic, space group P_21 with a = 7.2804(13) Å, b = 7.7406(15) Å, c = 11.197(3) Å, α = 90°, β = 104.549(12)°, γ = 90°, V = 610.8(2), T = 100 K, R1 = 0.0855, wR2 = 0.2298 on observed data, z = 2, $F(000)$ = 224, absorption coefficient = 0.543, λ = 1.54178 Å, 4950 reflections were collected on a Bruker APEX-III, 1574 observed reflections ($I \geq 2\sigma(I)$).

*6-Methyl-2-(2-(methylthio)ethyl)-1,5,6,7-tetrahydro-4H-indol-4-one (**3l**).* Prepared according to procedure A using (*S*)-(−)-2-amino-4-methylthio-1-butanol (67 mg, 0.50 mmol) and 5-methyl-1,3-cyclohexanedione (63 mg, 0.50 mmol), and the residue was purified by 100−200 mesh silica gel column chromatography (EtOAc/hexane = 40:60) to afford 6-methyl-2-(2-(methylthio)ethyl)-1,5,6,7-tetrahydro-4*H*-indol-4-one **3l** (44 mg, 40%) as a dark brown solid. Melting point: 115−120 °C. ^1H NMR (400 MHz, $CDCl_3$) δ 9.27 (s, 1H), 6.22 (s, 1H), 2.84 (m, 3H), 2.73 (t, J = 8.0 Hz, 2H), 2.48 (dd, J = 12.0 Hz, 8.0 Hz, 2H), 2.38 (m, 1H), 2.21 (m, 1H), 2.11 (s, 3H), 1.12 (d, J = 4.0 Hz, 3H). $^{13}C\{^1H\}$ NMR (100 MHz, $CDCl_3$) δ 194.5, 143.4, 132.5, 120.0, 102.7, 46.4, 34.1, 32.1, 31.2, 27.2, 21.4, 15.6. IR (neat): 3222, 3154, 2920, 1623, 1480 cm^{-1}. HRMS (ESI-TOF) m/z: $[M + H]^+$ calcd for $C_{12}H_{18}NOS$ 224.1109; Found 224.1112.

*2-Benzyl-7,7-dimethyl-1,5,6,7-tetrahydro-4H-indol-4-one (**3m**).* Prepared according to procedure A using (*S*)-2-amino-3-phenylpropan-1-ol (76 mg, 0.50 mmol) and 4,4-dimethyl-1,3-cyclohexanedione (70 mg, 0.50 mmol), and the residue was purified by 100−200 mesh silica gel column chromatography (EtOAc/hexane = 35:65) to afford 2-benzyl-7,7-dimethyl-1,5,6,7-tetrahydro-4*H*-indol-4-one **3m** (77 mg, 61%) as a dark brown solid. Melting point: 175−177 °C. ^1H NMR (400 MHz, $CDCl_3$) δ 8.02 (s, 1H), 7.28 (m, 2H), 7.20 (m, 3H), 6.24 (d, J = 1.8 Hz, 1H), 3.87 (s, 2H), 2.69 (t, J = 8.0 Hz, 2H), 1.91 (t, J = 8.0 Hz, 2H), 1.13 (s, 6H). $^{13}C\{^1H\}$ NMR (100 MHz, $CDCl_3$) δ 199.3, 141.7, 138.6, 132.0, 128.8, 126.6, 119.1, 104.3, 41.4, 37.8, 34.0, 29.8, 24.6, 20.0. IR (neat): 3234, 3160, 2919, 1622, 1478 cm^{-1}. HRMS (ESI-TOF) m/z: $[M + H]^+$ calcd for $C_{17}H_{20}NO$ 254.1545; Found 254.1546.

*2,7,7-Trimethyl-1,5,6,7-tetrahydro-4H-indol-4-one (**3n**).* Prepared according to procedure A using (*S*)-2-aminopropan-1-ol (37 mg, 0.50 mmol) and 4,4-dimethyl-1,3-cyclohexanedione (70 mg, 0.50 mmol), and the residue was purified by 100−200 mesh silica gel column chromatography (EtOAc/hexane = 40:60) to afford 2,7,7-trimethyl-1,5,6,7-tetrahydro-4*H*-indol-4-one **3n** (74 mg, 84%) as a dark brown solid. Melting point: 1181−183 °C. ^1H NMR (400 MHz, $CDCl_3$) δ 8.76 (s, 1H), 6.14 (s, 1H), 2.78 (t, J = 6.3 Hz, 2H), 2.22 (s, 3H), 1.96 (t, J = 6.3 Hz, 2H), 1.17 (s, 6H). $^{13}C\{^1H\}$ NMR (100 MHz, $CDCl_3$) δ 199.8, 142.0, 129.6, 119.3, 103.7, 41.7, 38.2, 24.9, 20.3, 13.2. IR (neat): 3228, 3166, 2922, 1621, 1476 cm^{-1}. HRMS (ESI-TOF) m/z: $[M + H]^+$ calcd for $C_{11}H_{16}NO$ 178.1232; Found 178.1237.

*2-Ethyl-7,7-dimethyl-1,5,6,7-tetrahydro-4H-indol-4-one (**3o**).* Prepared according to procedure A using (*S*)-2-aminobutan-1-ol (45 mg, 0.50 mmol) and 4,4-dimethyl-1,3-cyclohexanedione (70 mg, 0.50 mmol), and the residue was purified by 100−200 mesh silica gel column chromatography (EtOAc/hexane = 40:60) to afford 2-ethyl-7,7-dimethyl-1,5,6,7-tetrahydro-4*H*-indol-4-one **3o** (34 mg, 36%) as a brownish black solid. Melting point: 119−124 °C. ^1H NMR (400 MHz, $CDCl_3$) δ 9.05 (s, 1H), 6.16 (s, 1H), 2.79 (t, J = 6.26 Hz, 2H), 2.57 (q, J = 7.52 Hz, 15.08 Hz, 2H), 1.96 (t, J = 6.24 Hz, 2H), 1.22 (t, J = 7.56 Hz, 3H), 1.17 (s, 6H). $^{13}C\{^1H\}$ NMR (100 MHz, $CDCl_3$) δ 200.0, 142.1, 136.3, 118.8, 101.8, 41.7, 38.2, 24.9, 21.0, 20.3, 13.5. IR (neat): 3242, 3168, 2962, 1623, 1476 cm^{-1}. HRMS (ESI-TOF) m/z: $[M + H]^+$ calcd for $C_{12}H_{18}NO$ 192.1388; Found 192.1392.

*2-Isopropyl-7,7-dimethyl-1,5,6,7-tetrahydro-4H-indol-4-one (**3p**).* Prepared according to procedure A using (*S*)-2-amino-3-methylbutan-1-ol (52 mg, 0.50 mmol) and 4,4-dimethyl-1,3-cyclohexanedione (70 mg, 0.50 mmol), and the residue was purified by 100−200 mesh silica gel column chromatography (EtOAc/hexane = 40:60) to afford 2-isopropyl-7,7-dimethyl-1,5,6,7-tetrahydro-4*H*-indol-4-one **3p** (43 mg, 42%) as a pale brown solid. Melting point: 191−196 °C. ^1H NMR (400 MHz, $CDCl_3$) δ 9.17 (s, 1H), 6.15 (s, 1H), 2.87 (m, 1H), 2.80 (t, J = 6.2 Hz, 2H), 1.97 (t, J = 6.2 Hz, 2H), 1.23 (d, J = 6.9 Hz, 6H), 1.18 (s, 6H). $^{13}C\{^1H\}$ NMR (100 MHz, $CDCl_3$) δ 199.9, 141.9, 140.8, 118.5, 100.4, 41.5, 38.1, 27.2, 24.8, 22.4, 20.0. IR (neat): 3208, 3142, 2964, 1613, 1477 cm^{-1}. HRMS (ESI-TOF) m/z: $[M + H]^+$ calcd for $C_{13}H_{20}NO$ 206.1545; Found 206.1548.

*2-sec-Butyl-7,7-dimethyl-1,5,6,7-tetrahydro-4H-indol-4-one (**3q**).* Prepared according to procedure A using (2S)-2-amino-3-methylpentan-1-ol (59 mg, 0.50 mmol) and 4,4-dimethyl-1,3-cyclohexanedione (70 mg, 0.50 mmol), and the residue was purified by 100−200 mesh silica gel column chromatography (EtOAc/hexane = 40:60) to afford 2-(sec-butyl)-6-methyl-1,5,6,7-tetrahydro-4*H*-indol-4-one **3q** (77 mg, 71%) as a yellowish brown solid. Melting point: 1154−160 °C. ^1H NMR (400 MHz, $CDCl_3$) δ 8.34 (s, 1H), 6.18 (s, 1H), 2.79 (t, J = 6.24 Hz, 2H), 2.62 (m, 1H), 1.97 (t, J = 6.24 Hz, 2H), 1.57 (m, 2H), 1.22 (d, J = 6.9 Hz, 3H), 1.18 (s, 6H), 0.88 (t, J = 7.4 Hz, 3H). $^{13}C\{^1H\}$ NMR (100 MHz, $CDCl_3$) δ 199.6, 141.1, 139.2, 118.9, 101.5, 41.5, 38.0, 34.2, 29.9, 24.8, 20.2, 19.9, 11.8. IR (neat): 3207, 3143, 2964, 1617, 1477 cm^{-1}. HRMS (ESI-TOF) m/z: $[M + H]^+$ calcd for $C_{14}H_{22}NO$ 220.1701; Found 220.1704.

*7,7-Dimethyl-2-(2-(methylthio)ethyl)-1,5,6,7-tetrahydro-4H-indol-4-one (**3r**).* Prepared according to procedure A using (*S*)-(−)-2-amino-4-methylthio-1-butanol (67 mg, 0.50 mmol) and 4,4-dimethyl-1,3-cyclohexanedione (70 mg, 0.50 mmol), and the residue was purified by 100−200 mesh silica gel column chromatography (EtOAc/hexane = 40:60) to afford 6-methyl-2-(2-(methylthio)ethyl)-1,5,6,7-tetrahydro-4*H*-indol-4-one **3r** (51 mg, 43%) as a brown solid. Melting point: 126−131 °C. ^1H NMR (400 MHz, $CDCl_3$) δ 8.82 (s, 1H), 6.23 (s, 1H), 2.80

https://doi.org/10.1021/acs.joc.1c00714
J. Org. Chem. 2021, 86, 8805−8828

(m, 6H), 2.14 (s, 3H), 1.97 (t, J = 6.1 Hz, 2H), 1.17 (s, 6H). $^{13}C\{^1H\}$ NMR (100 MHz, $CDCl_3$) δ 199.7, 141.7, 132.5, 118.9, 103.6, 41.6, 37.9, 34.2, 29.8, 24.7, 20.2, 15.7. IR (neat): 3240, 3165, 2921, 1624, 1477 cm^{-1}. HRMS (ESI-TOF) m/z: $[M + H]^+$ calcd for $C_{13}H_{20}NOS$ 238.1266; Found 238.1270.

*2-Benzyl-6,6-dimethyl-1,5,6,7-tetrahydro-4H-indol-4-one (**3s**).* Prepared according to procedure A using (*S*)-2-amino-3-phenylpropan-1-ol (76 mg, 0.50 mmol) and 5,5-dimethyl-1,3-cyclohexanedione (70 mg, 0.50 mmol), and the residue was purified by 100−200 mesh silica gel column chromatography (EtOAc/hexane = 35:65) to afford 2-benzyl-6,6-dimethyl-1,5,6,7-tetrahydro-4*H*-indol-4-one **3s** (85 mg, 68%) as a dark brown solid. Melting point: 202−206 °C. ^1H NMR (400 MHz, $CDCl_3$) δ 8.00 (s, 1H), 7.31 (m, 3H), 7.21 (m, 2H), 6.29 (s, 1H), 3.91 (s, 2H), 2.56 (s, 2H), 2.31 (s, 2H), 1.08 (s, 6H). $^{13}C\{^1H\}$ NMR (100 MHz, $CDCl_3$) δ 194.1, 142.6, 138.6, 132.1, 128.9, 126.9, 119.5, 103.6, 52.0, 36.9, 35.9, 34.1, 29.8, 28.8. IR (neat): 3234, 3162, 2925, 1627, 1479 cm^{-1}. HRMS (ESI-TOF) m/z: $[M + H]^+$ calcd for $C_{17}H_{20}NO$ 254.1545; Found 254.1552.

*2,6,6-Trimethyl-1,5,6,7-tetrahydro-4H-indol-4-one (**3t**).*[30] Prepared according to procedure A using (*S*)-2-aminopropan-1-ol (37 mg, 0.50 mmol) and 5,5-dimethyl-1,3-cyclohexanedione (70 mg, 0.50 mmol), and the residue was purified by 100−200 mesh silica gel column chromatography (EtOAc/hexane = 40:60) to afford 2,6,6-trimethyl-1,5,6,7-tetrahydro-4*H*-indol-4-one **3t** (84 mg, 95%) as a dark brown solid. Melting point: 184−187 °C. ^1H NMR (400 MHz, $CDCl_3$) δ 8.33 (s, 1H), 6.17 (s, 1H), 2.62 (s, 2H), 2.32 (s, 2H), 2.23 (s, 3H), 1.10 (s, 6H). $^{13}C\{^1H\}$ NMR (100 MHz, $CDCl_3$) δ 194.2, 142.4, 129.3, 119.9, 103.1, 52.4, 37.3, 36.3, 29.1, 13.3. IR (neat): 3237, 3176, 2950, 1625, 1478 cm^{-1}. HRMS (ESI-TOF) m/z: $[M + H]^+$ calcd for $C_{11}H_{16}NO$ 178.1232; Found 178.1243.

*2-Ethyl-6,6-dimethyl-1,5,6,7-tetrahydro-4H-indol-4-one (**3u**).* Prepared according to procedure A using (*S*)-2-aminobutan-1-ol (45 mg, 0.50 mmol) and 5,5-dimethyl-1,3-cyclohexanedione (70 mg, 0.50 mmol), and the residue was purified by 100−200 mesh silica gel column chromatography (EtOAc/hexane = 40:60) to afford 2-ethyl-6,6-dimethyl-1,5,6,7-tetrahydro-4*H*-indol-4-one **3u** (68 mg, 72%) as a brown solid. Melting point: 140−145 °C. ^1H NMR (400 MHz, $CDCl_3$) δ 8.51 (s, 1H), 6.20 (s, 1H), 2.63 (s, 2H), 2.57 (q, J = 7.5 Hz, 15.1 Hz, 2H), 2.32 (s, 2H), 1.23 (t, J = 7.5 Hz, 3H), 1.10 (s, 6H). $^{13}C\{^1H\}$ NMR (100 MHz, $CDCl_3$) δ 194.1, 142.1, 135.8, 119.2, 101.1, 52.1, 36.9, 35.9, 28.8, 20.8, 13.2. IR (neat): 3232, 3161, 2960, 1625, 1479 cm^{-1}. HRMS (ESI-TOF) m/z: $[M + H]^+$ calcd for $C_{12}H_{18}NO$ 192.1388; Found 192.1398.

*2-Isopropyl-6,6-dimethyl-1,5,6,7-tetrahydro-4H-indol-4-one (**3v**).* Prepared according to procedure A using (*S*)-2-amino-3-methylbutan-1-ol (52 mg, 0.50 mmol) and 5,5-dimethyl-1,3-cyclohexanedione (70 mg, 0.50 mmol), and the residue was purified by 100−200 mesh silica gel column chromatography (EtOAc/hexane = 40:60) to afford 2-isopropyl-6,6-dimethyl-1,5,6,7-tetrahydro-4*H*-indol-4-one **3v** (85 mg, 83%) as a brown solid. Melting point: 176−178 °C. ^1H NMR (400 MHz, methanol-d_4) δ 6.08 (s, 1H), 2.84 (hept, J = 6.8 Hz, 1H), 2.66 (s, 2H), 2.29 (s, 2H), 1.24 (s, 3H), 1.22 (s, 3H), 1.09 (s, 6H). $^{13}C\{^1H\}$ NMR (100 MHz, methanol-d_4) δ 196.9, 145.9, 142.5, 119.1, 100.1, 52.5, 37.3, 36.9, 28.7, 28.2, 22.7. IR (neat): 3239, 3160, 2958, 1627, 1481 cm^{-1}. HRMS (ESI-TOF) m/z: $[M + H]^+$ calcd for $C_{13}H_{20}NO$ 206.1545; Found 206.1554.

*2-sec-Butyl-6,6-dimethyl-1,5,6,7-tetrahydro-4H-indol-4-one (**3w**).* Prepared according to procedure A using (2S)-2-amino-3-methylpentan-1-ol (59 mg, 0.50 mmol) and 5,5-dimethyl-1,3-cyclohexanedione (70 mg, 0.50 mmol), and the residue was purified by 100−200 mesh silica gel column chromatography (EtOAc/hexane = 40:60) to afford 2-*sec*-butyl-6,6-dimethyl-1,5,6,7-tetrahydro-4*H*-indol-4-one **3w** (85 mg, 76%) as a brown solid. Melting point: 145−151 °C. ^1H NMR (400 MHz, $CDCl_3$) δ 8.59 (s, 1H), 6.18 (s, 1H), 2.63 (m, 3H), 2.32 (s, 2H), 1.57 (m, 2H), 1.21 (d, J = 6.9 Hz, 3H), 1.10 (s, 6H), 0.86 (t, J = 7.4 Hz, 3H). $^{13}C\{^1H\}$ NMR (100 MHz, $CDCl_3$) δ 194.2, 142.0, 139.1, 119.1, 100.6, 52.1, 36.9, 35.9, 34.1, 29.8, 28.8, 28.7. 19.8, 11.7. IR (neat): 3244, 3159, 2958, 1625, 1479 cm^{-1}. HRMS (ESI-TOF) m/z: $[M + H]^+$ calcd for $C_{14}H_{22}NO$ 220.1701; Found 220.1707.

*6,6-Dimethyl-2-(2-(methylthio)ethyl)-1,5,6,7-tetrahydro-4H-indol-4-one (**3x**).* Prepared according to procedure A using (*S*)-(−)-2-amino-4-methylthio-1-butanol (67 mg, 0.50 mmol) and 5,5-dimethyl-1,3-cyclohexanedione (70 mg, 0.50 mmol), and the residue was purified by 100−200 mesh silica gel column chromatography (EtOAc/hexane = 40:60) to afford 6-methyl-2-(2-(methylthio)ethyl)-1,5,6,7-tetrahydro-4*H*-indol-4-one **3x** (30 mg, 25%) as a brown solid. Melting point: 153−158 °C. ^1H NMR (400 MHz, $CDCl_3$) δ 8.95 (s, 1H), 6.23 (s, 1H), 2.85 (t, J = 6.8 Hz, 2H), 2.74 (t, J = 6.9 Hz, 2H), 2.64 (s, 2H), 2.32 (s, 2H), 2.11 (s, 3H), 1.10 (s, 6H). $^{13}C\{^1H\}$ NMR (100 MHz, $CDCl_3$) δ 194.1, 142.4 132.4, 119.2, 102.8, 52.1, 36.9, 35.9, 34.2, 28.8, 27.1, 15.7. IR (neat): 3240, 3155, 2926, 1624, 1479 cm^{-1}. HRMS (ESI-TOF) m/z: $[M + H]^+$ calcd for $C_{13}H_{20}NOS$ 238.1266; Found 238.1274.

*3,6,6-Trimethyl-1,5,6,7-tetrahydro-4H-indol-4-one (**3y**).*[31] Prepared according to procedure A using (*R*)-(−)-1-amino-propanol (37 mg, 0.50 mmol) and 4,4-dimethyl-1,3-cyclohexanedione (70 mg, 0.50 mmol), and the residue was purified by 100−200 mesh silica gel column chromatography (EtOAc/hexane = 40:60) to afford 3,6,6-trimethyl-1,5,6,7-tetrahydro-4*H*-indol-4-one **3y** (35 mg, 40%) as a white solid. Melting point: 149−153 °C. ^1H NMR (400 MHz, $CDCl_3$) δ 8.13 (s, 1H), 6.40 (s, 1H), 2.62 (s, 2H), 2.32 (s, 2H), 2.28 (s, 3H), 1.10 (s, 6H). $^{13}C\{^1H\}$ NMR (100 MHz, $CDCl_3$) δ 194.6, 142.3, 119.1, 117.6, 115.9, 52.8, 37.2, 35.7, 28.6, 11.5. IR (neat): 3239, 2934, 1696, 1476 cm^{-1}. HRMS (ESI-TOF) m/z: $[M + H]^+$ calcd for $C_{11}H_{16}NO$ 178.1232; Found 178.1239.

*6-(4-(Dimethylamino)phenyl)-2-isopropyl-1,5,6,7-tetrahydro-4H-indol-4-one (**3z**).* Prepared according to procedure A using (*S*)-2-amino-3-methylbutan-1-ol (36 mg, 0.35 mmol) and 5-(4-(dimethylamino)phenyl)cyclohexane-1,3-dione (81 mg, 0.35 mmol), and the residue was purified by 100−200 mesh silica gel column chromatography (EtOAc/hexane = 40:60) to afford 6-(4-(dimethylamino)phenyl)-2-isopropyl-1,5,6,7-tetrahydro-4*H*-indol-4-one **3z** (50 mg, 48%) as a blackish brown solid. Melting point: 120−124 °C. ^1H NMR (400 MHz, $CDCl_3$) δ 8.54 (s, 1H), 7.15 (d, J = 8.5 Hz, 2H), 6.73 (m, 2H), 6.25 (s, 1H), 3.42 (m, 1H), 2.98 (m, 1H), 2.93 (s, 6H), 2.87 (m, 2H), 2.68 (m, 2H), 1.25 (d, J = 6.9 Hz, 6H). $^{13}C\{^1H\}$ NMR (100 MHz, $CDCl_3$) δ 193.9, 149.7, 142.6, 140.6, 131.7, 127.5, 120.2, 112.9, 100.1, 45.5, 41.9, 40.8, 31.2, 27.1, 22.5. IR (neat): 2961, 2926,1623, 1523, 1483 cm^{-1}. HRMS (ESI-TOF) m/z: $[M + H]^+$ calcd for $C_{19}H_{25}N_2O$ 297.1967; Found 297.1963.

*6,6-Dimethyl-1,2,3,5,6,7-hexahydro-8H-pyrrolo[1,2-a]indol-8-one (**3aa**).* Prepared according to procedure A using (*S*)-(+)-2-pyrrolidinemethanol (51 mg, 0.50 mmol) and 5,5-dimethyl-1,3-cyclohexanedione (70 mg, 0.50 mmol), and the residue was purified by 100−200 mesh silica gel column chromatography (EtOAc/hexane = 40:60) to afford 6,6-dimethyl-1,2,3,5,6,7-hexahydro-8*H*-pyrrolo[1,2-*a*]indol-8-one **3aa** (47 mg, 47%) as a blackish brown solid. Melting point: 124−128 °C. ^1H NMR (400 MHz, $CDCl_3$) δ 6.16 (s, 1H), 3.81 (m, 2H), 2.81 (t, J = 6.9 Hz, 2H), 2.57 (s, 2H), 2.51 (m, 2H), 2.31 (s, 2H), 1.11 (s, 6H). $^{13}C\{^1H\}$ NMR (100 MHz, $CDCl_3$) δ 193.7, 138.1, 137.7, 123.3, 96.2, 52.2, 44.1, 36.3, 35.7, 28.9, 27.9, 23.7. IR (neat): 2954, 2868, 1645, 1464, 1369 cm^{-1}. HRMS (ESI-TOF) m/z: $[M + H]^+$ calcd for $C_{13}H_{18}NO$ 204.1388; Found 204.1384.

*6-(4-(Dimethylamino)phenyl)-1,2,3,5,6,7-hexahydro-8H-pyrrolo-[1,2-a]indol-8-one (**3ab**).* Prepared according to procedure A using (*S*)-(+)-2-pyrrolidinemethanol (35 mg, 0.35 mmol) and 5-(4-(dimethylamino)phenyl)cyclohexane-1,3-dione (81 mg, 0.35 mmol), and the residue was purified by 100−200 mesh silica gel column chromatography (EtOAc/hexane = 40:60) to afford 6-(4-(dimethylamino)phenyl)-1,2,3,5,6,7-hexahydro-8*H*-pyrrolo[1,2-*a*]-indol-8-one **3ab** (62 mg, 61%) as a blackish brown solid. Melting point: 200−205 °C. ^1H NMR (400 MHz, $CDCl_3$) δ 7.17 (m, 2H), 6.73 (m, 2H), 6.21 (s, 1H), 3.83 (m, 2H), 3.42 (m, 1H), 2.94 (s, 6H), 2.84 (m, 4H), 2.69 (m, 2H), 2.51 (m, 2H). $^{13}C\{^1H\}$ NMR (100 MHz, $CDCl_3$) δ 193.4, 149.6, 138.2, 131.6, 127.4, 124.1, 112.9, 96.3, 45.3, 44.1, 41.7, 40.7, 30.5, 27.8, 23.7. IR (neat): 2922, 2854, 1644, 1613, 1520, 1462 cm^{-1}. HRMS (ESI-TOF) m/z: $[M + H]^+$ calcd for $C_{19}H_{23}N_2O$ 295.1793; Found 295.1798.

*2-Isopropyl-5,6-dihydrocyclopenta[b]pyrrol-4(1H)-one (**3ac**).* Prepared according to procedure A using (*S*)-2-amino-3-methylbu-

https://doi.org/10.1021/acs.joc.1c00714
J. Org. Chem. 2021, 86, 8805−8828

tan-1-ol (52 mg, 0.50 mmol) and cyclopentane-1,3-dione (49 mg, 0.50 mmol), and the residue was purified by 100−200 mesh silica gel column chromatography (EtOAc/hexane = 40:60) to afford 2-isopropyl-5,6-dihydrocyclopenta[b]pyrrol-4(1*H*)-one **3ac** (34 mg, 42%) as a brown solid. Melting point: 180−185 °C. ^{1}H NMR (400 MHz, $CDCl_3$) δ 9.30 (s, 1H), 5.96 (s, 1H), 2.88 (m, 5H), 1.25 (d, J = 6.9 Hz, 6H). ^{13}C{^{1}H} NMR (100 MHz, $CDCl_3$) δ 193.9, 149.7, 142.6, 140.6, 131.7, 127.5, 120.2, 112.9, 100.1, 45.5, 41.9, 40.8, 31.2, 27.1, 22.5. IR (neat): 3237, 2961, 2925, 1659, 1576, 1487 cm^{-1}. HRMS (ESI-TOF) m/z: [M + H]$^+$ calcd for $C_{10}H_{14}NO$ 164.1075; Found 164.1070.

*(Z)-3-((1-Hydroxy-3-phenylpropan-2-yl)amino)-1,3-diphenylprop-2-en-1-one (**3ad**).* Prepared according to procedure A using (*S*)-2-amino-3-phenylpropan-1-ol (76 mg, 0.50 mmol) and 1,3-diphenylpropane-1,3-dione (112 mg, 0.50 mmol), and the residue was purified by 100−200 mesh silica gel column chromatography (EtOAc/hexane = 40:60) to afford (Z)-3-((1-hydroxy-3-phenylpropan-2-yl)amino)-1,3-diphenylprop-2-en-1-one **3ad** (78 mg, 44%) as a yellow semisolid. ^{1}H NMR (400 MHz, $CDCl_3$) δ 11.42 (d, J = 10.4 Hz, 1H), 7.86 (m, 2H), 7.35 (m, 9H), 7.05 (m, 2H), 6.81 (d, J = 7.3 Hz, 2H), 5.55 (s, 1H), 3.91 (s, 1H), 3.74 (m, 2H), 3.64 (m, 1H), 2.86 (m, 2H). ^{13}C{^{1}H} NMR (100 MHz, $CDCl_3$) δ 188.6, 167.6, 140.6, 137.9, 135.8, 130.8, 129.8, 129.2, 128.6, 128.4, 128.3, 127.9, 127.5, 126.6, 94.3, 65.4, 59.0, 39.8. IR (neat): 3364, 3059, 3026, 2922, 1581, 1479, 1330 cm^{-1}. HRMS (ESI-TOF) m/z: [M + H]$^+$ calcd for $C_{24}H_{24}NO_2$ 358.1807; Found 358.1805.

*(Z)-3-((1-Hydroxypropan-2-yl)amino)-1,3-diphenylprop-2-en-1-one (**3ae**).* Prepared according to procedure A using (*S*)-2-aminopropan-1-ol (37 mg, 0.50 mmol) and 1,3-diphenylpropane-1,3-dione (112 mg, 0.50 mmol), and the residue was purified by 100−200 mesh silica gel column chromatography (EtOAc/hexane = 40:60) to afford (Z)-3-((1-hydroxypropan-2-yl)amino)-1,3-diphenylprop-2-en-1-one **3ae** (45 mg, 32%) as a yellowish brown semisolid. ^{1}H NMR (400 MHz, $CDCl_3$) δ 11.29 (d, J = 9.4 Hz, 1H), 7.86 (m, 2H), 7.40 (m, 8H), 5.72 (s, 1H), 3.65 (m, 1H), 3.59 (d, J = 3.6 Hz, 2H), 1.26 (s, 1H), 1.19 (d, J = 6.4 Hz, 3H). ^{13}C{^{1}H} NMR (100 MHz, $CDCl_3$) δ 188.7, 167.2, 140.3, 135.9, 130.9, 129.6, 128.7, 128.4, 127.9, 127.2, 67.1, 52.3, 29.8, 18.8. IR (neat): 3358, 3058, 2926, 1561, 1480 cm^{-1}. HRMS (ESI-TOF) m/z: [M + H]$^+$ calcd for $C_{18}H_{20}NO_2$ 282.1494; Found 282.1499.

*(Z)-3-((1-Hydroxy-3-methylbutan-2-yl)amino)-1,3-diphenylprop-2-en-1-one (**3af**).* Prepared according to procedure A using (*S*)-2-amino-3-methylbutan-1-ol (52 mg, 0.50 mmol) and 1,3-diphenylpropane-1,3-dione (112 mg, 0.50 mmol), and the residue was purified by 100−200 mesh silica gel column chromatography (EtOAc/hexane = 40:60) to afford (*Z*)-3-((1-hydroxy-3-methylbutan-2-yl)amino)-1,3-diphenylprop-2-en-1-one **3af** (39 mg, 25%) as a yellowish brown solid. Melting point: 99−101 °C. ^{1}H NMR (400 MHz, $CDCl_3$) δ 11.41 (d, J = 10.6 Hz, 1H), 7.87 (d, J = 7.6 Hz, 2H), 7.38 (m, 8H), 5.70 (s, 1H), 3.70 (m, 2H), 3.36 (m, 1H), 1.84 (m, 1H), 1.26 (s, 1H), 0.97 (d, J = 6.8 Hz, 3H), 0.86 (d, J = 6.8 Hz, 3H). ^{13}C{^{1}H} NMR (100 MHz, $CDCl_3$) δ 188.4, 168.5, 140.2, 135.9, 130.9, 129.4, 128.9, 128.3, 128.2, 127.3, 64.4, 61.9 30.6, 19.8, 18.2. IR (neat): 3365, 3060, 2958, 1568, 1479 cm^{-1}. HRMS (ESI-TOF) m/z: [M + H]$^+$ calcd for $C_{20}H_{24}NO_2$ 310.1807; Found 310.1809. Crystal preparation: The crystal is grown by simple recrystallization method where pure compound isolated after column chromatography is dissolved in dichloromethane and layered with hexane to get pure crystal. Crystal data: $C_{20}H_{23}NO_2$, M = 309, monoclinic, space group *C*2 with a = 22.889(8) Å, b = 8.478(3) Å, c = 9.441(4) Å, α = 90°, β = 104.65(2)°, γ = 90°, V = 1772.5(12), T = 100 K, R1 = 0.0563, wR2 = 0.1807 on observed data, z = 4, F(000)= 664, Absorption coefficient = 0.585, λ= 1.54178 Å, 9240 reflections were collected on a Bruker APEX-III, 2661 observed reflections ($I \geq 2\sigma$ (I)).

*3-((1-Hydroxy-3-phenylpropan-2-yl)amino)cyclohex-2-en-1-one (**11a**).* Prepared according to procedure B using (*S*)-2-amino-3-phenylpropan-1-ol (755 mg, 5 mmol) and 1,3-cyclohexanedione (560 mg, 5 mmol), and the residue was purified by 100−200 mesh silica gel column chromatography (EtOAc/methanol = 99:1) to afford 3-((1-hydroxy-3-phenylpropan-2-yl)amino)cyclohex-2-en-1-one **11a** (1029 mg, 84%) as a pale brown solid. Melting point: 128−133 °C. ^{1}H NMR (400 MHz, $CDCl_3$) δ 7.32 (m, 2H), 7.25 (m, 3H), 5.70 (s, 1H), 5.29 (s, 1H), 3.67 (m, 3H), 2.95 (d, J = 6.2 Hz, 2H), 2.34 (m, 4H), 1.95 (s, 2H). ^{13}C{^{1}H} NMR (100 MHz, $CDCl_3$) δ 197.9, 164.9, 137.6, 129.4, 128.7, 126.8, 73.83, 61.7, 55.4, 36.3, 30.0, 21.9, 14.3. IR (neat): 3259, 3077, 2940, 1535, 1446 cm^{-1}. HRMS (ESI-TOF) m/z: [M + H]$^+$ calcd for $C_{15}H_{20}NO_2$ 246.1494; Found 246.1494. Crystal preparation: The crystal is grown by simple recrystallization method. The isolated **11a** pure compound after column chromatography is dissolved in methanol and layered with hexane and kept at room temperature for 3 days to get pure crystal. Crystal data: $C_{15}H_{19}NO_2$, M = 245, orthorhombic, space group $P2(1)2(1)2(1)$ with a = 4.6957(2) Å, b = 12.4256(6) Å, c = 22.8195(10) Å, α = 90°, β = 90°, γ = 90°, V = 1331.45(10), T = 100 K, R1 = 0.0341, wR2 = 0.1028 on observed data, z = 4, F(000) = 528, Absorption coefficient = 0.081, λ= 0.71073 Å, 24521 reflections were collected on a Bruker APEX-III, 3142 observed reflections ($I \geq 2\sigma$ (I)).

*3-((1-Hydroxypropan-2-yl)amino)cyclohex-2-en-1-one (**11b**).*[22] Prepared according to procedure B using (*S*)-2-aminopropan-1-ol (37 mg, 0.50 mmol) and 1,3-cyclohexanedione (56 mg, 0.50 mmol), and the residue was purified by 100−200 mesh silica gel column chromatography (EtOAc/methanol = 99:1) to afford 3-((1-hydroxypropan-2-yl)amino)cyclohex-2-en-1-one **11b** (80 mg, 95%) as a dark brown semisolid. ^{1}H NMR (400 MHz, DMSO-d_6) δ 6.81 (s, 1H), 4.84 (s, 1H), 3.25 (m, 2H), 2.88 (s, 1H), 2.72 (s, 1H), 2.29 (t, J = 6.0 Hz, 2H), 2.05 (t, J = 6.2 Hz, 2H), 1.76 (m, 2H), 1.06 (d, J = 6.3 Hz, 3H). ^{13}C{^{1}H} NMR (100 MHz, DMSO-d_6) δ 194.5, 164.0, 94.7, 63.6, 49.5, 36.5, 28.8, 21.7, 16.6. IR (neat): 3253, 3093, 2941, 1518, 1379 cm^{-1}. HRMS (ESI-TOF) m/z: [M + H]$^+$ calcd for $C_9H_{16}NO_2$ 170.1181; Found 170.1187.

*3-((1-Hydroxy-4-(methylthio)butan-2-yl)amino)cyclohex-2-en-1-one (**11f**).* Prepared according to procedure B using (*S*)-(−)-2-amino-4-methylthio-1-butanol (67 mg, 0.50 mmol) and 1,3-cyclohexanedione (56 mg, 0.50 mmol), and the residue was purified by 100−200 mesh silica gel column chromatography (EtOAc/methanol = 99:1) to afford 3-((1-hydroxy-4-(methylthio)butan-2-yl)amino)cyclohex-2-en-1-one **11f** (88 mg, 77%) as a brown semisolid. ^{1}H NMR (400 MHz, DMSO-d_6) δ 6.80 (d, J = 7.52 Hz, 1H), 4.89 (s, 1H), 4.85 (s, 1H), 3.33 (m, 4H), 2.41 (m, 2H), 2.31 (m, 2H), 2.06 (t, J = 6.12 Hz, 2H), 2.03 (s, 3H), 1.77 (m, 2H), 1.64 (m, 1H). ^{13}C{^{1}H} NMR (100 MHz, DMSO-d_6) δ 194.6, 164.6, 94.7, 62.0, 52.9, 36.5, 30.2, 30.0, 28.8, 21.7, 14.7. IR (neat): 3353, 3058, 2926, 1650, 1012 cm^{-1}. HRMS (ESI-TOF) m/z: [M + H]$^+$ calcd for $C_{11}H_{20}NO_2S$ 230.1215; Found 230.1222.

*3-((1-Hydroxy-3-phenylpropan-2-yl)amino)-5-methylcyclohex-2-en-1-one (**11g**).* Prepared according to procedure B using (*S*)-2-amino-3-phenylpropan-1-ol (76 mg, 0.50 mmol) and 5-methyl-1,3-cyclohexanedione (63 mg, 0.50 mmol), and the residue was purified by 100−200 mesh silica gel column chromatography (EtOAc/methanol = 99:1) to afford 3-((1-hydroxy-3-phenylpropan-2-yl)amino)-5-methylcyclohex-2-en-1-one **11g** (49 mg, 37%) as a dark brown solid. Melting point: 163−166 °C. Diastereomer ratio % (major/minor): 58:42. ^{1}H NMR (400 MHz, MeOH-d_4) δ 7.29−7.16 (m, 10.26 H), 3.78−3.69 (m, 0.9H), 3.64−3.51 (m, 3.64H), 2.96 (dd, J = 13.8, 5.8 Hz, 2H), 2.80−2.71 (m, 1.7H), 2.46−1.88 (m, 9.8H), diastereomer 2:1.03 (d, J = 5.9 Hz, 2.19H), diastereomer 1:1.00 (d, J = 6.0 Hz, 3H). ^{13}C{^{1}H} NMR (100 MHz, MeOH-d_4) δ 199.6, 169.2, 139.3, 130.3, 129.5, 127.5, 95.3, 63.5, 57.4, 44.8, 38.3, 37.6, 30.1, 21.1. IR (neat): 3257, 3078, 2928, 1532, 1450 cm^{-1}. HRMS (ESI-TOF) m/z: [M + H]$^+$ calcd for $C_{16}H_{22}NO_2$ 260.1651; Found 260.1659.

*3-((1-Hydroxy-3-phenylpropan-2-yl)amino)-4,4-dimethylcyclohex-2-en-1-one (**11m**).* Prepared according to procedure B using (*S*)-2-amino-3-phenylpropan-1-ol (76 mg, 0.50 mmol) and 4,4-dimethyl-1,3-cyclohexanedione (70 mg, 0.50 mmol), and the residue was purified by 100−200 mesh silica gel column chromatography (EtOAc/methanol = 99:1) to afford 3-((1-hydroxy-3-phenylpropan-2-yl)-amino)-4,4-dimethylcyclohex-2-en-1-one **11m** (92 mg, 67%) as a yellowish brown solid. Melting point: 126−131 °C. ^{1}H NMR (400 MHz, $CDCl_3$) δ 7.28 (m, 2H), 7.21 (m, 3H), 5.13 (s, 1H), 3.63 (m, 3H), 2.92 (d, J = 7.0 Hz, 2H), 2.34 (s, 2H), 1.75 (s, 2H), 1.09 (s, 6H). ^{13}C{^{1}H} NMR (100 MHz, DMSO-d_6) δ 195.6, 158.1, 129.9, 120.8, 119.9, 118.0, 85.1, 53.9, 47.8, 30.8, 28.3, 27.3, 17.7, 16.1. IR (neat): 3271, 2927, 1534, 1458 cm^{-1}. HRMS (ESI-TOF) m/z: [M + H]$^+$ calcd for $C_{17}H_{24}NO_2$ 274.1807; Found 274.1815.

https://doi.org/10.1021/acs.joc.1c00714
J. Org. Chem. 2021, 86, 8805−8828

*3-((1-Hydroxypropan-2-yl)amino)-4,4-dimethylcyclohex-2-en-1-one (**11n**).* Prepared according to procedure B using (*S*)-2-aminopropan-1-ol (37 mg, 0.50 mmol) and 4,4-dimethyl-1,3-cyclohexanedione (70 mg, 0.50 mmol), and the residue was purified by 100−200 mesh silica gel column chromatography (EtOAc/methanol = 99:1) to afford 3-((1-hydroxypropan-2-yl)amino)-4,4-dimethylcyclohex-2-en-1-one **11n** (66 mg, 67%) as a brown solid. Melting point: 100−103 °C. ^{1}H NMR (400 MHz, DMSO-d_6) δ 6.66 (s, 1H), 4.79 (s, 1H), 4.73 (s, 1H), 3.39 (m, 2H), 3.24 (m, 1H), 2.32 (t, J = 6.2 Hz, 2H), 1.64 (t, J = 6.2 Hz, 2H), 1.06 (d, J = 6.4 Hz, 3H), 0.95 (s, 6H). ^{13}C{^{1}H} NMR (102 MHz, DMSO-d_6) δ 199.4, 162.5, 93.3, 63.8, 49.7, 35.5, 25.8, 25.3, 16.8. IR (neat): 3302, 2927, 1525, 1457 cm^{-1}. HRMS (ESI-TOF) m/z: [M + H]$^+$ calcd for $C_{11}H_{20}NO_2$ 198.1494; Found 198.1503.

*3-((1-Hydroxy-4-(methylthio)butan-2-yl)amino)-4,4-dimethylcyclohex-2-en-1-one (**11r**).* Prepared according to procedure B using (*S*)-(−)-2-amino-4-methylthio-1-butanol (67 mg, 0.50 mmol) and 4,4-dimethyl-1,3-cyclohexanedione (70 mg, 0.50 mmol), and the residue was purified by 100−200 mesh silica gel column chromatography (EtOAc/methanol = 99:1) to afford 3-((1-hydroxy-4-(methylthio)-butan-2-yl)amino)-4,4-dimethylcyclohex-2-en-1-one **11r** (105 mg, 82%) as a pale brown semisolid. ^{1}H NMR (400 MHz, DMSO-d_6) δ 6.66 (d, J = 7.0 Hz, 1H), 4.83 (s, 1H), 4.78 (s, 1H), 3.41 (d, J = 8.9 Hz, 2H), 3.30 (m, 2H), 2.39 (m, 4H), 2.02 (s, 3H), 1.87 (m, 1H), 1.64 (t, J = 6.2 Hz, 2H), 0.95 (s, 6H). ^{13}C{^{1}H} NMR (100 MHz, DMSO-d_6) δ 199.4, 162.9, 93.2, 62.1, 52.9, 38.7, 35.4, 30.3, 30.0, 25.7, 25.1, 14.7. IR (neat): 3358, 2926, 1631, 1443 cm^{-1}. HRMS (ESI-TOF) m/z: [M + H]$^+$ calcd for $C_{13}H_{24}NO_2S$ 258.1528; Found 258.1535.

*3-((1-Hydroxypropan-2-yl)amino)-5,5-dimethylcyclohex-2-en-1-one (**11t**).* Prepared according to procedure B using (*S*)-2-aminopropan-1-ol (37 mg, 0.50 mmol) and 5,5-dimethyl-1,3-cyclohexanedione (70 mg, 0.50 mmol), and the residue was purified by 100−200 mesh silica gel column chromatography (EtOAc/methanol = 99:1) to afford 3-((1-hydroxypropan-2-yl)amino)-5,5-dimethylcyclohex-2-en-1-one **11t** (88 mg, 90%) as a yellowish brown solid. Melting point: 142−146 °C. ^{1}H NMR (400 MHz, DMSO-d_6) δ 6.70 (s, 1H), 4.84 (s, 1H), 4.75 (t, J = 4.8 Hz,1H), 3.39 (m, 2H), 3.24 (m, 1H), 2.16 (s, 2H), 1.94 (s, 2H), 1.07 (d, J = 6.2 Hz, 3H), 0.95 (s, 6H). ^{13}C{^{1}H} NMR (100 MHz, DMSO-d_6) δ 193.8, 162.2, 93.4, 63.6, 50.3, 49.5, 42.3, 32.2, 28.0, 27.9, 16.6. IR (neat): 3251, 3076, 2940, 1521, 1376 cm^{-1}. HRMS (ESI-TOF) m/z: [M + H]$^+$ calcd for $C_{11}H_{20}NO_2$ 198.1494; Found 198.1502.

*3-((1-Hydroxy-4-(methylthio)butan-2-yl)amino)-5,5-dimethylcyclohex-2-en-1-one (**11x**).* Prepared according to procedure B using (*S*)-(−)-2-amino-4-methylthio-1-butanol (67 mg, 0.50 mmol) and 5,5-dimethyl-1,3-cyclohexanedione (70 mg, 0.50 mmol), and the residue was purified by 100−200 mesh silica gel column chromatography (EtOAc/methanol = 99:1) to afford 3-((1-hydroxy-4-(methylthio)-butan-2-yl)amino)-5,5-dimethylcyclohex-2-en-1-one **11w** (115 mg, 92%) as a yellowish brown semisolid. ^{1}H NMR (400 MHz, DMSO-d_6) δ 6.82 (s, 1H), 4.96 (s, 1H), 4.91 (s, 1H), 3.42 (m, 7H), 2.25 (s, 2H), 2.10 (s, 3H), 2.02 (s, 2H), 1.03 (s, 3H), 1.02 (s, 3H). ^{13}C{^{1}H} NMR (100 MHz, DMSO-d_6) δ 193.9, 162.9, 93.3, 62.2, 52.9, 50.3, 42.4, 32.2, 30.3, 29.9, 28.1, 27.8, 14.8. IR (neat): 3250, 3058, 2931, 1520, 1375, 1264, 1150, 1051 cm^{-1}. HRMS (ESI-TOF) m/z: [M + H]$^+$ calcd for $C_{13}H_{24}NO_2S$ 258.1528; Found 258.1534.

*3,4-Dihydroacridin-1(2H)-one (**13a**).*[32] Prepared according to procedure D using (2-aminophenyl)methanol (61 mg, 0.50 mmol) and 1,3-cyclohexanedione (56 mg, 0.50 mmol), and the residue was purified by 100−200 mesh silica gel column chromatography (EtOAc/hexane = 30:70) to afford 3,4-dihydroacridin-1(2*H*)-one **13a** (64 mg, 65%) as a brown solid. Melting point: 96−101 °C. ^{1}H NMR (400 MHz, $CDCl_3$) δ 8.83 (s, 1H), 8.03 (d, J = 8.5 Hz, 1H), 7.91 (d, J = 7.4 Hz, 1H), 7.79 (t, J = 8.6 Hz, 1H), 7.53 (t, J = 7.0 Hz, 1H), 3.30 (t, J = 6.0 Hz, 2H), 2.79 (m, 2H), 2.26 (m, 2H). ^{13}C{^{1}H} NMR (100 MHz, $CDCl_3$) δ 198.0, 162.1, 149.8, 137.2, 132.5, 129.9, 128.7, 126.9, 126.8, 126.4, 39.2, 33.6, 21.9. IR (neat): 2939, 1688, 1595, 1500, 755 cm^{-1}. HRMS (ESI-TOF) m/z: [M + H]$^+$ calcd for $C_{13}H_{12}NO$ 198.0919; Found 198.0924. Crystal preparation: The crystal is grown by simple recrystallization method. The isolated pure compound **13a** after column chromatography is dissolved in dichloromethane and layered with hexane and kept at room temperature for 2 days to get pure crystal. This crystal structure was previously reported (CCDC 2048643).[40] Crystal data: $C_{13}H_{11}NO$, M = 197, monoclinic, space group $P21/c$ with a = 8.1821(13) Å, b = 9.5096(18) Å, c = 12.598(2) Å, α = 90°, β = 99.337(5)°, γ = 90°, V = 967.2(3), T = 100 K, R1 = 0.0399, wR2 = 0.1157 on observed data, z = 4, F(000) = 416, Absorption coefficient = 0.086, λ= 0.71073 Å, 14102 reflections were collected on a Bruker APEX-III, 1591 observed reflections (I ≥ 2σ (I)).

*3-Methyl-3,4-dihydroacridin-1(2H)-one (**13b**).* Prepared according to procedure D using (2-aminophenyl)methanol (61 mg, 0.50 mmol) and 5-methyl-1,3-cyclohexanedione (63 mg, 0.50 mmol), and the residue was purified by 100−200 mesh silica gel column chromatography (EtOAc/hexane = 30:70) to afford 3-methyl-3,4-dihydroacridin-1(2*H*)-one **13b** (65 mg, 62%) as a brown solid. Melting point: 94−99 °C. ^{1}H NMR (400 MHz, $CDCl_3$) δ 8.83 (s, 1H), 8.04 (d, J = 8.5 Hz, 1H), 7.93 (d, J = 8.2 Hz, 1H), 7.80 (m, 1H), 7.55 (t, J = 7.1 Hz, 1H), 3.39 (dd, J = 14.9, 3.2 Hz, 1H), 3.00 (dd, J = 16.8, 10.6 Hz, 1H), 2.87 (m, 1H), 2.48 (m, 2H), 1.23 (d, J = 6.2 Hz, 3H). ^{13}C{^{1}H} NMR (100 MHz, $CDCl_3$) δ 198.1, 161.5, 149.9, 137.0, 132.4, 129.9, 128.7, 126.9, 125.9, 47.2, 41.8, 29.2, 21.4. IR (neat): 2947, 1689, 1599, 1506, 756 cm^{-1}. HRMS (ESI-TOF) m/z: [M + H]$^+$ calcd for $C_{14}H_{14}NO$ 212.1075; Found 212.1077.

*4,4-Dimethyl-3,4-dihydroacridin-1(2H)-one (**13c**).* Prepared according to procedure D using (2-aminophenyl)methanol (61 mg, 0.50 mmol) and 4,4-dimethyl-1,3-cyclohexanedione (70 mg, 0.50 mmol), and the residue was purified by 100−200 mesh silica gel column chromatography (EtOAc/hexane = 30:70) to afford 4,4-dimethyl-3,4-dihydroacridin-1(2*H*)-one **13c** (63 mg, 56%) as a brown semisolid. ^{1}H NMR (400 MHz, $CDCl_3$) δ 8.84 (s, 1H), 8.02 (d, J = 8.5 Hz, 1H), 7.90 (d, J = 8.1 Hz, 1H), 7.77 (t, J = 8.2 Hz, 1H), 7.51 (t, J = 8.1 Hz, 1H), 3.31 (t, J = 6.3 Hz, 2H), 2.09 (t, J = 6.5 Hz, 2H), 1.27 (s, 6H). ^{13}C{^{1}H} NMR (100 MHz, $CDCl_3$) δ 202.4, 161.3, 149.7, 138.1, 132.3, 129.7, 128.6, 126.9, 126.6, 125.3, 41.9, 35.3, 29.6, 24.4. IR (neat): 3057, 2925, 1687, 1590, 1495, 754 cm^{-1}. HRMS (ESI-TOF) m/z: [M + H]$^+$ calcd for $C_{15}H_{16}NO$ 226.1232; Found 226.1237.

*3,3-Dimethyl-3,4-dihydroacridin-1(2H)-one (**13d**).*[32] Prepared according to procedure D using (2-aminophenyl)methanol (61 mg, 0.50 mmol) and 5,5-dimethyl-1,3-cyclohexanedione (70 mg, 0.50 mmol), and the residue was purified by 100−200 mesh silica gel column chromatography (EtOAc/hexane = 30:70) to afford 3,3-dimethyl-3,4-dihydroacridin-1(2*H*)-one **13d** (75 mg, 67%) as a brown solid. Melting point: 105−110 °C. ^{1}H NMR (400 MHz, $CDCl_3$) δ 8.83 (s, 1H), 8.05 (d, J = 8.5 Hz, 1H), 7.94 (d, J = 8.1 Hz, 1H), 7.80 (t, J = 7.2 Hz, 1H), 7.55 (t, J = 7.1 Hz, 1H), 3.20 (s, 2H), 2.65 (s, 2H), 1.15 (s, 6H). ^{13}C{^{1}H} NMR (100 MHz, $CDCl_3$) δ 198.1, 160.9, 150.2, 136.7, 132.4, 129.9, 128.7, 126.9, 125.4, 52.6, 47.6, 32.9, 28.5. IR (neat): 3050, 2947, 1689, 1513, 1409, 758 cm^{-1}. HRMS (ESI-TOF) m/z: [M + H]$^+$ calcd for $C_{15}H_{16}NO$ 226.1232; Found 226.1238.

*3-(4-(Dimethylamino)phenyl)-3,4-dihydroacridin-1(2H)-one (**13e**).* Prepared according to procedure D using (2-aminophenyl)-methanol (43 mg, 0.35 mmol) and 5-(4-(dimethylamino)phenyl)-cyclohexane-1,3-dione (81 mg, 0.35 mmol), and the residue was purified by 100−200 mesh silica gel column chromatography (EtOAc/hexane = 40:60) to afford 3-(4-(dimethylamino)phenyl)-3,4-dihydroacridin-1(2*H*)-one **13e** (68 mg, 62%) as a brown solid. Melting point: 185−190 °C. ^{1}H NMR (400 MHz, $CDCl_3$) δ 8.88 (s, 1H), 8.07 (d, J = 8.5 Hz, 1H), 7.96 (d, J = 8.1 Hz, 1H), 7.82 (t, J = 7.2 Hz, 1H), 7.57 (t, J = 7.5 Hz, 1H), 7.21 (d, J = 8.6 Hz, 2H), 6.75 (d, J = 8.7 Hz, 2H), 3.60 (m, 1H), 3.50 (m, 2H), 3.09 (m, 1H), 2.94 (s, 6H), 2.92 (m, 1H). ^{13}C{^{1}H} NMR (100 MHz, $CDCl_3$) δ 197.9, 161.5, 150.1, 149.8, 137.1, 132.5, 130.7, 129.9, 128.8, 127.5, 126.9, 125.9, 113.0, 46.6, 41.5, 40.8, 38.6, 29.8. IR (neat): 3052, 1687, 1590, 1497 cm^{-1}. HRMS (ESI-TOF) m/z: [M + H]$^+$ calcd for $C_{21}H_{21}N_2O$ 317.1654; Found 317.1644.

*2,3-Dihydro-1H-cyclopenta[b]quinolin-1-one (**13f**).*[33] Prepared according to procedure D using (2-aminophenyl)methanol (62 mg, 0.50 mmol) and 1,3-cyclopentanedione (49 mg, 0.50 mmol), and the residue was purified by 100−200 mesh silica gel column chromatography (EtOAc/hexane = 30:70) to afford 2,3-dihydro-1*H*-cyclopenta-[b]quinolin-1-one **13f** (40 mg, 44%) as a black solid. Melting point:

https://doi.org/10.1021/acs.joc.1c00714
J. Org. Chem. 2021, 86, 8805−8828

145−147 °C. ^{1}H NMR (400 MHz, $CDCl_3$) δ 8.58 (s, 1H), 8.14 (d, J = 8.6 Hz, 1H), 7.98 (d, J = 8.2 Hz, 1H), 7.86 (t, J = 7.7 Hz, 1H), 7.60 (t, J = 7.6 Hz, 1H), 3.46 (t, J = 6 Hz, 2H), 2.91 (t, J = 6 Hz, 2H). ^{13}C{^{1}H} NMR (100 MHz, $CDCl_3$) δ 205.0, 171.1, 151.8, 133.7, 132.9, 130.6, 129.1, 127.9, 127.0, 36.4, 29.0. IR (neat): 2922, 2852, 1700, 1623, 1585, 1493 cm^{-1}. HRMS (ESI-TOF) m/z: [M + H]$^+$ calcd for $C_{12}H_{10}NO$ 184.0762; Found 184.0761.

*1,3-Dimethylpyrimido[4,5-b]quinoline-2,4(1H,3H)-dione (**13g**).*[34] Prepared according to procedure D using (2-aminophenyl)methanol (62 mg, 0.50 mmol) and 1,3-dimethylpyrimidine-2,4,6(1*H*,3*H*,5*H*)-trione (78 mg, 0.50 mmol), and the residue was purified by 100−200 mesh silica gel column chromatography (EtOAc/hexane = 40:60) to afford 1,3-dimethylpyrimido[4,5-*b*]quinoline-2,4(1*H*,3*H*)-dione **13g** (45 mg, 38%) as a black solid. Melting point: 197−199 °C. ^{1}H NMR (400 MHz, $CDCl_3$) δ 8.96 (s, 1H), 7.94 (dd, J = 22.0, 8.4 Hz, 2H), 7.81 (m, 1H), 7.50 (m, 1H), 3.80 (s, 3H), 3.51 (s, 3H). ^{13}C{^{1}H} NMR (100 MHz, $CDCl_3$) δ 161.5, 151.7, 149.9, 148.5, 140.1, 133.2, 129.3, 128.2, 125.9, 124.8, 110.9, 29.7, 28.6. IR (neat): 3055, 2920, 1704, 1659, 1616, 1496, 1468, 1421 cm^{-1}. HRMS (ESI-TOF) m/z: [M + H]$^+$ calcd for $C_{13}H_{12}N_3O_2$ 242.0930; Found 242.0937.

*9-Methyl-3,4-dihydroacridin-1(2H)-one (**13h**).*[35] Prepared according to procedure D using 1-(2-aminophenyl)ethan-1-ol (68 mg, 0.50 mmol) and 1,3-cyclohexanedione (56 mg, 0.50 mmol), and the residue was purified by 100−200 mesh silica gel column chromatography (EtOAc/hexane = 30:70) to afford 9-methyl-3,4-dihydroacridin-1(2*H*)-one **13h** (45 mg, 42%) as a brown semisolid. ^{1}H NMR (400 MHz, $CDCl_3$) δ 8.19 (d, J = 8.5 Hz, 1H), 8.01 (d, J = 8.4 Hz, 1H), 7.76 (m, 1H), 7.55 (m, 1H), 3.27 (m, 2H), 3.03 (s, 3H), 2.79 (t, J = 6.6 Hz, 2H), 2.19 (m, 2H). ^{13}C{^{1}H} NMR (100 MHz, $CDCl_3$) δ 200.7, 162.2, 131.7, 129.1, 127.8, 126.5, 125.6, 116.7, 41.2, 34.7, 21.4, 16.2. IR (neat): 2930, 2853, 1679, 1613, 1563 cm^{-1}. HRMS (ESI-TOF) m/z: [M + H]$^+$ calcd for $C_{14}H_{14}NO$ 212.1075; Found 212.1081.

*3,3,9-Trimethyl-3,4-dihydroacridin-1(2H)-one (**13h**).*[35] Prepared according to procedure D using 1-(2-aminophenyl)ethan-1-ol (68 mg, 0.50 mmol) and 5,5-dimethyl-1,3-cyclohexanedione (56 mg, 0.50 mmol), and the residue was purified by 100−200 mesh silica gel column chromatography (EtOAc/hexane = 30:70) to afford 3,3,9-trimethyl-3,4-dihydroacridin-1(2*H*)-one **13i** (40 mg, 34%) as a yellow solid. Melting point: 88−90 °C. ^{1}H NMR (400 MHz, $CDCl_3$) δ 8.22 (d, J = 8.5 Hz, 1H), 8.02 (d, J = 8.4 Hz, 1H), 7.77 (t, J = 7.6 Hz, 1H), 7.57 (t, J = 7.8 Hz, 1H), 3.19 (s, 2H), 3.07 (s, 3H), 2.67 (s, 2H), 1.14 (s, 6H). ^{13}C{^{1}H} NMR (100 MHz, $CDCl_3$) δ 200.7, 161.2, 131.7, 129.2, 127.8, 126.6, 125.7, 124.3, 54.9, 48.6, 32.3, 28.4, 16.2. IR (neat): 2928, 2866, 1680, 1562, 1371 cm^{-1}. HRMS (ESI-TOF) m/z: [M + H]$^+$ calcd for $C_{16}H_{18}NO$ 240.1388; Found 240.1398.

*6,8-Dibromo-3-(4-(dimethylamino)phenyl)-3,4-dihydroacridin-1(2H)-one (**13j**).* Prepared according to procedure D using (2-amino-3,5-dibromophenyl)methanol (40 mg, 0.14 mmol) and 5-(4-(dimethylamino)phenyl)cyclohexane-1,3-dione (32 mg, 0.14 mmol), and the residue was purified by 100−200 mesh silica gel column chromatography (EtOAc/hexane = 40:60) to afford 6,8-dibromo-3-(4-(dimethylamino)phenyl)-3,4-dihydroacridin-1(2*H*)-one **13j** (58 mg, 68%) as a yellow solid. Melting point: 196−201 °C. ^{1}H NMR (400 MHz, $CDCl_3$) δ 8.74 (s, 1H), 8.23 (d, J = 1.8 Hz, 1H), 8.07 (d, J = 2.0 Hz, 1H), 7.19 (t, J = 5.8 Hz, 2H), 6.76 (d, J = 8.1 Hz, 2H), 3.71 (m, 1H), 3.52 (m, 2H), 3.11 (m, 1H), 2.95 (s, 6H), 2.94 (s, 1H). ^{13}C{^{1}H} NMR (100 MHz, $CDCl_3$) δ 197.2, 162.9, 138.4, 136.4, 131.4, 128.7, 127.4, 126.9, 125.4, 119.9, 113.0, 46.5, 41.5, 40.8, 38.3. IR (neat): 2952, 2800, 1692, 1600, 1582, 1522, 1458 cm^{-1}. HRMS (ESI-TOF) m/z: [M + H]$^+$ calcd for $C_{21}H_{19}Br_2N_2O$ 472.9864; Found 472.9856.

*6,8-Dibromo-9-methyl-2,3-dihydro-1H-cyclopenta[b]quinolin-1-one (**13k**).* Prepared according to procedure D using 1-(2-amino-4,6-dibromophenyl)ethan-1-ol (146 mg, 0.5 mmol) and 1,3-cyclopentanedione (49 mg, 0.50 mmol), and the residue was purified by 100−200 mesh silica gel column chromatography (EtOAc/hexane = 30:70) to afford 6,8-dibromo-9-methyl-2,3-dihydro-1*H*-cyclopenta[b]-quinolin-1-one **13k** (60 mg, 34%) as a light purple solid. Melting point: 219−220 °C. ^{1}H NMR (400 MHz, $CDCl_3$) δ 8.30 (d, J = 2.1 Hz, 1H), 8.25 (d, J = 2.1 Hz, 1H), 3.43 (m, 2H), 3.05 (s, 3H), 2.89 (m, 2H). ^{13}C{^{1}H} NMR (100 MHz, $CDCl_3$) δ 205.9, 172.2, 147.6, 138.2, 134.6, 130.6, 129.5, 127.8, 126.0, 119.8, 36.8, 28.6, 12.8. IR (neat): 2921, 2851, 1600 cm^{-1}. HRMS (ESI-TOF) m/z: [M + H]$^+$ calcd for $C_{13}H_{10}Br_2NO$ 353.9129; Found 353.9130.

*1,3,5-Trimethylpyrimido[4,5-b]quinoline-2,4(1H,3H)-dione (**13l**).*[35] Prepared according to procedure D using 1-(2-aminophenyl)-ethan-1-ol (68 mg, 0.50 mmol) and 1,3-dimethylpyrimidine-2,4,6-(1*H*,3*H*,5*H*)-trione (78 mg, 0.50 mmol), and the residue was purified by 100−200 mesh silica gel column chromatography (EtOAc/hexane = 40:60 to afford 1,3,5-trimethylpyrimido[4,5-*b*]quinoline-2,4(1*H*,3*H*)-dione **13l** (60 mg, 47%) as a white solid. Melting point: 221−223 °C. ^{1}H NMR (400 MHz, $CDCl_3$) δ 8.15 (s, 1H), 7.91 (s, 1H), 7.76 (t, J = 7.5 Hz, 1H), 7.50 (t, J = 7.5 Hz, 1H), 3.78 (s, 3H), 3.47 (s, 3H), 3.23 (s, 3H). ^{13}C{^{1}H} NMR δ 162.31 (s), 153.9, 151.3, 148.6, 148.1, 132.5, 128.7, 125.3, 108.7, 30.0, 28.5, 16.1. IR (neat): 2923, 2852, 1661, 1579 cm^{-1}. HRMS (ESI-TOF) m/z: [M + H]$^+$ calcd for $C_{14}H_{14}N_3O_2$ 256.1086; Found 256.1087.

*3-((2-(Hydroxymethyl)phenyl)amino)cyclohex-2-en-1-one (**14a**).* Prepared according to procedure B using (2-aminophenyl)methanol (61 mg, 0.50 mmol) and 1,3-cyclohexanedione (56 mg, 0.50 mmol), and the residue was purified by 100−200 mesh silica gel column chromatography (EtOAc/methanol = 98:2) to afford 3-((2-(hydroxymethyl)phenyl)amino)cyclohex-2-en-1-one **14a** (101 mg, 92%) as a yellow solid. Melting point: 163−167 °C. ^{1}H NMR (400 MHz, MeOH-d_4) δ 7.55 (m, 1H), 7.34 (m, 2H), 7.21 (m, 1H), 4.98 (s, 1H), 4.57 (s, 2H), 2.63 (t, J = 6.2 Hz, 2H), 2.32 (t, J = 6.4 Hz, 2H), 2.01 (m, 2H). ^{13}C {^{1}H} NMR (100 MHz, MeOH-d_4) δ 200.8, 169.3, 138.9, 136.8, 129.5, 129.3, 128.6, 128.1, 98.3, 61.4, 36.8, 29.7, 22.9. IR (neat): 3841, 3741, 3613, 1696, 1520 cm^{-1}. HRMS (ESI-TOF) m/z: [M + H]$^+$ calcd for $C_{13}H_{16}NO_2$ 218.1181; Found 218.1184.

*3-((2-(Hydroxymethyl)phenyl)amino)-5-methylcyclohex-2-en-1-one (**14b**).* Prepared according to procedure B using (2-aminophenyl)-methanol (61 mg, 0.50 mmol) and 5-methyl-1,3-cyclohexanedione (63 mg, 0.50 mmol), and the residue was purified by 100−200 mesh silica gel column chromatography (EtOAc/methanol = 98:2) to afford 3-((2-(hydroxymethyl)phenyl)amino)-5-methylcyclohex-2-en-1-one **14b** (94 mg, 82%) as a yellow solid. Melting point: 168−170 °C. ^{1}H NMR (400 MHz, MeOH-d_4) δ 7.54 (m, 1H), 7.33 (m, 2H), 7.21 (m, 1H), 4.97 (s, 1H), 4.57 (s, 2H), 2.61 (m, 1H), 2.36 (m, 2H), 2.24 (m, 1H), 2.07 (m, 1H), 1.12 (d, J = 6.5 Hz, 3H). ^{13}C{^{1}H} NMR (100 MHz, MeOH-d_4) δ 200.6, 168.7, 138.8, 136.8, 129.5, 129.3, 128.6, 128.0, 97.9, 61.4, 45.0, 37.7, 30.7, 21.1. IR (neat): 3843, 3741, 3615, 1690, 1525 cm^{-1}. HRMS (ESI-TOF) m/z: [M + H]$^+$ calcd for $C_{14}H_{18}NO_2$ 232.1338; Found 232.1345.

*3-((2-(Hydroxymethyl)phenyl)amino)-4,4-dimethylcyclohex-2-en-1-one (**14c**).* Prepared according to procedure B using (2-aminophenyl)methanol (61 mg, 0.50 mmol) and 4,4-dimethyl-1,3-cyclohexanedione (70 mg, 0.50 mmol), and the residue was purified by 100−200 mesh silica gel column chromatography (EtOAc/methanol = 98:2) to afford 3-((2-(hydroxymethyl)phenyl)amino)-4,4-dimethylcyclohex-2-en-1-one **14c** (98 mg, 80%) as a white solid. Melting point: 128−132 °C.^{1}H NMR (400 MHz, MeOH-d_4) δ 7.53 (dd, J = 8.1, 5.6 Hz, 1H), 7.32 (m, 2H), 7.22 (m, 1H), 4.57 (s, 2H), 2.65 (t, J = 6.3 Hz, 2H), 1.88 (t, J = 6.3 Hz, 2H), 1.12 (s, 6H). ^{13}C{^{1}H} NMR (100 MHz, MeOH-d_4) δ 205.9, 166.9, 138.7, 137.1, 129.5, 129.3, 128.3, 127.9, 97.1, 61.5, 40.5, 36.8, 26.7, 25.4. IR (neat): 3841, 3739, 3614, 1694, 1523 cm^{-1}. HRMS (ESI-TOF) m/z: [M + H]$^+$ calcd for $C_{15}H_{20}NO_2$ 246.1494; Found 246.1497.

*3-((2-(Hydroxymethyl)phenyl)amino)-5,5-dimethylcyclohex-2-en-1-one (**14d**).* Prepared according to procedure B using (2-aminophenyl)methanol (61 mg, 0.50 mmol) and 5,5-dimethyl-1,3-cyclohexanedione (70 mg, 0.50 mmol), and the residue was purified by 100−200 mesh silica gel column chromatography (EtOAc/methanol = 98:2) to afford 3-((2-(hydroxymethyl)phenyl)amino)-5,5-dimethylcyclohex-2-en-1-one **14d** (104 mg, 85%) as a yellow solid. Melting point: 177−182 °C. ^{1}H NMR (400 MHz, MeOH-d_4) δ 7.56 (m, 1H), 7.35 (m, 2H), 7.20 (m, 1H), 4.95 (s, 1H), 4.58 (s, 2H), 2.49 (s, 2H), 2.20 (s, 2H), 1.13 (s, 6H). ^{13}C{^{1}H} NMR (100 MHz, MeOH-d_4) δ 198.7, 166.4, 137.5, 135.4, 127.9, 127.3, 126.7, 95.7, 59.9, 49.2, 41.9, 32.5, 26.9. IR (neat): 3842, 3740, 3615, 1694, 1523 cm^{-1}. HRMS (ESI-

https://doi.org/10.1021/acs.joc.1c00714
J. Org. Chem. 2021, 86, 8805−8828

TOF) m/z: $[M + H]^+$ calcd for $C_{15}H_{20}NO_2$ 246.1494; Found 246.1496.

*2,3,4,9-Tetrahydro-1H-xanthen-1-one (**16a**).*[36] Prepared according to procedure F using cyclohexane-1,3-dione (56 mg, 0.50 mmol) and 2-hydroxybenzyl alcohol (124 mg, 1 mmol), and the residue was purified by 100−200 mesh silica gel column chromatography (EtOAc/hexane = 10:90) to afford 2,3,4,9-tetrahydro-1*H*-xanthen-1-one (**16a**) (cat. **10**: 82 mg, 82%, cat. **8**: 85 mg, 85%) as a pale yellow crystalline solid. Melting point: 80−84 °C. ^{1}H NMR (400 MHz, $CDCl_3$): δ 7.15 (m, 2H), 7.05 (m, 1H), 6.95 (d, J = 8.2 Hz, 1H), 3.50 (s, 2H), 2.56 (t, J = 6.2 Hz, 2H), 2.46(t, J = 6.6 Hz, 2H), 2.05 (m, 2H). ^{13}C{^{1}H} NMR (100 MHz, $CDCl_3$) δ 198.3, 167.0, 149.8, 129.8, 127.7, 124.7, 120.9, 116.5, 110.1, 36.7, 27.8, 21.2, 20.7. IR (neat): 2929, 1638, 1452, 1220, 1180 cm^{-1}. HRMS (ESI-TOF) m/z: $[M + H]^+$ calcd for $C_{13}H_{13}O_2$ 201.0916; Found 201.0915. Crystal preparation: The crystal is grown by simple recrystallization method. The isolated pure compound **16a** after column chromatography is dissolved in dichloromethane and layered with hexane and kept at room temperature for 2 days to get pure crystal. Crystal data: $C_{13}H_{12}O_2$, M = 200, triclinic, space group P-1 with a = 5.7502(3) Å, b = 8.1975(4) Å, c = 10.7100(5) Å, α = 98.716(2)°, β = 101.290(2)°, γ = 98.159(2)°, V = 481.60(4), T = 296 K, R1 = 0.0433, wR2 = 0.1196 on observed data, z = 2, F(000) = 212, absorption coefficient = 0.092, λ= 0.71073 Å, 8779 reflections were collected on a Bruker APEX-II CCD, 2033 observed reflections ($I \geq 2\sigma$ (I)).

*5-Methoxy-2,3,4,9-tetrahydro-1H-xanthen-1-one (**16b**).* Prepared according to procedure F using cyclohexane-1,3-dione (56 mg, 0.50 mmol) and 2-hydrox-3-methoxybenzyl alcohol (154 mg, 1 mmol), and the residue was purified by 100−200 mesh silica gel column chromatography (EtOAc/hexane = 10:90) to afford 5-methoxy-2,3,4,9-tetrahydro-1*H*-xanthen-1-one (**16b**) (cat. 10:79 mg, 69%, cat. 8:77 mg, 67%) as orange yellow crystalline solid. ^{1}H NMR (400 MHz, $CDCl_3$): δ 7.0 (t, J = 7.96 Hz, 1H), 6.75 (m, 2H), 3.89 (s, 3H), 3.51 (s, 2H), 2.64 (t, J = 6.28 Hz, 2H), 2.47 (t, J = 6.3 Hz, 2H), 2.06 (m, 2H). ^{13}C{^{1}H} NMR (100 MHz, $CDCl_3$) δ 198.6, 167.1, 148.2, 139.6, 124.7, 122.3, 121.7, 110.5, 110.4, 56.5, 37.1, 28.2, 21.6, 21.1. IR (neat): 2933, 2847, 1639, 1585, 1270, 1187, 1077 cm^{-1}. HRMS (ESI-TOF) m/z: $[M + H]^+$ calcd for $C_{14}H_{15}O_3$ 231.1021; Found, 231.1027.

*7-Nitro-2,3,4,9-tetrahydro-1H-xanthen-1-one (**16c**).* Prepared according to procedure F using cyclohexane-1,3-dione (56 mg, 0.50 mmol) and 2-hydroxy-5-nitrobenzyl alcohol (169 mg, 1 mmol), and the residue was purified by 100−200 mesh silica gel column chromatography (EtOAc/hexane = 10:90) to afford 7-nitro-2,3,4,9-tetrahydro-1*H*-xanthen-1-one (**16c**) (cat. **10**: 89 mg, 73%, cat. **8**: 87 mg, 71%) (as white yellow crystalline solid. Melting point: 158−163 °C. ^{1}H NMR (400 MHz, $CDCl_3$): δ 8.08 (m, 2H), 7.10 (m, 1H), 3.61 (s, 2H), 2.63 (t, J = 6.3 Hz, 2H), 2.51 (t, J = 6.3 Hz, 2H), 2.12 (m, 2H). ^{13}C{^{1}H} NMR (100 MHz, $CDCl_3$) δ 198.0, 166.3, 154.7, 144.6, 126.0, 124.1, 122.6, 117.7, 110.2, 37.0, 27.8, 21.7, 20.9. IR (neat): 3059, 2925, 1643, 1511, 1229, 1175, 1120 cm^{-1}. HRMS (ESI-TOF) m/z: $[M + H]^+$ calcd for $C_{13}H_{12}NO_4$ 246.0766; Found 246.0767.

*3-Methyl-2,3,4,9-tetrahydro-1H-xanthen-1-one (**16d**).*[36] Prepared according to procedure F using 5-methylcyclohexane-1,3-dione (62 mg, 0.50 mmol) and 2-hydroxybenzyl alcohol (124 mg, 1 mmol), and the residue was purified by 100−200 mesh silica gel column chromatography (EtOAc/hexane = 10:90) to afford 3-methyl-2,3,4,9-tetrahydro-1*H*-xanthen-1-one (**16d**) (cat. **10**: 68 mg, 65%, cat. **8**: 71 mg, 66%) as white crystalline solid. Melting point: 89−91 °C. ^{1}H NMR (400 MHz, $CDCl_3$): δ 7.15 (m, 2H), 7.07 (m, 1H), 6.96 (d, J = 8.4 Hz, 1H), 3.51 (m, 2H), 2.54 (m, 2H), 2.31 (s, 2H), 2.19 (m, 1H), 1.13 (d, J = 6.2 Hz, 3H). ^{13}C{^{1}H} NMR (100 MHz, $CDCl_3$) δ 198.3, 166.4, 145.0, 129.9, 127.7, 124.7, 120.9, 116.6, 109.7, 45.1, 35.9, 28.5, 21.23, 21.1. IR (neat): 2926, 1640, 1451, 1222, 1190 cm^{-1}. HRMS (ESI-TOF) m/z: $[M + H]^+$ calcd for $C_{14}H_{15}O_2$ 215.1072; Found 215.1075.

*5-Methoxy-3-methyl-2,3,4,9-tetrahydro-1H-xanthen-1-one (**16e**).* Prepared according to procedure F using 5-methylcyclohexane-1,3-dione (62 mg, 0.50 mmol) and 2-hydroxy-3-methoxybenzyl alcohol (154 mg, 1 mmol), and the residue was purified by 100−200 mesh silica gel column chromatography (EtOAc/hexane = 10:90) to afford 5-methoxy-3-methyl-2,3,4,9-tetrahydro-1*H*-xanthen-1-one (**16e**) (cat. **10**: 54 mg, 44%, cat. **8**: 51 mg, 42%) as a white crystalline solid. Melting point: 105−105 °C. ^{1}H NMR (400 MHz, $CDCl_3$): δ 6.99 (t, J = 8.0 Hz, 1H), 6.74 (dd, J = 7.5 Hz, 2H), 3.87 (s, 3H), 3.49 (m, 2H), 2.60 (dd, J = 11.3, 8.4 Hz, 2H), 2.34 (d, J = 15.1 Hz, 2H), 2.16 (m, 2H), 1.11 (d, J = 6.2 Hz, 3H). ^{13}C{^{1}H} NMR (100 MHz, $CDCl_3$) δ 198.3, 166.1, 147.8, 139.5, 124.4, 121.9, 121.0, 110.3, 109.5, 56.1, 45.0, 35.9, 28.4, 21.3, 21.0. IR (neat): 2924, 1645, 1583, 1268, 1197, 1087 cm^{-1}. HRMS (ESI-TOF) m/z: $[M + H]^+$ calcd for $C_{15}H_{17}O_3$ 245.1178; Found 245.1178.

*3-Methyl-7-nitro-2,3,4,9-tetrahydro-1H-xanthen-1-one (**16f**).* Prepared according to procedure F using 5-methylcyclohexane-1,3-dione (62 mg, 0.50 mmol) and 2-hydroxy-5-nitrobenzyl alcohol (169 mg, 1 mmol), and the residue was purified by 100−200 mesh silica gel column chromatography (EtOAc/hexane = 10:90) to afford 3-methyl-7-nitro-2,3,4,9-tetrahydro-1*H*-xanthen-1-one (**16f**) (cat. **10**: 62 mg, 48%, cat. **8**: 53 mg, 41%) as white crystalline solid. Melting point: 106−111 °C. ^{1}H NMR (400 MHz, $CDCl_3$): δ 8.05 (m, 2H), 7.08 (m, 1H), 3.87 (s, 3H), 3.58 (m, 2H), 2.57 (m, 2H), 2.31 (m, 2H), 2.18 (m, 2H), 1.15 (d, J = 6.2 Hz, 3H). ^{13}C{^{1}H} NMR (100 MHz, $CDCl_3$) δ 198.2, 166.8, 154.4, 144.3, 125.7, 123.8, 122.2, 117.5, 109.4, 44.9, 35.5, 28.3, 21.3, 21.0. IR (neat): 2923, 2862, 1648, 1522, 1232, 1190, 1085 cm^{-1}. HRMS (ESI-TOF) m/z: $[M + H]^+$ calcd for $C_{14}H_{14}NO_4$ 260.0923; Found 260.0927.

*3,3-Dimethyl-2,3,4,9-tetrahydro-1H-xanthen-1-one (**16g**).*[36] Prepared according to procedure F using 5,5-dimethylcyclohexane-1,3-dione (70 mg, 0.50 mmol) and 2-hydroxybenzyl alcohol (124 mg, 1 mmol), and the residue was purified by 100−200 mesh silica gel column chromatography (EtOAc/hexane = 10:90) to afford 3,3-dimethyl-2,3,4,9-tetrahydro-1*H*-xanthen-1-one (**16g**) (cat. **10**: 55 mg, 48%, cat. **8**: 56 mg, 49%) as white crystalline solid. ^{1}H NMR (400 MHz, $CDCl_3$): δ 7.15 (t, J = 6.9 Hz, 2H), 7.05 (t, J = 7.4 Hz, 1H), 6.95 (d, J = 7.9 Hz, 1H), 3.51 (s, 2H), 2.42 (s, 2H), 2.32 (s, 2H), 1.12 (s, 6H). ^{13}C{^{1}H} NMR (100 MHz, $CDCl_3$) δ 197.8, 164.9, 149.8, 129.5, 127.4, 124.4, 120.6, 116.3, 108.5, 50.4, 45.7, 31.9, 28.2 (2C), 20.8. IR (neat): 2924, 1639, 1453, 1231, 1180 cm^{-1}. HRMS (ESI-TOF) m/z: $[M + H]^+$ calcd for $C_{15}H_{17}O_2$ 229.1229; Found 229.1230.

*3,3-dimethyl-7-nitro-2,3,4,9-tetrahydro-1H-xanthen-1-one (**16h**).*[37] Prepared according to procedure F using 5,5-dimethylcyclohexane-1,3-dione (70 mg, 0.50 mmol) and 2-hydroxy-5-nitrobenzyl alcohol (169 mg, 1 mmol), and the residue was purified by 100−200 mesh silica gel column chromatography (EtOAc/hexane = 10:90) to afford 3,3-dimethyl-7-nitro-2,3,4,9-tetrahydro-1*H*-xanthen-1-one (**16h**) (cat. **10**: 41 mg, 30%, cat. **8**: 45 mg, 33%) as white crystalline solid. Melting point: 106−108 °C.^{1}H NMR (400 MHz, $CDCl_3$): δ 8.06 (d, J = 6.9 Hz, 2H), 7.11 (d, J = 9.5 Hz, 1H), 3.57 (s, 2H), 2.53 (m, 2H), 1.93 (m, 2H), 1.34 (s, 6H). ^{13}C{^{1}H} NMR (100 MHz, $CDCl_3$) δ 197.6, 171.7, 154.1, 144.3, 127.5, 123.7, 122.2, 117.6, 108.3, 35.6, 35.0, 33.7, 25.5 (2C), 21.7. IR (neat): 2925, 2863, 1639, 1229, 1087 cm^{-1}. HRMS (ESI-TOF) m/z: $[M + H]^+$ calcd for $C_{15}H_{16}NO_4$ 274.1079; Found 274.1082..

*5-Methoxy-3,3-dimethyl-2,3,4,9-tetrahydro-1H-xanthen-1-one (**16i**).* Prepared according to procedure F using 5,5-dimethylcyclohexane-1,3-dione (70 mg, 0.50 mmol) and 2-hydroxy-3-methoxybenzyl alcohol (154 mg, 1 mmol), and the residue was purified by 100−200 mesh silica gel column chromatography (EtOAc/hexane = 10:90) to afford 5-methoxy-3,3-dimethyl-2,3,4,9-tetrahydro-1*H*-xanthen-1-one (**16i**) (cat. **10**: 38 mg, 30%, cat. **8**: 41 mg, 32%) as yellowish crystalline solid. Melting point: 76−81 °C. ^{1}H NMR (400 MHz, $CDCl_3$): δ 7.0 (t, J = 7.9 Hz, 1H), 6.76 (t, J = 8.0 Hz, 2H), 3.88 (s, 3H), 3.51 (s, 2H), 2.52 (s, 2H), 2.33 (s, 2H), 1.12 (s, 6H). ^{13}C{^{1}H} NMR (100 MHz, $CDCl_3$) δ 198.2, 165.0, 147.8, 139.5, 124.4, 121.9, 121.3, 110.10, 108.7, 56.1, 50.7, 41.5, 32.3, 28.5 (2C), 21.2. IR (neat): 2949, 1646, 1583, 1273, 1083 cm^{-1}. HRMS (ESI-TOF) m/z: $[M + H]^+$ calcd for $C_{16}H_{19}O_3$ 259.1334; Found 259.1335.

*4,4-Dimethyl-2,3,4,9-tetrahydro-1H-xanthen-1-one (**16j**).* Prepared according to procedure F using 4,4-methylcyclohexane-1,3-dione (70 mg, 0.50 mmol) and 2-hydroxybenzyl alcohol (124 mg, 1 mmol), and the residue was purified by 100−200 mesh silica gel column chromatography (EtOAc/hexane = 10:90) to afford 4,4-dimethyl-2,3,4,9-tetrahydro-1*H*-xanthen-1-one (**16j**) (cat. **10**: 82 mg, 72%, cat. **8**: 83 mg, 73%) as white crystalline solid. Melting point: 69−73 °C. ^{1}H

https://doi.org/10.1021/acs.joc.1c00714
J. Org. Chem. 2021, 86, 8805−8828

NMR (400 MHz, $CDCl_3$): δ 7.15 (d, J = 6.8 Hz, 2H), 7.05 (m, 1H), 6.99 (m, 1H), 3.48 (s, 2H), 2.57 (t, J = 6.3 Hz, 2H), 1.88 (t, J = 6.3 Hz, 2H), 1.16 (s, 6H). $^{13}C\{^1H\}$ NMR (100 MHz, $CDCl_3$) δ 203.0, 165.0, 149.9, 129.8, 127.6, 124.6, 121.0, 116.4, 108.1, 40.3, 34.4, 24.8, (2C), 21.7. IR (neat): 2925, 1641, 1456, 1229, 1182 cm^{-1}. HRMS (ESI-TOF) m/z: $[M + H]^+$ calcd for $C_{15}H_{17}O_2$ 229.1229; Found 229.1230.

*4,4-Dimethyl-7-nitro-2,3,4,9-tetrahydro-1H-xanthen-1-one (**16k**).* Prepared according to procedure F using 4,4-methylcyclohexane-1,3-dione (70 mg, 0.50 mmol) and 2-hydroxy-5-nitrobenzyl alcohol (169 mg, 1 mmol), and the residue was purified by 100−200 mesh silica gel column chromatography (EtOAc/hexane = 10:90) to afford 4,4-dimethyl-7-nitro-2,3,4,9-tetrahydro-1*H*-xanthen-1-one (**16k**) (cat. **10**: 79 mg, 58%, cat. **8**: 75 mg, 55%) as white crystalline solid. Melting point: 179−182 °C. ^1H NMR (400 MHz, $CDCl_3$): δ 8.06 (d, J = 12.2 Hz, 2H), 7.06 (d, J = 8.8 Hz, 1H), 3.56 (s, 2H), 2.60 (t, J = 6.3 Hz, 2H), 1.91 (t, J = 6.3 Hz, 2H), 1.16 (s, 6H). $^{13}C\{^1H\}$ NMR (100 MHz, $CDCl_3$) δ 201.8, 163.4, 153.1, 143.7, 125.2, 123.2, 121.8, 116.79, 107.3, 39.9, 33.7, 29.3, 24.1 (2C), 21.3. IR (neat): 2926, 2861, 1642, 1516, 1231, 1184 cm^{-1}. HRMS (ESI-TOF) m/z: $[M + H]^+$ calcd for $C_{15}H_{16}NO_4$ 274.1079; Found 274.1087.

*5-Methoxy-4,4-dimethyl-2,3,4,9-tetrahydro-1H-xanthen-1-one (**16l**).* Prepared according to procedure F using 4,4-methylcyclohexane-1,3-dione (70 mg, 0.50 mmol) and 2-hydroxy-3-methoxybenzyl alcohol (154 mg, 1 mmol), and the residue was purified by 100−200 mesh silica gel column chromatography (EtOAc/hexane = 10:90) to afford 5-methoxy-4,4-dimethyl-2,3,4,9-tetrahydro-1*H*-xanthen-1-one (**16l**) (cat. **10**: 61 mg, 47%, cat. **8**: 53 mg, 41%) as white crystalline solid. Melting point: 115−120 °C. ^1H NMR (400 MHz, $CDCl_3$): δ 6.99 (t, J = 7.9 Hz, 1H), 6.76 (t, J = 7 Hz, 2H), 3.98 (s, 3H), 3.48 (s, 2H), 2.65 (t, J = 6.3 Hz, 2H), 1.89 (d, J = 12.7 Hz, 2H), 1.15(s, 6H). $^{13}C\{^1H\}$ NMR (100 MHz, $CDCl_3$) δ 203.0, 164.7, 147.8, 139.5, 124.3, 121.4, 113.6, 110.1, 108.1, 46.1, 40.4, 34.5, 31.9, 29.8, 24.8, 21.8. IR (neat): 2925, 2867, 1578, 1475, 1236, 1078 cm^{-1}. HRMS (ESI-TOF) m/z: $[M + H]^+$ calcd for $C_{16}H_{19}O_3$ 259.1334; Found 259.1338.

*3-(4-(Dimethylamino)phenyl)-7-nitro-2,3,4,9-tetrahydro-1H-xanthen-1-one (**16m**).* Prepared according to procedure F using 5-(4-(dimethylamino)phenyl)cyclohexane-1,3-dione (115 mg, 0.50 mmol) and 2-(hydroxymethyl)-4-nitrophenol (169 mg, 1 mmol), and the residue was purified by 100−200 mesh silica gel column chromatography (EtOAc/hexane = 20:80) to afford 3-(4-(dimethylamino)-phenyl)-7-nitro-2,3,4,9-tetrahydro-1*H*-xanthen-1-one **16m** (cat. **10**: 69 mg, 38%, cat. **8**: 60 mg, 33%) as a yellow solid. Melting point: 216−222 °C. ^1H NMR (400 MHz, $CDCl_3$) δ 8.08 (m, 2H), 7.12 (dd, J = 25.0, 8.7 Hz, 3H), 6.75 (d, J = 6.6 Hz, 2H), 3.63 (m, 2H), 3.38 (m, 1H), 2.96 (s, 6H), 2.94 (s, 2H), 2.80 (d, J = 8.1 Hz, 2H). $^{13}C\{^1H\}$ NMR (100 MHz, $CDCl_3$) δ 197.3, 165.4, 144.4, 127.5, 125.8, 123.8, 122.3, 117.6, 109.7, 44.1, 37.9, 35.5, 29.8, 21.5. IR (neat): 2923, 2853, 1652, 1608, 1586, 1522 cm^{-1}. HRMS (ESI-TOF) m/z: $[M + H]^+$ calcd for $C_{21}H_{21}N_2O_4$ 365.1501; Found 365.1497.

*4a-Hydroxy-9a-methyl-2,3,4,4a,9,9a-hexahydro-1H-xanthen-1-one (**16n**).* Prepared according to procedure F using 2-methyl-1,3-cyclohexanedione (63 mg, 0.50 mmol) and 2-(hydroxymethyl)phenol (124 mg, 1 mmol), and the residue was purified by 100−200 mesh silica gel column chromatography (EtOAc/hexane = 30:70) to afford 4a-hydroxy-9a-methyl-2,3,4,4a,9,9a-hexahydro-1*H*-xanthen-1-one **16n** (cat. **10**: 91 mg, 78%, cat. **8**: 87 mg, 75%) as a white solid. Melting point: 134−137 °C. Diastereomer ratio % (major/minor): 58:42. Selected signal for major diastereomer: ^1H NMR (400 MHz, $CDCl_3$) δ 7.17−6.71 (m, 4H), 3.35 (d, J = 16.7 Hz, 1H), 2.85−2.54 (m, 2H), 2.52−1.86 (m, 6H), 1.20 (s, 3H). $^{13}C\{^1H\}$ NMR (100 MHz, $CDCl_3$) δ 211.6, 210.4, 151.0, 150.3, 130.6, 128.9, 127.4, 121.8, 121.5, 116.9, 100.2, 51.5, 49.6, 36.1, 35.6, 33.2, 31.9, 29.3, 22.4, 21.2, 19.6. IR (neat): 3417, 2950, 1702, 1488, 1457 cm^{-1}. HRMS (ESI-TOF) m/z: $[M + H]^+$ calcd for $C_{14}H_{17}O_3$ 233.1178; Found 233.1183. Crystal preparation: The crystal is grown by simple recrystallization method where pure compound isolated after column chromatography is dissolved in dichloromethane and layered with hexane and kept at room temperature for 2 days to get pure crystal. Crystal data: $C_{14}H_{16}O_3$, M = 232, monoclinic, space group $P21/n$ with a = 11.470(2) Å, b = 6.1988(13) Å, c = 32.304(7) Å, α = 90°, β = 97.018(7)°, γ = 90°, V = 2279.6(8), T = 273 K, R1 = 0.0589, wR2 = 0.1407 on observed data, z = 8, $F(000)$ = 992, Absorption coefficient = 0.094, λ= 0.71073 Å, 31952 reflections were collected on a Bruker APEX-II CCD, 3826 observed reflections ($I \geq 2\sigma(I)$).

*7-Nitro-3,9-dihydrocyclopenta[b]chromen-1(2H)-one (**16o**).* Prepared according to procedure F using 1,3-cyclopentanedione (49 mg, 0.50 mmol) and 2-(hydroxymethyl)-4-nitrophenol (169 mg, 1 mmol), and the residue was purified by 100−200 mesh silica gel column chromatography (EtOAc/hexane = 10:90) to afford 7-nitro-3,9-dihydrocyclopenta[b]chromen-1(2*H*)-one **16o** (cat. **10**: 53 mg, 42%, cat. **8**: 54 mg, 43%) as a yellow solid. Melting point: 155−160 °C. ^1H NMR (400 MHz, $CDCl_3$) δ 8.07 (m, 2H), 7.12 (m, 1H), 3.60 (s, 2H), 2.77 (m, 2H), 2.59 (m, 2H). $^{13}C\{^1H\}$ NMR (100 MHz, $CDCl_3$) δ 203.1, 178.5, 126.4, 125.6, 124.6, 124.2, 121.4, 118.3, 33.7, 25.8, 21.2. IR (neat): 2923, 2853, 1663, 1522, 1435 cm^{-1}. HRMS (ESI-TOF) m/z: $[M + H]^+$ calcd for $C_{12}H_{10}NO_4$ 232.0610; found, 232.0608.

*1,3-Dimethyl-7-nitro-1,5-dihydro-2H-chromeno[2,3-d]-pyrimidine-2,4(3H)-dione (**16p**).* Prepared according to procedure F using 1,3-dimethylpyrimidine-2,4,6(1*H*,3*H*,5*H*)-trione (78 mg, 0.50 mmol) and 2-(hydroxymethyl)-4-nitrophenol (169 mg, 1 mmol), and the residue was purified by 100−200 mesh silica gel column chromatography (EtOAc/hexane = 30:70) to afford 1,3-dimethyl-7-nitro-1,5-dihydro-2*H*-chromeno[2,3-*d*]pyrimidine-2,4(3*H*)-dione **16p** (cat. **10**: 112 mg, 78%, cat. **8**: 110 mg, 76%) as a brown solid. Melting point: 281−284 °C. ^1H NMR (400 MHz, DMSO-d_6) δ 7.99 (dd, J = 9.1, 2.8 Hz, 1H), 7.83 (d, J = 1.9 Hz, 1H), 6.89 (d, J = 9.1 Hz, 1H), 3.41 (s, 3H), 3.36 (s, 2H), 2.93 (s, 3H). $^{13}C\{^1H\}$ NMR (100 MHz, DMSO-d_6) δ 169.9, 161.9, 150.4, 139.2, 126.7, 124.9, 123.2, 115.2, 55.6, 38.2, 28.1. IR (neat): 3015, 1673, 1625, 1588, 1542, 1501, 1342 cm^{-1}. HRMS (ESI-TOF) m/z: $[M]^+$ calcd for $C_{13}H_{12}N_3O_5$ 289.0699; Found 289.0696.

*6H,7H-Chromeno[4,3-b]chromen-6-one (**16q**).*[38] Prepared according to procedure F using 4-hydroxy-2*H*-chromen-2-one (81 mg, 0.50 mmol) and 2-(hydroxymethyl)phenol (124 mg, 1 mmol), and the residue was purified by 100−200 mesh silica gel column chromatography (EtOAc/hexane = 10:90) to afford 6*H*,7*H*-chromeno[4,3-*b*]chromen-6-one **16q** (cat. **10**: 50 mg, 40%, cat. **8**: 53 mg, 42%) as a white solid. Melting point: 216−223 °C. ^1H NMR (400 MHz, acetone-d_6) δ 7.89 (dd, J = 7.9, 1.4 Hz, 1H), 7.60 (ddd, J = 8.3, 7.4, 1.6 Hz, 1H), 7.35 (m, 3H), 7.09 (m, 1H), 6.94 (dd, J = 8.1, 1.1 Hz, 1H), 6.85 (td, J = 7.5, 1.2 Hz, 1H), 3.90 (s, 2H). $^{13}C\{^1H\}$ NMR (100 MHz, acetone-d_6) δ 164.1, 160.9, 153.9, 153.4, 132.7, 131.7, 128.7, 126.8, 124.7, 124.1, 121.8, 117.2, 117.0, 116.0, 105.5, 24.5. IR (neat): 3078, 2956, 1660, 1618, 1566, 1505, 1425 cm^{-1}. HRMS (ESI-TOF) m/z: $[M + H]^+$ calcd for $C_{16}H_{11}O_3$ 251.0708; Found 251.0714.

*3-Ethyl-2-methyl-1,5,6,7-tetrahydro-4H-indol-4-one (**17a**).*[39] Prepared according to procedure G using 2-methyl-1,5,6,7-tetrahydro-4*H*-indol-4-one (25 mg, 0.17 mmol) and ethanol in excess, and the residue was purified by 100−200 mesh silica gel column chromatography (EtOAc/hexane = 50:50) to afford 3-ethyl-2-methyl-1,5,6,7-tetrahydro-4*H*-indol-4-one **17a** (18 mg, 61%) as a white solid. Melting point: 191−196 °C. ^1H NMR (400 MHz, $CDCl_3$) δ 8.53 (s, 1H), 2.74 (t, J = 6.2 Hz, 2H), 2.65 (q, J = 14.9, 7.4 Hz, 2H), 2.43 (t, J = 5.9 Hz, 2H), 2.15 (s, 3H), 2.09 (m, 2H), 1.12 (t, J = 7.4 Hz, 3H). $^{13}C\{^1H\}$ NMR (100 MHz, $CDCl_3$) δ 195.1, 142.3, 123.9, 120.8, 118.4, 38.9, 24.1, 23.1, 18.2, 15.6, 10.4. IR (neat): 3227, 3187, 2956, 2854, 1623, 1469 cm^{-1}. HRMS (ESI-TOF) m/z: $[M + H]^+$ calcd for $C_{11}H_{16}NO$ 178.1232; Found 178.1236.

*3-Hexyl-2-methyl-1,5,6,7-tetrahydro-4H-indol-4-one (**17b**).* Prepared according to procedure G using 2-methyl-1,5,6,7-tetrahydro-4*H*-indol-4-one (50 mg, 0.34 mmol) and hexan-1-ol in excess and the residue was purified by 100−200 mesh silica gel column chromatography (EtOAc/hexane = 50:50) to afford 3-hexyl-2-methyl-1,5,6,7-tetrahydro-4*H*-indol-4-one **17b** (37 mg, 48%) as a white solid. Melting point: 93−98 °C. ^1H NMR (400 MHz, $CDCl_3$) δ 7.88 (s, 1H), 2.73 (t, J = 6.2 Hz, 2H), 2.60 (t, J = 7.5 Hz, 2H), 2.42 (t, J = 5.9 Hz, 2H), 2.13 (s, 3H), 2.09 (m, 2H), 1.61 (s, 2H), 1.50 (m, 2H), 1.29 (m, 4H), 0.86 (t, J = 6.7 Hz, 3H). $^{13}C\{^1H\}$ NMR (100 MHz, $CDCl_3$) δ 194.6, 141.7, 123.8, 119.5, 118.7, 38.7, 31.8, 30.9, 29.3, 24.8, 23.9, 23.1, 22.8, 14.2,

https://doi.org/10.1021/acs.joc.1c00714
J. Org. Chem. 2021, 86, 8805−8828

10.5. IR (neat): 3222, 3185, 2923, 2853, 1620, 1467 cm^{-1}. HRMS (ESI-TOF) m/z: $[M + H]^+$ calcd for $C_{15}H_{24}NO$ 234.1858; Found 234.1861.

2-Benzyl-3-ethyl-1,5,6,7-tetrahydro-4H-indol-4-one (17c). Prepared according to procedure G using 2-benzyl-1,5,6,7-tetrahydro-4*H*-indol-4-one (32 mg, 0.14 mmol) and ethan-1-ol in excess and the residue was purified by 100−200 mesh silica gel column chromatography (EtOAc/hexane = 50:50) to afford 2-benzyl-3-ethyl-1,5,6,7-tetrahydro-4*H*-indol-4-one **17c** (14 mg, 40%) as a white solid. Melting point: 150−152 °C. ^1H NMR (400 MHz, $CDCl_3$) δ 7.77 (s, 1H), 7.32 (m, 2H), 7.21 (m, 3H), 3.88 (s, 2H), 2.74 (q, J = 14.8, 7.4 Hz, 2H), 2.67 (t, J = 6.2 Hz, 2H), 2.42 (t, J = 6.9 Hz, 2H), 2.08 (m, 2H), 1.17 (t, J = 7.4 Hz, 3H). $^{13}C\{^1H\}$ NMR (100 MHz, $CDCl_3$) δ 194.9, 142.7, 139.2, 128.9, 128.7, 126.8, 126.4, 121.8, 118.6, 38.8, 31.3, 24.0, 23.2, 18.3, 15.9. IR (neat): 3843, 3740, 2926, 1629,1525, 1469 cm^{-1}. HRMS (ESI-TOF) m/z: $[M + H]^+$ calcd for $C_{17}H_{20}NO$ 254.1545; Found 254.1551.

3-(Hexylamino)cyclohex-2-en-1-one (18). Prepared according to procedure A using hexan-1-amine (54 mg, 0.50 mmol) and 1,3-cyclohexanedione (56 mg, 0.50 mmol), and the residue was purified by 100−200 mesh silica gel column chromatography (EtOAc/methanol = 99:1) to afford 3-(hexylamino)cyclohex-2-en-1-one **18** (55 mg, 56%) as a black semisolid. ^1H NMR (400 MHz, $CDCl_3$) δ 5.11 (s, 1H), 4.86 (s, 1H), 3.04 (dd, J = 12.4, 6.4 Hz, 2H), 2.31 (m, 4H), 1.93 (m, 2H), 1.56 (m, 2H), 1.31 (m, 6H), 0.87 (t, J = 6.3 Hz, 3H). $^{13}C\{^1H\}$ NMR (100 MHz, $CDCl_3$) δ 197.5, 164.9, 96.7, 43.1, 36.4, 31.6, 29.8, 28.6, 26.7, 22.4, 21.7, 14.1. IR (neat): 3842, 3741, 2932, 1696, 1538 cm^{-1}. HRMS (ESI-TOF) m/z: $[M + H]^+$ calcd for $C_{12}H_{22}NO$ 196.1701; Found 196.1703.

3-Hydroxy-2-(3-methoxybenzyl)cyclohex-2-en-1-one (19). Prepared according to procedure A using 2-hydroxy-3-methoxybenzyl alcohol (69 mg, 0.5 mmol) and 1,3-cyclohexanedione (56 mg, 0.50 mmol), and the residue was purified by 100−200 mesh silica gel column chromatography (EtOAc/hexane = 20:80) to afford 5-methoxy-2,3,4,9-tetrahydro-1*H*-xanthen-1-one **19** (66 mg, 57%) as a brown semisolid. ^1H NMR (400 MHz, $CDCl_3$): δ 8.71 (s, 1H), 7.51 (dd, J = 7.5, 1.6 Hz, 1H), 7.19 (m, 1H), 6.94 (t, J = 7.4 Hz, 1H), 6.89 (d, J = 8.2 Hz, 1H), 3.96 (s, 3H), 3.62 (s, 2H), 2.40 (t, J = 6.2 Hz, 2H), 2.33 (t, J = 6.4 Hz, 2H), 1.90 (m, 2H). $^{13}C\{^1H\}$ NMR (100 MHz, $CDCl_3$) δ 198.3, 172.2, 154.9, 132.1, 128.9, 127.6, 122.4, 115.1, 110.6, 55.9, 36.8, 28.9, 21.0, 20.7. IR (neat): 3740, 2926, 1710, 1596, 1455, 1243 cm^{-1}. HRMS (ESI-TOF) m/z: $[M + H]^+$ calcd for $C_{14}H_{17}O_3$ 233.1178; Found 233.1180.

■ ASSOCIATED CONTENT

Supporting Information

The Supporting Information is available free of charge at https://pubs.acs.org/doi/10.1021/acs.joc.1c00714.

Experimental procedures, Characterization data and Copies of the NMR spectra for the compounds (PDF)

FAIR data, including the primary NMR FID files, for compounds **3a−z**, **3aa−af**, **11a,b**, **11f,g**, **11m,n**, **11r**, **11t**, **11w**, **13a−l**, **16a−q**, **17a−c**, **18**, and **19** (ZIP)

Accession Codes

CCDC 2048435, 2048437, 2048643−2048644, 2051625, and 2064954 contain the supplementary crystallographic data for this paper. These data can be obtained free of charge via www.ccdc.cam.ac.uk/data_request/cif, or by emailing data_request@ccdc.cam.ac.uk, or by contacting The Cambridge Crystallographic Data Centre, 12 Union Road, Cambridge CB2 1EZ, UK; fax: +44 1223 336033.

■ AUTHOR INFORMATION

Corresponding Author

Boopathy Gnanaprakasam − *Department of Chemistry, Indian Institute of Science Education and Research, Pune 411008, India;* orcid.org/0000-0002-3047-9636; Email: gnanaprakasam@iiserpune.ac.in

Authors

Akanksha M. Pandey − *Department of Chemistry, Indian Institute of Science Education and Research, Pune 411008, India*

Naveen Kumar Digrawal − *Department of Chemistry, Indian Institute of Science Education and Research, Pune 411008, India*

Nirmala Mohanta − *Department of Chemistry, Indian Institute of Science Education and Research, Pune 411008, India*

Akash Bandu Jamdade − *Department of Chemistry, Indian Institute of Science Education and Research, Pune 411008, India*

Moreshwar B. Chaudhari − *Department of Chemistry, Indian Institute of Science Education and Research, Pune 411008, India*

Girish Singh Bisht − *Department of Chemistry, Indian Institute of Science Education and Research, Pune 411008, India*

Complete contact information is available at: https://pubs.acs.org/10.1021/acs.joc.1c00714

Notes

The authors declare no competing financial interest.

■ ACKNOWLEDGMENTS

This research was supported by the SERB (CRG/2018/003935) and Council of Scientific and Industrial Research [02(0296/17/EMR-II)], India. A.M.P, N.D., and N.M thanks IISER-Pune for the research fellowship. A.J. thanks CSIR for a research fellowship. B.G. thanks SERB, CSIR, and IISER-Pune for the financial support. We thank Dr. C. S. Gopinath (NCL-Pune) for the GC analysis for the detection of hydrogen liberation.

■ REFERENCES

(1) (a) Keller, P. A. In *Comprehensive Heterocyclic Chemistry III*; Katritzky, A. R., Ramsden, C. A., Scriven, E. F. V., Taylor, R. J. K., Eds.; Elsevier: Oxford, U.K., 2008; Vol. 7, pp 217−308. (b) *The Alkaloids: Chemistry and Biology*; Cordell, G. A., Ed.; Academic Press: San Diego, CA, 2000; Vol. 54. (c) *Pharmaceuticals: Classes, Therapeutic Agents, Areas of Application*; McGuire, J. L., Ed.; Wiley−VCH: Weinheim, Germany, 2000; Vols. 1−4. (d) Brown, B. R. *The Organic Chemistry of Aliphatic Nitrogen Compounds*; Cambridge University Press: Cambridge, U.K., 2004. (e) Joule, J. A.; Mills, K. *Heterocyclic Chemistry*, 5th ed.; Wiley: Chichester, U.K., 2010.

(2) (a) Allais, C.; Grassot, J. M.; Rodriguez, J.; Constantieux, T. Metal-Free Multicomponent Syntheses of Pyridines. *Chem. Rev.* **2014**, *114*, 10829−10868. (b) Hill, M. D. Recent Strategies for the Synthesis of Pyridine Derivatives. *Chem. - Eur. J.* **2010**, *16*, 12052−12062. (c) Broere, D. L. J.; Ruijter, E. Recent Advances in Transition-Metal-Catalyzed [2 + 2 + 2]-Cyclo(co)trimerization Reactions. *Synthesis* **2012**, *44*, 2639−2672.

(3) Acceptorless dehydrogenation of alcohols chemistry. Reviews: (a) Crabtree, R. H. Homogeneous Transition Metal Catalysis of Acceptorless Dehydrogenative Alcohol Oxidation: Applications in Hydrogen Storage and to Heterocycle Synthesis. *Chem. Rev.* **2017**, *117*, 9228−9246. (b) Gunanathan, C.; Milstein, D. Applications of Acceptorless Dehydrogenation and Related Transformations in Chemical Synthesis. *Science* **2013**, *341*, 1229712. (c) Filonenko, G. A.; van Putten, R.; Hensen, E. J. M.; Pidko, E. A. Catalytic (de)hydrogenation promoted by non-precious metals − Co, Fe and Mn: recent advances in an emerging field. *Chem. Soc. Rev.* **2018**, *47*, 1459−1483.

(4) Catalytic borrowing hydrogen chemistry in chemical synthesis. Reviews: (a) Corma, A.; Navas, J.; Sabater, M. Advances in One-Pot Synthesis through Borrowing Hydrogen Catalysis. *Chem. Rev.* **2018**,

118, 1410−1459. (b) Obora, Y. Recent Advances in α-Alkylation Reactions using Alcohols with Hydrogen Borrowing Methodologies. *ACS Catal.* **2014**, *4*, 3972−3981.
(5) (a) Hamid, M. H. S. A.; Slatford, P. A.; Williams, J. M. J. Borrowing Hydrogen in the Activation of Alcohols. *Adv. Synth. Catal.* **2007**, *349*, 1555−1575. (b) Reed-Berendt, B. G.; Polidano, K.; Morrill, L. C. Recent Advances in Homogeneous Borrowing Hydrogen Catalysis Using Earth-Abundant First Row Transition Metals. *Org. Biomol. Chem.* **2019**, *17*, 1595−1607.
(6) (a) Nandakumar, A.; Midya, S. B.; Landge, V. G.; Balaraman, E. Transition-Metal-Catalyzed Hydrogen-Transfer Annulations:Access to Heterocyclic Scaffolds. *Angew. Chem., Int. Ed.* **2015**, *54*, 11022−11034. (b) Huang, F.; Liu, Z.; Yu, Z. C-Alkylation of Ketones and Related Compounds by Alcohols: Transition-Metal-Catalyzed Dehydrogenation. *Angew. Chem., Int. Ed.* **2016**, *55*, 862−875.
(7) (a) Michlik, S.; Kempe, R. A Sustainable Catalytic Pyrrole Synthesis. *Nat. Chem.* **2013**, *5*, 140−144. (b) Michlik, S.; Kempe, R. Regioselectively Functionalized Pyridines from Sustainable Resources. *Angew. Chem., Int. Ed.* **2013**, *52*, 6326−6329.
(8) Srimani, D.; Ben-David, Y.; Milstein, D. Direct Synthesis of Pyrroles by Dehydrogenative Coupling of β-Aminoalcohols with Secondary Alcohols Catalyzed by Ruthenium Pincer Complexes. *Angew. Chem., Int. Ed.* **2013**, *52*, 4012−4015.
(9) Iida, K.; Miura, T.; Ando, J.; Saito, S. The Dual Role of Ruthenium and Alkali Base Catalysts in Enabling a Conceptually New Shortcut to N-Unsubstituted Pyrroles through Unmasked α-Amino Aldehydes. *Org. Lett.* **2013**, *15*, 1436−1439.
(10) Zhang, M.; Neumann, H.; Beller, M. Selective Ruthenium-Catalysed Three-Component Synthesis of Pyrroles. *Angew. Chem., Int. Ed.* **2013**, *52*, 597−601.
(11) Pan, B.; Liu, B.; Yue, E.; Liu, Q.; Yang, Z.; Wang, Z.; Sun, W. A Ruthenium Catalyst with Unprecedented Effectiveness for the Coupling Cyclization of γ-Amino Alcohols and Secondary Alcohols. *ACS Catal.* **2016**, *6*, 1247−1253.
(12) Kallmeier, F.; Dudziec, B.; Irrgang, T.; Kempe, R. Manganese-Catalyzed Sustainable Synthesis of Pyrroles from Alcohols and Amino Alcohols. *Angew. Chem., Int. Ed.* **2017**, *56*, 7261−7265.
(13) Chai, H.; Wang, L.; Liu, T.; Yu, Z. A Versatile Ru(II)-NNP Complex Catalyst for the Synthesis of Multisubstituted Pyrroles and Pyridines. *Organometallics* **2017**, *36*, 4936−4942.
(14) Deng, D.; Hu, B.; Yang, M.; Chen, D. NNN-Ruthenium Catalysts for the Synthesis of Pyridines, Quinolines, and Pyrroles by Acceptorless Dehydrogenative Condensation. *Organometallics* **2018**, *37*, 2386−2394.
(15) Midya, S.; Landge, V.; Sahoo, M.; Rana, J.; Balaraman, E. Cobalt-catalyzed Acceptorless Dehydrogenative Coupling of Aminoalcohols with Alcohols: Direct Access to Pyrrole, Pyridine and Pyrazine Derivatives. *Chem. Commun.* **2018**, *54*, 90.
(16) (a) Singh, K.; Vellakkaran, M.; Banerjee, D. A Nitrogen-ligated Nickel-catalyst Enables Selective Intermolecular Cyclisation of β- and γ-Aminoalcohols with Ketones: Access to Five and Six Membered N-Heterocycles. *Green Chem.* **2018**, *20*, 2250. (b) Alanthadka, A.; Bera, S.; Vellakkaran, M.; Banerjee, D. Nickel-Catalyzed Double Dehydrogenative Coupling of Secondary Alcohols and β-Amino Alcohols to Access Substituted Pyrroles. *J. Org. Chem.* **2019**, *84*, 13557−13564.
(17) Mastalir, M.; Glatz, M.; Pittenauer, E.; Allmaier, G.; Kirchner, K. Rhenium-Catalyzed Dehydrogenative Coupling of Alcohols and Amines to Afford Nitrogen-Containing Aromatics and More. *Org. Lett.* **2019**, *21*, 1116−1120.
(18) Chai, H.; Zhang, G.; Tan, W.; Ma, J. A. Robust NNP-type Ruthenium (II) Complex for Alcohols Dehydrogenation to Esters and Pyrroles. *Appl. Organomet. Chem.* **2020**, *34*, e5367.
(19) (a) Gholap, S. S. Pyrrole: An Emerging Scaffold for Construction of Valuable Therapeutic Agents. *Eur. J. Med. Chem.* **2016**, *110*, 13−31. (b) Rigby, J. H.; Cavezza, A.; Heeg, M. J. Total Synthesis of (±)-Tazettine. *J. Am. Chem. Soc.* **1998**, *120*, 3664−3670. (c) Li, W.; Usman, M.; Wu, L.-Y.; Liu, W.-B. Synthesis of 2,3-Ring Fused Pyrroles via Cu-Catalyzed 5-exo-dig Annulation of Alkyne-Tethered Enaminones. *J. Org. Chem.* **2019**, *84*, 15754−15763.
(20) (a) Patil, S. A.; Patil, R.; Pfeffer, L. M.; Miller, D. D. Chromenes: Potential New Chemotherapeutic Agents for Cancer. *Future Med. Chem.* **2013**, *5*, 1647−1660. (b) Shaheen, F.; Ahmad, M.; Nahar, K. S.; Samreen, H. S.; Anjum, S.; Tashkhodjaev, B.; Turgunov, K.; Sultankhodzhaev, M. N.; Choudhary, M. I.; Ahmad, M.; Attaur, R. New α-Glucosidase Inhibitors and Antibacterial Compounds from Myrtus communis L. *Eur. J. Org. Chem.* **2006**, *2006*, 2371−2377. (c) Morkunas, M.; Dube, L.; Götz, F.; Maier, M. E. Synthesis of the Acylphloroglucinols Rhodomyrtone and Rhodomyrtosone B. *Tetrahedron* **2013**, *69*, 8559−8563. (d) Cottiglia, F.; Dhanapal, B.; Sticher, O.; Heilmann, J. New Chromanone Acids with Antibacterial Activity from Calophyllum Brasiliense. *J. Nat. Prod.* **2004**, *67*, 537.
(21) Muthaiah, S.; Hong, S. H. Acceptorless and Base-Free Dehydrogenation of Alcohols and Amines using Ruthenium-Hydride Complexes. *Adv. Synth. Catal.* **2012**, *354*, 3045−3053.
(22) Aoyagi, Y.; Mizusaki, T.; Shishikura, M.; Komine, T.; Yoshinaga, T.; Inaba, H.; Ohta, A.; Takeya, K. Efficient synthesis of pyrroles and 4,5,6,7-tetrahydroindoles via palladium-catalyzed oxidation of hydroxyenamines. *Tetrahedron* **2006**, *62*, 8533−8538.
(23) (a) Yates, P.; Bichan, D. J.; McCloskey, J. E. Condensation of Cyclohexane-1,3-Diones with o-Hydroxybenzyl alcohol. Synthesis of 3,4-dihydro-1(2H)-xanthenones. *J. Chem. Soc., Chem. Commun.* **1972**, *14*, 839a. (b) Kidwai, M.; Jain, A. Zn[(L)Proline]$_2$: An Eligible Candidate for the Synthesis of Xanthenediones in Water. *Appl. Organomet. Chem.* **2012**, *26*, 528−535. (c) Yoshioka, E.; Kohtani, S.; Miyabe, H. A. Multicomponent Coupling Reaction Induced by Insertion of Arynes into the C-O Bond of Formamide. *Angew. Chem., Int. Ed.* **2011**, *50*, 6638−6642. (d) Ghosh, P. P.; Das, A. R. Nano Crystalline and Reusable ZnO Catalyst for the Assembly of Densely Functionalized 4H-Chromenes in Aqueous Medium via One-Pot Three Component Reactions: A Greener "NOSE" Approach. *J. Org. Chem.* **2013**, *78*, 6170−6181. (e) He, X.; Tao, J.; Hu, X.; Wang, H.; Shang, Y. $FeCl_3$-Mediated One-Pot Domino Reactions for the Synthesis of 9-Aryl/9-Arylethynyl-2,3,4,9-tetrahydro-1*H*-xanthen-1-ones from Propargylic Amines/Diaryl Amines and 1,3-Cyclohexanediones. *J. Org. Chem.* **2016**, *81*, 2062−2069. (f) Sudheendran, K.; Malakar, C. C.; Conrad, J.; Beifuss, U. Cu(I)-Catalyzed Domino Reactions: Efficient and Selective Synthesis of 4H-Chromenes and Naphthalenes. *J. Org. Chem.* **2012**, *77*, 10194−10210.
(24) Hanbauer, M.; Nazir, Z.; Hildebrand, P.; Figini, A.; Liang, L.; Fumagalli, T. Methods of producing Molindone and its salts. US2014/0081020 A1, 2014.
(25) Stanovnik, B. Enaminone, Enaminoesters, and Related Compounds in the Metal-Free Synthesis of Pyridines and Fused Pyridines. *Eur. J. Org. Chem.* **2019**, *2019*, 5120−5132.
(26) (a) Zbieg, J. R.; Yamaguchi, E.; McInturff, E. L.; Krische, M. J. Enantioselective C-H Crotylation of Primary Alcohols via Hydro hydroxyalkylation of Butadiene. *Science* **2012**, *336*, 324−327. (b) Murahashi, S.-I.; Naota, T.; Ito, K.; Maeda, Y.; Taki, H. Ruthenium-Catalyzed Oxidative Transformation of Alcohols and Aldehydes to Esters and Lactones. *J. Org. Chem.* **1987**, *52*, 4319−4327. (c) Xie, X.; Huynh, H. V. Tunable Dehydrogenative Amidation versus Amination Using a Single Ruthenium-NHC Catalyst. *ACS Catal.* **2015**, *5*, 4143. (d) Dam, J. H.; Osztrovszky, G.; Nordstrøm, L. U.; Madsen, R. Amide Synthesis from Alcohols and Amines Catalyzed by Ruthenium N-Heterocyclic Carbene Complexes. *Chem. - Eur. J.* **2010**, *16*, 6820. (e) Kuwahara, T.; Fukuyama, T.; Ryu, I. Ruthenium Hydride/Nitrogen Tridentate Ligand-catalyzed α-Alkylation of Acetamides with Primary Alcohols. *RSC Adv.* **2013**, *3*, 13702.
(27) Reddy, C. R.; Reddy, M. D.; Srikanth, B. Phosphine Mediated Cascade Reaction of Azides with MBH-acetates of Acetylenic Aldehydes to Substituted Pyrroles: A Facile Access to N-fused Pyrrolo-Heterocycles. *Org. Biomol. Chem.* **2012**, *10*, 4280−4288.
(28) Luo, J.; Lu, D.; Peng, Y.; Tang, Q. Paal−Knorr Furan Synthesis Using TiCl4 as Dehydrating Agent: A Concise Furan Synthesis from a-Haloketones and b-Dicarbonyl Compounds. *Asian J. Org. Chem.* **2017**, *6*, 1546−1550.

https://doi.org/10.1021/acs.joc.1c00714
J. Org. Chem. 2021, 86, 8805−8828

(29) Hu, L.; Luo, J.; Lu, D.; Tang, Q. Urea Decomposition: Efficient Synthesis of Pyrroles Using the Deepeutectic Solvent Choline Chloride/Urea. *Tetrahedron Lett.* **2018**, *59*, 1698−1701.
(30) To, Q. H.; Lee, Y. R.; Kim, S. H. One Step Synthesis of Tetrahydroindoles by Ceric(IV) Ammoniumnitrate Promoted Oxidative Cycloaddition of Enaminones and Vinyl Ethers. *Tetrahedron* **2014**, *70*, 8108−8113.
(31) Huang, K.; Veal, J. M.; Fadden, R. P.; Rice, J. W.; Eaves, J.; Strachan, J. P.; Barabasz, A. F.; Foley, B. E.; Barta, T. E.; Ma, W.; Silinski, M. A.; Hu, M.; Partridge, J. M.; Scott, A.; DuBois, L. G.; Freed, T.; Steed, P. M.; Ommen, A. J.; Smith, E. D.; Hughes, P. F.; Woodward, A. R.; Hanson, G. J.; McCall, W. S.; Markworth, C. J.; Hinkley, L.; Jenks, M.; Geng, L.; Lewis, M.; Bert Pronk, J. O.; Verleysen, K.; Hall, S. E. Discovery of Novel 2-Aminobenzamide Inhibitors of Heat Shock Protein 90 as Potent, Selective and Orally Active Antitumor Agents. *J. Med. Chem.* **2009**, *52*, 4288−4305.
(32) Sridharan, V.; Ribelles, P.; Ramos, M. T.; Menéndez, J. C. Cerium(IV) Ammonium Nitrate Is an Excellent, General Catalyst for the Friedländer and Friedländer−Borsche Quinoline Syntheses: Very Efficient Access to the Antitumor Alkaloid Luotonin A. *J. Org. Chem.* **2009**, *74*, 5715−5718.
(33) Cini, E.; Petricci, E.; Truglio, G. I.; Vecchio, M.; Taddei, M. Ruthenium Catalysed C-Alkylation of 1,3-Dicarbonyl Compounds with Primary Alcohols and Synthesis of 3-Keto-quinolines. *RSC Adv.* **2016**, *6*, 31386−31390.
(34) Panday, A. K.; Mishra, R.; Jana, A.; Parvin, T.; Choudhury, L. Synthesis of Pyrimidine Fused Quinolines by Ligand-Free Copper-Catalyzed Domino Reactions. *J. Org. Chem.* **2018**, *83*, 3624−3632.
(35) Na, J. E.; Lee, K. Y.; Park, D. Y.; Kim, J. N. Modified Friedlander Synthesis of Quinolines from N-Phenyl Cyclic Enaminones. *Bull. Korean Chem. Soc.* **2005**, *26*, 323−326.
(36) Sudheendran, K.; Malakar, C. C.; Conrad, J.; Beifuss, U. Copper(I)-Catalyzed Intramolecular O-Arylation for the Synthesis of 2,3,4,9-Tetrahydro-1*H*-xanthen-1-ones with Low Loads of CuCl. *J. Org. Chem.* **2012**, *77*, 10194−10210.
(37) Ramachary, D. B.; Reddy, V. Y.; Kishor, M. Multi-catalysis Reactions: Direct Organocatalytic Sequential One Pot Synthesis of Highly Functionalized Cyclopenta[b]chromen-1-ones. *Org. Biomol. Chem.* **2008**, *6*, 4188−4197.
(38) Zhang, X. Y.; Fang, L. L.; Liu, N.; Wu, H. Y.; Fan, X. S. Copper-catalyzed Tandem Reaction of 2-Bromobenzyl Bromides with 1,3-Dicarbonyl Compounds Leading to 4H-Chromenes. *Chin. Chem. Lett.* **2012**, *23*, 1129−1132.
(39) Fukada, N.; Trudell, M. L.; Johnson, B.; Cook, J. H. Synthetic Studies in the l3-Carbonile Area New Entry into 4-Substituted and 3,4-Disubstituted B-Carbolines. *Tetrahedron Lett.* **1985**, *26*, 2139−2142.
(40) Rajawinslin, R. R.; Gawande, S. D.; Kavala, V.; Huang, Y.; Kuo, C.; Kuo, T.; Chen, M.; He, C.; Yao, C. Iron/acetic acid mediated intermolecular tandem C−C and C−N bond formation: an easy access to acridinone and quinoline derivatives. *RSC Adv.* **2014**, *4*, 37806−37811.

https://doi.org/10.1021/acs.joc.1c00714
J. Org. Chem. 2021, 86, 8805−8828

Continuous-Flow Direct Azidation of Alcohols and Peroxides for the Synthesis of Quinoxalinone, Benzooxazinone, and Triazole Derivatives

Author: Akanksha M. Pandey, Shankhajit Mondal, Boopathy Gnanaprakasam
Publication: The Journal of Organic Chemistry
Publisher: American Chemical Society
Date: Aug 1, 2022

PERMISSION/LICENSE IS GRANTED FOR YOUR ORDER AT NO CHARGE

This type of permission/license, instead of the standard Terms and Conditions, is sent to you because no fee is being charged for your order. Please note the following:

- Permission is granted for your request in both print and electronic formats, and translations.
- If figures and/or tables were requested, they may be adapted or used in part.
- Please print this page for your records and send a copy of it to your publisher/graduate school.
- Appropriate credit for the requested material should be given as follows: "Reprinted (adapted) with permission from {COMPLETE REFERENCE CITATION}. Copyright {YEAR} American Chemical Society." Insert appropriate information in place of the capitalized words.
- One-time permission is granted only for the use specified in your RightsLink request. No additional uses are granted (such as derivative works or other editions). For any uses, please submit a new request.

If credit is given to another source for the material you requested from RightsLink, permission must be obtained from that source.

BACK CLOSE WINDOW

Catalytic Acceptorless Dehydrogenation of Amino Alcohols and 2-Hydroxybenzyl Alcohols for Annulation Reaction under Neutral Conditions

Author: Akanksha M. Pandey, Naveen Kumar Digrawal, Nirmala Mohanta, et al
Publication: The Journal of Organic Chemistry
Publisher: American Chemical Society
Date: Jul 1, 2021

PERMISSION/LICENSE IS GRANTED FOR YOUR ORDER AT NO CHARGE

This type of permission/license, instead of the standard Terms and Conditions, is sent to you because no fee is being charged for your order. Please note the following:

- Permission is granted for your request in both print and electronic formats, and translations.
- If figures and/or tables were requested, they may be adapted or used in part.
- Please print this page for your records and send a copy of it to your publisher/graduate school.
- Appropriate credit for the requested material should be given as follows: "Reprinted (adapted) with permission from {COMPLETE REFERENCE CITATION}. Copyright {YEAR} American Chemical Society." Insert appropriate information in place of the capitalized words.
- One-time permission is granted only for the use specified in your RightsLink request. No additional uses are granted (such as derivative works or other editions). For any uses, please submit a new request.

If credit is given to another source for the material you requested from RightsLink, permission must be obtained from that source.

BACK CLOSE WINDOW